**Saskatchewan
Energy and Mines**

Saskatchewan
Geological Survey

Miscellaneous Report 2000-4.2

Summary of Investigations 2000, Volume 2, Saskatchewan Geological Survey

Printed under the authority of the
Minister of Energy and Mines

Although the Department of Energy and Mines has exercised all reasonable care in the compilation, interpretation, and production of this report, it is not possible to ensure total accuracy, and all persons who rely on the information contained herein do so at their own risk. The Department of Energy and Mines and the Government of Saskatchewan do not accept liability for any errors, omissions or inaccuracies that may be included in, or derived from, this report.

Cover:
This photo is of the east end of the Deilmann Pit at Key Lake. Note in the center of the photo, sandstones and conglomerates of the Manitou Falls Formation, Athabasca Group, on lap maroon weathering gneisses of the Wollaston Group. The incised unconformity surface is part of the north limb of an east-trending paleovalley (see papers by Harvey and Bethune, this volume; Yeo *et al.*, this volume). Photo by G.D. Delaney, Saskatchewan Energy and Mines.

Additional copies of this report may be obtained by contacting:

Saskatchewan Energy and Mines
Communications Branch
2101 Scarth Street, 3rd floor
Regina, SK S4P 3V7
(306) 787-2528
FAX: (306) 787-2527
E-mail: enquiry@sem.gov.sk.ca

Editors:
G.D. Delaney
C.T. Harper

Production Editor:
C.L. Brown

ISSN 0228 5657
Printed by Houghton Boston Printers • Lithographers

102-06700/

Foreword

The Summary of Investigations 2000, Volume 2 presents the results of geoscience field projects carried out by Saskatchewan Energy and Mines and other geoscience investigators who were active in Saskatchewan. An associated volume published in the spring focuses on Phanerozoic geoscience projects.

Most of the projects summarized within this volume are cooperative endeavors with other agencies conducting research in the province. Examples include the Athabasca Basin EXTECH IV project designed to study the multifaceted context of Saskatchewan's uranium deposits. Partners providing funding are Natural Resources Canada, Cameco Corporation, COGEMA Resources Inc., Saskatchewan Energy and Mines, and the Alberta Geological Survey. Included in the research team is the Saskatchewan Research Council (SRC), the Universities of Regina and Saskatchewan, and Laurentian University.

Two large multi-discipline studies, including airborne geophysical surveys and geological mapping, were started in northern Saskatchewan: one in the Uranium City area, in the northwest of the province, and the second in the Phelps Lake area, in the northeast. Both airborne projects received funding through the Geological Survey of Canada's Targeted Geoscience Initiative and Saskatchewan's Northern Affairs Centenary Fund.

The digital Geology Atlas of Saskatchewan has been expanded to include new information including lake-bottom sediment geochemistry and oil and gas dispositions. The previous version received an award of excellence from ESRI Canada. Saskatchewan Energy and Mines plans to add 1:250 000 scale geology maps to next year's version.

Several new land-use planning projects, the representative areas network, and other land-based issues have increased the demand for mineral assessments. Currently, two staff members are working full-time and two staff part-time to meet this demand. The mineral assessments done by department staff are reviewed by industry representatives. Industry participation in the land-use plans is critical to the success of the these plans.

Saskatchewan Energy and Mines is in the process of reviewing its five-year plan, based on a completed audit of Saskatchewan's geoscience database. This information, along with a questionnaire, was distributed to the exploration industry. Preliminary results confirm industry's need for geological maps, but also the increasing demand for digital products.

The department hired a new Project Geologist, J. Kraus and a new Resident Geologist, G. Tourigny, last spring, and plans to hire an additional project geologist during 2001.

George C. Patterson
Executive Director
Exploration and Geological Services

December 2000

Contents

page

Foreword .... *iii*

Contents .... *iv*

A. Northern Papers Exclusive of the Athabasca Basin

* Uranium City Revisited: A New Look at the Rocks of the Beaverlodge Mining Camp .... *K.E. Ashton, J. Kraus, R.P. Hartlaub, and R. Morelli* 3

* New Insights into the Structural Geology and Tectonic Setting of the Uranium City area, Northwestern Saskatchewan .... *J. Kraus and K.E. Ashton* 16

Airborne Multisensor (Gamma Ray Spectrometric/Magnetic/VLF-EM) Surveys in Northern Saskatchewan: A Status Report .... *R.B.K. Shives, J.M. Carson, P.B. Holman, K.L. Ford, J.A. Grant, K.E. Ashton, C.T. Harper, and G.D. Delaney* 26

* The Final Pieces of the 'Bridge': Geology of the Southern Reindeer Lake and Laurie Lake Areas .... *Ralf O. Maxeiner and Cameron J. Demmans* 30

Constraints on Metamorphic Conditions in the Milton Island Metasedimentary Assemblage, Reindeer Lake .... *Anthony E. Williamson, Kevin M. Ansdell, and Ralf O. Maxeiner* 51

Geochemistry of Volcanic and Intrusive Rocks of the May Lake Area, La Ronge Domain .... *C.T. Harper* 59

The Round Lake Stock: A Structural Trap for the Emplacement of the Fracture-controlled Komis Gold Deposit in the La Ronge Domain, Northern Saskatchewan .... *Bruno Lafrance* 74

Nd Isotope Geochemistry of Igneous Rocks in the Glennie Domain and its Immediate Sub-Phanerozoic Extension: Evidence for Interactions with the Sask Craton? .... *Tim C. Prokopiuk and Kevin M. Ansdell* 79

Geochemical Character of the Tonalite-Trondhjemite Suite of the Tonalite-Migmatite Complex, Deception Lake, Saskatchewan .... *Chris T. Coolican, Kevin M. Ansdell, Rob Kerrich, and Mel Stauffer* 86

Mineralized Core Collection .... *A.J. Gracie* 95

B. Athabasca Basin: EXTECH IV Papers

EXTECH IV – Athabasca Uranium Multidisciplinary Study – Overview .... *C.W. Jefferson and G.D. Delaney* 99

Seismic Modeling Prior to the EXTECH IV Athabasca Basin Seismic Reflection Survey .... *Z. Hajnal, B. Reilkoff, B. Pandit, D. White, E. Adam, B. Powell, and R. Koch* 104

Multiparameter Borehole Geophysical Logging at the Shea Creek and McArthur River Projects: Parameters for Exploration, Stratigraphy, and High-resolution Seismic Studies .... *C.J. Mwenifumbo, K.A. Pflug, B.E. Elliott, C.W. Jefferson, R. Koch, J. Robbins, and R. Matthews* 110

* Practical Stratigraphy and Flashy Sedimentology in the Paleoproterozoic Manitou Falls Formation, Eastern Athabasca Basin, Saskatchewan – An EXTECH IV Progress Report .... *Gary Yeo, Charles W. Jefferson, Jeanne B. Percival, Dan Jiricka, Scott McHardy, Pat Munholland, Brent Collier, Amanda Gaze, and Cathy Williamson* 123

Architecture and Origin of Fluvial Facies in the Athabasca Group at McClean Lake, Northern Saskatchewan .... *Darrel Long, Cathy Williamson, Philippe Portella, and Steve Wilson* 140

* Structural Setting of the Sue C Uranium Deposit, McClean Lake Mine, Northern Saskatchewan .... *Ghislain Tourigny, Steve Wilson, Guy Breton, and Philippe Portella* 146

Detection of K-enrichment (Illite) Chimneys Using Ground Gamma Ray Spectrometry, McArthur River Area, Northern Saskatchewan .... *R.B.K. Shives, K. Wasyliuk, and G. Zaluski* 160

Status Report on the Surficial Geological Framework for the NEA-IAEA Study Area, Eastern Athabasca Basin .... *Janet Campbell and Rob Shives* 170

Synchrotron X-radiation Study of Illitic Clays from the Cigar Lake Uranium Deposit, Northern Saskatchewan .... *J.B. Percival, S. Skanthakumar, L. Soderholm, P.C. Burns, and A. Locock* 173

C. Athabasca Basin: Other Contributed Papers

Paleotopography and Clay Mineral Alteration Associated with the Deilmann Uranium Orebody, Key Lake, Saskatchewan .... *S.E. Harvey and K.M. Bethune* 181

Paleoproterozoic Thermotectonic Evolution of the Eastern Sub-Athabasca Basement, Northern Saskatchewan: Integrated Geophysical and Geological Data......... *Philippe Portella and Irvine R. Annesley* 191

Uraninite-bearing Granitic Pegmatite, Moore Lakes, Saskatchewan: Petrology and U-Th-Pb Chemical Ages...................... *Irvine R. Annesley, Catherine Madore, Richard T. Kusmirski, and Tom Bonli* 201

D. Industrial Minerals Studies

Origin of Saskatchewan Sodium Sulphate Deposits – A Progress Report .... *Lynn I. Kelley* 215

Electrical Resistivity Imaging of a Brine Plume under the Margin of a Sodium Sulphate Lake................ *E.P. Zimmerman, L.R. Bentley, M. Hayashi, L.I. Kelley, and C. Holmden* 218

The Diamond Potential of Saskatchewan 2000: A Study in Progress................ *Brent C. Jellicoe, Phil Robertshaw, Gary Billingsley, and Bruce Kjarsgaard* 223

E. Appendices

Titles and Abstracts of Recent Saskatchewan Energy and Mines Publications and Papers by Staff of the Saskatchewan Geological Survey 227

Acknowledgments 241

Organization Chart 242

Staff List .... inside back cover

---

* Asterisked reports are accompanied by maps, which are available separately for purchase, and are listed in full in the map package.

A. Northern Papers Exclusive of the Athabasca Basin

Uranium City Revisited: A New Look at the Rocks of the Beaverlodge Mining Camp

K.E. Ashton, J. Kraus, R.P. Hartlaub [1], and R. Morelli [2]

Ashton, K.E., Kraus, J., Hartlaub, R.P., and Morelli, R. (2000): Uranium City revisited: A new look at the rocks of the Beaverlodge mining camp; *in* Summary of Investigations 2000, Volume 2, Saskatchewan Geological Survey, Sask. Energy Mines, Misc. Rep. 2000-4.2.

Abstract

The geology of the Uranium City area is complex and characterized by widespread intense brittle to brittle-ductile deformation. Circa 3.0 Ga granitoid basement is unconformably overlain by the moderately to highly metamorphosed Archean Murmac Bay Group, a dominantly siliciclastic sequence comprising basal orthoquartzite, pelite, and psammite, with minor basalt and associated iron formation and dolostone. Serpentinized ultramafic intrusive rocks with komatiitic affinities are also considered part of the sequence and suggest a komatiite-quartzite association.

Following an early thermotectonic event, the Murmac Bay Group was intruded by extensive granitoid and gabbroic rocks, some of which have yielded preliminary 2.64 Ga ages. A second, locally intense deformation and metamorphic event was followed by emplacement of diabase dykes and granitoid rocks prior to a period of widespread brittle and brittle-ductile deformation. This later event resulted in extensive cataclasis and numerous high-strain zones, which were instrumental in forming the region's numerous uranium and gold deposits. The 1800 to 1750 Ma Martin Group of redbed siliciclastics was unconformably deposited towards the end of this third deformational event and slightly predated deposition of the flat-lying 1750 to 1700 Ma Athabasca Group.

The Murmac Bay Group is now known to dominate both the Nevins Lake Block and Beaverlodge Belt/Domain, and to extend into the Black Bay Domain. Hence, the justification for three distinct lithotectonic domains is tenuous. The term "Beaverlodge Domain" is suggested to refer to all three in future.

The "Foot Bay Gneiss" appears to be an intensely deformed mix of granitoid rocks seen elsewhere in the area and therefore does not require distinct lithological status. Nor does the "Donaldson Lake Gneiss", which is a complex mix of Murmac Bay Group supracrustal rocks and intrusive granitoids.

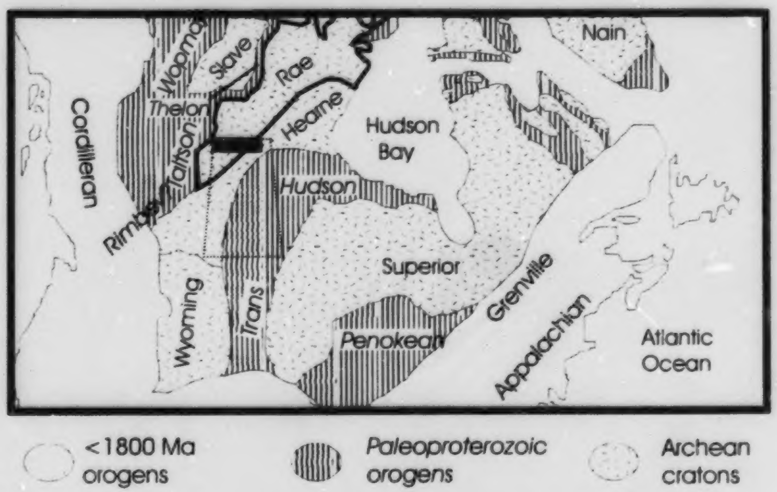

Figure 1 - Orogenic map of North America showing location of the Rae lithotectonic province (highlighted in black) in northern Saskatchewan (dotted outline) (modified from Hoffman, 1988). Area of Figure 2 denoted by black rectangle.

1. Introduction

The Rae Northeast project was initiated in 1998 to determine the tectonic setting and mineral potential of the northeastern Rae Province north of Lake Athabasca (Figures 1 and 2). To date, the study has involved both reconnaissance mapping within the Nevins Lake Block, Train Lake Domain, and Dodge Domain (Ashton and Card, 1998; Ashton *et al.*, 1999), as well as 1:20 000 scale coverage of Murmac Bay Group rocks (Hartlaub and Ashton, 1998; Hartlaub, 1999) and the Oldman-Bulyea Shear Zone (Card and Bethune, 1999). In 2000, the northwestern corner of the province, bounded by the northern shore of Lake

---

[1] Department of Earth and Atmospheric Sciences, University of Alberta, Edmonton, AB T6G 2E3

[2] Department of Geological Sciences, University of Saskatchewan, 114 Science Place, Saskatoon, SK S7N 5E2

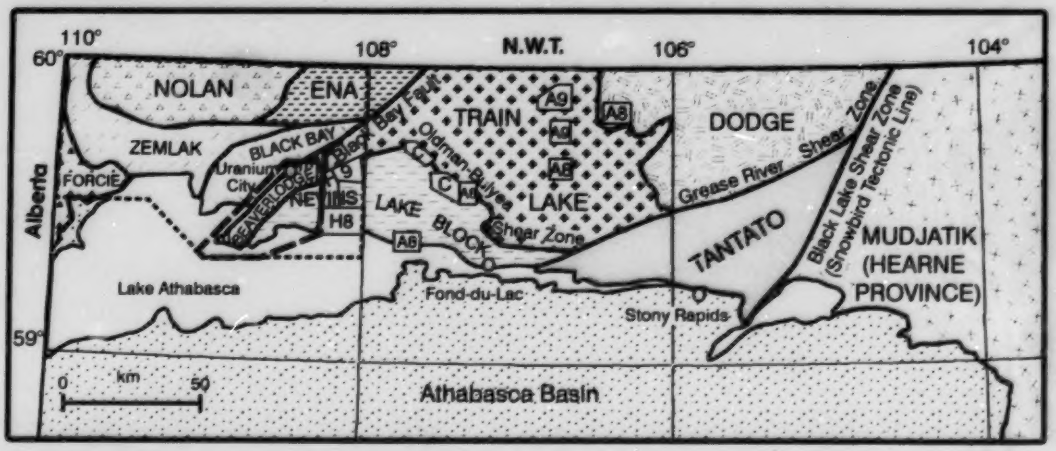

Figure 2 - Location map showing existing lithotectonic domains. Area of GSC multi-parameter airborne survey outlined by short-dashed line; SEM 1:20 000 scale mapping coverage in 2000 outlined by heavy long-dashed line; areas previously mapped outlined by thin lines (A8, Ashton and Card, 1998; H8, Hartlaub and Ashton, 1998; A9, Ashton et al.***, 1999; C, Card and Bethune, 1999; and H9, Hartlaub, 1999).***

Athabasca, the Alberta and Northwest Territorial borders, and 108° longitude, was designated for a three-year collaborative study by Saskatchewan Energy and Mines (SEM) and the Geological Survey of Canada (GSC) (Figure 2). In this first year, the GSC, with partial financial support from Saskatchewan Northern Affairs through the provincial centenary fund, is conducting a combined radiometric-magnetic-VLF-EM airborne survey of the region, while SEM began systematic 1:20 000 scale mapping of the Uranium City area. This report summarizes the general geology of the approximately 850 km^2 area mapped in 2000 (Figure 2), which adjoins and partly overlaps the Murmac Bay Group study to the east (Hartlaub and Ashton, 1998; Hartlaub, 1999). A complementary paper deals more specifically with the structural and tectonic history of the Uranium City area (Kraus and Ashton, this volume).

Since the discovery of uranium at Goldfields on the northern shore of Lake Athabasca in 1934, the Uranium City area has been the site of numerous mapping and exploration programs. The early work has been summarized by Tremblay (1972), whereas the more recent regional mapping has been referenced in the 1:100 000 scale geological compilation of the Greater Beaverlodge area (Macdonald and Slimmon, 1985). Of particular interest to this study is the recent detailed mapping of the Lodge Bay (Sibbald and Lewry, 1980), Nicholson Bay (Sibbald, 1982), and Mickey Lake (Thomas, 1982) map areas, which was conducted in more detail than the present work. It collectively provides an excellent foundation upon which to build, and an attempt has been made to incorporate this detailed data into the new geological maps accompanying this report.

A synthesis of the uranium deposits and showings was compiled by Beck (1969). Although the importance of Uranium City has diminished since closing of the Beaverlodge operation in 1982, a small settlement of about 200 people remains. At a town meeting during the summer of 2000, Greater Lenora Resources Corporation announced plans to re-open the Box gold mine as a small open pit operation. The potential for uranium, copper, and platinum group metals also remains high in the region.

2. General Geology

The broad geological history of the Uranium City area is summarized in Table 1. Circa 3.0 Ga granitic basement (Van Schmus *et al.*, 1986) is unconformably overlain by a dominantly siliciclastic sedimentary sequence containing abundant quartzite and subordinate amounts of basalt, iron formation, carbonate, psammite, and pelite, along with gabbroic to komatiitic intrusive rocks (Figure 3). This dominantly sedimentary package was originally considered part of the Tazin Group (e.g. Alcock, 1936; Christie, 1953), but was subsequently termed the Fay Mine Complex in the vicinity of Eldorado's Ace-Fay-Verna mine complex, and Murmac Bay Formation (Tremblay, 1972; subsequently modified to Murmac Bay Group, e.g. Macdonald, 1983) south of the St. Louis Fault in the Beaverlodge Lake area. Previous workers have suggested that Fay Mine Complex and Murmac Bay Group are correlative. Since the findings of this study support that view, the term Murmac Bay Group has been adopted.

The Murmac Bay Group was deformed and metamorphosed (M1) at conditions locally reaching as high as upper amphibolite facies prior to intrusion of an apparently single suite of coarse-grained granitic plutons including the Gunnar, Mackintosh Bay, Cameron Island, Stephens Lake, and Dead Man Channel granites. Previous attempts to date this suite have yielded U-Pb zircon ages ranging from ca. 2180 to 2440 Ma (Persons, 1983; Van Schmus *et al.*, 1986; Bickford *et al.*, 1987), although ongoing

Table 1 - Inferred geological history of the Uranium City area.

1750 to 1700 Ma	Deposition of Athabasca Group
	---------- Unconformity (F4 folding & sub-greenschist facies metamorphism) ----------
	Diabase Dykes
1800 to 1750 Ma	Deposition of Martin Group
	---------- Unconformity (D3 deformation & M3 metamorphism) ----------
	Medium-grained to pegmatitic granite Diabase
	---------- (D2 deformation & M2 metamorphism) ----------
	Gabbro-diorite
	Pink leucogranite
Ca. 2.64 Ga?	Pink, coarse-grained granite (Gunnar)
	Inclusion-rich to migmatitic leucocratic granite to tonalite
	---------- (D1 deformation & M1 metamorphism) ----------
	Murmac Bay Group
	---------- Unconformity ----------
Ca. 3.05 Ga	Basement granite

geochronological studies suggest that at least the Dead Man Granite may be as old as ca. 2640 Ma.

The Murmac Bay Group was also intruded by abundant gabbroic sills and by medium-grained leucocratic granites including an inclusion-rich variety which invades the supracrustal rocks in the northeast (formerly referred to as "Donaldson Lake Gneiss") and a pink homogeneous variety which occurs as small intrusions throughout (e.g. Box Mine Granite). The inclusion-rich granitoid component of the former "Donaldson Lake Gneiss" previously yielded a U-Pb zircon age of ca. 2180 Ma (Tremblay *et al.*, 1981), although preliminary geochronological work in this study is indicating an older age of about 2640 Ma. There may be several ages of pink leucogranite. The Foot Bay Gneiss, which appears to be a variably sheared and cataclastic portion of a large pink leucogranite intrusion, has yielded a U-Pb zircon age of ca. 2513 Ma (Tremblay *et al.*, 1981), whereas the smaller, sheet-like, Box Mine Granite has yielded 1950 to 2000 Ma ages by both single-zircon Pb-evaporation (O'Hanley *et al.*, 1994) and conventional U-Pb (Van Schmus *et al.*, 1986) techniques.

A second, younger set of mafic intrusions in the form of locally cross-cutting dykes is distinguished from the older gabbro sills based on their thinner nature, the more acicular habit of the hornblende, and by their lower metamorphic grade (the gabbro sills exhibit local M2? partial melting). Together with rare medium-grained to pegmatitic granite dykes, they are considered ramifications of the Paleoproterozoic Trans-Hudson Orogen, which is also thought to have produced a third metamorphic event (M3) along with the dominant northeast-trending folds.

The siliciclastic package was later unconformably overlain by both the ca. 1800 to 1750 Ma Martin Group redbeds, which are themselves folded about a north-northeast-trending axis, and by the flat-lying, ca. 1750 to 1700 Ma Athabasca Group.

3. Unit Descriptions

a) Basement

The circa 3.0 Ga Lodge Bay and Elliot Bay granites comprise homogeneous, medium-grained, leucocratic granitoid rocks containing up to 3% chlorite replacing biotite. As with most rocks in the region, the basement granites are variably strained, ranging from weakly foliated to mylonitic. Due to the masking effects of this deformation and the broad similarity of younger granitoid rocks, the basement granites may be more abundant than presently recognized. Analytical studies are underway to better document the modal and chemical characteristics of all of the granitoid suites.

b) Murmac Bay Group

Quartzite

Quartzite occurs throughout the area but is particularly abundant in the east. Most is white orthoquartzite containing minor sericite, although hematization related to the Martin and Athabasca group unconformities has produced widespread ferruginous varieties, particularly along the eastern Crackingstone Peninsula. Rarely preserved primary features include trough and planar crossbedding and ripple marks (Figure 4). The contact with the basement granites is generally a high-strain zone up to several metres thick, but the local absence of this deformation suggests that it is an unconformity which has been variably affected by contact strain.

Variants of the quartzite include oligomictic conglomerate, grits, feldspathic quartzite, and calcareous quartzite. The oligomictic conglomerate ranges from clast to matrix supported, is poorly sorted, and is characterized by sub-angular to sub-rounded ovoid quartz(ite?) pebbles up to 3 cm long by 1.5 cm wide in a fine-grained to gritty quartzitic matrix (Figure 5). It is interlayered with finer-grained quartzite on a centimetre to metre scale and apparently forms a continuous unit several metres to tens of metres thick. The main unit is intraformational, occurring about 100 m stratigraphically above the basement unconformity, which infers a beach or shallow marine rather than fluvial setting for the

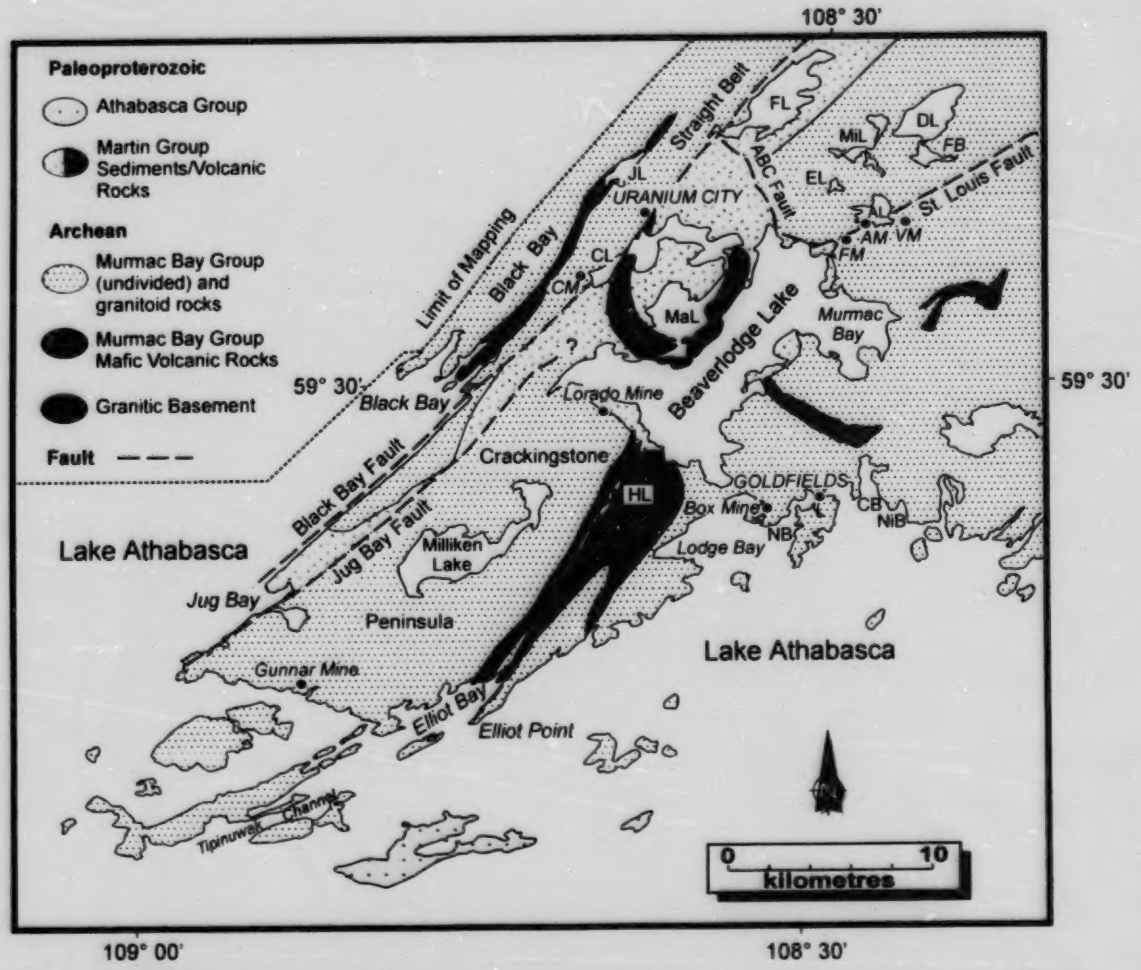
108° 30'
Paleoproterozoic
Athabasca Group
Martin Group Sediments/Volcanic Rocks
Archean
Murmac Bay Group (undivided) and granitoid rocks
Murmac Bay Group Mafic Volcanic Rocks
Granitic Basement
Fault
Limit of Mapping
Black Bay
Straight Belt
FL
DL
MiL
FB
JL
URANIUM CITY
ABC Fault
EL
St. Louis Fault
AL
AM
VM
FM
CL
CM
MaL
Beaverlodge Lake
Murmac Bay
?
59° 30'
Black Bay
Lorado Mine
59° 30'
Crackingstone
Black Bay Fault
HL
GOLDFIELDS
Box Mine
CB
NiB
NB
Lake Athabasca
Jug Bay Fault
Milliken Lake
Lodge Bay
Jug Bay
Peninsula
Lake Athabasca
Gunnar Mine
Elliot Bay
Elliot Point
Tipinuwak Channel
0
10
kilometres
109° 00'
108° 30'

Figure 3 - Simplified geological map of the study area; AL, Ace Lake; CL, Cinch Lake; DL, Donaldson Lake; EL, Eagle Lake; FL, Fredette Lake; HL, Howland Lake; JL, Jean Lake; MaL, Martin Lake; MiL, Mickey Lake; CB, Cornwall Bay; FB, Foot Bay; NB, Neiman Bay; NiB, Nicholson Bay; AM, Ace Mine; CM, Cinch Lake Mine, FM, Fay Mine; and VM, Verna Mine.

Figure 4 - Trough crossbedding in orthoquartzite from eastern Crackingstone Peninsula.

quartzite unit. Assuming that the clasts are locally derived from earlier lithified quartzites, the oligomictic conglomerate could mark a marine transgression (i.e. a disconformity), a storm deposit, or an episode of dip-slip faulting. The conglomerate is especially common at the southern end of Beaverlodge Lake, where one occurrence is underlain by a metre-scale wedge of cobble to boulder conglomerate typified by more angular quartz(ite?) clasts ranging from 5 to 10 cm in size. This may represent one of several channel deposits which were supplying sediment to the more continuous conglomerate sheet.

The "grits" comprise 1 to 2 mm quartz grains in a finer quartzite matrix. They are most common in the southeastern Crackingstone Peninsula, where they occur as lenticular sheets typically interlayered with

CENTIMETRES

Figure 5 - Oligomictic quartz(ite) pebble conglomerate, southwestern Beaverlodge Lake.

finer-grained orthoquartzite on a scale of a few centimetres.

Feldspathic quartzite occurs both as gradational units between quartzite and more psammitic sedimentary rocks and in some of the more highly metamorphosed areas where the quartzites may have been feldspathized during the emplacement of abundant syn-metamorphic granitic dykes and sheets. Calcareous quartzite similarly occurs as a transitional unit into dolostone and is characterized by minor tremolite and/or diopside.

Mafic Volcanic Rocks

Mafic volcanic rocks form several thin units generally in sharp contact with quartzite. Most are weakly layered, fine-grained hornblende-plagioclase amphibolites, but near-massive outcrops on the islands in Elliot Bay (Figure 3) exhibit primary flow contacts, cooling cracks, and amygdules. Features previously interpreted as pillow selvedges on one of these islands are re-interpreted here as polygonal cooling cracks due to their angular and intersecting nature. Although pillows have been reported from the Howland Lake area (C. Harper, pers. comm., 2000), most flows appear massive and may be sub-aerial. The Elliot Bay volcanic belt is characterized by a high aeromagnetic signature. This is in sharp contrast to other supracrustal and granitoid rocks which appear devoid of magnetite, presumably due to replacement by hematite during subaerial exposure associated with the Martin and Athabasca unconformities.

Pale green, fine-grained, intermediate(?) volcanic rocks also occur in the Howland Lake area. Rare volcanic breccia suggests that some of these more intermediate rocks may be volcaniclastic.

In the most highly metamorphosed rocks, the amphibolites are intruded by abundant granite. This is particularly evident in the Donaldson Lake area, where agmatites have resulted. West of the Black Bay Fault, the combination of amphibolites and thin granite intrusions have produced straight gneisses in zones of high strain. The replacement of hornblende by fine-grained biotite in some rocks is attributed to metasomatism associated with these late granitoid rocks.

Centimetre-scale oxide-facies iron formation was noted in quartzite a few centimetres from the mafic volcanic contact near Jean Lake (Figure 3). It also occurs as several thin units up to 0.8 m within intermediate rocks north of Elliot Bay. Both occurrences contribute to the high aeromagnetic signature associated with the mafic volcanic rocks. The oxide facies iron formation is thought to mark a period of chemical sedimentation related to volcanism.

Several occurrences of fine-grained, homogeneous felsite within the mafic volcanic rocks are tentatively interpreted as shallow, syn-volcanic intrusions.

Dolostone

Fine-grained, buff dolostone is found at several localities in the Goldfields and Cornwall Bay areas (Figure 3), where it is spatially associated with quartzite and mafic volcanic rocks. It is commonly interlayered with quartzite on a scale of centimetres to metres. Pegmatitic diopsidite formed along contacts with the quartzite is attributed to the well-known amphibolite facies metamorphic reaction involving quartz and dolomite. Less pure reactants result in more heterogeneous calc-silicate rocks containing abundant tremolite±biotite. The patchy distribution and stratigraphic setting of the dolostone suggest that it was deposited as chemical sediment from hydrothermal vents during the main period of volcanism, rather than as continuous, uniform sedimentary sheets.

Serpentinite-Gabbro

A large ultramafic body at Nicholson Bay has been interpreted as a komatiitic intrusion (Schwann, 1985). It exhibits rare spinifex texture along its chilled contact and has been intruded into quartzite and dolostone, the latter giving rise to thin skarn deposits. Several smaller bodies occur in the Cornwall Bay area. These units appear to grade into gabbros which are considered coeval.

Psammopelitic to Pelitic Rocks

In the more weakly metamorphosed northern Crackingstone Peninsula and Murmac Bay areas, rare argillaceous rocks occur as well-layered mica schists or hornblende-biotite foliates. With increasing grade, biotite-rich varieties become partially melted, culminating in pelitic migmatites west of the Black Bay Fault, which contain about 50% leucosome and garnet±sillimanite in the melanosome.

The pelitic rocks tend to be spatially associated with the quartzite and/or the mafic volcanic rocks, and therefore probably occur stratigraphically below the psammites, although they are commonly missing from the sequence.

Psammitic Rocks

The extent and distribution of psammitic sedimentary rocks is uncertain due to their similarity to widespread sheared granitoid rocks. In the least deformed and metamorphosed Elliot Bay area, feldspathic sediments containing about 20 to 50% glassy quartz eyes and abundant sericite locally contain ripple marks (Figure 6). These grade into fine-grained siltstones and argillites interlayered on a scale of centimetres to tens of centimetres. Both varieties are in contact with quartzite and all of these rocks are ferruginous due to long periods of exposure related to the Martin and Athabasca unconformities. In higher grade rocks of the eastern and northern Crackingstone Peninsula, rocks thought to be psammitic in origin include white to pink, fine- to medium-grained quartzofeldspathic rocks containing varying amounts of white mica and biotite, and rare garnet or micaceous lenses thought to be retrogressed sillimanite faserkiesel. Psammitic rocks of the southern Crackingstone Peninsula and west of the Black Bay Fault weather grey and have been metamorphosed at even higher grades to produce a centimetre-scale partial melt fraction and rare garnet in the biotite-rich melanosome.

c) Intrusive Rocks

Inclusion-rich to Migmatitic Leucocratic Granite to Tonalite (Former Donaldson Lake Gneiss)

Heterogeneous leucocratic granitoid rocks occur as sheets and transposed dykes throughout the more highly metamorphosed parts of the area. They are particularly common in the Donaldson Lake area where they invade the Murmac Bay Group, and range from inclusion-rich intrusions to agmatitic and arteritic migmatites (Figure 7). Confusion over the origin of these rocks led earlier workers to treat them as a distinct unit, which was termed the "Donaldson Lake Gneiss" (e.g. Tremblay, 1972), but the presence of quartzite within the supracrustal component is taken as strong evidence that the rocks are simply a complex mixture of the Murmac Bay Group and intrusive granitoids. Other supracrustal components include abundant amphibolite and subordinate pelite. The character of the granitoid rocks appears to vary depending on the host rock type: white granodioritic to tonalitic rocks are most commonly associated with amphibolitic hosts, whereas rocks invading the quartzites and pelitic rocks are more commonly pink to grey and more granitic. Interaction of the host and injected granitoid rocks is further suggested by the presence of up to 20% feldspar in the quartzites, which locally form discontinuous units up to several metres thick. The pelitic rocks occur as rare partially melted garnet-biotite-sillimanite gneisses. More commonly, the granitoid rocks are nebulitic with an unusually high biotite content and rare sillimanite, possibly suggesting an anatectic origin. In many places, magmatic portions of the migmatite contain inclusions of amphibolite, quartzite and/or pelite separated by only a few metres. Centimetre-scale lenses of pelitic restite containing biotite, garnet, and rare sillimanite appear locally overprinted by randomly oriented pink andalusite(?) porphyroblasts. The heterogeneous nature of the inclusion-rich to migmatitic leucocratic granite to tonalite suggests a crustal origin, possibly by anatexis of Murmac Bay Group rocks at depth. In light of this re-interpretation, it is recommended that the term "Donaldson Lake Gneiss" be discontinued since it infers a distinct package of rocks with a unique geological history.

CENTIMETRES

Figure 6 - Gritty psammite from small island west of Johnson Island.

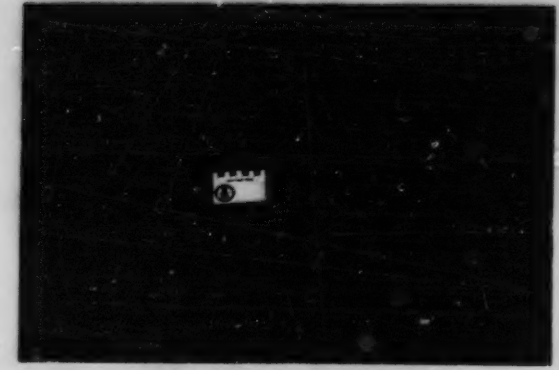

Figure 7 - Agmatite derived from intrusion of white medium-grained granitoid rock into Murmac Bay Group mafic volcanic rocks (former "Donaldson Lake Gneiss"); from Donaldson Lake.

Granite (North Shore Plutons)

A suite of pink, coarse-grained, homogeneous granite plutons in the region (e.g. Mackintosh Bay, Cameron Island, Stephen's Lake, and Dead Man Channel granites) is represented in the study area by the Gunnar Granite, which occurs as a central main body and as sheets tens of metres thick. The migmatitic host rocks occur locally as xenoliths suggesting that an episode of partial melting took place prior to granite emplacement

(Figure 8). The variably strained, massive to well foliated main phase is coarse grained with K-feldspar grains reaching 3 cm in size, and contains 5 to 10% variably chloritized biotite (Figure 9). As mentioned above, this suite of coarse-grained granites has historically been considered Paleoproterozoic, but recent work has suggested that at least some of the plutons were emplaced ca. 2640 Ma. Along the southern shore of the Crackingstone Peninsula west of the Gunnar Mine, cross-cutting relationships confirm at least two phases of co-magmatic quartz- and quartz-feldspar-phyric porphyries. Similar pink coarse-grained granite sheets in the highly strained migmatites west of the Black Bay Fault occur as augen foliates.

Pink Leucogranite

Medium-grained leucogranite, characterized by its dark pink K-feldspar and sharply contrasting white quartz, is most common in the area northeast of Beaverlodge Lake, where it occurs as large plutons exhibiting variable ductile and cataclastic strain (Figure 3). A belt of Murmac Bay Group rocks in that region is flanked by large bodies of pink leucogranite. The best preserved rocks are medium grained, homogeneous, potassic, and contain up to 3% chloritized biotite. Rocks deformed in ductile fashion contain quartz ribbons, whereas cataclastic varieties exhibit a hackly fracture pattern on weathered surfaces and may contain as much as 60% chlorite. These large pink leucogranites are thought to intrude the Murmac Bay Group, although contacts are generally sheared. Their age relative to the inclusion-rich to migmatitic leucogranite to tonalite and to the pink coarse-grained granites is uncertain. Small dykes and metre-scale irregular bodies of pink leucogranite occur within the former, but they may postdate the large pink leucogranite plutons. Elsewhere, the inclusion-rich to migmatitic leucogranite to tonalite grades into similar-looking pink leucogranite, but in general, the two are separated by structural discontinuities.

Figure 8 - Gneissic xenoliths of psammitic(?) quartzofeldspathic gneiss showing evidence of partial melting in Gunnar Granite; from southern shore of Crackingstone Peninsula, west of the Gunnar Mine.

Figure 9 - Coarse-grained Gunnar Granite exhibiting dextral shear bands; from southern shore of Crackingstone Peninsula, west of the Gunnar Mine.

Smaller sheets and transposed dykes of pink leucogranite occur throughout the area. One such body, hosting the Box gold mine, appears to have been emplaced in a mylonite zone towards the end of the shearing event. Assuming that all of the pink leucogranites are broadly coeval, this spatial relationship to high-strain zones may indicate that they were emplaced along structural discontinuities during periods of intense tectonism. Appleyard (1990) noted that the Box Granite has the approximate composition of a eutectic granite and suggested that it formed by anatexis of Murmac Bay Group sedimentary rocks at depth. The findings of this study are broadly compatible with that model, which can be applied to all of the pink leucogranite. It is suggested, however, that the metaluminous composition of the pink leucogranites may indicate a supplementary melt contribution from the basement granites, which could also represent a source for the gold mineralization.

Gabbro

A suite of large gabbro sills are best preserved and exposed in the topographically rugged Lodge Bay area, where they intrude the basement granite and overlying Murmac Bay Group quartzite. The main phase weathers black and is characterized by about 50% medium-grained hornblende which commonly occurs as centimetre-scale aggregates replacing primary coarse-grained pyroxene(?). Elsewhere, hornblende has an equigranular habit. The remainder of the rock is dominated by plagioclase, although iron sulphides are a common accessory. Several phases of finer-grained gabbro crosscut the main phase demonstrating the composite nature of the intrusions.

The abundance of the gabbro sills in the basement and overlying quartzites in the Lodge Bay area (almost exclusively on the 1:100 000 scale compilation map of Macdonald and Slimmon, 1985) led to an early idea that they were feeders to the stratigraphically overlying mafic volcanic rocks. However, abundant gabbro sills and/or transposed dykes of similar appearance were also found in the psammitic rocks, the Gunnar Granite, and the pink leucogranite, suggesting that these intrusions postdate the Murmac Bay Group. Geochemical analyses are planned to further explore the relationship between the gabbroic and mafic volcanic rocks.

Quartzofeldspathic Rocks of Uncertain Origin

As mentioned above, the effects of alteration and deformation preclude easy distinction of rock types in many areas. In places, grain size and texture is sufficient to distinguish granitoid from supracrustal rocks but inadequate to place a rock or unit in a particular granitoid suite. In these cases, the rocks are generally pink to white, medium grained, and well foliated to mylonitic. Elsewhere, finer grain size, higher strain, and/or spatial association to the quartzite preclude easy distinction between psammitic and granitoid rocks.

Diabase

Thin dykes and sills of black fine-grained diabase were noted on the southern Crackingstone Peninsula and in migmatites west of the Black Bay Fault. These differ from the older gabbro in several ways: 1) they have a generally finer grain size, and are characterized by a more acicular habit to the approximately 50% hornblende, 2) they locally crosscut the main regional foliation, and 3) they do not exhibit evidence of partial melting (as does the older gabbro) in areas of high metamorphic grade. They have, however, been affected by the main period of shearing west of the Black Bay Fault. This set of diabase dykes is tentatively correlated with relatively late diabases reported to the east in the eastern Nevins Lake Block (Harper, 1986) and Train Lake Domain (Ashton and Card, 1998).

Late Medium-grained to Pegmatitic Granite Dykes

A variety of late, medium-grained to pegmatitic granite dykes occur throughout the area. They are most obvious in mylonitic rocks west of the Black Bay Fault and north of the St. Louis Fault, where they crosscut the sheared fabric but are variably deformed, suggesting emplacement late in the shearing event. They may be pink or white and generally contain less than 3% biotite and/or chlorite.

Several white massive muscovite pegmatite dykes intrude the Gunnar Granite on the southern Crackingstone Peninsula. They are straight sided with sharp contacts and appear randomly oriented, suggesting emplacement very late in the deformational history. They are zoned with large muscovite books and accessory tourmaline in the main granitic margin and a core dominated by quartz.

d) Martin Group

The Martin Group is a siliciclastic redbed sequence dominated by conglomerates, siltstones, and sandstones, lying unconformably above all of the rocks previously described. It occurs on the eastern side of the Black Bay Fault, which has clearly truncated its western extent. The sequence has been affected by late upright folding, but evidence of metamorphism is restricted to a sheen resulting from very fine-grained sericite on bedding planes. A distinctive red polymictic basal conglomerate is characterized by angular, cobble- to boulder-sized clasts, which can generally be correlated with rocks from the immediate area, suggesting local derivation. The Martin Group is generally not well exposed, with some of the best outcrops occurring in road cuts, washed surfaces at some of the old uranium mines (e.g. Larado Mine), and along the shores of Beaverlodge Lake. Sandstone and conglomerate dykes are common in the Murmac Bay Group quartzites along the eastern shore of the Crackingstone Peninsula, where extensive fracturing has provided conduits for fluids which have precipitated abundant specular and earthy hematite. Conglomerate infill along fractures in the quartzite and specular hematite veins within tens of metres of the Murmac Bay Group–basement granite unconformity near the road west of Beaverlodge Lake are also thought to be features associated with the Martin unconformity.

The Martin Group has been previously described (e.g. Mazimhaka and Hendry 1984, 1985) and has been designated as the target for a stratigraphic and sedimentological study by SEM in the near future. Therefore, it was not remapped during this study; however, the red-brown weathering, locally amygdaloidal basaltic flows, and associated gabbro sills were sampled for a geochemical study by R. Morelli at the University of Saskatchewan. It is hoped that this will help establish the tectonic setting of volcanism, which should in turn provide information on the depositional setting of the entire Martin Group. The Martin Group is thought to have been deposited at about 1800 to 1750 Ma.

A set of red-brown weathering, essentially unmetamorphosed diabase dykes occurs in a wide area surrounding the Martin Group. The intrusive relationship of these dykes into the Martin Group as implied on Dewar Island in Fredette Lake (Tremblay, 1972) was confirmed. The dykes are centimetre- to metre-scale in thickness and dip steeply to the south-southwest. They are fine grained and contain primary pyroxene. Their proximity to the Martin Group, together with their similar age relationships, suggest that they may be broadly coeval with the Martin volcanic rocks. This idea is also being geochemically tested in Morelli's study.

e) Athabasca Group

Siliciclastic rocks of the Manitou Falls Formation (Athabasca Group) are known to unconformably overlie Murmac Bay Group sedimentary rocks on islands south of the Crackingstone Peninsula (Macdonald and Slimmon, 1985). Rare exposures consist of flat-lying white quartz-rich sandstone which was deposited in small depressions in the basement topographic surface. Liesegang rings are common in both the Athabasca quartzite and in the basement. A red-weathering polymictic basal conglomerate unconformably overlying Murmac Bay Group quartzite on an island southwest of Gunnar Mine differs from Martin basal conglomerate mainly in the more rounded nature of the cobble- to boulder-sized clasts. The Athabasca Group is thought to have been deposited at about 1750 to 1700 Ma.

4. Metamorphism

The degree of metamorphism is difficult to characterize due to the general dearth of indicator minerals. The best indicator is partial melting, although its usefulness is broadly restricted to pelitic to psammitic metasedimentary rocks and granitoids. The least metamorphosed of the pre-Martin Group rocks appear to be in the Beaverlodge Lake area, easternmost Crackingstone Peninsula and on the islands farther south and southwest (Figure 3). Primary features are locally preserved in volcanic rocks and quartzites in this area, and the presence of slates in the Eagle Lake area suggest patchy preservation of greenschist facies assemblages. Rare occurrences of andalusite in siltstones and garnet-biotite±staurolite±andalusite± cordierite assemblages in pelitic rocks are consistent with low-pressure, lower to middle amphibolite facies conditions. The transition to upper amphibolite facies assemblages has several different faces. East of Beaverlodge Lake, the degree of metamorphism increases steadily through the Mackintosh Bay area, where pelitic and psammitic metasedimentary rocks are partially melted and contain faserkiesel and sillimanite-K-feldspar assemblages (Hartlaub and Ashton, 1998). Still farther east, granulite facies conditions are reported from Murmac Bay Group rocks of the eastern Nevins Lake Block (Harper, 1986; Ashton and Card, 1998).

Northeast of Beaverlodge Lake, there appears to be a very steep gradient between the greenschist to lower amphibolite facies slates of the Eagle Lake area and the upper amphibolite facies migmatites at Donaldson Lake. Pelitic rocks intruded by the inclusion-rich to migmatitic leucocratic granite to tonalite contain a high proportion of partial melt and sillimanite-garnet-biotite assemblages. Restite inclusions containing the same assemblage are locally overprinted by pink andalusite(?) porphyroblasts, which possibly record a later low-pressure metamorphic overprint. This is supported by the presence of a new partial melt phase rimming some restite inclusions within granodioritic to tonalitic rocks at Donaldson Lake.

A layer-parallel structural discontinuity on the southeastern Crackingstone Peninsula apparently places lower to middle amphibolite facies rocks to the east against upper amphibolite facies rocks exhibiting *lit-par-lit* melt leucosome to the west. Farther north, both sides of the fault appear to have been metamorphosed under lower to middle amphibolite facies conditions and the discontinuity is less obvious. An increasing southwestward metamorphic gradient over the rest of the Crackingstone Peninsula is inferred from the distribution of partially melted rocks, but is difficult to document due to the lack of appropriate rock types and indicator minerals.

The Black Bay Fault broadly marks another discontinuity in metamorphic conditions. Immediately west of the fault, in the Uranium City area, sheared to mylonitized pink leucogranite appears much the same as it does in the lower to middle amphibolite facies rocks north of Beaverlodge Lake. At Jean Lake, however, Murmac Bay Group pelitic rocks are migmatitic. These pelitic migmatites extend southward through Bushell Inlet where they contain sillimanite-garnet-biotite assemblages, and associated psammitic to psammopelitic gneisses exhibit garnetiferous melanosomes. Granulite facies rocks, observed about 10 km farther west along the northern shore of Lake Athabasca during a brief reconnaissance, infer a steadily westward increasing gradient.

Crosscutting relationships imply multiple metamorphic events in the Uranium City area. An early M1 thermotectonic event is implied by the presence of melt leucosome in quartzofeldspathic xenoliths within the unmelted ca. 2.64(?) Ga Gunnar Granite (Figure 8). This M1 event is broadly correlated with the first phase of deformation (D1). The Gunnar Granite is intruded by gabbro sills and/or transposed dykes which elsewhere exhibit partial melting, inferring a second locally high-grade thermotectonic event. This M2 event is broadly correlated to the second phase of regional deformation. The younger, locally crosscutting diabase dykes have also attained amphibolite facies but have not been partially melted, suggesting a third metamorphic event. This M3 event is also considered synchronous with a major Paleoproterozoic overprint since the diabase dykes exhibit shearing and folding related to the third phase of regional deformation (D3) west of the Black Bay Fault. The pink andalusite(?) porphyroblasts overprinting the sillimanite-garnet-biotite restites, together with the new melt material rimming some of the restite lenses in the Donaldson Lake area, are tentatively attributed to this M3 event, and suggest relatively low-pressure yet locally high-temperature conditions. This is consistent with the presence of cordierite-bearing melts axial planar to F3 folds in the central Nevins Lake Block (Figure 2; Hartlaub and Ashton, 1998). Preliminary geochronological work on the inclusion-rich to migmatitic leucocratic granite to tonalite at Donaldson Lake suggests a lower intercept age of ca. 1800 Ma, which is considered the best estimate for the M3 event. The metamorphic gradient described above is thought to have been established during M1/M2 time, although the extent and intensity of M3 is poorly constrained.

5. Structure

The following is a brief summary of the structural relationships in the Uranium City area. A more detailed treatment is provided in a companion paper by Kraus and Ashton (this volume).

a) Early Deformation (D1 and D2)

Primary structures are rare and restricted to areas of lowest grade metamorphism, along the eastern Crackingstone Peninsula. Bedding (S0) can only rarely be distinguished from the dominant overprinting S1 foliation in Murmac Bay Group rocks, which is assumed to be axial planar to rare transposed F1 folds. Since this S1 foliation is exhibited by randomly oriented quartzofeldspathic xenoliths in the Gunnar Granite, the near-co-planar foliation exhibited by the granite is considered an S2 fabric. The main regional foliation is, therefore, a composite of S0, S1, and S2.

F2 folds outlined by the S1 foliation in Murmac Bay Group rocks are difficult to distinguish from later F3 folds, and F2/F3 fold interference is rarely observed. Tight to isoclinal, high-amplitude folds seen in the Elliot and Black bays areas have been tentatively attributed to D2, which is thought to be responsible for the main repetition of Murmac Bay Group rock types. Rare down-dip tectonic stretching lineations in discrete layer-parallel shear zones, such as the one through Howland Lake which apparently places basement granites on top of Murmac Bay Group quartzite, may indicate west- and/or north-verging D1 and/or D2 thrust faulting. A similar relationship exists in mylonitic granitoid rocks hosting the Box Mine Granite and gold deposit, although it is not yet clear whether those rocks are part of the basement or a younger granite.

b) D3 Deformation

The D3 event was responsible for producing widespread shearing (Figure 9), cataclasis, and folding. Most of the F3 folds have axial planes dipping steeply to the southeast, but reversals are not uncommon. Fold axes plunge gently to moderately to the northeast or southwest. A disproportionately high percentage of the F3 folds display "z" asymmetry on the Crackingstone Peninsula, consistent with development during a period of regional dextral shear.

Rocks affected by a high degree of ductile strain are particularly common in the vicinity and north of the St. Louis Fault and west of the Black Bay Fault. In the St. Louis Fault area, the ductile strain is extremely heterogeneous, with zones of near-massive (though cataclastic) rocks alternating with distinct mylonitic to ultramylonitic zones up to hundreds of metres wide. Mylonitic rocks vary in appearance with both the protolith and the shear regime. The most obvious mylonites are characterized by ribbon quartz exhibiting up to 50:1 aspects. Such zones are commonly silicified and easily confused with quartzites and/or rocks derived from psammitic protoliths. Elsewhere, however, high-ductile strain is recognized by the development of "mica schists" composed of medium- to coarse-grained platy feldspars sheathed in fine-grained sericite. Such rocks are also difficult to distinguish from metasedimentary rocks of similar composition. Two of these layer-parallel ductile mylonite zones were recognized in the northern Mickey Lake area and two others were noted on either side of the St. Louis Fault, although many other smaller zones occur throughout this area. Tectonic stretching lineations in the middle two zones consistently plunge at a gentle angle to the southwest, consistent with a dominantly transcurrent sense of displacement. The other zones are more contorted due to folding, which has resulted in more randomly oriented tectonic stretching lineations. Sinistral shear bands were noted in the two northern mylonite zones and in several outcrop-scale zones elsewhere north of the St. Louis Fault; dextral shear bands were recognized at one locality at the eastern end of the northernmost zone.

The entire study area was subsequently subjected to a brittle-ductile to brittle deformational event which resulted in heterogeneous but widespread development of faulting, fracturing, brecciation, and feldspar beading. This was accompanied by pervasive chloritization, hematization, and silicification, indicating that much of this cataclastic deformation took place under greenschist facies conditions. The St. Louis and ABC faults are poorly exposed, thin, discrete structures which have developed during this later more brittle deformational event. There are several conflicting models regarding the sense of displacement on the St. Louis Fault, although most are based on apparent offsets and are on the order of only a few kilometres or less (Beck, 1969 and references therein). Based on a petrographic study, Krupicka and Sassano (1972) attributed the ductile and overprinting brittle deformation in the area of the St. Louis Fault and north to multiple periods of tectonic activity taking place at successively higher levels in the crust.

The area west of the Black Bay Fault exhibits a more uniform record of D3 ductile deformation. The area is a straight zone comprising variably sheared to mylonitic tectonites. Strain gradients and abundant centimetre-scale zones of slip marked by biotite schists imply widespread mylonitization. A doubly-plunging, near-horizontal tectonic stretching lineation, together with widespread low- and high-angle shear bands (Figure 10), asymmetric pull-aparts, and rare ∂-

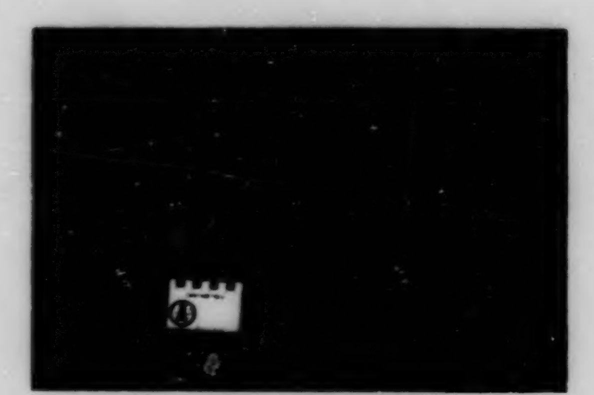

Figure 10 - Dextral shear bands in mylonitic migmatite derived from psammite intruded by granitoid rocks, west of Bushell Inlet on shore of Lake Athabasca.

porphyroclasts consistently indicate a dextral sense of shear. In contrast to the St. Louis Fault area, the absence of overprinting greenschist facies minerals implies that this dextral shearing event took place under amphibolite-facies conditions and probably deeper crustal levels.

Minor folds ranging from isoclinal to open are abundant in these highly strained rocks west of the Black Bay Fault. Their axial planes dip steeply to the southeast or northwest and their fold axes are gently northeast or southwest plunging, essentially co-linear with the tectonic stretching lineation. Some are curvilinear suggesting rotation into their present orientation, perhaps by a mechanism similar to sheath folding. Most exhibit "z" asymmetry, consistent with a dextral sense of shear, but "s" and "w" folds are also common. Their relative age, orientation, and interlimb angles suggest that most are F3 folds, however, the repetition of Murmac Bay Group units in this area indicates that some are likely of F1/F2 age.

c) Late Deformation (D4 and D5)

The north-trending, upright fold defined by Martin Group volcanic rocks is tentatively thought to be a fourth-generation feature postdating the main period of northeast-trending D3 structures, although some of the more open, northeast-trending folds on the Crackingstone Peninsula and west of the Black Bay Fault may also have developed at this time. The non-folded character and near-perpendicular orientation of the late unmetamorphosed diabase dykes to the axial plane of this F4 fold, suggests that the dykes were emplaced along extension fractures and normal faults during a late east-west shortening event responsible for the folding.

Late kink and box folds display a variety of orientations and have been grouped together as F5 structures. At several localities, pairs of these structures are consistent with derivation as conjugate sets resulting from north-south shortening.

6. Economic Potential: Uranium and Gold

The Uranium City area is best known for its multitude of vein-type uranium deposits which were actively mined between 1953 and 1982. The spatial correlation of these deposits with faults and high-strain zones has long been recognized (e.g. Beck, 1969), as has a spatial relationship with the Martin Group, although a genetic link has yet to be established. It is noteworthy that the Athabasca Group unconformity is also nearby, and likely extended farther north to cover the Uranium City area at one time leaving doubt as to whether it played a significant role in mineralization. One of the outstanding problems in developing a model for uranium deposits is the source of the uranium. In addition to potential reservoirs in the Athabasca and Martin groups, the Murmac Bay Group quartzites have been suggested as a possible source (Tremblay, 1972). Recognition of Archean granitic basement and an implied Archean age for the Murmac Bay Group adds additional potential sources for the uranium. In the inferred reducing atmosphere during Archean time, detrital uranium minerals derived from granitic basement rocks (e.g. the Lodge and Elliot Bay granites) would have survived the weathering process and been concentrated in sediments, much as sulphides have in Murmac Bay Group quartzites. Subsequent oxidizing fluids moving through the quartzites and basement granites during Paleoproterozoic thermotectonic events or diagenesis could be expected to leach the uranium and carry it along structural discontinuities until encountering reducing conditions where it would be precipitated. The more extensive nature of the basement suggested by this work would only enhance the potential role of a reducing Archean atmosphere.

The Box gold mine was discovered in 1934 and operated between 1939 and 1942. Goldfields Operating Company currently plans to bring it back into production as an open pit operation with a projected life span of three years. The geology of the Box Mine has been investigated several times. Early suggestions that the host Mine Granite and mineralization resulted from "granitization" of metasedimentary rocks (Sibbald, 1984 and references therein; Sibbald and Jiricka, 1986) have given way to a model involving intrusion of a gold-bearing eutectic granite, derived by partial melting of Murmac Bay Group sedimentary rocks at depth, into higher-level sedimentary rocks (Appleyard, 1990). The findings of the present study are consistent with Appleyard's model, except for his interpretation of the "older granites" hosting the Mine Granite, which were thought to be altered Murmac Bay Group sedimentary rocks. Current treatment of this problem has been far from exhaustive, but comparison with other variably deformed granitoid rocks throughout the Uranium City area suggests that these host rocks are indeed older deformed igneous granites. Petrographic and geochemical studies are planned to test this model and to determine whether these "older granites" are correlative with one of the other known suites in the area. An increasing strain gradient extending from Neiman Bay to the Mine Granite contact suggests that the latter, a pink leucogranite strongly resembling other rocks of that unit elsewhere, and its gold mineralization were emplaced in a ductile high-strain zone. Therefore, the Mine Granite may have resulted from partial melting of the older host granite instead of, or in addition to, Murmac Bay Group sedimentary rocks. Other similar pink leucogranites spatially associated with high-strain zones represent potential targets for further gold exploration.

There has also been speculation regarding the potential for Olympic Dam and base metal mineralization related to the Martin Group. In addition, rare anthophyllite-rich rocks observed in Murmac Bay Group basalts in the Tipinuwak Channel area probably result from the metamorphism of alkali-depleted and/or Mg-enriched volcanic protoliths. Such alteration commonly accompanies volcanogenic massive sulphide mineralization.

7. Discussion and Summary

In this first year of study in the immediate Uranium City area, several tentative conclusions can be drawn.

1) Rocks of the Fay Mine Complex are correlative with those of the Murmac Bay Group. Thus it is recommended that the former term be dropped.

2) Based on ongoing geochronological work by Hartlaub, it appears that the Murmac Bay Group was deposited prior to 2.64 Ga, rather than in the Paleoproterozoic as previously suggested (e.g. O'Hanley *et al.*, 1994).

3) Although granitoid rocks and Murmac Bay Group psammites are difficult to distinguish due to locally intense deformation and alteration, both are present, and granitoid rocks forming the basement to the Murmac Bay Group are likely more abundant than previously recognized.

4) As in many places in Saskatchewan, subdivision of the region based on various parameters (e.g. lithological makeup, degree of deformation and metamorphism) led to a complicated classification scheme (e.g. Macdonald, 1983), which was further complicated over time by the general adoption of many of these subdivisions as lithotectonic domains (e.g. Macdonald and Slimmon, 1985, 1998). Dominance of the Murmac Bay Group and intrusive granitoid rocks throughout the Uranium City area leaves no obvious lithological justification for distinguishing the "Beaverlodge Belt/Domain" from the "Nevins Lake Block"; nor does there appear to be any major lithological change moving westward across the Black Bay Fault into the "Black Bay Domain". In order to help clarify the confusion, the new term "Beaverlodge Domain" is being introduced to refer to all three previous lithotectonic elements. In future, it is recommended that new terminology include the parameter being distinguished, and that it be made clear that the subdivision is a part of a larger lithotectonic domain. For example, the "Black Bay Straight Belt" (e.g. Macdonald, 1983; Kraus and Ashton, this volume) is a tectonic element based on structural style which occurs west of the Black Bay Fault and within the Beaverlodge lithotectonic domain.

5) The terms "Donaldson Lake Gneiss" and "Foot Bay Gneiss" appear to have been introduced to refer to areas northeast of Beaverlodge Lake in which the effects of deformation, metamorphism, and alteration combined to mask protoliths and age relationships. It now appears that the "Donaldson Lake Gneiss" is an injection migmatite formed by intrusion of leucocratic granitic rocks into the Murmac Bay Group sequence of quartzites, basalts, and pelites exposed immediately along strike to the west. The "Foot Bay Gneiss" appears to be a variably mylonitic and cataclastic extension of the pink leucogranite exposed to the west. It has been affected by intense ductile and brittle deformational events, but in that regard, it is not unlike other pink leucogranites in the area (e.g. the one north of Mickey Lake). Since neither the "Donaldson Lake Gneiss" nor the "Foot Bay Gneiss" is lithologically or tectonically unique to the area, it is recommended that these terms also be dropped.

8. Acknowledgments

This project could not have been completed without the able and enthusiastic assistance of E. Chorney, S. Ehman, D. Boivin, and A. Yanko, the former two of whom continue to contribute to the project in the form of field-based B.Sc. thesis studies of the area north of the St. Louis Fault. R. Morelli is similarly following up his contributions with a geochemical comparison of the Martin Group basalts and young diabase dykes. Discussions during a five-day visit by G. Delaney, C. Harper, K. Bethune, and C. Card were both instructive and appreciated, as was a three-day visit by L. Heaman and T. Chacko. G. Yeo has provided valuable insights into the sedimentology and depositional environments of quartzites.

9. References

Alcock, F.J. (1936): Geology of Lake Athabaska region, Saskatchewan; Geol. Surv. Can., Mem. 196, 41p.

Appleyard, E.C. (1990): Petrogenetic aspects of the Goldfields Granites, Saskatchewan; *in* Summary of Investigations 1990, Saskatchewan Geological Survey, Sask. Energy Mines, Misc. Rep. 90-4, p84-93.

Ashton, K.E. and Card, C.D. (1998): Rae Northeast: A reconnaissance of the Rae Province northeast of Lake Athabasca; *in* Summary of Investigations 1998, Saskatchewan Geological Survey, Sask. Energy Mines, Misc. Rep. 98-4, p3-16.

Ashton, K.E., Card, C.D., Heaman, L.M., and Coolican, J. (1999): Rae Northeast: Analytical update and new field results from the north-central Train Lake Domain; *in* Summary of Investigations 1999, Volume 2, Saskatchewan Geological Survey, Sask. Energy Mines, Misc. Rep. 99-4.2, p3-16.

Beck, L.S. (1969): Uranium deposits of the Athabasca region, Saskatchewan; Sask. Dep. Miner. Resour., Rep. 126, 139p.

Bickford, M.E., Van Schmus, W.R., Collerson, K.D., and Macdonald, R. (1987): U-Pb zircon geochronology project: New results and interpretations; *in* Summary of Investigations 1987, Saskatchewan Geological Survey, Sask. Energy Mines, Misc. Rep. 87-4, p76-79.

Card, C.D. and Bethune, K.M. (1999): The Oldman-Bulyea Shear Zone: Studies across the Nevins Lake Block–Train Lake Domain boundary in the

Rubus-Bulyea lakes and Oldman Lake areas; *in* Summary of Investigations 1999, Volume 2, Saskatchewan Geological Survey, Sask. Energy Mines, Misc. Rep. 99-4.2, p27-37.

Christie, A.M. (1953): Goldfields–Martin Lake Map-area, Saskatchewan; Geol. Surv. Can., Mem. 269, 126p.

Harper, C.T. (1986): Geology of the Nevins-Forsyth lakes area; Sask. Energy Mines, Open File Rep. 86-4, 57p.

Hartlaub, R.P. (1999): New insights into the geology of the Murmac Bay Group, northeastern Rae Province, northwest Saskatchewan; *in* Summary of Investigations 1999, Volume 2, Saskatchewan Geological Survey, Sask. Energy Mines, Misc. Rep. 99-4.2, p17-26.

Hartlaub, R.P. and Ashton, K.E. (1998): Geological investigations of the Murmac Bay group, Lake Athabasca North Shore Transect; *in* Summary of Investigations 1998, Saskatchewan Geological Survey, Sask. Energy Mines, Misc. Rep. 98-4, p17-28.

Hoffman, P.F. (1988): United plates of America, the birth of a craton: Early Proterozoic assembly and growth of Laurentia; Ann. Rev. Earth Planet. Sci., v16, p543-603.

Krupicka, J. and Sassano, G.P. (1972): Multiple deformation of crystalline rocks in the Tazin Group, Eldorado Fay Mine, NW Saskatchewan; Can. J. Earth Sci., v9, p422-433.

Macdonald, R. (1983): Geology and regional context of the Oldman Lake area; *in* Summary of Investigations 1983, Saskatchewan Geological Survey, Sask. Energy Mines, Misc. Rep. 83-4, p19-23.

Macdonald, R. and Slimmon, W.L. (1985): Bedrock geology of the Greater Beaverlodge Area, NTS 74N-6 to -11; Sask. Energy Mines, Map 241A, 1:100 000 scale.

__________ (compilers) (1998): Geological map of Saskatchewan; Sask. Energy Mines, 1:1 000 000 scale.

Mazimhaka, P.K. and Hendry, H.E. (1984): The Martin Group, Beaverlodge area; *in* Summary of Investigations 1984, Saskatchewan Geological Survey, Sask. Energy Mines, Misc. Rep. 84-4, p53-62.

__________ (1985): The Martin Group, Charlot Point and Jug Bay areas; *in* Summary of Investigations 1985, Saskatchewan Geological Survey, Sask. Energy Mines, Misc. Rep. 85-4, p67-80.

O'Hanley, D.S., Kyser, T.K., and Sibbald, T.I.I. (1994): The age and origin of the North Shore Plutons in the Rae Province, Goldfields area, Saskatchewan; Can. J. Earth Sci., v31, p1397-1406.

Persons, S.S. (1983): U-Pb geochronology of Precambrian rocks in the Beaverlodge area, northwestern Saskatchewan; unpubl. M.Sc. thesis, Univ. Kansas, 68p.

Schwann, P.L. (1985): Geochemistry and petrology of the Nicholson Bay Ultramafic Complex, northwestern Saskatchewan; unpubl. B.Sc. thesis, Univ. Regina, 67p.

Sibbald, T.I.I. (1982): Uranium metallogenic studies: Nicholson Bay area; *in* Summary of Investigations 1982, Saskatchewan Geological Survey, Sask. Energy Mines, Misc. Rep. 82-4, p43-45.

__________ (1984): Gold metallogenic studies, Goldfields area; *in* Summary of Investigations 1984, Saskatchewan Geological Survey, Sask. Energy Mines, Misc. Rep. 84-4, p116-121.

Sibbald, T.I.I. and Jiricka, D.E. (1986): Geology of the gold deposits, Goldfields, Saskatchewan; *in* Clark, L.A. (ed.), Gold in the Western Shield; CIM, Spec. Vol. 38, p412-414.

Sibbald, T.I.I. and Lewry, J.F. (1980): Uranium metallogenic studies: Lodge Bay area, Lake Athabasca; *in* Summary of Investigations 1980, Saskatchewan Geological Survey, Sask. Energy Mines, Misc. Rep. 80-4, p44-48.

Thomas, D.J. (1982): Uranium metallogenic studies: Mickey Lake area; *in* Summary of Investigations 1982, Saskatchewan Geological Survey, Sask. Energy Mines, Misc. Rep. 82-4, p51-55.

Tremblay, L.P. (1972): Geology of the Beaverlodge mining area, Saskatchewan; Geol. Surv. Can., Mem. 367, 265p.

Tremblay, L.P., Loveridge, W.D., and Sullivan, R.W. (1981): U-Pb ages of zircons from the Foot Bay Gneiss and the Donaldson Lake Gneiss, Beaverlodge area, northern Saskatchewan; *in* Current Research, Part C, Geol. Surv. Can., Pap. 81-1C, p123-126.

Van Schmus, W.R., Persons, S.S., Macdonald, R., and Sibbald, T.I.I. (1986): Preliminary results from U-Pb zircon geochronology of the Uranium City region, northwest Saskatchewan; *in* Summary of Investigations 1986, Saskatchewan Geological Survey, Sask. Energy Mines, Misc. Rep. 86-4, p108-111.

New Insights into the Structural Geology and Tectonic Setting of the Uranium City area, Northwestern Saskatchewan

J. Kraus and K.E. Ashton

Kraus, J. and Ashton, K.E. (2000): New insights into the structural geology and tectonic setting of the Uranium City area, northwestern Saskatchewan: *in* Summary of Investigations 2000, Volume 2, Saskatchewan Geological Survey, Sask. Energy Mines, Misc. Rep. 2000-4.2.

Abstract

The Uranium City area, in the south-central Rae province of northwestern Saskatchewan, records a protracted deformation history from the Neoarchean to the Paleoproterozoic. Five generations of structures (F_1 to F_5) related to four compressive deformation events (D_1 to D_4) have been identified in the Murmac Bay Group, a Neoarchean rift sequence or basin deposit. Three structural domains (A to C) have been distinguished on the basis of variation in bulk deformation paths and deformation histories. D_1 and/or D_2, although partly obscured by subsequent deformation, appear to be characterized by overthrusting accommodated by thick fold nappes. Models for D_3, the last regionally significant event, are presented according to which the rocks of the Uranium City area were subjected to dextral shearing (with or without a transpressive component) resulting in a large Z-asymmetrical fold structure and related faults. D_4, which is expressed by small-scale structures only, may have recorded weak sinistral shearing during the waning stages of deformation.

1. Introduction

Mapping at 1:20 000 scale was conducted in the Uranium City area during the first field season of a three-year collaborative project between the Saskatchewan Geological Survey and the Geological Survey of Canada. The area is located in the south-central Archean Rae province (Figures 1 and 2). The southern Rae portion is welded to the Buffalo Head terrane in the west, and to the Hearne province in the east by the Taltson magmatic arc and the Snowbird tectonic zone, respectively (e.g. Hoffman, 1988, 1989). The lithological units exposed around Uranium City are described in detail in a companion paper (Ashton *et al.*, this volume). In brief, the study area hosts a possible passive continental margin (or intracratonic basin) sequence of weakly to highly metamorphosed supracrustal Archean rocks of the Murmac Bay Group, which unconformably overlie ca. 3.0 Ga Archean granitic basement (Figure 3) (Tremblay, 1972; Macdonald, 1983; Van Schmus *et al.*, 1986; Hartlaub and Ashton, 1998, Hartlaub, 1999, Ashton *et al.*, this volume). Both contain several suites of felsic and mafic intrusive rocks. The Murmac Bay Group is unconformably overlain by weakly deformed and essentially unmetamorphosed sediments of the Paleoproterozoic Martin Group. The whole sequence is unconformably overlain by largely undeformed Paleoproterozoic Athabasca sandstone. There is evidence that the Archean rocks experienced deformation in at least two and possibly three events: first, in the Neoarchean and subsequently during the Paleoproterozoic. Here, we present a preliminary synthesis of the structural and tectonic history of this small part of the Rae province.

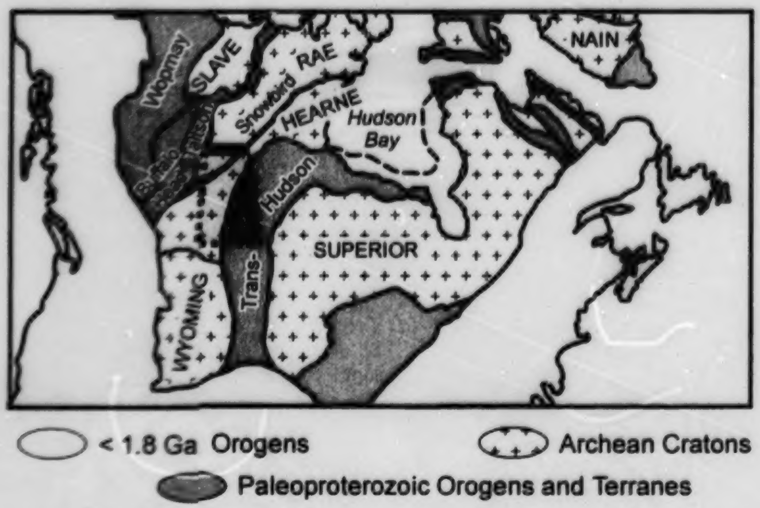

***Figure 1** - Simplified map of the tectonic elements of Laurentia. Saskatchewan is outlined by dotted line and the black rectangle refers to the area of Figure 2 (after Hoffman, 1988).*

2. Previous Work

A few regional scale structural analyses of the Uranium City area have been conducted, the most important of which are summarized as follows.

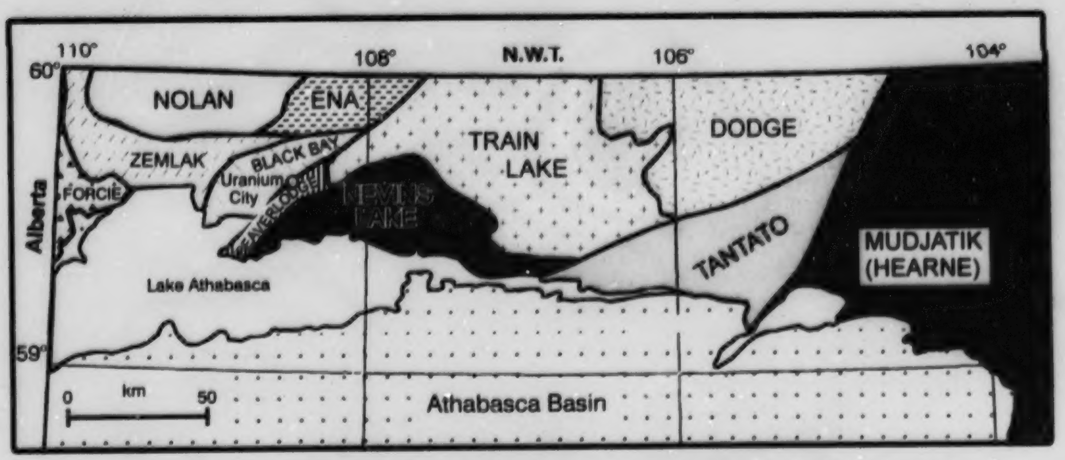
110°
108°
N.W.T.
106°
104°
60°
NOLAN
ENA
TRAIN LAKE
DODGE
ZEMLAK
BLACK BAY
Uranium City
FORCIE
BEAVERLODGE
NEVINS LAKE
Alberta
TANTATO
MUDJATIK (HEARNE)
Lake Athabasca
59°
0
km
50
Athabasca Basin

Figure 2 - Regional geology of the Rae province in northwestern Saskatchewan.

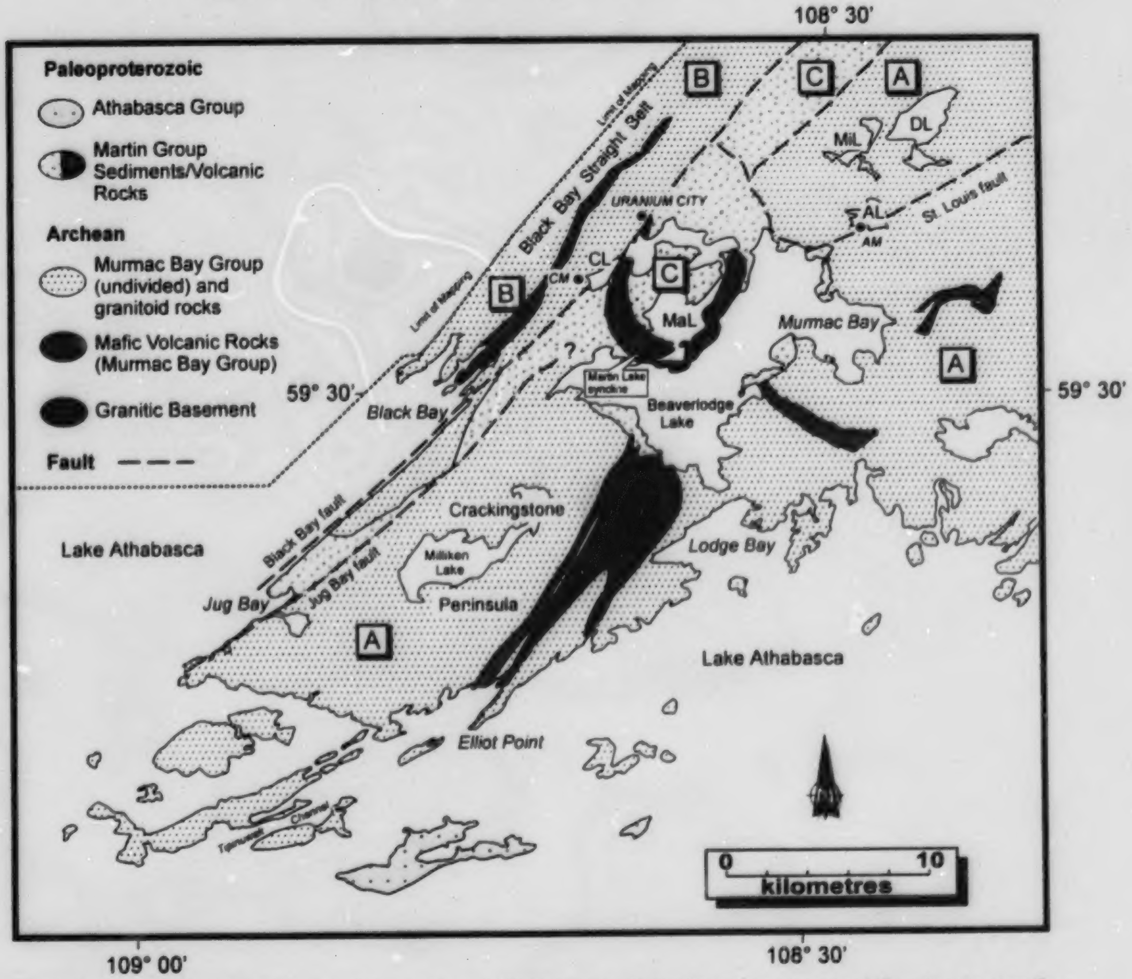
108° 30'
Paleoproterozoic
Athabasca Group
Martin Group Sediments/Volcanic Rocks
Archean
Murmac Bay Group (undivided) and granitoid rocks
Mafic Volcanic Rocks (Murmac Bay Group)
Granitic Basement
Fault
B
C
A
DL
MiL
Limit of Mapping
Black Bay Straight Belt
URANIUM CITY
AL
AM
St. Louis fault
CL
CM
MaL
Murmac Bay
?
Martin Lake syncline
Beaverlodge Lake
59° 30'
Black Bay
Black Bay fault
Jug Bay fault
Crackingstone
Milliken Lake
Peninsula
Lake Athabasca
Jug Bay
Lodge Bay
Elliot Point
0
10
kilometres
109° 00'
108° 30'

Figure 3 - Simplified geological map of the study area. The letters A, B, and C refer to structural domains (see text for details). AL, Ace Lake; AM, Ace Lake mine; CL, Cinch Lake; CM, Cinch Lake mine; DL, Donaldson Lake; MaL, Martin Lake; and MiL, Mickey Lake.

Tremblay (1972) described two generations of folds in the Beaverlodge Lake area, the first of which affects both the Murmac Bay Group and Martin Group rocks. He attributed the sinuous trace of a large first-generation fold (Martin Lake syncline; Figure 3) to refolding.

Sibbald and Lewry (1980) recognized two generations of structures (F_1 and F_2) for the Lodge Bay area, which they attributed to two episodes of deformation (D_1 and D_2), each of which is characterized by strong variations in strain intensity. They attributed the intercalation of supracrustal and igneous rocks to D_1 folding and thrusting. Minor F_1 folds contain a stretching lineation parallel to their hinges and an axial planar S_1 fabric. The F_1 folds are overprinted by major F_2 folds with steeply east- to southeast-dipping axial surfaces and northerly and southerly plunging axes. The F_2 folds are accompanied by an S_2 axial-plane cleavage.

Since 1998, there has been renewed mapping activity in the "Rae Northeast" between Uranium City and the Tantato domain (Figure 2) (Ashton and Card, 1998; Hartlaub and Ashton, 1998; Ashton *et al.*, 1999; Hartlaub, 1999, Ashton *et al.*, this volume). Hartlaub and Ashton (1998) reported three fold generations for the north shore of Lake Athabasca immediately east of our study area. Their F_1 folds are tight to isoclinal and associated with an axial-plane S_1 foliation. Close to tight F_2 folds, which contain an S_2 axial plane foliation, plunge shallowly in northerly and southerly directions. The map picture is dominated by shallowly to intermediately south-southwest-plunging open to closed S_3-cleaved F_3 folds with northwest- and southeast-dipping axial planes, which fold F_1 and F_2 structures. This interpretation was also applied to the neighbouring study areas of Ashton and Card (1998) and Hartlaub (1999).

All authors mentioned above reported brittle structures following ductile folding.

3. Structural Generations

The Uranium City area records a protracted deformation history possibly exceeding 0.7 Ga from the Neoarchean to the Paleoproterozoic. At least five generations of structures (F_1 to F_5) exist in the Murmac Bay Group rocks, which we relate to four distinct compressive deformation events (D_1 to D_4) (Table 1). We distinguish three structural domains (A to C) based on variation in bulk deformation paths and deformation histories (Figure 3). The spatial orientations of structural features for each domain are given in Figure 4. **Domain A** comprises the area east of the Jug Bay fault hosting Archean basement, Murmac Bay Group rocks, and intrusive rocks. It is representative for the regional-scale deformation and can therefore be correlated with the adjacent areas investigated by workers mentioned above. **Domain B** constitutes the area west of the Black Bay fault. It hosts essentially the

Table 1 - Tentative summary of the tectonometamorphic history of the Uranium City area.

Deformation		Structures	Magmatic Events	Metamorphism	Speculative Age (Ga)	Tectonic Setting
		Unconformity	Gabbro		? 2.7	Deposition of Murmac Bay Group during rifting of Archean basement
D_1	F_1	Transposed folds; stretching lineation; S_1 parallel to primary layering	Leucogranite	M_1 metamorphism, locally at high grade (anatexis)	? 2.6	Crustal thickening by north-west-directed overthrusting; Rae-Hearne collision?
			Gunnar granite cutting F_1 structures, followed by gabbro dykes and sills			
D_2	F_2	Isoclinal folds; stretching lineation; S_1/S_2 transposition foliation parallel to primary layering	Leucogranite	M_2 metamorphism, locally at high grade (partial melting of post-Gunnar-granite gabbro	? 2.0 to 1.9	East-west shortening related collision with Taltson orogen?
D_3	F_3	North-northwest-northeast-trending dominantly Z-folds at all scales; local S_3; Black Bay straight belt with shallow L parallel to hinges of Z-folds, dextral shear bands	Leucogranite	M_3 metamorphism at lower medium grade		Transpression during approx. east-west shortening related to Rae/Hearne–Superior collision?
					? ca. 1.8	Deposition of Martin Group in dextral pull-apart basin and on erosional surface
	F_4	Dominantly Z-folds; dextral shear bands and refolding of L in Black Bay high-strain zone	Diabase sills; west- to northwest-trending diabase dykes			
D_4	F_5	Gentle folds, box folds, and kink bands			post-1.8	
						Deposition of Athabasca Group in an intracratonic basin

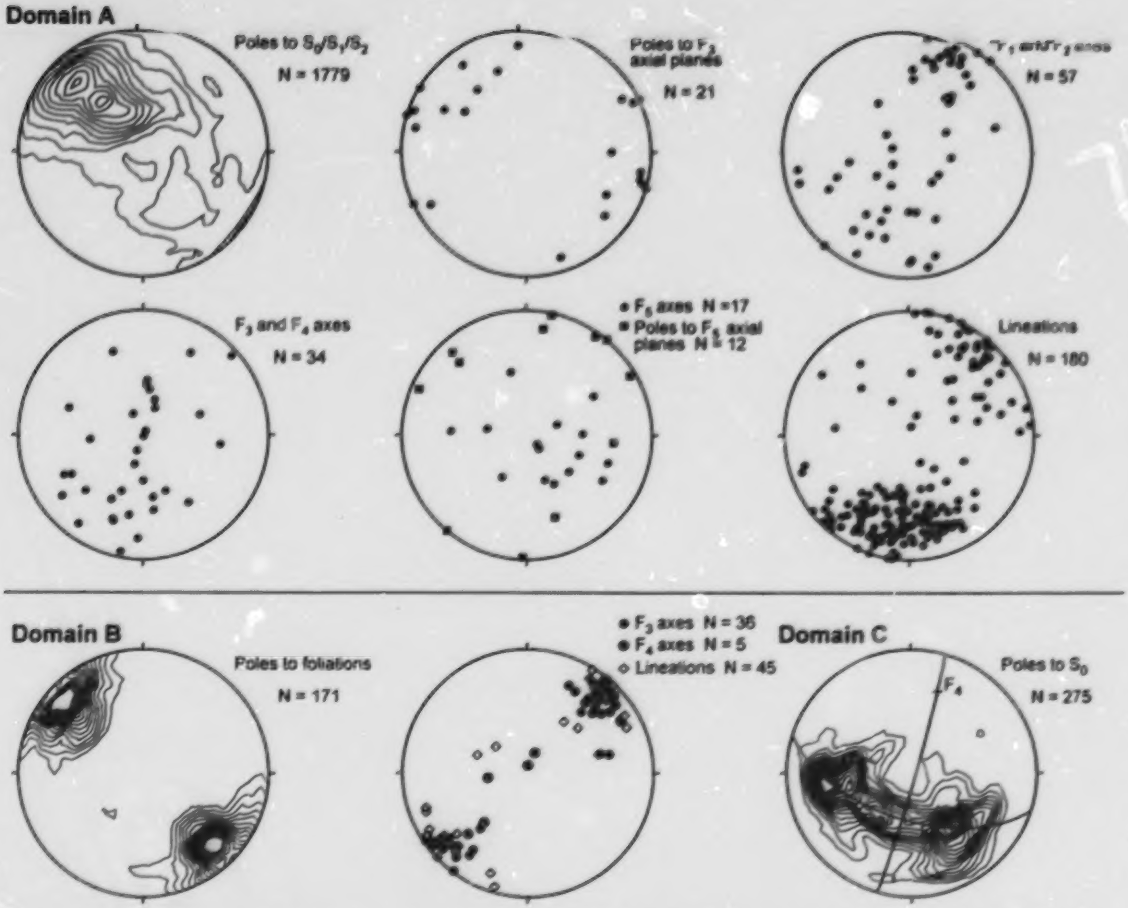

Figure 4 - Equal-area projections (lower hemisphere, Schmidt net) of structural data for the three structural domains. Contours at 0.5, 1.0, 1.5,…8.0 (multiples of random distribution). In domain C, the pole to the great-circle girdle defined by bedding poles is the axis of the F_4 Martin Lake syncline. The great circle containing the F_4 axis constitutes the syncline's axial plane.

same rocks as domain A, but it has experienced much higher F_3 strains so that Macdonald (1983) referred to it as the 'Black Bay straight belt'. **Domain C** is a lithological domain as well in that it hosts only Martin Group sediments and late mafic volcanic rocks. These rocks postdate F_2 and M_2 and thus do not record the early deformation history of the Murmac Bay Group.

a) Domain A

F_1 and F_2 Folds and Related Thrusts

F_1 and F_2 folds, each of which may represent one or several fold generations, are in most cases indistinguishable in terms of style and orientation. Both are isoclinal to transposed with shallowly to intermediately plunging hinges (Figure 4) and are typically observed at decimetre to metre scale. They can be distinguished where rare overprinting and cross-cutting relationships are preserved: the F_2 folds postdate and the F_1 folds predate and/or coincide with M_1 metamorphism and related granitic magmatism (Ashton *et al.*, this volume). Locally, however, the F_2 folds are not as tightly apressed as the F_1 folds. Psammite xenoliths in post-F_1 Gunnar granite (Ashton *et al.*, this volume) contain an S_1 fabric defined by migmatitic schlieren, which is indicative of local partial melting associated with F_1 folding. This granite and all other post-F_1 granites contain an S_2 fabric defined by flattened quartz and feldspar grains enveloped by phyllosilicate grains. S_2 is parallel to lithological boundaries. In the Murmac Bay Group supracrustal rocks, the main planar fabric is an S_1/S_2 transposition foliation, which is parallel to primary layering on the F_1/F_2 fold limbs (Figure 4). This fabric is defined by aligned hornblende grains in mafic rocks, by gneissic layering in psammites, by aligned phyllosilicates in pelites, and as a fracture cleavage in quartzites. In psammites, at several locations around Milliken Lake, this fabric envelops sillimanite faserkiesel (Figure 5). The poles to $S_0/S_1/S_2$ plot on a broad girdle (Figure 4), which is composed of a number of northwest-southeast-trending great-circle girdles. The poles to these great-circle girdles represent the large F_3 fold axes, and the broad girdle reflects the variation in F_3 axis orientations. The maximum of $S_0/S_1/S_2$ poles in the northwest quadrant of the stereonet reflects the prevailing southeasterly dips on the Crackingstone Peninsula.

Relict crenulations of S_1 are preserved in insular domains within the S_1/S_2 transposition fabric at Beaverlodge Lake. In F_1/F_2 hinges in sedimentary rocks, an axial-plane cleavage is restricted to phyllosilicate-rich layers. Minor F_2 folds are rare. They occur, for example, as transposed leucogranite stringers in Gunnar granite or as isoclinal structures in siltstone. F_2 folds appear to be associated with M_2 metamorphism, which culminated in partial melting of all rocks including post-F_1/pre-F_2 gabbro dykes and sills (Figure 6; Table 1; Ashton *et al.*, this volume).

Owing to the strong degree of transposition followed by granite intrusion, few large-scale F_1 folds (but no large F_2 folds) have been identified. On the northeastern Crackingstone Peninsula, a kilometre-scale, northwesterly verging F_1 anticlinorium cored by granitic basement reveals a shallow, slightly curvilinear fold axis. The strain increases dramatically to the western termination of the basement, where northwest-vergent drag folds are developed, too. This zone of elevated strain may be the base of an F_1 fold nappe juxtaposing basement rocks over its Murmac Bay Group cover. Shear bands and CS fabrics observed elsewhere, as well as near-down-dip stretching lineations, may constitute another piece of evidence for early northwest-directed transport.

CENTIMETRE

Figure 5 - Faserkiesel enveloped by the S_1/S_2 transposition foliation at southwestern Milliken Lake.

Figure 6 - Patches of M_2 leucosome in post-F_1 gabbro sill, Black Bay.

F_3 to F_5 Folds

Open to tight, northerly trending (in northeast-trending rocks) mainly Z-asymmetrical F_3 folds are ubiquitous at all scales in the Uranium City area (Figures 4 and 7). They have rather mildly thickened hinges compared to the F_1 and F_2 folds. Minor F_3 folds appear to be related to a map-scale fold with its hinge in the Beaverlodge Lake–Lodge Bay area (Figure 3), which is responsible for a change in structural grain from northeasterly on the Crackingstone Peninsula to east-southeasterly farther east. On a regional scale, the structure appears to be a large Z-fold. An axial-plane S_3 fabric is developed in rocks which contain phyllosilicates. At one location at Beaverlodge Lake, $S_{1/2}$ and S_3 alternate in adjacent beds, displaying a chevron pattern in a way described by Henderson (1997). In some places, the S_1/S_2 transposition foliation is crenulated but did not develop into a new cleavage.

F_4 folds, which are Z-asymmetrical on the Crackingstone Peninsula, are in most cases impossible to tell apart from F_3 folds (Figure 4). The F_4 folds may be more open than their F_3 counterparts. Both generations may have formed in essentially the same tectonic regime, but not simultaneously (see below). Along the eastern shore of the Crackingstone

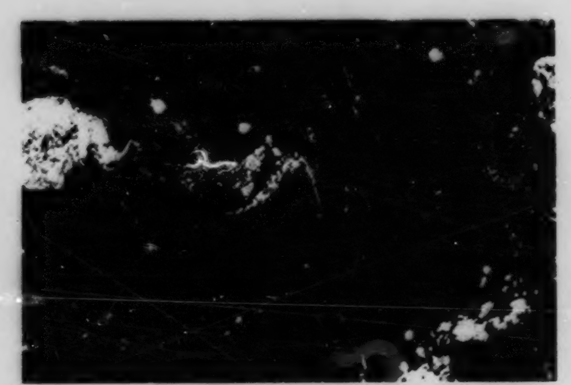

Figure 7 - Train of mildly Z-asymmetrical F_3 folds with varying degrees of tightness in Murmac Bay Group siltstone near Elliot Point. This pattern is a microcosm of the regional scale F_3 folds along the north shore of Lake Athabasca, east of Lodge Bay (see Figure 3 and the compilation map of Macdonald and Slimmon, 1985). Note the folded F_2-boudinaged conformable leucogranite stringers.

Peninsula, between Lodge Bay and Elliot Point, conglomeratic horizons in the basal quartzite locally contain a foliation defined by a shape fabric in the quartz clasts. The intersection of this shape fabric with S_0 yields a dextral asymmetry in all places (Figure 8). Based on the consistent asymmetry and northerly trend, we believe that this fabric constitutes an S_3 or an S_4, despite the lack of minor folds in those outcrops.

The waning stages of deformation are manifested by gentle, small-scale, mostly S-asymmetric chevron-type F_5 folds, box folds, and kink bands. These structures are not significant at the map scale.

Lineations

There is a variety of lineations of different ages in both the Murmac Bay Group and intrusive rocks, defined by stretched quartz grains, quartz rods, clasts, crenulations, and preferred mineral orientations. In a few places, where two different kinds of lineation appear together, they are approximately parallel. The early near-down-dip stretching lineations (see above) appear to be related to early thrusting, but not all early lineations are near down-dip. For example, in southeasterly dipping psammites in one outcrop on Milliken Lake (Figure 3), F_1-related faserkiesel define a lineation, which ranges from subhorizontal to intermediately plunging. Further, a quartz-stretching lineation in the generally shallow F_1 and F_2 folds is parallel to their hinges. The best-developed stretching lineations are parallel to the subhorizontal axes of hundreds-of-metres- to kilometre-scale northeasterly trending open folds, one through Milliken Lake and a trail of them through a group of islands east of Elliot Point (Figure 3). Although there is no unambiguous evidence whether these folds are F_2 or F_3 structures, their relatively large interlimb angles (varying between 60° and 90°) and some small open parasitic folds on Milliken Lake, which deform the transposition foliation (and also contain the shallow, hinge-parallel stretching lineation) suggest that they are F_3 structures. Hence, this lineation is likely an L_3, which formed during stretching of the F_3 fold hinges (see last section for a detailed explanation). In summary, the lineations in the study area are of different ages, but no overprinting relationships were observed.

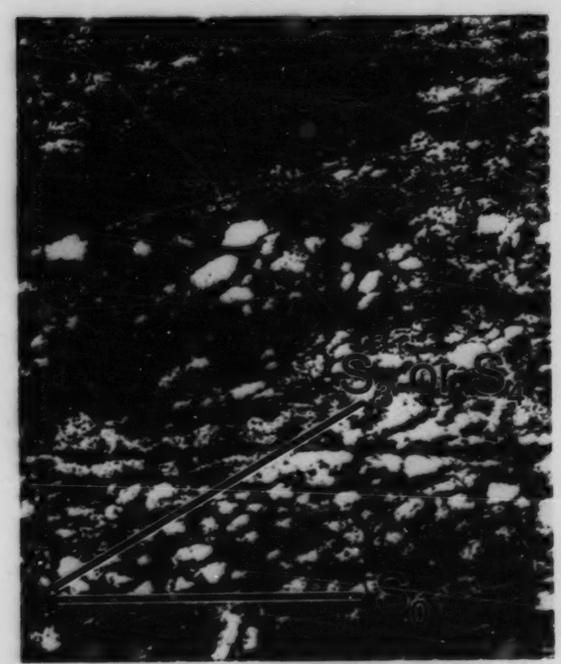

Figure 8 - Shape fabric of clasts defining an S_3 or S_4 in conglomeratic portions of the basal quartzite, Lodge Bay. Note the dextral asymmetry of bedding and cleavage.

Shear Zones and Faults

St. Louis Fault

The St. Louis fault is a complicated structure exhibiting low-temperature mylonitization and later cataclastic deformation (Krupicka and Sassano, 1972). We examined the kinematics of an east-northeast-trending segment of the structure in two locations: east of Donaldson Lake and on the Ace Lake mine (Figure 3), but our results are inconclusive and microstructural work is needed. A complicating factor is that the structure appears to be gently folded by F_3 and/or F_4.

Other Shear Zones

Low-temperature, retrograde mylonite zones, commonly several tens to a few hundred metres wide, are common in the leucogranites of the Mickey Lake–Donaldson Lake area (Figure 3). These mylonites are typically characterized by quartz ribbons with aspect ratios of up to 1:50 and locally show some brittle-ductile overprinting. Some of these ribbon mylonites are bleached and so fine grained, that they had been mistaken for quartzites in previous mapping. Others are strongly sericitic and had therefore been mapped as sericite schists. These late mylonite zones, particularly the overprinted ones, are commonly accompanied by strong chloritization. Owing to their fine grain size and the lack of visible kinematic indicators, the determination of shear sense will rely on our forthcoming microstructural study. At present we can only report that some brittle-ductile shear bands indicate a predominantly apparent sinistral shear sense.

b) Domain B

Domain B is the eastern part of the Black Bay straight belt (Figures 3, 4, and 9). The straight belt constitutes an at least 10 km wide, northeast-trending corridor of intensely deformed and attenuated Murmac Bay Group rocks and intrusive rocks. It is bounded by the Black Bay fault to the east.

Our mapping covered the eastern part of the straight belt (Figure 3). Here, M_1 and M_2 metamorphic grades are indistinguishable, but the combined grade is

Figure 9 - Attenuated, highly strained high-grade gneisses in the Black Bay straight belt. Hammer (circled) for scale.

characterized by partial melting (Figure 6) and leucogranite injection. The following post-M_2 structural features have been observed (Figure 4):

1) Shearing was accommodated along the gneissic layering, which dips steeply towards the northwest and southeast (Figure 4). These dip reversals occur at all scales and appear to be the result of shallow boudinage together with relatively open folding.

2) Abundant close to transposed Z-asymmetrical folds with shallowly northerly plunging axes both deform the shear-zone fabric and, with increasing tightness, contain the shear-zone fabric along their axial-planes. The F_3 axial planes appear rotated towards the shear fabric with increasing tightness. A strong, gently northeast- and southwest-plunging stretching lineation is developed parallel to the fold axes. In some locations, both curve through the horizontal. Some of these folds have been intruded by synkinematic leucogranite both along and across their axial planes. In the first situation, the stringers are undeformed to slightly boudinaged (Figure 10), because they remained in the extensional sector throughout folding whereas, in the second situation, the stringers were irregularly folded during tightening of the host fold. There are also a few S-folds, mainly plunging shallowly southwesterly, and some earlier rootless folds. We correlate both the Z-folds and shearing with the ubiquitous F_3 Z-folds outside the shear zone, and interpret the granite intrusion as related to the M_3 event.

3) Open, more brittle style F_4 Z-folds have typically intermediately plunging axes and they are locally dismembered by brittle faults parallel to the shear-zone fabric (Figure 11). They deform boudinaged conformable granite stringers and the shallow stretching lineation.

4) Other F_3 and/or F_4 structures such as ubiquitous decimetre-scale brittle to brittle-ductile shear bands, asymmetrical boudinage (with steep boudin axes; Figure 12), and asymmetrical granite fish are all indicative of a component of dextral shear.

At Cinch Lake mine (Figure 3), the S_3 mylonitic fabric in leucogranite dips steeply northwestward and the stretching lineation plunges shallowly southwest. This is consistent with shallowly oblique dextral reverse movement of the west side over the east side.

Figure 10 - Z-asymmetrical F_3 fold in Black Bay straight belt with syn-F_3 axial-planar leucogranite intrusion in plan view.

Figure 11 - Z-asymmetrical F_4 fold that has been dismembered by shearing along its long limb. In contrast to the F_3 fold in Figure 10, this one folds the shallow L_3 lineation.

0 1 2 3 4 5 6 7
CENTIMETRES

Figure 12 - Shear bands indicating dextral movement in the Black Bay straight belt (plan view).

In summary, this high-strain corridor constitutes a dextrally oblique reverse high-strain zone, possibly with a transpressive component. Considering the combination of shallow stretching lineations, abundant shear bands, and the strong attenuation of the package, the transpressive interpretation appears the more plausible one.

c) Domain C

Domain C comprises the area between the Black Bay fault and Jug Bay fault, and part of the Beaverlodge Lake shore (Figure 3). It hosts only Martin Group sediments and related volcanic rocks, which were deposited after F_2 and M_2, possibly during F_3. Thus, the rocks of domain C do not record the Archean history of the Murmac Bay Group. As evident from the map and the stereographic projection of bedding (Figures 3 and 4; data taken from Tremblay, 1972), the rocks are folded into the tight, shallowly to intermediately north-northeasterly plunging F_4 Martin Lake syncline (e.g. Tremblay, 1972) with a steeply east-southeast-dipping axial plane. The significance of this fold is discussed below. In one location west of Milliken Lake, small Z-asymmetrical F_4 folds with intermediately to steeply northeasterly plunging axes were observed.

The steep Black Bay fault and the parallel, moderately to steeply northwest-dipping Jug Bay fault delimit a narrow, at least 50 km long belt, which we interpret as a dextral pull-apart basin (Figure 3). Both structures appear to be brittle-ductile and have a strong brittle overprint associated with pervasive chloritization in a zone tens of metres wide. We could not gather any kinematic information on the Black Bay fault other than some dextral ductile-brittle shear bands on an adjacent small island, but there is no proof that the shear bands and the fault are related. At Jug Bay, Martin Group siltstones and weakly foliated to massive Gunnar granite are exposed two metres apart, but the faulted contact of the Jug Bay fault is missing. Farther away from the contact, in the granite, there are fault sets near-parallel to the main structure. In their vicinity, the granite is hydrothermally altered, locally beyond recognition. The Jug Bay fault thus appears to represent a set of faults rather than a single discrete structure. The Black Bay fault was active longer than the Jug Bay fault, as the former truncates late easterly trending dykes, whereas these dykes cut across the latter.

d) Correlation with Previous Work

Our sequence of structural generations (Table 1) correlates well with Ashton and Hartlaub (1998) and Hartlaub (1999). As the only difference, we report two additional late fold generations (F_4 and F_5). Sibbald and Lewry (1980) grouped our early F_1 and F_2 folds together so that our F_3 correlates with their F_2. Our interpretations are in stark contrast to Tremblay (1972), whose F_1 is our F_4. Further, the sinusoidal fold-axial plane of the Martin Lake syncline did not result from refolding but is a primary feature common in folds at all scales.

4. Tectonic Synthesis

D_1 is characterized by northwest-directed folding and thrusting (in terms of present day coordinates), as indicated by the northwest vergent F_1 anticlinorium cored by basement on the northeastern Crackingstone Peninsula, and by local near-down-dip stretching lineations in southeasterly dipping rocks. Considering the local high M_1 metamorphic grade which led to partial melting, D_1 deformation was likely not accommodated in a foreland fold-and-thrust belt, but in thick, internally deformed ductile nappes. Preliminary monazite chemical ages from upper medium-grade pelitic rocks sampled 20 km to the east of the study area suggest that D_1 occurred at or close to the Archean-Proterozoic boundary (Hartlaub, pers. comm., 2000). The significance of D_2 is uncertain. F_2 folds are distinguished solely on the basis of their relationships with respect to post-F_1 granites and their accompanying M_2 metamorphism. Considering that F_2 structures did not introduce any complex F_1/F_2 interference patterns, the D_2 and D_1 settings may have been similar. D_2 is likely of Paleoproterozoic age and, so we speculate, it may be related to the collision of the Taltson orogen with the Rae plate at 2.0 to 1.9 Ga.

We present three preliminary models for the D_3 deformation history. In the first model, the large F_3 fold hinge in the Beaverlodge Lake–Lodge Bay area belongs to a symmetrical synform with a steep, northeast-trending axial plane and abundant large M-shaped folds in its hinge area, formed during northwest-southeast shortening. According to this geometry, we expect the sequence exposed on the eastern shore of the Crackingstone Peninsula to re-appear to the east (under the Athabasca sandstone cover and Lake Athabasca). The fold's axis, east of the Crackingstone Peninsula and south of Lodge Bay, must be shallow to subhorizontal in order to be in agreement with the northeasterly trend of the rocks exposed on the peninsula and on the islands to the east of it.

The other two models (Figure 13) consider the large F_3 fold as Z-asymmetrical, with the rocks of the

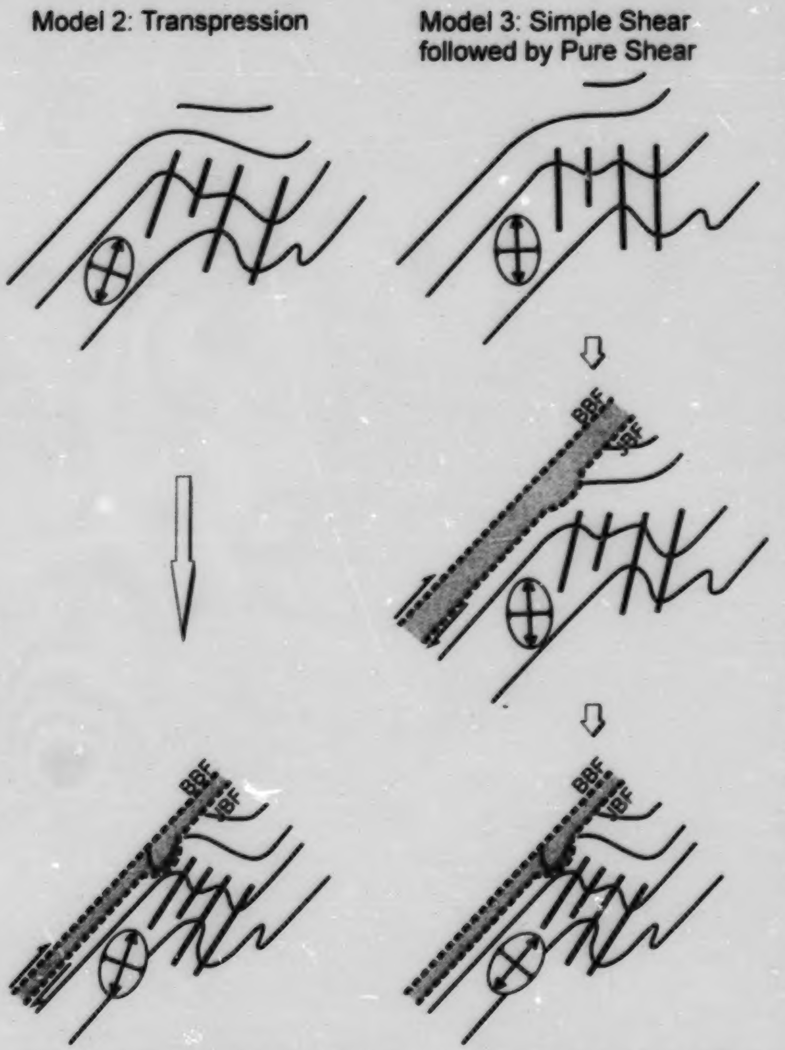

Figure 13- Sequence of diagrams that schematically depict the D_3 history according to models two and three, as discussed in the text. The thick black lines depict fold axial planes and the ellipses indicate the directions of instantaneous maximum and minimum stretching. BBF, Black Bay fault and JBF, Jug Bay fault.

Crackingstone Peninsula being located on one of the long limbs. This is consistent with the structural grain and the prevailing map-scale Z-asymmetrical folds west of Uranium City (see compilation map of Macdonald and Slimmon, 1985).

According to the second model, the Uranium City area was subjected to dextral transpression (i.e. a combination of simple shear and pure shear, which results in thinning of the deformation zone). In this situation, the direction of the maximum shortening direction was at an angle higher than 45° with the then prevalent structural grain (which we assume to have been the same northeast grain as on the present-day Crackingstone Peninsula). In this setting, the F_3 folds formed at an angle to the northeast structural grain in a shear environment that progressively rotated them towards parallelism with this direction. During rotation, the fold hinges were in the extensional sector and a stretching lineation parallel to the fold axes developed. The reason for the locus of the large fold hinge straddling the Beaverlodge Lake area, and the abundance of kilometre-scale parasitic symmetrical folds in this hinge area, may be related to a large-scale flow perturbation initiated around flow-inhibiting voluminous granite bodies. During tightening of the large fold structure, a northeast-trending dextral pull-apart basin developed (shaded area in Figure 13), flanked by the Black Bay shear zone/fault and the Jug Bay fault, the latter of which dismembered the large F_3 fold along its long limb and possibly cut out part of the hinge. While the basin was becoming narrower during transpression, its Martin Group fill was constrained to become folded (Martin Lake syncline; Figures 3 and 4). In the Black Bay straight belt and, to a minor extent in the extended Donaldson Lake area, sets of west- to west-northwest-trending, undeformed late mafic dykes may represent the "frozen" azimuth of the maximum shortening direction at the end of D_3, which is consistent with the transpression interpretation.

Model three is a variation of model two, and considers simple shear and pure shear deformation as not having operated simultaneously. According to this model, the large Z-fold developed as a drag fold in dextral simple shear related to approximately east-west shortening. During continued dextral shearing, the F_3 axial planes rotated towards parallelism with the structural grain and the Martin basin developed as a strike-slip basin developed (shaded area in Figure 13). This was followed by pure shear associated with northwest-southeast shortening, during which the parasitic F_3 folds in the large F_3 hinge area east of Beaverlodge Lake were locally tightened, their axial planes were rotated farther towards parallelism with the northeast structural grain, and the Martin Lake syncline formed.

The fundamental difference between models two and three is that model two does not require a shift in the shortening direction during D_3, and it offers the best explanation for the pervasive, relatively shallow L_3 stretching lineations. Model one may explain the large apparent thickness of the quartzite, but it cannot account for the shallow stretching lineations parallel to the F_3 hinges, nor for the pull-apart basin.

We therefore favour model two at the present stage of investigations in the Uranium City area. After the D_3 deformation outlined in these models, small, gentle, S-asymmetrical folds recorded on the Crackingstone Peninsula, which are frequently associated with kink bands and box folds, are thought to indicate of weak sinistral shearing during D_4. D_4 may represent the waning stages of deformation and, since there are no large-scale D_4 structures, it is rather insignificant. D_3 and D_4 are possibly related to the Hudsonian orogeny, a worldwide event at ca. 1.8 Ga, which, for example, included the Rae/Hearne-Superior collision.

5. Acknowledgments

We thank Russell Hartlaub, Ryan Morelli, Erin Chorney, and Sarah Ehman for acquiring some of the structural data presented in Figure 4. We further acknowledge the dedicated field assistance of Danielle Boivin, Erin Chorney, Sarah Ehman, and Asha Yanko. Discussion in the field with Kathy Bethune, Colin Card, Tom Chacko, Gary Delaney, Charlie Harper, Russell Hartlaub, Larry Heaman, and Ryan Morelli is appreciated.

6. References

Ashton, K.E. and Card, C.D. (1998): Rae Northeast: A reconnaissance of the Rae Province northeast of Lake Athabasca; *in* Summary of Investigations 1998, Saskatchewan Geological Survey, Sask. Energy Mines, Misc. Rep. 98-4, p3-16.

Ashton, K.E., Card, C.D., Heaman, L.M., and Coolican, J. (1999): Rae Northeast: Analytical update and new field results from the north-central Train Lake Domain; *in* Summary of Investigations 1999, Volume 2, Saskatchewan Geological Survey, Sask. Energy Mines, Misc. Rep. 99-4.2, p3-16.

Hartlaub, R.P. (1999): New insights into the geology of the Murmac Bay Group, northeastern Rae Province, northwest Saskatchewan; *in* Summary of Investigations 1999, Volume 2, Saskatchewan Geological Survey, Sask. Energy Mines, Misc. Rep. 99-4.2, p17-28.

Hartlaub, R.P. and Ashton, K.E. (1998): Geological investigations of the Murmac Bay group, Lake Athabasca North Shore Transect; *in* Summary of Investigations 1998, Saskatchewan Geological Survey, Sask. Energy Mines, Misc. Rep. 98-4, p17-28.

Henderson, J.R. (1997): Development of a chevron cleavage pattern and porphyroblast rotation in graded metaturbidites, Slave structural province, Northwest Territories, Canada; J. Struc. Geol., v19, p653-661.

Hoffman, P.F. (1988): United plates of America, the birth of a craton: Early Proterozoic assembly and growth of Laurentia; Ann. Rev. Earth Planet. Sci., v16, p543-603.

__________ (1989) Precambrian geology and the tectonic history of North America; *in* Bally, A.W. and Palmer, A.R. (eds.), The Geology of North America – An overview, Vol. A, Geol. Soc. Amer., p447-512.

Krupicka, J. and Sassano, G.P. (1972): Multiple deformation of crystalline rocks in the Tazin Group, Eldorado Fay Mine, NW Saskatchewan; Can. J. Earth Sci., v9, p1422-433.

Macdonald, R. (1983): Geology and regional context of the Oldman Lake area; *in* Summary of Investigations 1983, Saskatchewan Geological Survey, Sask. Energy Mines, Misc. Rep. 83-4, p44-48.

Macdonald, R. and Slimmon, W.L. (1985): Bedrock geology of the greater Beaverlodge area, NTS 74N-6 to -11; Sask. Energy Mines, Map 241A (1:100 000 scale).

Sibbald, T.I.I. and Lewry, J.F. (1980): Uranium metallogenic studies: Lodge Bay area, Lake Athabasca; *in* Summary of Investigations 1980, Saskatchewan Geological Survey, Sask. Energy Mines, Misc. Rep. 80-4, p19-23.

Tremblay, L.P. (1972): Geology of the Beaverlodge Mining Area, Saskatchewan; Geol. Surv. Can., Mem. 367, 265p.

Van Schmus, W.R., Persons, S.S., Macdonald, R., and Sibbald, T.I.I. (1986): Preliminary results from U-Pb zircon geochronology of the Uranium City Region; *in* Summary of Investigations 1986, Saskatchewan Geological Survey, Sask. Energy Mines, Misc. Rep. 86-4, p108-111.

Airborne Multisensor (Gamma Ray Spectrometric/Magnetic/VLF-EM) Surveys in Northern Saskatchewan: A Status Report

R.B.K. Shives [1], J.M. Carson [1], P.B. Holman [1], K.L. Ford [1], J.A. Grant [1], K.E. Ashton, C.T. Harper, and G.D. Delaney

---

Shives, R.B.K., Carson, J.M., Holman, P.B., Ford, K.L., Grant, J.A., Ashton, K.E., Harper, C.T., and Delaney, G.D. (2000): Airborne multisensor (gamma ray spectrometric/magnetic/VLF-EM) surveys in northern Saskatchewan: A status report; *in* Summary of Investigations 2000, Volume 2, Saskatchewan Geological Survey, Sask. Energy Mines, Misc. Rep. 2000-4.2.

Abstract

For more than four decades, gamma ray spectrometry surveys have been applied to geological mapping, mineral and hydrocarbon exploration, and environmental monitoring, worldwide. In northern Saskatchewan, the entire Precambrian Shield has been covered with reconnaissance surveys using 5000 m line spacing. Selected areas have been re-flown with 2000 to 300 m line spacings, for improved resolution.

In 2000, new surveys were completed in the Uranium City and Phelps Lake areas, combining gamma ray spectrometric, aeromagnetic, and VLF-EM sensors, to support new integrated geoscience projects. Results will be presented, as available, at the annual SEM Open House, November 2000 in Saskatoon, and will be published by Spring 2001.

Under the National Gamma Ray Spectrometry Program (NATGAM), the Radiation Geophysics Section obtains, maintains, and distributes data acquired during various airborne gamma ray spectrometer (AGRS) surveys, throughout Canada. During the first 10 years of data acquisition, only AGRS data were routinely measured. For the past 20 years, NATGAM surveys also acquired magnetic total field and very low frequency electromagnetic (VLF-EM) data.

In northern Saskatchewan, the entire Precambrian Shield has been covered with reconnaissance gamma ray spectrometric surveys flown under the Uranium Reconnaissance Program in 1975-1978, using 5000 m line spacing (Figure 1). While these surveys continue to provide useful regional geology information at 1:1 000 000 and 1:250 000 scales, they lack the resolution necessary for presentation at larger scales. Many areas have been re-flown with line spacings from 2000 to 300 m, as illustrated. The resulting data, has improved resolution and supports 1:50 000, 1:20 000, and property-scale, bedrock and surficial geological mapping, and mineral exploration for a variety of commodities (Shives *et al.*, 1995; Shives *et al.*, this volume; Campbell and Shives, this volume).

Recently, the Section has taken on the task of converting all the data in the NATGAM database from several old digital formats and analogue products to a single, consistent, digital database for the entire country. This will support improved data distribution and new compilations at a variety of scales. Emphasis has been placed on the Saskatchewan data to support the new Geological Survey of Canada (GSC)–Saskatchewan Energy and Mines (SEM) EXTECH IV Athabasca Uranium Multidisciplinary Study (Yeo *et al.*, this volume).

In 2000, under a joint federal-provincial agreement, new AGRS, magnetometer, and VLF surveys were flown in the Uranium City and Phelps Lakes areas, in support of integrated geoscience mapping projects led by Ashton *et al.* (this volume), Kraus and Ashton (this volume), and C. Harper, respectively. Survey funding was provided under the federal Targeted Geoscience Initiative and by Saskatchewan Northern Affairs through the Saskatchewan Centenary Fund.

The new surveys were flown under contract to Sander Geophysics Limited, using an Islander twin-engine fixed wing aircraft (Figure 2). On-board sensors included an Exploranium GR820 gamma ray spectrometer linked to 40 liters of NaI detectors (32 liters main detector, 8 liters upward-looking), a Scintrex cesium-vapour magnetometer, and Hertz-totem 2A VLF-EM unit. Lines were flown at 1000 m (Phelps Lakes regional) and 500 m (Uranium City survey, and the Ennadai block in-fill, in the northwest corner of the Phelps Lakes area) intervals. Nominal terrain clearance was 120 m. Flight lines were optimally oriented for local geological strike.

At the time of writing the surveys had been flown, but only preliminary field plots have been viewed. Highlights will be presented at the Saskatchewan Energy and Mines annual Open House in Saskatoon, November 2000. All data will be available for purchase in map and digital formats by spring 2001.

---

[1] Radiation Geophysics Section, Geological Survey of Canada, 573 - 601 Booth Street, Ottawa, ON K1A 0E8.

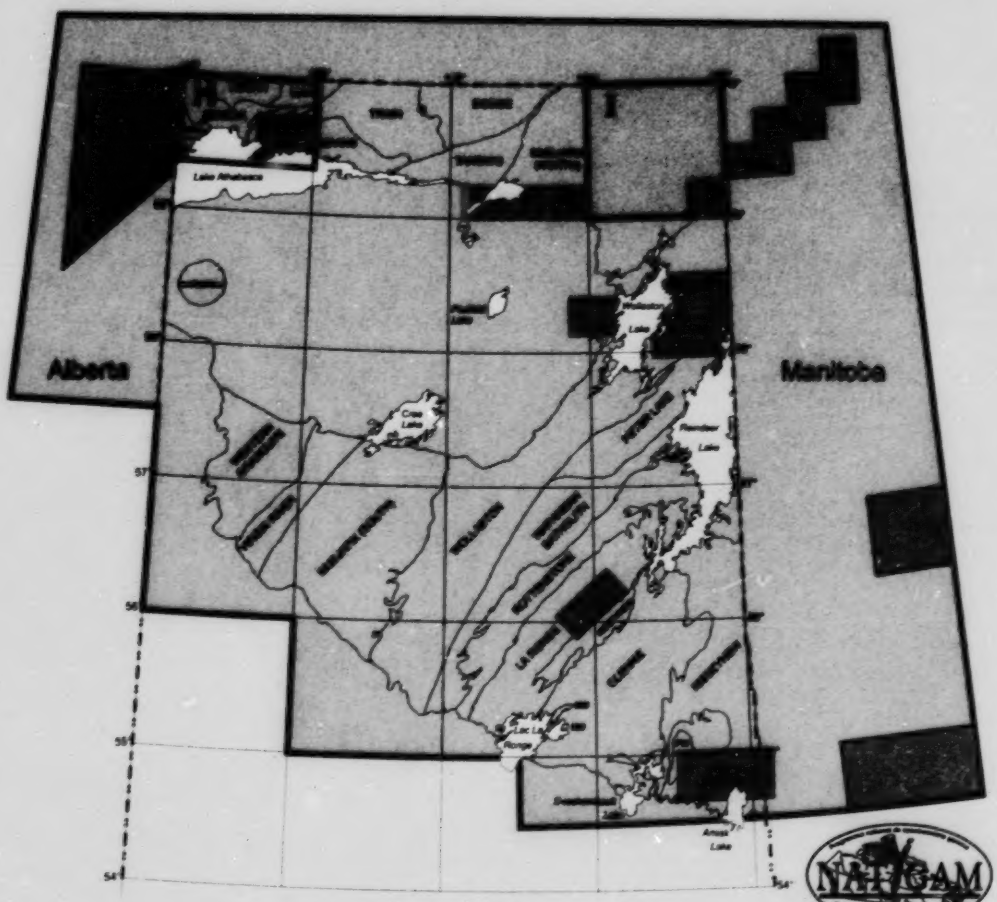
Lake Athabasca
Alberta
Manitoba
Cree Lake
Wollaston Lake
Reindeer Lake
Lac La Ronge
Amisk Lake
57°
56°
55°
54°
54°
NATGAM

			Flight line spacing (in m)
░	Uranium Recconnaissance Program Surveys		5000
▓	Detail Surveys:	A. Uranium City	2000
		B. Black Lake	800
		C. Hara Lake	1000
		D. NEA-IAEA	300
		E. Wollaston Lake	1600
		F. Star - Waddy lakes	500
		G. Hanson Lake -Flin Flon	500
▣	***New*** 2000 Surveys: (includes magnetic total field and VLF-EM)	H. Uranium City	500
		I. Phelps Lakes/Ennadai Detail	1000/ 500

Figure 1 - Index to airborne gamma ray spectrometer surveys in northern Saskatchewan. For some of these, including the recently completed 2000 surveys, aeromagnetic and VLF-EM data were also collected. Archean basement windows are: HW, Hunter Window; NW, Nistowiak Window; and PW, Pelican Window.

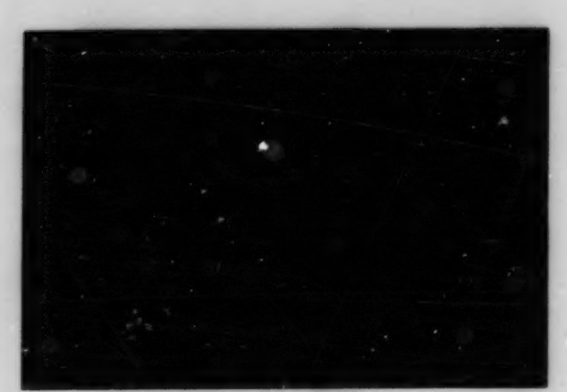

Figure 2 - Islander twin-engine fixed wing aircraft used to conduct the new, multisensor (gamma ray spectrometric/magnetic/VLF-EM) airborne geophysical surveys in the Phelps Lakes and Uranium City areas. The aircraft is owned and operated by Sander Geophysics Limited.

1. References

Shives, R.B.K., Ford, K.L., and Charbonneau, B.W. (1995): Applications of gamma ray spectrometric/magnetic/VLF-EM surveys - Workshop Manual; Geol. Surv. Can., Open File 3061, 82p.

The Final Pieces of the 'Bridge': Geology of the Southern Reindeer Lake and Laurie Lake Areas

Ralf O. Maxeiner and Cameron J. Demmans [1]

Maxeiner, R.O. and Demmans, C.J. (2000): The final pieces of the 'Bridge': Geology of the southern Reindeer Lake and Laurie Lake areas; *in* Summary of Investigations 2000, Volume 2, Saskatchewan Geological Survey, Sask. Energy Mines, Misc. Rep. 2000-4.2.

Abstract

The field component of the La Ronge–Lynn Lake Bridge Project was completed in 2000 by 1:20 000 scale mapping in three separate areas. An approximately 130 km² area between Laurie Lake and Dumont Lake along the Manitoba border is largely underlain by migmatized upper amphibolite facies Sickle Group feldspathic psammite and Burntwood Group pelite to psammopelite. Supracrustal rocks of the Lynn Lake Belt and the Levesque Bay supracrustal assemblage represent a lesser component of the area. Many of the units of the Lynn Lake Belt and Kisseynew Domain at Laurie Lake, including the host rocks of the Lar deposit, are correlative with parts of Saskatchewan's Central Metavolcanic Belt and MacLean Lake Belt.

At Reindeer Lake, an approximately 140 km² area centered on Westlake Island in southern Numabin Bay is underlain by upper amphibolite facies supracrustal successions of the La Ronge Domain, Kisseynew Domain (MacLean Lake Belt), and Glennie Domain. The boundary between the Kisseynew and Glennie domains is overprinted by a several kilometre wide mylonite zone, which is cut by the Tabbernor Fault System. The unknown age of the various sedimentary successions of the Kisseynew Domain remains a fundamental obstacle in deciphering the lithotectonic history of the region.

Mapping of a 40 km² area over Brenton-Priestly islands is the framework for a current undergraduate thesis investigation of the geochemical affinity of amphibolites and tonalites of the Levesque Bay supracrustal assemblage.

No major economic mineral occurrences exist in the area. Several new minor disseminated pyrite-pyrrhotite-chalcopyrite occurrences were encountered at Laurie Lake.

1. Introduction

In this final year of fieldwork on the La Ronge–Lynn Lake Bridge project (Maxeiner, 1996; Corrigan *et al.*, 1997), two separate areas at opposite ends of the 'bridge' were mapped. In addition, mapping was undertaken in the Brenton-Priestly islands area as part of a B.Sc. thesis project (Figure 1).

The Laurie Lake area, situated along the Manitoba border, was mapped to better understand the geology of the Sickle and Burntwood groups as well as their relationship with the Lynn Lake Belt, and to compare and integrate this acquired knowledge with elements of the newly defined lithotectonic framework developed at Reindeer Lake (e.g. Corrigan *et al.*, 1999a; Maxeiner, 1999).

Based on previous mapping (Pyke, 1960; Gilboy, 1980; Johnston and Thomas, 1984), the Laurie-Dumont lakes area is known to be underlain by psammopelitic 'garnet-biotite gneisses' and derived migmatites of the Burntwood Group (Zwanzig, 1990), as well as psammitic sediments and derived migmatites of the Sickle Group. Mapping by the Manitoba Geological Survey (Gilbert *et al.*, 1980; Syme, 1990; Zwanzig *et al.*, 1999), as well as mapping and exploration by mining companies, has traced the Lynn Lake Belt to the east side of Laurie Lake. In Manitoba, the Lynn Lake Belt hosts several volcanogenic massive sulphide (VMS) occurrences. The most westerly, the Lar deposit (e.g. Elliott-Meadows and Appleyard, 1991), is located on Laurie Lake, just 7 km east of the Saskatchewan-Manitoba border. Of equal economic interest is the Johnson Shear Zone, an important gold-bearing structure located along the southern edge of the Lynn Lake Belt (e.g. Beaumont-Smith and Rogge, 1999), and its possible extension into Saskatchewan.

The Westlake Island area, previously mapped by Johnston (1983) and also part of the 1:250 000 scale Reindeer Lake South compilation (Johnston and Thomas, 1984), is located at the southern end of Numabin Bay on Reindeer Lake, just north of the settlement of Southend. It joins previous maps of the La Ronge–Lynn Lake Bridge project (Maxeiner, 1996; 1998; Harper, 1998) and contains the southward transition from the La Ronge Domain into the Kisseynew Domain (MacLean Lake Belt) and Glennie Domain. The area is overprinted and complicated by a several kilometre wide mylonite zone and the brittle to ductile Tabbernor Fault system.

In the Brenton-Priestly islands area, 1:20 000 scale mapping was undertaken to provide a framework for

---

[1] Department of Geology, University of Regina, Regina, SK S4S 0A2.

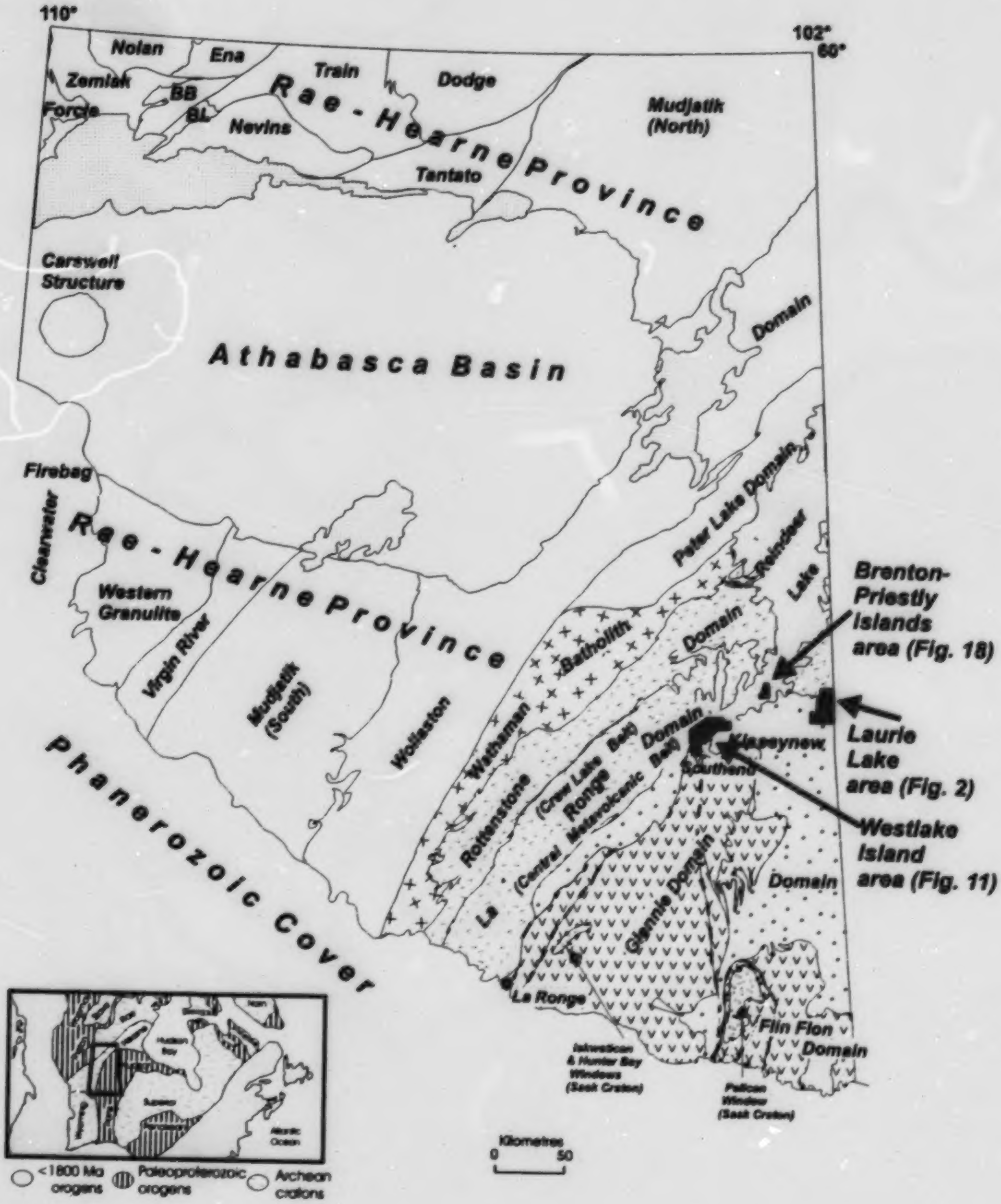
110°
102°
60°
Nolan
Ena
Train
Dodge
Zemlak
BB
Forcie
BL
Nevins
Rae-Hearne Province
Mudjatik (North)
Tantato
Carswell Structure
Athabasca Basin
Domain
Peter Lake Domain
Firebag
Clearwater
Rae-Hearne Province
Western Granulite
Virgin River
Mudjatik (South)
Wollaston
Reindeer
Lake
Domain
Batholith
Wathaman
Rottenstone
La
(Crew Lake Belt)
Ronge
(Central Metavolcanic Belt)
Domain
Kisseynew
Southend
Glennie Domain
Domain
Brenton-Priestly islands area (Fig. 18)
Laurie Lake area (Fig. 2)
Westlake Island area (Fig. 11)
Phanerozoic Cover
La Ronge
Flin Flon Domain
Iskwatikan & Hunter Bay Windows (Sask Craton)
Pelican Window (Sask Craton)
Kilometres
0
50
Hudson Bay
Superior
Atlantic Ocean
<1800 Ma orogens
Paleoproterozoic orogens
Archean cratons

Figure 1 - Location of the Westlake Island, Laurie Lake, and Brenton-Priestly islands areas with respect to the main lithotectonic elements of the Precambrian Shield of northern Saskatchewan. Geological map of North America after Hoffman (1990); domainal map of Saskatchewan after Ashton (1999); BB, Black Bay and BL, Beaverlodge Lake.

an undergraduate thesis investigation of the geochemical affinity of amphibolites and tonalites of the Levesque Bay supracrustal assemblage.

2. Laurie Lake: The Final Stone of the 'Bridge'?

An 8 by 17 km corridor between Laurie Lake and Dumont Lake along the Manitoba border was mapped at 1:20 000 scale. This adjoins previous reconnaissance mapping in the Wapus-Dumont lakes area (Maxeiner, 1999) and provides a link with Manitoba geology. Field relationships of the Lynn Lake Belt and Kisseynew Domain in western Manitoba were also examined during a field trip with Herman Zwanzig and Chris Beaumont-Smith of the Manitoba Geological Survey.

Glacial cover and overall poor accessibility between Wapus Bay of Reindeer Lake and Laurie Lake, does not allow physical tracing of units of the La Ronge Domain into the Lynn Lake Belt. However, many of the observed rocks at Laurie Lake, which have physical continuity with the Lynn Lake Belt and the Sickle and Burntwood groups of the Kisseynew Domain, are identical to the Reindeer Lake rocks. For example, the unconformity between Sickle Group and Wasekwan Group of the Lynn Lake Belt (Gilbert *et al.*, 1980) was observed on Reindeer Lake in 1997 (Maxeiner, 1997). Moreover, the exact same succession of tectonized serpentinites, emerald-green weathering actinolite schist, and structurally underlying polymictic conglomerate was observed in a sliver of the Lower Lynn Lake Belt (Zwanzig, pers. comm., 2000), and is equated by us with the Lawrence Point Assemblage at Reindeer Lake (Table 1).

a) Regional Geology

The Laurie Lake area (Figure 2) is underlain by migmatitic sedimentary rocks of the Sickle Group and Burntwood Group of the Kisseynew Domain, as well as minor volcanic rocks of the Lynn Lake Belt (Gilbert *et al.*, 1980; Gordon *et al.*, 1990; Zwanzig, 1990). The high-grade equivalents of the two groups are referred to as the Sickle Metamorphic Suite and the Burntwood River Metamorphic Suite (Zwanzig, 1990). In Manitoba, the Burntwood Group is the most abundant and oldest component of the Kisseynew Domain (Gilbert *et al.*, 1980); deposition of sediments along the south flank of the belt occurred between 1.855 and 1.84 Ga (David *et al.*, 1996). Psammitic rocks from the southwestern MacLean Lake Belt, which are correlated with the Burntwood Group, have yielded Pb-Pb evaporation ages from detrital zircons that suggest deposition after 1.855 Ga (Ansdell and Yang, 1995).

The Sickle Group is correlated with the McLennan Group in Saskatchewan (e.g. Lewry *et al.*, 1990). West of Laurie Lake, in the Macfarlane Island area at Reindeer Lake, cross-bedded psammite overlying basal polymictic conglomerate of the McLennan Group (Maxeiner, 1998), contains a major population of 1.85 to 1.845 Ga detrital zircons (SHRIMP U-Pb data; Ansdell *et al.*, 1999). Work in the southwestern MacLean Lake Belt, suggested an even younger age for deposition of the McLennan Group, with detrital zircon Pb/Pb ages (Pb evaporation technique) between 1.835 and 1.854 Ga (Ansdell and Yang, 1995). However, pink 'felsite' in the North Lake area, interpreted as felsic dykes and sills intrusive into the McLennan Group (Maxeiner and Sibbald, 1995), yielded a conventional U-Pb zircon age of 1.843 ±2 Ga obtained by Heaman and reported in Kyser *et al.* (1992).

Metavolcanic rocks of the Lynn Lake Belt have historically been referred to as the Wasekwan Group (Table 1; Gilbert *et al.*, 1980). Based on a more recent geochemical investigation of the belt, Zwanzig *et al.* (1999) have identified a number of unrelated, in part 1.91 Ga old (Baldwin *et al.*, 1987) tectonostratigraphic assemblages. On a first order basis, the Lynn Lake Belt can be subdivided into a northern and a southern belt (Gilbert *et al.*, 1980; Zwanzig *et al.*, 1999).

Geochemically, the southern Lynn Lake Belt contains arc tholeiites and felsic to intermediate calc-alkaline arc rocks, as well as mid-ocean ridge tholeiitic basalts (Zwanzig *et al.*, 1999). The northern Lynn Lake Belt is made up of enriched mid-ocean ridge basalts, as well as light rare earth element-enriched arc tholeiites.

b) Local Geology

Rock units of the Laurie Lake area are broadly similar to those identified during mapping in previous years (Table 2; Maxeiner, 1997, 1998, 1999; Corrigan *et al.*, 1998). Naming of sedimentary rocks follows the

Table 1 - Correlation of major lithotectonic divisions of the northwestern Reindeer Zone.

Lewry, 1983 McLennan - Jaysmith lakes area: La Ronge Domain / MacLean Lake Belt	Thomas, 1990; 1993 Otter Lake area: La Ronge Domain / MacLean Lake Belt	Maxeiner, 1996 to 1999, this study; Corrigan *et al.*, 1997 Reindeer Lake area: La Ronge Domain / MacLean Lake Belt / Kisseynew Domain	Gilbert *et al.*, 1980 Lynn Lake area, Manitoba: Lynn Lake Domain / Kisseynew Domain
McLennan Group (granitoid meta-arkose, meta-arkose, arkosic greywacke, arkosic quartzite, arkosic conglomerate) oooooooooooooooo Central Metavolcanic Belt (volcanics and synvolcanic sediments) Gradational contacts MacLean Lake gneisses (psammitic-semipelitic greywacke (biotite gneisses), pelite, hornblendic-amphibolite; calc-silicate gneiss)	McLennan Group (K-spar > plagioclase meta-arenites, metaconglomerate, granitic meta-arkose, also subordinate quartzitic meta-'arkose', meta-arkosic wacke and meta-arkosic muscovite schist) unconformable, in part sheared Central Metavolcanic Belt (volcanics and synvolcanic sediments) Crew Lake Belt (mixed metasediments) MacLean Lake gneisses (calcareous to noncalcareous psammitic to pelitic metagreywacke, metaconglomerate, hornblende gneiss, amphibolite, calc-silicate gneiss)	Sickle / McLennan groups (Sickle Metamorphic Suite) (feldspathic psammite, in part calcic or aluminous, conglomerate) ? Burntwood Group / MacLean Lake gneisses (Burntwood River Metamorphic Suite) (graphitic pelite and psammopelite) oooooooooooooooooooooo LA RONGE DOMAIN Reed Lake Assemblage (CMB) (felsic to intermediate volcanic rocks, and sedimentary rocks) Duck Lake Assemblage (pelite to psammite) ? Levesque Bay supracrustal assemblage Lawrence Point Assemblage (CMB) (mafic to ultramafic volcanic and plutonic rocks) ? (calcic psammopelite, quartzite, amphibolite)	Sickle Group (greywacke, conglomerate, cross-bedded arkose, biotite gneiss, calcareous sandstone and arkosic sandstone) oooooooooooo Wasekwan Group (volcanic rocks and synvolcanic sediments) Burntwood Group (graphitic pelite and psammopelite)

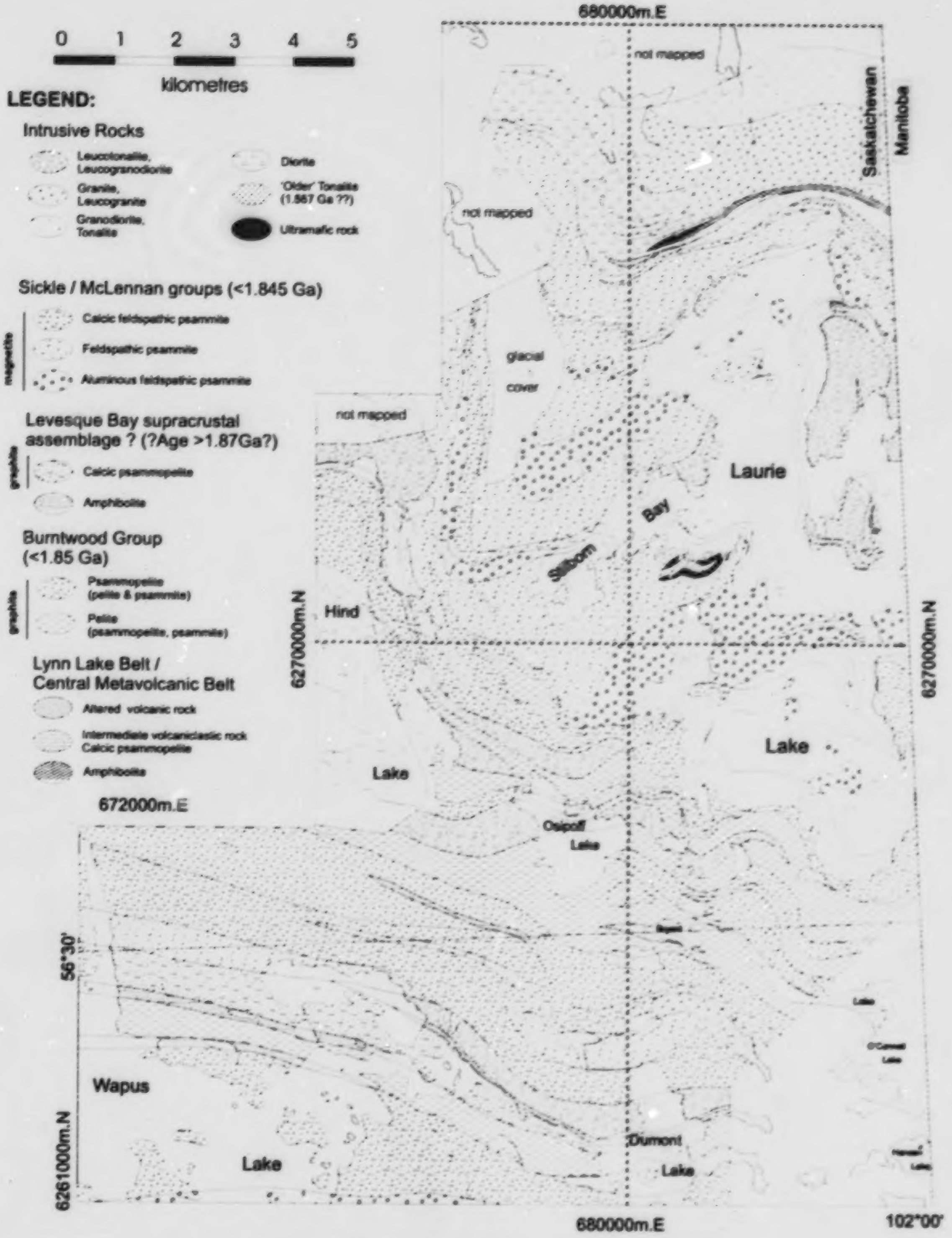
0 1 2 3 4 5
kilometres
LEGEND:
Intrusive Rocks
Leucotonalite, Leucogranodiorite
Granite, Leucogranite
Granodiorite, Tonalite
Diorite
'Older' Tonalite (1.867 Ga ??)
Ultramafic rock
Sickle / McLennan groups (<1.845 Ga)
magnetite
Calcic feldspathic psammite
Feldspathic psammite
Aluminous feldspathic psammite
Levesque Bay supracrustal assemblage ? (?Age >1.87Ga?)
graphite
Calcic psammopelite
Amphibolite
Burntwood Group (<1.85 Ga)
graphite
Psammopelite (pelite & psammite)
Pelite (psammopelite, psammite)
Lynn Lake Belt / Central Metavolcanic Belt
Altered volcanic rock
Intermediate volcaniclastic rock Calcic psammopelite
Amphibolite
680000m.E
not mapped
Saskatchewan
Manitoba
not mapped
glacial cover
not mapped
Laurie
Bay
Sillborn
Hind
6270000m.N
6270000m.N
Lake
Lake
Osipoff Lake
672000m.E
56°30'
Wapus
Lake
Dumont Lake
6261000m.N
680000m.E
102°00'

Figure 2 - Simplified geological sketch map of the Laurie Lake area.

Table 2 - Characteristics of the main rock units in the Westlake Island, Brenton-Priestly islands, and Laurie Lake areas.

Rocktype	**Map Code**	**Colour (weathered surface)**	**Grain-size**	**Texture and Association**	**Structure**	**Mineralogy**	**Thickness**	**Magnetic Susceptibility**
● Intrusive Rocks								
Leucogranodiorite (post-D3)	Lgd	Light grey, light pinkish grey to pink	Medium to coarse	Equigranular, homogeneous	Massive to weakly foliated	Plagioclase, quartz (20 to 25%), microcline (5 to 15%), biotite (<5%), ±magnetite	NA	Very Low 0.1
Leucogranite	Lg	Pinkish grey to moderate orange pink	Medium to coarse	Equigranular, homogeneous	Massive to weakly foliated-lineated	Plagioclase, microcline (20 to 30%), quartz (20 to 30%), biotite (<<5%), ±magnetite±hornblende	NA	High 1 to 5
Leucotonalite	Lt	White to very light grey	Coarse to medium	Equigranular, homogeneous	Massive to weakly foliated-lineated	Plagioclase, quartz (25 to 35%), biotite (<5%)	NA	Low (~0.1) 0.1 to 5
Granite	G	Pinkish grey to moderate orange pink	Medium to coarse	Equigranular, homogeneous	Massive to weakly foliated-lineated	Plagioclase, quartz (15 to 20%), microcline (20 to 30%), biotite (5 to 10%), magnetite±hornblende	NA	Variable 1 to 5
Granodiorite	Gd	Light grey to light pinkish grey	Medium to coarse	Equigranular, homogeneous, Gdx - heterogeneous and agmatitic	Massive to weakly foliated-lineated	Plagioclase, quartz (15 to 20%), microcline (10 to 15%), hornblende>biotite>epidote (5 to 15%), sphene	NA	1.1 0.1 to 8
Diorite / Quartz-diorite	Di, Diq	Medium grey to brownish grey, peppered	Medium to coarse	Homogeneous, locally hornblende-blastic	Massive to weakly foliated-lineated	Plagioclase, hornblende > retrograde biotite>epidote (15 to 30%), quartz (0 to 15%)	NA	0.41 0.09 to 1
Tonalite	T	Light grey	Coarse to medium	Equigranular, homogeneous, Tg - mylonitic garnetiferous ± opx tonalite	Massive to strongly foliated-lineated	Plagioclase, quartz (20 to 30%), microcline (<<5%), hornblende>biotite>epidote (5 to 15%), magnetite±opx	NA	High (~1.6) 0.2 to 8.5
Gabbro	Ga	Dark greenish grey to greenish black	Medium to coarse	Commonly hornblende porphyroblastic	Massive to weakly foliated-lineated	Hornblende (40 to 65%), plagioclase, relict pyroxene, ±quartz±biotite±pyrite±pyrrhotite	NA	1.7 0.2 to 4.0
Amphibolite	Am	Dark green to greenish black	Fine (to medium)	Homogeneous, locally banded, granoblastic, rarely hornblende-blastic	Massive to strongly foliated	Plagioclase, hornblende(40 to 50%), tremolite-actinolite±diopside±garnet±orthopyroxene±cummingtonite	~1 to 50 m	~0.57 0.4 to 0.7
Ultramafic rock	Ua	Emerald green to dusky yellow green	Fine to coarse	Locally with relict olivine or olivine blasts, in part magnetic, Ua - emerald green actinolite schist, Us - bluish to brownish grey serpentinite, Up - dusky green pyroxenite	Massive-strongly foliated, locally schistose	±hornblende±tremolite-actinolite±serpentine±olivine±orthopyroxene±clinopyroxene±plagioclase ±chromite±magnetite±anthophyllite±talc±chloritoid±pyrite, ±pyrrhotite	NA	0.4 (typical) 0.2 to 40
● Supracrustal Rocks								
→ McLennan / Sickle groups								
Psammopelite to pelite	MPsp	Light grey to medium grey	Fine to medium	Granoblastic, locally layered. Possibly not part of McLennan-Sickle groups	Well foliated, 10 to 20% granitic leucosome	Plagioclase, quartz, microcline (10 to 20%), sillimanite (10%), biotite (5%), ±retrograde muscovite	200 to 500 m	~0.2 0.15 to 0.25
Feldspathic psammite	MAr	Light grey to light pinkish grey	Fine to medium	Granoblastic, thinly to medium bedded, local trough cross-bedding and lag deposits, 0.2 to 2 m thick mafic-ultramafic amphibolite dykes, 0.2 to 0.4 m thick calc-silicate layers	20 to 30% *lit-par-lit* granitic leucosome	Plagioclase, quartz, microcline (10 to 20%), biotite (5 to 10%), magnetite, ±muscovite±hornblende	400 to 800 m	High (~7.1) 0.1 to 40
Aluminous feldspathic psammite to psammopelite	MArs	Light grey to light pinkish grey	Fine to medium	Granoblastic, up to 10% sillimanite faserkiesel axial planar to F2 folds, MArg-garnetiferous feldspathic psammopelite	20 to 30% *lit-par-lit* granitic leucosome	Plagioclase, quartz, microcline (10 to 20%), sillimanite (10%), biotite (<5%), magnetite, ±retrograde muscovite	200 m to 2 km	High (~8.6) 0.1 to 44
Calcic feldspathic psammite to psammopelite	MArc	Light grey, pinkish grey to greenish grey	Fine to medium	Thinly to medium bedded, granoblastic, abundant 0.2 to 0.4 m thick calcic beds. MArp-calcic psammopelite, low magnetic susceptibility	20 to 30% *lit-par-lit* granitic leucosome	Plagioclase, quartz, microcline (10 to 20%), diopside and hornblende (<10%), biotite (<5%), magnetite, ±diopside	100 m to 1 km	High (~6.2) 0.1 to 36
Polymictic conglomerate	MCg	Grey, pinkish grey to brownish grey	Fine matrix	Pebble- to cobble-sized clasts (volcanic>plutonic>sedimentary), hornblende- to biotite-rich matrix, rare sandy layers	Clast elongation up to 200:1	Plagioclase, quartz, microcline, biotite, hornblende, ±garnet, ±muscovite	100 to 300 m	7.4 0.3 to 18

→ Burntwood River Group								
Diatexite	**BDt**	Grey	Medium to very coarse	Inequigranular; heterogeneous	Migmatitic, >70% tonalitic leucosome	Plagioclase, quartz, biotite(20 to 25%), ±garnet (0 to 10%) ±graphite	200 m	$\frac{\sim 0.20}{0.15 \text{ to } 0.25}$
Pelite	**BPp**	Grey to dark grey	Fine to medium	Heterogeneous, granoblastic, variable from pelitic to psammopelitic, in part cordierite-bearing (**BPpc**)	Migmatitic, gneissic, 20 to 30% tonalitic leucosome	Plagioclase, quartz, biotite (20 to 25%), garnet (5 to 10%), graphite	100 to 300 m	$\frac{\sim 0.20}{0.15 \text{ to } 0.25}$
Psammopelite	**BPsp**	Medium grey to brownish grey	Fine to medium	Heterogeneous, granoblastic, variable from psammopelitic to psammitic	Migmatitic, gneissic, 10 to 30% tonalitic leucosome	Plagioclase, quartz, biotite (10 to 20%), garnet (<5%), graphite (1 to 2%)	400 to >1000 m	$\frac{\sim 0.20}{0.15 \text{ to } 0.25}$
→ Levesque Bay supracrustal assemblage								
Ferruginous psammite	**LWfe**	Brownish grey, medium grey to rusty brown	Fine	Compositionally layered, thin to medium bedded, interlayered chert	Well foliated	Quartz, plagioclase, biotite and/or hornblende (<15%), ±tremolite±garnet±diopside±pyrite±pyrrhotite±graphite	20 m	$\frac{\text{Variable}}{0.5 \text{ to } 2.0}$
Calcic psammopelite	**LPcs**	Grey, greenish grey to rusty brown	Fine (to medium)	Poorly layered, granoblastic, interlayered with rare beds of marble, quartzite, silicate-facies iron formation	Well foliated, migmatitic, 20% tonalitic leucosome	Plagioclase, quartz, diopside, hornblende, tremolite, garnet, biotite, graphite, ± microcline (up to 30%), ±orthopyroxene, ±carbonate±pyrrhotite±chalcopyrite±cummingtonite	10 to 100 m	$\frac{0.3 \text{ (typical)}}{0.2 \text{ to } 0.5}$ also 20 to 50
Banded amphibolite	**LCm**	Banded greenish black, pale green, rusty brown	Fine (to medium)	Banded on centimetre- to decimetre-scale, granoblastic, with garnet-amphibolite (**PCmg**) bands	Well foliated, boudinaged layers	Plagioclase, hornblende and diopside (40 to 50%), ±garnet±carbonate	~1 to 50 m	$\frac{\sim 0.50}{0.4 \text{ to } 0.7}$
→ Duck Lake Assemblage								
Pelite	**DPp**	Grey	Fine to medium	Thinly to medium bedded	Well foliated	Plagioclase, quartz, biotite (20 to 25%), sillimanite (<10%), garnet (<5%), ±staurolite±muscovite±tourmaline	<500 m	$\frac{\sim 0.2}{0.15 \text{ to } 0.25}$
Psammopelite	**DPsp**	Medium grey to brownish grey	Fine to medium	Medium to thickly bedded, granoblastic	Well foliated, 10-20% *lit-par-lit* tonalitic leucosome	Plagioclase, quartz, biotite (10 to 15%) ±sillimanite (<5%), ±garnet (<5%) ±muscovite±tourmaline	<400 m	$\frac{\sim 0.25}{0.20 \text{ to } 0.30}$
Psammite	**DPs**	Light medium grey to dark grey	Fine to medium	Granoblastic, poorly layered, monotonous, equigranular.	Well foliated, 10% *lit-par-lit* tonalitic leucosome	Plagioclase (50%), quartz (40%), biotite (5 to 10%), garnet (<5%), ±tourmaline±graphite±sillimanite±diopside±epidote	400 to 1200 m	$\frac{\sim 0.20}{0.10 \text{ to } 0.30}$
→ Central Metavolcanic Belt–Lynn Lake Belt								
Calcic psammopelite	**CCs**	Light greenish grey to dark grey, locally rusty brown	Fine (to medium)	Heterogeneous, centimetre-scale banding and compositionally layered, includes calcic psammite, psammopelite, minor felsic tuffs, chert and iron formation	Schistose, well foliated.	Plagioclase, hornblende, quartz, diopside, tremolite-actinolite, garnet, biotite, ±carbonate±graphite±pyrrhotite±pyrite	~100 m	$\frac{0.70}{0.2 \text{ to } 0.9}$
Altered volcanic rock	**CAv**	Light grey, buff to rusty brown	Fine to coarse	Garnet-cummingtonite schist (**CAvc**) and cordierite-garnet schist (**CAvg**), heterogeneous and compositionally variable	Well foliated, granoblastic	Plagioclase, quartz, biotite, ±garnet±cummingtonite±anthophyllite±cordierite±hornblende±pyrite±pyrrhotite±chalcopyrite	<20 m	$\frac{\text{Variable}}{0.1 \text{ to } 50}$
Intermediate volcaniclastic rock	**CIv**	Medium grey to dark grey	Fine	Granoblastic, in part poorly layered	Well foliated to lineated	Plagioclase, hornblende (20 to 25%), quartz, ±biotite	50 to 100 m	$\frac{0.40 \text{ (typical)}}{0.2 \text{ to } 40}$
Banded amphibolite	**CCm**	Banded greenish black to pale green	Very fine to fine	Colour banded on centimetre scale, garnetiferous banded amphibolite (**CCmg**)	Well foliated and boudinaged layers	Plagioclase, hornblende, diopside, tremolite, ±garnet±carbonate±epidote	<50 m	$\frac{\sim 0.65}{0.4 \text{ to } 0.9}$
→ Glennie Domain								
Calcic psammopelite	**GPcs**	Grey, greenish grey to brownish grey, locally rusty	Fine (to medium)	Poorly layered, granoblastic, with rare amphibolite and garnet-amphibolite layers, ultramafic pods	Well foliated, migmatitic, 20% tonalitic leucosome	Plagioclase, quartz, diopside, hornblende, tremolite, garnet, biotite, graphite, ±orthopyroxene ±cummingtonite±carbonate±pyrrhotite±pyrite	10 to 100 m	$\frac{0.3 \text{ (typical)}}{0.2 \text{ to } 0.5}$ also 20 to 50
Amphibolite	**GAm**	Greenish black to black	Fine (to medium)	Heterogeneous to homogeneous, locally banded/laminated, in part hornblende-blastic, **GAmx**-amphibolite breccia, equivalent of **LCm** and/or **CCm** / **CMv**	Massive to well foliated, locally with incipient melt	Plagioclase, hornblende, ±garnet±diopside±magnetite±pyrite	20 to 200 m	$\frac{\sim 0.56}{0.4 \text{ to } 0.8}$

suggestions of Maxeiner *et al.* (1999). Where UTM coordinates are provided in the text they are in NAD 1927. All rocks have been overprinted by regional thermotectonism and for convenience, the prefix meta- has been omitted throughout the text (with the exception of names). The metamorphic grade at western Laurie Lake is upper amphibolite facies and anatectic melt phases are abundant, particularly in pelitic and psammopelitic rocks. Due to the high degree of recrystallization, partial melting, folding, refolding and faulting, stratigraphic relationships are hard to decipher.

Lynn Lake Belt–Central Metavolcanic Belt

North of Laurie Lake, thin units of highly strained supracrustal and minor intrusive rock, including banded amphibolite (unit CCm), intermediate volcanic rocks (unit CIv), garnet-cordierite schist, and cummingtonite-garnet schist (unit CAv), as well as ultramafic actinolite schist (unit Ua), occur in the same relative structural position as the Laurie Lake assemblage in Manitoba (Zwanzig *et al.*, 1999). All of these rocks are strongly recrystallized and tectonized, and injected by leucogranite or diorite. The Laurie Lake banded amphibolite is identical in appearance to rocks of both the ca. >1.89 Ga (Corrigan, pers. comm., 1999) Levesque Bay supracrustal assemblage mapped in the Brenton Island area, and amphibolites of the Lawrence Point Assemblage (? age) in the Duck Lake area (Maxeiner, 1997, 1998). In both cases these rocks are interpreted as calcium-metasomatized, strongly deformed, pillowed basaltic flows. Structurally overlying the Laurie Lake banded amphibolite is a thin unit of actinolite schist which is believed to represent a tectonized ultramafic intrusive similar to those of the Lawrence Point Assemblage (Maxeiner, 1999).

Banded amphibolite (unit CCm) is also present as thin slivers in two isolated localities in the east central part of the area. It is closely associated with a prominent, approximately 100 m thick unit of calcic sedimentary rock (unit CCs) and is intruded by leucogranodiorite (Figure 3). Most outcrops of the banded amphibolite show centimetre-scale banding defined by variations in mafic mineral content and overall mineralogy. The overall composition of the rock is intermediate, but some layers have mafic or even ultramafic composition.

Two 20 m thick units of garnet-cummingtonite schist (unit CAvc) and cordierite-garnet schist (unit CAvg) at the north end of Laurie Lake form large rafts in the dioritic to quartz-dioritic intrusion and are on strike of the banded amphibolite and ultramafic tectonite. They are interpreted as syngenetically altered intermediate to mafic volcanic rocks.

Calcic psammopelite (unit CCs) is distinct from the intermediate volcanic unit (CIv) in that it contains abundant biotite and quartz, in addition to hornblende. Several thin units of migmatitic pelite (unit BPp) and psammopelite (unit BPsp) occur near a leucogranodiorite intrusion at east central Laurie Lake and likely represent tectonic slivers of the Burntwood Group. Alternatively, their association with intermediate and mafic supracrustal rocks may suggest that they are correlative with the Lynn Lake Belt or the Levesque Bay supracrustal assemblage.

Burntwood Group

An approximately 3 km thick succession of migmatitic pelite to psammopelite (units BPp and BPsp), intruded by leucotonalite to leucogranodiorite, occurs at the south end of Laurie Lake (Figure 4). These are similar to rocks of the Jones Peninsula area (Maxeiner, 1998) and southwest Numabin Bay–Deep Bay area (this report) at Reindeer Lake. On the regional aeromagnetic map (Geological Survey of Canada, 1964), the Laurie Lake pelitic to psammopelitic succession shows up as a distinctive low and is traceable into the psammopelitic rocks of the Jones Peninsula area, which we are tentatively interpreting as belonging to the ca. 1.87 Ga Duck Lake Assemblage.

Figure 3 - Xenolith of banded amphibolite within leucogranodiorite; station M00-0491, east central Laurie Lake.

Figure 4 - Tonalitic leucosome and biotite-rich melanosome within migmatitic pelite; station M00-0301, south Laurie Lake.

Burntwood-Sickle Transition

Amphibolite, garnet-amphibolite, mafic calc-silicate rock (Unit LCm), and minor calcic psammopelite (unit LPcs) mark the transition between the Burntwood Group and the Sickle Group in many locations. In Manitoba (e.g. Zwanzig, 1990), these rocks are included in the upper part of the Burntwood Group, and are generally interpreted as being derived from volcanic, volcaniclastic and intrusive protoliths. A similar succession was mapped at Reindeer Lake in Saskatchewan (Maxeiner, 1998; Corrigan *et al.*, 1999b), where they were named the Levesque Bay supracrustal assemblage (Corrigan *et al.*, 1998).

South of Laurie Lake in Saskatchewan, a unit of amphibolite (LCm), varying in thickness from 1 to 50 m, occurs on opposing limbs of an early east-west-trending syncline cored by feldspathic psammite of the Sickle Group. The amphibolite (LCm) is interpreted to be derived from mafic volcanic, and volcaniclastic rocks. It is very similar to banded amphibolites of the Levesque Bay supracrustal assemblage, as well as the Lawrence Point Assemblage at Reindeer Lake (Maxeiner, 1999).

A compositionally variable unit of calcic psammopelite (unit LPcs), interbedded pyrrhotite-bearing grunerite-hornblende rock (silicate facies iron formation), impure marble, and chert is closely associated with the amphibolite.

Sickle Group

Rocks of the Sickle Group underlie a large part of the Laurie Lake area and are similar to those in the Macfarlane Island area and the northern part of Hodgson Island at Reindeer Lake (Maxeiner, 1997, 1998). An approximately 8 km thick belt in the central part of the lake, as well as an approximately 3 km thick belt south of the lake, were identified. Feldspathic psammite (referred to as meta-arkose by previous workers) is the main rock type (unit MAr), subordinate units include calcic feldspathic psammite (MArc) and aluminous feldspathic psammite (MArs). Mafic to ultramafic, strongly boudinaged conformable amphibolite bands between 0.2 to 2 m thick (Figure 5) are characteristic of all the units, as well as up to 0.4 m thick boudinaged calc-silicate layers (Figure 6). The amphibolite bands are interpreted as mafic dykes. The calc-silicate layers, comprising quartz, plagioclase, diopside, epidote, and garnet, likely represent original beds of a more calcic and quartz-rich composition.

Calcic feldspathic psammite to psammopelite (MArc) comprising alternating layers of hornblende-diopside-rich beds and microcline-rich beds (Figure 7) likely reflect primary rhythmic layering (but see description of similar rocks on Priestly Island at Reindeer Lake below). Unit MArc occurs at the structural base of the Sickle Group at Laurie Lake, but the stratigraphic base is known to be a polymictic conglomerate (e.g. Gilbert *et al.*, 1980; Maxeiner, 1997).

Figure 5 - Boudinaged amphibolite dyke in aluminous feldspathic psammite; station M00-0107, southwest Laurie Lake.

Figure 6 - Boudinaged calc-silicate layer (epidote-quartz rich) in aluminous feldspathic psammite; station M00-107, southwest Laurie Lake.

Figure 7 - Rhythmic layering in calcic feldspathic psammite; station M00-0354, south Laurie Lake.

Aluminous feldspathic psammite to psammopelite (MArs) contains as much as 10% sillimanite, some as crystals up to 10 cm long (Figure 8).

Intrusive Rocks

Intrusive rocks, including diorite to quartz-diorite (Di), granodiorite (Gd) and granite (G), are abundant north of Laurie Lake.

In the central part of Laurie Lake, intrusive rocks comprise leucocratic tonalite to granite (units Lt, Lgd, Lg) and most of these plutons have been transposed and folded on a kilometre scale. A leucogranodiorite intrusion at east-central Laurie Lake is quite circular and contains xenoliths and larger rafts of a foliated hornblende granodiorite (Figure 9), banded amphibolite (Figure 3), and graphitic pelite. A small gabbroic body cross-cuts feldspathic psammite at east-central Laurie Lake.

c) Structure and Metamorphism

Same as elsewhere in the 'bridge', three main deformation events are distinguished (e.g. Maxeiner, 1999). D_1 produced outcrop- to kilometre-scale isoclinal folds with layer parallel axial planes, which were later refolded by tight northeast-plunging F_2 folds. Sillimanite or biotite is commonly axial planar to the F_2 structures, which are consecutively refolded by co-axial northeast-plunging, close to open F_3 folds. Quartz and plagioclase within leucosome are commonly flattened parallel to the axial plane of the F_3 structures.

Upper amphibolite facies mineral assemblages are common throughout the entire Laurie Lake area in Saskatchewan. Anatectic tonalite to granodiorite is prevalent in all psammitic to pelitic rocks of the Burntwood Group, granitic leucosome predominates in feldspathic psammite of the Sickle Group. Microcline and sillimanite co-exist in the leucosome of aluminous feldspathic psammite (MArs). In mafic rocks, clinopyroxene-hornblende-plagioclase-bearing assemblages are common. The peak metamorphic event is contemporaneous with D_2, as peak metamorphic minerals are refolded by F_3 structures (Figure 10).

Metamorphic grade decreases eastward to northeastward across Laurie Lake, with lower amphibolite to middle amphibolite facies mineral assemblages typical in rocks around the Fox Mine in Manitoba (e.g. Elliott-Meadows *et al.*, 1999).

d) Economic Geology

Outcrops around the Lar Cu-Zn VMS deposit (Elliott-Meadows *et al.*, 1999), located on Laurie Lake, 5 km east of the Saskatchewan-Manitoba border, were examined. The Lar Deposit is in rocks that structurally overlie the Laurie Lake assemblage of the southern Lynn Lake Belt (Zwanzig *et al.*, 1999); it is uncertain as to which of the two sub-domains of the Lynn Lake

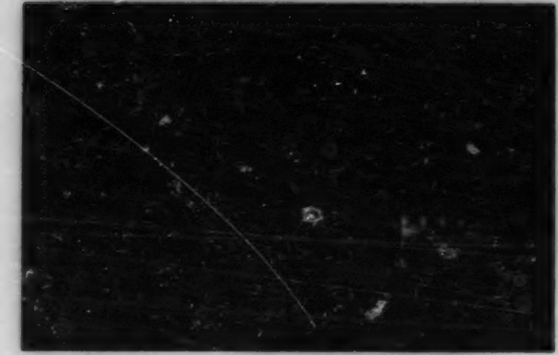

Figure 8 - Large sillimanite faserkiesel define main foliation (S_2) in aluminous feldspathic psammite; station M00-0209, west Laurie Lake.

Figure 9 - Massive leucogranodiorite with xenolith of foliated granodiorite; station M00-0492, central Laurie Lake.

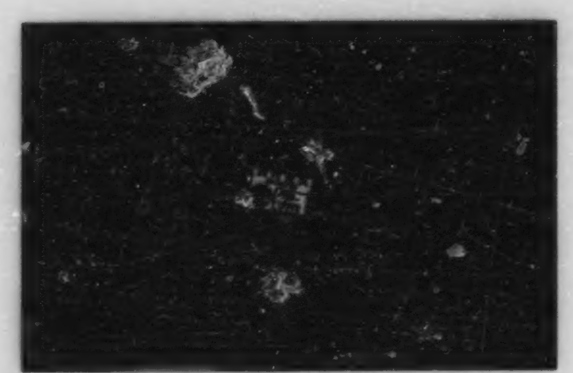

Figure 10 - Open F_3 folds in migmatitic aluminous feldspathic psammite; note coarse-grained granitic leucosome in fold hinges and folded faserkiesel; station M00-0193, north Laurie Lake.

Belt the deposit lies in. Fifteen kilometres to the east of the Lar deposit, the Fox VMS orebody is hosted by rocks of the southern Lynn Lake Belt. In contrast, however, the Lynn Lake Ni-Cu deposit is hosted in rocks of the northern Lynn Lake Belt.

The massive sulphide lenses of the Lar deposit are not exposed, but lakeshore outcrops along strike and structurally above and below the mineralized horizon were inspected. Outcrops along strike of the deposit comprise a sequence of rusty, strongly foliated and compositionally variable mafic to felsic rocks. The mafic rocks are likely altered equivalents of hornblende-diopside-bearing banded amphibolites occurring both above and below the mineralized sequence and are interpreted to be derived from mafic volcanics and lesser mafic sediments. The felsic components are fine-grained, white- to beige-weathering rocks containing abundant garnet and cummingtonite and represent strongly altered mafic volcanics (Elliott-Meadows and Appleyard, 1991). Discontinuous units of felsic volcanics were also reported (Elliott-Meadows *et al.*, 1999).

Mineral occurrences have not previously been known on the Saskatchewan side of Laurie Lake. In the Wapus-Dumont lakes area, south of the present map area, several copper and molybdenum occurrences have been described (e.g. Scott, 1991).

During four weeks of mapping and inspection of over 600 outcrops at Laurie Lake, only a few rather insignificant mineral occurrences were encountered. A small copper showing was discovered just east of Hind Lake and approximately 2 km west of Stilborn Bay (UTM: 676995, 6270041). A granite pegmatite dyke, approximately 0.5 m wide and exposed over a strike length of 4 m, is mineralized with antlerite (a secondary green copper sulphate mineral) and up to 1 to 2% chalcocite. The pegmatite is intrusive into feldspathic psammite of the Sickle Group, and is not seen to contain any other economic minerals.

Supracrustal rocks in the transition zone between the Burntwood and Sickle groups contain several occurrences of disseminated pyrite and pyrrhotite. In one location, approximately 1 km west of Hind Lake and one kilometre southwest of Stilborn Bay (UTM: 677976, 6269490), a ferruginous psammite at the boundary between migmatitic pelite of the Burntwood Group and calcic psammopelite of the Sickle Group, contains up to 2% disseminated pyrrhotite, pyrite, and minor chalcopyrite. In another location, about 1.5 km south of Osipoff Lake (UTM: 679070, 6264340), disseminations of pyrrhotite, pyrite, and minor chalcopyrite account for up to 5% of a calcic sedimentary rock.

Disseminated pyrrhotite occurs in strongly banded and compositionally variable calcic graphitic psammopelite, surrounding the concentric leucogranodiorite intrusion in the east central part of Laurie Lake.

3. Westlake Island: Porphyroclastic Mylonites and the La Ronge–Kisseynew–Glennie Domains Transition

The second half of the summer was spent in the southern part of Numabin Bay at Reindeer Lake (Figure 1), where the boundary relationships between the La Ronge, Kisseynew, and Glennie domains were studied (Figure 11). An approximately 140 km^2 area was mapped with overlap into the 1996 and 1998 map areas, as well as into Harper's 1998 map area.

The Westlake Island area is significantly different from the areas investigated between 1996 and 1999. Similar to the Street Lake area to the south (Harper, 1998), it contains an early mylonite zone that separates two of Lewry *et al.*'s (1990) allochthonous thrust sheets, the Wapassini sheet (Glennie Domain) in the footwall from the Kyaska sheet (MacLean Lake Belt/Kisseynew Domain) in the hanging wall. Most of the area is dominated by this approximately 3 km-wide mylonite zone which is tightly folded, doubling up the mylonite zone to about 5 km. The mylonites cannot be traced eastward across the main splay of the Tabbernor fold and fault zone. Instead, they appear to continue southward, before bending to the east and the north where they should re-emerge at the south end of Deep Bay.

a) Geology

From northwest to southeast, the Westlake Island area is underlain by supracrustal rocks of the Lawrence Point and Duck Lake assemblages (La Ronge Domain), pinkish grey porphyroclastic feldspathic psammite of the Sickle/McLennan groups (alias Sickle Metamorphic Suite) and pelitic porphyroclastic gneisses of the Burntwood Group of the Kisseynew Domain, as well as heterogeneous, granodioritic to dioritic orthogneisses, amphibolite and calcic psammopelite of the Glennie Domain. Rock descriptions are again summarized in Table 2.

La Ronge Domain (Lawrence Point and Duck Lake Assemblages)

The southeastern edge of the Central Metavolcanic Belt is exposed northwest of Hayward Rapids (Figure 11) and comprises sheared pillow basalts (unit CCm), calcic psammopelite (unit CCs), and migmatitic psammite to psammopelite (units DPs, DPsp; Maxeiner, 1996). In the current interpretation, mafic rocks are included as part of the Lawrence Point Assemblage and the sedimentary rocks are here re-interpreted as belonging to the ~1.87 Ga Duck Lake Assemblage (see Maxeiner, 1999), which is in structural contact with the Lawrence Point Assemblage in its type area (Maxeiner, 1997; Table 1). The calcic psammopelite (CCs) is a very mixed and heterogeneous rock unit (Table 2), that may in part be derived from hydrothermal alteration, reworking and/or shearing of the mafic volcanic rocks.

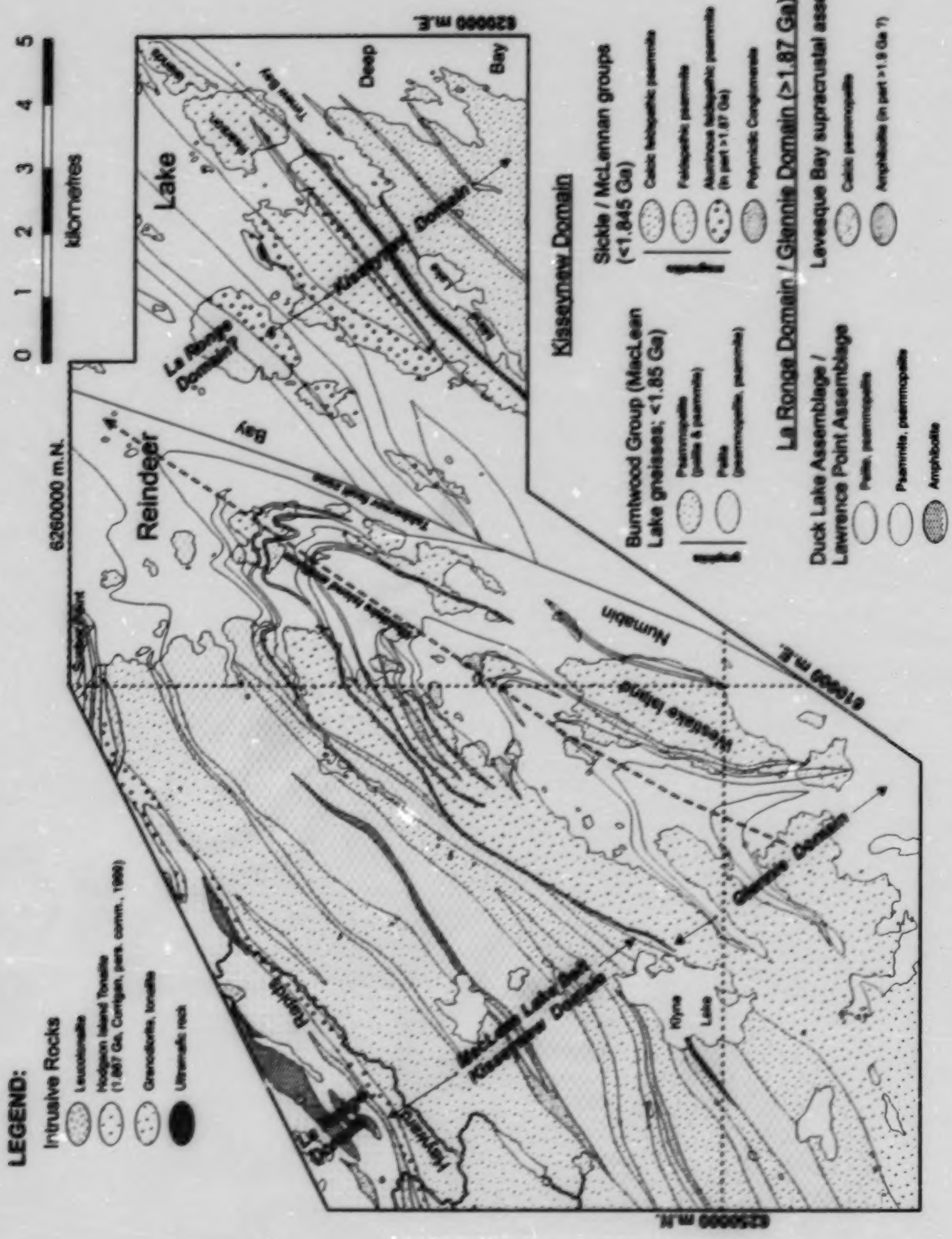
LEGEND:
Intrusive Rocks
Leucotonalite
Hodgson Island Tonalite (1.857 Ga, Corrigan, pers. comm., 1999)
Granodiorite, tonalite
Ultramafic rock
Kisseynew Domain
Burntwood Group (MacLean Lake gneisses; <1.85 Ga)
Psammopelite (pelite & psammite)
Pelite (psammopelite, psammite)
Sickle / McLennan groups (<1.845 Ga)
Calcic feldspathic psammite
Feldspathic psammite
Aluminous feldspathic psammite (in part >1.87 Ga)
Polymictic Conglomerate
La Ronge Domain / Glennie Domain (>1.87 Ga)
Duck Lake Assemblage / Lawrence Point Assemblage
Pelite, psammopelite
Psammite, psammopelite
Amphibolite
Levesque Bay supracrustal assemblage ?
Calcic psammopelite
Amphibolite (in part >1.9 Ga ?)
0 1 2 3 4 5
kilometres
6260000 m.N.
6250000 m.N.
620000 m.E.
610000 m.E.
Reindeer
Lake
Deep
Bay
Numabin
Bay
Westlake Island
La Ronge Domain?
Kisseynew Domain
MacLean Lake Belt Kisseynew Domain
Glennie Domain
Klyne
Lake
Rapids
Sucker Point

Figure 11 - Simplified geological sketch map of the Westlake Island (Reindeer Lake) area.

An interesting set of leucotonalite to leucogranodiorite sheets (Lgd) crosscuts the Duck Lake and Lawrence Point assemblages in the Hayward Rapids area. In most localities, this light grey, medium-grained rock is homogeneous and massive, however, protomylonitic varieties with ribboned quartz and feldspar also exist. Emplacement of the leucotonalite post-dated deposition of the Sickle/McLennan groups, as well as some of the earlier deformational events (D_{-1} to D_2), but clearly predated some of the latest ductile deformation and folding.

Kisseynew Domain

The area between Klyne Lake and Sucker Point is underlain by pelitic to psammitic rocks of the Kisseynew Domain (MacLean Lake gneisses). These rocks resemble the rocks of the Laurie Lake area, comprising elements of both the Burntwood and Sickle/McLennan groups. However, a several kilometre-wide ductile mylonite zone has overprinted the Klyne Lake–Sucker Point succession.

Southwest Numabin Bay

Grey to light pinkish grey, fine to medium grained, magnetite-bearing feldspathic psammite (unit MAr) is the dominant lithology of the Sickle/McLennan groups in the Klyne Lake–Sucker Point area. It typically contains between 20 to 30% highly dismembered, porphyroclastic granitic leucosome, which locally becomes very abundant, making distinction of protoliths difficult.

Over much of its length, the contact with psammitic to psammopelitic rocks of the La Ronge Domain (Duck Lake Assemblage equivalents?) is marked by aluminous feldspathic psammite (MArs), but towards the northeast a calcic variety (MArc) intervenes. The southeastern margin of the Sickle Group is poorly defined. It is characterized by a heterogeneous zone containing thin, highly strained and discontinuous units of feldspathic psammite, amphibolites of uncertain affinity, and pelitic to psammopelitic rocks belonging to the Burntwood Group or the Levesque Bay supracrustal assemblage. The feldspathic psammite is strongly migmatized with generally 20 to 30% pink, medium-grained granitic leucosome, in strongly transposed lenses which are in many locations highly dismembered and porphyroclastic in appearance. Some parts contain abundant late to post-tectonic granite pegmatite.

Migmatitic pelite to psammopelite (units BPp and BPsp) of the Burntwood Group are characterized by abundant garnet and biotite, and local cordierite and sillimanite (Unit BPpc; Figure 12). Graphite is ubiquitous, as is a high proportion of tonalitic leucosome, which is generally dismembered, and porphyroclastic (Figure 13).

Thin slivers of graphite-bearing calcic psammopelite, amphibolite, garnet amphibolite, and banded amphibolite are present at the structural top of the pelitic-psammopelitic succession, near the contact with feldspathic psammites of the Sickle Group. This transitional succession resembles rocks of the Levesque Bay supracrustal assemblage, as well as the transition between the Burntwood and Sickle groups at Laurie Lake.

Figure 12 - Migmatitic pelite of the Burntwood Group (MacLean Lake gneisses); pen points to 2 cm long blocky cordierite crystal in tonalitic leucosome; station M00-0726, southwest Numabin Bay.

Figure 13 - Coarse-grained garnet porphyroblasts in highly migmatized pelite of the Burntwood Group (MacLean Lake gneisses); tonalitic leucosome is strongly transposed resulting in porphyroclastic texture; station M00-0709, southwest Numabin Bay.

One outcrop of unquestionable serpentinite with relict coarse-grained textures of pyroxene and olivine defines a unit that occurs along the boundary between porphyroclastic sillimanite-cordierite-biotite-garnet pelite and biotite-garnet psammopelite west of Klyne Lake. The serpentinite looks identical to ultramafic harzburgites of the Lawrence Point Assemblage (Maxeiner, 1997).

Southeast Numabin Bay

East of the main splay of the Tabbernor Fault, on the peninsula between Numabin Bay and Deep Bay, psammite and aluminous psammite of the Sickle Group are also exposed. They are intruded by decimetre-scale mafic to ultramafic sills, which locally form larger pyroxenite intrusions, as on the north tip of the Deep Bay peninsula. One 20 to 40 m thick ultramafic unit is traceable for several kilometres, along the southeast margin of the Hodgson Island tonalite. It structurally overlies a thin amphibolite unit, which is also traceable for several kilometres. Despite the high state of strain, several examples of cross-bedding are preserved within the Deep Bay aluminous feldspathic psammite (Figure 14).

The feldspathic psammite and aluminous feldspathic psammite are in contact with garnet-biotite psammite and sillimanite-garnet psammopelite of the Jones Peninsula succession to the northwest. The Hodgson Island tonalite intrudes the aluminous feldspathic psammite, as well as associated amphibolite and ultramafic rocks. The homogeneous, xenolith-rich, largely massive intrusion has been dated using conventional U-Pb zircon methods and yielded crystallization ages of ca. 1.87 Ga (Corrigan, pers. comm., 1999) for samples collected from two different locations.

The feldspathic psammite unit between Milne Lake and Timew Bay is strongly porphyroclastic with shearing along both of its contacts. A 50 m thick unit of calcic psammopelite separates the feldspathic psammite from locally highly graphitic (30% graphite) pelitic to psammopelitic rocks of the Burntwood Group to the southeast.

Glennie Domain

West of the Tabbernor Fault Zone, between Klyne Lake and Westlake Island, highly deformed orthogneisses and minor supracrustal slivers define the core of a tight north-northeast-plunging antiform, herein named the Westlake Island antiform. The main rock types are heterogeneous granodiorite to quartz-diorite gneisses (units Gdx, Qdix). Agmatitic textures are common with abundant large rafts of supracrustal rocks (Figure 15), including fine-grained, granoblastic amphibolite, garnet-amphibolite, pelite, and calcic psammopelite. There are several generations of granite pegmatite, including both pre- and post-shearing varieties. All these units can be found on a single outcrop.

Towards the core of the antiform, southwest of Westlake Island, intrusive rocks dominate and become more homogeneous and less deformed. Massive, medium- to coarse-grained diorite and gabbro coexist with granodiorite and quartz-diorite.

Overall, supracrustal components, mostly amphibolite and calcic psammopelite (GAm, GPcs), appear to be more abundant in the neck of the antiform north of Westlake Island. The amphibolite is commonly fine grained, greenish black to black weathering, granoblastic, and highly recrystallized. Banding, that may in part represent transposed primary layering, is the sole recognizable primary texture (Figure 15). The mineralogy of the amphibolites is most commonly plagioclase plus hornblende, with mafic content typically varying between 40 and 50%. Locally, the amphibolite contains diopside or orthopyroxene, partly replaced by cummingtonite. Some of the garnet-amphibolite units contain a small proportion of plagioclase-hornblende-diopside±quartz leucosome, interpreted to be *in situ* melt (Figure 16).

In many places, the amphibolite is intruded by abundant granodiorite to quartz-diorite material, resulting in very messy and heterogeneous exposures of amphibolite breccia (Figure 15, subunit GAmx). This appears to be particularly characteristic of the strongly transposed units along the eastern limb of the Westlake Island antiform.

Calcic psammopelite (unit GPcs) is closely associated with the amphibolite in the hinge of Westlake Island antiform. These rocks are generally grey to brownish grey weathering, fine to medium grained, and typically compositionally variable and quite heterogeneous. They generally contain between 20 and 30% tonalitic partial melt, which has been tectonically dismembered

Figure 14 - Cross-bedding in aluminous feldspathic psammite of the Sickle Group (=McLennan Group); station M00-0977, from island west of 'Deep Bay peninsula' (under-water picture).

Figure 15 - Agmatitic tonalite with rafts of banded and folded amphibolite, likely derived from mafic volcanic protolith; station M00-0946, southwest Numabin Bay.

Figure 16 - In situ plagioclase-hornblende-diopside ±quartz melt in garnet amphibolite; station M00-1165, southwest Numabin Bay.

resulting in porphyroclastic textures. Thin, partly boudinaged layers of banded amphibolite and garnet amphibolite are common, as are homogeneous dusky green mafic to ultramafic pods. Graphitic garnet-biotite pelite is interbedded locally. Graphite, hornblende, and biotite are ubiquitous in these quartzofeldspathic gneisses, and locally they may contain garnet, cummingtonite, clinopyroxene or orthopyroxene, as well as trace amounts of sulphides, usually pyrrhotite or pyrite.

Plutonic rocks of the Westlake Island area are also strongly deformed, heterogeneous, and migmatized (Figure 17). They can generally be subdivided into two groups. Granodioritic to tonalitic rocks are more abundant than quartz dioritic to dioritic varieties; gradational relationships are common.

Thin sheets of strongly deformed garnet- and orthopyroxene-bearing tonalite to granodiorite (unit Tg), generally not more than 40 m thick, but traceable for several kilometres, are found along both flanks of the Westlake Island antiform. These grey to brown, generally medium-grained rocks are characterized by ribboned protomylonitic textures, silicification, a high magnetic susceptibility (Table 2) and an overall homogeneous, igneous texture. Garnet, magnetite, and hornblende, as well as minor orthopyroxene are common constituents.

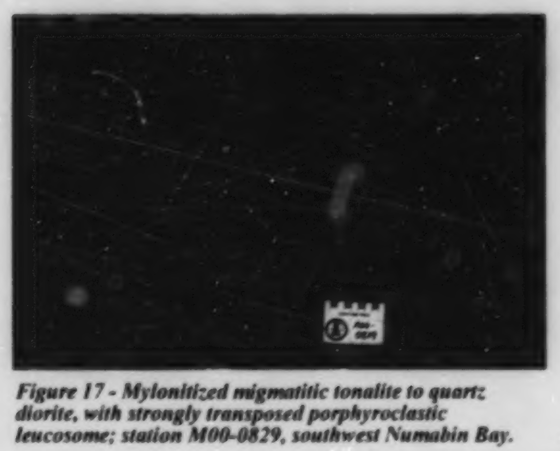

Figure 17 - Mylonitized migmatitic tonalite to quartz diorite, with strongly transposed porphyroclastic leucosome; station M00-0829, southwest Numabin Bay.

The contact between migmatitic pelite of the Burntwood Group and the orthogneisses of the Glennie Domain is marked by a several kilometre-wide mylonite zone. Because of the highly sheared nature and the multiply folded aspect of the contact, as well as the similarity between some of the supracrustal units on either side, it is difficult to decide on a dividing line between the two domains. For the purpose of the existing map, we have used the first appearance of granodioritic to dioritic rocks as the boundary between the Kisseynew Domain and the Glennie Domain.

b) Structure and Metamorphism

The overall regional structural geology of this area has been discussed by Maxeiner (1996, 1998) and is not repeated here.

The Westlake Island area is generally characterized by upper amphibolite to granulite facies metamorphic conditions. All rocks show signs of partial melting, which is most pronounced in the pelites. Feldspathic psammite of the Sickle Group is characterized by magnetite-bearing granitic leucosome; pelitic to psammopelitic rocks of the Burntwood Group have a tonalitic to granodioritic leucosome, which may locally contain graphite, garnet or cordierite. Abundant leucosome, interpreted as *in situ* partial melt indicates temperatures in access of 650° to 700°C (Bucher and Frey, 1994).

Biotite-garnet-cordierite-sillimanite is a characteristic mineral assemblage for pelitic rocks of the Westlake Island area and is indicative of 3 to 5 kbar and 650° to 750°C (Bucher and Frey, 1994). Calcic psammopelite contains the assemblage biotite-cummingtonite-hornblende±orthopyroxene±garnet. Cummingtonite in these rocks likely represents retrograde replacement of orthopyroxene. Mafic rocks are typified by assemblages containing hornblende-diopside-plagioclase±garnet. The first appearance of diopside in an amphibolite marks the beginning of upper amphibolite facies conditions at approximately 650°C. Prograde formation of orthopyroxene from hornblende, cummingtonite, and garnet in calcic psammopelite as well as some of the amphibolite occurs at approximately 750°C (Bucher and Frey, 1994).

The appearance of orthopyroxene in quartzofeldspathic pelite, calcic psammopelite, and amphibolite throughout the Westlake Island area marks the transition from upper amphibolite to granulite facies conditions. But hydrous mineral assemblages, including amphibole and biotite, remain stable indicating that most of the area hovers around the transition between upper amphibolite to granulite facies conditions. Based on the qualitative work, conditions of metamorphism in the Westlake Island area are tentatively estimated to have been between 750° to 800°C, at pressures above 3 to 5 kbar.

Relative age of metamorphism is believed to be syn-D_2 (Maxeiner, 1998; Wright *et al.*, 1999), which has been dated in the region using U-Pb zircon methods to between 1.818 and 1.805 Ga in the Levesque Bay supracrustal assemblage, but as late as 1.795 Ga in the Milton Island metasedimentary assemblage (Ansdell *et al.*, 1999).

A qualitative metamorphic study of cordierite-bearing rocks in the Mooney Island (Reindeer Lake) area by Ashton (1979) indicated temperatures of 660° to 710°C and pressures between 4.2 and 5.7 kbar, which was later refined to between 680° and 710°C and an upper pressure constraint of approximately 4.8 to 6.5 kbar by Wright *et al.* (1999). The turbiditic Milton Island metasedimentary assemblage (Williamson, 2000; Williamson *et al.*, this volume), constrained peak metamorphic conditions to between 4 and 9.75 kbar and 650° to 780°C.

c) Economic Geology

Other than a number of graphite occurrences on the east side of Numabin Bay, no major mineral occurrences are known from previous mapping or exploration in the Westlake Island area. Most of the higher grade graphite showings are located in the Pollon Lake area, within Indian Reservation #209, just south of the area presently mapped (see MacDougall, 1998). Minor copper and molybdenite occurrences on the north shore of the peninsula (e.g. Johnston, 1972) are of no significance (MacDougall, 1998).

A number of new minor sulphide occurrences, containing mainly pyrrhotite, pyrite, and trace amounts of chalcopyrite, were found. They are located in three distinct settings:

1) Many exposures of calcic psammopelite within the Glennie Domain and along the Glennie Domain–Kisseynew Domain transition are rusty weathering and contain minor disseminated pyrrhotite and pyrite, locally reaching 2 to 4%.
2) On the west side of Deep Bay, a unit of ferruginous psammite and associated cherty sediments within graphitic psammopelite of the Burntwood Group, several metres thick and traceable for several kilometres, contains between 5 to 10% pyrite and minor pyrrhotite, in disseminated as well as stringer form.
3) Along the transition between the Burntwood Group and the Sickle Group, a unit of pinkish weathering calcic feldspathic psammite contains rare occurrences with up to 5% disseminated sulphides. One such occurrence is located along the calcic feldspathic psammite southeast of the Hodgson Island pluton, the others are located on the west side of Numabin Bay. They are dominated by pyrrhotite, with minor amounts of pyrite and chalcopyrite. One occurrence (UTM: 602080, 6251580) is richer in copper, with minor malachite on weathered surface, as well as small stringers of chalcopyrite. It is associated with a pegmatite dyke that intrudes the feldspathic psammite, a setting that is remarkably similar to the occurrences at Laurie Lake.

4. Brenton-Priestly Islands Area: The McLennan Group and Levesque Bay Supracrustal Assemblage

The Brenton-Priestly islands area (Figures 1 and 18), which offers a unique cross-section through the imbricate stack of <1.845 Ga fluvial sedimentary rocks of the Sickle/McLennan groups and >1.87 Ga rocks of the Levesque Bay supracrustal assemblage (Corrigan *et al.*, 1998), was mapped as part of an undergraduate thesis project. The main purpose of this project is to geochemically characterize the amphibolite and tonalite components of the Levesque Bay supracrustal assemblage and to critically compare it to volcanic rocks of the Reed Lake and Lawrence Point assemblages of the La Ronge–Lynn Lake Belt, as well as to volcanic assemblages of the Glennie Domain.

a) Brenton Island Area

The Levesque Bay supracrustal assemblage as defined by Corrigan *et al.* (1998) comprises a heterogeneous succession of "garnet amphibolite with light green diopside-bearing calc-silicate streaks and pods, garnet-biotite±sillimanite meta-psammite and pelite, impure quartzite, calc-silicate gneiss and rare diopside marble, and minor sillimanite-anthophyllite±cordierite gneiss". The assemblage contains some of the oldest rocks of the Reindeer Lake area (Corrigan *et al.*, 1998) and it has been suggested that it is tectonically imbricated with the younger sedimentary rocks of the McLennan/Sickle groups. A leucotonalite dyke cutting banded amphibolite, sampled on the northwest side of 'Rabbit' Island, provided a U-Pb zircon age of 1.897 Ga (Corrigan, pers. comm., 1999). The larger tonalite intrusion, located on the same island but dated several kilometres along strike to the east and west, yielded a U-Pb zircon age of ca. 1.87 Ga (Corrigan *et al.*, 1998).

The Brenton Island area is underlain by a succession of amphibolite (LCm, Am), graphitic and partly sulphidic calcic psammopelite (LPcs), feldspathic psammopelite (MArg), as well as tonalite (T) and leucotonalite intrusions. Two different amphibolite units were distinguished. A banded amphibolite (LCm) occurs as two 10 to 20 m thick units, which are traceable for a few kilometres within the Hodgson Island tonalite. It is also found in two other locations between the sulphidic calcic psammopelite and tonalite, and between the sulphidic calcic psammopelite and sillimanite±garnet bearing feldspathic psammopelite. The 1.897 Ga leucotonalite dyke (Corrigan, pers. comm., 1999), cuts the banded amphibolite (Figure 19).

Massive amphibolite (Am) occurs as decimetre- to metre-sized, partly boudinaged layers within calcic psammopelite of the Levesque Bay supracrustal assemblage (unit LPcs), as well as in the sillimanite ±garnet-bearing feldspathic psammopelite (unit MArg), likely of Sickle/McLennan groups affinity

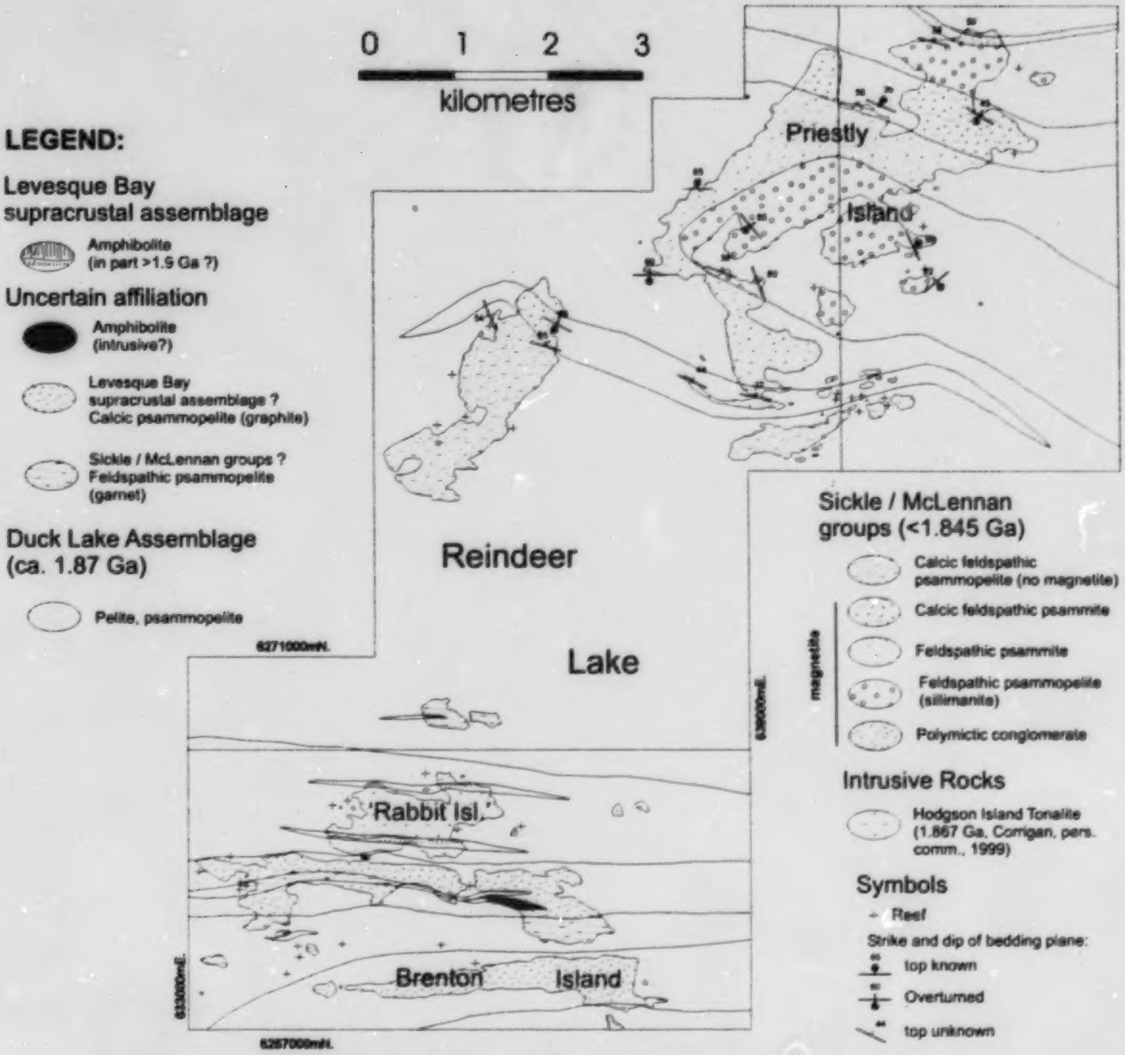
0
1
2
3
kilometres
LEGEND:
Levesque Bay supracrustal assemblage
Amphibolite (in part >1.9 Ga ?)
Uncertain affiliation
Amphibolite (intrusive?)
Levesque Bay supracrustal assemblage ? Calcic psammopelite (graphite)
Sickle / McLennan groups ? Feldspathic psammopelite (garnet)
Duck Lake Assemblage (ca. 1.87 Ga)
Pelite, psammopelite
6271000mN.
Priestly
Island
Reindeer
Lake
'Rabbit Isl.'
Brenton
Island
633000mE.
6267000mN.
639000mE.
Sickle / McLennan groups (<1.845 Ga)
Calcic feldspathic psammopelite (no magnetite)
magnetite
Calcic feldspathic psammite
Feldspathic psammite
Feldspathic psammopelite (sillimanite)
Polymictic conglomerate
Intrusive Rocks
Hodgson Island Tonalite (1.867 Ga, Corrigan, pers. comm., 1999)
Symbols
Reef
Strike and dip of bedding plane:
top known
Overturned
top unknown

Figure 18 - Simplified geological sketch map for the Brenton-Priestly islands area.

Figure 19 - Thin leucotonalite dyke cutting banded amphibolite; station D00-0131,island northwest of Brenton Island.

(Figure 20). Because of its crosscutting relationship with McLennan Group feldspathic psammopelite, it is interpreted to be intrusive in origin and likely younger than the banded amphibolite.

The contact between the tonalite and calcic psammopelite on Brenton Island shows evidence of high strain and local garnet development, and thrust imbrication between these two units seems likely. The north side of the Hodgson Island tonalite also shows signs of high strain, as does the sillimanite±garnet-bearing feldspathic psammopelite immediately to the north.

Sillimanite±garnet-bearing feldspathic psammopelite is intercalated with the partly sulphidic calcic psammopelite at several structural levels, but contacts between the two units were not observed. However,

Figure 20 - Boudinaged amphibolite (dyke?) within McLennan Group feldspathic psammopelite; station D00-0107, island northeast of Brenton Island.

rocks in close proximity to the contact did not show any sign of high strain. Our field evidence suggests instead that McLennan Group feldspathic psammopelite and Levesque Bay supracrustal assemblage calcic psammopelite are stratigraphically intercalated. A nonconformity, however, cannot be ruled out.

b) Priestly Island Area

Feldspathic psammite (unit MAr), calcic feldspathic psammite (unit MArc), calcic feldspathic psammopelite (unit MArp), and aluminous feldspathic psammite (unit MArs) underlie the Priestly Island area, 5 km northeast of Brenton Island. Metamorphic grade is considerably lower, generally in the middle amphibolite facies range, and the sedimentary rocks have not been affected by partial melting except for the very northern end of Priestly Island. The feldspathic psammite units are composed of plagioclase, quartz, microcline, magnetite or hematite, as well as biotite and muscovite. Primary sedimentary structures are abundant and include trough cross-bedding, and decimetre-scale pebbly conglomerate layers (Figure 21). The calcic component of the feldspathic psammite (unit MArc) is of ambiguous origin. Some calcic layers are parallel to bedding and probably primary in origin. Elsewhere, hornblende-bearing feldspathic psammite crosscuts feldspathic psammite (Figure 22). This may be due to diagenesis or metamorphic remobilization.

At the very north end of Priestly Island, a few outcrops of graphite-bearing sillimanite-garnet-biotite psammopelitic turbidities of the Duck Lake Assemblage (unit DPsp) are exposed, and are structurally underlain by a thin layer of highly strained polymictic conglomerate of the Sickle/McLennan groups (MCg).

Figure 21 - Thin polymictic conglomerate layers, interbedded with feldspathic psammite; pen parallel to bedding, long axis of card parallel to oblique foliation; station M00-0652, Priestly Island.

Figure 22 - Cross-cutting medium-grained calcic component within feldspathic psammite; station M00-1266, Priestly Island.

5. Discussion and Conclusions

a) Can the Lynn Lake Belt and La Ronge Domain be Correlated?

Historically, the Lynn Lake Belt has been equated with the La Ronge Domain and a common evolution for the two has been proposed by many workers (e.g. Van Schmus *et al.*, 1987; Lewry *et al.*, 1990). Yet Syme (1990 and references therein) views the Lynn Lake Belt as a "discrete entity, distinct geologically, geochemically, and geochronologically … from the adjacent La Ronge [Domain]". Baldwin *et al.* (1987) suggested that the La Ronge–Lynn Lake–Rusty Lake belts developed from two separate arcs an older one and a younger one. Age of rhyolite volcanism of the older northern Lynn Lake Belt was dated at 1.91 Ga, and quartz-diorite and tonalite plutonism at 1.876 Ga. In a recent geochemical investigation of the Lynn Lake Belt, Zwanzig *et al.* (1999) have further subdivided it into a plethora of distinct tectonostratigraphic and geochemical assemblages, recognizing geotectonic settings ranging from N-MORB, E-MORB, back-arc, arc, ocean island to ocean plateau.

Recently, the northeastern La Ronge Domain was subdivided into two volcanic assemblages, the predominantly intermediate to felsic Reed Lake Assemblage and the mafic-ultramafic Lawrence Point Assemblage (Maxeiner, 1999). Deposition of the turbiditic Duck Lake Assemblage is estimated to be syn- to late-volcanic at ~1.87 Ga (Maxeiner *et al.*, 1999). Age of felsic volcanism in the southwestern part of the La Ronge Domain is constrained to between 1.875 to 1.885 Ga (Van Schmus *et al.*, 1987). At Reindeer Lake, volcanic rocks were not successfully dated. Some of the tonalitic to granitic plutons of the Rottenstone Domain, which was reinterpreted as the intrusive root of the "La Ronge arc", were dated at ca. 1.88 to 1.89 Ga (Corrigan *et al.*, 1998; Maxeiner *et al.*, 1999).

Several units on the east side of Laurie Lake (Manitoba) are identical in outcrop appearance, mode of formation and tectonic setting to rocks at Reindeer Lake. In particular, the Laurie Lake Assemblage (Zwanzig *et al.*, 1999), a sliver of the southern Lynn Lake Belt, can be equated with the Lawrence Point Assemblage with a high degree of certainty.

On a large scale, the La Ronge Domain can be equated with the Lynn Lake Belt as both occupy the same structural position within the Trans-Hudson Orogen and both comprise juvenile volcanoplutonic rocks 1.91 to 1.87 Ga old. Yet each of the two domains contains a number of geochemically and possibly geochronologically distinct lithotectonic assemblages, which are fault bounded and may only be traceable for tens of kilometres. However, one lithotectonic assemblage (Lawrence Point Assemblage) has been documented to be continuous for 100 to possibly 200 km along the southeastern, structurally lowest part of the La Ronge Domain and Lynn Lake Belt. It provides a definite link between both domains.

b) Age of Supracrustal Rocks in the Kisseynew Domain?

One of the most fundamental problems that emerges from this five year mapping project is the inability to tell different successions of supracrustal rocks of the Kisseynew Domain apart. While it is recognized that pelitic gneisses of the Burntwood River Group and the MacLean Lake gneisses are ca. 1.85 Ga (e.g. Baldwin *et al.*, 1987; Ansdell *et al.*, 1995) and feldspathic psammite of the McLennan/Sickle groups are ca. 1.845 Ga (e.g. Ansdell and Yang, 1995; Ansdell *et al.*, 1999), it has also been documented that at least part of the Kisseynew Domain, namely the Levesque Bay supracrustal assemblage is older than ca. 1.87 Ga and ca. 1.9 Ga (Corrigan *et al.*, 1998; Maxeiner *et al.*, 1999).

As alluded to by Maxeiner (1999), separation of these sedimentary assemblages is not straightforward. Calcic psammopelite of the Levesque Bay supracrustal assemblage, for example, is reported to be closely associated with a banded amphibolite which is cut by a ca. 1.9 Ga leucotonalite dyke (Corrigan *et al.*, 1998). North of Deep Bay this same (?) calcic psammopelite is gradational into pelitic rocks of the 1.85 Ga Burntwood Group. This implies thrust imbrication between two differently aged calcic psammopelite successions, or thrust imbrication between the calcic psammopelite and the amphibolite, or a disconformity. Field relationships discussed in this paper would suggest that the calcic psammopelite may not be part of the relatively old Levesque Bay supracrustal assemblage (Corrigan *et al.*, 1998), and the extent of this assemblage therefore needs to be more clearly defined.

c) Are the Sickle Group and McLennan Group Identical?

Rocks belonging to the Sickle Group, as observed on the Manitoba and Saskatchewan side of Laurie Lake, are identical to the Macfarlane Island succession at Reindeer Lake (Maxeiner, 1998). One fundamental problem emerges from the aluminous feldspathic psammite, found from east Laurie Lake to Henry Lake and farther on to the southwest (Harper, 1986; Thomas, 1990). Most workers (e.g. Gilbert *et al.*, 1980; Thomas, 1990; Zwanzig, 1990; Harper,1997; Maxeiner, 1998) have included aluminous feldspathic psammite (MArs) and feldspathic psammite (MAr) as part of the same sequence, generally referred to as McLennan Group in Saskatchewan and Sickle Group in Manitoba. Both groups are generally interpreted as relatively young fluvial-littoral sedimentary successions that unconformably overlie rocks of the Central Metavolcanic Belt and the Lynn Lake Belt, respectively (e.g. Gilbert *et al.*, 1980; Maxeiner, 1997). Recent U-Pb dating of single zircons from cross-bedded feldspathic psammite at Macfarlane Island suggested a <1.845 Ga age of deposition for the McLennan Group (Ansdell *et al.*, 1999). This is consistent with age constraints established at the southwestern end of the La Ronge Domain (Ansdell and Yang, 1995).

One of the fundamental problems with the McLennan/Sickle groups story is that our fieldwork in the Deep Bay–Pearson Islands area strongly suggests an intrusive relationship between the Hodgson Island Pluton (T) and the aluminous feldspathic psammite (MArs). Recent geochronology by David Corrigan (GSC) has provided two precise U-Pb zircon ages of ca. 1.87 Ga from two different samples of this tonalitic intrusion. This implies that sediments of the McLennan Group were deposited prior to 1.87 Ga.

A number of explanations are possible:

1) There are two feldspathic psammite successions within the McLennan-Sickle groups, with one succession predating 1.87 Ga, and one postdating 1.85 Ga. The lithologies of the two differently aged successions are so similar that they cannot be mapped apart. At first glance, one obvious break

may lie between the feldspathic psammite (MAr) and the aluminous feldspathic psammite (MArs), but there is a gradational relationship between these two units at Laurie Lake, Macfarlane Island, and Priestly Island.

2) The intrusive relationship between the Hodgson Island tonalite and the aluminous feldspathic psammite has been misinterpreted. On southwest Pearson Islands, however, an exposure of the contact clearly suggests an intrusive relationship. The contact parallels the main foliation, but there is no evidence of high strain in either the tonalite or the supracrustal rocks. There is no evidence for the existence of an unconformity, either. In the Brenton Island–Levesque Bay area, however, Corrigan *et al.* (1998) interpreted a thrust contact between the tonalite and feldspathic psammite.
3) The relatively young age suggested by the detrital zircon work may not adequately portray the age of deposition. There is little doubt, however, that the McLennan Group polymictic conglomerate and overlying cross-bedded feldspathic psammite, unconformably overlie the ca. 1.87 Ga Duck Lake assemblage, the Lawrence Point Assemblage, and likely the 1.858 Ga Butler Island diorite (e.g. Maxeiner, 1998; Corrigan *et al.*, 1998).

The first option is the most appealing one, yet from a standpoint of geological mapping it is also the most frustrating option, as it clearly illustrates the inability to separate similar lithologies of different assemblages.

A systematic U-Pb detrital zircon study of all sedimentary assemblages between Lawrence Point and Deep Bay, including the Duck Lake Assemblage, McLennan/Sickle groups, and Levesque Bay supracrustal assemblage, may provide a way to answer some of these questions.

6. Acknowledgments

Doug Hobson provided excellent and cheerful field assistance during the entire summer. Hermann Zwanzig and Chris Beaumont-Smith of the Manitoba Geological Survey are thanked for an enlightening field trip on the Manitoba side of Laurie Lake. Osprey Wings, Lawrence Bay Airways, and La Ronge Aviation are acknowledged for efficient air support. Dave MacDougall and Gary Delaney are thanked for reviewing an earlier version of the manuscript.

7. References

Ansdell, K., Corrigan, D., Stern, R., and Maxeiner, R. (1999): Shrimp U-Pb geochronology of complex zircons from Reindeer Lake, Saskatchewan: Implications for timing of sedimentation and metamorphism in the northwestern Trans-Hudson Orogen; Geol. Assoc. Can.–Mineral. Assoc. Can., Jt. Ann. Meet., May 26-28, Sudbury, abstr., p3.

Ansdell, K.M., Lucas, S.B., Connors, K., and Stern, R.A. (1995): Kisseynew metasedimentary gneiss belt, Trans-Hudson Orogen (Canada): Back-arc origin and collisional inversion; Geol., v23, p1039-1043.

Ansdell, K.M. and Yang, H. (1995): Detrital zircons in the McLennan Group meta-arkoses and MacLean Lake Belt, Western Trans-Hudson Orogen; *in* Z. Hajnal and J.F. Lewry (eds.), LITHOPROBE Trans-Hudson Orogen Transect, Rep. No. 48, p190-198.

Ashton, K.E. (1979): The geology of the Milton Island map sheet (east half), Saskatchewan (64D-10E); unpubl. M.Sc. thesis, Univ. Sask., 131p.

__________ (1999): A proposed lithotectonic domainal re-classification of the southeastern Reindeer Zone in Saskatchewan; *in* Summary of Investigations 1999, Volume 1, Saskatchewan Geological Survey, Sask. Energy Mines, Misc. Rep. 99-4.1, p92-100.

Baldwin, D.A., Syme, E.C., Zwanzig, H.V., Gordon, T.M., Hunt, P.A., and Stevens, R.D. (1987): U-Pb ages from the Lynn Lake and Rusty Lake metavolcanic belts, Manitoba: Two ages of Proterozoic magmatism; Can. J. Earth Sci., v24, p1053-1063.

Beaumont-Smith, C.J. and Rogge, D.M. (1999): Preliminary structural analysis and gold metallogeny of the Johnson Shear Zone, Lynn Lake greenstone belt (parts of NTS 64C-10, -11, -15); *in* Report of Activities, 1999, Manit. Ind. Trade Min., Geol. Serv., p61-66.

Bucher, K. and Frey, M. (1994): Petrogenesis of Metamorphic rocks; Springer Verlag, Berlin, 318p.

Corrigan, D., Bashforth, A., and S. Lucas (1997): Geology and structural evolution of the La Ronge–Lynn Lake Belt in the Butler Island area (parts of 64D-9 and -10), Reindeer Lake, Saskatchewan; *in* Summary of Investigations 1997, Saskatchewan Geological Survey, Sask. Energy Mines, Misc. Rep. 97-4, p18-30.

Corrigan, D., Lucas, S.B., Theriault, R., Maxeiner, R.O., and Ansdell, K. (1999a): Terrane assembly and tectonomagmatic evolution of the northwestern Reindeer Zone, Trans-Hudson Orogen: Towards a new paradigm?; Geol. Assoc. Can.–Mineral. Assoc. Can., Jt. Ann. Meet., May 26-28, Sudbury, abstr., p26.

Corrigan, D., MacHattie, D.G., Piper, L., Wright, D., Pehrsson, S., Lassen, B., and Chakungal, J. (1998): La Ronge–Lynn Lake Bridge Project: New mapping results from Deep Bay (parts of 64D-6 and -7) to North Porcupine Point (top of 64E-7 and -8), Reindeer Lake; *in* Summary of Investigations 1998, Saskatchewan Geological

Survey, Sask. Energy Mines, Misc. Rep. 98-4, p111-122.

Corrigan, D., Pehrsson, S.J., MacHattie, T.G., Piper, L., Wright, D., Lassen, B., and Chakungal, J. (1999b): Lithotectonic framework of the Trans-Hudson Orogen in the northwestern Reindeer Zone, Saskatchewan: An update from recent mapping along the Reindeer Lake transect; *in* Current Research 1999-C, Geol. Surv. Can., p169-178.

David, J., Bailes, A.H., and Machado, N. (1996): Evolution of the Snow Lake portion of the Paleoproterozoic Flin Flon and Kisseynew belts, Trans-Hudson Orogen, Manitoba, Canada; Precamb. Resear., v80, p107-124.

Elliott-Meadows, S.R. and Appleyard, E.C. (1991): The alteration geochemistry and petrology of the Lar Cu-Zn deposit, Lynn Lake area, Manitoba, Canada; Econ. Geol., v86, p486-505.

Elliott-Meadows, S.R., Froese, E., and Appleyard, E.C. (1999): Cordierite-anthophyllite-cummingtonite from the Lar Deposit, Laurie Lake, Manitoba; Can. Mineral., v37, p375-380.

Geological Survey of Canada (1964): Aeromagnetic map, Reindeer Lake South (NTS 64D), Saskatchewan, Geol. Surv. Can., Map 7152G, 1:250 000 scale.

Gilbert, H.P., Syme, E.C., and Zwanzig, H.V. (1980): Geology of the metavolcanic and volcaniclastic metasedimentary rocks in the Lynn Lake area; Min. Resour. Div., Manit. Energy Mines, GP80-1, 118p.

Gilboy, C.F. (1980): Geology of the Reindeer Lake South (Southeast) Area; Sask. Dep. Miner. Resour., Rep. 198, 62p.

Gordon, T.M., Hunt, P.A., Bailes, A.H., and Syme, E.C. (1990): U-Pb zircon ages from the Flin Flon and Kisseynew belts, Manitoba: Chronology of crust formation at an Early Proterozoic accretionary margin; *in* J.F. Lewry and M.R. Stauffer (eds.), The Early Proterozoic Trans-Hudson Orogen of North America, Geol. Assoc. Can. Spec. Pap. 37, p177-199.

Harper, C.T. (1986): Bedrock geological mapping, Windrum Lake area (part of NTS 64D-4, 73P-16, and 74A-1); *in* Summary of Investigations 1986, Saskatchewan Geological Survey, Sask. Energy Mines, Misc. Rep. 86-4, p8-17.

__________ (1997): Sucker Lake–Flemming Lake update; *in* Summary of Investigations 1997, Saskatchewan Geological Survey, Sask. Energy Mines, Misc. Rep. 97-4, p42-51.

__________ (1998): The La Ronge Domain–Glennie Domain transition: Street Lake area (parts of NTS 64D-3 and -6); *in* Summary of Investigations 1998, Saskatchewan Geological Survey, Sask. Energy Mines, Misc. Rep. 98-4, p66-80.

Hoffman, P.F. (1990): Subdivision of the Churchill Province and extent of the Trans-Hudson Orogen; *in* J.F. Lewry and M.R. Stauffer (eds.), The Early Proterozoic Trans-Hudson Orogen of North America, Geol. Assoc. Can., Spec. Pap. 37, p15-39.

Johnston, W.G.Q. (1972): 64D-6-E: Southend (east half); *in* Summary Report of Investigations Conducted in the Precambrian Area of Saskatchewan, Sask. Dep. Miner. Resour., p15-21.

__________ (1983): Geology of the Southend area; Sask. Energy Mines; Open File Rep. 82-4, 151p.

Johnston, W.G.Q. and Thomas, M.W. (1984): Compilation bedrock geology, Reindeer Lake South, NTS area 64D; Sask. Energy Mines; Rep. 230 (1:250 000 scale map with marginal notes).

Kyser, T.K., Fayek, M., and Sibbald, T.I.I. (1992): Geochronological studies in the La Ronge and Glennie domains; *in* Summary of Investigations 1992, Saskatchewan Geological Survey, Sask. Energy Mines, Misc. Rep. 92-4, p130-134.

Lewry, J.F. (1983): Character and structural relations of the McLennan Group meta-arkoses, McLennan-Jaysmith lakes area; *in* Summary of Investigations 1983, Saskatchewan Geological Survey, Sask. Energy Mines, Misc. Rep. 83-4, p49-55.

Lewry, J.F., Thomas, D.J., Macdonald, R., and Chiarenzelli, J. (1990): Structural relations in accreted terranes of the Trans-Hudson Orogen, Saskatchewan: Telescoping in a collisional regime?; *in* J.F. Lewry and M.R. Stauffer (eds.), The Early Proterozoic Trans-Hudson Orogen of North America, Geol. Assoc. Can. Spec. Pap. 37, p75-94.

MacDougall, D.G. (1998): La Ronge–Lynn Lake Bridge Project: Metallogenic studies; *in* Summary of Investigations 1998, Saskatchewan Geological Survey, Sask. Energy Mines, Misc. Rep. 98-4, p100-110.

Maxeiner, R.O. (1996): Bedrock geology of the Henry Lake area (parts of NTS 64D-6 and -11), northern La Ronge Domain; *in* Summary of Investigations 1996, Saskatchewan Geological Survey, Sask. Energy Mines, Misc. Rep. 96-4, p51-66.

__________ (1997): Geology of the Lawrence Bay (Reindeer Lake) area, northeastern La Ronge Domain; *in* Summary of Investigations 1997, Saskatchewan Geological Survey, Sask. Energy Mines, Misc. Rep. 97-4, p3-17.

__________ (1998): Geology of the Birch Point (Reindeer Lake) Area, northeastern La Ronge

Domain; *in* Summary of Investigations 1998, Saskatchewan Geological Survey, Sask. Energy Mines, Misc. Rep. 98-4, p81-99.

__________ (1999): La Ronge–Lynn Lake Bridge: Geology of the Wapus Bay–Lowdermilk Bay (Reindeer Lake) Area; *in* Summary of Investigations 1999, Volume 2, Saskatchewan Geological Survey, Sask. Energy Mines, Misc. Rep. 99-4.2, p143-158.

Maxeiner, R.O., Gilboy, G.F., and Yeo, G.M. (1999): Classification of metamorphosed clastic sedimentary rocks: A proposal; *in* Summary of Investigations 1999, Volume 1, Saskatchewan Geological Survey, Sask. Energy Mines, Misc. Rep. 99-4.1, p89-92.

Maxeiner, R.O. and Sibbald, T.I.I. (1995): Controversial Rocks in the Hebden-MacKay lakes area, southern La Ronge Domain; *in* Summary of Investigations 1995, Saskatchewan Geological Survey, Sask. Energy Mines, Misc. Rep. 95-4, p79-86.

Pyke, M.W. (1960): The Geology of the Wapus Bay Area (east half), Saskatchewan; Sask. Dep. Miner. Resour., Rep. 40, 32p.

Scott, B.P. (1991): Metallogenic Map Series, Reindeer Lake South, NTS Area 64D; Sask. Energy Mines; Rep. 253, 18p (accompanied by 1:250 000 scale map).

Syme, E.C. (1990): Stratigraphy and geochemistry of the Lynn Lake and Flin Flon metavolcanic belts; *in* J.F. Lewry and M.R. Stauffer (eds.), The Early Proterozoic Trans-Hudson Orogen of North America, Geol. Assoc. Can. Spec. Pap. 37, p143-161.

Thomas, D.J. (1985): Geological mapping, Roundish-Bervin lakes area (part of NTS 73P-15 and -16); *in* Summary of Investigations 1985, Saskatchewan Geological Survey, Sask. Energy Mines, Misc. Rep. 85-4, p18-27.

__________ (1990): North Lake Gold deposit: A model for arenite-hosted gold; *in* Summary of Investigations 1990, Saskatchewan Geological Survey, Sask. Energy Mines, Misc. Rep. 90-4, p21-24.

__________ (1993): Geology of the Star Lake–Otter Lake Portion of the Central Metavolcanic Belt, La Ronge Domain; Saskatchewan Geological Survey, Sask. Energy Mines, Rep. 236, 132p.

Van Schmus, W.R., Bickford, M.E., Lewry, J.F., and Macdonald, R. (1987): U-Pb geochronology in the Trans-Hudson Orogen, northern Saskatchewan, Canada; Can. J. Earth Sci., v24, p407-424.

Williamson, A.E. (2000): The metamorphic history of the Milton Island metasedimentary assemblage; unpubl. B.Sc. thesis, Univ. Sask., 76p.

Wright, D.M., Ansdell, K.M., Corrigan, D., and Maxeiner, R.O. (1999): Geology and metamorphic petrology of variably altered volcanic rocks in the southern Reindeer Lake area, northern Saskatchewan; *in* Summary of Investigations 1999, Volume 2, Saskatchewan Geological Survey, Sask. Energy Mines, Misc. Rep. 99-4.2, p159-166.

Zwanzig, H.V. (1990): Kisseynew gneiss belt in Manitoba stratigraphy, structure, and tectonic evolution; *in* Lewry, J.J. and Stauffer, M.R. (eds.), The Early Proterozoic Trans-Hudson Orogen of North America, Geol. Assoc. Can., Spec. Pap. 37, p95-120.

Zwanzig, H.V., Syme, E.C., and Gilbert, H.P. (1999): Updated trace element geochemistry of ca. 1.9 Ga metavolcanic rocks in the Paleoproterozoic Lynn Lake Belt; Manit. Ind. Trade Min., Geol. Serv., 46p (plus accomp. map and diskette).

Constraints on Metamorphic Conditions in the Milton Island Metasedimentary Assemblage, Reindeer Lake

Anthony E. Williamson [1], *Kevin M. Ansdell* [1], *and Ralf O. Maxeiner*

Williamson, A.E., Ansdell, K.M., and Maxeiner, R.O. (2000): Constraints on metamorphic conditions in the Milton Island Metasedimentary Assemblage, Reindeer Lake; *in* Summary of Investigations 2000, Volume 2, Saskatchewan Geological Survey, Sask. Energy Mines, Misc. Rep. 2000-4.2.

Abstract

The metamorphic evolution of the turbiditic Milton Island metasedimentary assemblage is investigated through field and petrographic methods. Field work focused on the contact between the Milton Island metasedimentary assemblage and the Central Metavolcanic Belt, which is conformable and sharp with the former overlying the latter; it is locally sheared. Laboratory work focused on the qualitative and quantitative analysis of pelite, amphibolite and calc-silicate rock of the Milton Island metasedimentary assemblage. It reveals peak metamorphic conditions of between 3.5 and 9.75 kbar and 650° to 775°C, indicative of upper amphibolite facies. Re-equilibrated garnet-phyllosilicate pairs in calc-silicate layers give lower temperature and pressure results preserved by conditions of retrograde metamorphism.

1. Introduction

In 1996, Saskatchewan Energy and Mines and the Geological Survey of Canada initiated a joint mapping project in the northwestern Reindeer Zone of the Trans-Hudson Orogen (e.g. Maxeiner, 1996, Corrigan *et al.*, 1998). Mapping along the boundary between the La Ronge Domain and the Rottenstone Domain identified a new assemblage, the Milton Island metasedimentary assemblage (MIA; Corrigan *et al.*, 1997). The turbiditic MIA consists of interbedded pelitic to psammopelitic layers which contain key metamorphic indicator minerals and assemblages that are well suited for a metamorphic study. This paper provides a detailed description of the MIA in the study area, based on both field and petrographic work, and gives the results of the qualitative and quantitative analysis of its metamorphic evolution. The nature of the contact between the MIA and the Central Metavolcanic Belt (CMB) will also be discussed, based on field relationships.

2. Geological Framework

First named and described by Corrigan *et al.* (1997) and Maxeiner (1997), but previously mapped by Ashton (1979) and Stauffer *et al.* (1979), the MIA underlies an area of about 30 by 40 km between Park Island and Milton Island on Reindeer Lake, Saskatchewan (Figure 1). Based on its lithological characteristics and structural setting above the Central Metavolcanic Belt, it is considered to be correlative with the Crew Lake Belt (Corrigan *et al.*, 1997; Maxeiner, 1997), which lies along much of the northwestern edge of the La Ronge Domain (e.g. Thomas, 1993). The MIA, however, overlaps the currently defined boundary between the La Ronge and Rottenstone domains (Corrigan *et al.*, 1999). The age of the MIA is constrained by detrital zircons, which range from 1864 ±11 Ma to 2829 ±8 Ma (Ansdell *et al.*, 1999) and a cross-cutting diorite, correlated with the 1858 ±2 Ma Butler Island diorite (Corrigan *et al.*, 1997). The MIA has experienced at least three phases of ductile deformation and, during the second phase, amphibolite facies metamorphism was achieved. This metamorphic event is dated to between 1818 to 1805 Ma, but may be as young as 1795 Ma in the MIA (Ansdell *et al.*, 1999).

3. Field Relationships

During the summer of 1999, fieldwork was performed at Asimwok Bay, Lowdermilk Bay, Upistutik Island and Milton Island of Reindeer Lake (Figure 1). Twenty outcrops of MIA were studied, from which 34 samples were collected. Subsequently, twenty MIA samples were cut for petrographic and microprobe analysis.

a) Lithological Description

In the study area, the MIA comprises a sequence of interbedded light grey to light brown, fine- to medium-grained migmatitic psammite, psammopelite and pelite, containing variable amounts of tonalitic to granodioritic, coarse-grained anatectic melt.

Pelitic layers contain plagioclase, quartz, up to 25% biotite, as well as sillimanite faserkiesel, which are partly retrogressed to muscovite (Figure 2). Weathered surfaces are a light to medium grey, whereas fresh surfaces are medium grey. Graphite is ubiquitous and locally as high as 2%, causing outcrops to weather rusty brown. Pelitic layers are typically interbedded with psammopelite on a millimetre to decimetre scale and locally gradation from medium-grained psammopelite to coarse-grained pelite (reversed metamorphic grading) allows identification of tops (Figure 2).

---

[1] Department of Geological Sciences, University of Saskatchewan, 114 Science Place, Saskatoon, SK S7N 5E2.

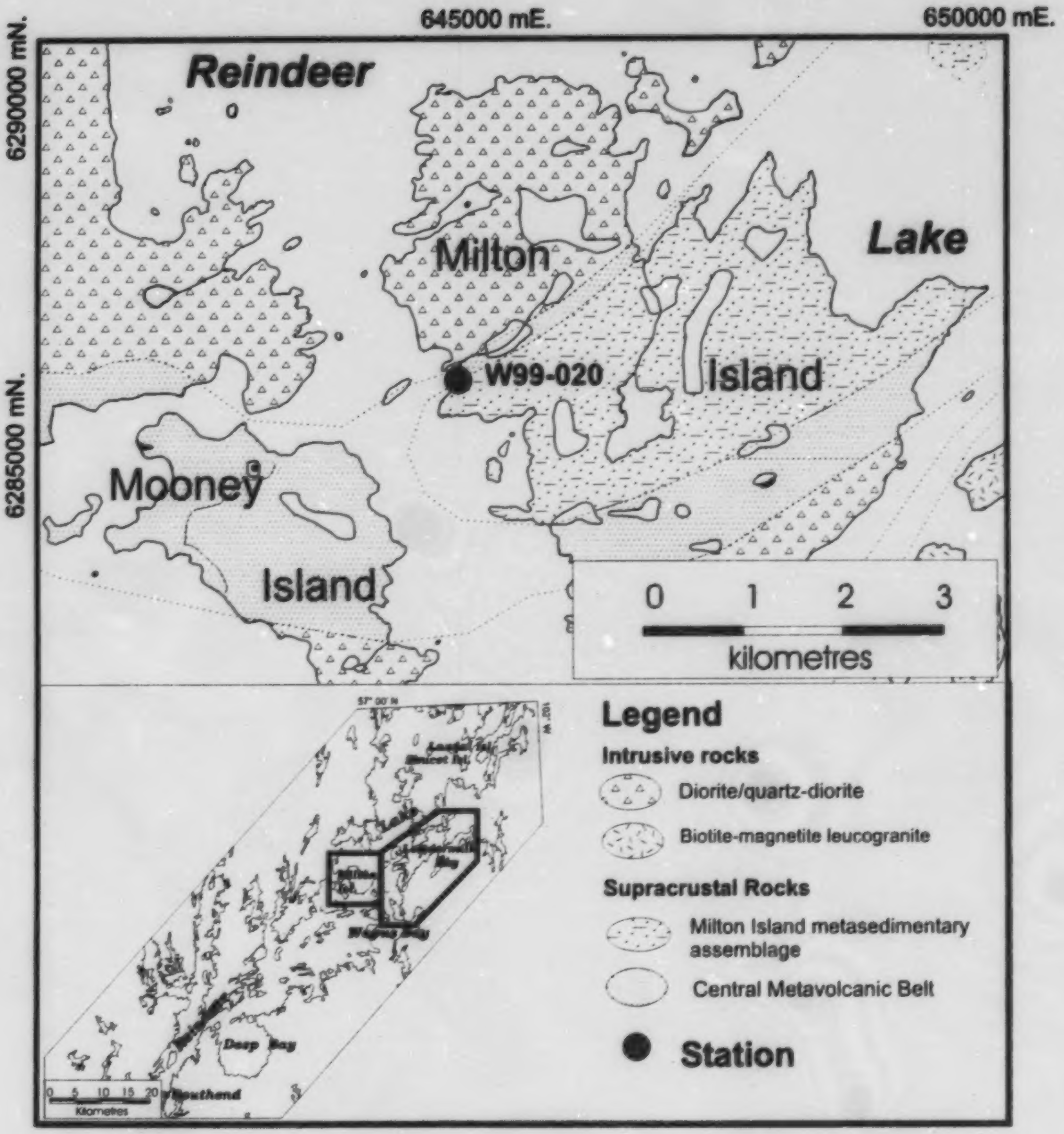
645000 mE.
650000 mE.
6290000 mN.
6285000 mN.
Reindeer
Lake
Milton
Island
W99-020
Mooney
Island
0
1
2
3
kilometres
Deep Bay
Southend
0 5 10 15 20
Kilometres
Legend
Intrusive rocks
Diorite/quartz-diorite
Biotite-magnetite leucogranite
Supracrustal Rocks
Milton Island metasedimentary assemblage
Central Metavolcanic Belt
Station

Figure 1 - Field locations and geographical extent

Rare boudinaged layers of a calc-silicate rock are characterized by greenish-grey quartz-rich psammite with a dark grey rim (Figure 3), which typically contains garnet, hornblende and pyrite±diopside. The rim is interpreted as a reaction zone that probably formed by infiltration of Ca-bearing fluids into the more permeable psammitic layers.

Tonalitic to granodioritic anatectic leucosome forms 5 to 30% of the MIA. The leucosome, ranging from millimetre- to centimetre-scale, layer-parallel veins (*lit-*

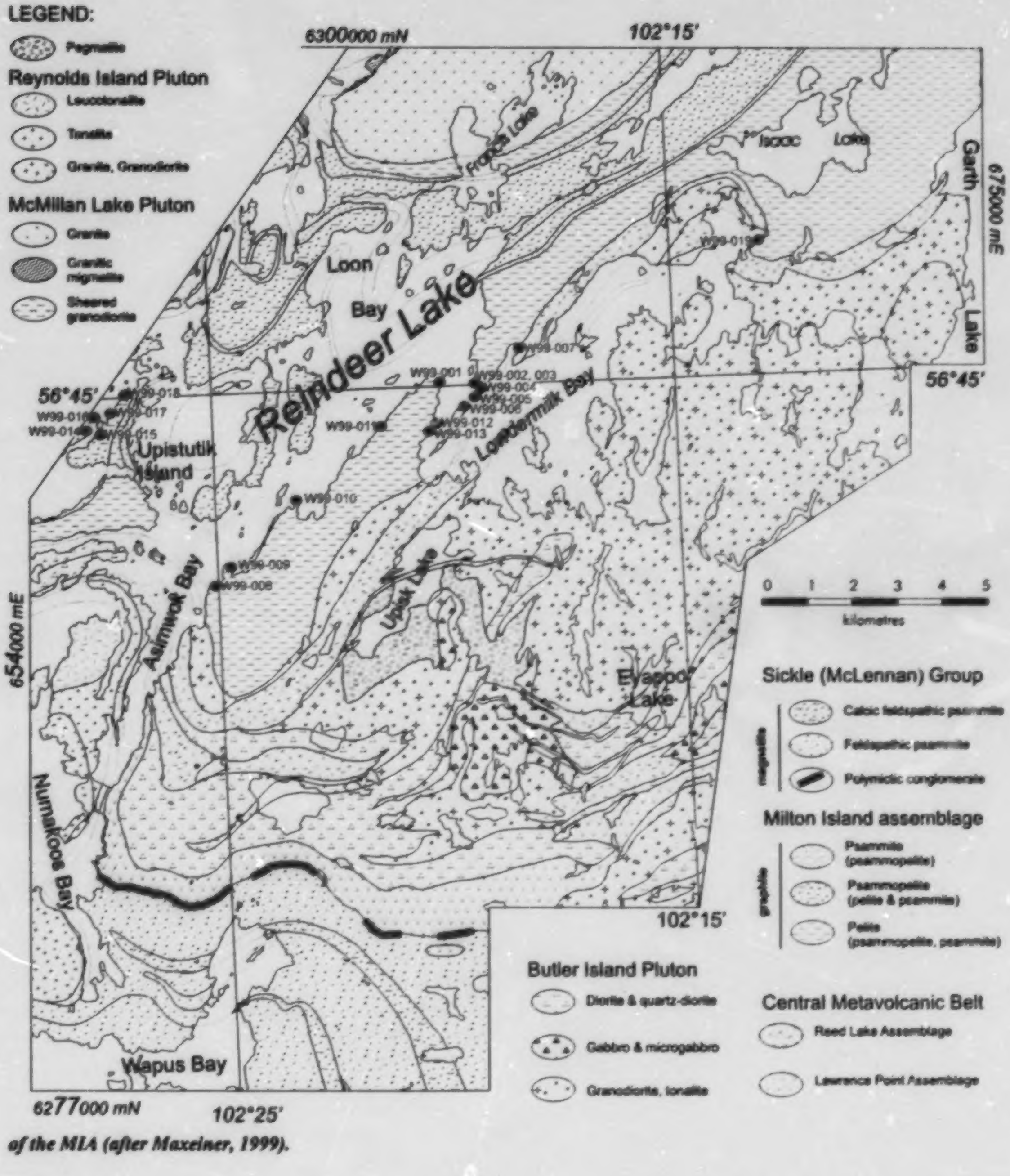
LEGEND:
Pegmatite
Reynolds Island Pluton
Leucotonalite
Tonalite
Granite, Granodiorite
McMillan Lake Pluton
Granite
Granitic migmatite
Sheared granodiorite
6300000 mN
102°15'
Francis Lake
Isaac Lake
Garth Lake
675000 mE
Loon Bay
Reindeer Lake
W99-019
W99-007
W99-001
W99-002, 003
W99-004
W99-005
W99-006
W99-011
W99-012
W99-013
Lowdermilk Bay
56°45'
W99-018
W99-016
W99-017
W99-014
W99-015
Upistutik Island
W99-010
W99-009
W99-008
Asimwok Bay
Upisk Lake
654000 mE
Eyapoo Lake
Numakoos Bay
102°15'
Wapus Bay
6277000 mN
102°25'
0
1
2
3
4
5
kilometres
Sickle (McLennan) Group
Calcic feldspathic psammite
Feldspathic psammite
Polymictic conglomerate
Milton Island assemblage
Psammite (psammopelite)
Psammopelite (pelite & psammite)
Pelite (psammopelite, psammite)
Butler Island Pluton
Diorite & quartz-diorite
Gabbro & microgabbro
Granodiorite, tonalite
Central Metavolcanic Belt
Reed Lake Assemblage
Lawrence Point Assemblage

of the MIA (after Maxeiner, 1999).

par-lit) to cross-cutting metre-scale bodies, is composed of quartz, plagioclase, muscovite, ±sillimanite, ±apatite, ±K-feldspar, and is typically bordered by thin biotite selvages (Figure 4).

Also found within the MIA are 10 to 40 cm thick transposed bands of amphibolite, which are interpreted as dykes and sills. They typically contain ~90% hornblende and biotite in varying proportions, with thin (millimetre-scale) bands of plagioclase and minor quartz. The amphibolite shares deformational features of the MIA, and therefore was emplaced prior to the onset of deformation.

Figure 2 - Reversed metamorphic grading: fine- to medium-grained psammopelite grading upwards into coarse-grained sillimanite-biotite pelite (top of photograph).

Figure 3 - Folded and boudinaged quartz-rich psammite layer with surrounding garnet-hornblende bearing reaction zone.

b) Deformation

Maxeiner (1997) identified four main phases of ductile deformation in the southern Reindeer Lake area. The first phase is not observable in the MIA, but only preserved in supracrustal xenoliths found within the nearby Butler Island diorite.

The next deformational event, termed D1 by Corrigan *et al.* (1998), resulted in the development of a regional foliation (S1), defined by biotite aligned parallel to primary lithological banding (S0). *Lit-par-lit* anatectic melt is indicative of upper amphibolite facies conditions during D1.

The D2 deformational event created tight to isoclinal, northerly plunging folds that deform the S0=S1 fabric. A locally well-developed, generally northwest-dipping axial planar S2 fabric is defined by parallel alignment of either biotite or sillimanite (Figure 5), as well as local anatectic melt. Thus, metamorphic conditions during D2 were probably similar to those during D1. The MIA lies in the core of a regional F_2 fold.

The final deformational event (D3) folded earlier structures into north-northeast plunging, map-scale open folds, also preserved as metre-scale fold interference patterns, locally.

c) CMB-MIA Contact

Two outcrops that reveal the contact between the CMB and MIA were examined, one in northeastern Lowdermilk Bay, and one on the western shore of Milton Island (Figures 1 and 6). In both, a heterogeneously strained succession of protomylonitic conglomerate, volcaniclastic, and calc-silicate rocks of the CMB (Reed Lake assemblage?) is in apparent conformable contact with psammite and psammopelite of the MIA. At the Lowdermilk Bay locality, glacial cover masks the actual contact between the uppermost volcaniclastic layer and the MIA, which does not allow the stratigraphic interpretation of the CMB-MIA

Figure 4 - Layer-parallel, sillimanite-bearing, anatectic leucosome bordered by a thin biotite selvage. Pencil for scale.

Figure 5 - F2 folds exhibiting axial-planar biotite and sillimanite faserkiesel (S2).

contact. At the Milton Island outcrop a 1.5 m wide tonalitic pegmatite dyke obscures the contact between the two assemblages (Figure 6).

Although the rocks close to the MIA-CMB contact at the two localities are in part sheared, the best interpretation is that the MIA stratigraphically overlies the CMB. A significant age gap may, however, mark the boundary, as the first appearance of MIA psammopelite appears to be rather abrupt, without any obvious interlayering. This is consistent with the observations of Corrigan *et al.* (1998) on an outcrop south of Upistutik Island (Figure 1), and with findings of Maxeiner (1999).

4. Qualitative Metamorphic Petrology

a) Pelites, Psammopelites, and Associated Leucosome

The pelitic and psammopelitic MIA samples studied have consistent mineral assemblages of quartz+plagioclase+biotite+muscovite+graphite. The more psammitic layers contain 10 to 15% biotite and 1 to 2% muscovite, whereas the pelitic layers have 20 to 25% biotite and 5 to 10% muscovite. The pelitic samples also contain 2 to 5% sillimanite+K-feldspar. Faserkiesel within these rocks consists of lenses of fibrous sillimanite enclosed by large, millimetre to centimetre-sized muscovite poikiloblasts (Figure 7).

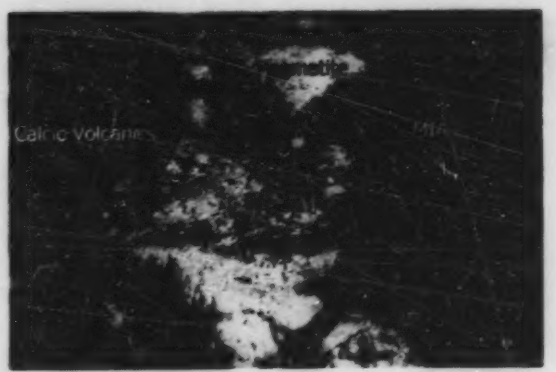

Figure 6 - The CMB-MIA contact on west Milton Island, marked by a tonalitic pegmatite.

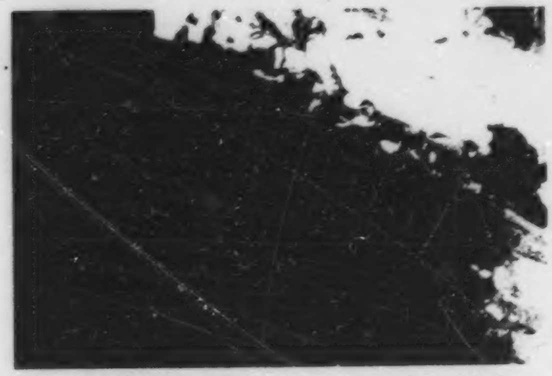

Figure 7 - Fibrolitic sillimanite in a muscovite poikiloblast. Field of view is 4.5 mm.

Two generations of muscovite are present. One is aligned parallel to sillimanite and the S2 fabric, the second is randomly oriented. Sillimanite within the aligned muscovite poikiloblasts is locally characterized by a swirling pattern, suggesting that it grew prior to or early during D2. Some muscovite growth occurred after the development of the S2 fabric. Therefore, formation of muscovite began late in the second phase of deformation and outlasted it. K-feldspar is seen to co-exist with sillimanite in the leucosome as well as in the paleosome and likely formed through the breakdown of muscovite via the reaction:

muscovite+quartz=K-feldspar+sillimanite+H_2O (Spear, 1993)[2]

The reverse of this reaction is likely to have been important in the formation of the muscovite poikiloblasts.

The presence of plagioclase in the MIA suggests that the following melting reaction may have been important in the production of the leucosome:

muscovite+quartz+plagioclase=sillimanite+K-feldspar +melt (Ashworth, 1985) [3]

Reaction [3] establishes minimum peak metamorphic conditions in the MIA, placing the P-T conditions to the right of the corresponding reaction curves in Figure 8. Apparent replacement of K-feldspar by plagioclase-muscovite intergrowths along with associated myrmekite is also observed, and based on similar observations by Ashworth (1985), it has been interpreted to be the reverse of reaction [3] during the crystallization of anatectic leucosome. Absence of the assemblage cordierite-garnet-K-feldspar in these samples indicates that the P-T conditions must have been to the left of reaction curve [4] and above reaction [5] in Figure 8. This combined with the constraints set by reactions [1] and [3] places the P-T conditions for the MIA between 3 and 9.75 kbar and 650° to 780°C (Figure 8).

Leucosome pods in the MIA are interpreted to be a result of anatexis of the pelitic host rocks via reaction [3], which is consistent with the characteristic mineral assemblage of quartz+plagioclase+K-feldspar+apatite+sillimanite. In outcrop it was observed that melt proportion increased, as the rock become more pelitic; this is consistent with greater water content in rocks that are more pelitic. Recrystallization via the reverse of reaction [3] is thought to have occurred in the leucosome as K-spar replacement features similar to those mentioned previously were observed in the leucosome.

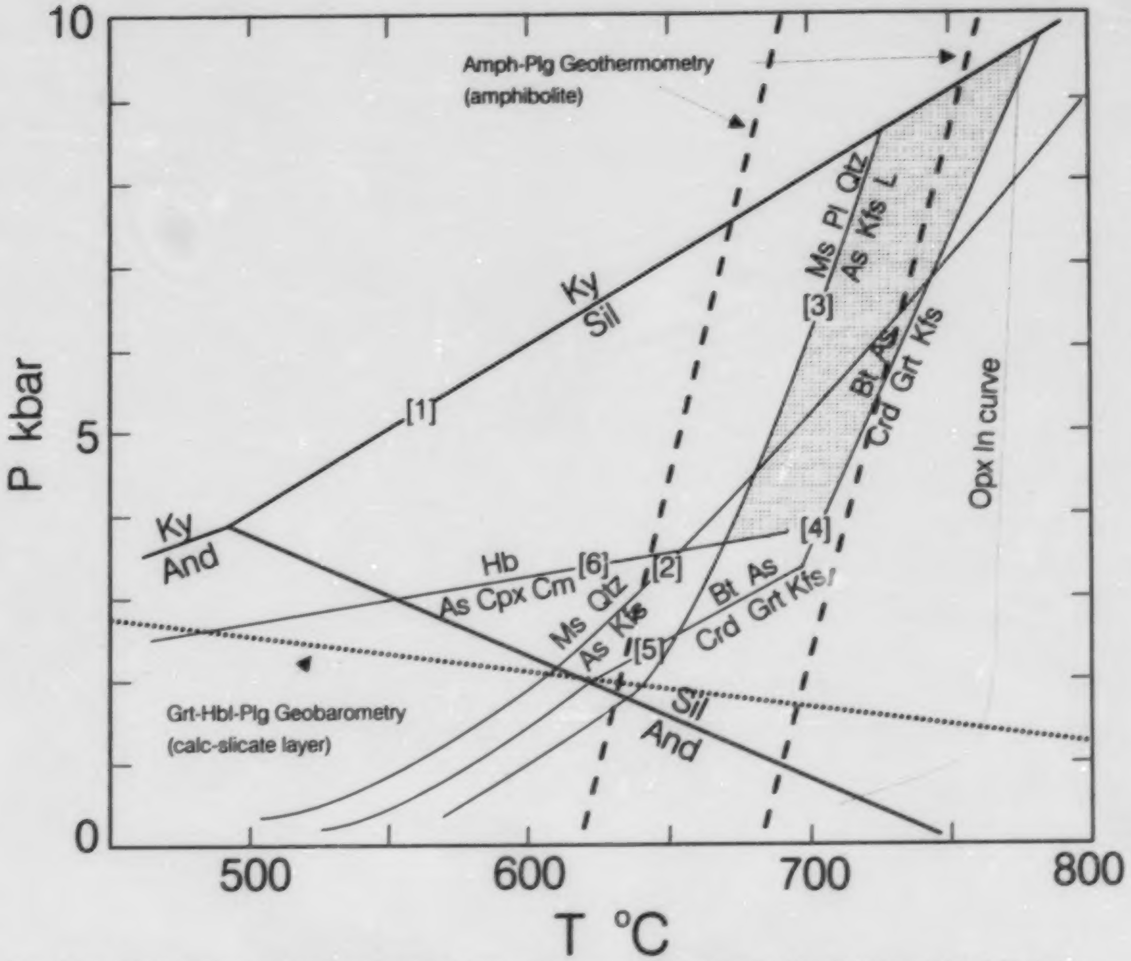

Figure 8 - P-T grid displaying the inferred metamorphic conditions experienced by the MIA (shaded region). Curves after Spear (1981, 1993) and Froese (1997). Temperature and pressure calibrations generated using Spear and Kohn (1999).

b) Calc-silicate Layers

Thin section analysis of the reaction zone surrounding some of the quartz-rich psammite layers revealed a mineral assemblage consisting of quartz+plagioclase +biotite+hornblende+calcite+garnet+titanite+chlorite+ pyrite+graphite. This assemblage is interpreted to result from the interaction of Ca-rich fluids with psammite. We suggest that the presence of hornblende and the lack of orthopyroxene support the contention that these rocks have not attained granulite grade metamorphic conditions.

c) Amphibolite

Amphibolites from the MIA, which are interpreted as dykes, have a mineral assemblage of hornblende+ plagioclase+biotite+quartz. As mentioned previously, plagioclase is seen to be concentrated in millimetre-scale bands within the amphibolite. The transition from amphibolite to granulite grade can be described by the general reaction:

$$\text{hornblende+quartz=orthopyroxene+clinopyroxene} \\ \text{+plagioclase +}H_2O$$

The lack of pyroxene in these rocks suggests that temperatures did not exceed 775°C (Figure 8), based on the experimental studies of Spear (1981).

Overall, the presence of sillimanite and lack of cordierite, evidence for partial melting in the pelitic and psammopelitic rocks, and the lack of orthopyroxene in the calc-silicate layers and amphibolite, constrain P-T conditions in the MIA during peak metamorphism to between 3.5 and 9.75 kbar, and 670° and 775°C (Figure 8).

5. Quantitative Metamorphic Petrology

In order to obtain quantitative determinations of temperature and pressure, samples from calc-silicate layers and amphibolites that appeared to contain suitable mineral assemblages, were selected. Minerals were analyzed using a JEOL-8600 Superprobe equipped with three automated wavelength-dispersion spectrometers at the University of Saskatchewan. Analytical procedures and compositional data are tabulated in Williamson (2000). Results from the amphibole-plagioclase geothermometer and the garnet-hornblende-plagioclase geobarometer are reported here.

The amphibole-plagioclase geothermometer uses the exchange reaction:

edenite+albite=richterite+anorthite

and assumes textural equilibrium between the two minerals. Mineral compositions from two amphibole-plagioclase sets from the amphibolites were entered into the Spear and Kohn (1999) program, with the calibration of Holland and Blundy (1994) to create the projections seen in Figure 8. The mineral chemistry appears to be appropriate for this calibration as electron microprobe analyses indicate that the amphibole is an edenite. These projections yield temperatures between 620° and 760°C, which correspond closely with the peak temperature values determined using petrogenetic grids (Figure 8).

The garnet-hornblende-plagioclase geobarometer was calibrated for a range of rock types (Kohn and Spear, 1990), and involved the reaction:

6 anorthite+3 tremolite=2 grossular+1 pyrope+3 tschermakite +6 quartz

One projection was produced for minerals from a calc-silicate layer, using the program of Spear and Kohn (1999). This yielded a pressure range of 1.25 to 2.75 kbar (Figure 8), which is considerably lower than the minimum of 3.5 kbar given by the peak metamorphic mineral assemblages.

a) Summary of Quantitative Data

The small number of suitable mineral phases within the psammopelitic and pelitic rocks of the MIA restricted the use of calibrated geothermometers and geobarometers to a small number of samples collected from calc-silicate layers and amphibolites. Suitable minerals in textural equilibrium were also rare, and so only a small number of temperature and pressure determinations could be made.

The highest temperatures were obtained from an amphibolite sample with the amphibole-plagioclase geothermometer, reported here, whereas the other calibrations (garnet-biotite, and garnet-chlorite geothermometers) yielded significantly lower temperatures than suggested by the mineral assemblages present in the rock (Williamson, 2000). The mineral compositions of the amphibole and plagioclase in the amphibolite are interpreted to have preserved peak metamorphic conditions. The one determination of pressure using the garnet-hornblende-plagioclase geobarometer also yielded a lower pressure than suggested by peak metamorphic mineral assemblages. Possible explanations for the discrepancy between the qualitative and quantitative estimates of temperature and pressure are: (1) re-equilibration of mineral compositions during slow cooling during retrograde metamorphism, (2) the use of calibrations normally used for pelitic rocks rather than calc-silicate rocks, and (3) the lack of samples available to constrain consistency in P and T across the area.

6. Summary

Petrological analysis of the MIA has revealed a peak metamorphic environment corresponding to between 3.5 and 9.75 kbar and 650° to 775° C, indicative of upper amphibolite facies. These findings also correspond to similar work performed on CMB rocks in the area by Wright *et al.* (1999). It revealed peak metamorphic temperatures to be between 680° and 710°C with an upper pressure constraint of approximately 4.8 to 6.5 kbar. Peak metamorphism appears to have taken place during the D2 deformation event, as peak metamorphic minerals define the F2 axial-planar fabric.

Geothermometry performed on an amphibolite dyke corresponds to the metamorphic conditions defined by the peak metamorphic mineral assemblage, however geothermometry and geobarometry performed on calc-silicate layers gave consistently lower temperatures and pressure. Most likely, the conditions represented by calc-silicate geothermobarometry are that of retrograde metamorphism preserved in re-equilibrated garnets and phyllosilicate pairs. This could imply relatively slow cooling during the retrograde path allowing the garnets time to re-equilibrate.

7. Acknowledgments

The assistance of Ryan Morelli, Don Wright, Curt Huebert, and Dave MacDougall in the field are appreciated. Blaine Novakowski and Tom Bonli assisted with thin section preparation and electron microprobe analysis, respectively. Discussions with Yuanming Pan and Luke Ootes, and a review by Ken Ashton were extremely helpful. The electron microprobe facility at the University of Saskatchewan is partially funded by an NSERC Major Facilities Access Grant, and analyses were funded by Saskatchewan Energy and Mines and an NSERC Research Grant to Ansdell.

8. References

Ansdell, K., Corrigan, D., Stern, R., and Maxeiner, R. (1999): Shrimp U-Pb geochronology of complex zircons from Reindeer Lake, Saskatchewan: implications for timing of sedimentation and metamorphism in the northwestern Trans-Hudson Orogen; Geol. Assoc. Can./Mineral. Assoc. Can. Joint Annual Meeting, May 26-28, Sudbury, Canada, abstr., p3.

Ashton, K.E. (1979): The geology of the Milton Island map sheet (east half), Saskatchewan (64D-10E); unpubl. M.Sc. thesis, Univ. Sask., 131p.

Ashworth, J. R. (ed.) (1985): Migmatites; Blackie and Son Limited, Bishopbriggs, Glasgow, 302p.

Corrigan, D., Bashforth, A., and Lucas, S. (1997): Geology and structural evolution of the La Ronge–Lynn Lake Belt in the Butler Island area (parts of 64D-9 and -10), Reindeer Lake, Saskatchewan; *in* Summary of Investigations 1997, Saskatchewan Geological Survey, Sask. Energy Mines, Misc. Rep. 97-4, p18-30.

Corrigan, D., Maxeiner, R.O., Bashforth, A., and Lucas, S.B. (1998): Preliminary report on the geology and tectonic history of the Trans-Hudson Orogen in the northwestern Reindeer Zone, Saskatchewan; *in* Current Research 1998-1C, Geol. Surv. Can., p95-106.

Corrigan, D., Pehrsson, S.J., MacHattie, T.G., Piper, L., Wright, D., Lassen, B., and Chakungal, J. (1999): Lithotectonic framework of the Trans-Hudson Orogen in the northwestern Reindeer Zone, Saskatchewan: An update from recent mapping along the Reindeer Lake transect; *in* Current Research 1999-C, Geol. Surv. Can., p169-178.

Froese, E. (1997): Metamorphism in the Weldon Bay–Syme Lake area, Manitoba; *in* Current Research 1997-E, Geol. Surv. Can., p35-44.

Holland, T. and Blundy, J. (1994): Non-ideal interactions in calcic amphiboles and their bearing on amphibole-plagioclase geothermometry; Contrib. Mineral. Petrol., v116, p433-447.

Kohn, M.J. and Spear, F.S. (1990): Two new geobarometers for garnet amphibolite, with applications to southeastern Vermont; Amer. Mineral., v75, p89-96.

Maxeiner, R.O. (1996): Bedrock geology of the Henry Lake area (parts of NTS 64D-6 and -11), northern La Ronge Domain; *in* Summary of Investigations 1996, Saskatchewan Geological Survey, Sask. Energy Mines, Misc. Rep. 96-4, p51-66.

__________ (1997): Geology of the Lawrence Bay (Reindeer Lake) area, northeastern La Ronge Domain; *in* Summary of Investigations 1997, Saskatchewan Geological Survey, Sask. Energy Mines, Misc. Rep. 97-4, p3-17.

__________ (1999): La Ronge–Lynn Lake Bridge: Geology of the Wapus Bay–Lowdermilk Bay (Reindeer Lake) Area; *in* Summary of Investigations 1999, Volume 2, Saskatchewan Geological Survey, Sask. Energy Mines, Misc. Rep. 99-4.2, p143-158.

Spear, F.S. (1981): An experimental study of hornblende stability and compositional variability in amphibolite; Amer. J. Sci., v281, p697-734.

__________ (1993): Metamorphic Phase Equilibria and Pressure-Temperature-Time Paths; Mineral. Soc. Amer. Mono., 799p.

Spear, F.S. and Kohn, M.J. (1999): Program GTB: Geothermo-barometry, Version 2.1; Dept. Earth Environ. Sci., Rensselaer Polytechnic Institute; http://www.rpi.edu/dept/geo/spear/GTB_Prog/GTB.html, accessed 12 April 2000.

Stauffer, M.R., Langford, F.F., Coleman, L.C., and Mossman, D.J. (1979): Geology of the Area Around Amiskit Island, Reindeer Lake; Sask. Dep. Miner. Resour., Rep. 191, 21p.

Thomas, D.J. (1993): Geology of the Star Lake–Otter Lake Portion of the Central Metavolcanic Belt, La Ronge Domain; Sask. Energy Mines, Rep. 236, 132p.

Williamson, A.E. (2000): The metamorphic history of the Milton Island Metasedimentary Assemblage; unpubl. B.Sc. thesis, Univ. Sask., 76p.

Wright, D.M., Ansdell, K.M., Corrigan, D., and Maxeiner, R.O. (1999): Geology and metamorphic petrology of variably altered volcanic rocks in the southern Reindeer Lake area, northern Saskatchewan; *in* Summary of Investigations 1999, Volume 2, Saskatchewan Geological Survey, Sask. Energy Mines, Misc. Rep. 99-4.2, p159-166.

Geochemistry of Volcanic and Intrusive Rocks of the May Lake Area, La Ronge Domain

C.T. Harper

Harper, C.T. (2000): Geochemistry of volcanic and intrusive rocks of the May Lake area, La Ronge Domain; *in* Summary of Investigations 2000, Volume 2, Saskatchewan Geological Survey, Sask. Energy Mines, Misc. Rep. 2000-4.2.

Abstract

Geochemical analyses were carried out on a variety of volcanic, intrusive and mineralized rock samples from the May Lake area of the Paleoproterozoic La Ronge Domain. The May Lake volcanics, mainly considered to be ca. 1880 Ma, are typically subalkaline, tholeiitic to calc-alkaline in character, and representative of subduction-related, island arc volcanics. A group of rhyolites that occur near the stratigraphic top of the volcanics appear to have a different magma source and are suspected of belonging to a younger period, ca. 1830 to 1840 Ma, of Reindeer Zone magmatism. The intrusive rocks in the May Lake area are predominantly of the ca. 1850 to 1860 Ma magmatic event and are typical of the La Ronge Domain, being strongly subalkaline and calc-alkaline, and displaying a volcanic arc affinity. The presence of anomalous Au concentrations in different geologic settings indicates a good potential for finding such occurrences in the under-explored May Lake area.

1. Introduction

As part of the 1:20 000 scale geological mapping of the May Lake area during 1999 (Harper, 1999), 52 samples were collected for geochemical analyses. These included 23 volcanic, 17 intrusive, nine altered and/or mineralized volcanic and intrusive rocks, and three quartz veins. Their locations are shown in Figure 1 and the results in Tables 1 and 2. For a description of the geology, the reader is referred to the paper by Harper (1999).

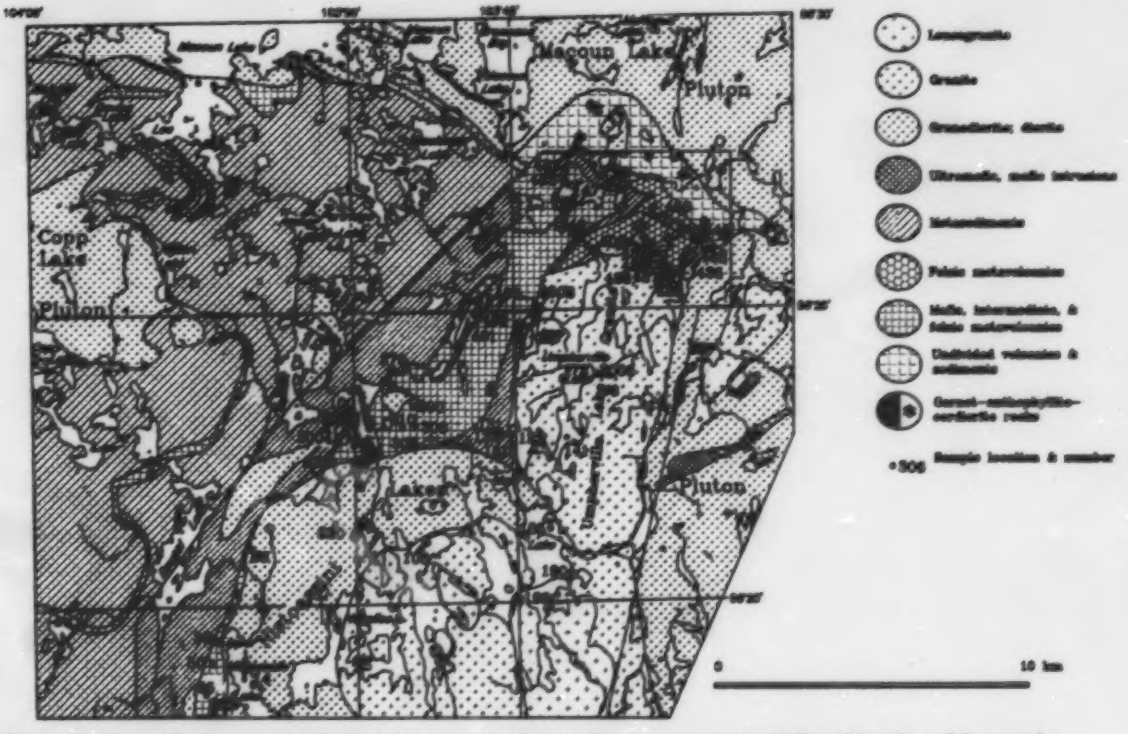
Magoun Lake
Pluton
Copp Lake
Pluton
Lake
Pluton
0
10 km
Leucogranite
Granite
Granodiorite; diorite
Ultramafic, mafic intrusions
Metasediments
Felsic metavolcanics
Mafic, intermediate, & felsic metavolcanics
Undivided volcanics & sediments
Garnet-anthophyllite-cordierite rocks
•306 Sample location & number

Figure 1 - Generalized geology of the May Lake region, showing the area mapped in 1999 and location of the samples described in this report. Geology is in part taken from Byers (1948) and Johnston (1970, 1973).

Table 1 - Major, trace, and rare earth element analyses for volcanic and related rocks from the May Lake area. Majors in wt %.

Sample No. 9911-	0232	0093	0502	0050	0477	0481	0035	0096	0290	0483	0036	0097	0161	0309
UTM East	571362	572382	578134	567518	579138	578754	567241	572070	573732	578645	567644	572073	576530	573653
UTM North	6240361	6248480	6253361	6241713	6256889	6257405	6240530	6249021	6249786	6257144	6242324	6249176	6248224	6249173
Rock Type	K	K	K	Mpp	M	M	M (min)	I	I	I	FD	FD	FD	FD
SiO_2	48.63	47.43	50.95	53.67	53.22	45.71	53.49	56.12	54.59	53.69	64.49	69.86	68.24	65.46
Al_2O_3	11.75	12.45	8.06	18.03	14.90	8.86	16.23	16.33	18.71	17.35	16	15.21	15.88	14.54
Fe_2O_3	10.77	10.60	10.47	11.35	11.58	11.81	10.84	9.41	9.05	11.48	5.78	3.03	3.17	6.95
MnO	0.18	0.165	0.196	0.18	0.209	0.196	0.12	0.18	0.19	0.166	0.1	0.05	0.04	0.12
MgO	14.43	13.45	13.52	3.5	3.98	16.48	3.89	2.22	2.66	2.95	1.36	0.92	1.32	1.39
CaO	10.5	8.74	13.60	7.1	10.17	10.45	6.11	5.57	5.78	8.07	3.6	3.5	3.04	4.99
Na_2O	1.65	1.96	0.39	4	3.27	1.00	5.12	4.51	3.81	4.07	4.64	3.49	4.18	1.24
K_2O	0.42	1.64	0.29	1.47	0.85	0.52	0.72	2.76	3.88	1.06	1.98	2.24	1.74	3.06
TiO_2	0.475	0.563	0.127	0.737	0.547	0.676	1.089	0.666	0.757	0.782	0.8	0.251	0.343	0.628
P_2O_5	0.13	0.21	0.04	0.19	0.19	0.08	0.16	0.4	0.45	0.21	0.29	0.09	0.12	0.19
LOI	1.77	1.90	1.41	0.67	0.78	2.80	2.68	1.43	0.86	0.11	1.61	0.84	2.03	2.15
Total	100.71	99.10	99.04	100.89	99.69	98.57	100.45	99.6	100.73	99.95	100.65	99.48	100.09	100.71
Be	<1	<1	<1	<1	<1	<1	1	1	2	<1	1	<1	<1	<1
V	212	223	149	248	177	211	275	150	163	182	51	43	39	59
Co	53	55	25	30	22	66	18	15	15	11	8	6	6	9
Cr	962	1500	1900	86	100	1000	113	125	17	27	129	93	81	38
Ni	332	406	141	28	<20	423	<15	38	663	<20	<15	<15	<15	<15
Cu	33	82	32	146	<10	39	240	174	150	32	38	62	<10	36
Zn	79	44	<30	104	60	50	63	107	113	<30	96	50	45	88
Ga	11	13	4	16	13	14	19	17	16	9	20	17	19	16
Ge	1.8	1.4	<0.5	1	<0.5	2.0	1.1	2	1.3	<0.5	1.1	0.7	0.8	1.3
Rb	8	32	5	29	12	11	7	55	76	27	45	43	44	70
Sr	315	278	117	440	339	156	819	529	687	413	293	307	352	389
Y	13.4	14.2	1.8	15.4	20.6	12.2	21.7	19.3	21.4	18.3	32.3	3.5	3.5	27.2
Zr	28	29	7	49	44	28	85	64	64	39	207	83	107	134
Nb	1.1	2.4	0.4	1.7	2.0	1.9	4.2	2.8	3.7	1.3	5.8	3.1	3.4	4.2
Mo	<2	<2	<2	<2	<2	<2	<2	<2	3	<2	<2	<2	<2	<2
Ag	<0.5	<0.5	<0.5	<0.5	<0.5	<0.5	<0.5	<0.5	<0.5	<0.5	<0.5	<0.5	<0.5	<0.5
In	<0.1	<0.1	<0.1	<0.1	<0.1	<0.1	<0.1	<0.1	<0.1	<0.1	<0.1	<0.1	<0.1	<0.1
Sn	<1	<1	<1	<1	<1	2	<1	<1	<1	<1	2	<1	<1	1
Cs	1.5	3.2	0.8	0.8	0.4	5.5	<0.1	1.6	2.4	1.3	1	1	0.8	4
Ba	148	454	20	712	188	239	156	898	1290	839	628	728	505	876
La	3.03	4.80	0.77	3.57	6.97	4.93	6.79	13.3	20.8	2.64	24.7	8.61	13.1	13.8
Ce	8.6	11.5	1.61	9.7	15.2	12.3	16.7	29.4	38.9	8.26	56.3	18.8	25.7	30.8
Pr	1.27	1.78	0.20	1.28	2.07	1.74	2.22	3.63	4.97	1.02	6.99	1.81	2.65	3.9
Nd	6.28	8.21	0.94	6.1	8.95	7.75	9.99	16.2	21.1	5.19	29.8	6.27	9.45	17
Sm	1.75	2.12	0.26	1.74	2.37	1.96	2.68	3.69	4.59	1.91	6.16	1.18	1.48	3.94
Eu	0.682	0.671	0.132	0.651	0.842	0.901	0.972	1.22	1.46	0.713	1.66	0.368	0.694	1.16
Gd	2.02	2.23	0.27	2.09	2.81	2.21	3.17	3.5	4.31	2.42	5.91	0.86	1.12	4.21
Tb	0.38	0.38	0.06	0.42	0.53	0.37	0.62	0.59	0.67	0.48	0.97	0.13	0.15	0.73
Dy	2.23	2.26	0.34	2.6	3.28	2.16	3.7	3.38	3.68	2.96	5.56	0.65	0.66	4.54
Ho	0.5	0.49	0.07	0.57	0.72	0.44	0.84	0.73	0.78	0.64	1.17	0.12	0.13	0.98
Er	1.56	1.52	0.21	1.75	2.28	1.31	2.58	2.21	2.3	1.98	3.5	0.35	0.32	3.05
Tm	0.237	0.221	0.032	0.285	0.338	0.171	0.414	0.337	0.343	0.290	0.536	0.047	0.041	0.47
Yb	1.49	1.44	0.26	1.72	2.20	1.11	2.69	2.1	2.23	1.89	3.29	0.32	0.25	2.92
Lu	0.223	0.224	0.042	0.258	0.366	0.163	0.407	0.318	0.332	0.314	0.482	0.047	0.039	0.422
Hf	0.9	0.9	0.2	1.5	1.4	1.0	2.5	1.8	1.8	1.3	5.4	2.2	2.5	3.7
Ta	<0.1	0.10	0.04	<0.1	0.10	0.10	0.3	0.2	0.2	0.09	0.5	0.3	0.3	0.3
W	0.4	<0.5	<0.5	0.5	<0.5	<0.5	98.4	0.4	0.3	<0.5	1.6	0.4	0.3	1.1
Tl	0.08	0.12	<0.05	0.17	<0.05	<0.05	<0.05	0.27	0.28	<0.05	0.22	0.09	0.18	0.29
Pb	6	<5	<5	6	7	<5	7	10	8	<5	7	<5	<5	8
Bi	0.36	0.6	<0.1	<0.06	<0.1	0.4	<0.06	<0.06	<0.06	<0.1	<0.06	<0.06	0.12	0.07
Th	0.98	0.98	0.22	1.31	1.21	0.76	1.41	2.71	3.09	1.11	5.11	2.82	1.73	2.76
U	0.39	0.38	0.06	0.42	0.54	0.31	0.87	0.73	0.93	0.51	2.15	0.53	0.48	1.41
Au	4	<2	<2	17	<2	2	25	<2	5	<2	<2	<2	10	<2
As	3.5	<5	<5	8.3	<5	<5	<0.5	4	1.7	<5	8.3	10.9	6.1	3.7
Br	<0.5			<0.5			<0.5	<0.5	<0.5		<0.5	<0.5	3.6	<0.5
Sb	1	0.4	<0.2	0.6	<0.2	0.4	0.4	0.6	0.7	<0.2	0.6	0.9	0.9	0.6
Sc	35.9	34	46	32.6	32	34	37.9	23.2	17.8	30	12.6	6	5.6	20.4

Notes:

K, ultramafic volcanic; M, basalt; Mpp, plagioclase phyric basalt; I, andesite; FD, dacitic; FDalt, altered dacitic to rhyolitic; FR, rhyolitic; FRpy, pyritic rhyolite; GAC, plus Ba, Sr, Y, Zr, Sc, Be, and V were analyzed by fusion and ICP. The trace element and rare earth element package (also included Ba, Sr, Y, Zr, and V) was analyzed by *trace and rare elements in ppm, and gold in ppb.*

0349	0366	2004	0429	0432	0446	0269	0278	0310	0310(Dup)	0367	0491	0492	0493	0409	0426	0427	0455
579166	574760	572125	581967	581657	583026	571997	573634	573473	573473	574415	575956	576011	576302	580891	582029	582029	581999
6255254	6249722	6248912	6254312	6254810	6255154	6249368	6251029	6249180	6249180	6249343	6252654	6252796	6253267	6255070	6254209	6254209	6255749
FD	FD	FD	FDalt	FDalt	FDalt	FR	FR	FR	FR	FR	FR	FR	FR	FRpy	GAC	GAC	IFs
69.32	67.00	68.07	68.08	76.17	72.57	75.47	75.15	76.29	76.32	73.66	75.53	75.53	75.42	72.67	55.09	46.03	55.34
15.68	15.56	16.25	13.75	11.79	12.30	14.74	14.55	14.3	14.35	15.96	14.23	14.59	14.36	12.70	13.68	18.55	13.67
3.28	4.51	3.44	5.29	3.01	5.76	1.13	0.9	1.1	1.09	1.09	0.84	0.96	0.96	5.09	21.77	23.24	14.99
0.062	0.069	0.047	0.078	0.066	0.060	0.03	0.03	0.06	0.06	0.035	0.058	0.039	0.052	0.015	0.351	0.695	0.175
1.54	1.68	1.31	3.52	0.89	1.72	0.24	0.13	0.27	0.27	0.26	0.12	0.12	0.13	1.70	6.21	7.12	1.91
4.51	4.25	3.65	0.62	2.26	1.27	1	1.37	0.87	0.86	1.10	1.34	0.35	0.55	1.77	0.85	1.20	7.15
3.46	3.99	4.81	3.22	2.52	4.36	5.1	4.62	2.75	2.76	2.50	4.91	4.54	4.14	2.89	0.27	0.37	0.70
1.14	1.92	1.28	1.52	1.80	0.66	1.8	3.36	3.62	3.71	4.14	2.19	3.35	3.68	0.60	0.39	0.44	0.33
0.398	0.573	0.367	0.413	0.257	0.371	0.06	0.062	0.083	0.079	0.085	0.049	0.038	0.046	0.409	0.421	0.598	0.341
0.10	0.20	0.12	0.08	0.04	0.06	0.05	0.03	0.05	0.05	0.04	0.04	0.04	0.03	0.09	0.02	0.14	0.06
0.71	0.73	0.56	2.29	0.98	1.11	0.69	0.44	1.37	1.23	1.29	0.82	0.75	0.98	2.45	<0.26	0.69	4.23
100.19	100.09	99.89	98.85	99.78	100.25	100.31	100.63	100.74	100.79	100.16	100.12	100.29	100.34	100.37	98.79	99.07	98.51
<1	1	<1	<1	<1	<1	1	2	2	2	1	1	2	1	<1	<1	<1	<1
54	66	40	12	<5	20	<5	<5	<5	<5	<5	<5	<5	<5	37	215	26	172
7	10	6	5	1	4	<1	<1	<1	<1	<1	<1	<1	<1	9	31	4	19
180	85	38	52	100	100	24	29	10	11	20	82	20	40	41	240	160	76
<20	<20	<20	<20	<20	<20	<15	<15	<15	<15	<20	<20	<20	<20	<20	<20	<20	115
<10	31	<10	61	<10	<10	<10	<10	<10	<10	<10	<10	<10	<10	17	<10	<10	166
34	77	<30	38	<30	<30	69	<30	<30	<30	<30	40	34	30	<30	93	<30	<30
15	18	11	13	9	11	21	18	19	19	19	20	18	17	15	12	3	10
0.7	1.0	0.7	0.6	0.6	<0.5	1.2	1	1.3	1.5	1.3	0.9	0.6	0.7	<0.5	0.9	<0.5	<0.5
27	43	27	30	24	6	32	64	54	55	74	49	71	82	8	12	9	6
409	437	375	59	73	103	327	399	257	260	525	337	294	320	85	3	7	106
6.5	10.1	4.3	13.7	16.8	20.0	9.6	7.8	10	10.3	11.3	7.0	5.8	6.3	20.1	5.5	31.9	11.3
105	123	57	75	87	81	57	57	87	107	106	43	41	42	87	16	83	39
5.5	8.9	3.3	2.7	3.4	2.9	7.9	7.5	7.8	7.8	9.7	6.7	7.0	6.9	4.3	1.4	2.6	2.1
<2	5	<2	<2	<2	<2	<2	<2	<2	<2	<2	<2	<2	<2	<2	<2	<2	7
<0.5	<0.5	<0.5	<0.5	<0.5	<0.5	<0.5	<0.5	<0.5	<0.5	<0.5	<0.5	<0.5	<0.5	<0.5	<0.5	<0.5	<0.5
<0.1	<0.1	<0.1	<0.1	<0.1	<0.1	<0.1	<0.1	<0.1	<0.1	<0.1	<0.1	<0.1	<0.1	<0.1	<0.1	<0.1	<0.1
1	1	<1	<1	<1	<1	<1	<1	<1	<1	<1	<1	<1	<1	<1	<1	<1	<1
1.2	1.3	1.5	1.7	0.5	0.2	0.8	2	0.7	0.7	2.2	0.8	1.8	1.7	0.3	0.8	0.6	0.2
435	491	374	260	346	78	1420	1540	1600	1620	"1,580"	955	"1,360"	"1,260"	171	96	99	55
15.2	20.0	15.1	7.18	4.67	7.75	11.2	4.6	5.1	4.75	12.8	8.63	8.52	5.81	7.14	1.51	5.31	3.06
29.4	39.7	27.1	14.8	8.14	16.9	24.2	10.2	14.5	13.6	26.7	17.9	17.9	12.4	15.9	3.42	15.6	7.14
3.14	4.54	3.33	1.89	1.47	2.24	2.75	1.23	1.44	1.37	3.24	2.22	2.19	1.48	2.17	0.44	1.96	1.06
11.0	15.9	12.0	7.76	6.43	9.86	10.5	5.13	5.64	5.37	12.3	8.19	8.21	5.51	9.41	1.95	8.73	4.56
1.91	2.80	1.95	1.82	1.73	2.60	2.14	1.42	1.7	1.56	2.70	1.87	1.75	1.34	2.48	0.56	2.67	1.36
0.662	0.904	0.624	0.670	0.499	0.875	0.641	0.519	0.562	0.617	0.651	0.498	0.380	0.368	0.878	0.219	0.855	0.498
1.55	2.38	1.48	2.11	2.02	2.92	1.93	1.35	1.55	1.56	2.21	1.57	1.36	1.21	2.84	0.80	4.01	1.56
0.23	0.34	0.17	0.38	0.42	0.55	0.31	0.23	0.29	0.3	0.33	0.23	0.20	0.20	0.52	0.15	0.77	0.31
1.20	1.81	0.86	2.33	2.79	3.47	1.49	1.21	1.54	1.56	1.74	1.12	0.99	1.02	3.28	0.98	4.88	1.78
0.22	0.33	0.14	0.48	0.62	0.74	0.28	0.25	0.31	0.31	0.31	0.19	0.18	0.19	0.70	0.20	1.03	0.39
0.60	0.97	0.35	1.50	2.09	2.34	0.81	0.74	1	0.98	0.89	0.55	0.48	0.49	2.22	0.65	3.14	1.26
0.079	0.132	0.042	0.212	0.336	0.348	0.112	0.112	0.145	0.154	0.129	0.070	0.062	0.066	0.338	0.098	0.452	0.174
0.48	0.82	0.24	1.43	2.46	2.32	0.73	0.77	0.93	0.99	0.86	0.46	0.39	0.41	2.23	0.68	2.97	1.13
0.069	0.117	0.030	0.221	0.440	0.375	0.101	0.122	0.148	0.146	0.126	0.055	0.057	0.055	0.356	0.118	0.508	0.196
2.7	3.2	2.0	2.1	2.6	2.4	2.3	2.2	2.8	3.2	3.1	1.8	2.0	1.8	2.6	0.5	2.5	1.3
0.45	0.68	0.35	0.18	0.26	0.19	0.9	0.8	0.6	0.6	0.67	0.50	0.57	0.55	0.23	0.07	0.30	0.15
<0.5	<0.5	<0.5	<0.5	<0.5	<0.5	0.7	0.7	1.3	1.4	<0.5	0.6	0.8	<0.5	0.6	<0.5	<0.5	<0.5
0.07	0.18	<0.05	0.10	<0.05	<0.05	0.33	0.39	0.31	0.32	0.41	0.35	0.53	0.53	<0.05	<0.05	<0.05	<0.05
<5	26	<5	<5	<5	<5	10	6	6	7	52	47	41	35	<5	<5	<5	<5
<0.1	2.2	<0.1	<0.1	<0.1	<0.1	0.18	<0.06	0.1	0.15	6.0	0.3	0.2	0.1	<0.1	<0.1	<0.1	<0.1
2.98	3.30	1.57	1.15	1.62	1.24	3.69	2.24	4.53	4.6	5.16	2.78	2.83	2.52	1.32	0.30	1.10	0.86
0.93	0.96	0.70	0.56	0.46	0.45	1.9	1.81	3.52	3.68	4.46	1.86	1.48	0.96	0.50	0.10	0.40	2.39
<2	<2	<2	<2	<2	<2	<2	3	<2	<2	<2	<2	<2	<2	<2	<2	<2	12
<5	5	<5	<5	<5	<5	2.1	4.2	3	2.8	<5	<5	<5	<5	<5	<5	<5	<5
						<0.5	<0.5	<0.5	<0.5								
<0.2	0.4	<0.2	<0.2	<0.2	<0.2	0.7	0.5	0.5	0.5	<0.2	<0.2	<0.2	<0.2	0.2	<0.2	<0.2	0.5
8	9	5	17	13	15	2.7	1.6	1.6	1.6	2	1	1	1	16	43	38	23

garnet-anthophylite-cordierite rocks; IFs, sulphide zone mineralization. Analyses by Activation Laboratories Ltd., Ancaster, Ontario. Major oxides, loss on ignition (LOI), a combined fusion, ICP/MS method at research grade. Gold analyses were by the INAA method.

Table 2 - Major, trace, and rare earth element analyses for intrusive rocks and quartz veins from the May Lake area. Majors in wt %, trace and rare earth elements in ppm, and gold in ppb.

Sample No	9911-0006	0072	0141	2005	2005 (dup)	0122	0425	0086	0014	0185	0108	0190	0192	0220	0025	0100	0435	0463	0131	0132	0271	0306
UTM East	580008	578830	579010	579632	579632	577991	581996	568603	568764	578215	574061	578869	578095	571331	567318	571909	582815	582525	576551	576551	571997	573758
UTM North	6250380	6251150	6248733	6251006	6251006	6248654	6254049	6245182	6241005	6246021	6245330	6244454	6243534	6246022	6240361	6249702	6254136	6254924	6249103	6249103	6249368	6248587
Rock Type	ULG	ULG	ULG	ULG	ULG	ULGdd	ULGd	NLPdi	NLPgd	NLPgd	NLPgr	NLPgr	NLPlg	NLPlg	PX	GD	GD(NE)	GD(NE)	MinDi	QV	QV	QV
SiO_2	73.31	69.11	68.52	74.03	74.39	55.85	68.14	57.75	65.99	63.79	67.84	70.88	72.46	76.28	45.88	71.71	61.02	62.16	58.02	78.4	96.49	91.01
Al_2O_3	15.02	15.55	15.05	14.37	14.27	16.23	15.21	17.97	15.01	15.26	15.23	15.02	14.45	12.67	5.24	15.33	18.20	19.44	14.24	6.88	1.2	2.86
Fe_2O_3	1.92	2.91	2.94	1.80	1.76	7.45	3.17	6.38	4.81	5.89	3.49	2.2	1.91	1.52	11.39	1.66	5.06	3.45	7.75	3.82	0.36	2.68
MnO	0.04	0.04	0.05	0.038	0.038	0.12	0.064	0.08	0.08	0.1	0.06	0.06	0.04	0.02	0.18	0.03	0.072	0.051	0.12	0.07	<0.01	0.03
MgO	0.53	0.97	0.99	0.44	0.44	4.73	1.50	3.48	2.54	3.08	1.71	0.9	0.66	0.58	24.39	0.57	2.32	1.34	4.1	3.17	0.04	0.76
CaO	2.55	3.66	3.59	2.03	2.01	6.36	4.10	6.02	4.18	5.2	3.62	2.54	2.31	1.54	6.8	1.76	6.27	3.93	7.19	4	0.09	1.28
Na_2O	4.46	4.24	4.2	4.77	4.60	3.59	3.71	4.73	3.94	3.94	4.48	4.68	4.69	3.74	0.77	4.26	3.76	5.54	1.12	0.96	0.58	0.62
K_2O	2.22	1.53	1.49	2.25	2.08	3.09	1.18	2.07	1.91	1.24	2.06	1.98	1.85	3.27	0.09	4.11	1.37	1.45	5.06	0.8	0.09	0.25
TiO_2	0.17	0.285	0.288	0.131	0.135	0.798	0.388	0.686	0.436	0.522	0.325	0.201	0.159	0.116	0.33	0.164	0.611	0.418	0.346	0.195	0.007	0.07
P_2O_5	0.08	0.09	0.09	0.06	0.05	0.71	0.09	0.17	0.1	0.13	0.09	0.08	0.07	0.04	0.12	0.09	0.19	0.10	0.11	0.08	0.01	0.06
LOI	0.49	0.83	1.65	0.45	0.41	1.41	1.30	1.59	0.89	1.39	0.86	0.69	0.87	0.74	5.08	0.67	1.34	1.33	1.9	1.42	0.22	1.11
Total	100.77	99.21	98.87	100.36	100.19	100.33	98.83	100.92	99.89	100.53	99.77	99.21	99.48	100.53	100.24	100.33	100.21	99.21	99.93	99.79	99.08	100.74
Be	1	1	1	1	1	2	1	1	1	<1	1	1	1	<1	<1	2	<1	2	<1	<1	<1	<1
V	16	35	34	14	14	125	48	130	76	100	54	21	15	15	137	19	83	43	125	71	<5	33
Co	3	6	6	2	2	23	7	9	12	13	8	4	3	3	76	3	13	6	15	13	<1	12
Cr	45	238	148	140	140	82	160	106	163	189	135	43	68	58	2200	114	66	100	208	126	24	44
Ni	<15	<15	<15	<20	<20	30	<20	<15	31	37	18	19	16	<15	775	21	<20	<20	20	44	<15	77
Cu	21	26	20	<10	<10	36	11	20	24	27	<10	<10	<10	201	54	16	<10	<10	86	<10	<10	82
Zn	156	58	59	49	51	101	<30	58	57	72	54	43	<30	37	89	38	60	<30	75	42	<30	<30
Ga	19	18	18	20	19	19	14	20	17	17	17	15	15	12	6	17	20	18	14	6	1	3
Ge	0.9	1	1	0.8	0.9	1.3	0.6	1	1	0.9	1	0.9	1	0.9	1.3	0.8	0.5	0.7	3.9	1.6	0.8	0.7
Rb	35	26	29	39	39	56	24	37	43	23	41	41	35	48	3	73	27	35	95	31	<2	5
Sr	280	544	307	220	223	1040	336	554	350	437	437	434	415	148	163	557	459	685	304	90	27	90
Y	5	5.1	4.7	4.3	4.7	20.3	7.8	16.4	11.5	11.3	9.5	5.1	4.7	4.5	9.1	3.1	7.8	7.3	3.5	4.8	0.6	3.4
Zr	80	92	98	51	54	207	109	79	116	97	124	89	82	69	24	77	95	115	17	11	6	6
Nb	4.5	4	4.7	5.0	5.0	8.3	5.3	3.9	4.1	3	4	3.3	3.1	2.9	1	2.7	5.0	7.4	0.5	0.7	0.5	<0.5
Mo	<2	<2	<2	<2	<2	<2	<2	<2	<2	<2	<2	<2	<2	17	<2	<2	<2	<2	109	<2	<2	2
Ag	<0.5	<0.5	<0.5	<0.5	<0.5	<0.5	<0.5	<0.5	<0.5	<0.5	<0.5	<0.5	<0.5	<0.5	<0.5	<0.5	<0.5	<0.5	<0.5	<0.5	<0.5	<0.5
In	<0.1	<0.1	<0.1	<0.1	<0.1	<0.1	<0.1	<0.1	<0.1	<0.1	<0.1	<0.1	<0.1	<0.1	<0.1	<0.1	<0.1	<0.1	<0.1	<0.1	<0.1	<0.1
Sn	1	<1	<1	<1	<1	<1	<1	1	<1	<1	1	<1	<1	<1	<1	<1	<1	<1	<1	<1	<1	<1
Cs	1	0.7	0.8	0.8	0.8	1.7	0.5	1.3	1.2	0.7	1.3	0.7	0.5	0.6	0.2	1.6	1.0	1.2	6.6	7.4	<0.1	0.3
Ba	553	533	430	470	481	1130	401	411	586	419	523	757	548	575	22	965	323	722	4140	294	31	79
La	11.8	14.5	14.2	6.80	6.88	65.3	13.1	11.7	10.3	10.4	12.9	6.46	6.09	12.7	3.52	12.9	10.8	16.7	3	2.04	0.33	0.83
Ce	22.6	28.1	26.7	16.7	16.7	147	24.4	26.9	23.5	24	28.6	11.8	11.9	22.7	8.5	27.8	22.4	30.0	6.1	4.4	0.7	1.8
Pr	2.39	2.91	2.75	1.46	1.47	16.9	2.69	3.37	2.8	2.92	3.33	1.26	1.29	2.05	1.18	3.05	2.65	3.13	0.76	0.55	0.08	0.21
Nd	8.79	10.3	9.55	4.94	5.11	66.2	9.68	14.7	11.2	12.3	13.2	4.78	4.74	6.41	5.64	11.2	10.4	10.6	3.21	2.41	0.25	0.9
Sm	1.57	1.75	1.63	0.96	0.99	11.1	1.81	3.3	2.25	2.62	2.55	0.93	0.99	0.89	1.44	1.78	2.13	1.78	0.73	0.6	0.08	0.23
Eu	0.447	0.537	0.585	0.374	0.369	3.04	0.598	1.15	0.732	0.851	0.743	0.485	0.403	0.317	0.515	0.67	0.764	0.743	0.223	0.212	0.027	0.106
Gd	1.23	1.29	1.32	0.78	0.83	7.84	1.58	3.02	2.03	2.38	2.04	0.87	0.88	0.71	1.56	1.15	1.90	1.43	0.67	0.67	0.09	0.32
Tb	0.18	0.19	0.18	0.14	0.15	0.91	0.25	0.5	0.34	0.38	0.3	0.14	0.15	0.12	0.28	0.12	0.29	0.21	0.11	0.13	0.02	0.07
Dy	0.9	0.95	0.88	0.73	0.76	4.16	1.36	2.83	1.95	1.99	1.58	0.75	0.81	0.67	1.64	0.56	1.53	1.22	0.59	0.77	0.09	0.46
Ho	0.17	0.18	0.17	0.14	0.14	0.72	0.27	0.6	0.4	0.41	0.32	0.16	0.16	0.15	0.35	0.1	0.29	0.24	0.13	0.18	0.02	0.13
Er	0.47	0.51	0.43	0.37	0.39	1.89	0.74	1.82	1.26	1.22	0.93	0.51	0.47	0.49	1.04	0.27	0.78	0.71	0.4	0.54	0.06	0.49
Tm	0.061	0.069	0.059	0.050	0.052	0.236	0.107	0.268	0.197	0.182	0.145	0.082	0.068	0.083	0.166	0.036	0.096	0.095	0.058	0.092	0.01	0.081
Yb	0.4	0.46	0.36	0.34	0.35	1.41	0.67	1.68	1.25	1.11	0.97	0.57	0.46	0.62	1	0.27	0.64	0.66	0.44	0.58	0.05	0.55
Lu	0.063	0.068	0.061	0.051	0.051	0.221	0.103	0.242	0.195	0.161	0.155	0.087	0.076	0.106	0.147	0.045	0.085	0.095	0.084	0.081	0.01	0.093
Hf	2.4	2.6	2.6	1.9	1.9	4.7	3.0	2.1	3.1	2.5	3.3	2.2	2.2	2.3	0.8	2.3	2.4	3.2	0.5	0.3	0.2	0.1
Ta	0.6	0.5	0.6	0.82	0.83	0.5	0.55	0.3	0.4	0.2	0.5	0.3	0.3	0.5	<0.1	0.1	0.40	0.75	<0.1	<0.1	<0.1	<0.1
W	<0.2	0.3	<0.2	<0.5	<0.5	0.5	0.8	1	<0.2	0.3	<0.2	<0.2	<0.2	0.2	0.8	0.4	<0.5	<0.5	1.3	0.5	<0.2	<0.2
Tl	0.25	0.18	0.23	0.25	0.21	0.52	<0.05	0.22	0.28	0.15	0.21	0.21	0.21	0.22	0.07	0.38	0.15	<0.05	0.63	0.31	<0.05	0.05
Pb	11	11	9	23	21	16	<5	6	<5	7	6	<5	8	14	11	15	12	<5	12	<5	<5	<5
Bi	<0.06	<0.06	0.26	<0.1	<0.1	0.09	<0.1	<0.06	<0.06	0.08	<0.06	<0.06	<0.06	<0.06	<0.06	<0.06	0.9	<0.1	29.8	1.26	<0.06	0.28
Th	2.48	3.71	2.62	2.55	2.57	9.85	3.41	2	3.23	1.44	3.89	1.49	1.18	6.75	0.72	4.75	2.38	4.12	0.33	0.28	0.29	0.27
U	1.42	1.49	1.01	0.63	0.64	4.25	1.30	1.37	1.32	0.78	2.19	0.73	0.64	2.89	0.28	1.25	1.07	1.09	0.16	0.11	0.34	0.09
Au	4	<2	<2	<2	<2	<2	<2	3	5	21	<2	<2	8	69	<2	<2	<2	<2	1150	47	<2	17
As	2.6	26.8	20	<5	<5	4.1	<5	4.4	3.1	26.1	9.3	3.9	10.1	7.7	3.2	14.4	<5	<5	4.3	3.9	2.2	8
Br	<0.5	<0.5	<0.5			<0.5		<0.5	<0.5	<0.5	<0.5	<0.5	1.8	<0.5	<0.5	<0.5			<0.5	<0.5	<0.5	<0.5
Sb	0.3	1	0.8	<0.2	<0.2	<0.1	0.2	0.5	0.4	1.2	0.6	0.4	0.8	1	0.5	0.8	<0.2	<0.2	0.9	0.7	0.4	0.5
Sc	3.6	5	5.9	3	3	18.6	8	17.6	12.6	14.4	7.9	4	2.8	2.5	35.3	2.8	12	6	17	16	0.3	4.5

Notes: ULG, Umpherville Lake granite; ULGd, granodiorite; ULGdd, diorite dyke; NLPd, Nistoassini Lakes Pluton diorite; NLPgd, granodiorite; NLPgr, granite-leucogranite; PX, pyroxenite; GD, granodiorite; GD(NE), granodiorite from northeast; MinDi, mineralized diorite; QV, quartz vein. Analyses by Activation Laboratories Ltd., Ancaster, Ontario. Major oxides, loss on ignition (LOI), plus Ba, Sr, Y, Zr, Sc, Be, and V were analyzed by fusion and ICP. The trace element and rare earth element package (also included Ba, Sr, Y, Zr, and V) was analyzed by a combined fusion, ICP/MS method at research grade. Gold analyses were by the INAA method.

2. Volcanic Rocks

The volcanics from the May Lake area are correlated with those from the Waddy Lake area where a quartz-phyric rhyolite has yielded a U-Pb zircon age of 1880 ±7 Ma (Bickford *et al.*, 1986). The sampled volcanic rocks were classified in the field as ranging from ultramafic to rhyolitic in composition (Table 1), and is demonstrated in Winchester and Floyd's (1977) SiO_2 vs. Zr/TiO_2 diagram (Figure 2). The three altered felsic volcanics and pyritic rhyolite are noticeably offset from the main groupings indicating their relative compositional changes.

The Jensen (1976) cation ternary plot (Figure 3) shows a tholeiitic to calc-alkaline trend which is typical of volcanics in the Waddy Lake section of the Central Metavolcanic Belt (CMB) (Harper, 1985; Harper *et al.*, 1986; Watters and Pearce, 1987). The ultramafic volcanic samples and sample 9911-0481 plot in the basaltic komatiite field, consistent with their high MgO (13.45 to 16.23%), Cr (962 to 1900 ppm), and Ni (141 to 423 ppm) contents. Similar rocks, examined by the author (Harper, 1985, 1996, 1997, 1998) across the Waddy-Sucker-Fleming lakes area, display a trend from basaltic komatiite to high-magnesium basalts on the Jensen plot.

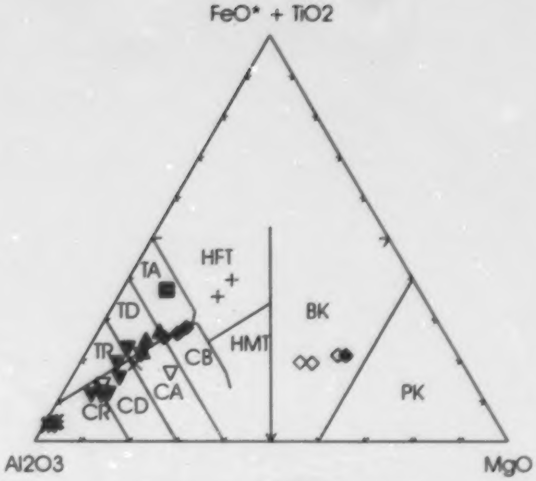

Figure 3 - Jensen (1976) cation plot for May Lake volcanics to distinguish tholeiitic and calc-alkaline series rocks. TR, TD, TA=tholeiitic rhyolite, dacite, andesite; CR, CD, CA, CB=calc-alkaline rhyolite, dacite, andesite, basalt; HFT, HMT=high-iron and high-magnesium tholeiites; and BK, PK=basaltic and peridotitic komatiites. Symbols as in Figure 2.

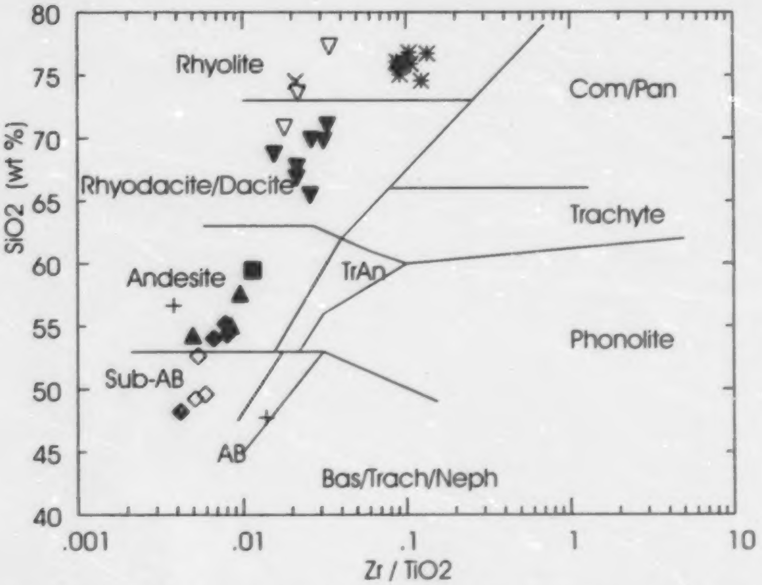

Figure 2 - SiO_2 vs. Zr/TiO_2 diagram illustrating the range of composition of volcanics from the May Lake area (Winchester and Floyd, 1977). Several altered and mineralized rocks are plotted for comparison. AB and Sub-AB=(sub-) alkaline basalt; Bas/Trach/Neph=basanite, trachyte, nephelinite; Com/Pan=comendite, pantellerite; and TrAn=trachyandesite. Open diamond=ultramafic volcanic; filled diamond=mafic volcanic; filled upward triangle=intermediate volcanic; filled downward triangle=dacitic/rhyodacitic volcanic; open downward triangle=altered felsic volcanic; asterisk=rhyolite; X=pyritic rhyolite; +=garnet-anthophylite-cordierite rocks; and solid square=sulphide zone.

Two diagrams that are useful in determining the tectonic setting of various basalts are Pearce and Cann's (1973) Ti/100-Zr-Y*3 and Wood *et al.* (1979) and Wood's (1980) Th-Ta-Hf/3 ternary plots. In the latter plot Nb/16 can be substituted for Ta as has been done for the May Lake volcanics. The ultramafic and mafic volcanics from May Lake mainly plot in, or just immediately adjacent to, field B on the Ti-Zr-Y diagram (Figure 4) which is an overlap field for volcanic arc basalts (VAB) and mid-ocean ridge basalts (MORB). Although the volcanic arc signature is not decisive in this plot, the rocks are clearly not within plate basalts (WPB). The tectonic distinction is much better on the Th-Nb-Hf diagram, which is also a good indicator of subduction zone affinity (Pearce, 1996). The ultramafic and mafic volcanics from the May Lake area all plot within the volcanic arc basalt (VAB) field (Field D, Figure 5) and show a strong linear trend toward the calc-alkaline (Th) corner of the diagram (Pearce, 1996).

Pearce (1996) has also used a group of MORB-normalized elements, including Th, Nb, Ce, Zr, Ti, and Y, to determine the tectonic setting of modern basalts and to characterize their related fractionation series. He found that VAB have a significant negative Nb anomaly with respect to Th and Ce. Tholeiitic VAB are characterized by relative depletion of Nb, Zr, Ti, and Y with respect to N-MORB, and calc-alkaline VAB have elevated Nb and Zr concentrations, but still have lower concentrations of Ti and Y relative to N-MORB. The negative Nb anomaly continues to occur with increasing fractionation through intermediate to dacitic rocks, but becomes less pronounced as Th concentrations increase. With increasing felsicity, Ti starts to develop a negative anomaly with respect to Zr and Y, and becomes very pronounced in rhyolites of both tholeiitic and alkaline fractionation series.

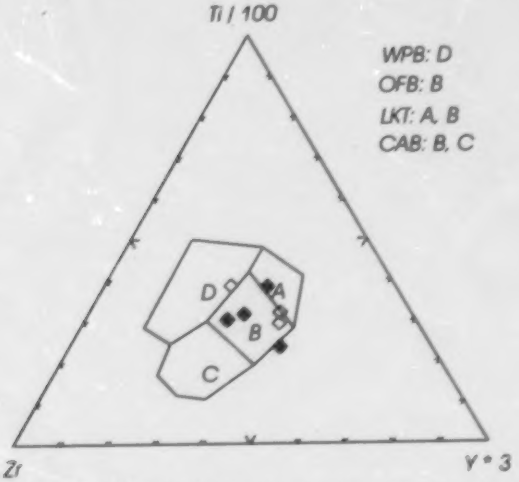

Figure 4 - May Lake basic volcanics plotted on Pearce and Cann's (1973) Ti/100-Zr-Y*3 basalt discrimination diagram. A=tholeiitic VAB; B=MORB+VAB; C=calc-alkaline VAB; and D=WPB. Symbols as in Figure 2.

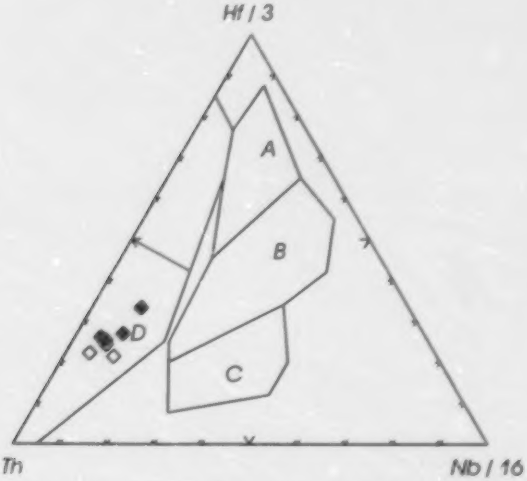

Figure 5 - Hf/3-Th-Nb/16 ternary discrimination diagram (Wood et al., 1979; Wood, 1980) to show the volcanic arc tectonic setting of the May Lake volcanics. A=MORB; B=MORB+WPB; C=WPB; and D=VAB. Symbols as in Figure 2.

The ultramafic and mafic volcanics of May Lake show the characteristic VAB profile (Figure 6A) as defined by Pearce (1996). One ultramafic sample, 9911-0502, however, shows a much more depleted profile for all elements. The intermediate volcanics show the same, but slightly elevated profiles (Figure 6B), as the VAB. Likewise the dacitic volcanics show parallel profiles (Figure 6C), but show two different trends from Ti to Y. Two samples show the negative Ti anomaly with respect to Y, whereas the other five show more depleted Y concentrations relative to N-MORB. The rhyolite samples (Figure 6D) have little or no negative Nb anomaly, but show a very strong negative Ti anomaly. The significant difference of the rhyolite profiles may be a function of them not being part of the same fractionation series, as these samples are representatives of the upper most volcanics in the sequence. More importantly they could be 40 to 50 Ma younger than the main period of volcanism ca. 1880 to 1890 Ma, and, therefore, could be derived from partial melting of subducted sediments or Archean crust (i.e. Sask Craton).

Chondrite normalized REE plots for the volcanics show flat profiles for the ultramafic and basaltic samples (Figure 7A and B), which is consistent with tholeiitic arc rocks (*c.f.* Syme *et al.*, 1996). Again ultramafic sample 9911-0502 has a parallel, but significantly more depleted profile with a small positive Eu anomaly. This rock comes from lower in the stratigraphic sequence and indicates that it may have a more primitive mantle source than the other ultramafic and mafic volcanics. Two of the intermediate (andesitic) volcanics have steeper light rare earth element (LREE) enriched patterns (Figure 7C) compared to a flatter pattern for the heavy rare earth elements (HREE) which is typical for calc-alkaline volcanic arc andesites. Sample 9911-0483 has a flat profile more akin to the mafic volcanics. The dacites (Figure 7D) and rhyolites (Figure 7E) have similar overall trends as the andesites, but the dacites display a distinct separation for the HREE, with two of the samples having significantly higher HREE than the other five samples. The upper pair resembles evolved arc patterns (Syme *et al.*, 1996), whereas the lower group is more like a tholeiitic arc pattern with a slight to noticeable positive Eu anomaly.

Christiansen and Keith (1996) have used the Rb vs. Nb+Y plot of Pearce *et al.* (1984) to distinguish granites and rhyolites in different tectonic settings or as S-, I-, A-, or OR-type granites, and relate them to their common metal associations (i.e. porphyry copper/epithermal settings). The May Lake rhyolite samples all plot in the volcanic arc granite (VAG) or I-type granite field (Figure 8), which indicates derivation by partial melting of metasomatized mantle (Christiansen and Keith, 1996). I-type granites and rhyolites are also commonly associated with precious

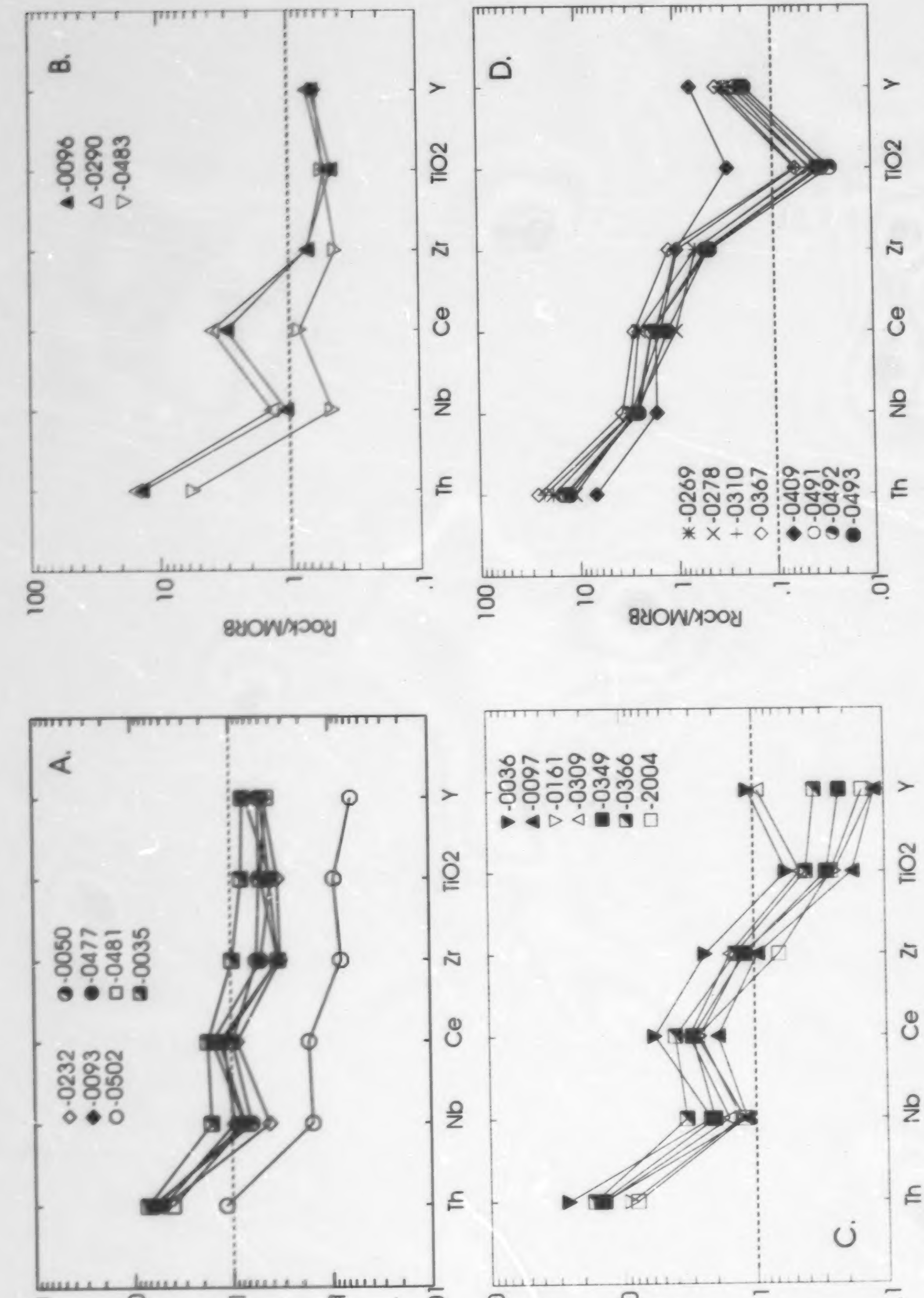

Figure 6 - N-type MORB normalized Th-Nb-Ce-Zr-TiO$_2$-Y profiles for May Lake volcanic rocks. A) ultramafic and mafic volcanics, B) intermediate volcanics, C) dacitic volcanics, and D) rhyolitic volcanics. Dashed line represents N-MORB profile based on normalizing values of Pearce (1996).

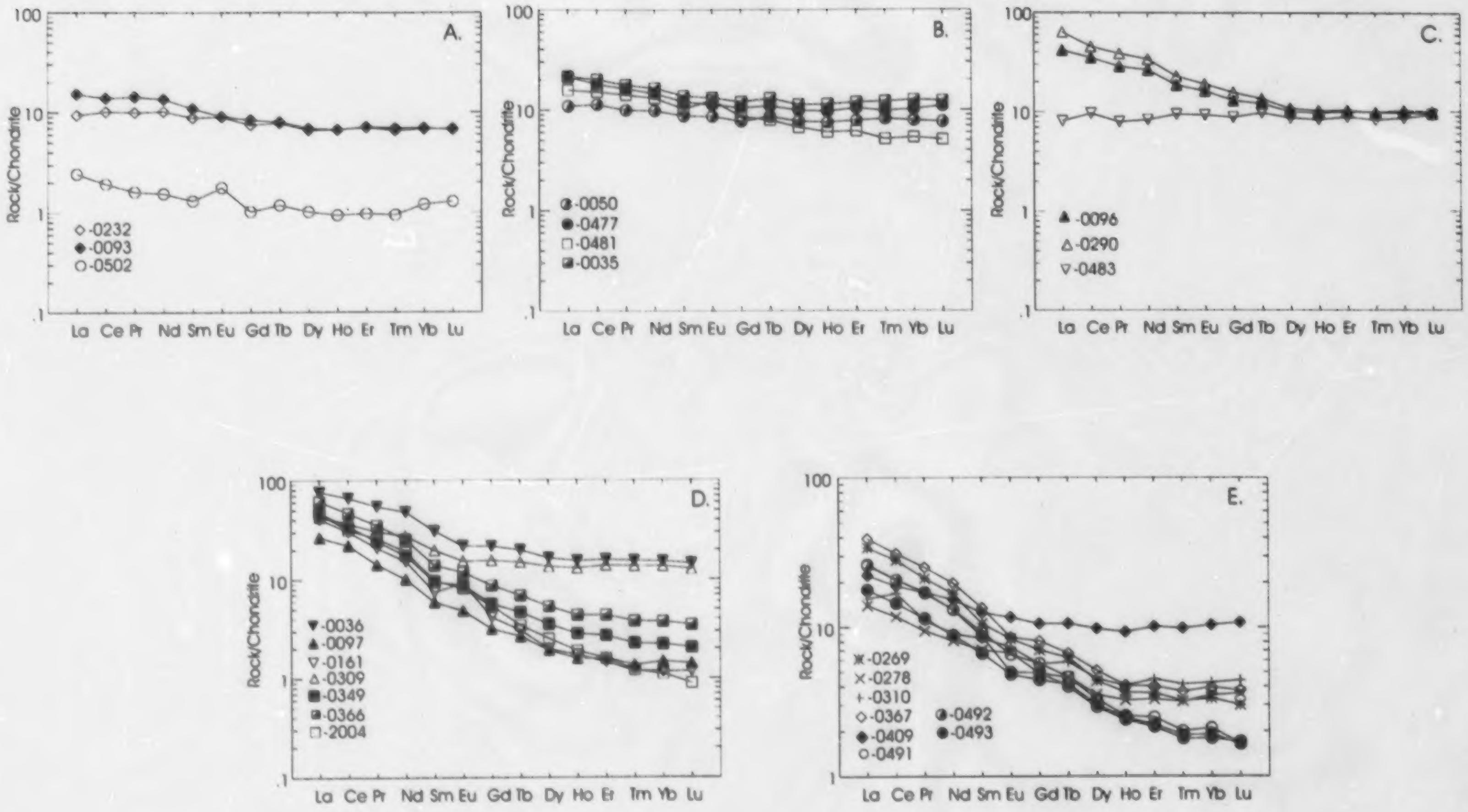

Figure 7 - Chondrite-normalized REE plot for May Lake volcanics. A) Ultramafic, B) mafic, C) intermediate, D) dacitic, and E) rhyolitic. Normalizing values from Sun (1982).

and base metal (VMS) deposits, which make the May Lake rhyolites more attractive exploration targets.

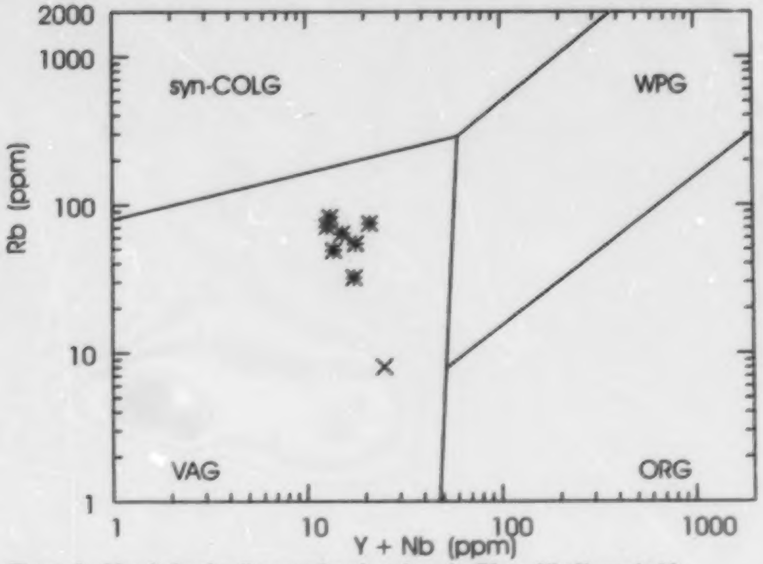

Figure 8 - May Lake rhyolite samples plotted on the Rb vs. Nb+Y granitoid discrimination diagram (Pearce* et al.*, 1984); VAG, volcanic arc granite or I-type granite; syn-COLG, syncollision granite or S-type granite; WPG, within-plate granite or A-type granite; and ORG, ocean ridge granite or OR-type granite.

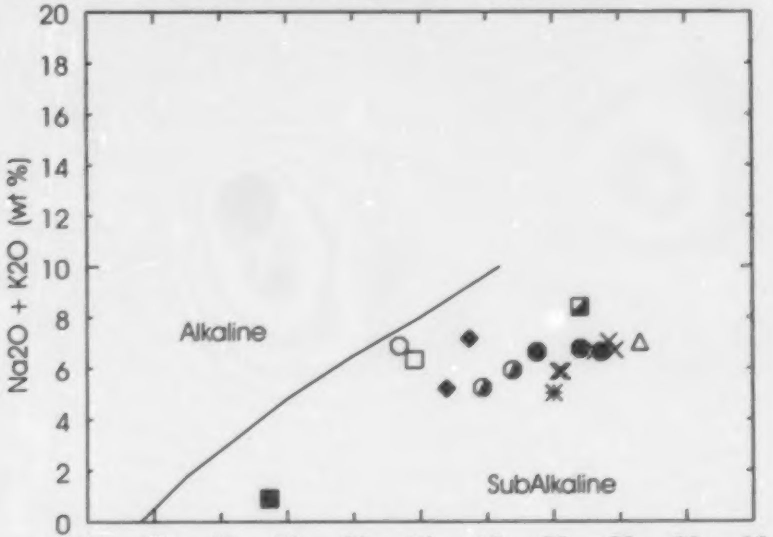

Figure 9 - May Lake area intrusive rocks plotted on the SiO_2 vs. Na_2O+K_2O diagram to distinguish alkaline and subalkaline rocks (Irvine and Baragar, 1971). ■, pyroxenite; half-filled square=McKenzie Lake granodiorite stock; □, altered diorite sill; ○, NLP diorite; half-filled circle=NLP granodiorite; ●, NLP granite-leucogranite; △, weakly mineralized leucogranite; ×, Umpherville Lake Granite; ✱, Umpherville Lake granodiorite; and ◆, granodiorite (northeast).

3. Intrusive Rocks

Intrusive rocks sampled include: five of the Umpherville Lake granite (ULG) plus a late diorite dyke that intrudes it; seven of the Nistoassini Lakes Pluton (NLP) ranging from diorite to leucogranite; a pyroxenite, which apparently intrudes both volcanics and Crew Lake Belt (CLB) sediments in the southwest; a biotite granodiorite sample from a stock intruding the CLB sediments at McKenzie Lake, and two granodiorite rocks from the northeast part of the area (Table 2). An altered diorite is included in most of the geochemical diagrams for comparative purposes. The NLP leucogranite sample, 9911-0220, which intrudes NLP granodiorite, is weakly mineralized with chalcopyrite, pyrite, and magnetite along a narrow silicified fracture. It, too, is included in the plots for comparison.

The May Lake intrusive rocks are strongly subalkaline as shown in Irvine and Baragar (1971) alkalis vs. SiO_2 plot (Figure 9). Except for the pyroxenite sample all of the intrusive rocks have a very well-defined calc-alkaline trend as depicted on the Irvine and Baragar (1971) tholeiitic-calc-alkaline ternary diagram (Figure 10). This is typical of the La Ronge Domain intrusions (Harper *et al.*, 1986). The five samples from the ULG have a parallel trend just slightly above the NLP trend, but the single granodiorite sample from the ULG lies on the NLP trend. Note also that the altered diorite sample, due to the total relative proportions of Na and K, still plots on the same trend as the other rocks as does the leucogranite.

On the Maniar and Piccoli (1989) multi-element plot (Figure 11) used to distinguish the nature of granitoid rocks, the hornblende dominant diorites, granodiorites and a hornblende-biotite granite plot in the metaluminous field. Biotite granites of both plutons and the small McKenzie Lake biotite granodiorite stock fall in the peraluminous field. The Umpherville Lake biotite granodiorite and a small biotite granodiorite stock in the northeast also plot in the peraluminous field.

On the Y+Nb versus Rb tectonic discrimination diagram (Pearce *et al.*, 1984), the May Lake intrusive rocks plot well into the volcanic arc granite (VAG) field (Figure 12) leaving little doubt that these are subduction-related intrusive rocks. On Batchelor and Bowden's (1985) multi-component diagram (Figure 13), the pyroxenite sample understandably plots in the mantle fractionates field. The NLP and ULG samples plot mainly in the syn-collision field, which supports the idea that the major period of plutonism, ca. 1855 Ma, coincided with the collision of the La Ronge arc with the Hearne Craton and emplacement of the Wathaman Batholith.

Chondrite-normalized rare earth element (REE) plots for the NLP (Figure 14A) and ULG (Figure 14B) display the characteristic signature of calc-alkaline volcanic arc plutons, having enriched LREE relative to the HREE. The granite end members of the NLP show a slight to strong positive Eu anomaly, whereas the ULG rocks have a steeper and much tighter clustering of profiles and display no or a slight positive Eu anomaly. The late diorite dyke has a parallel profile to the ULG rocks, but is significantly more enriched in all the REE (Figure 14C). The McKenzie Lake biotite granodiorite stock and the two northeast granodiorite samples (Figure 14C) have very similar LREE concentrations and have a small positive Eu anomaly, but the McKenzie Lake granodiorite has a much more pronounced depletion of the HREE. The altered diorite sample, although parallel to the NLP diorite profile (Figure 14C), is markedly depleted in overall REE concentrations. The pyroxenite sample has a low negative slope and resembles E-MORB profiles.

4. Mineralized Samples

The weakly pyritic mafic volcanic, sample 9911-0035 (Table 1), other than having slightly elevated concentrations of Cu and Au and anomalous W, has insignificant differences from the other mafic volcanic samples. The three altered felsic volcanic samples from the northeast part of the area, are listed as dacitic, but two samples have silica contents typical of rhyolites (Figure 2), indicating the potential for silicification. These rocks also contain variable amounts of garnet, magnetite, and biotite, which are interpreted as indications of weak to moderate hydrothermal alteration. With increasing alteration these minerals increase along with the development of anthophylite and cordierite. With respect to other dacitic rocks of the area, these three samples do not show distinctive changes in iron, but do show a slight increase in magnesium (Figure 3), and general losses of Ca, Na, and K, along with Sr, Ba, the LREE (Figure 15A). Compared to the MORB normalized discriminant plot for the dacites (Figure 6C), the three altered rocks have very similar profiles (Figure 15B), that fall along the lower limit of the unaltered dacites.

Compared to the other rhyolite samples, the pyritic rhyolite, 9911-0409, shows marked increases in Fe and Mg (shift to more mafic composition in Figure 3), less so in Ca and the HREE, and is depleted in Na, K, Sr, and Ba. None of the base or precious metals shows any increases beyond background (Table 1). The chondrite normalized REE pattern (Figure 15A) is identical to the altered dacitic volcanics, being rather flat because of the relative increase in the HREE. The MORB-normalized discriminant profile (Figure 15B) for this sample is very similar to that for the dacitic volcanics, suggesting perhaps that this rock is a silicified dacite, rather than a rhyolite.

Analyses of two samples of the garnet-anthophylite-cordierite rocks (9911-0426 and -0427), interpreted to have formed by synvolcanic hydrothermal alteration, are listed in Table 1. They are Fe, Mg, and Mn enriched (see Figure 3), generally Si poor and show low concentrations of Ca, Na, and K. They are Sr and Ba depleted and whereas one sample, 9911-0426, has low REE concentrations, the other, 0427, has nearly five times the concentrations (Figure 16A). Both have essentially flat profiles, most like tholeiitic mafic volcanics. Interestingly the sulphide-mineralized sample has a parallel profile approximately midway between these two (Figure 16A). In the MORB-normalized discriminant profile (Figure 16B) sample 0427, which has the lowest silica content (46.03%) has a profile that most closely resembles the altered dacites. Sample 0426 with the higher silica content (55.09%) is more like the ultramafic volcanics. Whether these are true indicators of the protoliths to these rocks is not clear, but warrants further investigation. Although Cr and Zn are weakly elevated in sample 0426, neither sample shows any elevated concentrations of the base or precious metals. Even the sulphide-mineralized sample has only weakly elevated concentrations of Cu, Ni, Au, and Mo.

A leucogranite dyke, sample 9911-0220 (Table 2), that intrudes granodiorite of the NLP is weakly mineralized along a narrow silicified fracture with trace amounts chalcopyrite, pyrite, malachite, and magnetite. The slight increases in SiO_2, and K_2O, and corresponding decreases in Al_2O_3, CaO, and Na_2O, had little overall effect on the various plots (Figures 9 and 10), and no effect on the trace elements used in the discrimination diagrams (Figures 12 to 14). This sample has anomalous concentrations of Cu, Mo, and Au, which are possibly indicative of porphyry-style hydrothermal processes having been active in the plutons.

The altered diorite, sample 9911-0131, has a marked increase in K_2O (5.06%), reflecting the biotitization of hornblende, and a corresponding decrease in Na_2O (1.12%), but in Figures 9 and 10, shows little difference from the unaltered diorite sample. This sample has a dramatic increase in Ba (4140 ppm) as well as having elevated concentrations of Cu, Zn, and Bi and anomalous Au (1150 ppb), and Mo (109 ppm) concentrations. This mineralization is similar to the Weedy Lake gold mineralization and represents a new discovery in the May Lake region.

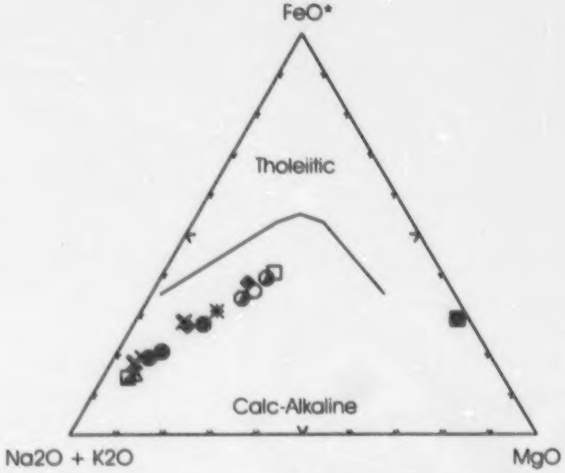

Figure 10 - May Lake intrusive rocks plotted on an AFM diagram (after Irvine and Baragar, 1971) to show their strong calc-alkaline trend. Symbols as in Figure 9.

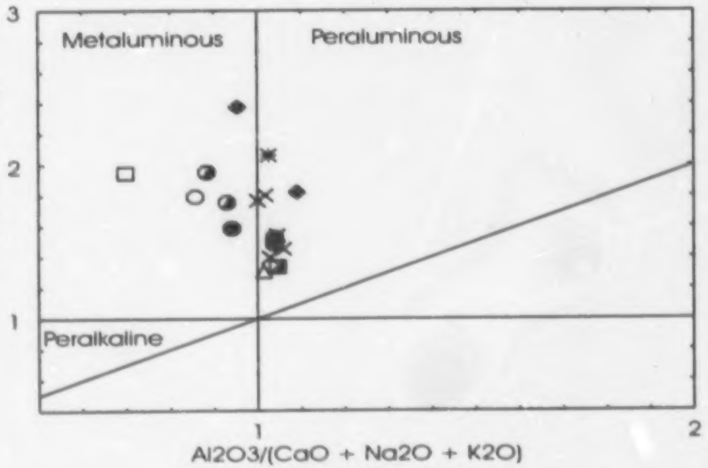

Figure 11 - May Lake intrusive rocks plotted on the Maniar and Piccoli (1989) granitoid rock discrimination diagram. Symbols as in Figure 9.

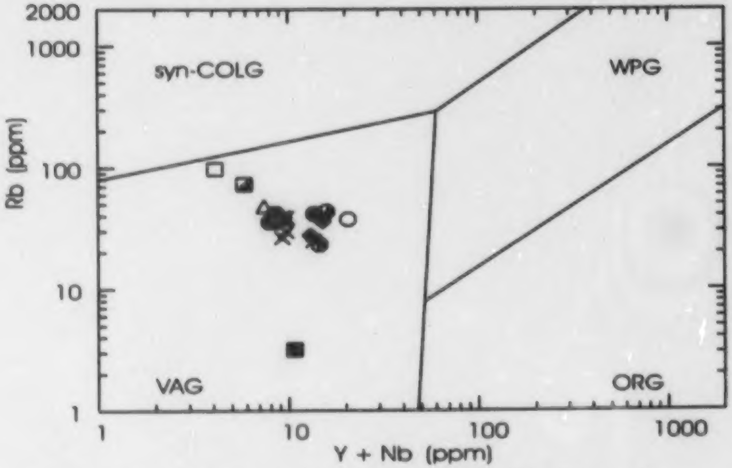

Figure 12 - May Lake intrusive rocks plotted on the Y+Nb vs. Rb tectonic discrimination diagram for granitic rocks (Pearce et al., 1984) showing fields for volcanic arc granites (VAG), ocean ridge granites (ORG), within-plate granites (WPG), and syn-collision granites (syn-COLG). Symbols as in Figure 9.

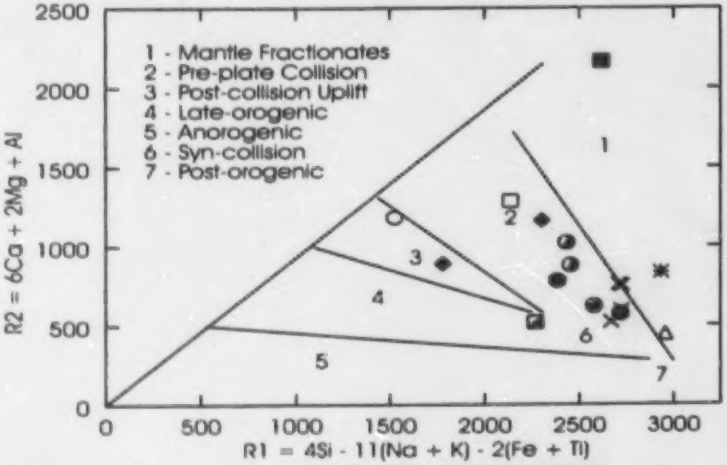

Figure 13 - May Lake intrusive rocks shown on the multi-component discrimination diagram for intrusive rocks (Batchelor and Bowden, 1985). Symbols as in Figure 9.

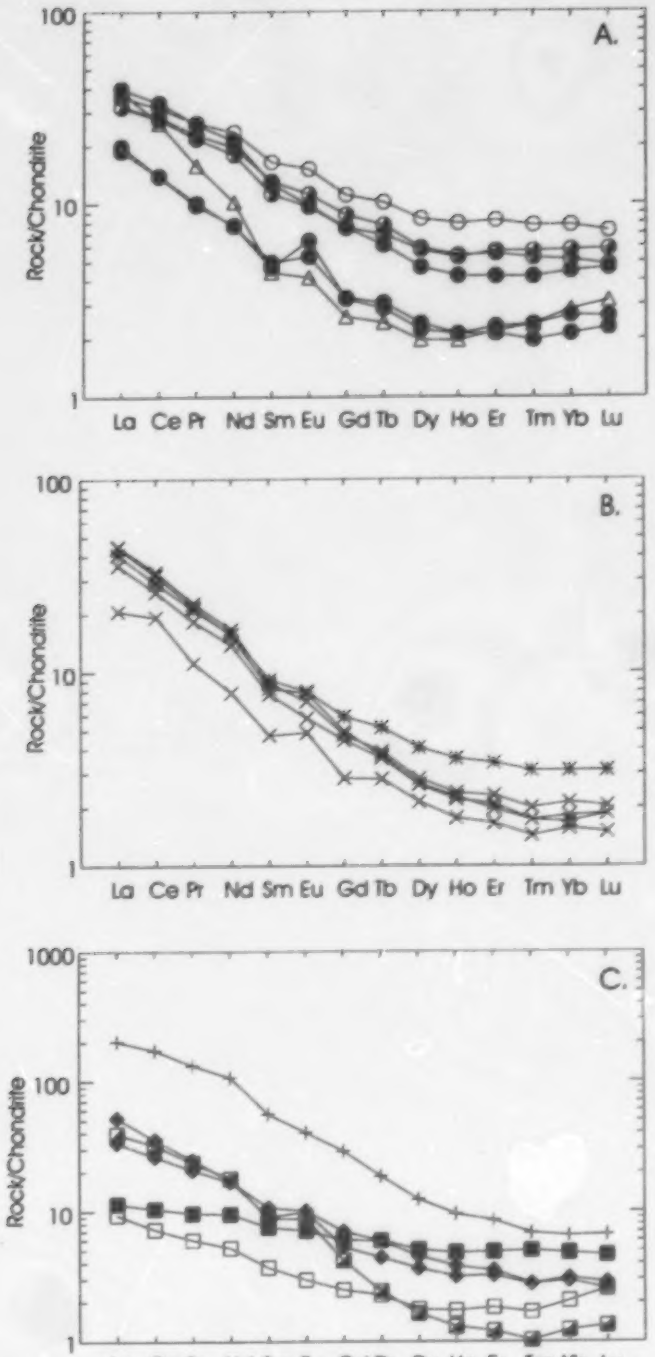

Figure 14 - Chondrite-normalized REE plots for the Nistoassini Lakes Pluton (A), Umpherville Lake Granite (B), and other intrusive rocks (C). Normalizing values are from Sun (1982). Symbols as in Figure 9.

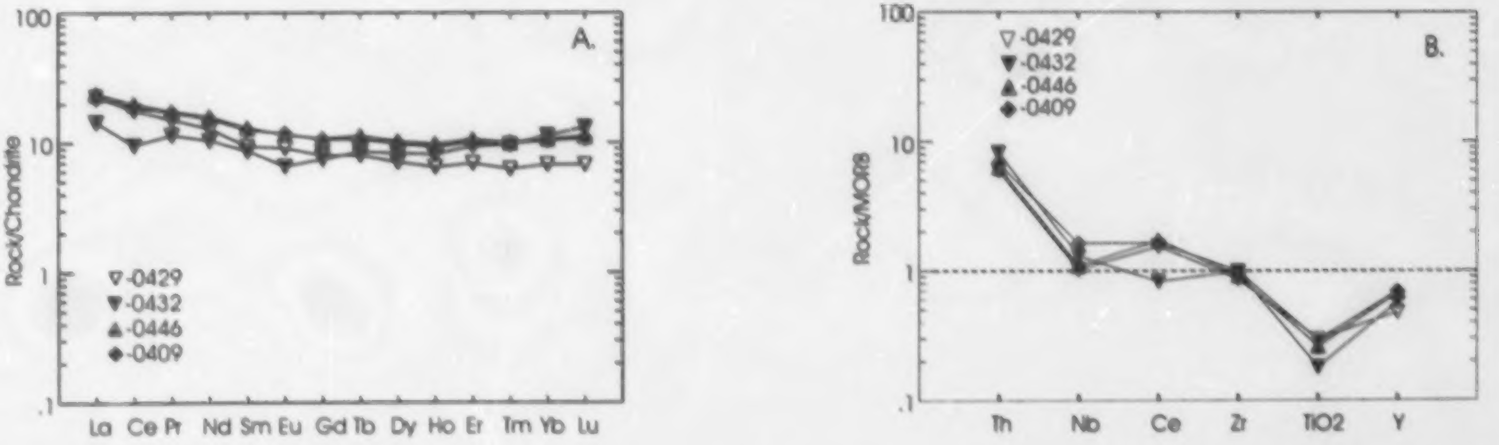

Figure 15 - Altered dacitic volcanics from May Lake area. A) Chondrite-normalized REE profiles; B) MORB-normalized discriminant profiles. Normalizing values as in Figures 7 and 6 respectively.

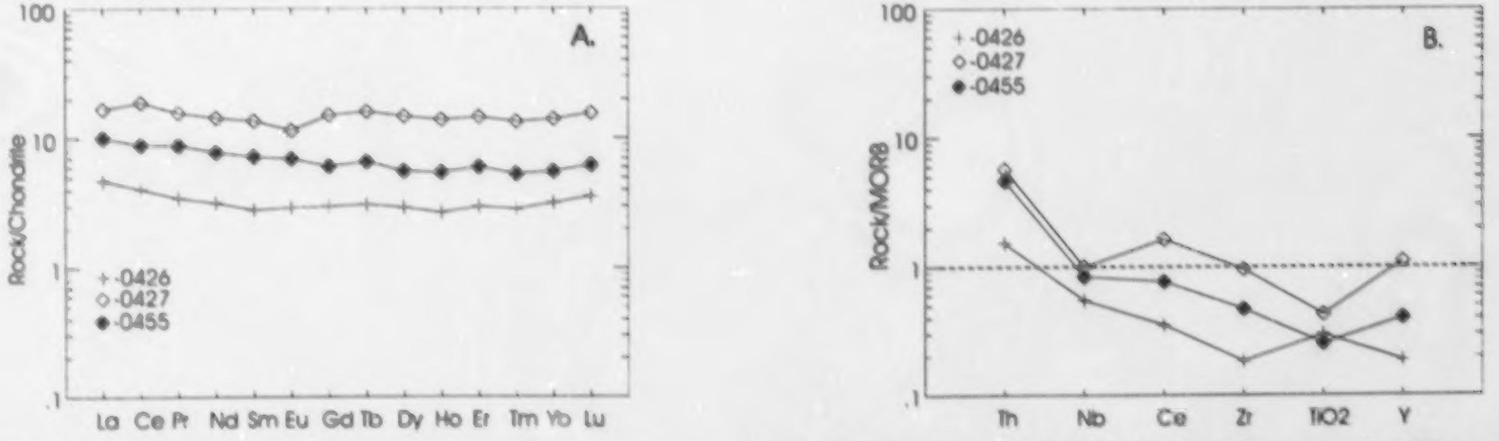

Figure 16 - Garnet-anthophylite-cordierite rocks and sulphide zone mineralization from northeast part of area. A) Chondrite-normalized REE profiles; B) MORB-normalized discriminant profiles.

Of the three quartz veins sampled, the one associated with the altered diorite, sample 9911-0132, has the highest Au content at 47 ppb (Table 2). This pyritic quartz vein contained fragments of altered wall rock, and thus has the lowest silica content, 78.4%, but has higher contents of the other major and trace elements. Sample 9911-0271, a smoky quartz vein cutting rhyolite at McKenzie Lake, was collected because of its dark colour. The material is almost pure quartz at 96.49% SiO_2, with nothing in its chemical composition indicates a cause for the smoky habit. In thin section the quartz exhibits strong undulose extinction, which might be a cause of the dark colour. Quartz vein sample 9911-0306 occurred in weakly altered mafic volcanics adjacent to Nistassini Lakes Pluton and, although it contains only weakly elevated Cu and Au concentrations, it is still indicative of hydrothermal processes having been active and; therefore, of the potential for gold mineralization to exist.

5. Summary

The available data for the May Lake volcanics indicates that they are typically subalkaline, with a predominantly tholeiitic to calc-alkaline trend, and are representative of subduction-related, island arc volcanics. The upper rhyolites probably have a different magma source as would be expected from the suspected younger, ca. 1830 to 1840 Ma, period of magmatism. The intrusive rocks are typical of the La Ronge Domain, as they are calc-alkaline, and display volcanic arc affinity. The presence of anomalous Au concentrations in rocks from different geologic settings indicates the potential for finding such occurrences in the under explored May Lake area.

6. References

Batchelor, R.A. and Bowden, P. (1985): Petrogenetic interpretation of granitoid rock series using multicationic parameters; Chem. Geol., v48, p43-55.

Byers, A.R. (1948): The geology of the Waddy Lake area, Rottenstone Mining Division, Saskatchewan; Sask. Dep. Miner. Resour., Rep. 1, 36p.

Christiansen, E.H. and Keith, J.D. (1996): Trace element systematics in silicic magmas: A metallogenic perspective; *in* Wyman, D.A. (ed.), Trace Element Geochemistry of Volcanic Rocks: Applications for Massive Sulphide Exploration, Geol. Assoc. Can., Short Course Notes Vol. 12, p115-152.

Harper, C.T. (1985): Bedrock geological mapping, Waddy-Tower lakes area (part of NTS 64D-4 and -5 and 74A-1 and -8); *in* Summary of Investigations 1985, Saskatchewan Geological Survey, Sask. Energy Mines, Misc. Rep. 85-4, p 6-17.

_________ (1996): La Ronge–Lynn Lake Bridge Project: Sucker Lake–Fleming Lake area; *in* Summary of Investigations 1996, Saskatchewan Geological Survey, Sask. Energy Mines, Misc. Rep. 96-4, p66-78.

_________ (1997): Sucker Lake–Fleming Lake update; *in* Summary of Investigations 1997, Saskatchewan Geological Survey, Sask. Energy Mines, Misc. Rep. 97-4, p42-50.

_________ (1998): The La Ronge Domain–Glennie Domain transition: Street Lake area (parts of NTS 64D-3 and -6); *in* Summary of Investigations 1998, Saskatchewan Geological Survey, Sask. Energy Mines, Misc. Rep. 98-4, p66-80.

_________ (1999): Geology and mineral potential of the northwest margin of the Central Metavolcanic Belt, May Lake area (part of 64D-05); *in* Summary of Investigations 1999, Volume 2, Saskatchewan Geological Survey, Sask. Energy Mines, Misc. Rep. 99-4.2, p181-195.

Harper, C.T., Thomas, D.J., and Watters, B.R. (1986): Geology and petrochemistry of the Star-Waddy lakes area, Saskatchewan; *in* Clark, L.A. (ed.), Gold in the Western Shield, CIM Spec. Vol. 38, p57-85.

Irvine, T.N. and Baragar, W.R. (1971): A guide to the chemical classification of the common volcanic rocks; Can. J. Earth Sci., v8, p523-548.

Jensen, L.S. (1976): A new cation plot for classifying subalkalic volcanic rocks; Ont. Geol. Surv., Misc. Pap. 66, 22p.

Johnston, W.G.Q. (1970): The geology of the May Lake area (east half), Saskatchewan; Sask. Dep. Miner. Resour., Rep. 130, 36p.

_________ (1973): The geology of the May Lake area (northwest quarter), Saskatchewan, Sask. Dep. Miner. Resour., Rep. 149, 43p.

Maniar, P.D. and Piccoli, P.M. (1989): Tectonic discrimination of granitoids; Geol. Soc. Amer. Bull., v101, p635-643.

Pearce, J.A. (1996): A user's guide to basalt discrimination diagrams; *in* Wyman, D.A. (ed.), Trace Element Geochemistry of Volcanic Rocks: Applications for Massive Sulphide Exploration, Geol. Assoc. Can., Short Course Notes, Vol. 12, p79-114.

Pearce, J.A. and Cann, J.R. (1973): Tectonic setting of basic volcanic rocks determined using trace element analysis; Earth Planet. Sci. Lett., v19, p290-300.

Pearce, J.A., Harris, N.B.W., and Tindle, A.G. (1984): Trace element discrimination diagrams for the tectonic interpretation of granitic rocks; J. Petrol., v25, p956-983.

Sun, S.S. (1982): Chemical composition and origin of the earth's primitive mantle; Geochim. Cosmochim. Acta, v46, p179-192.

Syme, E.C., Bailes, A.H., Stern, R.A., and Lucas, S.B. (1996): Geochemical characteristics of 1.9 Ga tectonostratigraphic assemblages and tectonic setting of massive sulphide deposits in the Proterozoic Flin Flon Belt, Canada; *in* Wyman, D.A. (ed.), Trace Element Geochemistry of Volcanic Rocks: Applications for Massive Sulphide Exploration, Geol. Assoc. Can., Short Course Notes Vol. 12, p279-328.

Watters, B.R. and Pearce, J.A. (1987): Metavolcanic rocks of the La Ronge Domain in the Churchill Province, Saskatchewan: Geochemical evidence for a volcanic arc origin; *in* Pharaoh, T.C., Beckinsale, R.D., and Rickard, D. (eds.), Geochemistry and Mineralization of Proterozoic Volcanic Suites, Geol. Soc., Spec. Publ. No. 33, p167-182.

Winchester, J.A. and Floyd, P.A. (1977): Geochemical discrimination of different magma series and their differentiation products using immobile elements; Chem. Geol., v20, p325-343.

Wood, D.A. (1980): The application of a Th-Hf-Ta diagram to problems of tectonomagmatic classification and to establishing the nature of crustal contamination of basaltic lavas of the British Tertiary volcanic province; Earth Planet. Sci. Lett., v50, p11-30.

Wood, D.A., Joron, J-L., and Treuil, M. (1979): A re-appraisal of the use of trace elements to classify and discriminate between magma series erupted in different tectonic settings; Earth Planet. Sci. Lett., v45, p326-336.

The Round Lake Stock: A Structural Trap for the Emplacement of the Fracture-controlled Komis Gold Deposit in the La Ronge Domain, Northern Saskatchewan

Bruno Lafrance [1]

Lafrance, B. (2000): The Round Lake Stock: A structural trap for the emplacement of the fracture-controlled Komis gold deposit in the La Ronge Domain, northern Saskatchewan; *in* Summary of Investigations 2000, Volume 2, Saskatchewan Geological Survey, Sask. Energy Mines, Misc. Rep. 2000-4.2.

Abstract

The Komis gold deposit occurs in ca. 1880 Ma andesite along the eastern flank of the 1834 Ma Round Lake Stock in the La Ronge Domain. Gold mineralization is associated with north-northwest-trending tensional quartz veins, which cut across andesite, and east-trending granodiorite and aplite dykes of the late stock. Gold occurs as free gold in quartz veins and as disseminations in biotite-pyrite-carbonate alteration haloes surrounding the quartz veins. Large pyrite cubes contain inclusions of recrystallized and deformed dyke material. Pyrite replaces magnetite in epidote-chlorite-magnetite veins cutting the dykes and andesite. The quartz veins and gold mineralization therefore postdate the emplacement of the dykes and stock. The dykes acted as brittle structural traps which localized the flow of the hydrothermal fluids, the emplacement of the quartz veins, and the gold mineralization. Shear-hosted gold occurrences along the Byers Fault, 3 km south of the deposit, have the same alteration and mineralization style as the Komis deposit, suggesting that they formed during the same regional hydrothermal and structural event.

1. Introduction

The Komis deposit is located in the La Ronge Domain, approximately 30 km northwest of the community of Brabant. The deposit was discovered in 1956 by Eric F. Partridge. In 1994, Waddy Lake Resources Ltd. completed an underground exploration drilling program and extracted a bulk sample of the ore. Two years later, the deposit was brought into production. The mine produced 26,885 ounces of gold before it closed down a few months later in 1997 due to declining gold prices (Gracie and Bennett, 1999).

The Komis deposit occurs in metamorphosed andesite and rhyolite [2] along the eastern flank of the Round Lake Stock (Figure 1). Gold mineralization is associated with north-northwest-trending narrow quartz veins, which cut across the northwest-trending metavolcanic rocks. The quartz veins were preferentially emplaced in fractures transecting east-trending granodiorite and aplite dykes, which are apophyses of the Round Lake Stock. Late hydrothermal silica-rich fluids, generated during the emplacement and cooling of the Round Lake Stock, are interpreted as the source of the gold mineralization and quartz (Asbury, 1986).

This study combines observations from surface mapping of mine site exposures, with those from core from six drill holes through the deposit. The study shows that gold mineralization was emplaced during a late hydrothermal event which overprinted the Round Lake Stock and associated dykes. Shear-hosted gold occurrences along the Byers Fault (Lafrance, 1998, 1999), a major east-trending fault zone located only 3 km south of the deposit, have the same mineralization and alteration styles as the Komis deposit. The Komis deposit, and other shear-hosted occurrences in the area, are therefore interpreted as products of the same regional hydrothermal and structural event.

2. Rock Types

The Komis mine is in andesite and rhyolite cut by granodiorite and aplite dykes of the Round Lake Stock (Harper, 1984, 1985). Andesite is the most abundant rock type on the mine site. It occurs as massive flows, lapilli tuffs, and agglomerates. The massive flows are generally light to dark greenish grey, fine-grained, and commonly contain up to 5% hornblende porphyroblasts (2 to 4 mm in size), surrounded by narrow rims of white feldspar. The lapilli tuffs and agglomerates are massive, and consist of 0.3 cm to 75 cm wide mafic volcanic fragments in a fine-grained, grey-green andesitic matrix. They contain rare rhyolite fragments, which are similar to massive rhyolite flows interlayered in the mine sequence. The rhyolite flows are aphanitic, light grey on fresh surface, and weather orange-brown. The outcrop surfaces are typically cut by multiple sets of small fractures, which are conchoidal on fresh surface. A sample of rhyolite collected from the northeasterly trending peninsula in Waddy Lake yielded an U-Pb zircon age of 1880 ±7 Ma (Bickford *et al.*, 1986).

In drill core, a porphyritic andesite or basalt occurs that is coarser-grained than varieties seen in outcrop. This

---

[1] Department of Earth Sciences, Laurentian University, 935 Ramsey Lake Road, Sudbury, ON P3E 2C6.

[2] As all volcanic rocks are metamorphosed, the prefix 'meta' will be dropped in the following discussion.

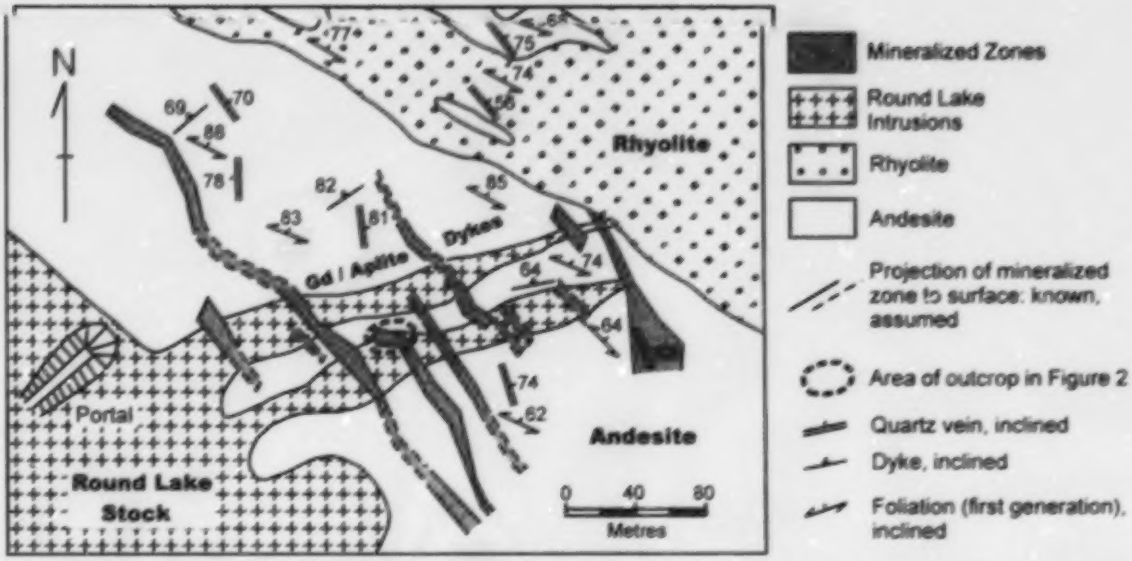

Figure 1 - Surface geological map of the Komis mine site, modified from map by geologists of Waddy Lake Resources Inc. (SEM Assessment File 64D04-NW-0181). Structural measurements by author. Komis Deposit is located at lat. 56° 12' 35" and long. 103° 54' 7".

massive unit called porphyritic greenstone by Asbury (1986), is about 100 m thick (SEM Assessment File 64D04-NW-0181). It is dark green, and medium-grained, with up to 20% hornblende porphyroblasts (grain size of 0.5 cm). This porphyry is interpreted to have formed as a thick massive flow, or a subvolcanic intrusion.

Granodiorite and aplite dykes are apophyses of the 1834 ±13 Ma (Bickford *et al.*, 1986) Round Lake Stock. The granodiorite dykes are compositionally and texturally similar to the granodioritic stock. They are generally less than 1 m wide, medium grained (1 to 2 mm grain size), pale brown to grey on outcrop surface, and light grey on fresh surface. They are massive, unfoliated intrusions, containing approximately 50 to 65% feldspar, 25 to 35% quartz, and 5 to 15% biotite and hornblende. The granodiorite stock and dykes are cut by aplite dykes interpreted to represent the last phase of magma from the cooling intrusion. Some aplite dykes intruded the granodiorite dykes along fractures parallel to the margins of the dykes, whereas others cut across the granodiorite dykes. Aplite dykes are aphanitic to fine-grained, red to pale orange, and typically less than 20 cm wide. They are composed almost exclusively of quartz and feldspar with less than 2% mafic minerals. Some are zoned with cores of massive quartz.

3. Structure

A 30 m wide swarm of granodiorite and aplite dykes extends from the mine's portal, where the Round Lake Stock is exposed, to more than 100 m eastward across the west-northwest-trending volcanic rocks. An early tectonic foliation (S_1) that strikes 300° and dips 70° to the northeast is parallel to the lithological contacts in the volcanic rocks (Harper, 1984, 1985). In rhyolite, S_1 is defined by discrete, mafic mineral-rich surfaces, and in andesite, it is defined by flattened, elongate volcanic fragments, surrounded by amphibole- and biotite-rich films.

The aplite and granodiorite dykes are generally east-trending, with dips ranging from 40° to 80° to the north. The dykes cut across S_1, and appear undeformed, except for the many quartz-filled tensional fractures that dissect them (Figure 2). A few narrow dykes are boudinaged parallel to S_1. Other dykes, trending north, are folded. In the hinge of the folded dykes, S_1 is defined by a strong biotite-rich foliation, which acted as a dextral shear zone along one limb of a fold. Dextral dragging of S_1 is observed along a second 3 cm wide shear zone, striking 326° and dipping 88° to the northeast. In summary, the dykes overprint S_1, but S_1 was locally reactivated during the deformation of the dykes.

Quartz veins were emplaced in fractures, cutting through both volcanic rocks and dykes. The quartz veins are generally steeply dipping and less than 10 cm wide. They are massive and composed of milky white quartz containing minor biotite, muscovite, microcline, pyrite, and gold. A few veins have open median surfaces lined by drusy quartz. Vein walls are coated with chlorite and muscovite in the rhyolite and the dykes, and by biotite and actinolite in andesite.

Swarms of quartz veins invade the dykes. Some occur as ladder veins, which only span the width of the dykes; others are through-going varieties that extend

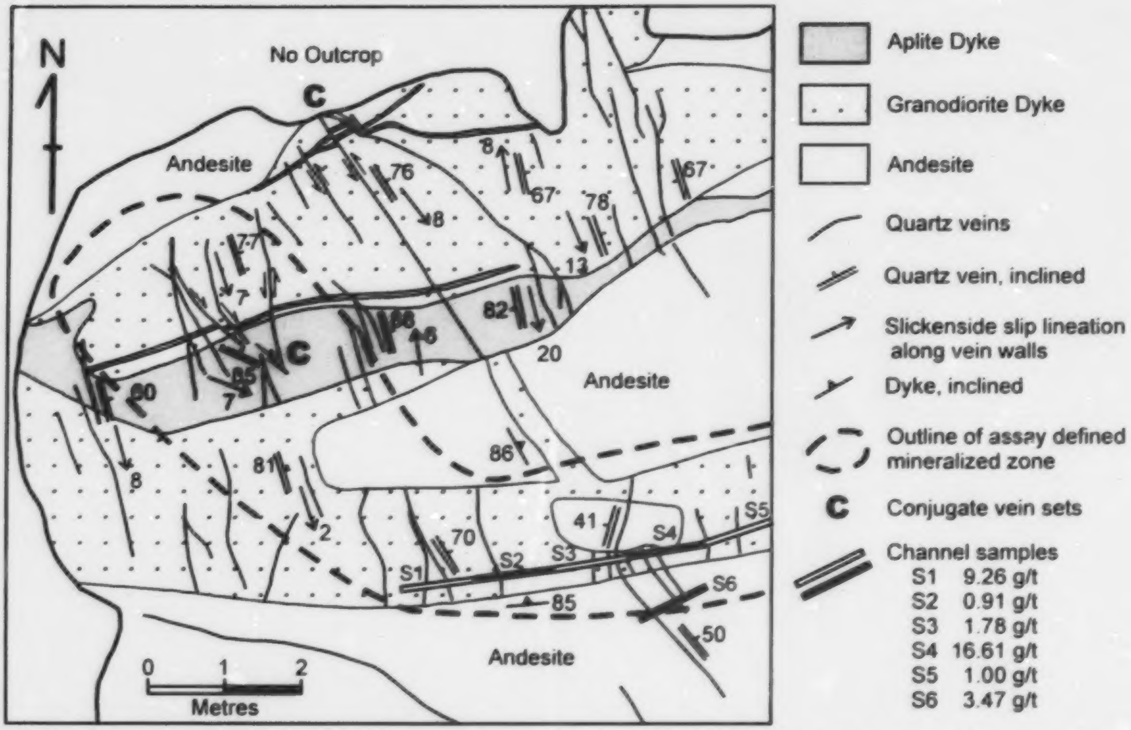
N
No Outcrop
C
Andesite
Andesite
Andesite
76
8
67
78
67
7
7
88
6
82
13
20
85
7
60
8
81
86
2
41
70
S1
S2
S3
S4
S5
S6
85
50
0
1
2
Metres
Aplite Dyke
Granodiorite Dyke
Andesite
Quartz veins
Quartz vein, inclined
Slickenside slip lineation along vein walls
Dyke, inclined
Outline of assay defined mineralized zone
Conjugate vein sets
Channel samples
S1 9.26 g/t
S2 0.91 g/t
S3 1.78 g/t
S4 16.61 g/t
S5 1.00 g/t
S6 3.47 g/t

Figure 2 - Outcrop map of east-trending dykes cut by north-northwest-trending quartz veins. The outline of the assay-defined mineralized zone is shown by heavy broken lines. Modified from map by Ian Fraser of Waddy Lake Resources Inc. (SEM Assessment File 64D04-NW-0181). Structural measurements and conjugate vein sets "C" added by author.

across the dykes into the volcanic rocks. The through-going quartz veins strike 335° in the volcanic rocks, but are refracted 5° clockwise as they pass into the more competent dykes. In a mineralized zone exposed on surface, a large dyke is transected by two conjugate sets of steeply-dipping quartz veins. One set of veins was emplaced along sinistral fractures trending 330° and the other along dextral fractures trending 290°. Slickensides along the vein walls of the sinistral veins plunge 12° towards 155°. The orientation of the veins and shallow plunge of the slickensides suggest that the fractures and veins formed during near horizontal north-northwest compression.

4. Alteration and Mineralization

Gold mineralization is associated with sulphidic and potassic alteration of andesite. Narrow quartz veins are surrounded by wide alteration haloes of biotite, carbonate, and pyrite, with minor epidote, microcline, and apatite. For example, a 3 cm wide vein is typically mantled by a 15 cm wide alteration halo. Altered andesite next to the quartz vein contains up to 5% well-formed pyrite cubes, referred to locally as "Komis pyrite". Andesite underwent strong silicification next to some quartz veins.

Several aplite and granodiorite dykes, up to 1 m wide, are surrounded by 4 to 10 cm thick sulphidic and potassic alteration haloes. Pyrite occurs as disseminations in the wall rocks, and as fracture-fillings in thin quartz-biotite-pyrite stockwork fractures. The granodiorite-aplite dykes were also weakly silicified and altered to muscovite, biotite, and chlorite during the hydrothermal event. Pyrite cubes in the dykes contain inclusions of deformed and partially recrystallized quartz and feldspar, suggesting that the deformation of the dykes occurred either before or during the quartz hydrothermal event.

Gold is associated with pyrite in the alteration envelopes of both quartz veins and dykes. It also occurs as free gold in the quartz veins. Although gold is found in the altered wall rocks of the dykes, gold grades increase significantly where through-going quartz veins pass into andesite (SEM Assessment File 64D04-NW-0181). Gold has also been found in rhyolite, but most economic mineralized zones are in andesite with crosscutting dykes and through-going quartz veins.

Irregular lenses and veins of epidote, chlorite, quartz, and magnetite cut across S_1, and the Round Lake intrusions. This metasomatic event possibly resulted from late hydrothermal activity during emplacement and cooling of the intrusions. Where quartz veins are in contact with the epidote-chlorite-magnetite veins, Komis pyrite replaces magnetite. Thus, this early metasomatic event predates that associated with the gold mineralization.

5. Discussion and Conclusions

The Komis deposit has been interpreted as an intrusion-related gold deposit, which formed during the emplacement and cooling of the Round Lake Stock (Asbury, 1986). Several lines of evidence, however, suggest that the deposit was emplaced during a late regional structural and hydrothermal event which overprinted the Round Lake Stock and dykes. These include:

1) The gold-bearing quartz veins cut across the Round Lake Stock and dykes. Hydrothermal muscovite, biotite, and chlorite overprint the dykes.
2) Although hydrothermal alteration haloes surround some of the dykes, gold grades are preferentially enriched where the dykes are cut by through-going quartz veins which extend into andesite. Komis pyrite in the dykes contains inclusions of deformed and recrystallized dyke material, indicating that the dykes underwent solid-state deformation prior to the formation of the quartz veins. Thus, the dykes acted as competent solid bodies which localized brittle fracturing and the flow of hydrothermal mineralizing fluids. They were therefore structural traps for the gold mineralization.
3) Komis pyrite replace magnetite in epidote-chlorite-magnetite veins. This early epidote metasomatic event, which overprints the dykes and the Round Lake Stock, possibly resulted from the activity of late hydrothermal fluids during the emplacement and cooling of the intrusions. Thus, the Komis pyrite and gold mineralization overprint an early metasomatic event possibly associated with the Round Lake intrusions.
4) Gold deposits along the Byers Fault system, to the south of Komis, are hosted by shear zones which cut the margins of late stocks that are mineralogically similar to the Round Lake Stock (Harper, 1984, 1985). Furthermore, the mineralized quartz veins are surrounded by potassic and sulphidic alteration envelopes which are similar to the alteration haloes surrounding quartz veins of the Komis deposit (Netolitzky, 1986; Schwann, 1990, 1991).
5) The contraction of north-trending dykes, together with the extension of the east-trending dykes and the formation of north-northwest-trending tensional quartz veins (≈330°), suggest that the dykes were deformed, and the quartz veins were emplaced, during a north-northwest-directed compressive event. The orientation of the conjugate vein systems, and the shallow plunge of slickenside lineations along the vein walls support this interpretation. North-northwest compression is consistent with dextral transpressional shearing along the east-trending Byers Fault system (Lafrance, 1999), which, as noted above, hosts several gold deposits that have similar alteration and mineralization styles as the Komis deposit.

6. Acknowledgments

Aaron Grimeau is thanked for excellent field assistance. The study was funded through a Laurentian University Research Fellowship and field support from Saskatchewan Energy and Mines.

7. References

Asbury, B.C. (1986): The Komis Gold Deposit and EP Zone, Waddy Lake area, Saskatchewan; *in* Clark, L.A. (ed.), Gold in the Western Shield, Can. Inst. Min. Metall., Spec. Vol. No. 38, p221-228.

Bickford, M.E., Van Schmus, W.R., Macdonald, R., Lewry, J.F., and Pearson, J.G. (1986): U-Pb zircon geochronology project for the Trans-Hudson Orogen: Current sampling and recent results; *in* Summary of Investigations 1986, Saskatchewan Geological Survey, Sask. Energy Mines, Misc. Rep. 86-4, p101-107.

Gracie, A.J. and Bennett, R.W. (1999): Saskatchewan exploration and development highlights 1999; Sask. Energy Mines, 14p.

Harper, C.T. (1984): Geological mapping, Waddy Lake area (part of NTS 64D-4 and -5); *in* Summary of Investigations 1984, Saskatchewan Geological Survey, Sask. Energy and Mines, Misc. Rep. 84-4, p6-20.

__________ (1985): Bedrock geological mapping, Waddy-Tower lakes area (part of NTS 64D-4 and -5 and 74A-1 and -8); *in* Summary of Investigations 1985, Saskatchewan Geological Survey, Sask. Energy and Mines, Misc. Rep. 85-4, p6-17.

Lafrance, B. (1998): Pre-tectonic and syn-faulting gold mineralization in the Byers Fault area, La Ronge Domain; *in* Summary of Investigations 1998, Saskatchewan Geological Survey, Sask. Energy and Mines, Misc. Rep. 98-4, p123-128.

__________ (1999): Gold studies in the Byers Fault-Waddy Lake area, La Ronge Domain; *in* Summary of Investigations 1999, Volume 2, Saskatchewan Geological Survey, Sask. Energy and Mines, Misc. Rep. 99-4.2, p202-207.

Netolitzky, R.K. (1986): An exploration review of the Weedy Lake, Tower Lake, and Wedge Lake gold deposits, Saskatchewan; *in* Clark, L.A. (ed.), Gold in the Western Shield, Can. Inst. Min. Metall., Spec. Vol. No. 38, p229-252.

Schwann, P.L. (1990): Field observations on the Corner Lake and Tower Lake East gold showings, Byers Fault area; *in* Summary of Investigations 1990, Saskatchewan Geological Survey, Sask. Energy Mines, Misc. Rep. 90-4, p60-63.

__________ (1991): Field observations on the Broken Hammer gold occurrence and NIKO gold deposits; *in* Summary of Investigations 1991, Saskatchewan Geological Survey, Sask. Energy Mines, Misc. Rep. 91-4, p93-100.

Nd Isotope Geochemistry of Igneous Rocks in the Glennie Domain and its Immediate Sub-Phanerozoic Extension: Evidence for Interactions with the Sask Craton?

Tim C. Prokopiuk [1] *and Kevin M. Ansdell* [1]

Prokopiuk, T.C. and Ansdell, K.M. (2000): Nd isotope geochemistry of igneous rocks in the Glennie Domain and its immediate Sub-Phanerozoic extension: Evidence for interactions with the Sask Craton?; *in* Summary of Investigations 2000, Volume 2, Saskatchewan Geological Survey, Sask. Energy Mines, Misc. Rep. 2000-4.2

Abstract

The Nd isotopic composition of mafic and granitoid igneous rocks from the Glennie Domain, and from drillcore immediately to the south of the Phanerozoic-Precambrian unconformity were used to provide: (1) constraints on the isotopic composition of the Paleoproterozoic mantle, (2) evidence for the initial interaction between the Archean Sask Craton and the juvenile rocks of the Trans-Hudson Orogen, and (3) the present extent of the Sask Craton. The age of the mafic volcanic rocks from the southern Glennie Domain and the Sub-Phanerozoic are not known, but are assumed to be ca. 1880 to 1850 Ma. The ε_{Nd} *(1850 Ma) values range from +3.8 to +1.3, which suggests that these mafic magmas were likely derived from a similar heterogeneous mantle to that which yielded the ocean floor rocks of the Flin Flon Domain. The lower values may provide evidence for a small amount of interaction of this magma with older crustal materials. Three granitoids in the southern Glennie Domain have U-Pb ages of ca. 1832 Ma and are thus broadly coeval with the collision between the Sask Craton and the Flin Flon–Glennie complex, whereas the Wapawekka Lake pluton is ca. 1850 Ma. The latter has an* ε_{Nd} *(1850 Ma) value of +3.2, whereas the former have* ε_{Nd} *(1832 Ma) values of +0.9 to +1.7. The Wapawekka Lake pluton was probably derived from a similar source as the mafic volcanic rocks or by melting of relatively young arc crust, whereas the younger plutons may have crystallized from magmas that had undergone up to 20% contamination by Archean crustal material. The nature of this older crust is unknown, but may represent the Sask Craton itself. These granitic magmas may thus be recording the arrival of the Sask Craton in the Trans-Hudson Orogen. The granitoid rocks from the Sub-Phanerozoic have significantly lower* ε_{Nd} *(1850 Ma) values ranging from -3.8 to -8.6, and thus have undergone significant interaction with older crust or are actually Archean in age. The lowest* ε_{Nd} *value obtained in this study is from a ca. 1780 Ma pegmatite from the northern Glennie Domain. The* ε_{Nd} *(1780 Ma) of -10.6 indicates that the pegmatitic melt was probably derived by melting of the northern buried extension of the Sask Craton, as imaged on LITHOPROBE seismic line S2b.*

1. Introduction

The Trans-Hudson Orogen (THO) is a Paleoproterozoic zone of orogenesis extending from Greenland, through central Canada, and into the northern United States (Hoffman, 1988). The THO comprises a collage of accreted intraoceanic terranes (Reindeer Zone) and reworked continental margins (Lewry and Collerson, 1990), and formed in response to the collision of the Archean Hearne and Superior cratons (Bickford *et al.*, 1990), and a third Archean craton, the Sask Craton, which drifted northwards between the Superior and Hearne cratons from about 1.83 to 1.80 Ga (Ansdell *et al.*, 1995).

The Sask Craton outcrops in structural windows located in the Flin Flon–Glennie complex (Figure 1; Chiarenzelli *et al.*, 1998; Ashton *et al.*, 1999), but extends into the subsurface as a crustal-scale anticlinorium which is separated from the bounding Superior and Hearne cratons by Paleoproterozoic crust. The geometry of this craton has been estimated from LITHOPROBE and COCORP seismic sections (Lucas *et al.*, 1993; Nelson *et al.*, 1993; Lewry *et al.*, 1994; Baird *et al.*, 1996), whereas its extent has been estimated from Nd and Pb isotope analyses of post-collisional pegmatites in the exposed THO (Steinhart *et al.*, 1997; Ansdell and Stern, 1997), and Precambrian rocks intersected in drill holes through the Phanerozoic cover (Collerson *et al.*, 1988). Together, these methods have shown that the Sask Craton extends over 1000 km under the Phanerozoic cover and tapers northwards towards the northern end of the Glennie Domain. Although geophysical anomalies have been used to extrapolate the Paleoproterozoic elements of the THO southwards (e.g. Green *et al.*, 1985), geochronological and isotopic data suggest that the volume of juvenile Paleoproterozoic crust is probably insignificant below the Phanerozoic cover (Collerson *et al.*, 1988). The character of this southward change in age and isotopic composition of the Precambrian rocks is, however, unknown.

One of the problems is that the Nd isotopic composition of magmatic rocks in the Glennie Domain, other than post-collisional pegmatites (Bickford *et al.*, 1992), are poorly known, and thus it is unclear whether the older igneous rocks may record

---

[1] Department of Geological Sciences, University of Saskatchewan, 114 Science Place, Saskatoon, SK S7N 5E2.

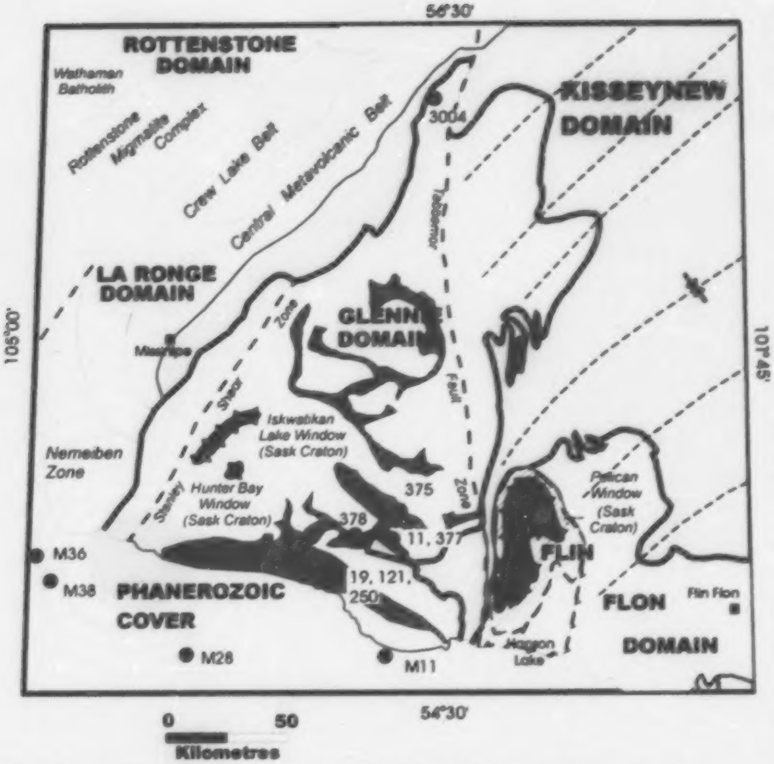
56°30'
ROTTENSTONE DOMAIN
Wathaman Batholith
Rottenstone Migmatite Complex
Crew Lake Belt
Central Metavolcanic Belt
3004
KISSEYNEW DOMAIN
Tabbernor Fault Zone
LA RONGE DOMAIN
105°00'
GLENNIE DOMAIN
Missinipe
Stanley Shear Zone
Iskwatikan Lake Window (Sask Craton)
Nemeiben Zone
Hunter Bay Window (Sask Craton)
375
378
11, 377
Pelican Window (Sask Craton)
101°45'
FLIN
M36
M38
PHANEROZOIC COVER
19, 121, 250
FLON
DOMAIN
Flin Flon
Hanson Lake
M28
M11
0
50
Kilometres
54°30'

Figure 1 - Simplified geological map of the Glennie Domain, and surrounding Paleoproterozoic terranes of the Reindeer Zone of the Trans-Hudson Orogen (after Ashton, 1999; Delaney, 1992). The Flin Flon–Glennie Complex comprises the Glennie and Flin Flon domains. The grey-shaded regions in the Glennie Domain are greenstone belts. The location of samples are indicated by the collar of the drill hole for the Sub-Phanerozoic samples, and the location of outcrops in the exposed shield. The complete sample numbers are shown in Table 1.

interaction with Archean crust. Thus, these rocks may have a significantly different Nd isotopic composition from lithologically similar arc and ocean floor rocks in the Flin Flon Domain (Stern *et al.*, 1995a, 1995b; Whalen *et al.*, 1999). In addition, extrapolation of geophysical anomalies over long distances is difficult, and in fact Green *et al.* (1985) indicate that the southward extension of the Glennie Domain is particularly inconclusive. Thus, it is difficult to relate the isotopic data obtained from drill holes across the whole of southern Saskatchewan with specific regions within the exposed THO. In order to address some of these problems, it was decided to determine the Nd isotopic composition of pre- and post-collisional igneous rocks in the Glennie Domain. The former included mafic volcanic rocks, which are assumed to provide an indication of the Nd isotopic composition of the Paleoproterozoic mantle. The latter included ca. 1.83 Ga granitoid rocks, interpreted to have been intruded synchronous with the development of regional scale thrust faults related to the first interactions between the Reindeer Zone and the Sask Craton (Ansdell *et al.*, 1995; Ashton *et al.*, 1999). It was also decided to analyze magmatic rocks from drill holes closest to the Phanerozoic unconformity to provide the most reasonable basis for the southward extrapolation of data from the exposed THO.

2. Sampling and Analytical Techniques

Samples (Figure 1) were chosen from the rock collections at Saskatchewan Energy and Mines, and consisted of either powders, outcrop samples, or drillcore. The absolute age of the samples was either known, or assumed from well-understood geological relationships. The only sample located at a significant distance from the contact with the Phanerozoic rocks is 9811-3004, a ca. 1780 Ma post-collisional pegmatite, which was used to help delineate the northern extent of the Sask Craton.

Nd isotope analyses were performed at the University of Saskatchewan, and the results reported in Table 1. Rock and drillcore samples were jaw-crushed and ground in a tungsten carbide swing mill. Powdered samples were completely spiked with the appropriate amount of a mixed ^{149}Sm-^{150}Nd tracer solution prior to digestion in HF-HNO$_3$ in screwtop Teflon containers. Sm and Nd were separated using standard cation-exchange procedures, prior to loading on outgassed rhenium filaments with H_3PO_4 and 2.0N HCl. Isotopic analyses were performed in static mode on a Finnigan MAT 261 mass spectrometer. Spike unmixing, and mass fractionation corrections were performed offline, and used the following normalization ratios: ^{146}Nd/^{144}Nd=0.7219 and ^{148}Sm/^{154}Sm=0.49419. Analyses of standards during the course of this project yielded the following values: La Jolla Nd standard yielded a ^{143}Nd/^{144}Nd value of 0.511835 ±9; Ames Nd standard yielded an average ^{143}Nd/^{144}Nd value of 0.512102 ±11 (n=3); and Ames Sm standard ^{149}Sm/^{154}Sm a value of 0.60751 ±3. The epsilon Nd (ε_{Nd}) values at the present or at the age of the rock were calculated using the following reference values: ^{143}Nd/^{144}Nd CHUR (present)=0.512638 and ^{147}Sm/^{144}Nd CHUR (present)=0.1966 (Goldstein *et al.*, 1984). The T_{DM} values were calculated using the following reference values: ^{143}Nd/^{144}Nd Depleted Mantle (present)=0.51316 and ^{147}Sm/^{144}Nd Depleted Mantle (present)=0.2141 (Goldstein *et al.*, 1984). Procedural blanks are about 100 pg Nd and 30 pg Sm, but are insignificant for these samples.

Table 1 - Analytical data.

Sample	UTM	UTM	Location	Rock Type	Sm (ppm)	Nd (ppm)	^{147}Sm/^{144}Nd	^{143}Nd/^{144}Nd*	εNd (0)	T_{DM} (Ga)	Age (Ma)	ε_{Nd} (Age)
Sub-Phanerozoic												
M11	6062071	589147	Selco Ballantyne Bay: 207'	granite pegmatite	8.88	36.19	0.14829	0.511853 ±20	-15.3	3.01	1850	-3.8
M28A	6053585	532278	Anglo-American Wapawekka #3: 1001'	mafic volcanic	4.54	22.71	0.12073	0.511908 ±21	-14.2	2.04	1850	+3.8
M28E	6053585	532278	Anglo-American Wapawekka #3: 1052'	mafic volcanic	4.78	20.59	0.14025	0.512018 ±07	-12.1	2.35	1850	+1.3
M36B	6096741	446716	DMR Morin Lake: 289'	granite	0.61	3.76	0.09736	0.511195 ±16	-28.2	2.55	1850	-4.6
M38A	6083570	466864	DMR La Ronge: 523'	granitic gneiss	7.53	50.85	0.08944	0.510894 ±12	-34.0	2.75	1850	-8.6
Southern Glennie Domain												
8822-11	6091500	561350	Brownell Lake	mafic volcanic	1.95	5.36	0.21956	0.513076 ±21	8.6	—	1850	+3.1
8922-121	6088740	547480	Wapawekka Lake	mafic volcanic	3.49	13.72	0.15363	0.512286 ±08	-6.9	2.19	1850	+3.4
8922-250	6087820	537150	Wapawekka Lake	mafic volcanic	2.01	7.70	0.15737	0.512293 ±20	-6.7	2.32	1850	+2.6
8822-375	6099590	583560	Carroll Lake Block	granodiorite	3.55	20.85	0.10287	0.511591 ±44	-20.4	2.14	1833†	+1.7
8822-377	6092960	581760	Brownell Lake Pluton	granite	5.10	33.94	0.09079	0.511420 ±19	-23.8	2.14	1831†	+1.1
8822-378	6095750	570360	Maynard Creek Pluton	granodiorite	3.64	25.59	0.08594	0.511346 ±10	-25.2	2.15	1832†	+0.9
8922-19	6092075	542400	Wapawekka Lake	granodiorite	2.23	12.83	0.10509	0.511684 ±09	-18.6	2.06	1850	+3.2
Northern Glennie Domain												
9811-3004	5981880	624092	Gloeckler Lake	granite pegmatite	5.67	19.02	0.18002	0.511900 ±39	-14.4	---	1780	-10.6

Notes: Footage represents depths measured down the length of the core.
* errors reported to $2\sigma \times 10^{-6}$
† U-Pb zircon ages (from McNicoll *et al.*, 1992); all other ages assumed for comparative purposes.

3. Discussion of Results

Analytical results are provided in Table 1 and include ε_{Nd} values at present ($\varepsilon_{Nd}(0)$) and at the assumed or U-Pb age of the rock (ε_{Nd} (Age)). These values are an indicator of the Nd isotopic composition of the sample relative to that of the bulk earth, or CHUR (chondritic uniform reservoir) (DePaolo and Wasserburg, 1976), at the present and at the age of the rock. Negative values for an igneous rock at its crystallization age implies that the magma resulted from partial melting of, or interaction with a long-term LREE-enriched source, such as older crust, whereas positive values suggest derivation direct from a LREE-depleted source, such as the depleted mantle. The depleted mantle model age (T_{DM}) represents the amount of time that has elapsed since the sample had the same ^{143}Nd/^{144}Nd ratio as the depleted mantle source region, and gives an approximate idea as to the age of the crust from which the magma was generated. The Nd isotopic composition of rocks are typically preserved during weathering, sedimentation, and metamorphism, although McCulloch and Black (1984) and Barovich and Patchett (1991) indicated that Sm and Nd can be redistributed during upper amphibolite to granulite facies metamorphism, and mylonitization, respectively. None of the samples analyzed exceed upper amphibolite facies conditions, nor are they highly deformed, and so it is assumed that the Sm-Nd isotope systematics are representative of their initial values. The Nd isotope evolution lines for the samples in this study are shown in Figure 2.

a) Mafic Rocks

Southern Glennie Domain

Samples 8822-11, 8922-121, and 8922-250 are tholeiitic arc or ocean floor basalts from the Brownell-Wapawekka lakes greenstone belt in the southern part of the Glennie Domain (Delaney, 1992). The age of these rocks is unknown, although they predate the ca. 1850 Ma granitoids and may be as old as ca. 1880 Ma (McNicoll *et al.*, 1992). The age used in Table 1 is 1850 Ma, and thus the ε_{Nd} (Age) value of the mafic rocks can be used to determine whether the mafic magmas may have resulted from melting of the recently formed volcanic pile. Extrapolation of the ε_{Nd} values to 1880 Ma does not affect the interpretations made here.

At 1850 Ma, the mafic rocks have ε_{Nd} values between +2.6 and +3.4, which indicate that the mafic melts could not be derived by melting of the depleted mantle of Goldstein *et al.* (1984) (Figure 2). However, Stern *et al.* (1995a) argued, from combined geochemical and isotopic data of mid-ocean ridge and ocean island basalts, that the Nd isotopic composition of the Paleoproterozoic mantle below the Flin Flon Domain was heterogeneous and ranged from +5.4 to +2.2. The three samples from the southern Glennie Domain are within this range, and thus could be explained by derivation from similar mantle sources. The extent of interaction with newly formed and thus slightly older Paleoproterozoic crust, or even small amounts of Archean crust, cannot be determined using Nd isotopes only and must await more detailed trace element analyses. In addition, a better understanding of the petrogenesis of these rocks requires trace element analyses.

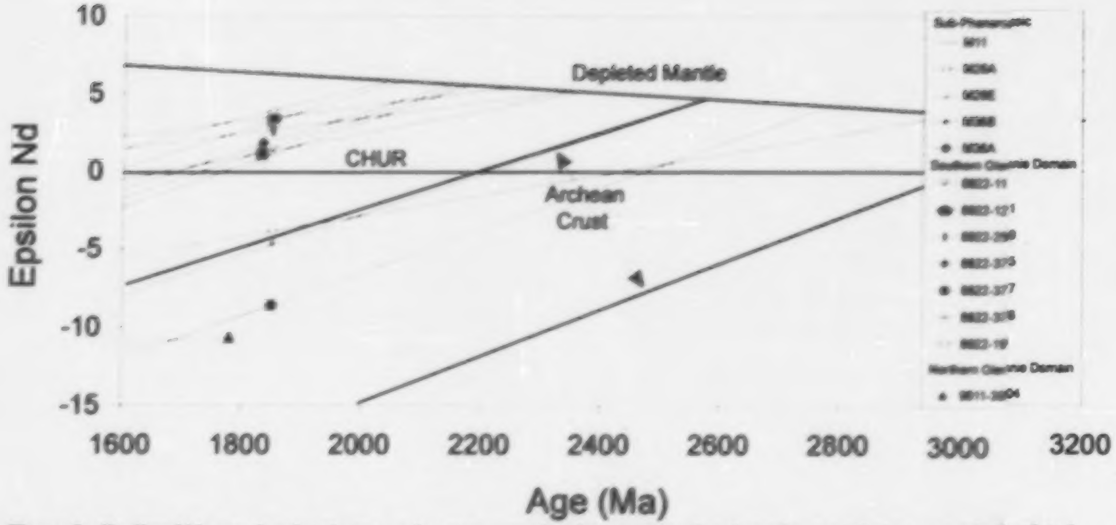

Figure 2 - Epsilon Nd-age plot showing ε_{Nd} value at assumed or known age of rock, and extrapolation towards Depleted Mantle. The field for Archean crust is after Collerson et al. *(1988) and Ansdell and Bleeker (1997), and Depleted Mantle is after Goldstein* et al. *(1984).*

Sub-Phanerozoic

M28A and M28E are samples of amphibolite grade mafic volcanic rocks from a drill hole located to the south of the Glennie Domain. They have ε_{Nd} values at 1850 Ma of +3.8 and +1.3, respectively. The best interpretation for M28A is that the mafic magma was derived from a similar source as the mafic volcanic rocks in the southern Glennie Domain, and is probably Paleoproterozoic in age. The ε_{Nd} value of +1.3 obtained from M28E is similar to the lower values obtained from arc rocks in the Flin Flon Domain (Stern *et al.*, 1995b), and may provide evidence for the interaction of this magma with older crustal materials. However, this material may have been Paleoproterozoic sediment which contained minor amounts of recycled Archean or earlier Proterozoic clastic detritus.

Overall, the ε_{Nd} values of the mafic volcanic rocks are similar to other juvenile Paleoproterozoic mafic volcanic rocks in the THO. The mafic rocks from the Sub-Phanerozoic drillcore do not provide evidence for large-scale interaction with older crust, although they probably formed in an oceanic environment prior to the arrival of the Sask Craton.

b) Granitoid Rocks

Southern Glennie Domain

Four granitoid rocks that intrude the supracrustal rocks of the southern Glennie Domain were analyzed. Three of these yielded similar U-Pb zircon ages of ca. 1832 Ma (Table 1; McNicoll *et al.*, 1992). These granitoids were emplaced broadly synchronous with the initiation of southwest-directed thrusting, which was related to the collision between the Sask Craton and the Flin Flon–Glennie complex (Ansdell *et al.*, 1995; Ashton *et al.*, 1999). Thus, these rocks may record some interaction with the newly arrived Sask Craton. The fourth, the Wapawekka Lake granodiorite, formed during the earlier phase of granitoid magmatism, and is thus assumed to be 1850 Ma.

The ca. 1832 Ma plutonic rocks have very similar Nd isotopic compositions at time of formation (ε_{Nd} values between +0.9 and +1.7; Table 1). In contrast, the Wapawekka Lake granodiorite, which is assumed to be older, has an ε_{Nd} value of +3.2 at 1850 Ma. The latter value lies within the range exhibited by the middle successor arc granitoids in the Flin Flon Domain, whereas the younger granitoids have significantly lower ε_{Nd} values than rocks of the same age in the Flin Flon Domain (Whalen *et al.*, 1999). However, these values are similar to those exhibited by older granitoid rocks (1860 to 1880 Ma) in the Flin Flon Domain, which are thought to have been generated by melting of mantle wedge or juvenile arc crust with subsequent small amounts of contamination by assimilation of older crust.

The best interpretation of the data from the southern Glennie Domain is that the Wapawekka Lake granodioritic magma was derived from a similar source as the mafic volcanic rocks, or by melting of relatively young mantle-derived crust. The 1832 Ma plutons have consistent calculated T_{DM} ages, which suggests that these magmas could have formed by partial melting of 2.14 Ga crust (Figure 2). There is no known crust of this age within the THO, and so these magmas could have formed by either: (1) melting of slightly older basaltic crust, similar in isotopic composition to sample M28E, or (2) contamination of +3.0 magmas with older Archean crust with an ε_{Nd} value of about -10.0 or less. A simple two-component mixing calculation using the following end-member components (granitic magma Nd=30 ppm and ε_{Nd}=+3.0; Archean crust Nd=30 ppm and ε_{Nd}=-10.0) indicates that the ε_{Nd} value of the 1832 Ma plutons could result from 20% contamination by Archean crust. If the Archean crust has a lower ε_{Nd} value or higher concentration of Nd then the weight fraction of older crust required would decrease accordingly. In addition, it is not known whether this Archean component would consist of Archean crystalline rocks, or Archean crust that had been recycled and deposited into Paleoproterozoic sedimentary basins and subsequently incorporated into the 1832 Ma magmas.

Northern Glennie Domain

An undeformed ca. 1780 Ma granitic pegmatite which intrudes mylonitized granitoid gneisses along the northern boundary of the Glennie Domain (Harper, 1998; Harper *et al.*, 2000) was analyzed to determine whether its Nd isotopic composition suggested interaction with significantly older crust. The ε_{Nd} value at the assumed age of intrusion is -10.6 (Table 1), which suggests extensive contamination by or direct derivation from Archean crust (Figure 2). This Archean crust is probably the northern extension of the Sask Craton, which is imaged on LITHOPROBE seismic line S2b (Hajnal *et al.*, 1996), and indicates that the Sask Craton had underthrust the Paleoproterozoic rocks of the THO at least as far north as this point by ca. 1780 Ma.

Sub-Phanerozoic

Three granitic samples were taken from drill holes that intersected the basement below the Phanerozoic sedimentary cover. The ages of these samples are not known, but are presumed to be Paleoproterozoic, because they are taken from drill holes that are as close as possible to the exposed THO. Drill holes M36 and M38 are situated within the extension of the La Ronge Domain, whereas M11 lies immediately to the south of the Glennie Domain in the Deschambault Lake area.

The samples from M36 and M38 have ε_{Nd} values of -4.6 and -8.6 at an assumed age of 1850 Ma, and T_{DM} ages of 2.55 and 2.75 Ga, respectively (Table 1, Figure 2). These magmas have thus interacted significantly with older crust, or are actually Archean in age. However, no geochronological data is available for these rocks. Similar ε_{Nd} values have been obtained from the Wathaman Batholith and the Tonalite-Migmatite Complex on Reindeer Lake (Kyser and Stauffer, 1992). These authors suggested that low ε_{Nd} values in the gneisses of the Tonalite-Migmatite Complex resulted from metamorphism of supracrustals containing detritus shed from the Hearne craton. The Wathaman Batholith formed from magmas that incorporated significant quantities of this older supracrustal material. A better understanding of the geological, age, and petrogenetic relationships in the southern La Ronge Domain is necessary before the Nd isotopic compositions of the granitoids in this study can be fully interpreted.

Sample M11 is a coarse-grained granitoid with a ε_{Nd} value of -3.8 at an assumed age of 1850 Ma. This value is significantly lower than the values obtained from the ca. 1832 Ma granitoids in the Glennie Domain. Therefore, even though the crystallization age of this rock is not known, the initial magma interacted with a substantial amount of older, possibly Archean, crust prior to crystallization.

4. Summary

1) The Nd isotopic composition of mafic volcanic rocks from the southern Glennie Domain and two samples from the Sub-Phanerozoic indicate derivation from a similar mantle to that from which the Flin Flon arc and ocean floor rocks were generated.
2) The ca. 1850 Ma Wapawekka Lake granodiorite has an ε_{Nd} value of +3.2, which is similar to the successor arc plutons of the Flin Flon Domain, and is thus probably derived by remelting of juvenile arc crust.
3) In contrast, the ca. 1832 Ma granitoids have lower ε_{Nd} values, which suggest up to approximately 20% contamination by older crustal material. The nature of this contaminant is unknown, but may be Paleoproterozoic sedimentary rocks containing Archean detritus, or actual Archean crust. If it is the latter, then these granitoids may be sampling a small component of the Sask Craton, which thus provides further constraints on the arrival of this craton in the THO.
4) The age of the granitoids from the Sub-Phanerozoic drillcore are unknown, although all three samples have negative ε_{Nd} values. These data suggest significant interaction with Archean crustal material, although the lack of age control makes interpretation difficult.
5) The ca. 1780 Ma pegmatite from the northern Glennie Domain has an ε_{Nd} value of -10.6, which suggests that the pegmatitic melt was probably generated from Archean crust. The location of this sample, and the interpretation of the LITHOPROBE seismic signature lends support to the theory that this Archean crust is the Sask Craton. This sample thus marks the northernmost limit of the Sask Craton.

More detailed and integrated geochronological, geochemical, and isotopic analysis is required to fully understand the development of the southern Glennie Domain and the southern extensions of the La Ronge Domain, in order to be able to extrapolate to the Sub-Phanerozoic basement. These new data, however, do suggest that the ca. 1832 Ma granitoids may be providing evidence for the arrival of the Sask Craton, which then underthrust as far north as the northern Glennie Domain.

5. Acknowledgments

This study was initiated while Tim Prokopiuk was a recipient of an NSERC Undergraduate Research Scholarship. The supplement to the scholarship, and sampling and analytical costs were borne by an NSERC Research Grant to Kevin Ansdell. Samples were collected in Regina with the assistance and advice of Gary Delaney, Ken Ashton, Charlie Harper, and Lynn Kelley. Technical support in the Isotope Laboratory at the University of Saskatchewan was provided by Diane Fox, Chris Holmden, and Kerrie Fanton. Tim Prokopiuk appreciated the midsummer break from lab work provided by Don Wright and Ralf Maxeiner. Bill Slimmon and Ken Ashton are thanked for a digital copy of a Glennie Domain map on which Figure 1 is based, and Gary Delaney is thanked for his comments on the manuscript. LITHOPROBE Publication #1103.

6. References

Ansdell, K.M. and Bleeker, W. (1997): The margin of the Superior Craton: Neodymium isotope constraints on the evolution of the Thompson Nickel Belt, Manitoba; Geol. Assoc. Can./Miner. Assoc. Can., Abst. Vol., v22, pA-4-5.

Ansdell, K.M., Lucas, S.B., Connors, K., and Stern, R.A. (1995): Kisseynew metasedimentary gneiss belt, Trans-Hudson Orogen (Canada): Back-arc origin and collisional inversion; Geol., v23, p1039-1043.

Ansdell, K.M. and Stern, R.A. (1997): The Scimitar Complex: Initial SHRIMP U-Pb and Nd isotope data from granitoid rocks; *in* Summary of Investigations 1997, Saskatchewan Geological Survey, Sask. Energy Mines, Misc. Rep. 97-4, p145-149.

Ashton, K.E. (1999): A proposed lithotectonic domainal reclassification of the southeastern Reindeer Zone in Saskatchewan; *in* Summary of Investigations 1999, Volume 1, Saskatchewan Geological Survey, Sask. Energy Mines, Misc. Rep. 99-4.1, p92-100.

Ashton, K.E., Heaman, L.M., Lewry, J.F., Hartlaub, R.P., and Shi, R. (1999): Age and origin of the Jan Lake Complex: A glimpse of the buried Archean craton of the Trans-Hudson Orogen; Can. J. Earth Sci., v36, p185-208.

Baird, D., Nelson, K., Knapp, J., Walters, J., and Brown, L. (1996): Crustal structure and evolution of the Trans-Hudson Orogen: Results from seismic reflection profiling; Tectonics, v15, p416-426.

Barovich, K.M. and Patchett, P.J. (1991): Behavior of isotopic systematics during deformation and metamorphism: A Hf, Nd and Sr isotopic study of mylonitized granite; Contrib. Mineral. Petrol., v109, p386-393.

Bickford, M.E., Collerson, K.D., Lewry, J.F., and Orrell, S.E. (1992): Pegmatites and leucogranites as probes of crust beneath allochthonous orogenic rocks in the Glennie and La Ronge domains; *in* Summary of Investigations 1992, Saskatchewan Geological Survey, Sask. Energy Mines, Misc. Rep. 92-4, p124-129.

Bickford, M., Collerson, K., Lewry, J., Van Schmus, R., and Chiarenzelli, J. (1990): Proterozoic collisional tectonism in the Trans-Hudson Orogen in Saskatchewan; Geol., v18, p14-18.

Chiarenzelli, J., Aspler, L., Villeneuve, M., and Lewry, J. (1998): Early Proterozoic evolution of the Saskatchewan Craton and its allochthonous cover, Trans-Hudson Orogen; J. Geol., v106, p247-267.

Collerson, K.D., Van Schmus, R.W., Lewry, J.F., and Bickford, M.E. (1988): Buried Precambrian basement in south-central Saskatchewan: Provisional results from Sm-Nd model ages and U-Pb zircon geochronology; *in* Summary of Investigations 1988, Saskatchewan Geological Survey, Sask. Energy Mines, Misc. Rep. 88-4, p142-150.

Delaney, G.D. (1992): Gold in the Glennie Domain; Sask. Energy Mines, Misc. Rep. 92-5, 71p.

DePaolo, D.J. and Wasserburg, G.J. (1976): Nd isotopic variations and petrogenetic models; Geophys. Resear. Lett., v3, p743-746.

Goldstein, S.L., O'Nions, R.K., and Hamilton, P.J. (1984): A Sm-Nd isotopic study of atmospheric dusts and particulates from major river systems; Earth Planet. Sci. Lett., v70, p221-236.

Green, A.G., Weber, W., and Hajnal, Z. (1985): Evolution of Proterozoic terrains beneath the Williston Basin; Geol., v13, p624-628.

Hajnal, Z., Stauffer, M.R., White, D.J., Lucas, S.B., Lewry, J., Clowes, M.R., and Ashton, K.E. (1996): Three-dimensional seismic crustal signature of the western Trans-Hudson Orogen, Saskatchewan; *in* LITHOPROBE Trans-Hudson Orogen Transect Meeting, Rep. 55, p113-124.

Harper, C.T. (1998): The La Ronge Domain–Glennie Domain transition: Street Lake area (parts of NTS 64D-3 and -6); *in* Summary of Investigations 1998, Saskatchewan Geological Survey, Sask. Energy Mines, Misc. Rep. 98-4, p66-80.

Harper, C.T., Heaman, L.M., and Prokopiuk, T.C. (2000): Glassy pseudotachylite in Paleoproterozoic Gloeckler Lake Mylonite Zone at the Kisseynew Domain–Glennie Domain boundary, Street Lake area, northern Saskatchewan; GeoCanada 2000, Calgary, May 2000, Conference CD, ext. abstr. #124.

Hoffman, P.F. (1988): United Plates of America, the birth of a craton: Early Proterozoic assembly and growth of Laurentia; Ann. Rev. Earth Planet. Sci., v16, p543-603.

Kyser, T.K. and Stauffer, M. (1992): Petrogenesis of the Wathaman Batholith; *in* LITHOPROBE Trans-Hudson Orogen Transect Meeting, Rep. 26, p126-128.

Lewry, J.F. and Collerson, K.E. (1990): The Trans-Hudson Orogen: Extent, subdivision, and problems; *in* Lewry, J.F. and Stauffer, M.R. (eds.), The Early Proterozoic Trans-Hudson Orogen of North America, Geol. Assoc. Can., Spec. Pap. No. 37, p1-14.

Lewry, J., Hajnal, Z., Green, A., Lucas, S., White, D., Stauffer, M., Ashton, K., Weber, W., and Clowes, R. (1994): Structure of a Paleoproterozoic continent-continent collision zone: A LITHOPROBE seismic reflection profile across the Trans-Hudson Orogen, Canada; Tectonophysics, v232, p143-160.

Lucas, S.B., Green, A., Hajnal, Z., White, D., Lewry, J., Ashton, K., Weber, W., and Clowes, R. (1993): Deep seismic profile across a Proterozoic collision zone: Surprises at depth; Nature, v363, p339-342.

McCulloch, M.T. and Black, L.P. (1984): Sm-Nd isotopic systematics of Enderby Land granulites and evidence for the redistribution of Sm and Nd during metamorphism; Earth Planet. Sci. Lett., v71, p46-58.

McNicoll, V.J., Delaney, G.D., Parrish, R.R., and Heaman, L.M. (1992): U-Pb age determinations from the Glennie Lake Domain, Trans-Hudson Orogen, Saskatchewan; *in* Radiogenic Age and Isotopic Studies: Report 6, Geol. Surv. Can., Pap. 92-2, p57-72.

Nelson, K., Baird, D., Walters, J., Hauck, M., Brown, L., Oliver, J., Ahern, J., Hajnal, Z., Jones, A., and Sloss, L. (1993): Trans-Hudson Orogen and Williston Basin in Montana and North Dakota: New COCORP deep profiling results; Geol., v21, p447-450.

Steinhart, W.E., Bickford, M.E., Lewry, J.F., and Mock, T.D. (1997): Common Pb and Sm-Nd study of the Glennie, Hanson Lake, and La Ronge domains, and the Hearne province, Trans-Hudson Orogen: Implications for tectonic evolution; Geol. Assoc. Can./Mineral. Assoc. Can., Abst. Vol., v22, pA-142.

Stern, R.A., Syme, E.C., and Lucas, J.B. (1995a): Geochemistry of 1.9 Ga MORB- and OIB-like basalts from the Amisk collage, Flin Flon belt, Canada: Evidence for an intra-oceanic origin, Geochim. Cosmochim. Acta, v59, p3131-3154.

Stern, R.A., Syme, E.C., Bailes, A.H., and Lucas, S.B. (1995b): Paleoproterozoic (1.90-1.86 Ga) arc volcanism in the Flin Flon belt, Trans-Hudson Orogen, Canada; Contrib. Mineral. Petrol., v119, p117-141.

Whalen, J.B., Syme, E.C., and Stern, R.A. (1999): Geochemical and Nd isotopic evolution of Paleoproterozoic arc-type granitoid magmatism in the Flin Flon belt, Trans-Hudson Orogen, Canada; Can. J. Earth Sci., v36, p227-250.

Geochemical Character of the Tonalite-Trondhjemite Suite of the Tonalite-Migmatite Complex, Deception Lake, Saskatchewan [1]

Chris T. Coolican [2], Kevin M. Ansdell [2], Rob Kerrich [2], and Mel Stauffer [2]

Coolican, C.T., Ansdell, K.M., Kerrich, R., and Stauffer, M. (2000): Geochemical character of the tonalite-trondhjemite suite of the Tonalite-Migmatite Complex, Deception Lake, Saskatchewan; *in* Summary of Investigations 2000, Volume 2, Saskatchewan Geological Survey, Sask. Energy Mines, Misc. Rep. 2000-4.2.

Abstract

Deception Lake straddles the boundary between the Wathaman Batholith and the Tonalite-Migmatite Complex in the Trans-Hudson Orogen. The focus of the geochemical study is the tonalite-trondhjemite suite of the Tonalite-Migmatite Complex. At outcrop scale, cross-cutting relationships indicate that multiple tonalite phases have been emplaced which both pre- and post-date the Wathaman Batholith. Although similarities in mineralogy hinder correlation of individual tonalite phases beyond the outcrop scale, it is possible to subdivide them on geochemical characteristics.

Geochemical characteristics of the tonalite-trondhjemite suite include high Al contents (14.1 to 18.3 wt %), high Sr (397 to 782 ppm), very low Rb/Sr ratio (0.029 to 0.092), low Y (<15.47 ppm), negative Nb anomaly, LREE enrichment, fractionated HREE, and slight negative or positive Eu anomaly. Based on differences in the magnitude of REE fractionation and Eu, Nb, Sr, and Ti anomalies, four groups of tonalite have been distinguished. Overall, these geochemical characteristics are typical of high-Al tonalite-trondhjemite-granodiorite suites, characteristic of Archean granitic gneiss terrains. They are interpreted to have crystallized from magmas derived from melting of subducted oceanic crust.

1. Introduction

The formation of the Trans-Hudson Orogen (THO) is a result of collisions between the Superior, Sask, and Hearne cratons and juvenile terrains of the Reindeer Zone (Chiarenzelli *et al.*, 1996; Lewry and Collerson, 1990). Collisional processes occurring between the northern margin of the THO and the Archean Hearne craton are poorly understood, and therefore more geological work is needed to unravel the history of this part of the Orogen. The relationships within the rocks comprising the Tonalite-Migmatite Complex (TMC) and the Wathaman Batholith (WB) are crucial to interpreting the northern margin of the THO.

Previous geochemical work by Clarke and Hendry (1993, 1994, 1995) in the Davin Lake area of the Tonalite-Migmatite Complex was undertaken to understand the origin and emplacement of granitoids in the Davin Lake Complex of the Tonalite-Migmatite Complex. Their data was interpreted to indicate that the pink and white granites were derived from metasedimentary and metavolcanic sources respectively, and that they were emplaced in a suture zone along the southeast margin of the Wathaman Batholith. In contrast, Lewry *et al.* (1981) suggested that the contact is a deformed intrusive relationship. This project was initiated to improve the understanding of the Tonalite-Migmatite Complex by mapping a transect across the contact between the Wathaman Batholith and the Tonalite-Migmatite Complex at Deception Lake. Using the structural constraints, geochemical analysis of the granitoid rocks will provide significant information about the origin and evolution of the TMC.

This report will discuss preliminary results from samples collected at Deception Lake in the summer of 1999 (Coolican *et al.*, 1999).

2. General Geology

Deception Lake, in the northwest margin of the Trans-Hudson Orogen, straddles the boundary between the Wathaman Batholith and the Tonalite-Migmatite Complex (Figure 1). The TMC consists of a migmatitic supracrustal sequence that has been intruded by a tonalitic to trondhjemitic intrusive suite. The contact between the WB and the TMC is marked by a zone of mainly granodioritic intrusions with increasing pegmatitic and aplitic dikes towards the WB. The WB comprises mainly porphyritic monzogranite to granodiorite that crosscuts all the other intrusive rocks, representing the youngest intrusive unit recognized.

Two ductile deformational events were distinguished. Early migmatization and deformation of the supracrustal rocks was followed by intrusion of the tonalite-trondhjemite suite and occurred during D_1. The dominant regional fabric, S_1, strikes southwest-northeast and dips northwest, and is axial planar to minor F_1 folds. An S_2 foliation strikes slightly oblique to S_1 and has a shallow westward dip. F_2 folds, the dominant folds, are isoclinal to tight, recumbent to near recumbent with hingelines trending north-northwest to

---

[1] Funded by NSERC LITHOPROBE Special Studies Grant; LITHOPROBE Publication # 1196.

[2] Department of Geological Sciences, University of Saskatchewan, 114 Science Place, Saskatoon, SK S7N 5E2.

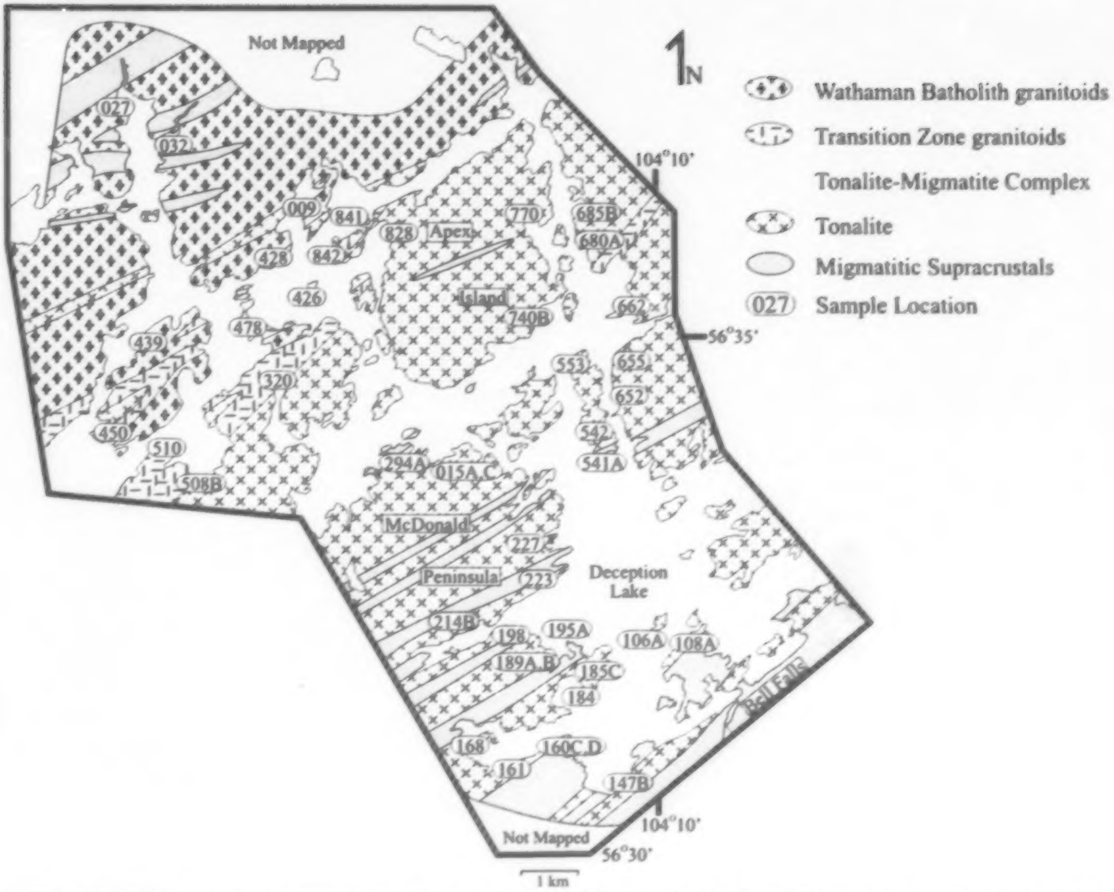
Not Mapped
N
104°10'
56°35'
104°10'
56°30'
Not Mapped
1 km
Wathaman Batholith granitoids
Transition Zone granitoids
Tonalite-Migmatite Complex
Tonalite
Migmatitic Supracrustals
027 Sample Location
027
032
009
841
828
Apex
770
685B
680A
428
842
426
Island
740B
662
478
439
320
553
655
652
450
542
510
541A
508B
294A
015A,C
McDonald
227
Peninsula
223
Deception Lake
214B
198
195A
106A
108A
189A,B
185C
184
Bell Falls
168
160C,D
161
147B

Figure 1 - Simplified geological map of the eastern Deception Lake area showing the locations of lithogeochemical samples (center of ellipse).

north-northeast, and shallow northwest dipping axial planes. D_2 fabrics continued to form during the intrusion of the WB, which acquired weak to intense S_2 foliation. Upper amphibolite grade metamorphic conditions were attained during D_1 as indicated by the hornblende-plagioclase assemblage in mafic volcanogenic units, and folded (F_1) *in situ* tonalitic leucosomes in the supracrustal units. Tonalitic leucosome folded by F_1, also indicates it was generated prior to the intrusion of the WB at ca. 1865 Ma (Ray and Wanless, 1980; Van Schmus *et al.*, 1987; Bickford *et al.*, 1990; Meyer *et al.*, 1992). In addition, foliated amphibolite xenoliths within the WB indicate that a considerable pre-Wathaman deformational event occurred.

3. Petrology of Intrusive Phases

a) Tonalite-Migmatite Complex

The earliest intrusive phases within the study area are the tonalite-trondhjemite suite of the TMC. At outcrop scale, three phases can be distinguished by intrusive relationships; these are highlighted by variations in deformational fabric or grain size (Coolican *et al.*, 1999). Generally, the older tonalite-trondhjemite phases have a more intense S_1 foliation and smaller grain size (Figure 2), and the youngest phase is pegmatitic tonalite. However, at outcrops with only one tonalite phase, identification of the specific phase is impossible because of the similar lithologies of the tonalite intrusives. This also makes it difficult to extend individual phases beyond outcrop scale, and therefore it is likely that more than three tonalite phases are present in the study area. Geochemically, the tonalites have been subdivided into four groups based on their trace element compositions, as discussed in the Geochemistry section.

Due to the similar lithologies of the tonalite intrusives, the following petrographic description is relative to all the tonalite phases. The tonalites are composed of quartz (20 to 35%), plagioclase (An_{25-35}; 45 to 65%), microcline (<5%), biotite (5 to 20%), and muscovite (<2%); with accessory zircon, apatite and magnetite. Alteration of plagioclase to sericite varies between samples and ranges from slight alteration along grain

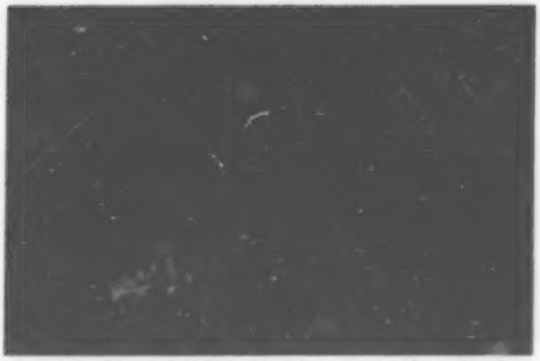

Figure 2 - Intensely foliated tonalite crosscut by a massive, coarser grained phase.

boundaries to pervasive throughout the crystal. Plagioclase grains are generally subhedral with well-developed twin planes, and commonly contain inclusions of quartz, biotite, and accessory minerals. Some grains are fractured or bent, and grain size ranges up to 4 mm, with some samples coarser grained than others. Quartz grains are anhedral, commonly fractured, and 0.1 to 2 mm wide. Microcline is generally anhedral to subhedral, and occurs either as grains up to 3 mm wide with inclusions or as myrmekitic intergrowths with quartz. Biotite commonly has a strong parallel orientation and may show a second oblique cleavage; however, random orientation also occurs. Biotite crystals are generally less than 2 mm in size; fine-grained muscovite is along grain boundaries of some samples.

b) Tonalite-Migmatite Complex–Wathaman Batholith Contact Zone

At the contact between the TMC and the WB is a zone up to 1 km wide in which there are a variety of intrusive phases ranging from tonalitic to granodioritic in composition. These intrusions are non-porphyritic, weakly foliated, and crosscut the strongly foliated tonalite-trondhjemite suite of the TMC.

The granodiorites from the contact zone are composed of quartz (20 to 30%), plagioclase (An_{20-30} 45 to 55%), microcline (15 to 25%), and biotite (10 to 15%); accessory phases include zircon, apatite, and/or magnetite. The rocks are hypidiomorphic granular, with alteration of plagioclase to sericite common, as is some degree of grain fracturing and warping of twin lamellae. Quartz and plagioclase grains are up to 5 mm wide, but 1 to 3 mm is common. Microcline occurs as small interstitial grains and/or larger grains up to 2 mm wide, commonly with plagioclase and biotite inclusions. Biotite occurs in flakes up to 3 mm long, and exhibit either a moderate parallel orientation or are randomly oriented.

c) Wathaman Batholith

The Wathaman Batholith comprises massive to strongly foliated granodiorite to monzogranite. The rocks are most commonly porphyritic with randomly oriented microcline phenocrysts up to 5 cm long; locally the phenocrysts exhibit a weak flow alignment. Hornblende-biotite-rich mafic xenoliths are most common, but pelitic to psammopelitic and tonalitic xenoliths also occur.

The granodiorites in the Wathaman Batholith are composed of quartz (20 to 30%), plagioclase (An_{25-30} 20 to 30%), microcline (35 to 45 %), biotite (5 to 15%), and muscovite (up to 2%); accessory minerals include zircon, apatite, magnetite, and chlorite. Microcline varies from fine interstitial grains to phenocrysts several centimetres long that commonly have inclusions of plagioclase, biotite, and/or magnetite. Carlsbad twinning is common, as is microperthite. Plagioclase grains are 0.5 to 3 mm long, and commonly altered to sericite along grain boundaries and fractures. Parallel orientation of biotite is well developed. Biotite grains are 0.2 to 2 mm long, and commonly have pleochroic haloes; rarely, muscovite occurs as intergrown microcrystalline flakes with biotite or along grain boundaries.

4. Geochemistry

A total of 44 whole rock samples were crushed and ground in agate, and analysed for major elements together with Rb, Sr, Y, Zr, Nb, and Ba using X-ray fluorescence spectrometry (XRF) at X-ray Assay Laboratories (Don Mills, Ontario). Twenty of these samples were then analysed at the University of Saskatchewan using inductively coupled plasma emission mass spectrometry (ICP-MS) to obtain a complete set of trace element data including high field strength element (HFSE) and rare earth element (REE) data.

Samples from the TMC and TMC-WB contact zone were initially selected given that the field relationships were most clearly understood. The remaining samples were selected to assure good geographic coverage of the study area, and on the basis of sample quality. Representative samples from the WB were collected and analysed to allow local comparison with the samples from the TMC and TMC-WB contact zone (Table 1).

The geochemistry of the Wathaman Batholith is well documented (Fumerton *et al.*, 1984; Halden *et al.*, 1990; Meyer *et al.*, 1992), and therefore the following geochemical discussion will focus on the tonalite-trondhjemite suite of the TMC.

a) Major Element Geochemistry

As suggested by its name, the dominant rock type within the TMC is tonalite; and trondhjemite is subordinate, although granodiorite intrusives occur in the WB-TMC contact zone. The dominantly tonalitic nature of the intrusives is illustrated on the normative Ab-An-Or ternary diagram (Figure 3) by a cluster of samples within the tonalite field; this also demonstrates the similarity of the various tonalite phases within the

Table 1 - Geochemical data of representative samples from the Deception Lake area.

Samples	WB 027	WB-TMC 320	TMC Gp 1 223	TMC Gp 2 294A	TMC Gp 3 189A	TMC Gp 4 189B
SiO_2 (wt %)	72.5	69.1	73.5	68.8	70.9	63.7
TiO_2	0.296	0.261	0.131	0.284	0.252	0.376
Al_2O_3	14.1	15.8	14.6	16.2	15.4	18.3
Fe_2O_3	2.29	3.32	1.27	2.93	2.05	3.02
MnO	0.03	0.05	0	0.02	0.01	0.03
MgO	0.66	1.35	0.48	1.22	0.88	1.33
CaO	1.63	3.49	2.8	3.53	3.73	4.76
K2O	3.54	1.62	2.31	1.65	1.16	1.63
Na_2O	4.15	4.29	4.18	4.87	4.49	5.21
P_2O_5	0.1	0.09	0.04	0.07	0.09	0.42
LOI	0.75	0.7	0.6	0.6	1.1	1.45
Sum	100.3	100.2	100.3	100.3	100.3	100.4
Rb (ppm)	99.87	15.08	14.59	14.34	24.77	32.99
Sr	412.42	399.92	505.65	425.86	731.92	782.72
Cs	0.7	0.47	0.43	0.42	0.4	0.61
Ba	1133.9	636.38	2678.23	519	716.68	847.81
Sc	5.44	8.22	1.75	4.18	2.86	5.85
V	20.6	34.84	15.89	36	22.93	37.1
Ta	0.42	0.35	0.1	0.29	0.1	0.25
Nb	10.16	5.08	3.22	8	3.59	7.86
Zr	228.02	61.84	37.79	85	54.35	47.68
Hf	6.59	3.24	1.74	2.69	1.71	2.5
Th	23.02	2.76	14.51	6.07	0.33	0.87
U	1.87	0.39	0.66	0.41	0.15	0.42
Y	12.36	5.11	3.24	4	3.77	15.47
La	58.76	5.56	42.11	18.70	6.32	10.3
Ce	107.53	22.86	114.7	38.62	11.05	24.32
Pr	11.66	1.6	11.36	4.21	1.26	2.99
Nd	39.95	6.55	42.24	15.7	4.99	13.73
Sm	6.41	1.68	7.06	2.75	0.97	3.6
Eu	0.78	0.46	1.3	0.85	0.95	1.1
Gd	4.79	1.57	4.96	2.07	0.97	3.73
Tb	0.55	0.23	0.39	0.22	0.11	0.53
Dy	2.93	1.49	1.5	0.98	0.61	3.15
Ho	0.45	0.28	0.19	0.16	0.12	0.6
Er	1	0.75	0.28	0.37	0.32	1.53
Tm	0.13	0.12	0.03	0.04	0.04	0.19
Yb	0.74	0.7	0.12	0.26	0.25	1.05
Lu	0.11	0.09	0.02	0.04	0.03	0.12

Note:
WB, Wathaman Batholith and WB-TMC, Wathaman Batholith–Tonalite-Migmatite Complex contact zone

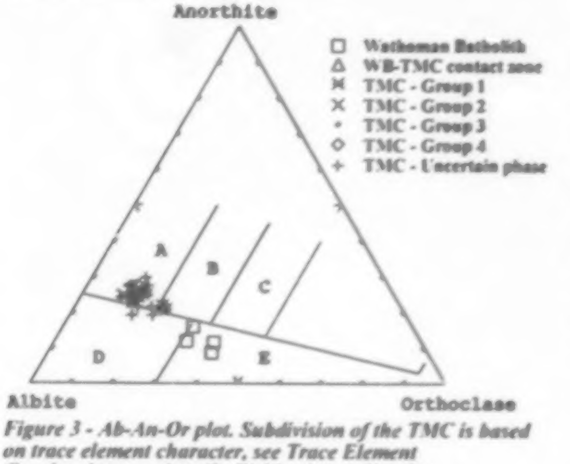

Figure 3 - Ab-An-Or plot. Subdivision of the TMC is based on trace element character, see Trace Element Geochemistry section 4b. Fields: A, tonalite; B, granodiorite; C, adamellite; D, trondhjemite; and E, granite. Fields according to Barker (1979).

TMC. Samples from the WB plot within the granite field, clearly separated from rocks of the TMC.

Selected elements for the granitoids from the TMC and WB are plotted on Harker diagrams (Figure 4). Tonalite samples contain a narrow range of SiO_2 between 65 to 75 wt %, and display a negative linear relationship with Al_2O_3, MgO, CaO, Na_2O, and TiO_2. The K_2O-SiO_2 trend demonstrates an extremely narrow range of K_2O in the TMC ranging from 1.5 to 2 wt %. WB monzogranites have a range of SiO_2 contents from 70 to 75 wt %, and can be distinguished from the tonalites by their higher K_2O, and lower CaO and Na_2O concentrations. Overall, the various phases of tonalite intrusions exhibit very similar major element compositions.

b) Trace Element Geochemistry

Rare Earth Elements

Chondrite normalized REE patterns for the tonalite-trondhjemite rocks of the TMC are coherent with enriched LREE, fractionated and depleted HREE, and only slight negative or positive Eu anomalies. Although there are general similarities, there are distinct differences in the magnitude of fractionation and anomalies which may be significant in understanding the origin of the granitoids. These differences, along with field relationships where possible, have been used to subdivide the tonalite-trondhjemites into four groups (Figure 5).

Group 1 tonalites exhibit the strongest LREE enrichment ($(La/Yb)_N$ = 105 to 265), and highest $(Gd/Yb)_N$ ratios (10 to 34), with slight to pronounced negative Eu anomalies. In addition, Group 1 tonalites have higher LREE abundances than the other groups. Group 2 tonalites have moderate LREE enrichment ($(La/Yb)_N$ = 50 to 105), $(Gd/Yb)_N$ values from 6 to 15 and slightly negative to slightly positive Eu anomalies. LREE abundances of Group 2 are less than Group 1, and higher than Group 3. Group 3 tonalites are less fractionated than Group 1 and 2 tonalites ($(La/Yb)_N$ = 18 to 52; $(Gd/Yb)_N$ = 3 to 6) and all have strong positive Eu anomalies relative to the other groups. Group 4 tonalites are the least fractionated ($(La/Yb)_N$ = 7 to 10; $(Gd/Yb)_N$ = 3 to 4), have only slight negative

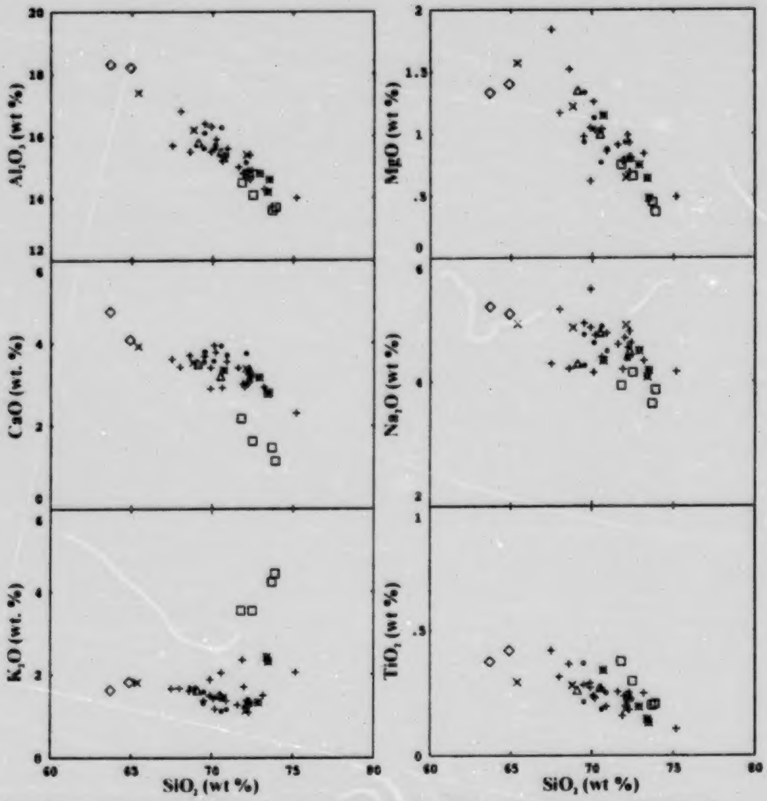

Figure 4 - Harker diagrams for selected major elements. Symbols as in Figure 3.

or positive Eu anomalies and higher HREE abundances than the other groups.

As previously mentioned, three phases of tonalite were distinguished in the field, however, geochemical analysis of pegmatitic tonalite, the youngest of the three phases, was not attempted due to difficulty in achieving sample homogeneity. The relative ages of the four geochemical groups can partially be determined based on field evidence. Intrusive relationships indicate that Group 3 tonalite is older than Group 4, unfortunately samples comprising Group 1 and Group 2 are from outcrops with only one tonalite phase, and therefore their relative age is uncertain.

The REE plots of two granodiorites from the TMC-WB contact zone are displayed in Figure 6a. Sample 320 has a comparatively unfractionated pattern ($(La/Yb)_N$ = 5.7) relative to sample 478 ($(La/Yb)_N$ = 92), although both samples display LREE enrichment and only slightly negative Eu anomalies.

Figure 6b also demonstrates the REE patterns of porphyritic granodiorite from the Wathaman Batholith. The two samples have similar fractionation trends ($(La/Yb)_N$ = 47 to 57) and abundances, and both samples have negative Eu anomalies.

The four tonalite/trondhjemite groups were also plotted on primitive mantle normalized multi-element plots (Figure 7). As with the REE plots, the four groups generally have similar patterns, including: (1) fractionated pattern; (2) weak to strong negative Nb, P, and Ti anomalies; and (3) relatively enriched Rb, Ba, K, and Sr.

Overall, Group 1 tonalites have elevated Ba and Th, and stronger negative Nb, P, and Ti relative to the other three groups. Groups 3 and 4 have depleted Th contents relative to Groups 1 and 2, and distinct negative Th anomalies.

Figure 8 shows multi-element plots for the TMC-WB contact zone and the Wathaman Batholith. These patterns are generally similar to those of the TMC, displaying a negative slope, negative Nb, P and Ti anomalies, and similar element abundances. Th and U systematics are similar to those in Groups 1 and 2 tonalites. Granodiorites from the TMC-WB contact zone have lower abundances in comparison to granodiorites from the WB.

c) Petrogenetic and Tectonic Implications of Tonalites/Trondhjemites

Classification

Granitoid rocks in this study have relatively high Na_2O (Na_2O>3.6; see Figure 3), metaluminous to slightly peraluminous character (Al-saturation index 0.95 to 1.05), and <1% normative corundum. These characteristics are typical of I-type granitoids as defined by Chappell and White (1974) and Chappell and Stephens (1988).

Further, samples from the TMC display features typical of Archean high-Al trondhjemite-tonalite-dacite (TTD) (Drummond and Defant, 1990; Drummond *et al.*, 1996) and TTG (trondhjemite-tonalite-granodiorite) (Martin, 1986, 1993) suites, including high Al contents (14.1 to 18.3 wt %), high Sr (397 to 782 ppm), very low Rb/Sr ratio (0.029 to 0.092), LREE enrichment ($(La/Yb)_N$ = 7 to 265) with slight Eu anomalies, low Y (<15.47 ppm) and negative Nb anomalies.

Granitoid Source and Petrogenetic Processes

The high Al content in the tonalite-trondhjemite suite may have resulted from the removal of hornblende

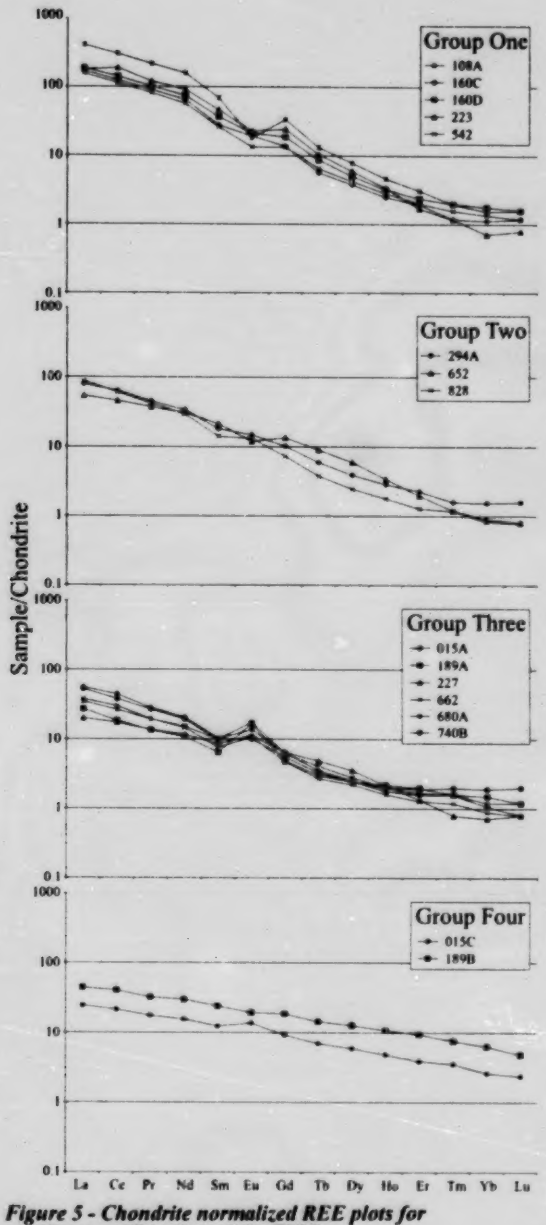

Figure 5 - Chondrite normalized REE plots for tonalites/trondhjemites of the TMC.

The REE plots (Figure 5) and multi-element plots (Figure 7) clearly display the geochemical signature of melts derived from oceanic crust and provide constraints on source material. Key features displayed by REE plots (Figures 5 and 7) include REE fractionation, HREE depletion, and no to minor positive or negative Eu anomalies. The enriched LREE character can be explained through partial melting of a basaltic source leaving a refractory phase assemblage with various proportions of clinopyroxene, hornblende, and garnet (Arth and Hanson, 1975; Gromet and Silver, 1987; Defant *et al.*, 1988). The lack of a strong negative Eu anomaly may imply that little feldspar was retained at the site of partial melting, or separated from the melt via crystal fractionation. Although to a lesser extent, refractory garnet, hornblende, and pyroxene have the opposite effect of plagioclase. The combined effects result in the weak Eu anomalies in Groups 1, 2, and 4, and the minor positive Eu anomaly in Group 3.

Refractory garnet can also explain the high Sr/Y ratio. Sr behaves incompatibly during high-pressure partial melting of basalt due to the instability of plagioclase; therefore, it will become concentrated in the melt (Drummond *et al.*, 1996). Conversely, Y is strongly compatible with garnet and therefore is controlled by the presence of garnet in the residue. The combined effect of Sr concentration in the melt and Y concentration in the refractory garnet results in the high Sr/Y ratio.

Multi-element plots (Figure 7) show clear negative Nb and Ti anomalies for all the tonalite/trondhjemites. Drummond and Defant (1990) postulate that retention of hornblende at the site of partial melting could account for these negative anomalies because of its strong affinity for Nb and Ti in siliceous melts. Hornblende exclusion from the melt may also be the cause of the low to moderate K/Rb ratios because of from the melt either as a residual phase at the source, or as a fractionation product (Barker and Arth, 1976; Barker, 1979). Further, the metaluminous to slightly peraluminous character of these rocks indicates that hornblende is unlikely to be the only refractory phase left at the source, because a basaltic parent with an exclusively hornblendic refractory residue would form strongly peraluminous magmas (Holloway and Burnham, 1972; Drummond and Defant, 1990).

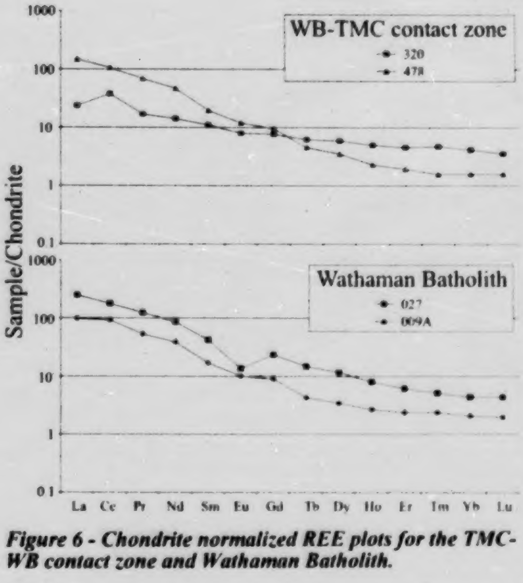

Figure 6 - Chondrite normalized REE plots for the TMC-WB contact zone and Wathaman Batholith.

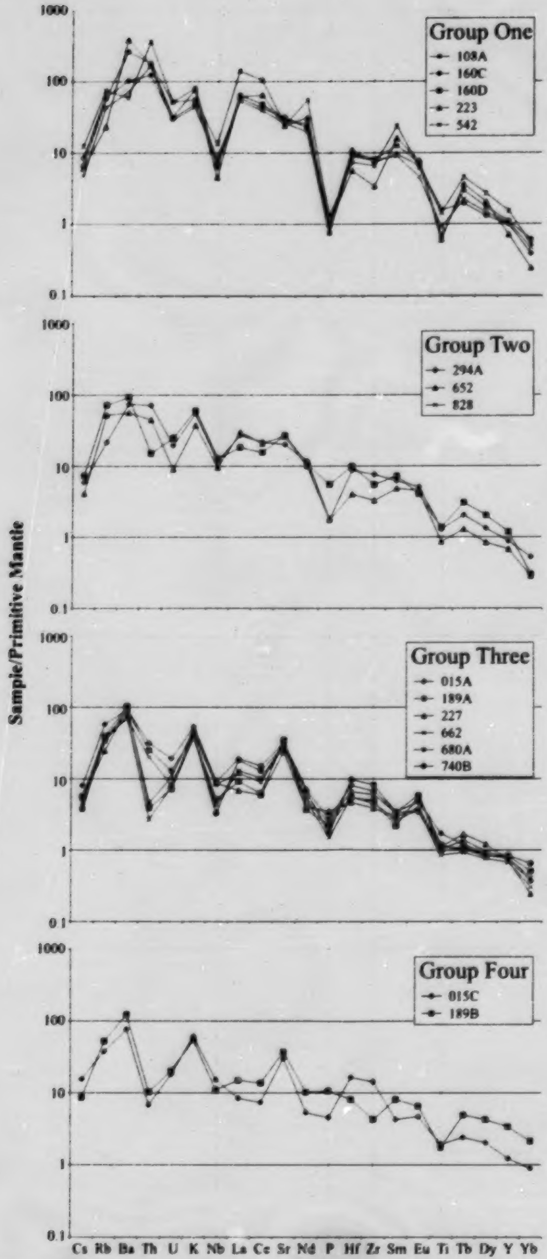

Figure 7 - Primitive mantle normalized multi-element plots for tonalites/trondhjemites of the TMC. Normalizing values after Sun and McDonough (1989).

the preference of hornblende to accommodate K relative to Rb (Arth and Hanson, 1975).

Tectonic Implications

The tonalite-trondhjemite rocks of the TMC are I-type granitoids, and have a trace element profile characteristic of arc environments. They display very similar characteristics to high-Al TTD granitoids that are interpreted to crystallize from magmas derived by melting of subducted oceanic crust, resulting in a hornblende eclogite residue. This conclusion has implications for the model for the tectonic evolution of the northwestern margin of the THO. Further refinement of this model will come with a better understanding of absolute age relationships.

5. Summary

1) In the Deception Lake area, the earliest intrusive phase in the Tonalite-Migmatite Complex is the tonalite-trondhjemite suite. At outcrop scale, three phases of tonalite were identified, however, the similarity of these phases make it difficult to correlate them across the area.

2) Chondrite normalized REE patterns for the tonalite-trondhjemite rocks of the TMC are coherent, with enriched LREE, fractionated HREE, and only slightly negative or positive Eu anomalies. These intrusive rocks were subdivided into four chemical groups based on distinct differences in magnitude of fractionation and anomalies displayed in their trace element geochemical patterns.

3) The tonalite-trondhjemite rocks of the TMC display very similar characteristics to high-Al TTD/TTG described by Martin (1986, 1993), Drummond and Defant (1990), and Drummond *et*

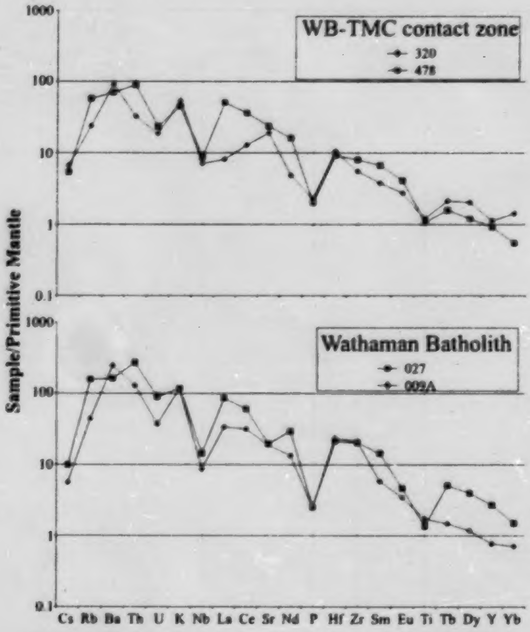

Figure 8 - Primitive mantle normalized multi-element plots for TMC-WB contact zone. Normalizing values after Sun and McDonough (1989).

al., (1996). The rocks were formed in an arc environment, and are interpreted to have crystallized from magmas derived by melting of subducted oceanic crust.

6. Acknowledgments

The project was funded by an NSERC LITHOPROBE Special Studies Grant. Thanks are due to Qianli Xie for assistance with preparation and analysis of geochemical samples, and Blaine Novakovski for thin section preparation. Logistical support for field work from the Geological Survey of Canada and Saskatchewan Energy and Mines, and the assistance of David Corrigan and Bill Slimmon in particular was greatly appreciated. Thanks to Erin Chorney for her valuable field assistance throughout the summer. I also thank Charlie Harper and Gary Delaney for reviewing the manuscript.

7. References

Arth, J.G. and Hanson, G.N. (1975): Geochemistry and origin of the early Precambrian crust of northeastern Minnesota; Geochim. Cosmochim. Acta, v39, p325-362.

Barker, F. and Arth, J.G. (1976): Generation of trondhjemitic-tonalitic liquids and Archean bimodal trondhjemite-basalt suites; Geol., v4, p596-600.

Barker, F. (1979): Trondhjemite: Definition, environment and hypothesis of origin; *in* Trondhjemites, Dacites and Related Rocks; Elsevier, Amsterdam, 356p.

Bickford, M.E., Collerson, K.D., Lewry, J.F., Van Schmus, W.R., and Chiarenzelli, J.R. (1990): Proterozoic collisional tectonism in the Trans-Hudson Orogen, Saskatchewan; Geol., v18, p14-18.

Chappell, B.W. and Stephens, W.E. (1988): Origin of infracrustal (I-type) granite Magmas; Trans. Roy. Soc. Edin. Earth Sci., v79, p2-3.

Chappell, B.W. and White, A.J.R. (1974): Two contrasting granite types; Pac. Geol., v8, p173-174.

Chiarenzelli, J.R., Aspler, L.B., and Villeneuve, M. (1996): Characterization, origin, and Paleoproterozoic history of the Saskatchewan craton and possible implications for the Trans-Hudson Orogen; *in* Hajnal, Z. and Lewry, J.F. (eds.), LITHOPROBE Trans-Hudson Orogen Transect, Rep. 55, p26-38.

Clarke, D.B. and Henry, A.S. (1993): Petrological and geochemical investigations in the Migmatite-Tonalite Belt of the Rottenstone Domain; *in* Hajnal, Z. and Lewry, J.F. (eds.), LITHOPROBE Rep. 34, p179-181.

__________ (1994): Petrochemical and structural evidence for the origin of granitoid rocks in the Rottenstone Domain; *in* Hajnal, Z. and Lewry, J.F. (eds.), LITHOPROBE Rep. 38, p188-195.

__________ (1995): Petrogenetic and tectonic significance of migmatites and granites in the Davin Lake area of the Rottenstone Domain; *in* Hajnal, Z. and Lewry, J.F. (eds.), LITHOPROBE Rep. 48, p104-110.

Coolican, C.T., Ansdell, K.M., Stauffer, M.R., and Kerrich, R. (1999): Geology of the Tonalite-Migmatite Complex, Deception Lake, Saskatchewan; *in* Summary of Investigations 1999, Volume 2, Saskatchewan Geological Survey, Sask. Energy Mines, Misc. Rep. 99-4.2, p196-201.

Defant, M.J., Drummond, M.S., Arthur, J.D., and Ragland, P.C. (1988): An example of trondhjemite petrogenesis: The Blakes Ferry pluton, Alabama, U.S.A.; Lithos, v21, p161-181.

Drummond, M.S. and Defant, M.J. (1990): A model for trondhjemite-tonalite-dacite genesis and crustal growth via slab melting: Archean to modern comparisons; J. Geophys. Res., v95, p21,503-21,521.

Drummond, M.S., Defant, M.J., and Kepezhinskas, P.K. (1996): Petrogenesis of slab-derived trondhjemite-tonalite-dacite/adakite magmas, Trans. Roy. Soc. Edin. Earth Sci., v87, p205-215.

Fumerton, S.L., Stauffer, M.R., and Lewry, J.F. (1984): The Wathaman Batholith: Largest known Precambrian pluton; Can. J. Earth Sci., v21, p1082-1097.

Gromet, P.L. and Silver, L.T. (1987): REE variations across the Peninsular Ranges Batholiths; implications for batholithic petrogenesis and crustal growth in magmatic arcs; J. Petrol., v28, p75-125.

Halden, N.M., Clark, G.S., Corkery, M.T., Lenton, P.G., and Schledewitz, D.C. (1990): Trace-element and Rb-Sr whole-rock isotopic constraints on the origin of the Chipewyan, Thorsteinson, and Baldock batholiths, Churchill Province, Manitoba; *in* Lewry, J.F. and Stauffer, M.R. (eds.), The Early Proterozoic Trans-Hudson Orogen of North America, Geol. Assoc. Can., Spec. Pap. 37, p201-214.

Holloway, J.R. and Burnham, C.W. (1972): Melting relations of basalt with equilibrium water pressure less than total pressure; J. Petrol., v13, p1-29.

Lewry, J.F., Stauffer, M.R., and Fumerton, S. (1981): A Cordilleran-type batholithic belt in the Churchill province in northern Saskatchewan; Precamb. Resear., v14, p277-313.

Lewry, J.F. and Collerson, K.D. (1990): The Trans-Hudson Orogen: Extent, subdivision, and problems; *in* Lewry, J.F. and Stauffer, M.R. (eds.), The Early Proterozoic Trans-Hudson Orogen of North America, Geol. Assoc. Can., Spec. Pap. 37, p1-14.

Martin, H. (1986): Effects of steeper Archean geothermal gradient on geochemistry of subduction-zone magmas; Geol., v14, p753-756.

__________ (1993): The mechanism of petrogenesis of the Archean continental crust: Comparison with modern processes; Lithos, v30, p373-388.

Meyer, M.T., Bickford, M.E., and Lewry, J.F. (1992): The Wathaman Batholith: An early Proterozoic continental arc in the Trans-Hudson orogenic belt, Canada; Geol. Soc. Amer. Bull., v104, p1073-1085.

Ray, G.E. and Wanless, R.K. (1980): The age and geological history of the Wollaston, Peter Lake, and Rottenstone domains in northern Saskatchewan; Can. J. Earth Sci., v17, p333-347.

Sun, S. and McDonough, W.F. (1989): Chemical and isotopic systematics of oceanic basalts: Implications for mantle composition and processes; *in* Saunders, A.D. and Norry, M.J. (eds.), Magmatism in the Ocean Basins, Geol. Soc. Spec. Publ. 42, p313-345.

Van Schmus, W.R., Bickford, M.E., Lewry, J.F., and Macdonald, R. (1987): U-Pb geochronology in the Trans-Hudson Orogen, northern Saskatchewan, Canada; Can. J. Earth Sci., v24, p407-424.

Mineralized Core Collection

A.J. Gracie

Gracie, A.J. (2000): Mineralized core collection; *in* Summary of Investigations 2000, Volume 2, Saskatchewan Geological Survey, Sask. Energy Mines, Misc. Rep. 2000-4.2.

Most of the mineralized core collection is housed at the Precambrian geological laboratory in La Ronge with some unmineralized stratigraphic uranium cores at the Subsurface Laboratory in Regina. The mineralized core collection has been described in previous summary reports (e.g. Gracie, 1999) and in an index to the collection (Gracie and Scutt, 1990). This index identifies the location of all cores by latitude and longitude on 1:250 000 scale maps, and gives full particulars of each hole: company, mineral disposition, exploration commodity, year, hole number, core size, hole bearing and inclination, length of sample, reference to other exploration data, and storage. The database has been converted to Microsoft Access97 and updated to August 31, 2000. Xerox and diskette (excluding location maps) copies of the database are available from the La Ronge office. Complete copies of the index (including maps) are available in La Ronge and Regina. Versions 2 and 3 of the Geological Atlas of Saskatchewan CD include the La Ronge mineralized core collection drill holes as a separate geological data set theme.

A total of 3156.13 m of core was collected in 1999-2000 (Table 1) from uranium (39.8 percent), base metals (28.2 percent), gold (17.8 percent), iron (13.9 percent), and PGM (0.3 percent).

The core collection has been augmented by an extensive suite of rock samples from mineral properties in northern Saskatchewan. The index to the sample collection lists all samples by NTS and number and briefly describes each sample by mineralization type, property, longitude, latitude, topographic location, lithology, mineral of interest, collector, and date. Xerox and diskette copies of this database are also available from the La Ronge office.

1. References

Gracie, A.J. (1999): Mineralized core collection; *in* Summary of Investigations 1999, Volume 2, Saskatchewan Geological Survey, Sask. Energy Mines, Misc. Rep. 99-4.2, p213.

Gracie, A.J. and Scutt, A.G. (1990): Index to La Ronge core collection; Sask. Energy Mines, Data File 15, 228p.

Table 1 - Core Acquisitions (September 1, 1999 to August 31, 2000).

Company or Joint Venture Operator	Commodity	NTS Area	No. of Holes	Core Size	Property/Deposit Location by Lake	Core Length (m)
Mineralized Core						
Cameco Gold	Au	73P-10	2	NQ	Greywacke Lake	250.1
Claude Resources	Au	63M-12	1	AQTK	Seabee Mine	67.3
Golconda Resources	Fe	73I-11	2	NQ	Ennis Lake	439.12*†
Golden Rule Resources	Au	64D-4	2	NQ	Komis Mine	242.95
Hudson Bay Exploration and Development	Cu/Zn	63K-13	1	BQ	Callinan Mine	458.9
Hudson Bay Mining and Smelting	Cu/Zn	63K-13	1	AW34	Callinan Mine	110.6
Leader Mining	Cu	63M-15	1	NQ	Mokoman Lake	38.6
Uranerz	Cu/Ni	74F-1	3	BQ	Jabba, Careen Lake East and West	283.52
Stratigraphic Core						
DF Exploration	U	74I-15	1	BQ	Hawkrock River	164.24
Golconda Resources	PGM	73I-10	1	NQ	Yaholnitsky Creek	9†
Uranerz	U	74G-16	1	NQ	Kearns Lake	1091.8

Notes:
* concentrated
† sections missing

B. Athabasca Basin: EXTECH IV Papers

EXTECH IV – Athabasca Uranium Multidisciplinary Study – Overview

C.W. Jefferson[1] *and G.D. Delaney*

This section of the Summary of Investigations reports on preliminary results from the first field season of the EXTECH IV Athabasca Uranium Multidisciplinary Study, a collaborative three year study of the Athabasca Basin and its uranium deposits. This is the fourth in a series of EXploration TECHnology projects undertaken by Natural Resources Canada and various partners. In addition to NRCan, represented by the Geological Survey of Canada (GSC), other funding partners are Saskatchewan Energy and Mines (SEM), Cameco Corporation, COGEMA Resources Inc., and Alberta Geological Survey (AGS). The research team also includes the Saskatchewan Research Council (SRC) as well as scientists from the universities of Regina, Saskatchewan, and Laurentian. EXTECH IV is coordinated by Dan Brisbin (Cameco), Gary Delaney (SEM), Charlie Jefferson (GSC), Philippe Portella (COGEMA), and Reg Olson (Alberta Geological Survey). There are two main objectives to this investigation: 1) to improve understanding of the Athabasca Basin and the context of its uranium deposits, and 2) to develop new technologies for exploring for uranium, particularly in the deeper part of the basin. A key goal of this work is to maintain the Athabasca Basin as the most attractive place in the world to explore for and mine uranium. Currently the Athabasca Basin produces 32% of the world's uranium. EXTECH IV comprises eight different sub-projects involving over two dozen researchers. A list of sub-projects, goals, and progress to-date in point form is provided below. Aspects of some of these investigations are highlighted in the papers that follow.

Sub-project 1: High-resolution Seismic Reflection Survey
Co-leaders: Zoli Hajnal (University of Saskatchewan) and Don White (Geological Survey of Canada)

Goal: To develop a viable seismic reflection survey technique for deep mineral exploration, and contribute to a 4-D geoscience framework for mineral exploration in the Athabasca Basin.

Work Plan: This project will entail a high-resolution, pseudo 3-D, seismic reflection survey across the McArthur River orebody.

Progress To-date:

- Preliminary seismic modeling has been done for the planned field survey area (Hajnal *et al.*, this volume). New data from borehole geophysics from summer 2000 (sub-project 2, Mwenifumbo *et al.*, this volume) is being incorporated in the models.
- Reassessment of the Athabasca extension to 1994 LITHOPROBE line S2b, in Points North area, indicates a different interpretation of stratigraphic and unconformity picks, but reaffirms the potential usefulness of high-resolution seismic data for both stratigraphy, basement topography, and structures transecting Athabasca Group and/or basement.
- Significant local relief on the basal unconformity requires use of lithologic logs from drill holes that are located within 1 km or less of the line. Ground-truthing and datum re-definition are in progress.

Sub-project 2: Multiparameter Borehole Geophysics
Leader: Jonathan Mwenifumbo (Geological Survey of Canada)

Goal: To enhance existing, and develop new, exploration technologies and strategies by improving knowledge of a complete spectrum of bulk geophysical characteristics of the Athabasca uranium deposits and their host rocks.

Work Plan: Characterize *in situ* acoustic, electrical, radioelement, thermal, and geotechnical/geophysical parameters of the uranium deposits and associated lithologic units and alteration.

---

[1] Geological Survey of Canada, 601 Booth Street, Ottawa, ON K1A 0E8.

Progress To-date:

- Multi-sensor geophysical measurements including spectrometric natural gamma-ray, spectral gamma-gamma density, full waveform sonic, magnetic susceptibility, inductive conductivity, resistivity, and induced polarization were made in two boreholes at each of Shea Creek and McArthur River sites (Mwenifumbo *et al.*, this volume).
- Lithology and uranium mineralization with associated alteration can be readily mapped by several of the geophysical parameters, correlate directly with geological logs, and offer new tools for stratigraphic correlation within the Athabasca Basin, facilitated by GSC's LogView geophysical plotting software.
- Heavy duty plastic casing preserves drill holes for geophysical logging and permits most parameters to be measured.
- *In situ* physical rock properties, such as compressional-wave velocities and densities, are providing necessary information to help design the high-resolution seismic survey and to interpret resulting data that will be acquired within the Athabasca Basin.

Sub-project 3: Bitumens, Hydrocarbons, Fluids, and Diagenesis

Leader: Lavern Stasiuk (Geological Survey of Canada)

Goal: To evaluate the origin and possible influence of bitumens/hydrocarbons associated with the uranium mineralization.

Work Plan: To undertake a regional study of the organic geochemistry of the Athabasca sandstones and detailed investigations of the organic geochemistry and petrography of bitumen-rich zones associated with uranium mineralization.

Progress To-date:

- Established protocol for handling, preparation, and analysis of NORM (Naturally Occurring Radioactive Materials) using an external consultant and the Canadian Nuclear Safety Commission.
- Seventy-five sandstone and potential hydrocarbon source rock samples were collected from three boreholes within the Athabasca Basin: Rumple Lake 74-J, Cluff Lake Car-114, and Amok Car-181. Twenty-five doubly polished thin sections are in preparation for aqueous fluid inclusion microthermometry and paragenetic evaluation of the Locker Lake Formation.
- RockEval system bulk organic geochemistry analyses were completed on 49 potential hydrocarbon source rock samples from Amok Car-181, including % Total Organic Carbon, Tmax).
- Fifty-one polished samples were prepared for organic petrology–microscopy from potential hydrocarbon sources from Douglas Formation in Car-181.
- Fluorescence and microspectrometric analyses were completed for 20 samples from Douglas Formation in Car-181.
- Twelve samples were collected by EXTECH colleagues from McArthur River site.
- Athabasca Basin samples, reports, etc. were compiled at GSC Ottawa and GSC Calgary; a database was established and input status brought up to date. Fifteen archived polished thin sections from V. Ruzicka's collection were selected for re-examination.
- Excellent Post-doctoral Fellowship (PDF) candidates are being investigated for this project, however, it is a challenge to attract them at traditional PDF salaries in Canadian institutions.

Sub-project 4: Athabasca Stratigraphy and Sedimentology

Co-leaders: Charlie Jefferson (Geological Survey of Canada) and Gary Yeo (Saskatchewan Energy and Mines)

Goal: Refine understanding of Athabasca stratigraphy and sedimentology and their relationships to uranium mineralization.

Work Plan: Characterize depositional facies architecture, sequence stratigraphy, provenance, and diagenesis for the Athabasca Group by logging diamond drill core selected to construct a series of transects across the basin.

Progress To-date:

- More than 30 drill holes were logged in five transects of the eastern part of the basin (Yeo *et. al.*, this volume).

- In northeastern transects, basal members are rich in detrital magnetite and thicken westward. In southeastern transects, eastern facies resemble those in open pits whereas western basal facies are distinctive red mudstones and conglomerates.
- The four-member subdivision of Manitou Falls Formation (MFa, MFb, MFc, and MFd), established by Ramaekers in the 1980s, remains widely applicable and represents an overall fining-upward sequence amenable to quantitative description by parameters such as grain size, cross-bed thickness, sorting, and abundance of clay.
- Preliminary detailed subdivisions of each member of the Manitou Falls Formation have been suggested by quantitative plots using GSC's LogView software.
- Stratigraphic studies are being integrated with borehole geophysics and high-resolution seismic, allowing cross-calibration and improved interpretation of all three. These studies will enhance practical and theoretical exploration models, to improve precision of drilling and interpretation of exploration holes.

Sub-project 4a: Detailed Stratigraphic Studies in Athabasca Basin

Co-leaders: Darrel Long (Laurentian University) and Gary Yeo (Saskatchewan Energy and Mines)

Goal: To improve understanding of Athabasca stratigraphy and sedimentology and its role in the localization of uranium mineralization at some of the major uranium deposits.

Work Plan: To undertake detailed investigations of facies relationships in the basal Manitou Falls Formation as revealed in open pits and areas of relatively good exposure.

Progress To-date:

- Detailed investigations of stratigraphic relationships in Manitou Falls Formation in the Sue C Pit at McClean Lake and the Deilmann Pit at Key Lake (Long *et al.*, this volume).
- Basal strata exposed in Sue and Key Lake Pits include two conglomeratic coarse sandstones separated by a stepped erosional surface and a basal conglomerate respectively.

Sub-project 5: Basement to Western Athabasca Basin

Goal: To better understand the basement geology of the western Athabasca Basin and its influence on mineralization.

Work Plan: Augment an earlier study of the sub-Athabasca basement geology and geochemistry by integrating geophysical data with the logging of selected drill core supported by geochronological and geochemical studies. Correlate with information about flanking shield rocks.

Progress To-date: This sub-project is scheduled to commence in year two of EXTECH IV.

Sub-project 5a: Detailed Structural Studies of Athabasca Uranium Deposits

Leader: Ghislain Tourigny (Saskatchewan Energy and Mines)

Goal: To understand the structural history of the basement/cover rocks at some of the major uranium deposits and the role of structure in the localization of uranium mineralization.

Work Plan: To undertake detailed structural investigations in open pits at some of the deposits and to integrate this work with that of the broader sub-Athabasca basement study.

Progress To-date: Detailed studies in Sue C (McClean Lake) and Deilmann (Key Lake) pits have demonstrated compatibility with structural styles established in previous regional projects and provided a detailed understanding of the structural context of these two ore deposits (Tourigny *et al.*, this volume; Harvey and Bethune, this volume).

Sub-project 6: Gamma Ray Geophysics

Leader: Rob Shives (Geological Survey of Canada)

Goal: To improve understanding of current regional radiometric data over the Athabasca Basin and evaluate its relevance to mineralogical alteration and other components of the project.

Work Plan: Conversion of previous regional and detailed analogue NATGAM gamma-ray spectrometer surveys to digital data and subsequent recompilation and reinterpretation. This will be supported by detailed ground surveys in specific areas.

Progress To-date:

- A brief field study in the McArthur River Mine area tested the hypothesis that gamma ray spectrometry can map radioactive element (K, eU, and eTh) variations associated with known illite enrichment in sandstone boulders (Shives *et al.*, this volume).
- Preliminary results indicate that ground spectrometry can provide cost-effective, *in situ* determination of potassium enrichment related to illite within sandstone boulders.
- Detailed airborne high-sensitivity gamma ray spectrometric surveys would identify differences in low eTh/K ratios, thereby providing exploration guidance.

Sub-project 6a: Surficial Geology

Co-leaders: Janet Campbell (Saskatchewan Research Council) and Rod Klassen (Geological Survey of Canada)

Goal: To establish a surficial geological framework for the Athabasca Basin to aid in mineral exploration and sustainable development.

Work Plan: Compilation of available Quaternary geological data for the NEA-IAEA test area in both digital database and map formats with follow up ground studies of selected areas to ground truth surficial relationships.

Progress To-date:

- Saskatchewan Research Council initiated digital compilation and upgrading of existing and limited new data on surficial geology and regional till geochemistry in the NEA-IAEA test area, where a previous jointly sponsored GSC-SEM program compared different methods of exploration for uranium.
- Eleven bulk till samples and field data were collected from sites along the Black Lake and Points North roads from a variety of till deposits with background and elevated total count airborne radiometric data (Campbell and Shives *et al.*, this volume). Compositional analyses will assist with ground calibration of the radiometric data.

Sub-project 7: Clay Mineral Studies

Leader: Jeanne Percival (Geological Survey of Canada)

Goal: To undertake investigations of the genesis of clay minerals in the pre-Athabasca regolith, Athabasca Group sandstones, and alteration haloes surrounding ore bodies so as to enhance the interpretation of stratigraphy, diagenesis, basement geology, gamma ray geophysics, and surficial geology.

Work Plan: Petrographic and geochemical analysis of clay minerals from regional stratigraphic and deposit-scale sample suites.

Progress To-date:

- Participated in core logging, sampling, processing of samples for polished thin sections, and clay-size separations co-ordinated with stratigraphic studies.
- Synchrotron study of uranium associated with illitic clays from the alteration halo around the Cigar Lake uranium deposit, is contributing to understanding of clays in Athabasca Basin and to design follow-up EXTECH studies on clay mineralogy. The new data are being used to assess whether U occurs as UO_2, is adsorbed onto the clay surface, or occurs within the illite interlayer in the alteration halo (Percival *et al.*, this volume).

Sub-project 8: Coordination

Co-leaders: Charlie Jefferson (Geological Survey of Canada) and Gary Delaney (Saskatchewan Energy and Mines)

Goal: Ensure co-operation, transparency, integration, timely delivery, and maximum impact of relevant results.

Work Plan: To plan and coordinate field activities, and the subsequent compilation and communication of scientific results.

Progress To-date:

- Coordinators ensured full cooperation of staff in all supporting organizations, and smoothed logistics for the many activities involved (staff accommodation, transportation, core logging, sampling, mapping, processing of samples, etc.).
- Communication plans were developed and implemented, including newspaper, newsletter and government publications, posters, and a Web-site (nearing completion), workshop, and Open House plans. Co-ordinators managed and accounted for cash and in-kind contributions of their respective sponsoring agencies.

Sub-project 8a: GIS Database
Leader: Bill Slimmon (Saskatchewan Energy and Mines)

Goal: Design and compile an ArcView GIS database of all project results including mapping, locations of diamond drill holes, mineral occurrences, assessment work, sections measured, seismic lines, borehole geophysics, gamma ray geophysics, etc.

Work Plan: To systematically develop as complete a GIS database as possible, beginning in year one with public domain data and incrementing in years two to three with project-generated data.

Progress To-date: An extensive GIS database, compiling previous work, is being constructed in ArcView. Data entry and analysis are ongoing, and the database is available for query by project participants through distribution of CD-ROM copies on request.

Seismic Modeling Prior to the EXTECH IV Athabasca Basin Seismic Reflection Survey

Z. Hajnal [1], B. Reilkoff [1], B. Pandit [1], D. White [2], E. Adam [2], B. Powell [3], and R. Koch [4]

Hajnal, Z., Reilkoff, B., Pandit, B., White, D., Adam, E., Powell, B., and Koch, R. (2000): Seismic modeling prior to the EXTECH IV Athabasca Basin seismic reflection survey; *in* Summary of Investigations 2000, Volume 2, Saskatchewan Geological Survey, Sask. Energy Mines, Misc. Rep. 2000-4.2.

Abstract

The objectives of the EXTECH IV high-resolution seismic reflection survey planned for the McArthur River mining camp are: 1) to seismically detect a known orebody, 2) to seismically characterize the geology of the prospective ore-bearing horizon, and 3) to assess and refine seismic reflection techniques for exploration within the Athabasca Basin. General design of a suitable high-resolution seismic reflection survey is considered in light of the known geology and information from borehole sonic logs. We conclude that: 1) the heterogeneity of the surface till layer favours Vibroseis as a seismic energy source over dynamite in drill holes; 2) near-surface multiples will be a major source of coherent noise that have to be attenuated during processing, 3) dense spatial sampling of the wavefield is essential in order that a full spectrum of sophisticated noise-suppression techniques can be applied during processing. Design of a pseudo 3-D survey is also considered.

1. Background

Seismic surveys fundamentally consist of generating seismic waves at the Earth's surface that propagate down into the Earth where they are reflected and or scattered from geological boundaries. Some portion of the reflected/scattered energy returns to the surface where it is captured by an extensive array of motion sensors (geophones) and digitally recorded. To obtain spatial coverage, the source of seismic waves is moved many times (usually along a profile line), and the process is repeated. Prior to the data acquisition process, assessments can be made about the expected signal quality, potential background noise conditions, and the selection of optimal survey parameters. The outcome of a seismic survey is a large data set that is subsequently processed to obtain a seismic reflection image of the subsurface geology.

Seismic methods have provided the chief tool for oil and gas exploration in sedimentary basin environments. Within the past 15 to 20 years, seismic methods have been adapted and used for deep seismic profiling (to depths exceeding 50 km) of the continents (e.g. LITHOPROBE). Most recently, the seismic reflection method has been adapted for use as a mineral exploration tool in crystalline rock (e.g. Milkereit *et al.*, 1997; Hajnal *et al.*, 1997; Adam *et al.*, 2000). To date, there has been no successful attempt at direct detection and characterization of unconformity-type uranium deposits using seismic techniques. We intend to design and conduct a seismic survey within the McArthur River uranium camp of the Athabasca Basin with the primary objective of attempting to directly detect and characterize a uranium deposit. Here we report on pre-survey parameter selection and survey design.

2. Geological Setting and Initial Survey Considerations

The known subsurface geology around and within the unconformity-type uranium deposits of the Athabasca Basin is complex (Lewry and Sibbald, 1980; Ramaekers, 1981; Sibbald, 1983, 1986; Hoeve and Quirt, 1984, 1987; Fouques *et al.*, 1986; Kotzer and Kyser, 1993, 1995; Raffensperger and Garven, 1995; Matthews *et al.*, 1997). Earlier seismic studies (Hobson and MacAuley, 1969; Scott, 1983; Hajnal *et al.*, 1997) indicate that these intricate geologic settings generate complicated seismic signals, thus challenging the imaging capabilities of standard seismic reflection techniques. The ore deposits are surrounded by a variably altered sandstone *halo zone*, floored by a highly weathered regolith layer within the basement, and they are often associated with graphitic fault zones. Variability in these elements of the ore deposit geology should have recognizable spatially variant seismic reflectivity properties and are very likely the sources of complicated seismic reflection and scattering events. A primary objective of the program is to seismically detect a known ore deposit. Secondly, we hope to seismically characterize the lateral variations in the geology of the prospective ore-bearing horizon. The observation of these ore-related reflection waveforms is a fundamental requirement for the assessment of the method as a viable exploration technique in the Athabasca Basin. In addition, the acquisition of the field data will further advance our understanding of effective seismic data collection techniques for the basin, advance customized data processing methods,

---

[1] Department of Geological Sciences, University of Saskatchewan, 114 Science Place, Saskatoon, SK S7N 5E2.
[2] Geological Survey of Canada, Continental Geoscience Division, 615 Booth Street, Ottawa, ON K1A 0E9.
[3] Cameco Corporation, 2121 - 11th Street West, Saskatoon, SK S7M 1J3.
[4] COGEMA Resources Inc., 817 - 825 45th Street West, Saskatoon, SK S7K 3X5.

and establish a template for interpreting and distinguishing the characteristic ore-related signatures from the reflection patterns characteristic of adjacent barren zones. A comprehensive understanding of both the local and regional structural framework of a portion of the basin is required for this study. The results of combined regional and high-resolution seismic surveys are intended to provide this information.

The predominantly thin (<40 m) glacial till, which blankets the entire basin is heavily contaminated by variably sized boulders. This near-surface irregular textural condition constitutes the first major problem for seismic data acquisition in this remote area by eliminating shothole drilling and explosives as a potential energy source. As an alternative source, we will test a truck mounted vibroseis system and will investigate the following source parameters: number of sources per vibration point required to achieve adequate signal-to-noise ratio in the recorded data from the target depth, array configuration, frequency spectra, and the use of linear or nonlinear signal sweeps. Appropriate resolution requirements of the ore geology necessitates seismic signal frequencies reaching at least 150 Hz.

Shallow till deposits unconformably overlie the unweathered Paleoproterozoic Athabasca Group sandstone strata of the basin fill. The contact of the low-velocity (>1100 m/s) glacial till and the high-velocity sandstone (~4000 m/s) has a reflection coefficient of ~0.6. Thus, this very prominent shallow interface is a strong signal scatterer and the source of coherent noise (e.g. near-surface multiples) that degrades the deeper reflection signal. Novel source and detector arrays and signal processing procedures are required to minimize the noise conditions relative to the deeper reflections.

a) Survey

Survey Design

The success of any seismic imaging experiment is dependent on proper survey design. As every geological environment is unique, utilization of as much *a priori* information as possible maximizes the likelihood of success. Existing geological knowledge of the target regions, released by the mine operators, is incorporated into the modeling process and survey design. Survey design will include the specification of suitable seismic equipment, the minimum number and layout pattern of the surface sensors (geophones) to ensure acceptable signal-to-noise levels (based on stack fold), adequate wavefield sampling (in space and time) to accommodate the application of advanced data processing methods, an aperture size suited to the depth and anticipated geometry of the principal geologic target, frequency range and sweep pattern of the source, source spacing and vibration effort.

Pre-survey Modeling

Velocity log information (Figure 1) from borehole MAC257, in the vicinity of the McArthur River orebody, indicates several distinct velocity contrasts (R_1 to R_7) from surface to 550 m depth (0.00 to 0.258 s travel time). R_1 is the interface between the glacial till and the sandstone. R_2 to R_5 are velocity changes within sandstone of the Manitou Falls Formation. The velocity variations in the zone of R_6 to R_7 are associated with the geology of the unconformity zone. Note that the velocity log does not include a sampling of the ore zone. The uniform 5600 m/s velocity below R_7 is considered as a representative segment of the acoustic unaltered crystalline basement. Figure 1 shows the seismic response (excluding intrabed multiples) calculated for the velocity log. The diagram clearly shows that in the region of interest (i.e. the vicinity of the unconformity), strong recognizable seismic reflections are generated by the sudden changes in acoustic properties. Several of the stratigraphic changes within the sandstone also appear to be identifiable on the seismic record. An important feature of the record is the strong interference between the powerful near-surface generated events (R_1, direct wave, reflections from the first interface) and the reflections of interest. The suppression of the near-surface generated energy will require special consideration during the processing phase of the data analysis. The complexity of the complete seismic response (with multiple reflections) is demonstrated by Figure 2. The near-surface reverberations of seismic energy completely overwhelm the reflections of interest. Systematic multi-step signal processing (Hajnal *et al.*, 1997) is required to minimize the influence of these coherent noise patterns.

The planned survey will attempt to image the orebody along one profile (5 to 10 km long) or two parallel profiles (3 to 5 km long) with 1200 m separation (Figure 3). There is also to be a "regional" 30 km long line. Pending budgetary conditions, a 960 channel recording system will be used in an attempt to acquire 3-D coverage of the orebody during the acquisition of the two parallel lines utilizing cross-spreads; 480 of the 960 channel system would be utilized for the cross-spreads. Figure 3 illustrates the fold and offset ranges of a scenario where the two cross-spreads also record shot from an auxiliary shot line parallel with the two main profiles. This survey design will not provide full 3-D coverage as the fold is only 16, the azimuths and the offsets distributions are not ideal, but it provides some reasonable data to test 3-D applications in this specific environment.

b) Data Acquisition

Data acquisition will be handled under contract by a Canadian seismic acquisition company under the supervision of the principal investigators. The seismic data will be delivered in suitable digital format by the contractor to the principal investigators who will verify the integrity of the data. It is anticipated that data acquisition will take approximately 10 to 14 days upon arrival of the seismic crew at the survey location.

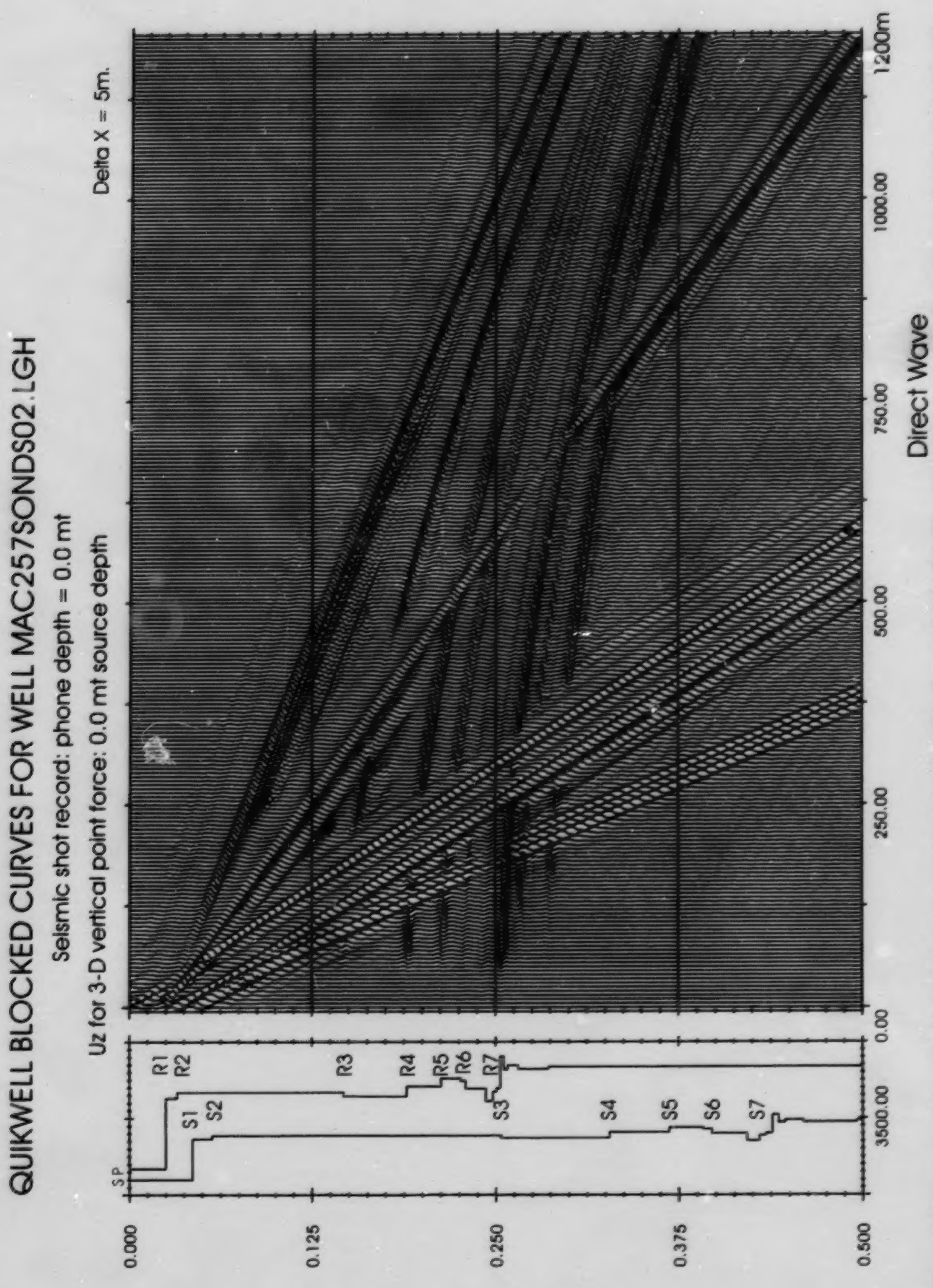

***Figure 1** - Velocity log (left) and calculated seismic record (right) for McArthur River well MAC257. The seismic record was calculated using a reflectivity algorithm with intrabed and free-surface multiples excluded. Reflections are generated from the velocity steps; R1 to R7 indicate the p-wave velocity steps and S1 to S7 the corresponding steps in s-wave velocity.*

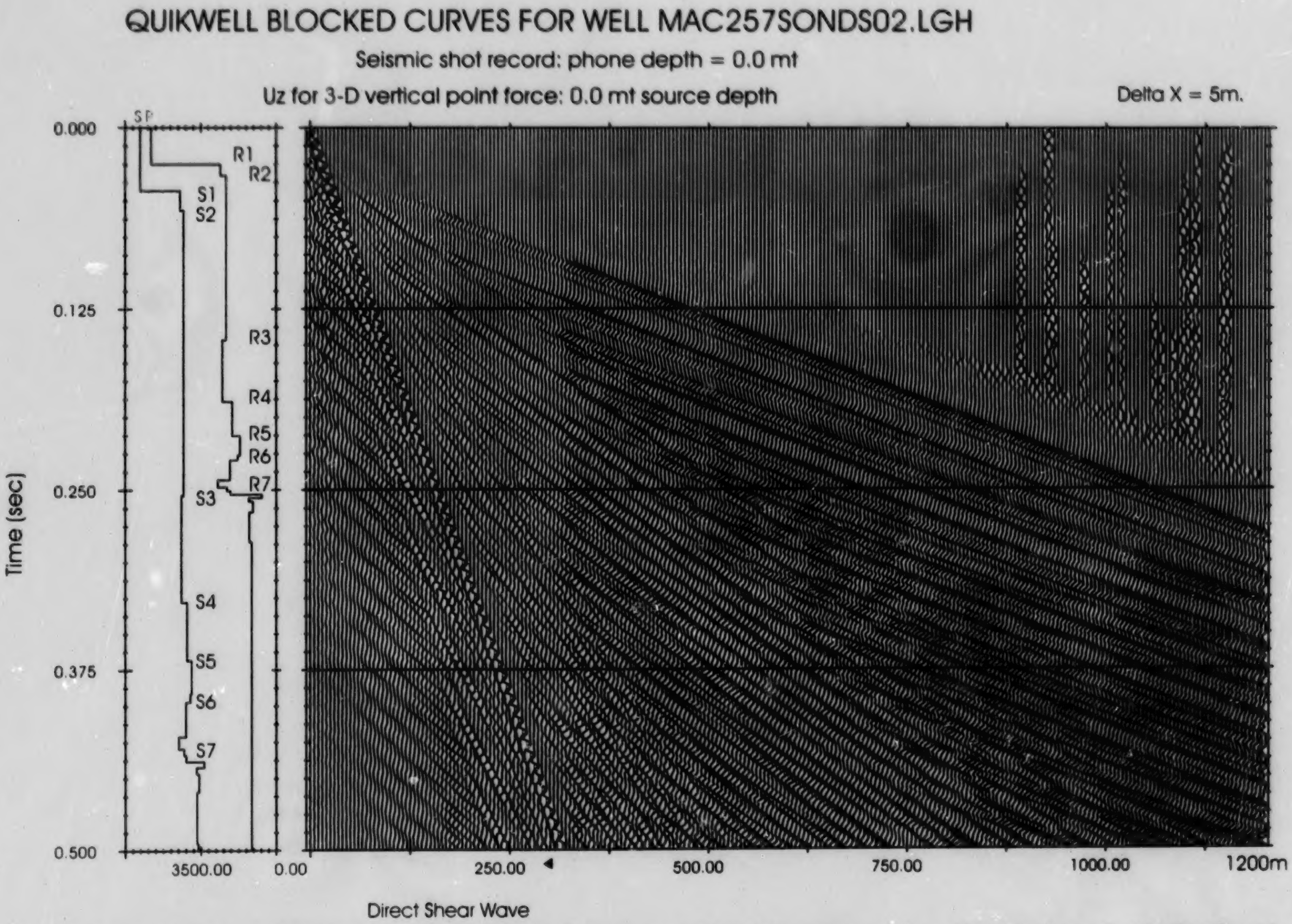

Figure 2 - Velocity log (left) and calculated seismic record (right) for McArthur River well MAC257. The seismic record was calculated using a reflectivity algorithm and includes the full wavefield (including intrabed and free-surface multiples). Reflections are generated from the velocity steps; R1 to R7 indicate the p-wave velocity steps and S1 to S7 the corresponding steps in s-wave velocity.

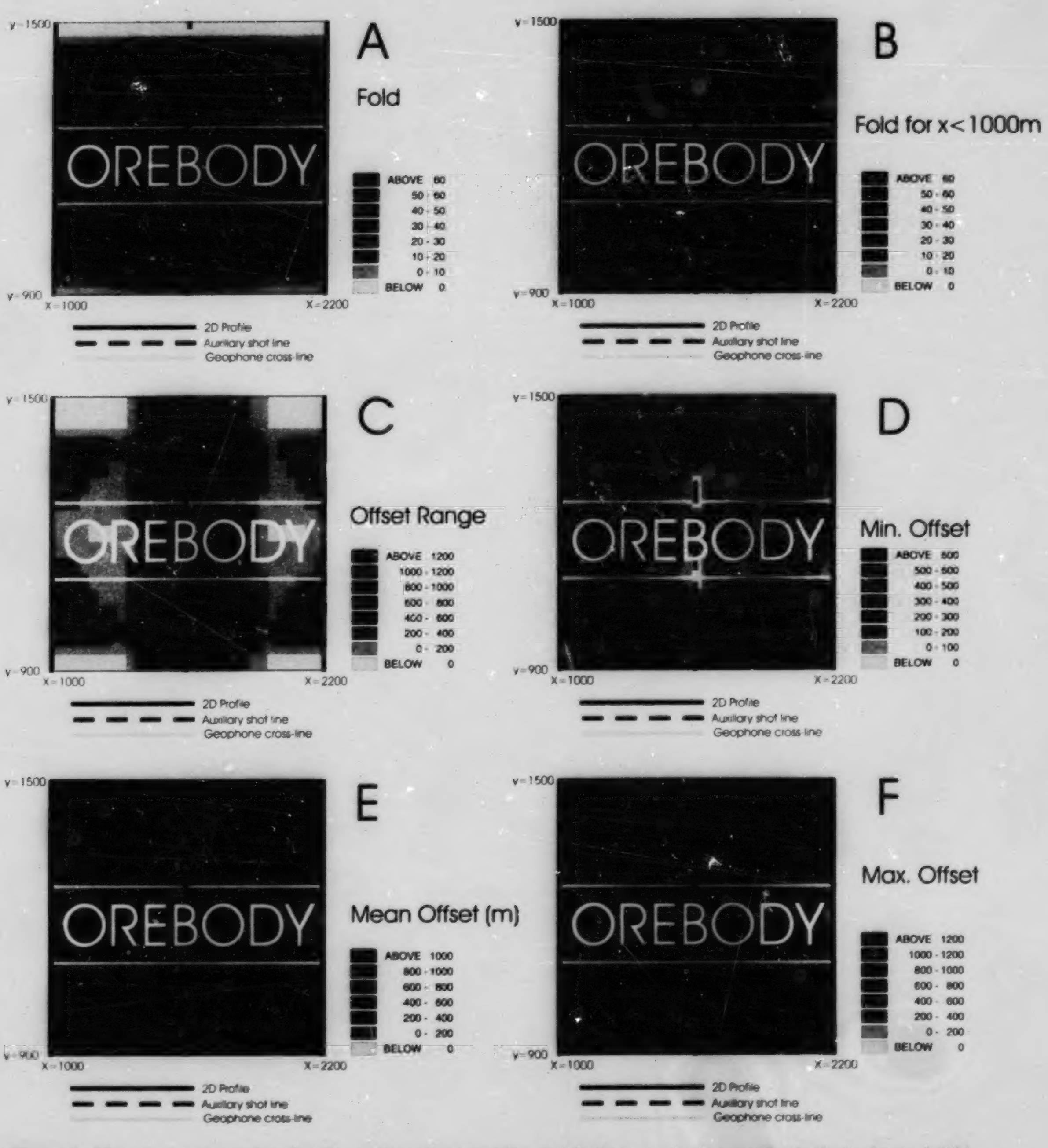

Figure 3 - Plan-view contour plots showing various characteristics of 3-D data acquired across the ore-body: A) stack fold using data from all offsets, B) stack fold using data for offsets of <1000 m , C) offset range, D) minimum offset, E) mean offset, and F) maximum offset. Shots from both of the two parallel 2-D profiles (located at x=1000 and x=2200 m) are recorded on the cross-spreads. The shot-interval is 20 m. Shots from 0 to 2400 m along the two parallel profiles are recorded by the cross-spreads. It is assumed that the target of primary interest is at a depth of 600 m, is 200 m wide (in the direction of the profiles), and is 1000 m long (in the direction normal to the profiles). The target runs along strike at y=1200 m. For fold determination, a 20 m x 20 m bin size is used. An additional line of shots is included along x=1600 m (20 m interval between y=600 m and y=1800 m; this is 60 shot points).

3. Data Processing and Interpretation

Data processing and interpretation will be conducted at the University of Saskatchewan Seismic Laboratory and at the Seismology and Electromagnetism Section of the Geological Survey of Canada. The two processing groups will work collaboratively, but will focus on different aspects of the data. University of Saskatchewan will concentrate on the regional seismic profile and detailed processing of the high-resolution lines whereas the Geological Survey of Canada will concentrate specifically on imaging the orebody.

4. Acknowledgments

Charlie Jefferson of the Geological Survey of Canada is thanked for his review of this manuscript. GSC contribution No. 2000182.

5. References

Adam, E., Perron, G., Milkereit, B., Wu, J., Calvert, A.J., Salisbury, M., Verpaelst, P., and Dion, D.-J. (2000): A review of high-resolution seismic profiling across the Sudbury, Selbaie, Noranda, and Matagami mining camps; Can. J. Earth Sci. v37, p503-516.

Fouques, J.P., Fowler, M., Knipping, H.D., and Schimman, K. (1986). The Cigar Lake uranium deposit: Discovery and general characteristics; *in* Evans, E.L. (ed.), Uranium deposits of Canada, Can. Inst. Min. Metal., Spec. Vol. 33, p218-229.

Hajnal, Z., Annesley, I.R., White, D., Matthews, R.B., Sopuk, V., Koch, R., Leppin, M., and Ahuja, S. (1997): Sedimentary-hosted mineral deposits: A high-resolution survey in the Athabasca Basin; *in* Gubins, A.G. (ed.), Proceedings of Exploration 97: Fourth Decennial International Conference on Mineral Exploration, Pap. 53, p421-432.

Hobson, G.D. and MacAuley, H.A. (1969): A seismic reconnaissance survey of the Athabasca Formation, Alberta and Saskatchewan; Geol. Surv. Can., Pap. 69-18, p35-47.

Hoeve, J. and Quirt, D. (1984): Uranium mineralization and host-rock alteration in relation to clay mineral diagenesis and evolution of the Middle-Proterozoic Athabasca Basin, Saskatchewan, Canada; Sask. Resear. Counc., Publ. R-855-2-B, 190p.

__________ (1987): A stationary redox form as a critical factor in the formation of high-grade, unconformity-type uranium ores in the Athabasca Basin, Saskatchewan, Canada; Bull. Mineral., v110, p157-171.

Kotzer, T.G. and Kyser, T.K. (1993): O, U, and Pb isotopic and chemical variations in uraninite: Implications for determining the temporal and fluid history of ancient terrains; Amer. Mineral., v78, p1262-1274.

__________ (1995): Petrogenesis of the Proterozoic Athabasca Basin, northern Saskatchewan, Canada, and its relation to diagenesis, hydrothermal uranium mineralization and paleohydrogeology; Chem. Geol., v120, p45-89.

Lewry, J.F. and Sibbald, T.I.I. (1980): Thermotectonic evolution of the Churchill Province in northern Saskatchewan, Canada; Can. J. Earth Sci., v68, p45-82.

Matthews, R., Koch, R., Leppin, M., Powell, B., and Sopuck, V. (1997): Advances in integrated exploration for unconformity uranium deposits in western Canada; *in* Gubins, A.G. (ed.), Proceedings of Exploration 97: Fourth Decennial International Conference on Mineral Exploration, Pap. 131, p993-1002.

Milkereit, B., Berrer, E.K., Watts, A., and Roberts, B. (1997): Development of 3-D seismic exploration technology for Ni-Cu deposits, Sudbury Basin; *in* Gubins, A.G. (ed.), Proceedings of Exploration 97: Fourth Decennial International Conference on Mineral Exploration, Pap. 55, p439-448.

Raffensperger, J.P. and Garven, G. (1995): The formation of unconformity-type uranium ore deposits 2: Coupled hydrochemical modeling; Amer. J. Sci., v295, p639-696.

Ramaekers, P. (1981): Hudsonian and Helikian basins of the Athabasca Basin; *in* Summary of Investigations, Saskatchewan Geological Survey, Sask. Miner. Resour., Misc. Rep. 79-10, p154-160.

Sibbald, T.I.I. (1983): Geology of the crystalline basement, NEA/IAEA test area; *in* Cameron, E.M. (ed.), Uranium exploration in the Athabasca Basin, Saskatchewan, Canada, Geol. Surv. Can., Pap. 82-11, p1-14.

__________ (1986): Overview of the Precambrian geology and aspects of the metallogenesis of northern Saskatchewan; *in* Gilboy, C.F. and Vigrass, L.W. (eds.), Economic Minerals of Saskatchewan, Sask. Geol. Soc., Spec. Publ. No. 8, p1-16.

Scott, F. (1983): Midwest Lake uranium discovery; *in* Cameron, E.M. (ed.), Uranium exploration in the Athabasca Basin, Saskatchewan, Canada, Geol. Surv. Can., Pap. 82-11, p41-50.

Multiparameter Borehole Geophysical Logging at the Shea Creek and McArthur River Projects: Parameters for Exploration, Stratigraphy, and High-resolution Seismic Studies

C.J. Mwenifumbo [1], K.A. Pflug [1], B.E. Elliott [1], C.W. Jefferson [1], R. Koch [2], J. Robbins [2], and R. Matthews [3]

Mwenifumbo, C.J., Pflug, K.A., Elliott, B.E., Jefferson, C.W., Koch, R., Robbins, J., and Matthews, R. (2000): Multiparameter borehole geophysical logging at the Shea Creek and McArthur River projects: Parameters for exploration, stratigraphy, and high-resolution seismic studies; *in* Summary of Investigations 2000, Volume 2, Saskatchewan Geological Survey, Sask. Energy Mines, Misc. Rep. 2000-4.2.

Abstract

Multi-sensor geophysical measurements including spectrometric natural γ-ray, spectral γ-γ density, full waveform sonic, magnetic susceptibility, inductive conductivity, resistivity, and induced polarization were made in several boreholes at Shea Creek and McArthur River in the Athabasca Basin of northern Saskatchewan. The objective was to determine the geophysical characteristics and signatures of the Athabasca uranium deposits and their host rocks. Preliminary analysis of these data indicates that lithology and uranium mineralization with associated alteration can be readily mapped by several of the geophysical parameters. The geophysical parameters also indicate that lithology can be refined and objectively characterized to provide a better framework for stratigraphic correlation within the Athabasca Basin. Geophysical logging at the Shea Creek project, carried out in plastic-cased boreholes, indicated that uranium ore delineation can be accomplished with spectral γ-γ density and natural γ-ray methods. Associated graphitic conductors can be accurately delineated on the inductive conductivity log. Logging data acquired at McArthur River, carried out in open boreholes, provided similar geophysical characteristics with the natural γ-ray data accurately mapping changes in lithology that can be matched with the drill core lithology data. In situ physical rock properties, such as compressional wave velocities and densities, are being determined and these will provide the necessary information for interpreting the high-resolution seismic survey data that will be acquired within the Athabasca Basin.

1. Introduction

This is a report of summer 2000 fieldwork for sub-project 2 of EXTECH IV - Athabasca Uranium Multidisciplinary Study. Multi-sensor borehole geophysical logs were acquired in two boreholes at the Shea Creek project, south of Cluff Lake mine, and two boreholes at the McArthur River P2 zone (Figure 1) with the Geological Survey of Canada (GSC) research and development (R&D) logging system (Killeen and Mwenifumbo, 1988).

2. Objectives and Strategies

The purpose of the borehole geophysics sub-project is to enhance existing, and develop new, exploration technology and strategies by improving knowledge of a complete spectrum of bulk geophysical characteristics of the Athabasca uranium deposits and their host rocks. This is addressed by:

1) Characterizing geophysical signatures of lithologic units and alteration associated with uranium deposits using state-of-the-art and new multiparameter borehole logging technologies of the Borehole Geophysics and Petrophysics Section.
2) Providing *in situ* physical properties: full waveform sonic (FWS – compressional (Vp) and shear (Vs) velocity) and density for high-resolution seismic interpretation; electrical (resistivity and induced polarization (IP)) for interpreting magnetotelluric, electromagnetic, and resistivity surveys; radioelement distribution for spectrometric γ-ray survey interpretations; temperature distribution for basin heat-flow modeling; and rock mass characteristics for exploration, geotechnical, and other mine development needs.
3) Improving the calibration of spectral γ-ray probes (K, U, and Th) in the extremely high-grade, Athabasca-type uranium deposits to assist in ore delineation and grade estimation.

3. Geophysical Logging

Multi-sensor borehole logs acquired (August 16 to 19, 2000) at the Shea Creek project area near Cluff Lake, include: natural γ-ray (one spectrometric probe and two

---

[1] Geological Survey of Canada, 601 Booth Street, Ottawa, ON K1A 0E8.
[2] COGEMA Resources Inc., 817 - 825 45th Street West, Saskatoon, SK S7K 3X5.
[3] Cameco Corporation, 2121 - 11th Street West, Saskatoon, SK S7M 1J3.

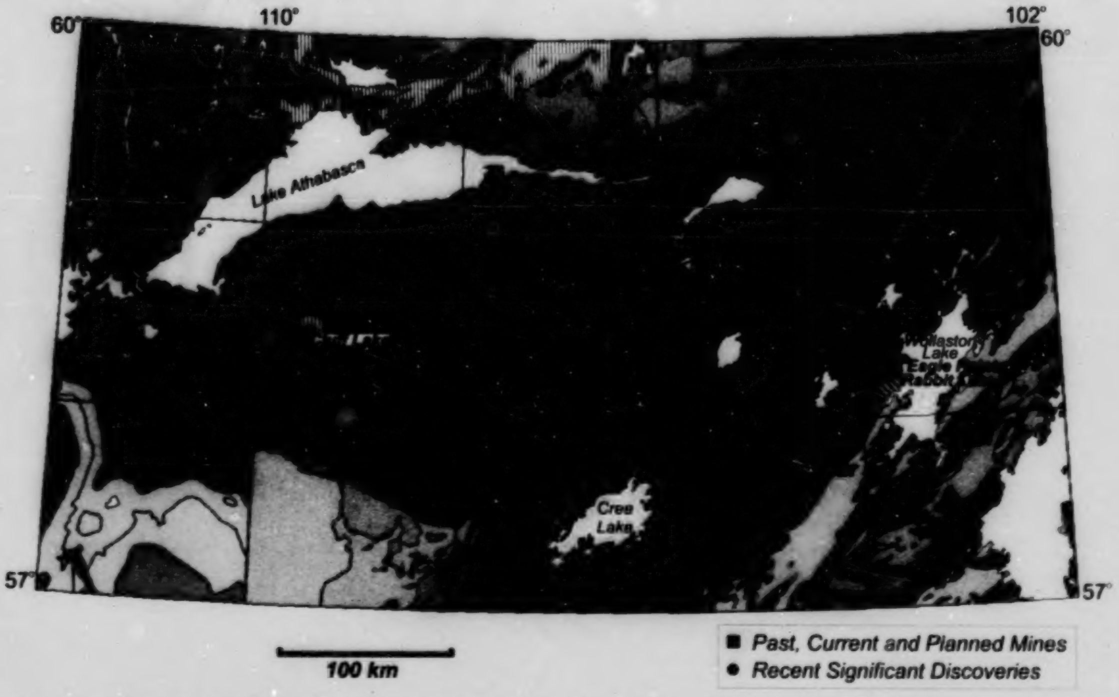

Figure 1 - Map of the Athabasca Basin showing the location of the Shea Creek Project and the McArthur River uranium deposits.

total counting probes), spectral γ-γ density, magnetic susceptibility, temperature, inductive conductivity, and full waveform sonic (Table 1). The two boreholes logged (SHE101-4 and SHE105-4) were plastic-cased and hence no galvanic electrical logging data (resistivity, IP, and self potential) were acquired.

Logging measurements acquired at McArthur River included: natural γ-ray spectrometry, spectral γ-γ density, magnetic susceptibility, inductive conductivity, resistivity, IP, full waveform sonic, and temperature (Table 1). These data were acquired in two boreholes, MAC218 and MAC197, from August 22 to 26, 2000.

The acquisition of the data was structured to address the reliability, calibration, and drift characteristics of each of the logging probes. Data were acquired while going down the borehole (downhole run) and coming back up (uphole run) thereby providing a check on the repeatability and quality of the data.

4. Shea Creek Project – Cluff Lake

The Shea Creek project, owned and operated by COGEMA Resources Inc., is located south of the Cluff Lake mine and south of the Carswell structure in the western part of the Athabasca Basin (Figure 1). Multiparameter borehole geophysical logging was conducted in boreholes SHE101-4 and SHE105-4 in the Anne zone. The overburden was penetrated with

Table 1 - Summary of logging conducted at Shea Creek and McArthur River, Athabasca Basin.

Area	Borehole	Logging Probe	Logging Date (2000)
Shea Creek	SHE101-4	Temperature	August 16
		Temperature	August 17
		Density	August 16
		Gamma	August 16
		Gamma*	August 17
		Multiparameter	August 17
		Acoustic	August 17
	SHE105-4	Temperature	August 18
		Density	August 18
		Gamma	August 19
		Multiparameter	August 19
		Acoustic	August 19
McArthur River	MAC218	Temperature	August 22
		IP	August 22
		Multiparameter	August 23
		Density	August 24
		Gamma	August 24
		Acoustic	August 24
	MAC197	Temperature	August 25
		IP	August 25
		Density	August 25
		Gamma	August 25
		Multiparameter	August 26
		Acoustic	August 26

* γ-ray data acquired with the small scintillation detector probe.

HW casing (114.3 mm in diameter) followed by HQ (96.1 mm) coring to approximately 400 m. The drill holes were completed by reducing them to NQ (75.7 mm) coring. SHE101-4 and SHE105-4 were drilled using navigational drilling techniques.

a) Local Geology

These two boreholes intersected overburden, the Athabasca Group (Ramaekers, 1990) and crystalline basement rocks. The overburden comprises Quaternary sediments ranging in thickness from 20 to 50 m in the project area. These sediments consist of glacial drift, outwash, and lacustrine sands. Paleoproterozoic sedimentary rocks of the Athabasca Group include basal conglomerate, sandstones, and minor siltstones of the non-marine Manitou Falls and marine Lazenby Lake, Wolverine Point (A and B members), and Locker Lake formations (see Table 4 of Yeo *et al.*, this volume, after Ramaekers, 1990).

The Athabasca Group is essentially flat lying, undeformed except for minor reverse faults, and unconformably overlies the gneissic basement rocks. The lowest strata intersected at the Shea Creek project is the Manitou Falls Formation, comprising members MFc and MFd. The lower member, MFc, is non-marine medium- to very coarse-grained sandstone and siltstone with thin (<2 cm) granule conglomerate and sparse clay intraclasts. The upper member comprises non-marine, medium- to fine-grained sandstone with common clay intraclasts. The overlying Lazenby Lake Formation is a marine succession of pebbly sandstone with illite and chlorite cement. Next, the Wolverine Point Formation consists of sandstone and siltstone with illite and chlorite cement. The uppermost strata intersected at Shea Creek is the Locker Lake Formation, pebbly sandstone, sandstone, and siltstone with illite as the predominant clay mineral. The Locker Lake Formation is highly fractured with rubble zones and randomly oriented fractures (geology from unpublished drill logs provided by COGEMA Resources Inc.).

Two mineralized zones have been intersected in the Shea Creek project area: the Colette and the Anne. Both boreholes logged for this sub-project are in the Anne zone. The basement rocks at the Anne zone consist of a lower felsic gneiss and a middle aluminous sequence. The felsic gneiss is composed of quartz-feldspar±garnet±biotite, depending on the degree of alteration. The unconformity is offset by several thrusted structures. The largest structure corresponds to the reactivated contact between the felsic and aluminous gneiss which is enriched in graphite due to intense shear deformation (Rippert *et al.*, 2000).

b) Uranium Mineralization

Mineralization at Shea Creek occurs along the Saskatoon Lake conductor that has been delineated by ground EM surveys. Mineralization is in chloritized sandstone at the base of the Manitou Falls Formation and consists of uraninite, pitchblende, and coffinite associated with hydraulic brecciated sandstone. Alteration haloes include kaolinite, sudoite, chlorite, and dravite (Rippert *et al.*, 2000).

In hole SHE101-4, massive pitchblende, accompanied by strong hematite alteration, was intersected above the unconformity from 735.2 to 738.1 m. Above this zone (733 to 735.2 m) coffinite (uranium silicate) is weakly disseminated in the breccia matrix and along fracture planes (drill core geology from J. Robbins, pers. comm., 2000).

In hole SHE105-4, there are two zones of mineralization. The upper zone between 696.2 and 700.7 m is located at and above the unconformity and the lower zone, from 717.0 to 723.0 m, is hosted entirely in the basement. The lower zone, associated with a graphitic structure (as noted between the aluminous and felsic gneiss), is semi-massive below the structure and grades downward into disseminated uranium mineralization as far as 723.0 m within the aluminous gneiss. The mineralization in the sandstone (the upper zone) consists mainly of coffinite and pitchblende in a chlorite breccia matrix (drill core geology from J. Robbins, pers. comm., 2000).

c) Alteration

The major alteration minerals associated with both basement and sandstone uranium mineralization are illite, kaolinite, dravite, and goyazite (strontium florencite) (Rippert *et al.*, 2000). Sudoite (c.f. Percival *et al.*, this volume) is mainly associated with basement alteration halos. Chloritic and illitic breccias indicate the proximity of sandstone-hosted and high-grade unconformity uranium mineralization, given the interpretation that they most probably resulted from the percolation of mineralizing hydrothermal solutions. Iron-rich kaolinite breccias indicate the proximity of high-grade mineralization as they are associated with uranium remobilization. At Shea Creek, the breccias are interpreted to have developed by hydraulic and solution-collapse processes (Lorilleux *et al.*, 2000).

d) Preliminary Geophysical Logging Results

Lithology and Geophysical Logs

Figure 2 shows the grain size (unpubl. drill logs provided by COGEMA Resources Inc.), natural γ-ray, density, and compressional-wave velocity (Vp) logs acquired in borehole SHE105-4. These data illustrate some of the challenges faced in interpreting the geophysical logs. The density log, for instance, shows negative densities in the mineralized zones (680 to 730 m) due to interferences between the backscattered γ-rays from the density probe source and the natural activity from the uranium ore. The densities are also slightly lower in the sandstone formations (<2 g/cm^3) than normal (>2.25 g/cm^3). These data are being recalibrated and corrected for the borehole environment. The two high-density zones between 520 and 540 m are wedges used for navigational drilling. The natural γ-ray log (plotted on a logarithmic scale) accurately delineates the four uranium ore zones. There

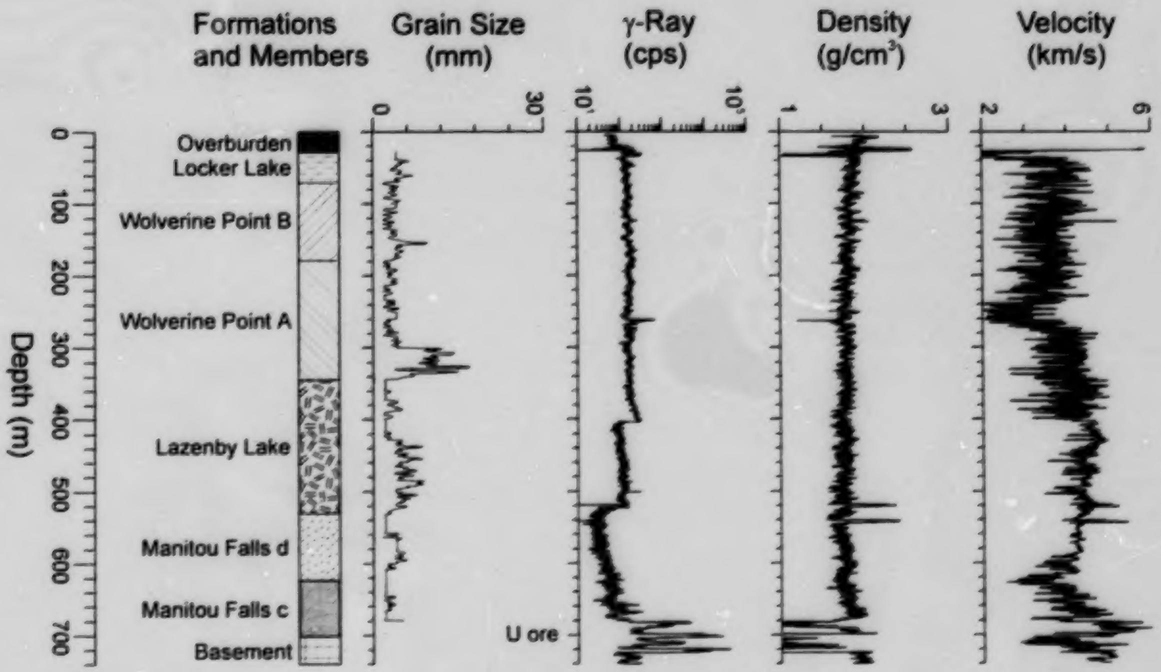

Figure 2 - Grain size, total count γ-ray, density, and compressional-wave velocity logs acquired in hole SHE105-4, Shea Creek project. Grain size log and formation data provided by COGEMA Resources Inc.

are, however, changes in activity around 400 and 520 m. These anomalous changes in activity are due to several factors: the use of bentonite to stabilize the borehole, change in hole diameter (from HQ to NQ around 400 m), and wedging (around 520 m). There is an interesting Vp distribution within the sandstone units. The low velocities around 260, 630, and 710 m are due to fracturing. The velocities also decrease steadily from about 420 to 610 m (Lazenby Lake Formation and Manitou Falls d member). This response may represent increasing porosity and alteration with depth in these sections. The velocities then start to increase from 620 m toward the uranium mineralization. The true Vp velocities of the uranium mineralization are going be difficult to determine because of the highly fractured nature of the mineralized rock. The Vp within the uranium ore zone ranges from 3 km/s (in fractured rock) to >5 km/s in more competent rock.

Temperature-Depth Profiles

The temperature distribution in a borehole is affected by several parameters including drilling fluid circulation, groundwater flow, lithology, and, as in the geological environment at the present project, the radiogenic heat from the uranium mineralization. Figure 3 shows the temperature-depth profile acquired in hole SHE105-4. Drilling of SHE105-4 was completed on August 14, 2000 and plastic casing was installed in the hole on August 15, 2000. The temperature logs were acquired on August 16, 2000. Also, in order to stabilize the hole in the highly fractured zone at the unconformity, bentonite was injected into the fracture zones before plastic installation. These procedures affected the temperature distribution in the borehole. The temperature anomaly around 610 m is interpreted to have been generated by the infiltration of the warmer drilling fluids and/or bentonite circulation into a permeable formation. This zone is highly fractured and correlates with low Vp and low tube-wave amplitudes (see Figure 4). This temperature anomaly should dissipate with time (Drury and Jessop, 1982; Mwenifumbo, 1993). The temperature anomaly in the mineralized zone (680 and 720 m) is lower than that described above. The mineralized zone is also highly fractured and permeable and it is difficult to determine if elevated temperatures are due to fluid circulation or to radiogenic heat generated by the high-grade uranium ore. To study the contribution of radiogenic heat to the temperature distribution within high-grade uranium mineralization, it is recommended that the boreholes be left open and not cemented and be logged during the summer 2001 field season.

Fractures and Full Waveform Sonic Logs

Figure 4 shows the fracture log (F/m), compressional-wave velocity (Vp), tube-wave amplitude, and variable

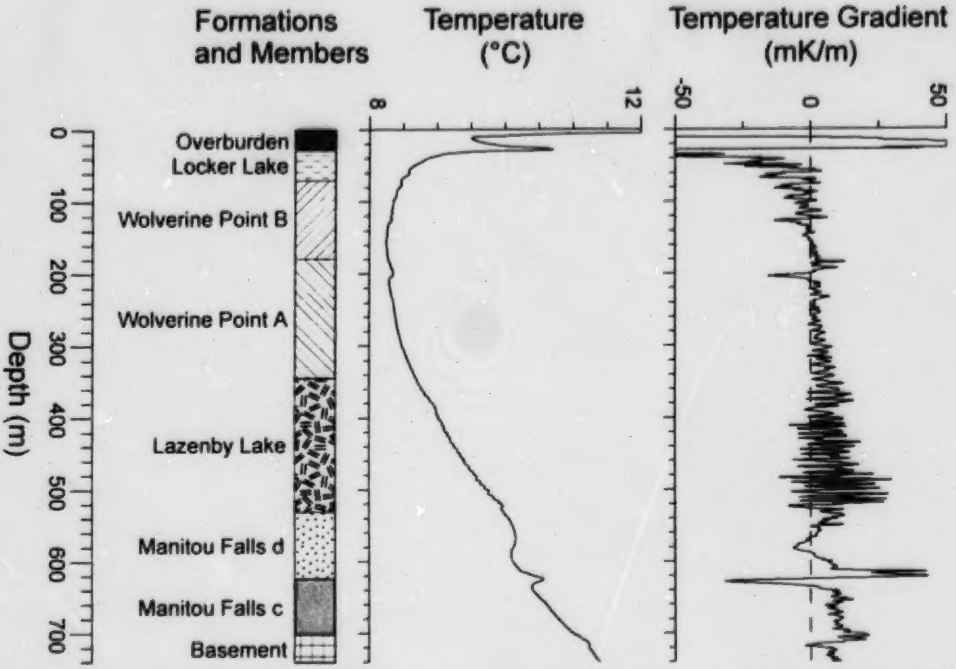

Figure 3 - Temperature and temperature gradient profiles acquired in hole SHE105-4, Shea Creek project.

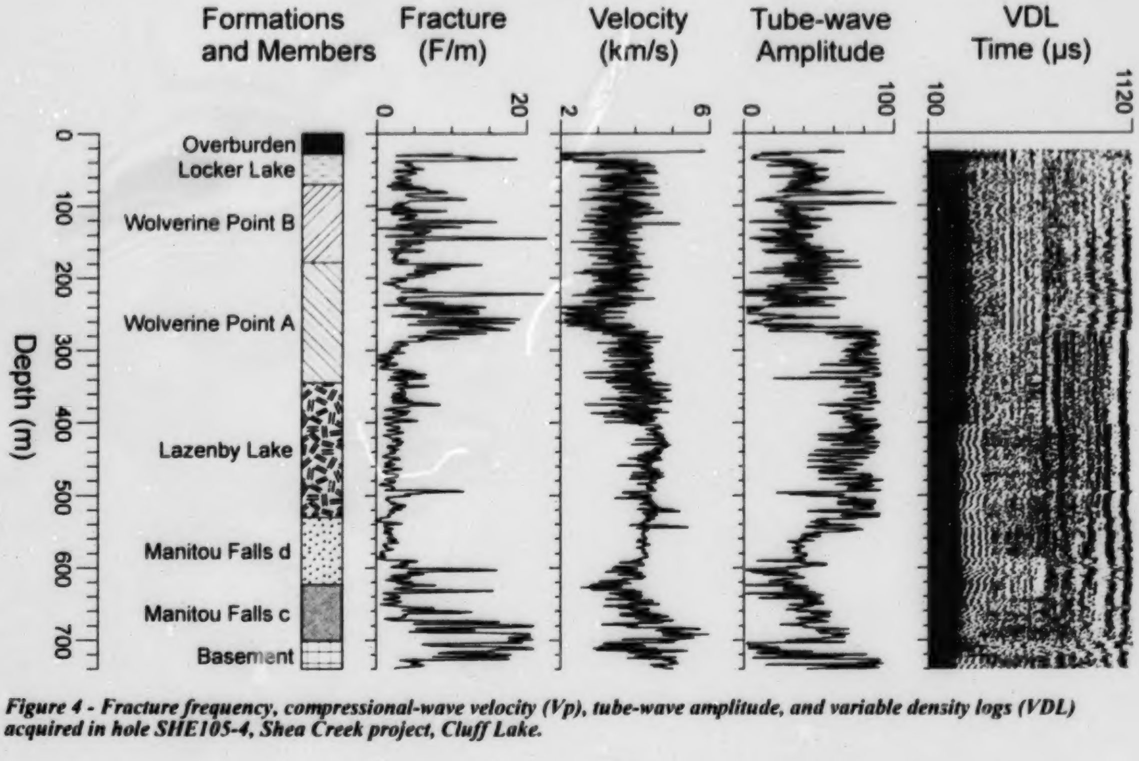

Figure 4 - Fracture frequency, compressional-wave velocity (Vp), tube-wave amplitude, and variable density logs (VDL) acquired in hole SHE105-4, Shea Creek project, Cluff Lake.

density (VDL) logs acquired in borehole SHE105-4. The fracture log was derived from the drill core (unpublished drill logs provided by COGEMA Resources Inc.). A high degree of fracturing occurs within the uppermost formations: Locker Lake, and Wolverine Point (A and B). The central part of the Wolverine Point A member is highly fractured. Within the sandstone and in the basement rocks, there is a remarkable correlation between the fracture frequency, Vp and the VDL. High-fracture frequency correlates with low Vp, low tube-wave amplitude and the VDL shows a high degree of attenuation across the entire wave train (100 to 1120 µs). The most competent rocks with low fracture density occur in Wolverine Point A, Lazenby Lake, and the upper part of Manitou Falls d. These zones also exhibit high tube-wave amplitude. The change in the acoustic character (Vp and VDL) at approximately 400 m is due to a change in hole diameter (from HQ at 96.1 mm to NQ at 75.7 mm). The acoustic data are fairly useful in delineating highly fractured zones within both the sandstones and the basement rocks. It is interesting to note that, although the fracture frequency increases toward mineralization in the basement, Vp also increases (620 to 700 m). This is probably due to changes in mineralogy of the Manitou Falls c member or that the fractures are healed and/or cemented by alteration minerals.

Geophysical Signature of Mineralization

Figure 5 shows the total count γ-ray, inductive conductivity and spectral γ-γ (density and spectral γ-γ ratio (SGG), a heavy element indictor) logs acquired in hole SHE105-4 through mineralization, illustrating their use in delineating the uranium ore zone and the graphitic conductive zone typically associated with uranium mineralization in the Athabasca deposits. There is a massive/nodular niccolite (NiAs) zone between 696.4 to 696.8 m within corroded polymict, non-oriented chlorite breccia. This zone, although narrow, shows up as a fairly conductive, high density and high SGG ratio zone with low γ-ray activity. The density log shows negative densities in the mineralized zones because of the extremely high γ-ray activity from the uranium ore that overwhelms the backscattered γ-rays from the density probe source (^{60}Co γ-ray source). The density data in the uranium mineralization are obviously incorrect. We are currently working on a method to extract density information in the ore. The graphitic R3 zone, occurring above the lower most uranium ore zone, exhibits high conductivity (conductivities in arbitrary units because the probe has not yet been calibrated to read in conductivity units of S/m).

5. McArthur River – P2 Zone

Several new holes were drilled west of McArthur River during the summer of 2000 and were planned to be geophysically logged as open holes (Figure 1). Several new and old holes that were suggested for the GSC logging operations could not be logged. A number were blocked, one was not cased in the overburden,

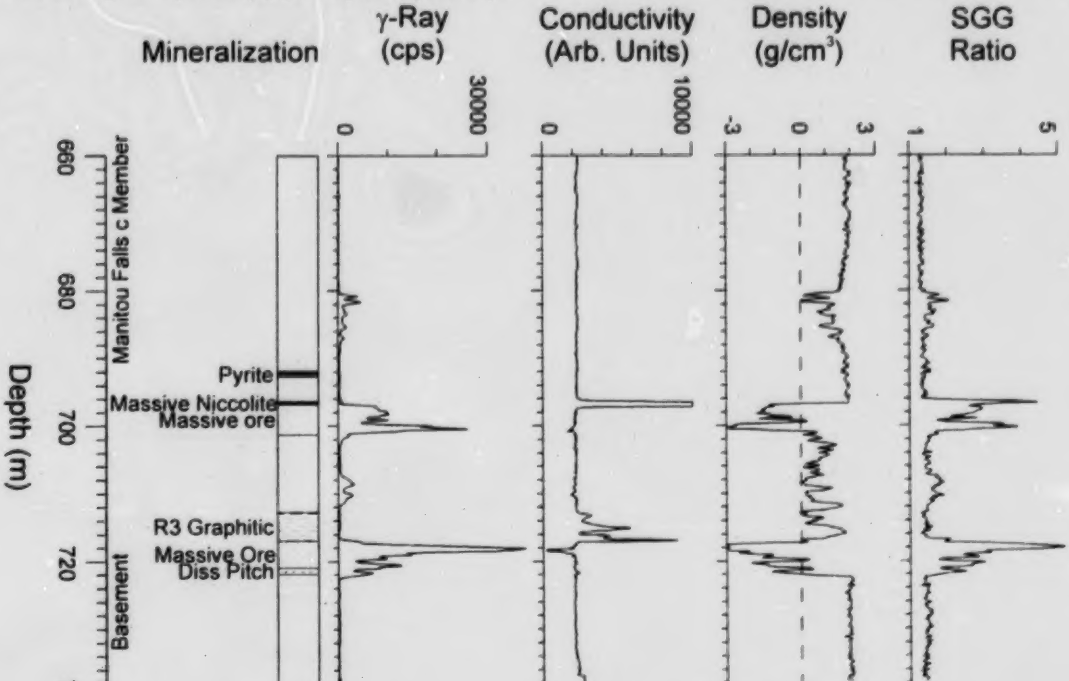

Figure 5 - Total count γ-ray, conductivity (uncalibrated probe data presented in arbitrary units), density, and the spectral γ-γ (SGG) ratio logs through uranium mineralization in borehole SHE105-4, Shea Creek project, Cluff Lake.

and a new hole collapsed in the highly fractured zone near the unconformity and a dummy probe was lost in the course of testing that hole. Two holes were, however, logged in the P2 zone: MAC218 and MAC197. These holes had intersected mineralization and a strong aquifer at the unconformity, and hence had to be cemented. Geophysical logging was, therefore, only done in the sandstones and no geophysical characteristics of the mineralization were determined.

a) Local Geology

The geology of the McArthur River area is summarized by McGill *et al.* (1993). The Manitou Falls Formation rests unconformably on Wollaston Group paragneisses and both are offset by 60 m to more than 80 m by the southeast-dipping P2 reverse fault. The Athabasca Group here comprises all four members of the Manitou Falls Formation (MFa, MFb, MFc, and MFd) (Yeo *et al.* (this volume) after Ramaekers (1990)). The upper two members generally are similar to those observed at the Shea Creek deposit.

McGill *et al.* (1993) described the Manitou Falls Formation in general terms for the vicinity of the McArthur River P2 North deposit. They determined that the total thickness above the hanging-wall unconformity is 480 m, comprising, in upward succession: a basal conglomerate averaging 10 m, 85 m of MFa, 125 m of MFb, 85 m of MFc, and 180 m of MFd. Holes drilled through the footwall sequence intersect some 560 m of Manitou Falls Formation, owing to structural repetition of the basal MFa member. In addition, the basal breccia is up to 25 m thick on the down-dropped side of the P2 fault. These different conglomerate thicknesses suggest that a precursor of the P2 fault was active during sedimentation.

b) Alteration

The following description of alteration is after McGill *et al.* (1993). The lower part of the Athabasca Group is intensely silicified and weakly bleached in the vicinity of the P2 North deposit. As a result, hydrothermal clay alteration is minimized in the immediate overlying sandstone. These characteristics contrast dramatically with the bleached, clay-altered haloes associated with most other unconformity-related uranium deposits of the Athabasca region. However, dravite (tourmaline) and drusy quartz is present in fractures. Dravite is interstitial to the framework sand grains in the upper MFc and MFd. Chlorite is also present in these upper members, and limonite (goethite) is a common late alteration related to recent circulation of oxidizing meteoric water. The surface effects of alteration are discussed by Shives *et al.* (this volume). In addition, visual estimates of clay in the matrix of sandstones increase systematically downward (Yeo *et al.*, this volume).

The upper 225 m of the Manitou Falls Formation (part of member MFc and all of MFd) are not silicified but pervasively bleached. As noted by McGill *et al.* (1993), these units rarely contain significant amounts of primary hematite so that bleaching is interpreted as regional. Local hydrothermal events may have been superimposed with little measurable effect. Silicification is weak and variable in the upper 375 m of sandstone, but increases dramatically below this.

c) Preliminary Stratigraphic Logging Results of MAC218

Drill hole MAC218 at the north end of the P2 trend at McArthur River was logged both geophysically (sub-project 2) and stratigraphically (sub-project 4, Yeo *et al.*, this volume) to cross-calibrate stratigraphic and borehole geophysical parameters. Throughout the course of sub-project 4, all drill holes were logged by entering data on a spreadsheet to facilitate numerical analysis and objective comparison between sub-projects. The most logical software for our purpose is LogView (Markarian *et al.*, 1996), which was developed at the Geological Survey of Canada for borehole geophysical purposes and has since realized a number of new applications. It uses ASCII or binary files that can be generated from spreadsheet data, and is both user-friendly and versatile. The stratigraphic plots shown here and in Yeo *et al.* (this volume) are its most recent adaptation. The numeric stratigraphic data that are compared with borehole geophysical data are briefly summarized in Table 2. These data were generated for each stratigraphic unit and plotted using LogView in a histogram form.

The Manitou Falls Formation in drill hole MAC218 rests unconformably on Wollaston Group paragneisses in the hanging wall of the southeast-dipping P2 reverse fault. The basal unconformity is at 493 m, the base of MFb was picked by Cameco at 407 m, the base of MFc at 260 m, the base of MFd at 180 m, and depth of overburden is 13 m. Borehole logging was conducted to 480 m, the top of the basal "fanglomerate" unit of Cameco. The following description is based on analysis of detailed spreadsheet data, a LogView plot of eight stratigraphic parameters (Figure 6) plus a comparison plot of selected geophysical and stratigraphic parameters (Figure 7).

The lowest stratigraphic unit recognized in MAC218 comprises, from bottom to top, a basal conglomerate (Facies 1 of Yeo *et al.*, this volume), a red mudstone-dominated sub-unit (Facies 3) and a coarse conglomerate (Facies 4). Contacts between these are interbedded, and the red coloration of Facies 3 is present throughout. As noted by Yeo *et al.* (this volume) these appear to be relatively undisturbed primary diagenetic red beds, in this locality somewhat bleached and significantly hardened by silicification. This member is indicated by FC in Figure 6 and, to avoid confusion with existing stratigraphic usage, is not included in MFa. Future work may resolve whether or not this member should be included in MFa.

The MFa member as defined by Cameco excludes the basal unit, but includes two preliminary sub-units recognized by EXTECH. Sub-unit MFa1 is the lowest

Table 2 - Numeric descriptors of stratigraphic-sedimentologic parameters.

Lithology	Numerical approximation of the overall modal grain size of the stratigraphic unit, taking into consideration both matrix and framework grains and plotted as minus phi equivalent ($\log_2$. D) where D is clast diameter.
MTG	Maximum transported grain size (visual average of the 10 largest grains observed), in millimetres, plotted as minus phi ($\log_2$. D) where D is clast diameter. This is a method of defining conglomerate together with %>2 mm.
% >2 mm	A visual estimate of the percentage of clasts in the unit whose diameters are greater than 2 mm (granule size or greater). This is a method of defining conglomerate together with MTG.
Cross Beds	xBcm = height of cross beds in cm, measured as the maximum distance between discordant sets of laminae in the unit being logged.
Rounding	A visual estimate of the largest clasts by number ranging from Very Angular (1) to Well Rounded (6). This is the weakest and least useful numerical attribute based on EXTECH logs.
Sorting	An overall visual estimate for the whole unit, by number ranging from Poor (1) to Very Well (4).
% Clay	The percentage of clay in matrix as proportion of whole rock; excluding clay in intraclasts.
Hematite	An overall visual estimate of the abundance and type of hematite in the rock expressed on a scale of 0 (Trace or no hematite) through 4 (Intensely hematitic, brick red to black-red) to 5 (abundant detrital hematite). This estimate does not include limonite which is commonly late, and is described in verbal descriptions in the logs.

for which borehole geophysical data could be obtained, and extends from about 483.6 to 450 m. It is much like MFa2 but has a higher proportion of sandstone, less conglomerate, and fewer mudstone interbeds. It is transitional between Facies 6 and 7 of Yeo *et al.* (this volume). This unit was somewhat generalized in the stratigraphic logging process and more analysis will be forthcoming.

The upper sub-unit MFa2 extends from about 450 to 407 m and comprises Facies 6, a coarse sandy conglomerate and gravelly sandstone. The conglomerates here are somewhat cleaner and mudstones less abundant than in Facies 8. Most characteristic is the abundance of coarse sand- and granule-sized grains in both cross-bedded and planar to low-angle cross-bedded sandstones. The granules are typically well rounded and very clean in appearance. In MAC218 these rocks are highly silicified, including the mudstone interbeds. The γ-ray log thus picks out the conglomerates, although with lower activity than the MFb conglomerates. Resistivity overall is high, likely reflecting the degree of silicification.

The MFb member is picked by Cameco to extend from 407 up to 259 m. Three sub-units are evident within Cameco's MFb in MAC218. The lowest member (MFb1, from 407 up to 362 m) is almost entirely Facies 7 of Yeo *et al.* (this volume), a medium to coarse sandstone, with a minor conglomerate zone at 380 m that is reflected in the γ-ray log. MFb1, with its better sorting and high degree of silicification, is reflected geophysically as having relatively high resistivity and lower γ-ray. The upper two facies (MFb2 and MFb3) extend up to 310 and 259 m respectively. These are variants of Facies 8, with the upper having a clearly smaller proportion of conglomerates, fewer and thinner mudstone interbeds, a generally greater maximum cross-bed height, and noticeably less hematite. The correlation between conglomerate and γ-ray log is powerful.

The MFc member continues the overall upward-fining nature of the Manitou Falls Formation, and is transitional between MFb and MFd: it contains some clay intraclasts as well as an upward-decreasing abundance, thickness and maximum transported grain size (MTG) of granule and fine-pebble conglomerates. Our picks of 259 m as the base and 161 m as the top of MFc are consistent with those of Cameco and are supported by the facies definitions of Yeo *et al.* (this volume).

MFc member is Facies 9 of Yeo *et al.* (this volume). Overall the height of cross beds appears to increase upward with upward-decreasing clay content of sandstone matrix and increased upward sorting. MFc is subdivided into three sub-units: MFc1, MFc2, and MFc3 reflecting upward-fining and thinning cycles recognized from one or more of grain size (lithology, MTG, and percent >2 mm) and cross-bed height.

The MFc2 sub-unit as logged by EXTECH begins with a small mixed interval from 231.55 to 227.73 m characterized by conglomerates more than 2 cm thick with diffuse contacts and MTG of 8 mm. From 259 m up to 231.55 m, conglomerates are absent in MFc1, so this thin unit of conglomerate is considered a marker at the base of the middle sub-unit MFc2. This marker clearly stands out on the γ-ray log, and has been observed in a number of other holes logged in the McArthur River area, suggesting that it has potential for practical use in constructing detailed structural and stratigraphic models. Regionally, this marker may represent a tongue of conglomerate that may be much thicker and more abundant to the east, and may thus become the pick for the base of MFc in eastern drill hole sections.

Our preliminary pick for the base of MFd is at 161 m, based on the absence of very sparse clay intraclasts below this depth, and this being the base of the third upward-thinning and fining cycle. This correlates with other holes, especially Close Lake CL77, but more

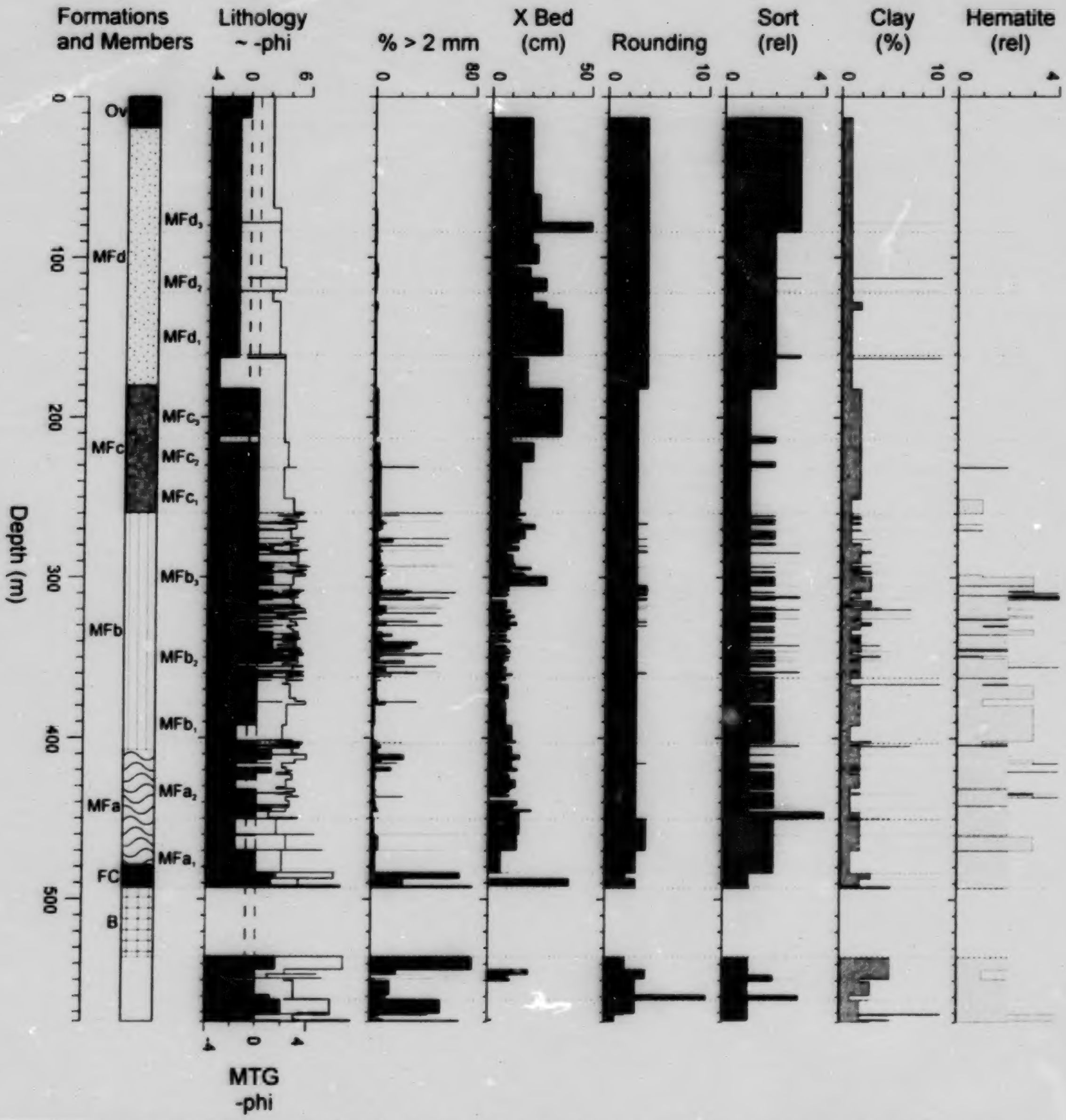

Figure 6 - Stratigraphic data from EXTECH drill core logging. See text for description of parameters. Formations column shows Cameco on the left and EXTECH on the right.

regional work is needed in consultation with industry colleagues before making this a firm pick. It does not appear to be a major sequence break: it is more of a punctuation of Manitou Falls Formation's overall upward-fining sequence.

The MFd member is characterized by medium- to fine-grained, pale yellow-grey sandstone with thin coarse sand to granule laminae and clay intraclasts constituting from 0.5 to 2% of the rock volume (Facies 10 of Yeo *et al.*, this volume). Intraclasts and the coarse sand/granule beds tend to be spatially associated with reactivation surfaces at the base of large cross beds. The sandstones are abundantly cross-bedded with three crude upward-thinning sequences suggested by maximum cross-bed thickness ranging from 10 to 50 cm (Figure 6). These sub-units, herein termed MFd$_1$, MFd$_2$, and MFd$_3$, appear to correspond to lithologic fining upward cycles and to subtle γ-ray activity cycles (Rider, 1986) at about the same scale. MTG fines upward overall with improved sorting. The upper contact of MFd is not preserved at this locality.

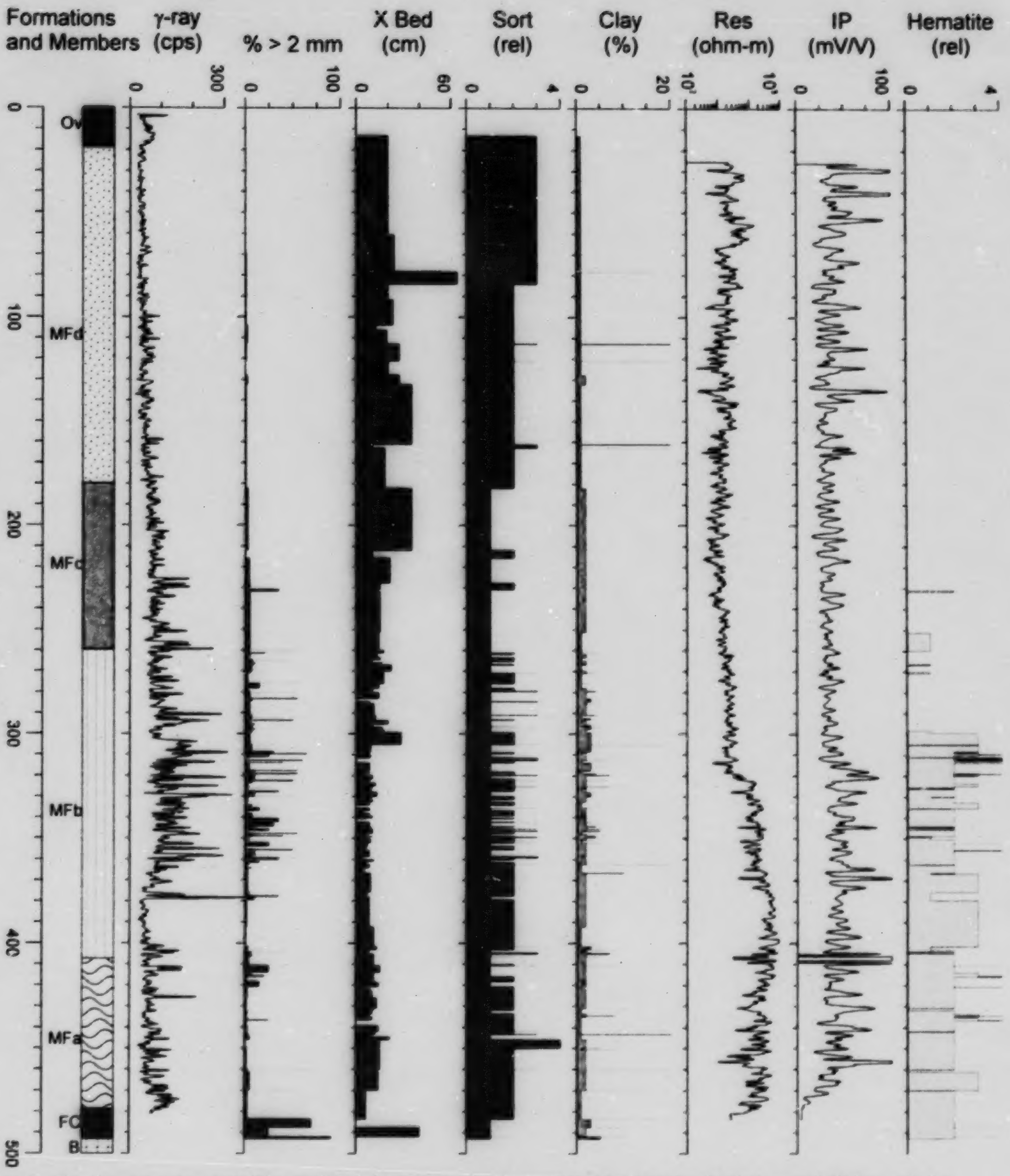

Figure 7 - Total count γ-ray, resistivity and IP logs compared with stratigraphic data (grain size, cross-bedding, relative sorting, percent clay, and relative hematite). Data acquired from hole MAC218, McArthur River.

d) Preliminary Geophysical Logging Results

The boreholes that were geophysically logged at McArthur River (MAC218 and MAC197) intersect overburden, sandstone of the Athabasca Group, and the crystalline basement rocks. However, these holes are cemented at the unconformity; therefore, no geophysical logging was conducted in either the mineralization or the crystalline basement.

Lithology and Multiparameters Logs

The suite of geophysical logs acquired at McArthur River comprised natural γ-ray spectrometry, spectral γ-γ density, magnetic susceptibility, temperature, inductive conductivity, single point resistivity, normal resistivity, IP, and FWS logs. Figure 7 shows only three of these geophysical parameters (γ-ray, resistivity, and IP) compared to the stratigraphic data.

The narrow, high γ-ray activity units correlate well with the increase in pebble size. The zones are conglomeratic and the elevated γ-ray activity in these zones is primarily due to thorium (from spectrometric γ-ray data, not shown). The IP and resistivity logs correlate fairly well with the hematite log. There is an increase in the IP effect in the upper part of the borehole that cannot be explained at the moment.

Temperature-Depth Profiles

Figure 8 shows the temperature- and temperature gradient-depth profiles acquired in hole MAC218. The temperature profile exhibits a response characteristic of an artesian well. Water is entering the borehole around 280 m and exiting close to the surface around 20 m at a fairly fast rate as indicated by the almost constant temperatures (20 to 280 m) or almost zero temperature gradients. Although the shallower part of the borehole exhibits high flow rates, the lower section appears to be reasonably stable. There is a minor temperature anomaly around 430 m that may be associated with localized groundwater flow along fractures. The temperature gradient near the bottom of the hole is approximately 12 mK/m. There are no significant changes in either the temperature or temperature gradient near the bottom of the hole that could be related to the influence of radiogenic heat from the uranium mineralization. The effects of uranium mineralization on the temperature distribution in the portion of the borehole that was logged may be subdued by groundwater flow.

Acoustic Properties of Sandstones

Figure 9 shows the density, compressional-wave velocity, and the acoustic impedance logs acquired in borehole MAC218. The lithology log was provided by Cameco. The density log shows low densities in the Manitou Falls c (at ~200 m) and d (at ~60 m and ~140 m) members probably due to fracturing. All the logs indicate a significant change around 320 m in the Manitou Falls b member. Above 320 m the density, Vp, and acoustic impedance are low (2.27 g/cm^3, 4.80 km/s, and 10.9 km/s g/cm^3, respectively) and below 320 m they are high (2.48 g/cm^3, 5.67 km/s, and 14.06 km/s g/cm^3, respectively). The reflectance at this interface is approximately 0.127. Both the density and Vp decrease towards the basement and, hence, the acoustic impedance also decreases, presumably because of approaching the highly fractured, mineralized zone at the unconformity. Unfortunately this borehole was cemented at the bottom to seal off the mineralization.

6. Discussions and Conclusions

Geophysical logging of the uranium deposits in the Athabasca Basin presents several challenges: first, is accessibility to borehole sites by a logging truck which could, in some cases, be overcome by improving the roads to the borehole sites; second, is maintaining the holes open long enough for logging operations to be carried out; and third, is extremely high-grade uranium mineralization produces very high γ-ray activity. To prevent the holes from collapsing, they have to be

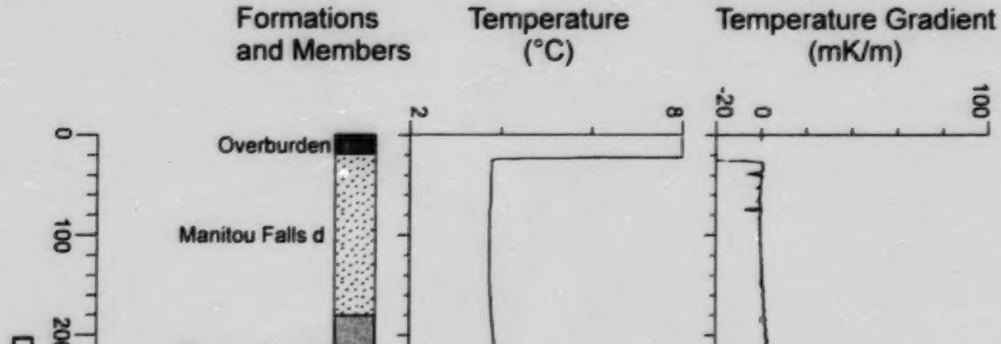

Figure 8 - Temperature and temperature gradient profiles acquired in hole MAC218, McArthur River.

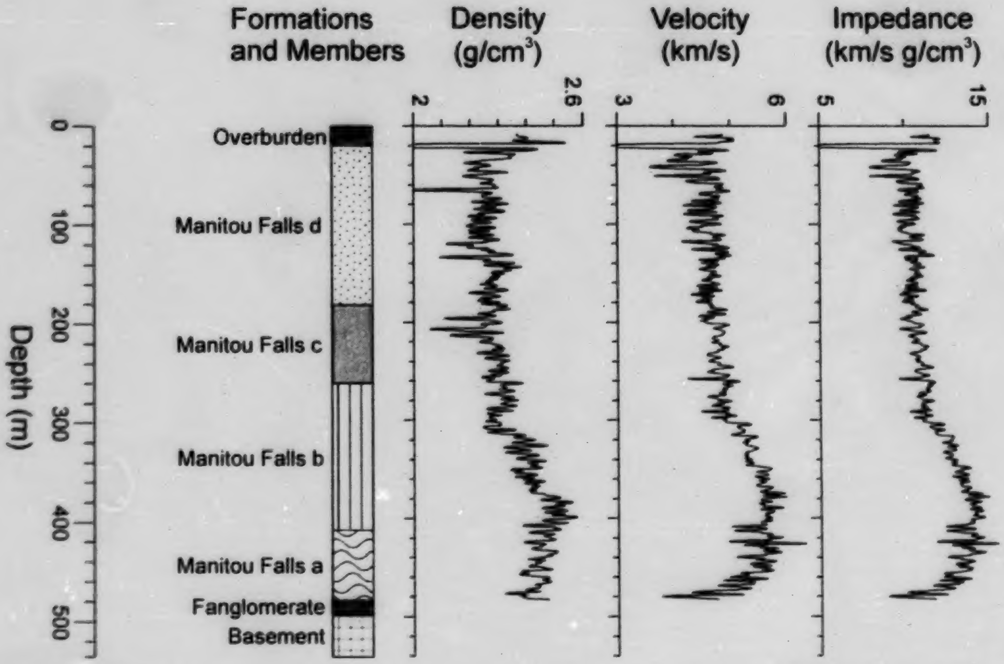

Figure 9 - Acoustic logs (density, velocity, and acoustic impedance) acquired in hole MAC218, McArthur River.

cased with plastic, but this means that certain geophysical parameters cannot be acquired in the boreholes (e.g. galvanic resistivity and IP). If logging is acquired immediately after drilling, the holes often have to be stabilized from collapsing by pumping bentonite mud into them, which introduces some complexity into data processing and interpretation (corrections for mudcake and the radioactivity from bentonite itself). The γ-ray logging probes have to be shielded in order to cope with the extremely high γ-ray activity in these deposits, which means that special calibration procedures have to be determined for *in situ* ore grade estimations.

The data that have been collected at the two deposits were acquired with these challenges in mind. Plastic casing was installed in the boreholes at the Shea Creek project and instead of shielding the γ-ray probe, a probe was designed with a fairly small detector to counteract the "deadtime" problem produced by the high-count rate in the ore. These data will be analyzed before the next summer of field data acquisition in 2001.

Mineralized zones are accurately delineated by the spectral γ-γ density and natural γ-ray techniques. The spectral γ-γ ratio, being a heavy element indicator, shows the relative uranium-grade distribution within the mineralized zones and, hence, there exists the possibility of calibrating this parameter for *in situ* ore grade estimation. The density responses within the mineralized zones yield high-count rate regions which incorrectly suggests that they are low density zones. The high-count rate is attributed to the high radioactivity from the uranium mineralization and methods of dealing with this problem are being investigated.

The full waveform acoustic data clearly shows the highly fractured zones within the sandstone and the basement. The highly fractured nature of the basement rocks in the boreholes that were logged show compressional-wave velocities being relatively lower than expected (4.86 km/s). The boreholes that were logged did not intersect fresh, unaltered basement rock, and therefore the true velocities of the unaltered basement could not be determined.

Use of the same plotting software for both geophysics and numerical representations of sedimentologic parameters demonstrates very strong benefits to both disciplines in confirming the importance of the various geophysical parameters discussed above, as well as improving our confidence in the stratigraphic parameters measured. In particular, the correlation between γ-ray and "percent >2 mm" grain size is powerful for defining conglomerates, resistivity appears to be a measure of sorting, and IP reflects zones of intense hematite. Other subtle geophysical and sedimentologic patterns appear to correlate and warrant further analysis. By providing acoustic data in this context, these initial borehole geophysical results strongly contribute to the EXTECH IV project proposal to calibrate and enhance the interpretation of high-resolution seismic reflection data.

7. Acknowledgments

This is sub-project 2 of EXTECH IV, a partnership funded by the Geological Survey of Canada (Targeted Geoscience Initiative and Proposal Approval System), Saskatchewan Energy and Mines, Alberta Geological Survey, COGEMA Resources Inc., and Cameco Corporation. We acknowledge the contributions to this work by Bill Hyatt and our summer student, Jason Boisvert with the field data acquisition. We also wish to acknowledge special logistical support from both COGEMA and Cameco personnel, especially John Robbins (COGEMA) for his technical support during the entire logging operation at Shea Creek.

8. References

Drury, M.J. and Jessop, A.M. (1982): The effect of a fluid-filled fracture on the temperature profile in a borehole; Geotherm., v11, no3, p145-152.

Killeen, P.G. and Mwenifumbo, C.J. (1988): Interpretation of new generation geophysical logs in Canadian mineral exploration; Second International Symposium on Borehole Geophysics for Minerals, Geotechnical and Groundwater Applications, Golden, October 1987, p167-178.

Lorilleux, G., Cuney, M., Jébrak, M., and Mondy, J. (2000): A new approach of unconformity-type uranium metallogenesis from a structural study (northern Saskatchewan, Canada); GeoCanada 2000, Calgary, May 2000, Conference CD, ext. abstr. #232.

Markarian, D., Grant, J.A., and Elliott, B.E. (1996): LogView - A Microsoft Windows 3.1 application to view borehole log (geophysical and geological) data; Geol. Surv. Can., Open File 3055, diskette.

McGill, B.D., Marlatt, J.L., Matthews, R.B., Sopuck, V.J., Homeniuk, L.A., and Hubregtse, J.J. (1993): The P2 North uranium deposit, Saskatchewan, Canada; J. Explor. Min. Geol., Can. Inst. Min. Metall. Petrol., v2, no4, p321-331.

Mwenifumbo, C.J. (1993): Temperature logging in mineral exploration; J. App. Geophys., v38, p297-313.

Ramaekers, P. (1990): Geology of the Athabasca Group (Helikian) in Northern Saskatchewan; Sask. Energy Mines, Rep. 195, 49p.

Rider, M.H. (1986): The Geological Interpretation of Well Logs; John Wiley and Sons, New York, 175p.

Rippert, J.C., Koning, E., Robbins, J., Koch, R., and Baudemont, D. (2000): The Shea Creek Uranium Project, West Athabasca Basin, Saskatchewan, Canada; GeoCanada 2000, Calgary, May 2000, Conference CD, ext. abstr. #570.

Practical Stratigraphy and Flashy Sedimentology in the Paleoproterozoic Manitou Falls Formation, Eastern Athabasca Basin, Saskatchewan – An EXTECH IV Progress Report

Gary Yeo, Charles W. Jefferson [1], Jeanne B. Percival [1], Dan Jiricka [2], Scott McHardy [2], Pat Munholland [3], Brent Collier [4], Amanda Gaze [5], and Cathy Williamson [4]

Yeo, G., Jefferson, C.W., Percival, J.B., Jiricka, D., McHardy, S., Munholland, P., Collier, B., Gaze, A., and Williamson, C. (2000): Practical stratigraphy and flashy sedimentology in the Paleoproterozoic Manitou Falls Formation, eastern Athabasca Basin, Saskatchewan – an EXTECH IV progress report; *in* Summary of Investigations 2000, Volume 2, Saskatchewan Geological Survey, Sask. Energy Mines, Misc. Rep. 2000-4.2.

Abstract

The Stratigraphy and Sedimentology sub-project of the Athabasca Uranium EXTECH IV aims to refine our understanding of Athabasca Basin stratigraphy and sedimentation, and their relationships to unconformity uranium deposits. This first year of the sub-project has involved three stratigraphers, a clay mineralogist, exploration project leaders and staff, and five students. We have documented basal Athabasca stratigraphy in the Sue C (McClean Lake) and Deilmann (Key Lake) pits, and logged more than 30 drill holes in five drill-hole transects that trend perpendicular to the margin of eastern Athabasca Basin.

Basal strata exposed in Sue C and Deilmann pits include two conglomeratic coarse sandstones separated by a stepped erosional surface and a basal conglomerate respectively. In northern transects, basal members are rich in detrital magnetite and thin westward. In southern transects, eastern basal facies resemble those in the open pits; southwestern basal facies include distinctive red mudstones interbedded with well rounded and sorted coarse quartz sandstones and texturally and compositionally immature conglomerates and breccias. The latter are interpreted to be of very local origin; some as being shed off local paleo-hills reaching 200 m or more in height. No convincing evidence for faulting during early sedimentation was observed, however.

The four-member subdivision of the Manitou Falls Formation (MFa, MFb, MFc, and MFd), established by Ramaekers in the 1980s, remains widely applicable and represents an overall fining upward assemblage amenable to quantitative description by parameters such as grain size, cross-bed thickness, sorting, and abundance of clay. Preliminary detailed subdivisions of each member of the Manitou Falls Formation have been defined by quantitative plots using the Geological Survey of Canada's LogView software, described in a companion paper by Mwenifumbo et al. (this volume). Stratigraphic studies are being integrated with borehole geophysical and high-resolution seismic investigations, allowing cross-calibration and improved interpretation of all three. These studies will enhance practical and theoretical exploration models, to improve precision of drilling and interpretation of exploration holes.

1. Introduction

The Stratigraphy and Sedimentology sub-project of Athabasca Uranium EXTECH IV aims to refine our understanding of Athabasca Basin stratigraphy and sedimentation, and their relationships to unconformity uranium deposits. Our strategy is to build on the substantial framework provided by Ramaekers (1990 and references therein), and its evolved versions in use by industry, by investigating the application of sequence stratigraphy to both marine and non-marine siliciclastic strata of this large, late Paleoproterozoic basin in northern Saskatchewan. The depositional facies architecture, sequence stratigraphy, provenance, and diagenesis will be determined for the entire basin, with focus on key mineralized areas with well-preserved drill core: McArthur River, Midwest–Dawn Lake–Rabbit Lake, Virgin River, and Cluff Lake–Shea Creek. Investigations in the McArthur River area will form the key link with other EXTECH IV sub-projects.

a) Scope and Objectives

This paper is based on review and compilation of existing public domain data (Ramaekers), examination of drill core on five preliminary transects developed by logging selected drill core archived at Cameco, COGEMA, DF Exploration, and JNR Resources camps and at SEM's Regina core laboratory (Figure 1) Documentation of accessible strata at the Sue C (McClean Lake; e.g. Long *et al.*, this volume) and Deilmann (Key Lake) open pits and detailed B.Sc. theses studies of closely spaces drill holes provide key information on expected lateral continuity of

---

[1] Geological Survey of Canada, 601 Booth Street, Ottawa, ON K1A 0E8
[2] Cameco Corporation, 2121 - 11th Street West, Saskatoon, SK S7M 1J3
[3] COGEMA Resources Inc., 817 - 825 45th Street, Saskatoon, SK S7K 3X5
[4] Department of Geology, University of Regina, Regina, SK S4S 0A2
[5] Department of Geological Sciences, University of Saskatchewan, 114 Science Place, Saskatoon, SK S7N 5E2

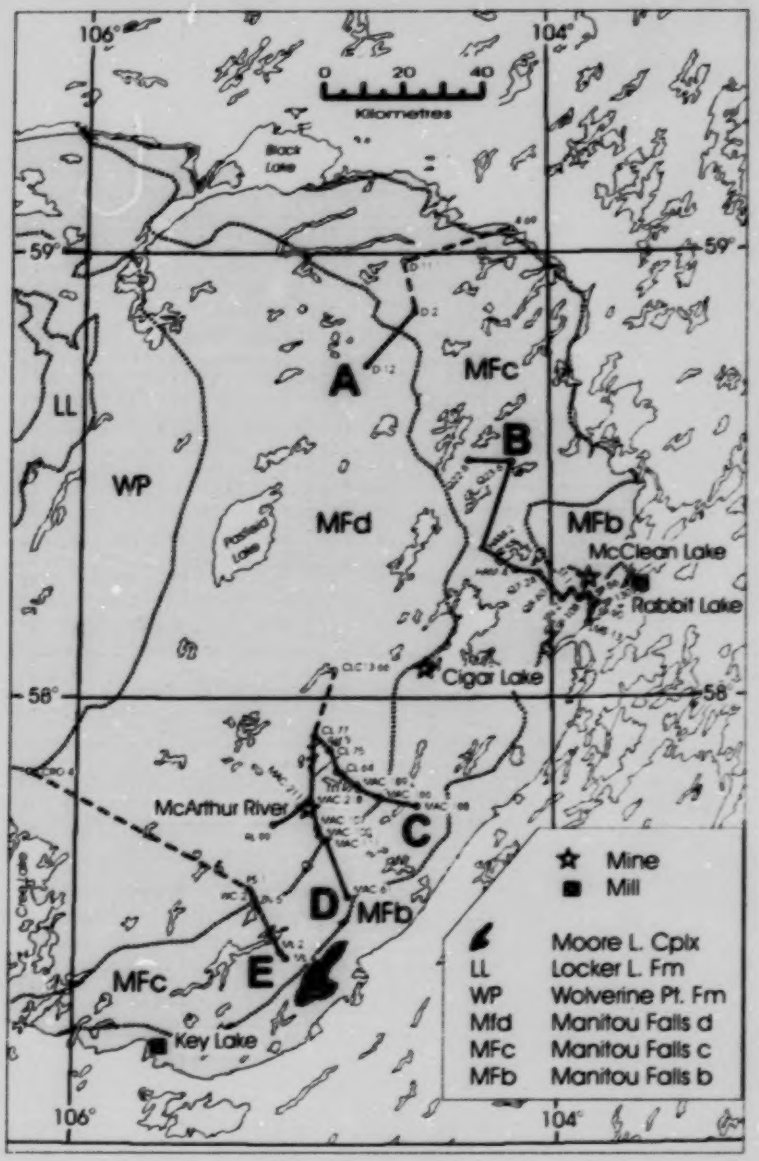

Figure 1 - Geological sketch map (after Ramaekers, 1990) of transects A to E and location of drill holes logged in the eastern Athabasca Basin for this project; ●, DDHs logged this season; ○, DDHs to be logged (stored in Regina); ★, operating mines; and ■, mill-sites and other facilities. See Table 6 for more details of the DDHs.

stratigraphic elements at different scales, and a more detailed 3-D understanding of the physical sedimentologic architecture revealed in the drill core transects. Standard lithologic descriptions, terminology, and logging software (see Mwenifumbo *et al.*, this volume) will be used for all components.

We are assessing a number of issues:

1) the continued applicability of the stratigraphic framework developed by Ramaekers through an objective, numerically-oriented logging method (discussed below);
2) the sedimentologic parameters most conducive to collecting and communicating rigorous and consistent data between personnel with varied experience;
3) adaptation of existing software to generate graphical plots for stratigraphic presentation, comparison with geophysical data and regional correlations (Mwenifumbo *et al.*, this volume); and
4) the status of stratigraphic terminology in use by various industry personnel in various localities, with an aim to providing tools for correlation between outcrop and drill core methods and mineral properties, leading to a more regionally consistent stratigraphic framework. We present clear definitions of the boundaries of units in the upper Manitou Falls Formation. We avoid setting out templates for units in the lower Manitou Falls Formation (MFa and MFb), because usage is as diverse as the actual stratigraphy. Instead, we set out potentially useful facies descriptions and parameters for application and testing over the next two years of the EXTECH IV project.

A number of other EXTECH IV sub-projects are closely associated with the Stratigraphy and Sedimentology sub-project. These include high-resolution seismic studies (Hajnal *et al.*, this volume), borehole geophysics (Mwenifumbo *et al.*, this volume), organic geochemistry, clay mineralogy, and geochronology. Stratigraphic parameters and sub-units most useful for correlation with borehole geophysical data (e.g. Mwenifumbo *et al.*, this volume) and high-resolution seismic data have been identified. Primary responsibilities for the first two authors are outlined in the three-year plan shown in Table 1.

Clay mineralogy has application to stratigraphy because primary clay minerals were deposited both as mudstone interbeds and as matrix to sandstone and

Table 1 - Provisional three year plan for stratigraphic and sedimentologic studies in the Athabasca Basin.

Year	Areas	Projects	Thesis Projects
2000-2001	Dawn Lake	Yeo: two transects during summer months.	Two detailed B.Sc. projects
	McArthur River	Jefferson: one transect, cross-calibrate borehole and seismic geophysical data during summer.	One detailed B.Sc. project
	Western Athabasca	Jefferson and Yeo: Examine drill core archived in Edmonton during winter.	
2001-2002	Cluff Lake	Yeo: Reconnaissance (40 x 40 km), Jefferson visit to coordinate. Two detailed sub-areas as B.Sc. projects.	Two M.Sc. projects in eastern basin (Dawn Lake? Key Lake?)
	Alberta	Jefferson: Reconnaissance (40 x 40 km), Yeo visit. Focus on logging DDH.	One in McArthur River area?
2002-2003	Virgin River	Yeo: Reconnaissance (40 x 40 km), Jefferson visit. Two detailed sub-areas as B.Sc. projects.	One or two in western basin; complete eastern basin
	Basin	Jefferson: follow-up, detailed studies.	One in Alberta area? Complete McArthur
2000-2003	Basin	Regional isopach maps (Yeo); basement-sandstone interface including primary and alteration facies (Jefferson).	
		Clay mineralogy as a regional stratigraphic element and as a local diagenetic or alteration marker.	Selected sections related to McArthur River/Shea Creek and regional

conglomerate. For example, several generations of illite, chlorite, and kaolinite are recognized in the basin. Regional burial diagenesis produced changes in polytypes (e.g. illite and kaolinite) and in crystallinity. Hydrothermal alteration related to mineralization also modified the clay minerals (e.g. presence of sudoite, a di-trioctahedral chlorite) and introduced elements such as boron to produce dravite. The sub-project led by Percival aims to determine changes in clay types related to stratigraphy and sedimentology to improve understanding of local and basin-scale provenance, depositional conditions, and diagenetic and alteration history.

Geochronology is key to both stratigraphic correlations and tracking of diagenetic changes associated with basin-wide processes and focussed mineralization. With the aid of GSC's SHRIMP (Stern, 2000), Rainbird and colleagues aim to calibrate the depositional and diagenetic history of Athabasca Basin and compare it with those of Dubawnt Supergroup in Thelon and Baker Lake basins. They are investigating the potential for using diagenetic xenotime (YPO_4, among other phosphatic cements) as a proxy for the age of deposition (McNaughton *et al.*, 1999). U-Pb dating of detrital zircons and phosphatic minerals (e.g. Heaman, 2000) will provide provenance information.

Industry authors selected appropriate drill cores for detailed study and provided guidance throughout the sub-project. Our emphasis is on basal units hosting uranium deposits and, throughout the Athabasca Basin section, on elements relevant to basin fluid-flow and metal provenance, including primary aspects such as depositional environments, facies architecture, lithology, porosity and permeability, diagenesis, and hydrothermal alteration. A number of focussed studies are providing detailed understanding of specific aspects, whereas correlation of cross-sections perpendicular to the basin margin are interpreted to provide a regional perspective. These are outlined in Table 2.

b) Core Logging Methods

Drill core was logged in a systematic fashion by measuring twelve parameters linked to depth in the drill hole: lithology, basal contact, facies (e.g. Miall, 1978, 1992), cross-bed height, grading, MTG (maximum transported grain size: the average of the largest observed grains), percent of grains greater than 2 mm, rounding, sorting, percent clay, colour, and hematite content (Table 3). Most of these parameters (all except basal contact, facies, grading, and colour) can be expressed as numerical values that have a minimum potential for bias and are conducive to use in available stratigraphic log plotting software packages (see Mwenifumbo *et al.* (this volume) for discussion of LogView plotting software). After logging was completed and initial graphic plots generated, the following parameters appear to have provided the most useful information: lithology, MTG , %>2 mm, cross-bed height, % clay, hematite, and presence of clay-rich intraclasts. While logging, qualitative subdivision into numbered units and alphabetic subunits was used to provide an immediate interpretation of stratigraphic grouping at various scales.

c) Regional Stratigraphy and Sedimentology of the Athabasca Basin

Regional Stratigraphic Framework

Since Ramaekers' ground-breaking study of the Athabasca Group was completed in 1981, many thousands of exploration holes have been drilled and several new uranium occurrences, including the Sue and Jeb deposits at McClean Lake, the P2 North deposit (McArthur River), the West Dominique–Janine deposit at Cluff Lake, the P-patch deposit at Key Lake, and the La Rocque Lake and Shea Creek deposits, have been found. The focus of exploration is shifting from the shallow, marginal parts of the basin, where traditional prospecting and geochemical exploration techniques have been effective, to deeper areas, where such methods have little application, but where more detailed understanding of basin stratigraphic relationships may be important. The stratigraphic classification developed by Ramaekers (1979a, 1979b, 1981, 1990) is summarized in Table 4.

Geochronological Constraints on Deposition and Diagenesis of the Athabasca Group

The Athabasca and Thelon basins, about 400 km to the north, are remnants of the extensive late Paleoproterozoic sedimentary cover of the Rae-Hearne craton. Initiation of sedimentation in both basins likely began before 1600 Ma. Cumming *et al.* (1987) inferred an age of greater than 1650 to 1700 Ma based on U-Pb dating of diagenetic fluorapatites from the Upper Wolverine Point and Fair Point formations. Miller *et al.* (1989) inferred an age of >1720 ±6 Ma for deposition of the correlative Thelon Formation in Nunavut, based on U-Pb dating of diagenetic phosphate minerals.

Kyser *et al.* (2000, p237) recently noted:

> "Given that the likely source for the basin-fill came from adjacent rocks to the east and uplifted during the Trans-Hudson Orogen, the temperature-time-pressure history of this orogen may help constrain the age of the basin. Peak metamorphism throughout the orogen is 1800-1820 Ma, so this age represents a minimum for deepest burial of the roots of the orogen (and maximum uplift). Ar-Ar ages of metamorphic and plutonic rocks throughout the orogen and presently exposed at the surface are consistent with a relatively rapid uplift beginning at ca. 1750 Ma. Therefore, major sedimentation in the basin was ca. 1750 Ma based on the thermal and temporal evolution of the most likely source terrains."

Much work remains to refine ages of sedimentation and diagenesis. For example the upper Athabasca strata may well have been deposited during the early Mesoproterozoic. Tuffs in the Wolverine Point Formation (Ramaekers, 1990) might be dateable by U-

Table 2 - Stratigraphic and sedimentologic studies in eastern Athabasca Basin.

Title	Responsibility
Stratigraphy of the Manitou Falls Formation in the Collins Creek area (along LITHOPROBE transect)	Amanda Gaze (B.Sc. thesis in progress at University of Saskatchewan)
Stratigraphy and paleoenvironments of the basal Manitou Falls Formation in the P2 area	Cathy Williamson (B.Sc. thesis in progress at University of Regina)
Depositional architecture of the Manitou Falls Formation in the Deilmann Pit, Key Lake	Brent Collier (B. Sc. Thesis in progress at University of Regina)
Stratigraphy and depositional architecture of the Sue Pit and adjacent drill holes, McClean Lake Mine	Darrel Long *et al.* (this volume)
Transects A (Hawkrock River), B (Rabbit Lake–La Rocque Lake), C (Close Lake), and E (Moore Lakes–Kearns Lake) in eastern Athabasca Basin	Gary Yeo (this study)
Transect D (McArthur River and link with proposed seismic transect), eastern Athabasca Basin	Charlie Jefferson (this study)
Clay mineralogy of depositional versus diagenetic clays	Jeanne Percival (this study)
Radiometric dating of diagenetic minerals (e.g. xenotime, monazite, and apatite) and detrital minerals such as zircon, apatite, thorite, and monazite	Rob Rainbird *et al.* (initial feasibility study in progress)

Table 3 - Sample spreadsheet-based core logging form. See Mwenifumbo** et al. **(this volume) for discussion.

SEM-GSC Athabasca Stratigraphy Short Logging Form

EXTECH IV Athabasca Uranium Project: AGS-Cameco-COGEMA-GSC-SEM

DDH# Q7-24	Disposition: CBS9332	NTS: 74 I/8	UTM: 6461300N 554800E	rev.
Page:	Property: Dawn Lake, Cameco	Storage: Dawn Lake	Logged by: G.M. Yeo & C.W. Jefferson	000616

Interval				Lithofacies			Structures		Clasts				Alteration			Remarks	Smpl #
Unit	Sub	Thick	To	Lithol	Base	Facies	xBon	Grading	MTG	%>2	Roun	Sort	%clay	Colour	Hem	NO core	(51-00-, PNA-00-)
		10	13.00													overburden	
1	A	13.00	60.80	fmS	T	Sx	20	cUF	2	0	4	3	1	plyelgy	0	1% clay intraclasts	PNA-00-801 @ 19.46-19.50m interbeds, PNA-00-802 @ 38.07-38.11, PNA-00-803 @ 60.53-60.58m

Table 4 - Formations and sediment source areas of the Athabasca Group (after Ramaekers, 1990, Table 1).

Sub-group	Environ-ment	Jackfish Basin (western Athabasca)	Mirror Basin (central Athabasca)	Cree Basin (eastern Athabasca)	Dominant Lithology	Source
Points Lake	marine	Carswell Fm. (C)			Stromatolitic and oolitic dolostone	northeast?
	marine	Douglas Fm. (D)			Black, red, and green mudstones, siltstones, and sandstones	
William River	marine	Tuma Lake Fm. (TL)			Pebbly sandstone	
	disconformity					
	marine	Otherside Fm. (OF)	Otherside Fm.		Sandstone and siltstone	south, east, and northeast
	marine	Locker Lake Fm. (LL)	Locker Lake Fm.		Pebbly sandstone	
	disconformity					
	marine	Wolverine Point B (WPb)	Wolverine Point B		Phosphatic, tuffaceous siltstone and clay-rich sandstone	south
	marine	Wolverine Point A (WPa)	Wolverine Point A	Wolverine Point A	Sandstone and siltstone	
	marine		Lazenby Lake Fm. (LzL)		Pebbly sandstone	
	disconformity					
	fluvial	Manitou Falls d (MFd)	Manitou Falls d	Manitou Falls d	Intraclast-rich sandstone	east and northeast
	fluvial	Manitou Falls c (MFc)	Manitou Falls c	Manitou Falls c	Sandstone	east, northeast, and south?
	fluvial			Manitou Falls b (MFb)	Conglomerate and sandstone	east, northeast, and south
	disconformity					
	fluvial	Fair Point Fm. (FP)	Manitou Falls a (MFa)		Sandstone, pebbly sandstone, and conglomerate	local; south, and east?
major unconformity						
Metamorphosed basement						

Pb methods. Diagenetic xenotime, discussed above, may also provide detailed breakdown of diagenetic events and age constraints of Athabasca deposition and diagenesis.

The Manitou Falls Formation

Detailed descriptions of facies assemblages in this paper are based on an initial focussed study of the Manitou Falls Formation in the eastern part of Athabasca Basin. Table 5 shows how the stratigraphy of the Manitou Falls Formation has changed over the past 20 years. Our initial results show that Ramaekers' (1990) framework is solid, and support his prediction that detailed subdivision of his regional formations is possible and relevant to analysis of the Athabasca Basin for its uranium potential.

In the course of his investigations, Ramaekers (1976, 1977, 1978a, 1978b) distinguished six fluvial depositional systems in the lower part of the Athabasca Group, chiefly on the basis of conglomerate types and paleocurrents. In his 1979 report, Ramaekers (1979a) recognized that the upper clastic formations of the Athabasca Group, which typically have higher paleocurrent variance than the lower ones, are probably coastal or shallow marine deposits, rather than braided river deposits like the lower ones. The summary of Manitou Falls stratigraphy below is based mainly on Ramaekers' 1981 and 1990 papers.

Table 5 - Comparison of characteristics of the Manitou Falls Formation as initially defined (Ramaekers, 1979a, 1979b, 1990) and as subsequently developed by some exploration geologists. The Cameco stratigraphy reflects current usage in the McArthur River area. The COGEMA stratigraphy is derived from assessment reports for the nearby Close Lake area.

	Ramaekers (1990)	Cameco	COGEMA (Close Lake)
MFd	Fine- to coarse-grained sandstones, typically with clay intraclasts concentrated above scoured surfaces. One layer granule and pebble beds are found locally, especially towards the base.	Well-sorted, medium-grained sandstone, characterized by clay intraclasts; faintly crossbedded; with grit horizons towards the base.	Fine-grained sandstone characterized by abundant clay intraclasts. Includes grit and clay intraclast layers.
MFc	Medium- to coarse-grained, less commonly granule-sized sandstone with pebble layers <2 cm thick in the lower part of the member. Rare, 1 to 2 cm clay layers and scattered clay intraclasts are present.	Moderately to poorly sorted, granule-rich sandstone with minor pebble layers <2 cm thick; well-developed, typically low-angle crossbedding; disseminated pebbles.	Sandstone with rare clay intraclasts. Variable thickness suggests contemporaneous tectonism. **MFc1**: a few upward fining cycles 10 to 20 m thick. **MFc2**: a succession of upward coarsening cycles.
MFb	Characterized by at least 2% clast-supported conglomerate beds >2 cm thick interbedded with sandstone. Quartz clasts predominate, but originally polymictic cobble conglomerates occur locally. Sandstones are typically poorly sorted, with heavy mineral (hematite, zircon, tourmaline, rutile, and anatase) laminae in the lower part. In the Cree Sub-basin 2 conglomeratic zones separated by sandstone are common.	Moderately to poorly sorted, medium to coarse grained sandstone, with intervals of grit, granules and pebbles >2 cm thick. Conglomerate thickness and clast size increases with depth.	Fine to coarse sandstones intercalated with conglomerates. **MFb1** (≈60 m): two fining upward cycles overlying a thin coarsening upward cycle. **MFb2** (≈145 m): characterized by abundant (40 to 70%) conglomerate beds 20 to 50 cm thick. **MFb3**: two upward coarsening cycles. Burial of basement topography at end of MFb3 time indicated by uniform thickness of overlying MFb2 and MFb1. **MFb4**: basal conglomerate, characterized by large (<150 mm) clasts.
MFa	Pebbly conglomerates interbedded with better sorted sandstones, locally with clay intraclast-rich layers.	Poorly sorted, medium- to coarse-grained sandstone with grit beds <1 cm and <15% conglomerate. Matrix-supported conglomerates and isolated clasts are common, but conglomerates are thinner and less abundant, and clasts are smaller than in the MFb.	Talus deposits, including fanglomerate, sandstone, and siltstone, associated with fault-related basement highs.

The MFa member is the basal unit of the Manitou Falls Formation, and was defined by Ramaekers (1990) as a thick succession of interbedded pebbly matrix-supported conglomerates and clay intraclast-bearing, well-sorted sandstones at the base of the Manitou Falls Formation along the southern margin of Athabasca Basin. Ramaekers (1980, 1990) initially considered the MFa member to be a mixed fluvial and marine package, but later interpreted it to be exclusively fluvial (Ramaekers, 1990), as the low angle and herringbone cross-beds typical of this member are more characteristic of marine upper shoreface deposition. The conglomerates are unequivocally fluvial. MFa was largely derived from south of the basin. The MFa member, as defined, is essentially restricted to the central Athabasca Basin, but may be partly correlative with the Fair Point Formation to the west (Table 4). Ramaekers (1990) suggested that a tongue of the MFa member might extend east to the Close Lake area. A lens of MFa is shown in this area on a geological sketch map (Ramaekers, 1981), but not on his later maps (Ramaekers, 1990). This feature has been retained, however, on various editions of the 1:1 000 000 Geological Map of Saskatchewan (e.g. Macdonald and Slimmon, 1999).

The MFb member is defined by the presence of more than 2% clast-supported conglomerates in beds more than 2 cm thick. It comprises an eastward thickening and coarsening succession of interbedded sandstones and conglomerates. Planar and trough cross-bedding are predominant in the sandstones, but clay intraclasts are uncommon. Over much of the eastern Athabasca Basin, two conglomerate units are separated by finer-grained strata. Regional paleocurrents suggest deposition from alluvial fans which radiated into the basin from the northeast and east. Ramaekers (1981) reported that debris flows were absent from these deposits, but as discussed below, these can be difficult to identify.

The MFc member is characterized by the absence of conglomerates thicker than 2 cm (although pebble layers are common in the transition to the underlying MFb member), and less than 1% layers with clay intraclasts. Abundant planar and trough cross-bedding and uniform westerly-directed paleocurrents indicate deposition in sandy, braided river systems.

The MFd member is characterized by well-sorted sandstones with more than 1% layers with clay intraclasts. The sands are typically better sorted and finer grained than those of the MFc member, with which it intertongues. Deposition on a braidplain with intermittent lakes was likely. The upper contact of the MFd member with the overlying Wolverine Point Formation was not observed, and their relationship is uncertain, although probably disconformable.

There have been few published studies of the basal Athabasca clastic strata done since Ramaekers' work. Pacquet and McNamara (1985) described the basal 78 m (Fair Point or Manitou Falls formations) in the Cluff Lake area from eight DDHs. They interpreted these strata as alluvial fan deposits (including debris flows). Harper (1996) also interpreted the Fair Point Formation in the Maurice Bay area, north of Lake Athabasca, as alluvial fan deposits.

2. Stratigraphic and Sedimentary Features of the Manitou Falls Formation

Our field work in 2000 focussed on examination of core from a series of five transects roughly perpendicular to the eastern margin of the Athabasca Basin (Figure 1; Table 6). Transect A (four DDHs) trends southwest from Moosoonees Lake to the Hawkrock River area. Transect B (14 DDHs) trends northwesterly from Lampin Lake to La Rocque Lake. Transect C (six DDHs) trends west-northwest from Whitford Lake through Close Lake to Cushing Lake. Transect D (seven DDHs) trends northwest from Wheeler River through the McArthur River mine area to Close Lake. Transect E trends north-northwest from Moore Lakes through the McDougall Lake area to Kearns Lake. In addition, a brief study was made of the exposures at the eastern end of the Deilmann Pit at Key lake. Transects B and D were designed to provide stratigraphic constraints on the Points North LITHOPROBE line (Hajnal *et al.*, 1997) and the planned McArthur River seismic line, respectively.

This paper presents results of stratigraphic studies restricted to the Manitou Falls Formation east of 106°. Plots of drill holes on stratigraphic fence diagrams are compiled in the map package accompanying this volume ("Geological Cross-sections through the Manitou Falls Formation in the eastern Athabasca Basin"). On these sheets we have subdivided the Manitou Falls Formation into previously established members from the upper contact of MFb through MFd, using criteria from Ramaekers (1990).

a) Preliminary Facies in Undifferentiated MFa-MFb Successions in the Eastern Athabasca Basin

Facies recognized in core from the Manitou Falls Formation are described below, and along with preliminary clay mineralogical analyses (the latter only in MAC-218), are consistent with stratigraphy and clay zoning reported by McGill *et al.* (1993).

Facies 1: Basal Conglomerate

Locally, a thin conglomerate or isolated cobbles and boulders directly overlie the basement. This sub-unit is commonly difficult to recognize in drill core due to the sparseness of the basal boulder-pebble lag. Clasts typically represent a variety of intensely weathered basement rock types – gneisses, schists, and granitoids, in addition to the predominant quartz. Grain size is typically in the 2 to 20 cm range, but in some holes is boulder size. The rounding of these clasts is interpreted to be a result of *in situ* climatic processes (c.f. Long *et al.*, this volume). Evidence for *in situ* rounding is preserved in some deep cracks in basement rock, where sub-rounded clasts or clast fragments can be seen (e.g. MAC-111).

Facies 2: Breccia

Highly angular, shard-like clasts of quartzite in a red muddy sandy matrix with seriate grain-size distribution, was observed only in RL-97, a core not logged as part of this project, but which intersects basement more than 100 m higher than adjacent holes, indicating significant local paleotopography. This facies is interpreted as a paleo-talus deposit.

Facies 3: Red Mudstone/Sandstone/Conglomerate

This facies is characterized by brick-red, wavy laminated mudstone in beds 1 to 40 cm thick, with abundant dewatering structures, clastic dykes, starved sand ripples, and sand-filled syneresis cracks ranging from millimetres to >4 cm across and up to 20 cm deep (Figure 2). The sandy mudstones have a fenestral appearance due to frosted quartz granules in the core. This facies was observed in the southern transects, at the eastern end of transect C, throughout transect D, and in transect E, although only weakly developed in the Moore Lakes area. The maximum observed thickness is about 30 m (e.g. MAC-111).

Interbeds of abundantly trough cross-bedded coarse sandstone are common and range in thickness from several centimetres to tens of centimetres. These sandstones are also brick red where they contain abundant mud matrix, but are pale grey where well-sorted with siliceous matrix. Mudstone on the margins of such beds is also bleached (Figure 3). Trough cross-

Table 6 - Summary of cores logged on transects A to E (see Figure 1 for locations). Thickness of Manitou Falls members (in metres) is taken from company logs, except D2, D12, MAC-111, MAC-100, MAC-107, RL-99, MAC-218, ML-4, and ML-2. Note that because of variations in definition of the MFa member, its presence or thickness, as reported in assessment reports, is not consistent. Basal units of MAC-188, -186, and -189 include MFa, MFb, and fanglomerate. MFc in CLC9S-64 includes COGEMA's subunits MFc1 and 2 (see Table 5). The basal unit of CLC9S-64, CLC10-76, CLC10-77, and CLC13-66 includes COGEMA's subunits MFb 1 to 4. Cores 4-69, D11, CLC13-66, and CRO-4 are stored at SEM's Regina Core Lab, but have not been logged at the time of writing.

Line	DDH	Company	Easting	Northing	Disposition	MFd	MFc	MFb	Mfa(?)	U/C (m)
A	4-69	Great Plains	547500	6553000	Permit # 4			31		46.3
	D2	DF Expl.	518400	6538200	S-99087		327	33		373.5
	D11	DF Expl.	518800	6538650	S-99086		125	30		163.5
	D12	DF Expl.	512800	6513850	S-106289	317	94	75		490.8
B	LMS-13	Eldorado	567750	6448100	CBS 6805			68		85.5
	SP-90	Cameco	567950	6450700	CBS 6805			59		81.5
	SP-130	Cameco	568514	6452168	CBS 6805		?	51		78.2
	SP-86	Cameco	568400	6453250	CBS 6802		?	69		90.6
	SP-108	Cameco	566097	6452279	CBS 6802		?	93	?in MFb	110.5
	SP-109	Cameco	566056	6452308	CBS 6802		?	119	?at base	143.5
	ST-1	SMDC	564550	6454250	CBS 7650		?	169		178.6
	SN-2	Cameco	560911	6452723	CBS 6804		?	180		183.4
	Q8-60	Cameco	558400	6456800	CBS 9330			152		161
	Q7-24	Cameco	554800	6461300	CBS 9332		27	156		196
	HAM-4	Cameco	547592	6462002	S-105331		86	158		263.8
	HAM-2	Cameco	541267	6465996	S-105329		161	176		340.8
	Q23-6	Cameco	548200	6487650	CBS 9339		88	140		273.1
	Q22-8	Cameco	537100	6488200	CBS 9338		117	171		306.2
C	MAC-188	Cameco	520427	6403195	S106851	112	36	10.5	9.6	173.9
	MAC-186	Cameco	514986	6405898	S105657	180	46	189		443.4
	MAC-189	Cameco	509543	6407425	S101722	146	72	188		411.6
	CLC9S-64	COGEMA	503460	6410540	S101494		92	286		421
	CLC10-77	COGEMA	499710	6419850	S104781	169	133	275		602.8
	CLC13-66	COGEMA	504100	6434900	S101503	209	117	301		651
D	MAC-61	SMDC	507546	6379404	ML5298		37	112		191.1
	MAC-111	SMDC	500144	6395115	S105665	106	95	117	92	410.8
	MAC-100	SMDC	499717	6395725	S105665	69	98	115	98	381
	MAC-107	SMDC	499663	6396633	S105665	94.5	140	86.6	70.1	391.1
	RL-99	Cameco	488950	6397410	CBS 8926	124	165	66	65	431.5
	MAC-218	Cameco	497567	6402797	ML5516	161	118	142	91.7	493.3
	CLC10-76	COGEMA	500125	6419700	S101497	154	123	301		585
E	ML-4	JNR Res.	492210	6363410	CBS 7839		64	207		277.1
	ML-2	JNR Res.	491650	6364480	CBS 7839		76	182		266.6
	ZN-5	Cameco	484656	6379707	S105530	132	87	158	83	463.2
	WC-2	Cameco	483767	6380852	S105530	100	100	124	92	429.8
	PS-1	Cameco	481702	6382122	S105531	82	140	37	5	280
	CRO-4	Uranerz	427450	6410450	S105389	530	144	145	172	1001.1

bedding appears to be unidirectional in most beds, but some beds have apparently opposing directions that may reflect either cuts of opposing unidirectional troughs, or actual bipolar paleocurrents.

Conglomerate interbeds 5 cm to tens of centimetres thick also have a sandy matrix (Figure 3) or a deep red muddy matrix (Figure 4). Very large clasts and a variety of basement rock types are common, either isolated in mud/sand, or as intact framework

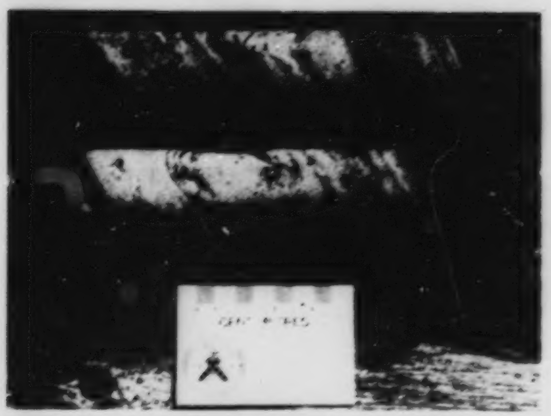

Figure 2 - Red mudstone/sandstone/conglomerate facies, illustrating synaeresis cracks (approx. 380 m in MAC-111) near McArthur River. Way up is to left; divisions on scale are 1 cm. Photo JP-00-88.

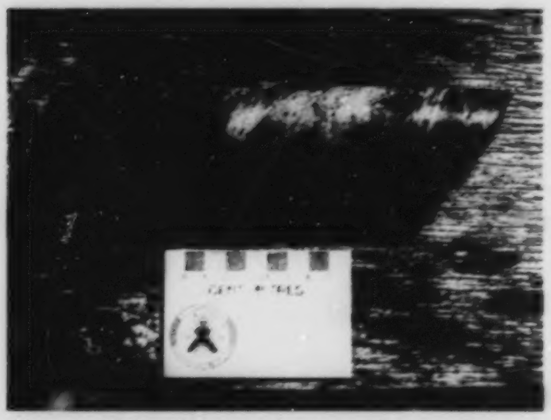

Figure 3 - Red mudstone/sandstone/conglomerate facies, illustrating upward-coarsening conglomeratic coarse sandstone with bleached basement clasts and bleached margins of bounding red mudstone (approx. 379 m in MAC-111). Way up is to left; divisions on scale are 1 cm. Photo JP-00-82.

conglomerates (Figure 4) containing mud/sand beds between clasts, infiltrated into facies assemblages 1, 2, or 4 as sieve texture. Inverse grading and protruding clasts draped by overlying mudstones are common.

The red colour of this facies is unique in its uniform brick red appearance and the extremely well-preserved fine grain size and textures. The unit appears to be relatively unaltered, except along clean sandstone beds. Mudstone intraclasts within these beds are commonly silicified and reduced to tan colour, as are mudstones located along their contacts (Figure 3). These features suggest that the red hematite colour is a well-preserved very early diagenetic result of vadose hematization processes (cf. Walker, 1967).

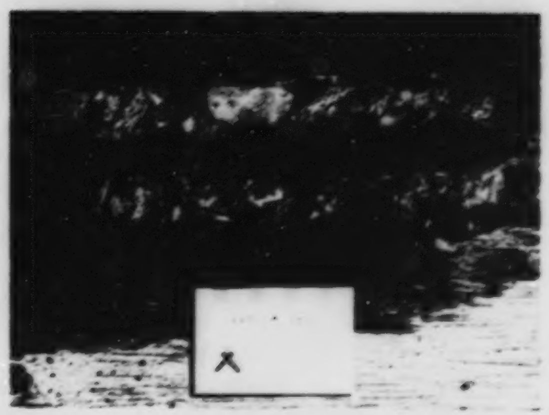

Figure 4 - Red mudstone/sandstone/conglomerate facies, illustrating matrix-supported disorganized conglomerate with a variety of highly clay altered clasts in a deep red mudstone matrix (approx. 390 m in MAC 111). Way up is to left; scale divisions in cm. Photo JP-00-91.

Facies 4: Coarse Conglomerate/Pebbly Sandstone

This facies comprises intercalated, intact framework, coarse to very coarse conglomerate and pebbly sandstone. It occurs low in the stratigraphic sequence, and is interpreted as being close to paleo-highs. Rounding is highly variable, with large round clasts interpreted as having been developed over short distances of transport by climatic effects at or near source (cf. Long *et al.*, this volume). Commonly, this unit is much coarser than stratigraphically lower strata, suggesting renewed uplift after basin initiation.

Facies 5: Heavy-mineral-rich Coarse Sandy Conglomerate and Gravelly Sandstone

Heavy mineral-bearing strata are most extensive in transects A, B and C; where they form a wedge on the order of 50 m thick that coarsens and then fines upward overall, with internal smaller coarsening- to fining-upward cycles. A broad peak in heavy mineral abundance and grain size occurs in the middle of each cycle. Upward transition to facies 6 is marked by decrease in heavy minerals and maximum grain size. In some northern drill holes, heavy minerals are abundant higher in the section. Heavy mineral laminae are common in the basal 20 m at Moore Lakes, but to the north and west on transects D and E, facies 5 thins to a very minor component, separated from basement by about 50 m of facies 1 to 4. It appears to be antipathetically related to facies 3 (i.e. heavy mineral laminae are absent where redbeds are well developed). Although diagenetic hematite predominates in the heavy mineral laminae (Figure 6), detrital magnetite occurs in nearly every lamina observed. Heavy mineral bands were not observed at McClean Lake (Long *et al.*, this volume), nor at Key Lake. Petrographic study is required to determine whether the heavy mineral bands were never deposited or the conspicuous magnetite

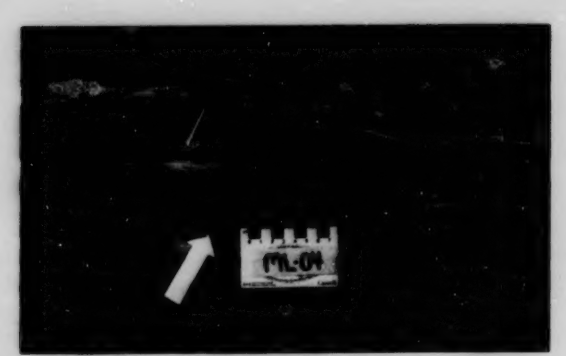

Figure 5 - Heavy mineral laminae outlined by dense detrital magnetite in facies 5 (at about 262 m in ML-4) near Moore Lakes. Way up is to left; scale divisions are 1 cm. Photo GY-00-36.

component was eliminated during diagenesis in these areas.

Facies 6: Coarse Sandy Conglomerate and Gravelly Sandstone

This assemblage is characterized by an abundance of sub-rounded coarse sand to granule-size material, and relatively few fine-grained interbeds. Trough cross-beds in the 2 to 10 cm range are common. Locally, as at Moore Lakes on the southern end of Transect E, horizontal or low angle cross-bedding is well developed. Facies 6 is intercalated with facies 7. This is an important component of the MFa subunit of Cameco and the lower MFb subunit of COGEMA (Table 5). In the northern transects it grades downward to facies 5 with the appearance of magnetite-bearing heavy mineral laminae and mudstone interbeds. In the southern transects it typically grades sharply downward to facies 3 through the introduction of red mudstone.

Facies 7: Medium to Coarse Sandstone

This coarse sandstone unit is relatively free of conglomerate and mudstone and separates lower coarse-sandy-muddy conglomerates of facies 6 from upper medium-sandy muddy conglomerates of facies 8. Facies 7 is relatively well sorted, has very little clay, silt, or fine sand in the matrix, and contains abundant large trough cross-beds. It is present at least in the McArthur River, Read Lake, and Close Lake areas. In some drill holes there are two intercalations of facies 6 and 7.

Facies 8: Intercalated Pebbly Sandstone, Sandy Conglomerate, and Mudstone

Poorly sorted, pebbly fine-medium sandstones and medium sandy conglomerates and mudstones to fine sandstones are intercalated on a scale of centimetres to decimetres, but overall this facie fines upward. Stacked coarsening-thickening and fining-thinning upward packages in the decimetre range appear to represent pulses of conglomerate mixed with moderately sorted medium-grained sandstone. Paleocurrents are unimodal westerly wherever measured (Figure 6). Conglomerates range from matrix-supported to intact framework and are generally massive and poorly organized. Both upward-fining and upward-coarsening beds are common. Contacts between sandstones and conglomerates are generally diffuse, whereas mudstones have sharp contacts, suggesting that following deposition of mud during quiet water periods, overlying gravels were deposited as a carpet rolled out onto the muds (Figure 7). Clast imbrication is rare, but interpreted to have been produced by mass flow, with clasts inclined down paleoflow (Figure 8). Comparable debris flow deposits are likely present in facies assemblages 3, 5, and 6. The mudstone layers commonly found in this facies assemblage (Figure 8), as well as facies 9, 10, and 11, are faintly laminated, rarely graded, well-sorted siltstones to very fine sandstones typically 1 to 10 cm thick.

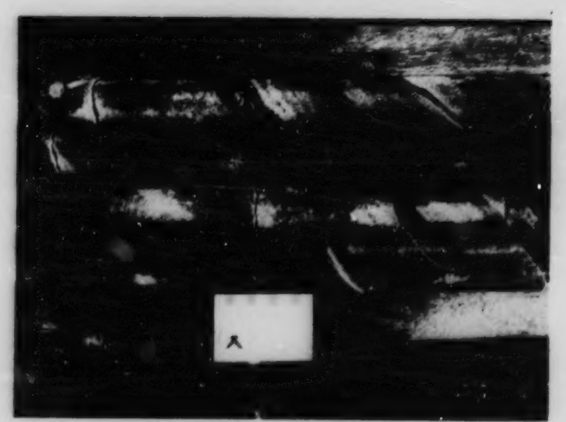

Figure 6 - Unidirectional sets of trough cross beds intersected in facies 8, from MAC-61, southeast of McArthur River. Way up is to the left; scale divisions are 1 cm. Photo JP-00-102.

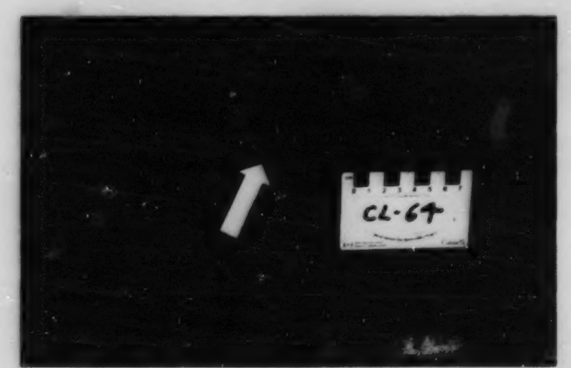

Figure 7 - Conglomerate overlying undisturbed sandy silt bed from CL-64 east of Close Lake. Way up is to left; scale divisions are 1 cm. Photo GY-00-28.

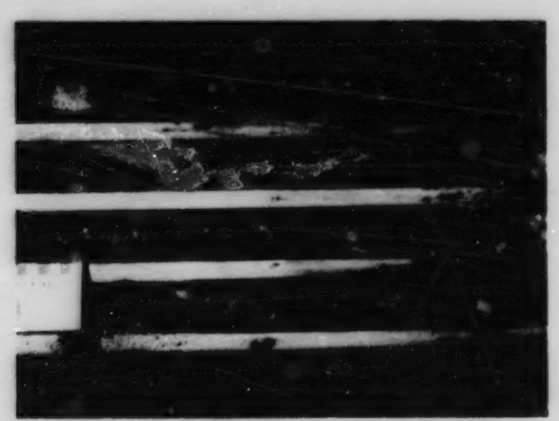

Figure 8 - Intercalated matrix- and framework-supported conglomerate with diffuse margins, and pebbly sandstone characteristic of facies 8, from MAC-61 southeast of McArthur River. Way up is to the left; divisions on scale are 1 cm. Photo JP-00-95.

Facies 9: Intercalated Granule-bearing Sandstone, Sandy Granulestone, and Mudstone

This assemblage is much like facies 8 but finer grained. The top of MFb is usually within this facies. On the numerical log (see Mwenifumbo *et al.*, this volume) the boundary is picked at a distinct unit that contains a minority of beds greater than 2 cm thick with granule to small-pebble conglomerate, in contrast to facies 8, which has up to 30% conglomerate beds.

b) Preliminary Subunits in MFc and MFd Successions in the Eastern Athabasca Basin

Facies 10: Clay Intraclast-bearing Sandstone and Gravelly Sandstone with Thin Pebbly Layers, and Mudstone

Facies 9 is transitional upwards into poorly to moderately sorted, fine to coarse sandstone interbedded with poorly to moderately sorted granule- and pebble-bearing sandstones. Scattered angular white clay intraclasts up to 50 mm long are present, but much less common than in facies 11. Pebbles up to 2 cm thick are locally common. This facies is typical of the lower MFc member.

Facies 11: Clay Intraclast-bearing Sandstone and Gravelly Sandstone

Facies 10 is transitional upwards into moderately to well-sorted, fine to medium sandstone interbedded with minor poorly to moderately sorted granule- and pebble-bearing sandstones, with abundant angular clay intraclasts up to 50 mm in length. Interbedded parallel-laminated fine sand to silt layers up to 10 cm thick are common. Pebble layers one clast thick are rare. This facies is typical of the upper MFc member.

Facies 12: Clay Intraclast-rich Fine to Medium Sandstone

Facies 10 and 11 are associated with moderately to well-sorted, fine to medium sandstone, commonly with angular clay intraclasts up to 25 mm long (Figure 9). Interbedded parallel-laminated fine sand to silt layers up to 10 cm thick are common. This facies is typical of the MFd member.

c) The Manitou Falls Formation in the Deilmann Pit

A series of 31 short sections, ranging from 2 to 17 m, were measured on the ramps in the eastern part of the Deilmann Pit at Key Lake, which is being flooded for use as a tailings storage pond. The structural geology and basement rocks of the pit were recently described by Harvey (1999), but little work has been done on the overlying Manitou Falls Formation. Previous workers (e.g. Harvey, 1999; Ramaekers, 1990) considered all the strata here to belong to the Manitou Falls b Member, but as shown below, at least two distinctive facies can be identified here.

On the north side of the Key Lake Fault Zone in the eastern area of the pit, the Manitou Falls Formation laps unconformably onto Wollaston Group paragneiss (Harvey, 1999; Figure 10). The basal Manitou Falls strata fill an easterly-trending paleovalley at least 60 m deep, whose axis lies south of the present-day pit (Harvey and Bethune, this volume). About 8 m of paleo-relief is evident in the pit. Development of a pre-Athabasca regolith is indicated by strong hematite and chlorite/illite content of the unconformably underlying Wollaston rocks (Harvey, 1999; Harvey and Bethune, this volume).

The lowest 15 m of Manitou Falls Formation exposed in the pit are predominantly trough cross-bedded, gravelly, medium to coarse sandstone in beds 20 to 220 cm thick, interbedded with massive and cross-bedded sandy conglomerate from 5 to 20 cm thick, and

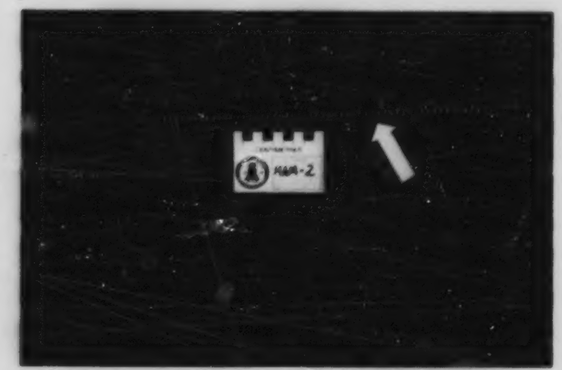

Figure 9 - Angular clay intraclasts in medium sandstone with well-developed liesegang banding, from HAM-2, south of Hamilton Lake. Way up is to left; scale divisions are 1 cm. Photo GY-00-46.

pebble layers one clast thick (Figure 11). Cyclic upward fining and upward-improved sorting are typical of the sandy beds. Conglomerate clasts range up to 80 cm. Cobble imbrication, observed in one bed, is consistent with northwesterly paleoflow indicated by cross-bedding. The one-clast-thick layers persist laterally for at least tens of metres, and are interpreted as lag deposits. These strata correspond mainly to facies 4 coarse conglomerate and pebbly sandstone and facies 6 coarse sandy conglomerate and gravelly sandstone observed in core. Cross-bed measurements from this interval on the south side and the east end of the pit indicate northerly transport.

The lowest exposed beds of the Manitou Falls Formation are overlain by a relatively thick succession of planar and trough cross-bedded sandstone and pebbly sandstone (Figure 12). Planar cross-bed sets are laterally continuous for tens to hundreds of metres.

Key Lake Fault Zone

Figure 10 - Unconformable onlap of Manitou Falls Formation onto Wollaston paragneisses on the northern slope of a Proterozoic paleovalley partly exposed at the east end of the Deilmann Pit. Note people to left on lowest bench for scale. Photo GY-00-53.

Figure 11 - Conglomerate and sandstone about 2 m above the basement unconformity on the south central face of the main Deilmann Pit. Scale divisions are 1 cm. Photo GY-00-38.

Figure 12 - Planar cross-bedding about 15 m above the basement unconformity on the south central face of the main Deilmann Pit. Divisions on staff are 10 cm. Photo GY-00-2.

Cyclic upward fining and upward-improved sorting are typical. Upward-decreased sorting also occurs. These strata correspond to facies 7 medium to coarse sandstone observed in core. Cross-bed measurements from this succession in the southeast and east parts of the pit indicate westerly and west-northwesterly transport.

3. Discussion

a) Stratigraphy of the Manitou Falls Formation

The distinction between Manitou Falls members MFa and MFb has been made in different ways by various workers (Table 5). Many have indicated the extensive distribution of MFa in the eastern Athabasca Basin. Ramaekers (1990), however, restricted MFa to the Mirror Sub-basin, northwest of Cree Lake, and well west of our study area. Furthermore, what is included in MFa varies according to location and author. We consider that insufficient information is available to resolve the distinction between MFa and MFb until we have personally investigated the type area for MFa designated by Ramaekers (1990). We have, however, subdivided the lower part of Manitou Falls Formation into numbered sub-units comprising different facies and facies assemblages (see also Mwenifumbo *et al.*, this volume). These sub-units will help to delineate correlations that can be made based on the numerical and qualitative values we have logged. We hope that as the project evolves, Table 5 will develop into a "Rosetta Stone" to facilitate development of a detailed regional stratigraphic terminology. Regional correlation of logs is illustrated in the fence diagrams in the accompanying map package.

b) Flashy Sedimentation in the Manitou Falls Formation

Depositional Environments of MFa and MFb Facies

Hematization of basement rocks up to 50 m below the Athabasca Group, and clay alteration immediately below the unconformity, reflect intense lateritic weathering prior to the onset of Manitou Falls deposition (Hoeve, 1977; Ramaekers, 1981, 1990). The geochemistry of this regolith is described by Tremblay (1982).

The association of variably sorted sands, gravels, and gravelly sands and unimodal paleocurrents (Ramaekers, 1981, 1990) are indicative of low-sinuosity, bedload-dominated (i.e. braided) river systems (Cant, 1982; Collinson, 1986). Pebbly streams predominated in the lower Manitou Falls (MFa and MFb), while sandy streams predominated in the upper Manitou Falls (MFc and MFd).

Alluvial fans may be subdivided into three distinctive parts, the upper, middle, and lower fan (Nilsen, 1982; Collinson, 1986). The upper fan, radiates out from a highland source valley and is characterized by a high ratio of coarse to fine gravel, plane-bedded sand, and channel down-cutting. The middle fan lies below the intersection point, where the upper fan channel emerges onto the fan surface and radiates into distributary channels, and is characterized by medium gravel, and both plane-bedded and cross-bedded sand. Sieve deposits and framework-supported conglomerates, typically occur just down-fan from the intersection point. The lower fan is characterized by fine gravel interbedded with cross-bedded and plane-bedded sand. Lower fan deposits are transitional to basin floor alluvial plain and other facies (Nilsen, 1982). Two dominant types of alluvial fans are recognized, "stream-dominated" fans and so-called "semi-arid" fans, associated with active faulting (Collinson, 1986).

Prevalence of cross-bedding, indicative of flow in channels, indicates that the Manitou Falls alluvial fans were generally closer to the "stream-dominated" end of the alluvial fan spectrum than the "semi-arid" type. Limited supply of fine sediment from the source area, indicated by scarcity of mudstones, is conducive to development of stream-dominated fans, even in semi-arid climates (Collinson, 1986). The extent of alluvial fan deposits (e.g. MFb) downdip suggests low gradients, another characteristic of stream-dominated fans.

Facies 1, the basal conglomerate, probably represents locally derived colluvial deposits. Large, matrix-supported clasts in this facies, suggest that sandy debris flows were involved in its deposition (e.g. Nilsen, 1982).

The angular nature of the clasts, local derivation, and association with paleorelief indicates that the facies 2 breccia beds are talus, deposited at the base of paleo-cliffs. They are evidence for considerable local paleorelief and possible syndepositional tectonism. This may have been basin-wide, as Pacquet and McNamara (1985) and Harper (1996) drew similar conclusions from basal Athabasca strata in the Cluff Lake and Maurice Bay areas in western Athabasca Basin, respectively. We have not yet observed convincing evidence for syndepositional faulting in eastern Athabasca Basin, however.

Reddening typical of facies 3 mudstone, sandstone, and conglomerate is interpreted to have occurred during early diagenesis because of the fine grain size and excellent preservation of very fine structures and textures in the red mudstones. Strata of this facies are, thus, classic redbeds (e.g. Walker, 1967), which probably developed in a relatively arid climate. We use the term arid in a relative sense, because some prime indicators of arid conditions are not yet observed here (e.g. eolianites, caliche, and evaporites) although they are present in the penecontemporaneous Dubawnt Group (Rainbird and Hadlari, 2000).

The coarse grain and intact framework of facies 4 subangular to rounded cobble to boulder conglomerates, is indicative of high energy deposition. The more organized and intact framework beds of conglomerate probably accumulated as longitudinal gravel bars in braided rivers (e.g. Collinson, 1986). Proximity to paleo-highs suggests that they are locally derived compared to associated strata, and may reflect local tectonic uplift.

The heavy mineral laminae characteristic of facies 5 coarse sandy conglomerates and gravelly sandstones are placer accumulations typical of mid-fan braided streams (Collinson, 1986). Although not recognized in this study, zircon, rutile, and tourmaline are known to be associated with magnetite in the Rabbit Lake (Ramaekers, 1979b) and Maurice Bay (Harper, 1996) areas, and are probably present elsewhere. This is an assemblage of very stable heavy minerals, typical of an older sedimentary provenance (e.g. Lewis and McConchie, 1994, Table 6-2). Taken with the overwhelming predominance of quartz, this indicates that these strata must be second cycle sediments.

The widespread occurrence of detrital magnetite has potential for refining the depositional age of the Manitou Falls Formation. The earliest magnetization recognized in Athabasca Basin (Kotzer *et al.*, 1992) corresponds to a 1600 to 1750 Ma paleopole, but was derived from early diagenetic hematite, not magnetite. As outcrops with heavy mineral laminae are rare, heavy mineral-bearing intervals from inclined DDHs could be sampled for this purpose.

The coarse sandy conglomerate and gravelly sandstone of facies 6 probably represent proximal braided rivers. The prevalence of facies 6 compared to facies 7 suggests that flow was relatively short-lived (i.e. ephemeral streams). Predominance of trough cross-bedding indicates that much of this facies assemblage represents deposition in channels by migrating sinuous-crested bars. Sedimentation in channels predominates on the upper parts of alluvial fans (Collinson, 1986, Figure 3.14). The low angle cross-bedding observed at Moore Lakes may represent downstream accumulation on longitudinal bars (c.f. Collinson and Thompson, 1982, Figure 7.5). Alternation of gravel-rich and gravel-poor layers may be due to slight fluctuations in stream velocity.

The medium to coarse sands of facies 7 may reflect more sustained flow conditions, which allowed better sorting.

Intercalated pebbly sandstone, sandy conglomerate, and mudstone of facies 8 are also interpreted as braided river deposits. Ramaekers (1990) observed that true debris flow deposits, typical of modern arid region alluvial fans, are rare in the Manitou Falls Formation, but the deposits of ephemeral streams and debris flows may be difficult to distinguish, as both have great textural immaturity. The normal and reverse grading observed in individual sandy conglomerate beds suggests that at least some are mass flow deposits . Further study is required to determine the depositional setting of facies 8. The base of conglomeratic facies 6 and 8 must correspond to episodes of channel downcutting, fan progradation, and lowered base level (i.e. the lowstand systems tracts of Hiatt and Kyser, 2000).

The fine grain-size of the mudstone layers common in facies 8, 9, 10, and 11 (e.g. Figure 7) is typical of suspension deposits, laid down as flow velocity dropped in the later stages of a flood, or in relatively quiet areas such as the "slough channels", developed downstream from bank-attached bars in braided river systems (e.g. Collinson, 1986, Figure 3.4a). Fine lamination of some of these beds, particularly those of silt to fine-sand grain-size, suggests upper plane-bed conditions (e.g. Lewis and McConchie, 1994). The tops of these mudstones resisted scour by later flows, as muddy sediments are relatively cohesive. On the other hand, mudstones in the MFc and MFd members are mainly present as rip-up intraclasts associated with granulestone at the base of trough cross-bedded sandstones, whereas mudstones in the MFa and MFb members are mainly present in beds directly overlain by pebbly sandstones or sandy conglomerates (e.g. Figure 7). Preservation of the latter mudstone beds indicates that they were buried rapidly and gently, and hence were more likely deposited in lows, such as slough channels, than on bar tops during flood stages. Coarse-grained beds overlain by slough channel muds must be channel deposits; not bars.

As noted above, the intercalated granule-bearing sandstone, sandy granulestone, and mudstone of facies 9 is similar to facies 8, and hence probably represents a similar, but more distal, depositional environment.

The decimetre-scale coarsening- to fining-upward packages, described in facies 8, are interpreted in terms of increasing and decreasing frequency and intensity of flood and/or debris-flows caused by sudden intense rainstorms and/or tectonic disturbances that caused pulses of pebble- and cobble-laden debris to course out into the basin from the tectonic hinterland.

In general, facies 1 to 9 correspond to the Donjek-type braided river model (Miall, 1978, 1992; Cant, 1982). Such rivers result from variable discharge (i.e. flashy) conditions and mixed sand and gravel bedload.

Depositional Environment of MFc and MFd Facies

The sandstones and gravelly sandstones of facies 10 and 11 differ from underlying strata by the scarcity of conglomerates, as well as the presence of clay intraclasts. They were probably deposited on alluvial plains; transitional and distal to the alluvial fans of facies 1 to 9. Cross-bedding appears to be mostly planar. This is typical of transverse bars (Collinson, 1986).

Although clay intraclasts are preserved in facies 10 and 11, clay beds are very rare (one was observed in facies 7 strata in the Deilmann pit). Mudstone layers, such as those in facies 8 discussed above, are typically silt to fine sand, rather than the silty clay or clay of the intraclasts. The clay beds, from which the intraclasts are derived, presumably formed as suspension deposits during the later stages of flood events, but did not survive subsequent exposure and flooding.

The increase in clay intraclasts, which distinguishes the sandstones and gravelly sandstones of facies 11 from those of facies 10, may reflect an increase in clay supply to the basin, and hence increased chemical weathering and a change to a more humid climate. This is in accord with evidence for a long term change from arid to wetter conditions reported from detailed stratigraphic studies in the Sue pit at McClean Lake (Long *et al.,* this volume).

Fine to medium sandstone of facies 12 has much better sorting than the associated facies. This may reflect either a more distal depositional environment, or increased fluvial transport associated with seasonally persistent rivers in a wetter climate.

In general, facies 10 to 12 correspond to the Platte-type braided river model (Miall, 1978, 1992; Cant, 1982), although the improved sorting and reduced range of grain size typical of facies 12 may be closer to the Bijou Creek-type model (Miall, 1978, 1992; Cant, 1982). Sandy bedload-dominated, Platte-type rivers result from more steady discharge than Donjek- or Bijou Creek-types (Cant, 1982).

Eolian features (e.g. Ahlbrandt and Fryberger, 1982), such as those described by Rainbird and Hadlari (2000) in the Thelon Basin, and Ross (1983) in the Hornby Bay Basin, have not been recognized in the Manitou Falls Formation. This is perhaps surprising, given the evidence for semi-arid conditions (redbeds and ephemeral stream systems). A possible explanation is that the water table may have been too deep for eolian deposits to be preserved. The well-sorted sands of facies 12 may have undergone eolian re-working prior to deposition in a fluvial system.

Paleocurrents

In addition to paleocurrent measurements at the Deilmann pit and outcrops near Collins Creek, a successful attempt was made to measure cross-bed azimuths in RL-99, an inclined hole from the McArthur River area, using a goniometer constructed by P. Ramaekers. In this core, direction of transport shows little variation from top (azimuth 320°) to bottom (azimuth 325°). Data are summarized in attached sections. More such measurements would allow construction of a 3-D picture of paleocurrent variability in the basin. This would be a valuable compliment to the outcrop paleocurrent maps of Ramaekers (1981, 1990).

Paleo-aquifers

Basal Manitou Falls strata were deposited as linear valley fills, as observed in the Deilmann Pit (Harvey and Bethune, this volume) and on Transect B in the Collins Creek area. Ongoing DDH compilations will probably identify more of these. In contrast, overlying Manitou Falls strata are laterally extensive. Minter (1978) described a similar relationship in the Bird Formation of the Proterozoic Witwatersrand Basin in South Africa. There, the Vaal gold placer sandstones and conglomerates form linear bodies, overlain by sheet-like sands. A two-part paleo-aquifer system is thus developed. In the lower, linear system, diagenetic and mineralizing fluids were channeled and concentrated. In the upper, planar system, fluids would have been relatively dispersed. There was probably little vertical exchange between the upper and lower paleo-aquifers (Hoeve *et al.*, 1981). Valleys were most likely to develop on the least competent (and geochemically most reactive) underlying lithologies, the Wollaston Group graphitic pelites and psammopelites.

4. Conclusions

Preliminary studies in eastern Athabasca Basin show that Ramaekers' (1990) stratigraphy has held up well over the past two decades, but, as Ramaekers (1990) suggested, it is possible to further subdivide the Manitou Falls Formation. At least 12 distinctive facies are recognized. Revision of the stratigraphy will be deferred until we have a more complete picture.

Syndepositional tectonic activity, at least during early Manitou Falls time, is suggested by the local occurrence of facies 2 breccia, but more evidence is needed to prove this. Uranium deposits, as at McArthur River and McClean Lake, may be associated with such fault rejuvenation.

Redbeds develop in arid regions under conditions of alternate wetting and drying (Walker, 1967). Alternation of sands, gravelly sands, and conglomerates indicates episodic flooding. Preservation of a range of clast types in the lower part of the Manitou Falls suggests that chemical weathering and alteration was not an important factor in sediment breakdown until later. These features all suggest that conditions were arid to semi-arid in early Manitou Falls time.

The lowermost parts of the Manitou Falls are locally quite variable, while the upper parts (upper MFb, MFc, and MFd) are relatively uniform on a regional basis. This supports evidence from Key Lake, McClean Lake, Collins Creek area, and elsewhere that the initial Manitou Falls deposits were ribbon-like valley fills, whose orientation was controlled by basement topography (and structural grain), while overlying ones are extensive sheet-like bodies. If there has been little inter-stratal fluid movement in the basin, as argued by Hoeve *et al.* (1981), identification of the linear paleo-aquifers (i.e. paleo-valleys) is important for understanding and modelling paleohydrology and uranium mineralization in the basin.

Magnetite (and other heavy minerals) previously noted by Ramaekers (1979b) in the lower MFb in Rabbit Lake area is widespread in the eastern Athabasca Basin. Paleomagnetic investigation of magnetite-bearing strata may yield a more precise depositional age than that determined by Kotzer *et al.* (1992) from early diagenetic hematite.

5. Acknowledgments

This sub-project is part of EXTECH IV – a multidisciplinary study of the Athabasca Basin and its unconformity-related uranium deposits. It is jointly funded by Alberta Geological Survey, Cameco Corp., COGEMA Resources Inc., Geological Survey of Canada (Proposal Approval System and Targeted Geoscience Initiative), NSERC grants to Long and Hajnal, and Saskatchewan Energy and Mines (Northern Geological Survey). This sub-project addresses one of the priorities set by the EXTECH IV Steering Committee, with key support from Gary Delaney, Dan Brisbin, Philippe Portella, and Vlad Sopuck. In-kind support by personnel, accommodations and analytical facilities of these agencies and participating universities (Laurentian, Saskatchewan, and Regina) is also gratefully acknowledged.

We are grateful for logistic support from Cameco Corporation at Rabbit Lake, McArthur River, and Key Lake. Bill Wakabayushi welcomed and introduced us to the Key Lake–McArthur River operation. Larry Richardson, Brian McGill, and Greg Leniuk facilitated logistic support at McArthur River, made themselves available to discuss results and ideas as our work progressed, and pointed out useful sources of information. We thank Daniel Faure for permission to examine DF Exploration Uranium Ltd. core in the Hawkrock River area, and Rick Kusmirski and Les Beck for permission to examine JNR Resources Inc. core at Moore Lakes. Lee Dauphin and Jason Bishop of Cameco selected many of the cores examined in the Rabbit Lake–La Rocque Lake area. Shawn Barbe of Cameco provided valuable support during the investigation of the Deilmann Pit. Aaron Grimeau and Mandy Sarfi were cheerful and able field assistants. Brenda Obina, and Phillip Pretz provided enthusiastic assistance in the GSC office and laboratory. We thank Rob Rainbird, Gary Delaney, and Charlie Harper for thorough and constructive critical reviews of this paper.

6. References

Ahlbrandt, T.S. and Fryberger, S.G. (1982): Introduction to eolian deposits; *in* Scholle, P.A. and Spearing, D. (eds.), Sandstone Depositional Environments, Amer. Assoc. Pet. Geol., Mem. 31, p11-47.

Cant, D.J. (1982): Fluvial facies models and their application; *in* Scholle, P.A. and Spearing, D. (eds.), Sandstone Depositional Environments, Amer. Assoc. Petrol. Geol., Mem. 31, p115-137.

Collinson, J.D. (1986): Alluvial Sediments; *in* Reading, H.G. (ed.), Sedimentary Environments and Facies, 2nd edition, Blackwell Scientific, Oxford, p20-62.

Collinson, J.D. and Thompson, D.B. (1982): Sedimentary Structures; George Allen and Unwin, London, 194p.

Cumming, G.L., Krstic, D., and Wilson, J.A. (1987): Age of the Athabasca Group, northern Alberta; *in* Geol. Assoc. Can./Mineral. Assoc. Can., Prog. Abstr., v12, p35.

Hajnal, Z., Annesley, I.R., White, D., Mathews, R.B., Sopuck, V., Koch, R., Leppin, M., and Ahuja, S. (1997): Sedimentary-hosted mineral deposits: A high-resolution seismic survey in the Athabasca Basin; *in* Gubins, A.G. (ed.), Proceedings of Exploration 97: Fourth Decennial International Conference on Mineral Exploration, p421-432.

Harper, C.T. (1996): Geology of the Maurice Bay Area (NTS 74N-5 and part of 74N-12); Saskatchewan Geological Survey, Sask Energy Mines, Rep. 219, 27p.

Harvey, S. (1999): Structural geology of the Deilmann Orebody, Key Lake, Saskatchewan; *in* Summary of Investigations 1999, Volume 2, Saskatchewan Geological Survey, Sask. Energy Mines, Misc. Rep. 99-4.2, p100-109.

Heaman, L. (2000): Refining the measurement of time with U-Pb geochronology; Geolog, Geol. Assoc. Can., v29, p13.

Hiatt, E.E. and Kyser, T.K. (2000): Sequence stratigraphy of Paleoproterozoic sedimentary successions: The relationships between basin evolution, systems tracts, and paleohydrology in non-actualistic depositional systems; GeoCanada 2000, Calgary, May 2000, Conference CD, abstr. #697.

Hoeve, J. (1977): Uranium metallogenic studies: II Rabbit Lake, mineralogy and geochemistry; *in* Summary of Investigations 1977 by the Saskatchewan Geological Survey, Sask. Dep. Miner. Resour., p124-135.

Hoeve, J., Rawsthorne, K., and Quirt, D., (1981): Uranium metallogenic studies: Clay mineral stratigraphy and diagenesis in the Athabasca Group; *in* Summary of Investigations 1981, Saskatchewan Geological Survey, Sask. Miner. Resour., Misc. Rep. 81-4, p76-89.

Kotzer, T.G., Kyser, T.K., and Irving, E. (1992): Paleomagnetism and the evolution of fluids in the Proterozoic Athabasca Basin, northern Saskatchewan, Canada; Can. J. Earth Sci., v29, p1474-1491.

Kyser, K., Hiatt, E., Renac, C., Durocher, K., Holk, G., and Deckart, K. (2000): Chapter 10. Diagenetic fluids in Paleo- and Mesoproterozoic sedimentary basins and their implications for long protracted fluid histories; *in* Kyser, K. (ed.), Fluids and Basin Evolution, Miner. Assoc. Can., GeoCanada 2000, Short Course, v28, p225-262.

Lewis, D.W. and McConchie, D. (1994): Practical Sedimentology; Chapman and Hall, New York, 213p.

Macdonald, R. and Slimmon, W.L. (1999): Geological Map of Saskatchewan, Sask. Energy Mines, 1:1 000 000 scale.

McGill, B.D., Marlatt, J.L., Matthews, R.B., Sopuck, V.J., Homeniuk, L.A., and Hubregtse, J.J. (1993): The P2 North Uranium deposit, Saskatchewan, Canada; Explor. Min. Geol., Can. Inst. Min. Metall. Petrol., v2, no4, p321-331.

McNaughton, N.J., Rasmussen, B., and Fletcher, I.R. (1999): SHRIMP uranium-lead dating of diagenetic xenotime in siliciclastic sedimentary rocks; Sci., v285, p78-80.

Miall, A.D. (1978): Lithofacies types and vertical profile models in braided river deposits: A summary; *in* Miall, A.D. (ed.), Fluvial Sedimentology, Can. Soc. Petrol. Geol., Mem. 5, p597-604.

__________ (1992): Alluvial deposits; *in* Walker, R.G. and James, N.P. (eds.), Facies Models – Response to Sea Level Change, Geol. Assoc. Can., Geotext 1, p119-142.

Miller, A.R., Cumming, G.L., and Krstic, D. (1989): U-Pb, Pb-Pb, and K-Ar isotopic study and petrography of uraniferous phosphate-bearing rocks of the Thelon Formation, Dubwant Group, Northwest Territories, Canada; Can. J. Earth Sci., v26, p867-880.

Minter, W.E.L. (1978): A sedimentological synthesis of placer gold, uranium and pyrite concentrations in Proterozoic Witwatersrand sediments; *in* Miall, A.D. (ed.), Fluvial Sedimentology, Can. Soc. Petrol. Geol., Mem. 5, p801-829.

Nilsen, T.H. (1982): Alluvial fan deposits; *in* Scholle, P.A. and Spearing, D. (eds.), Sandstone Depositional Environments, Amer. Assoc. Petrol. Geol. Mem. 31, p49-86.

Pacquet, A. and McNamara, S. (1985): The study of the basal Athabasca succession in the D, E, L, F, and S areas of the Carswell Structure; *in* Laine, R., Alonso, D., and Svab, M. (eds.), The Carswell Structure Uranium Deposits, Saskatchewan, Geol. Assoc. Can., Spec. Pap. 29, p81-86.

Rainbird, R.H. and Hadlari, T. (2000): Revised stratigraphy and sedimentology of the Paleoproterozoic Dubawnt Supergroup at the northern margin of Baker Lake Basin, Nunavut; GSC Current Research D2000-C, 9p.

Ramaekers, P. (1976): Athabasca Formation, northeast edge (64L, 74I, 74P): Part I reconnaissance geology; *in* Summary of Investigations 1976 by the Saskatchewan Geological Survey, Sask. Dep. Miner. Resour., p73-77.

__________ (1977): Athabasca Formation, south-central edge (74G): Part I reconnaissance geology; *in* Summary of Investigations 1977 by the Saskatchewan Geological Survey, Sask. Dep. Miner. Resour., p157-163.

__________ (1978a): Reconnaissance geology of the interior Athabasca Basin; *in* Summary of Investigations 1978, Saskatchewan Geological Survey, Sask. Miner. Resour., Misc. Rep 78-4, p133-135.

__________ (1978b): Athabasca Formation, southwestern edge: Part I - Reconnaissance geology (NTS areas 74F, 74K); *in* Summary of Investigations 1978, Saskatchewan Geological Survey, Sask. Miner. Resour., Misc. Rep 78-4, p124-128.

__________ (1979a): Stratigraphy of the Athabasca Basin; *in* Summary of Investigations 1979, Saskatchewan Geological Survey, Sask. Miner. Resour., Misc. Rep. 79-4, p154-160.

__________ (1979b): Surface geology of the Athabasca Group, NEA-IAEA test area; *in* Summary of Investigations 1979, Saskatchewan Geological Survey, Sask. Miner. Resour., Misc. Rep. 79-4, p161.

__________ (1980): Stratigraphy and tectonic history of the Athabasca Group (Helikian) of northern Saskatchewan; *in* Summary of Investigations 1980, Saskatchewan Geological Survey, Sask. Miner. Resour., Misc. Rep 80-4., p99-106.

__________ (1981): Hudsonian and Helikian basins of the Athabasca region, northern Saskatchewan; *in* Campbell, F.H.A. (ed.), Proterozoic Basins of Canada, Geol. Surv. Can., Pap. 81-10, p219-233.

__________ (1990): Geology of the Athabasca Group (Helikian) in Northern Saskatchewan; Sask. Energy Mines, Rep. 195, 49p.

Ross, G.M. (1983): Proterozoic aeolian quartz arenites from the Hornby Bay Group, Northwest Territories, Canada: Implications for Precambrian aeolian processes; Precamb. Resear., v20, p149-160.

Stern, R.A. (2000): Rapid contextual U-Pb geochronology at the micron scale using the SHRIMP: Good things also come in large packages; Geolog, Geol. Assoc. Can., v29, p13.

Tremblay, L.P. (1982): Geology of the Uranium Deposits related to the Sub-Athabasca Unconformity, Saskatchewan; Geol. Surv. Can., Pap. 81-20, 56p.

Walker, T.R. (1967): Formation of red beds in ancient and modern deserts; Bull. Geol. Soc. Amer., v78, p353-368.

Architecture and Origin of Fluvial Facies in the Athabasca Group at McClean Lake, Northern Saskatchewan

Darrel Long [1], Cathy Williamson [2], Phillipe Portella [3], and Steve Wilson [3]

Long, D., Williamson, C., Portella, P., and Wilson, S. (2000): Architecture and origin of fluvial facies in the Athabasca Group at McClean Lake, northern Saskatchewan; *in* Summary of Investigations 2000, Volume 2, Saskatchewan Geological Survey, Sask. Energy Mines, Misc. Rep. 2000-4.2

Abstract

Initial investigations into the character of basal strata of the Athabasca Group in COGEMA Resources Inc. Sue Pit, near the eastern margin of the Athabasca Basin indicate the presence of two distinct formations deposited under different climatic conditions. Lowermost strata consist predominantly of fine- to very coarse-grained sandstones with minor discontinuous cobble and boulder conglomerates and rare mudstones, and rest on a highly irregular unconformity developed on metamorphosed Hudsonian basement. Well-rounded clasts in the coarser conglomerates are all of local origin. These conglomerates and associated abundant massive and plane laminated sandstones in the basal member appear to have been deposited by sheet-flood and stream-flood processes in an arid to hyper-arid climatic setting. Overlying strata are predominantly coarse- to very coarse-grained sandstones with abundant cross-stratification and minor granules and small pebble conglomerates. These appear to have been deposited on a braidplain formed by semi-ephemeral or perennial braided rivers under more humid conditions. The contact between the two members is a stepped erosional surface, which is well represented in the core and in exposures within the pit. This surface represents development of an incised river system associated with the inferred climatic change.

1. Introduction

This sub-project of the Athabasca Uranium EXTECH IV project aims to complement a regional stratigraphic analysis (Ramaekers, 1990; Yeo *et al.*, this volume) by providing a link between drill core and geophysical studies and open pit/outcrop characteristics of the Athabasca Group.

In order to improve understanding of the stratigraphic framework and architecture of the group, it is essential to document its lithology, sedimentology, and detailed facies relationships. The best places to make such observations are at those deposits that have been, or are being, mined as open pits (e.g. Rabbit, McClean, Key, and Cluff lakes). Areas of relatively good exposure (e.g. southeast of Black Lake, Carswell Structure) will also be examined.

2. Three Year Plan

Work will be continued in cooperation with industry, Saskatchewan Energy and Mines, and the Geological Survey of Canada (Yeo *et al.*, this volume). Work in 2000-01 consisted of facies architecture analysis of the Sue Pit at McClean Lake and compilation and synthesis of relevant DDH core descriptions, and geophysical information. Investigations at Cluff Lake will coincide with Yeo's work there in 2001-02. B.Sc. and M.Sc. students will be involved in these projects.

3. New Observations

In order to understand the architecture of the basal strata at the McClean Lake Sue C Pit, architectural models were established on three accessible faces at the south end of the pit (adjacent to ramps or platforms). Observations were plotted directly on a series of overlapping instant photographs. Due to the instability of the pit walls, direct observations were limited to the lower two metres of exposure. In addition to these observations, twelve cores from closely spaced (10 to 20 m) boreholes were examined in order to fully document lithotypes within the pit and to allow direct comparison with temporary surface exposures in the pit.

Highly deformed, metamorphosed, and diagenetically altered basement rocks include coarse recrystallized "quartzite", metasediments including graphitic varieties, and pegmatitic intrusions. The "quartzites" may not have had a sedimentary protolith as they consist of an interlocking framework consisting of 70 to 90%, 4 to 8 mm crystals of polygonized and strained quartz, and 10 to 30% muscovite or kaolin. They may represent a "quartzite" or metamorphosed quartz-rich pegmatite. All the basement rocks show signs of intense diagenetic and possibly hydrothermal alteration (c.f. Kyser, 2000). Clay-filled fractures in the upper few metres of the formation may reflect development of deep weathering profiles (Figure 1, left).

---

[1] Department of Earth Sciences, Laurentian University, 935 Ramsey Lake Road, Sudbury, ON P3E 2C6; E-mail: dlong@nickel.laurentian.ca
[2] Department of Geology, University of Regina, Regina, SK S4S 0A2.
[3] COGEMA Resources Inc., 817 - 825 45th Street West, Saskatoon, SK S7K 3X5.

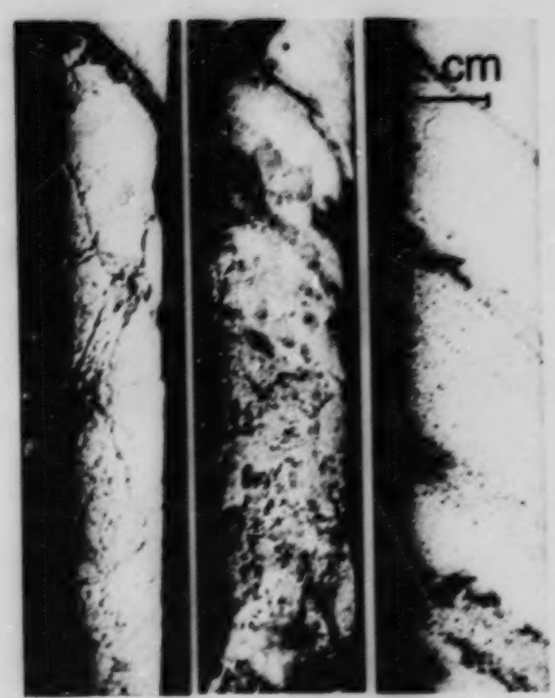

***Figure 1 - Left:** Brecciated "quartzite", with clay-filled seams, reflecting deep-weathering of the basement.*
***Center:** Detail of contact between large brecciated clast of "quartzite" (lower half) in a local basal conglomerate and massive to planar-stratified small pebble conglomerate and medium-grained sandstone in the lower member.*
***Right:** Detail of thin cosets of laminated medium- to coarse-grained sandstone of possible sheet-flood origin. Note minor concentration of coarse material between cosets.*

The contact between the basal strata (Manitou Falls Formation of Ramaekers, 1990) of the Athabasca Group and the basement rocks is an irregular unconformity with local slopes of 30° to 45° (Figure 2). Boulder and cobble conglomerates are present locally at the base of the formation and at higher levels within the lower member in proximity to basement highs (Figure 3). Most have very limited lateral continuity, and thin and fine away from basement highs. Clasts are predominantly "quartzite" of apparent local origin and are typically well rounded, although some show evidence of *in situ* brecciation (Figure 1, center). Matrix within the conglomerates is of medium to coarse sand grade, and locally shows evidence of draped stratification, with rare mudstone laminae.

Strata in the basal member are dominated by pink, moderately well-sorted to poorly sorted , medium- to coarse-grained sandstones, with minor granule and small pebble conglomerates. Most beds appear massive or weakly laminated (Figure 1, right; Figure 4) in composite sets 2 to 4 cm thick, which may be graded. Planar and trough cross-stratification is rare, as is ripple cross lamination. Beds appear to be laterally continuous for more than 20 m. Isolated, well-rounded "quartzite" clasts, of large pebble and cobble grade commonly rest on erosive surfaces at 1 to 3 m intervals.

The upper member of the sequence exposed in the Sue Pit (Manitou Falls Formation of Ramaekers, 1990) rests with an erosional discontinuity on strata within the lower member (Figure 2). Strata are predominantly medium to very coarse sandstones with minor granule

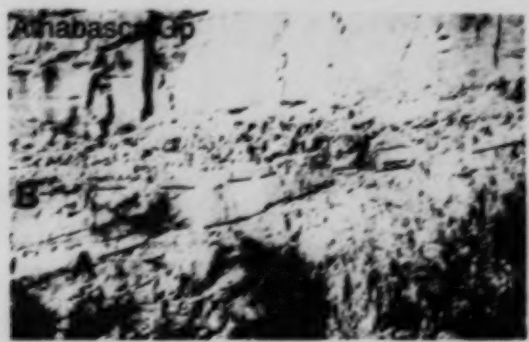

***Figure 2** - Basal contact (A) of predominantly flat laminated, medium- to coarse-grained sandstones of the basal unit of the Athabasca Group in the southwest wall of the Sue Pit, McClean Lake. Note that strata above the unconformity are truncated by the base of the upper unit (at B) which is dominated by coarse and very coarse cross-stratified sandstone. Note local absence of conglomerates at the base of this sequence.*

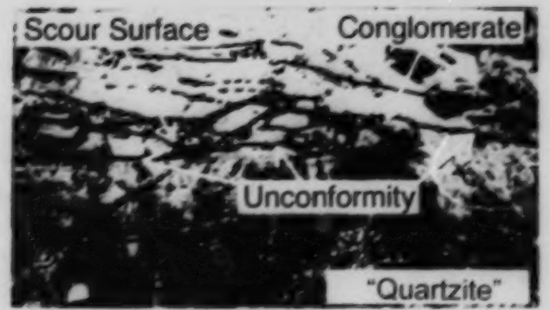

***Figure 3** - Annotated field photograph showing a 2 m wide, 35 cm thick lens of cobble conglomerate. This appears to have developed on and adjacent to the basement high during deposition of the lower member. Note inclined fractures in the "quartzite" that give the rock the appearance of a bedded quartzite.*

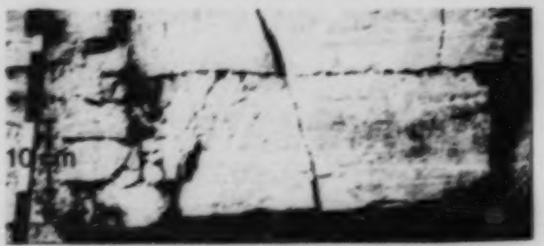

***Figure 4** - Thin cosets of thick plane-laminated, medium-grained sandstone in surface exposure of the lower member in the Sue Pit.*

conglomerates and granular very coarse-grained sandstones. Coarser grained conglomerates were not observed in the pit or in cores. Most of the sandstone appears to be massive or is characterized by planar or trough cross-stratification (Figures 5 and 6). Lateral continuity of beds is high (>100 m). No consistent cyclic fining, thinning, or coarsening upwards sequences were observed (Figure 7).

4. Sedimentology

Strata exposed in the Sue Pit are best explained by deposition in ephemeral to semi-permanent braidplain systems in hyper arid to semi-humid conditions. Specific interpretations are outlined below.

a) Basement and Lower Member

The presence of clay-filled fractures and enhanced alteration of deformed Hudsonian basement rocks beneath strata of the Athabasca Group suggest intense weathering during development of a sub-mature topographic surface. The probable local origin of well-rounded, and in part fractured "quartzite" clasts in the conglomerates suggests minimal transport distances from basement highs (inselbergs), with rounding caused by combined hydration and thermal spalling in an arid to hyper-arid climate. Minor stratified matrix in conglomerates at the base of the sequence suggests they were deposited as residual open-work gravel, with voids filled by later depositional events (i.e. sieve deposits: Bull, 1972).

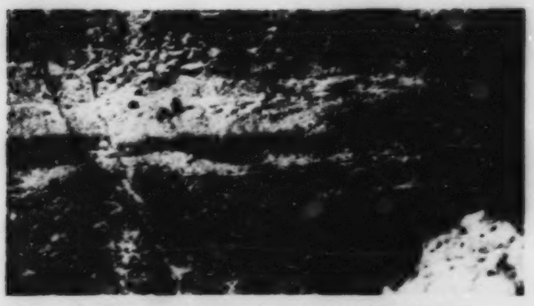

Figure 5 - Planar and trough cross-stratified coarse grained sandstone in the upper member of the sequence, adjacent to the ramp at the southeast end of Sue Pit. Field of view is approximately 20 cm.

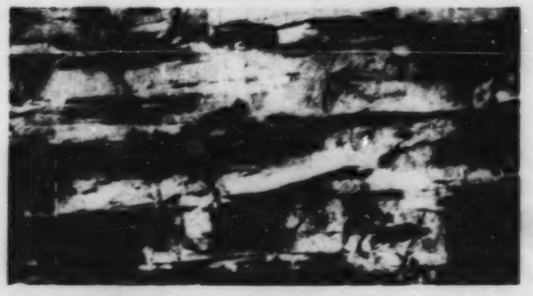

Figure 6 - Planar and trough cross-stratified sandstones in the upper member. Note discontinuous hematite staining along strike. Scale divisions on staff are 10 cm.

The predominance of flat laminated and massive sandstone in the lower member is suggestive of deposition by superimposed ephemeral sheet-flood and sheet-wash processes in the terminal parts of an arid to hyper-arid braidplain. (c.f. Williams, 1971; Frostick and Reid, 1977; Stear, 1985; Abdullatif, 1989; Tooth, 1999).

Thin sets of flat-laminated sandstones associated with planar and trough cross-stratified sets are common in modern and ancient fluvial deposits where they are typically interpreted as the rarely preserved products of deposition under upper flow regime conditions (Williams, 1971; Frostick and Reid, 1977). The presence of extensive stacked sets of apparently flat laminated sandstones, in the absence of interbedded cross-stratified sands is not typical of modern river deposits and may represent a distinctive pre-vegetative fluvial style produced by sheet-floods or stream-floods (c.f. Eriksson *et al.*, 1993; Bhattacharyya and Morad, 1993; Hjellbakk, 1993, 1997; Sønderholm and Tirsgaard, 1998; Tirsgaard and Øxnevad, 1998). The presence of rare parting lineations means that this facies could easily be confused with beach-face deposits. The absence of water-escape structures in the associated massive sets, combined with the lack of high-relief scour on basal contacts indicates that these were not produced by hyper-concentrated flow mechanisms as has been suggested for massive type sheet sandstones in Phanerozoic braided stream deposits by Martin and Turner (1998) and Proterozoic stream deposits by Røe and Hermansen (1993).

Thin cosets of massive to laminated strata (Figure 4) are analogous to deposits of Bijou Creek-type rivers (Miall, 1978). The type example of this highly ephemeral river type is characterized by flashy discharge and, due to source area characteristics, a lack of gravel. Plane lamination may develop under upper flow regime (sheet-wash) conditions, with a rare cap of mudstone (often removed by aeolian activity) reflecting waning flow conditions. Coarser grained laminae between cosets may reflect development of aeolian deflation lags, although direct evidence of aeolian deposition, such as adhesion ripples, warts, and coarsening upwards laminae (Ross, 1983; Tirsgaard and Øxnevad, 1998) were not seen.

The presence of isolated large pebbles and cobbles on scour surfaces at 1 to 3 m intervals throughout the lower member suggests occasional high energy sheet-flood events followed by periods of fluvial or aeolian deflation.

Thin intervals with medium-scale cross-beds and ripples suggest that some floods may have become channelized, with deposition in shallow fully turbulent ephemeral streams under lower flow-regime conditions.

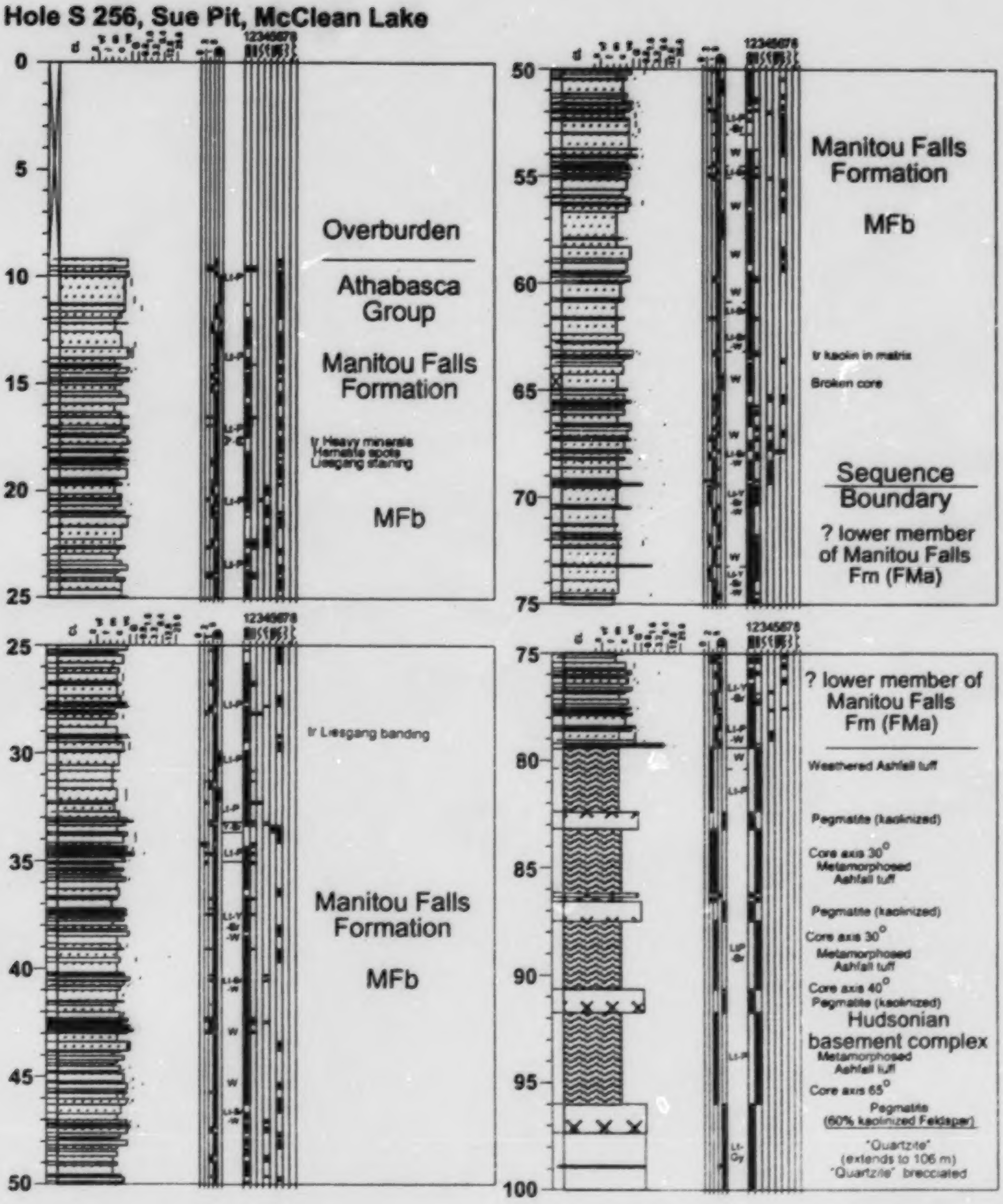

Figure 7 - Log of typical core from the Sue Pit, showing nature of contacts (First column: solid line, sharp contact; dash, transitional), median grain size (second column: deviations to right indicate coarse grained; scale at top is in phi divisions for sand and gravel grade material. Isolated bars to right of column indicate maximum grain size). Next five columns indicate median bed thickness in centimetres (0 to 0.2 cm, thin laminated; 0.2 to 1 cm, thick laminated; 1 to 5 cm, thin bedded; 5 to 60 cm, medium bedded; >60 cm, thick bedded). Letters in next column indicate colour (Lt, light; Gy, grey; W, white; Y, yellow; Br, brown; P, pink; and R, red). Next eight columns indicate apparent sedimentary structures (1, massive or indistinct; 2, plane bedding; 3, wavy ripple lamination; 4, ripple cross-stratification; 5, trough cross-stratification; 6, planar cross-bedding; 7, sedimentary intraclasts; and 8, desiccation cracks).

B

b) Upper Member

Architectural analysis (in progress) indicates the presence of a stepped erosion surface at the base of the (0 to 14 m thick) upper member. This surface truncates laminae sets in the lower member suggesting burial compaction of the sequence by tens to hundreds of metres of sandstones, prior to development of an incised valley system.

Medium-scale planar and, to a lesser extent, trough cross-stratified sandstones in the upper member reflect migration of straight and sinuous crested bedforms in shallow semi-ephemeral to perennial sandy braidplain systems (Long, 1978, 2000; Crowley, 1983; Roe and Hermansen, 1993; Miall, 1996). The sheet-like character of the sandstones, combined with the thickness of cross-stratification and apparent absence of sequences of bedforms and complex large-scale bed configurations (macroforms) indicates deposition in streams rarely more than a metre deep, and probably several hundreds to thousands of metres wide (c.f. Schumm, 1968; Long, 1978, 2000; Fuller, 1985; Martins-Neto, 1994).

5. Conclusions

Examination of the Athabasca Group exposed in the Sue Pit indicates initial deposition of flash-flood dominated strata in an arid to hyper-arid climatic regime predominantly by sheet-flood processes. The characteristics of modern flash-floods, including sheetwash (broad flows, a few centimetres thick), sheet-floods (several kilometres wide and 4 to 60 cm deep), and stream-floods (less than 1.5 m deep and up to 4.8 km wide) are poorly understood due to lack of direct measurements (Hogg, 1982; Graf, 1988). In modern dry land river settings, the presence of sparse to dense vegetation tends to break up sheet flows to produce turbulent flows in rills and small channels (Graf, 1988). Due to the absence of vascular plants, this would not be the case in Proterozoic settings, even in semi-humid to humid environments, hence upper flow regime deposits from sheet-floods might be expected to be more common. In terminal fluvial systems, rapid water infiltration should lead to increased sediment concentrations in the flows, resulting in deposition of massive beds, or beds with poorly defined lamination (Hjellbakk, 1993).

The absence of identifiable aeolian deposits in these and other Proterozoic fluvial deposits is enigmatic (Ross, 1983; Eriksson *et al.*, 1998). Tirsgaard and Øxnevad (1998) have suggested that this may be a function of preservation due to the position of the groundwater table which would have been too low in arid and semi-arid conditions to allow preservation of aeolian deposits. They suggest that optimal conditions for preservation occur in semi-ephemeral systems, in more humid settings, where a seasonally high water table is combined with preservation space created by subsidence.

Deposition of the lower member was followed by deposition from more substantial semi-ephemeral to perennial streams in a humid climatic setting. The change in depositional style was marked by significant erosion of the lower member, with development of an incised valley system. Preservation of relief on this major sequence boundary suggests partial consolidation, perhaps combined with the development of early diagenetic cements over a period of several thousand years.

The incised valley system was quickly buried beneath an extensive blanket of sheet-like fluvial deposits, characterized by broad, shallow braided channels dominated by transverse bedforms. Absence of aeolian bedforms in this setting may be related to low preservation potential as such deposits would be subject to erosion during flood events.

Strata along the eastern margin of the Athabasca Basin have been correlated with the Manitou Falls Formation by Ramaekers (1990). The presence of a major sequence boundary at the contact of the upper and lower members in the Sue Pit may indicate previously unsuspected local preservation of a remnant of the MFa member of the Manitou Falls Formation or an equivalent of the stratigraphically older Fair Point Formation.

The absence of extensive conglomerates in the upper member, combined with a lack of abundant mudstone intraclasts, suggests that these correlate with the MFb member of the Manitou Falls Formation, which Ramaekers (1990) shows to have overstepped the MFa member, and typically forms the oldest strata along the eastern margin of the basin.

6. Acknowledgments

This sub-project is funded in part by an NSERC grant to Dr. Darrel Long. Costs were shared by the Geological Survey of Canada, Saskatchewan Energy and Mines, Cameco Corporation, and COGEMA Resources Inc. for students and logistics. Accommodation at McClean Lake was provided by COGEMA Resources Inc.

7. References

Abdullatif, O.M. (1989): Channel-fill and sheet-flood facies sequences in the ephemeral terminal river Gash, Kassala, Sudan; Sed. Geol., v63, p171-184.

Bhattacharyya, A. and Morad, S. (1993): Proterozoic braided ephemeral fluvial deposits; an example from the Dhandraul Sandstone Formation of the Kaimur Group, Son Valley, central India; Sed. Geol., v84, p101-114.

Bull, W.B. (1972): Recognition of alluvial-fan deposits in the stratigraphic record; *in* Rigby, J.K. and Hamblin, W.K. (eds.), Recognition of ancient sedimentary environments, Soc. Econ. Paleontol. Mineral., Spec. Publ. 16, p63-83.

Crowley, K.D. (1983): Large-scale bed configurations (macroforms), Platte River Basin, Colorado and Nebraska: Primary structures and formative processes; Geol. Soc. Amer. Bull., v94, p117-133.

Eriksson, P.G., Condie, K.C., Tirsgaard, H., Mueller, W.U., Altermann, W., Miall, A.D., Aspler, L.A., Catuneanu, O., and Chiarenzelli, J.R. (1998): Precambrian clastic sedimentation systems; Sed. Geol., v120, p5-53.

Eriksson, P.G., Schreiber, U.M., van der Neut, M., Labuschagne, H., van der Schyff, W., and Potgieter, G. (1993): Alternative marine and fluvial models for the non-fossiliferous quartzitic sandstones of the Early Proterozoic Daspoot Formation, Transvaal Sequence of southern Africa; J. African Earth Sci., v16, p355-366.

Frostick, L.E. and Reid, I. (1977): The origin of horizontal laminae in ephemeral stream channel fill; Sediment., v24, p1-9.

Fuller, A.O. (1985): A contribution to the conceptual modeling of pre-Devonian fluvial systems; Trans. Geol. Soc. S. Africa, v88, p189-194.

Graf, W.L. (1988): Fluvial Processes in Dryland Rivers; Springer-Verlag, Berlin, 346p.

Hjellbakk, A. (1993): A 'flash-flood' dominated braid delta in the upper Proterozoic Næ ringselva Member, Varanger Peninsula, northern Norway; Norsk. Geolgisk Tidsskrift, v73, p63-80.

__________ (1997): Facies and fluvial architecture of a high-energy braided river: The Upper Proterozoic Seglodden Member, Varanger Penninsular, northern Norway; Sed. Geol., v114, p131-161.

Hogg, S.E. (1982): Sheetfloods, sheetwash, sheetflow, or –?; Earth Sci. Rev., v18, p56-76.

Kyser, K. (2000): Fluids and basin evolution; Mineral. Assoc. Can., Short Course Series, No.28, 262p.

Long, D.G.F. (1978): Proterozoic stream deposits: Some problems of recognition and interpretation of ancient sandy fluvial systems; *in* Miall, A.D. (ed.), Fluvial Sedimentology, Can. Soc. Petrol. Geol., Mem. 5, p313-341.

__________ (2000): Architecture of Proterozoic sand-dominated fluvial systems; GeoCanada 2000, Calgary, May 2000, Conference CD, ext. abstr. #342.

Martin, C.A.L. and Turner, B.R. (1998): Origins of massive-type sandstones in braided river systems; Earth Sci. Rev., v44, p15-38.

Martins-Neto, M.A. (1994): Braidplain sedimentation in a Proterozoic rift basin: The São João da Chapada Formation, southeastern Brazil; Sed. Geol., v89, p219-239.

Miall, A.D. (1978): Lithofacies types and vertical profile models in braided river deposits: A summary; *in* Miall, A.D. (ed.), Fluvial Sedimentology, Can. Soc. Petrol. Geol., Mem. 5, p597-604.

__________ (1996): The Geology of Fluvial Deposits: Sedimentary Facies, Basin Analysis, and Petroleum Geology; Springer-Verlag, Berlin, 582p.

Ramaekers, P. (1990): Geology of the Athabasca Group (Helikian) in Northern Saskatchewan; Sask. Energy Mines, Rep. 195, 49p.

Røe, S.L. and Hermansen, M. (1993): Processes and products of large, Late Precambrian sandy rivers in northern Norway; Int. Assoc. Sediment., Spec. Publ. No. 17, p151-166.

Ross, G.M. (1983): Proterozoic aeolian quartz arenites from the Hornby Bay Group, Northwest Territories, Canada: Implications for Precambrian aeolian processes; Precamb. Resear., v20, p149-160.

Schumm, S.A. (1968): Speculations concerning paleohydrologic controls of terrestrial sedimentation; Geol. Soc. Amer. Bull., v79, p1573-1588.

Sønderholm, M. and Tirsgaard, H. (1998): Proterozoic fluvial styles: Response to base-level changes and climate (Rivieradal sandstone, eastern North Greenland); Sed. Geol., v120, p257-274.

Stear, W.O. (1985): Comparison of the bedform distribution and dynamics of modern and ancient sandy ephemeral flood deposits in the southwestern Karoo Region, South Africa; Sed. Geol., v45, p209-230.

Tirsgaard, H. and Oxnevad, I.E.I. (1998): Preservation of pre-vegetational mixed fluvio-aeolian deposits in a humid climatic setting: An example from the Middle Proterozoic Rriksfjord Formation, southwest Greenland; Sed. Geol., v120, p295-317.

Tooth, S. (1999): Floodouts in central Australia; *in* Miller, A.J. and Gupta, A. (eds.), Varieties of Fluvial Form, John Wiley and Sons Ltd., Chichester, p219-247.

Williams, G.E. (1971): Flood deposits of the sand-bed ephemeral streams of central Australia; Sediment., v17, p1-40.

Structural Setting of the Sue C Uranium Deposit, McClean Lake Mine, Northern Saskatchewan

Ghislain Tourigny, Steve Wilson [1], Guy Breton [1], and Philippe Portella [1]

Tourigny, G., Wilson, S., Breton, G., and Portella, P. (2000): Structural setting of the Sue C uranium deposit, McClean Lake mine, northern Saskatchewan; *in* Summary of Investigations 2000, Volume 2, Saskatchewan Geological Survey, Sask. Energy Mines, Misc. Rep. 2000-4.2.

Abstract

The Sue C deposit is a structurally controlled, basement-hosted, high-grade uranium deposit located at the eastern edge of the Athabasca Basin of northern Saskatchewan. Strongly foliated and lineated metamorphic tectonites exposed in the pit display evidence of a complex structural evolution involving three main pre-mineralization ductile deformational events. The earliest deformation, D1, produced a flat-lying bedding-parallel foliation, S1, and two styles of folds due to a single progressive deformation. Primary lithological contacts have been folded by east-west-trending F1a folds. F1b folds are defined by folding of the S0-S1 surfaces and represent recumbent, concentric flexures associated with flat-lying thrust slices. The F1b flexures are observed in thin sheets of well-foliated gneiss and represent detached structures analoguous to rootless folds encountered in décollement thrust-fold assemblages. The D1 bulk strain records evidence of an early nappe–teconic event pre-dating ore emplacement.

The D2 generation of structures is chiefly characterized by the development of a moderately to steeply dipping, north-northeast- to northeast-trending S2 foliation with associated F2 folds. The early D1 structures are clearly refolded about north-northeast- to northeast-trending overturned to upright structures (folds). Steeply plunging mineral extension lineations observed on S2 surfaces recorded a subvertical transport direction during D2 deformation.

D3 deformation formed an east-west-trending fracture/crenulation cleavage axial planar to minor, open buckle folds that slightly distorted and reoriented D1 and D2 structures.

A late phase of compressional deformation (late to post-D3) is responsible for the development of major north-northeast- to northeast-trending, west-verging thrust faults developed parallel to the pervasive S2 foliation. These faults follow the trace of Aphebian graphitic clay-rich gneisses (Wollaston Group) observed on the western limb of the Collins Bay Dome.

Post-Athabasca deformation involves reactivation of late Hudsonian north-northeast- to northeast-trending faults as west-verging subvertical reverse faults and localized normal displacement. Uranium mineralization is essentially located within the prominent thrust fault system and appears controlled by ductile structures inherited from the pre-existing ductile deformation.

Northeast-southwest and northwest-southeast conjugate normal faults, minor strike-slip faults and a set of subhorizontal thrust faults are the youngest structures developed in the mine sequence.

1. Introduction

The Sue C deposit is a structurally controlled, basement-hosted, high-grade uranium deposit located at the eastern edge of the Athabasca Basin in northern Saskatchewan (Figure 1; Baudemont *et al.*, 1993). The deposit, discovered in 1989, is one of a cluster of uranium deposits spatially related to the unconformity separating the Helikian Athabasca Group sandstone from the underlying metasediments of the Paleoproterozoic Wollaston Group. The Sue C mineralization is located in a north-northeast-trending anastomosing deformation zone straddling the lithological contact between the Archean Collins Bay granitic dome and the Aphebian Wollaston Group metasediments (Baudemont *et al.*, 1993). This major fault zone is of great economic importance since it contains several lenses of uranium mineralization designated Sue A, Sue B, Sue C, Sue D, and Sue E.

In their previous detailed studies of drill core, Baudemont *et al.* (1993) and Baudemont and Pacquet (1996), illustrated the importance of ductile and brittle structural elements to the internal geometry of ore lenses as well as to the spatial distribution of uranium concentrations in these deposits. Recent open-pit exploitation of the Sue C deposit has produced newly exposed outcrops which have provided additional information on the structural setting of the Sue C deposit, and on the geometry of the deformation corridor hosting this typical basement-type uranium mineralization. A detailed structural study of this deposit was undertaken as a part of the EXTECH IV - Athabasca Uranium Project. This paper presents the initial results of this study and is based on detailed 1:100 scale structural mapping carried out between June and August 2000 of all open-pit exposures then avalaible. Most of our observations are from the west

---

[1] COGEMA Resources Inc., 817 - 825 45th Street West, Saskatoon, SK S7K 3X5.

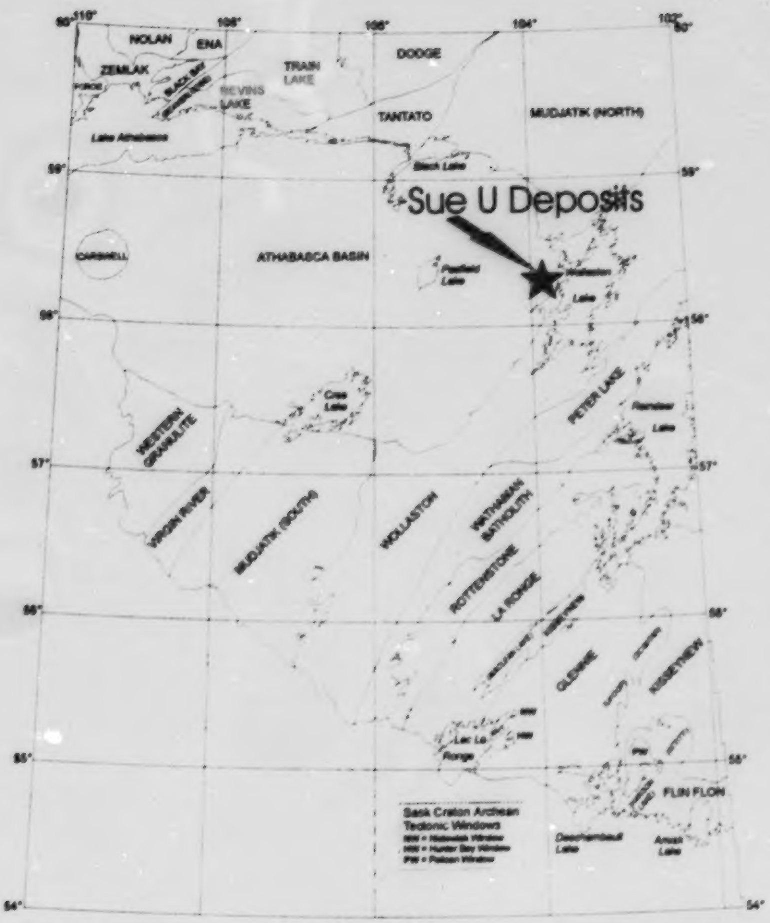
Sue U Deposits
NOLAN
ENA
ZEMLAK
TRAIN LAKE
BEVINS LAKE
DODGE
TANTATO
MUDJATIK (NORTH)
Lake Athabasca
Black Lake
CARSWELL
ATHABASCA BASIN
Cree Lake
PETER LAKE
Reindeer Lake
WESTERN GRANULITE
VIRGIN RIVER
MUDJATIK (SOUTH)
WOLLASTON
WATHAMAN BATHOLITH
ROTTENSTONE
LA RONGE
GLENNIE
KISSEYNEW
Lac La Ronge
FLIN FLON
Sask Craton Archean Tectonic Windows
Deschambault Lake
Amisk Lake
110°
108°
106°
104°
102°
60°
59°
58°
57°
56°
55°
54°

Figure 1 - Lithostructural subdivision of northern Saskatchewan and location of the Sue uranium deposits.

wall of the deposit where complexly deformed basement rocks have provided important information on the internal geometry and tectonic history of the host rock sequence. The present study shows that three main ductile deformational events predated mineralization, which might have been related to reactivation of previously developed deeply seated ductile faults.

2. Regional Setting and Property Geology

The Sue uranium deposits are located approximately 8.3 km northwest of the Rabbit Lake Mine and 2.5 km east of the McClean Lake uranium deposit (Figure 2). The regional geology of this area has been described by a number of authors and is briefly summerized here (see Wallis *et al.*, 1983; Baudemont *et al.*, 1993).

The property is situated in the central part of the Hearne Province (Hoffman, 1990) and straddles the transition zone between the Mudjatik Domain to the west and the Wollaston Domain to the east (Lewry and Sibbald, 1979). This transitional structural boundary represents the curvilinear deformation front of a foreland fold and thrust belt related to the Trans-Hudson Orogen (Portella and Annesley, 2000).

The outstanding geologic feature of the area is the presence of circular to elongate Archean granitic domes exposed in large antiformal structures (Figure 2). The domes comprise rocks ranging from granitoids in the core to foliated granitoids, gneissic rocks, and migmatites on the margins (Baudemont *et al.*, 1993). They are unconformably overlain by thin units of polydeformed Aphebian paragneissic rocks of the Wollaston Group (Figure 2).

The Wollaston Group comprises a lower package of arkose, quartzite, pelite, and graphitic gneiss interlayered with calc-silicate and minor marble (Sibbald, 1983). This Early Proterozoic metamorphic sequence is constrained by a 2075 ±2 Ma age from an inferred rift-related quartz-feldspar porphyry intruding basal rift-fill rocks of the Courtenay Lake–Cairns Lake fold belt at the base of the Wollaston Group (Ansdell *et al.*, 2000), and is intruded by ca. 1930 Ma pegmatitic granite (Annesley *et al.*, 1997). The main regional foliation strikes north-northeast to northeast, dips steeply east, and is intense with predominant down-dip mineral tectonic stretching lineations. Prograde metamorphic assemblages are typical of the regional high-T/low-P upper amphibolite facies.

The basement is unconformably overlain by the unmetamorphosed Helikian Athabasca Group, comprising clay-rich sandstone, mudstone, and siltstone with minor conglomerate (Ramaekers, 1990). Bray *et al.* (1987) used Ar/Ar and K/Ar techniques to determine minimum dates of 1484 ±55 and 1459 ±4 Ma for interstitial and sedimentary-layer illites, 1482 ±49 and 1453 ±49 Ma for regolithic illite, and 1319 ±3 Ma for illite derived by alteration at the McClean Lake deposits.

Both the metamorphosed basement rocks and the Athabasca Group have been intruded by late, northwest-trending Mackenzie diabase dykes which were introduced at approximately 1267 ±2 Ma (Slimmon, 1996).

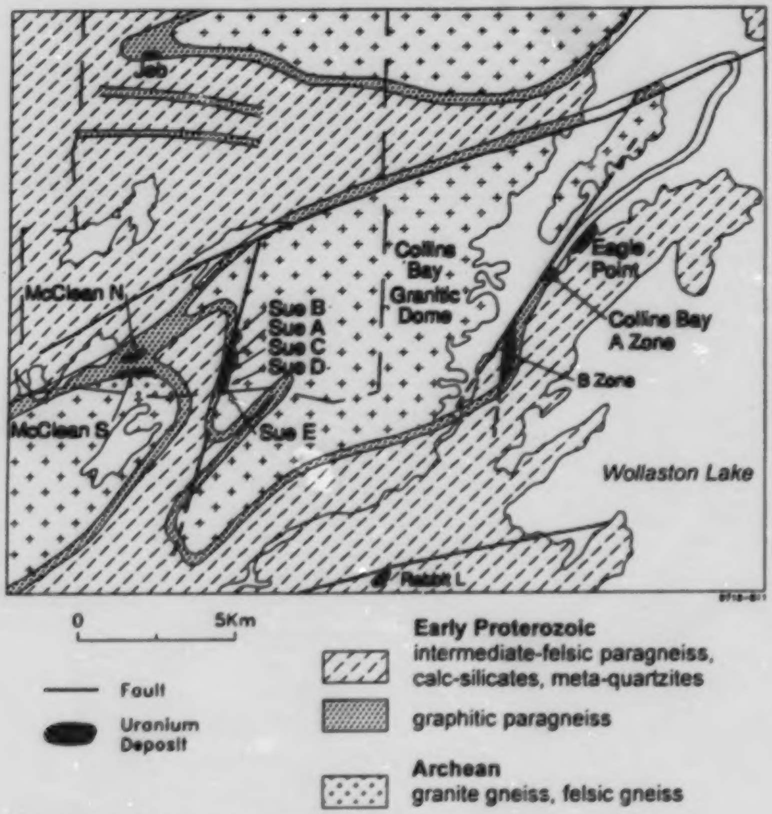

Figure 2 - General geology of the McClean Lake area showing the location of uranium deposits (from Baudemont and Pacquet, 1996).

North-northeast- and north-trending subvertical ductile and brittle-ductile faults zones, typically localized at the contact between the Collins Bay granitic dome and Wollaston Group graphitic paragneisses, are among the dominant structural features of the district (Figure 2). These graphitic structural discontinuities are excellent geophysical conductors and are considered one of the most reliable exploration guidelines at a regional scale. North-northeast- and northeast-trending faults are directly associated with hydrothermal activity and high-grade uranium mineralization.

The youngest tectonic structures are represented by northeast- and northwest-trending brittle faults that show a complex kinematic history involving strike-slip and/or extensional and/or compressional components of displacement. These structures have only minor geometric influence on the spatial distribution of rock types.

The uranium mineralization is essentially found on the western limb of the Collins Bay granitic dome where the distribution of highly strained rocks defined a wide deformational corridor called the Sue Trend (Figure 3). The rocks of this high-strain zone are cut by several minor and major ductile and brittle faults, several of which extend upwards into the Athabasca sandstone and induce variable-sized offsets of the unconformity (Baudemont *et al.*, 1993). The economic uranium mineralization is limited to two subparallel north-northeast-trending zones of graphitic paragneiss, which are up to about 25 m wide and marked by intense hydrothermal alteration. The Sue C and D basement-hosted mineralization is associated with the western graphitic unit; the eastern fault zone hosts the Sue A and B sandstone-unconformity mineralization. Sue E is located in the southern part of the Sue Trend at the junction of these two anastomosing deformation zones. Table 1 summarizes proven ore reserves for the Sue A, B, and C orebodies.

The geometric configuration of the orebodies appears largely controlled by the pervasive north-trending tectonic fabric and the regional structural elements that prevailed within the graphitic fault zones. The economic zones are north-northeast-trending and vary from subvertical to steeply east- or west-dipping. All of these lenses are pencil shaped and plunge 10° to 15° southward. This pitch angle is almost perpendicular to the extension lineation measured in adjacent rocks, but is at a very low angle to fold axes observed in the structural footwall of the Sue C deposit.

The present production at McClean Lake Mine is entirely from the Sue C deposit which represents more than 85% of the total reserves at the Sue deposits. The Sue C orebody is found at an average depth of 76 m and is unconformably overlain by ~68 m of Athabasca sandstone and 8 m of glacial till. The mineralization consists of massive pitchblende nodules and veinlets within a white, black, and red clay envelope (Baudemont *et al.*, 1993). Minor amounts of arsenides and nickel are also observed in the ore zone. Host-rock hydrothermal alteration pervades and surrounds the orebody and is typified by hematization, argillization, and silicification.

3. Mine Sequence

The mine sequence consists of a northeast- to north-trending and steeply dipping succession, composed of graphitic and non-graphitic gneiss including garnet-cordierite-sillimanite gneiss and hematite-rich gneiss containing foliated and brecciated quartzite. All of these rocks are typically invaded by narrow sheets,

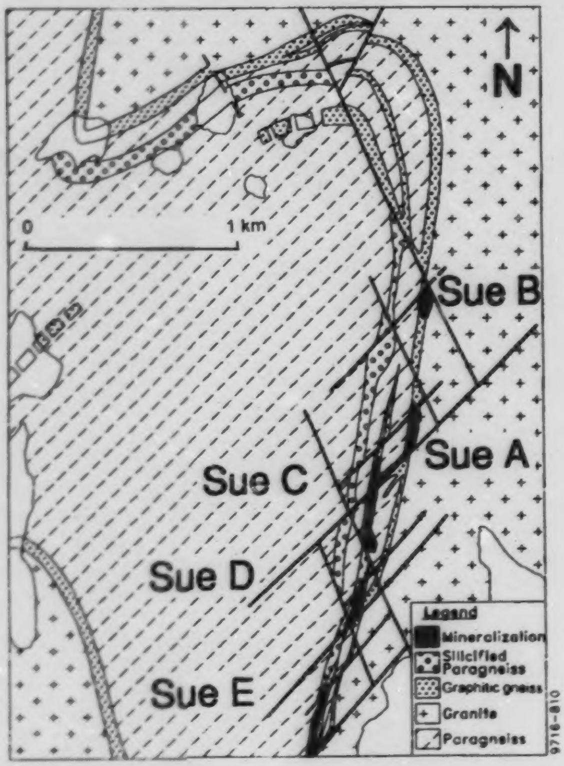

Figure 3 - Geological map of the Sue Trend (from Baudemont and Pacquet, 1996).

dykes and veins of granite, granitic pegmatite, and *lit-par-lit* quartz-feldspar melt leucosome.

Fault rocks include narrow mylonite layers with tectonic breccia and cataclasite (Figure 4).

a) Graphitic Gneiss

Grey to black graphitic gneiss with minor amounts of garnet forms fault-bounded lenses located in the most highly strained parts of the deposit and in its structural hanging wall (east side; Figure 4). The rock is strongly anisotropic and characterized by variably oriented slickensides on the foliation surfaces and by the presence of small drag folds along the foliation. Locally, graphite-rich slices (30 to 70% graphite) are tectonically interfingered with thin layers of garnet-cordierite-sillimanite gneiss. Pegmatite sheets and quartz-rich melt leucosome are locally observed in the unit.

Table 1 - In situ geological ore reserves for the Sue A, B, and C uranium deposits.

Orebody	Metric Tonnes	Grade (%U)
Sue A	606	0.74
Sue B	664	0.51
Sue C	10 516	2.81

b) Cordierite-Garnet-Sillimanite Gneiss

Cordierite-garnet-sillimanite-bearing gneiss is well exposed in the central part of the pit where it forms the immediate structural footwall (west) of the orebody (Figure 4). The rock is light gray to light brown, fine to medium grained and characterized by compositional layering ranging in thickness from a few millimetres to a few centimetres (Figure 5). The metamorphic layering is defined by a segregation of quartz-plagioclase-rich layers and biotite-cordierite-garnet-sillimanite layers. Major mineral components are quartz, feldspar and cordierite. Sillimanite and garnet are minor constituents. Patches of white mica, clay, and iron oxide appear to be retrograde products overprinting peak metamorphic minerals.

c) Hematite-rich Gneiss

Weakly to strongly foliated brick-red gneiss occurs close to the unconformity (Figure 4). The rock is fine grained and characterized by a red, dusty iron-rich staining on the weathered surface. It is mainly composed of fine-grained quartz and plagioclase in a biotite-chlorite-hematite-rich matrix. In places, the rock is in gradational contact with the cordierite-sillimanite-garnet gneiss. Within the hematite-rich gneiss, cordierite and garnet occur as trace remnants that have been almost completely retrograded to biotite-chlorite assemblages.

d) Quartzite

Quartzitic rocks are abundant and continuous on the structural footwall (west) of the orebody representing approximately 40% of the mappable rocks in the pit (Figure 4).

The rock is grey to pinkish-white, fine to coarse grained, and typified by alternating massive and strongly foliated layers. Both varieties are characterized by intense development of late fracture cleavages and joint sets. The rock consists almost entirely of recrystallized quartz (80 to 90%) and feldspar (<10%) with subordinate amounts of hematite, sillimanite, and clay.

This rock type has been previously interpreted as representing a large zone of intense silicification contemporaneous with the sandstone diagenesis, rather than an integral stratigraphic component of the mine sequence (Baudemont and Pacquet, 1996). Our recent structural mapping demonstrates that the quartzite forms a very continuous unit and records the same tectonic events as the surrounding Wollaston Group. It displays the regional pervasive foliation and is clearly folded and faulted. Furthermore, the presence of quartzite clasts in the breccia overlying the unconformity preclude the possibility that this unit is related to diagenetic processes (see Figure 4). All of this evidence suggests that the quartzite is an integral part of the Wollaston Group stratigraphic succession and must be considered as a primary depositional unit rather than a result of post-metamorphic silica-metasomatism.

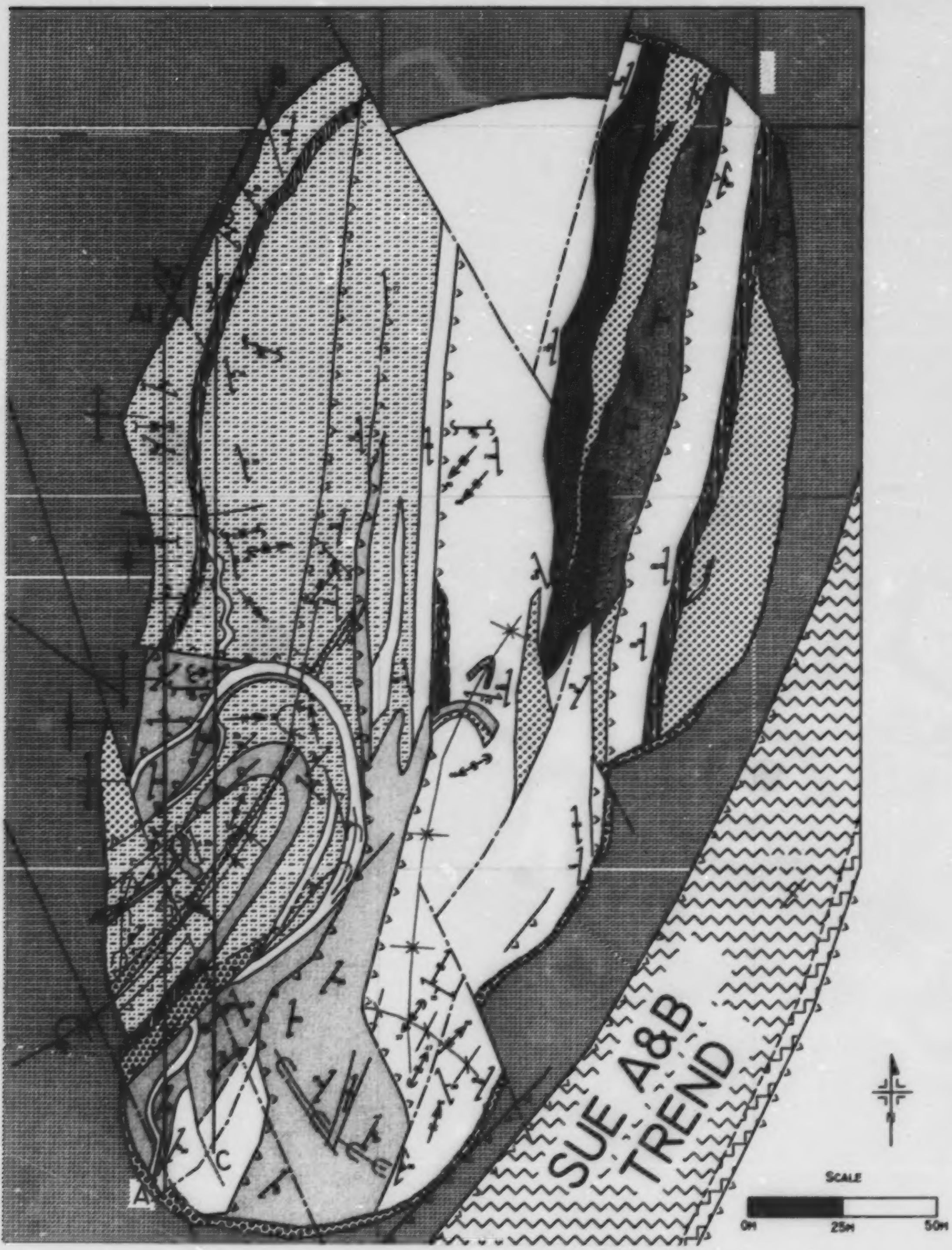
SUE A&B TREND
A
A'
C
SCALE
0M
25M
50M

Figure 4 - Simplified structural map of the Sue C pit (for legend, see the accompanying map separate).

Figure 5 - Well-foliated cordierite-garnet-sillimanite gneiss (plan view, trench 382).

e) Granitoid and Pegmatoid

Mappable granitic rocks occur sporadically in the pit, as concordant (foliation-parallel) or discordant sheets and pods ranging from less than one metre to tens of metres wide. The massive to moderately foliated, pinkish-white to grey granite is medium to coarse grained, and is strongly altered, consisting almost entirely of granular quartz in a white, clay-rich matrix. Some unaltered samples show that the primary mineralogy of the granite consists of a mixture of 15 to 35% quartz, 35 to 70% combined K-feldspar and plagioclase, 1 to 3% hornblende, and minor biotite and tourmaline.

White to pink, medium- to coarse-grained, massive pegmatitic rocks occur locally in the mine sequence. They form veins or dykes less than 1 m thick. Most pegmatites were emplaced along north-northwest-trending fractures, oriented 10° to 20° anticlockwise relative to the main regional foliation in the gneissic host rocks. The rock is composed of subhedral to euhedral, coarse tourmaline crystals, biotite and large K-feldspar crystals. The pegmatoids are probably contemporaneous with a late extensional-dilational tectonic pulse of the progressive deformation.

f) Mylonite and Fault Rocks

The most severely deformed and recrystallized rocks are found in fault zones (Figure 4). Mylonite (*sensus stricto*) is uncommon but was identified as narrow, centimetre- to metre-wide lenses truncating coarse-grained protoliths. In places, it represents zones of maximum shear strain that are tectonically interfingered with less deformed rocks. The individual mylonites are composed of spaced slip planes on which the displacement is marked by vertical striations. Grain-size reduction is clearly related to increasing deformation in the fault zone and affects large as well as small mineral grains. In the less deformed isotropic rock types (mainly granite), large grains of quartz, feldspar and mica are 1 to 15 mm wide. In the mylonite, quartz and feldspar constitute alternating ribbons that are 1 to 5 mm wide and generally bounded by discontinuous seams of mica and clay. Evidence of non-coaxial flow is rare but some mica and feldspars are rotated, bent and kinked.

The general term *fault rock* is used here to designate complexly deformed tectonites characterized by an irregular and chaotic ductile and/or brittle fabric. These rocks show neither mesoscopic evidence of non-coaxial flow, grain size reduction, nor cataclasis. The rock is composed of anastomosing, centimetre-scale fault gouges surrounding lens-shaped pods of competent wall rocks. The anastomosing deformation planes comprise clay- and hematite-rich fault gouges occurring adjacent to pinch-and-swell and boudinage structures developed in the adjacent, competent quartzitic rocks. When observed in the XZ plane of the finite strain ellipsoid, individual boudins have long axes parallel to the prominent flattening fabric developed in surrounding rocks.

g) Tectonic Breccia and Cataclasite

Tectonic breccia and cataclasite coexist in late northwest- and northeast-trending faults observed in the basement rocks. They form dark layers (<2 m width) composed of brecciated wallrock fragments either with a random fabric or are foliated cataclasites. Most of the clasts are subangular quartzite and hematite-rich gneiss fragments contained in a matrix of quartz, clay, and hematite. The alignment of elongate clasts defines the foliation within the cataclasites. Granular quartz resulting from crushing and granulation of competent wallrock makes up a large proportion of these rocks. Typically, granular quartz gives the rock a saccharoidal texture.

h) Athabasca Group

Sandstone, Conglomerate, and Breccia

The Athabasca Group, unconformably overlying the basement rocks in the pit area, belongs to the MFb and MFc units of the Manitou Falls Formation (Ramaekers, 1990; Figure 4). These units are composed of interbedded medium-grained quartz sandstone and conglomerate with minor layers of clay and silt. The sandstone is more than 80% quartz and is well cemented by silica, clay, and hematite. Basal conglomeratic beds reach 2 m in thickness. Clast size varies from 1 cm to over 50 cm.

Large zones of altered sandstone 20 to 100 m wide are present over the Sue A and B deposits (Figure 4). The white to pale grey, altered sandstone is characterized by a high-clay content. The argillized zones are most important in the immediate vicinity of the unconformity and appear to coincide with late northeast-trending faults. These wide alteration zones represent very favourable environments for the discovery of Athabasca Group sandstone-hosted uranium deposits.

A breccia lies on the unconformity principally in the south and southwest parts of the pit. This unit consists of angular pebble- and cobble-sized clasts of quartzite and minor sandstone cut by argillized extensional micro-fractures (Figure 6). Clasts are randomly oriented giving a chaotic fabric to the rock. The breccia's composition suggests that it could have formed by erosion along a second unconformity surface composed of basement quartzites overlapped by Athabasca Group sandstones during a period of syndepositional faulting and tectonic instability (Hudsonian). This rock type represents an environment dominated by erosional relief to the west and southwest. Local topographic control of the initial phase of sedimentation is indicated.

The ongoing stratigraphic and sedimentological study of the Athabasca Group will examine in greater detail the nature and significance of this breccia (see Long *et al.*, this volume).

Zone à Boule

Zone à boules are mature tectonic breccias observed close to north- and northeast-trending fault planes in the Athabasca Group along the Sue trend (Figures 4 and 7). The rock is composed of tilted and rotated clasts and blocks of sandstone contained in a strongly argillized matrix. Rounded to subrounded clasts with well-polished and striated surfaces are randomly oriented. Because the striation's trend and plunge are highly variable from one fragment to another, it cannot be used as a reliable paleostress indicator in these rocks.

Figure 6 - Chaotic fabric of the breccia overlying the unconformity (plan view, bench 382; SST, sandstone and QTZ, quartzite).

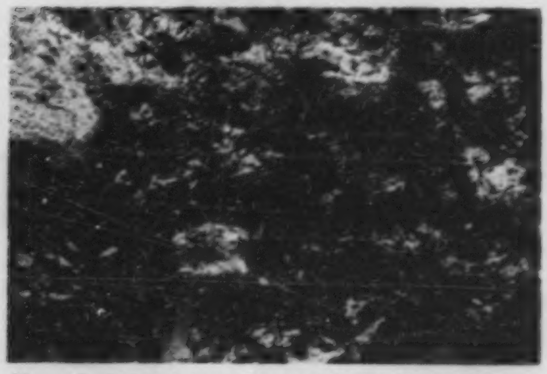

Figure 7 - Vertical view of a zone à boule observed along the Sue Trend (south wall, bench 418).

4. Structural Analysis

The following description and interpretation of the mine sequence's structural architecture is drawn from detailed structural, 1:100 scale, mapping of the pit area. Inhomogeneous and non-coaxial progressive deformation involved two principal generations of structures, D1 and D2, which produced two penetrative foliation surfaces, associated folds, elongation lineations and ductile faults. The D1 and D2 structures are responsible for the complex internal geometry of the basement rocks. Cross-cutting relationships suggest that these early plano-linear structures predate the main episode of uranium mineralization. All of these D1 and D2 structures are obliquely cut by cleavages plus late ductile and brittle-ductile faults. Uranium mineralization is primarily localized within and parallel to the late north-northeast- and north-trending fault systems (see Figure 4 and accompanying map separate).

a) Earliest Recognizable Compressional Deformation Features: D1 Structures

The earliest recognizable fabric (S1) is also the least well preserved. It is best preserved in metre-scale rock panels where D1 structures lie at a high angle to the dominant S2 schistosity. These areas, protected from transposition into the second regional foliation, were observed near the contact between the Archean basement and Wollaston Group sedimentary cover.

Field evidence from the cordierite-garnet-sillimanite gneiss and hematite-rich paragneisses in the southern part of the pit indicates that S1 corresponds to a fine bedding-parallel fissility and metamorphic layering. In detail, S1 is defined by millimetre- to centimetre-scale compositional layering as well as by the preferred alignment of metamorphic minerals and the long dimension of mineral grains. The enveloping surfaces of S1 planes are generally flat lying, except near the fold hinges of recumbent F1 folds where S1 is more steeply dipping (Figures 8, 9, and 10). Mineral and elongation lineations have not been observed with S1.

At least two styles of F1 folds were identified in the mine sequence: (i) poorly exposed F1a, primary bedding folds and (ii) recumbent F1b folds with subhorizontal hinges. A typical example of a small-scale F1a fold has been mapped in the cordierite-garnet-sillimanite gneiss on bench 382. In outcrop, the axial trace of F1a represents a hidden planar surface on both sides of which F2 fold axes and L2 intersection lineations plunge in opposite directions. Along the same F2 axial plane, the plunge of two adjacent F2 fold

Figure 8 - Vertical view of the subhorizontal S1 foliation in hematite-rich gneiss (west wall, bench 382).

hinges varies from 37° southwest (north limb of F1a) to 47° north-northeast (south limb of F1a). The east-trending surface separating these two F2 fold axes is the F1a fold hinge. This geometric relationship shows that the attitude of F1a fold limbs controls the orientation of F2 fold axes. Locally, the synformal open F1 fold is upright, east-southeast-trending and plunges subhorizontally to the southeast (Figure 9).

F1b folds are intrafolial folds defined by the S1 fabric and recognized within gently inclined metre- to tens of metre-scale structural panels dominated by a flat attitude of the S1 schistosity. These folds, devoid of an axial planar fabric, are tight to isoclinal, with an axial surface parallel to the overall trend of S1 (Figure 10), indicating that the formation of F1b folds was not accompanied by the development of a new foliation. The folds are rootless symmetrical flexures with closures outlined by S1. Their axial plane is subhorizontal and they plunge at a low angle towards the south (Figure 9). The F1b folds have rounded hinges and die out laterally like concentric folds. This geometric style is indicative of small-scale multilayer

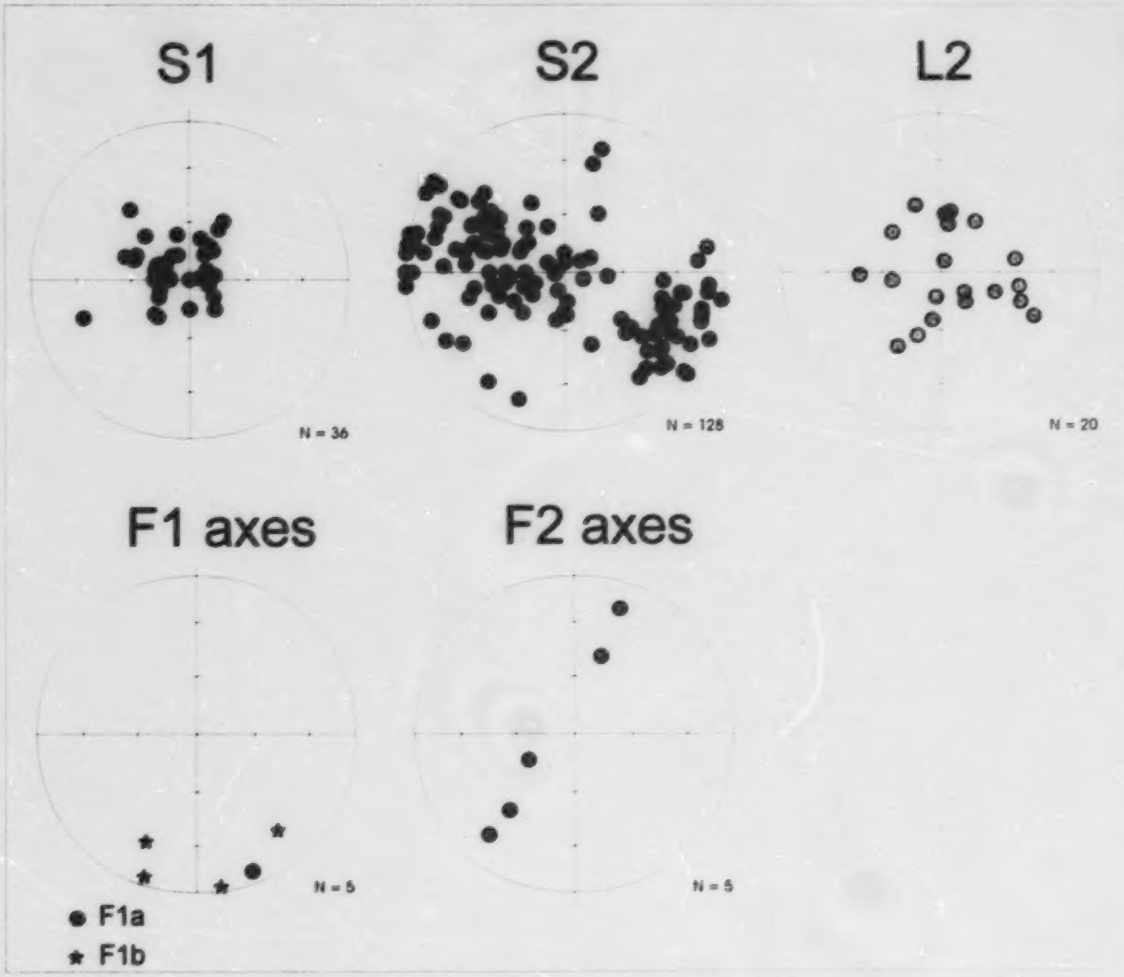

Figure 9 - Lower hemisphere stereographic projections of the principal structural elements of the mine sequence.

Figure 10 - Vertical view of a recumbent F1b fold in hematite-rich gneiss. Note the flat attitude of the limbs (south wall, bench 382).

buckling where S1 is subjected to tangential compression (Hudleston, 1986). Therefore F1b flexures likely represent buckled instabilities along the planar fabric that were subsequently amplified into folds by continued slip along S1 (Platt, 1983; Ghosh and Sengupta, 1987).

S1 is deformed by subhorizontal ductile faults interpreted here as late D1 thrust faults (Figure 4). These faults developed along the S1 foliation planes or at a very low angle to these surfaces, and formed the structural boundaries of panels with prominent flat-lying S1 schistosity. The late D1 faults are mostly located on the flat limbs of intrafolial F1b folds where transposition and increasing shear strain are evident. Sheared out intrafolial F1b folds, and development of anastomosing small-scale slip surfaces, mark the proximity of thrust planes. Slip planes anastomosing around intervening, rootless F1b folds, define duplex-like structures. Such structures are developed on a scale of metres to tens of metres and are particularly distinctive where there is a pronounced metamorphic layering along S1. One of these major D1 thrust faults is clearly folded by a major F2 synformal structure (Figure 4).

The relative transport direction along these discontinuities is still uncertain due to the paucity of reliable kinematic indicators. All pre-existing kinematic indicators seem to have been transposed and rotated parallel to D1 fault planes due to extreme flattening and shearing. However, similar gently inclined faults observed along the Archean basement/Wollaston cover contact and within the basement rocks of the Wollaston Group have already been described as thrust faults (Tran and Smith, 1999).

b) Second Phase of Deformation: D2 Structures

The second principal regional deformation (D2) is largely responsible for the finite geometry of the mine sequence. D2 was the main compressional deformation event and produced the prominent S2 schistosity, the F2 fold set, and the L2 mineral and stretching lineations (Figure 4).

Except in isotropic intrusive rocks, this S2 surface is highly penetrative. It clearly cuts the S1 flat-lying foliation at a high angle and the chronological relationships between the two planar surfaces is quite evident (see Figure 10). S2 is commonly expressed as the preferred alignment of metamorphic minerals such as biotite and amphibole, and by the flattening of porphyroblasts and porphyroclasts in coarse-grained rocks. Locally, the strike and dip of S2 is highly variable due to the presence of overprinting F3 folds and late (D3) brittle and ductile faults that distort and reorient D1 and D2 structures (Figure 9). Stereographic projection of the poles to the S2 surfaces shows that this schistosity chiefly strikes northeast and dips moderately (45° to 50°) to the southeast (Figure 9). Northeasterly trending D2 structures (S2, F2) dominate the structural west wall of the orebody, whereas north- and northeast-striking D2 structural elements predominate close to the mineralized fault zone (Figure 4). On the map, S2 surfaces and F2 folds measured in the western half of the pit are progressively rotated counterclockwise on approaching the deposit. In plan view, this apparent sinistral displacement probably reflects one component of the bulk displacement observed within and along the post-D2 graphitic faults.

The L2 tectonic stretching lineations are defined by oriented cordierite, plagioclase, and amphibole grains. The polar distribution of this linear fabric shows that L2 lineations plunge moderately to steeply in various directions (Figure 9). This distribution is clearly due to the post-D2 structures that reoriented S2 and L2. In general, L2 lineations are down dip on S2 surfaces. Close to the deposit they plunge steeply (>65°) south or north (Figure 4). This attitude is compatible with a prominent subvertical displacement along and within the mineralized fault zones.

Two major F2 folds can be recognized in the southern half of the pit (Figure 4). They consist of large flexures overprinting D1 structures including D1 flat-lying thrust zones. The large F2 folds are mostly developed along the faulted lithological contacts between competent quartz-rich units and the relatively incompetent hematite-rich gneiss. Well-preserved fold hinge segments indicate that the megaflexures are non-cylindrical synformal structures (Figure 4). The lack of antiformal F2 closures between these two synforms suggests that late D2 shearing was concentrated along the axial plane of the major F2 antiform. These folds are upright to gently overturned to the southeast and have a north-northeast-oriented axial planar surface. No F2 sheath folds were observed in the pit area.

An important point in the geometric analysis of the F2 folds is the variability in their axial plunge (Figure 9). F2 fold axes directly measured in outcrop have a remarkable, north-northeast–south-southwest-trending polar distribution along a great circle which coincides with the mean S2 plane of the folded domains. This variability in plunge may be interpreted as a consequence of the open character of the F1a folds.

The attitude of their limbs controls the orientation of F2 fold axes. If the F1 folds were isoclinal, the F2 fold axes would be relatively constant.

c) Third Phase of Deformational Structures: D3 Folds and Cleavages

Large-scale upright open folds (F3) refold D2 structures about east-plunging axes (Figure 4). The F3 folds consist of alternating synformal and antiformal flexures that are responsible for the undulating character of S2. These folds are open buckles with centimetre- to tens of metres-scale wavelength and have rounded hinges. They plunge variably from 30° to 50° towards the east. The tectonic fabric, axial planar to F3 folds, is a south-dipping to subvertical spaced fracture/crenulation cleavage (S3), typically oriented east-southeast to east-west.

At least two additional sets of steeply dipping northwest-southeast and northeast-southwest conjugate cleavages occur in the mine sequence. The chronological relationships between S3 and this conjugate set of fractures is still unknown. None of these late structures have any major influence on the internal geometry of the mine sequence.

d) Late Ductile and Ductile-Brittle Faults

Sets of ductile and brittle faults cutting the earlier fabrics and structures exist in addition to the late D1 flat-lying thrust faults (Figure 4). Most truncate both the basement rocks and the Athabasca sediments and are likely to be part of the late Helikian tectonic event involving re-activation of previously developed basement structures. Three principal sets of faults are present within the mine sequence: i) foliation-parallel thrusts and normal faults, ii) conjugate faults, and iii) late flat-lying thrust faults.

i) Foliation-parallel Thrust Faults and Normal Faults

Faults developed parallel to the pre-existing regional S2 foliations are one of the predominant structural features of the mine sequence (Figure 4) and host the principal orebodies of the property (Sue A, B, and C).

These structures are essentially parallel to S2 or cut this surface at a very low angle; they seem to have been formed at a late incremental stage of the main anisotropic phase of deformation (D2). They are preferentially developed along major lithological contacts where they juxtapose different rock types of highly contrasting rheological properties. Such ductile deformation zones imposed between pre-existing anisotropic rock masses formed in response to differences in mechanical constraints such as the degree of anisotropy and the viscosity contrast between deforming media (Jaeger, 1969; Mandl, 1988; Ramsay and Huber, 1987).

The main structures in the central part of the pit are subvertical or steeply inclined to the east or west. The north- to north-northeast-striking deformation zones associated with these faults are concentrated into narrow corridors, 1 to 20 m wide, and can be traced for several hundred metres along strike. Mineralized ore lenses occupy the most highly strained and altered segments of the fault zones.

Our analysis of the main mineralized fault zones has been restricted due to the lack of safe exposures at the time of mapping. However, important north-trending discontinuities observed very near to the orebody display mesoscopic features that probably mimic those present in the ore zone. Within the cordierite-garnet-sillimanite unit and along the contacts between this unit and the quartzite, faulting is expressed by development of mylonitic and clay-rich discontinuous deformation bands (c.f. Cobbold, 1977). The S2 foliation is strongly accentuated near tectonic discontinuities and finite deformation resulted in the development of L > S tectonites. Foliation-boudinage structures are also locally developed in the quartz-rich tectonites. Fault planes are generally defined by clay or mica-rich slip surfaces displaying elongation lineations and vertical striations. Vertical sections parallel to the extension lineations show rotated foliation segments indicating that these discontinuities are high-angle, west-verging thrust faults. This interpretation agrees well with that of Baudemont *et al.* (1993).

Several smaller-scale thrust faults are also observed on the west side of the pit (Figure 4). These foliation-parallel structures have a general orientation of 025° to 035° and a general dip of single line 50° north-northwest. Because they display the same structural features as the principal fault zones, they are interpreted as second-order structures subsidiary to the larger north-south structures. The main sense of displacement along these faults is given by well-developed drag folds of the S2 foliation as well as by the sigmoidal pattern of S2 between adjacent slip planes. These structures are therefore interpreted as southeast-verging thrust faults and are considered synchronous with the main north-south thrust set.

North- to northeast-trending thrust faults have also been observed within the Athabasca Group where faulting is expressed by intense fracturing, brecciation (zone à boule), block rotation and tilting, and is accompanied by pervasive clay alteration. These structures clearly represent the upward propogation of the basement thrusts. Within the sandstone, the faults are refracted and flattened, and have a general dip of less than 50° towards the east (Figure 11). Two locations underlying the Sue A and B trend (Figure 4) show this reverse sense of displacement by a counterclockwise rotation of sandstone beds and by displaced conglomeratic beds (Figure 11). The offset of the bedding along these faults is less than 2 m.

North-striking faults observed near the unconformity have induced normal displacement in the mine sequence (Figure 4). These foliation-parallel, extensional structures are mainly identified south of the orebody. One, located in the southern extemity of the pit, juxtaposed the sediments and the basement rocks at a same elevation (Bench 382). The normal fault has clearly downthrown the unconformity and overlying sediments by approximately 10 m. This normal sense of displacement has also been confirmed by the presence of extensional structures developed at the southern end of the deposit (Figure 12). They likely post-date the main high-angle reverse faulting observed along the major north- and northeast-trending thrust system.

ii) Late Flat-lying Thrust Faults

Narrow, late, subhorizontal thrust faults are recognized within the quartz-rich units and interlayered hematite-rich gneiss (Figure 4). The main fault in this set reaches dimensions on the order of 150 m laterally with an average thickness of about 2 m. The penetrative foliation within the fault zone is the rotated and reoriented S2 foliation which has the same strike and dip as the fault zone: i.e. east-west striking and subhorizontal to gently dipping (<30°) north or south. Several brittle fractures are commonly observed at the margin of the main fault planes. Pinch-and-swell and boudinage structures are also locally developed in competent quartzite layers. The faults have produced south-verging reverse displacements of 1 m or less.

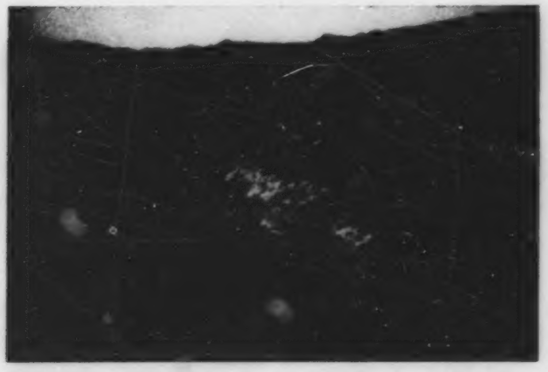

Figure 11 - Vertical view of a west-verging thrust fault in the Athabasca sandstone (north wall, bench 418).

Figure 12 - Vertical view of a west-dipping normal fault (3 m wide) cutting the cordierite gneiss. The attitude of the internal schistosity indicates the normal displacement (south wall, bench 358).

The hypothesis that the flat lying faults are D1 thrusts or reactivated D1 horizontal discontinuities is rejected for the following reasons: 1) late flat-lying faults clearly reorient and cut D2 structures at a high angle; 2) the internal fabric is the inherited S2 foliation; and 3) deformation in the fault panels and splay fractures has a pronounced brittle character that greatly contrasts with ductile character displayed by the earlier D1 discontinuities.

These late faults are likely riedel fractures induced by reverse displacement along the major high-angle reverse faults of the mine sequence.

iii) Conjugate Faults

A conjugate set of northeast and northwest brittle faults has produced important, vertical displacements of the mine sequence. These younger discontinuities cut the S2 and earlier north-south fabrics at variable angles ranging from about 25° to 55° in a clockwise or anticlockwise sense. They also show a wide variation in their internal deformational characteristics ranging from discrete, millimetre-scale striated slip planes to fault zones up to tens of metres thick.

Northeast-trending faults have been mainly observed along the Sue A and B trend where they consist of steeply dipping centimetre-scale clay-rich discontinuities, slightly discordant to the enveloping surface of the Sue Trend (Figure 4). The sense of displacement is still uncertain along these structures but some subhorizontal striations suggest strike slip movement.

The northwest-trending structures are predominant in the western, structural footwall of the Sue C deposit. They are generally less than 1 m wide and are marked by fault gouges, tectonic breccias, and cataclasites. The listric character of these structures is visible in vertical sections. The faults typically dip at 60° to 75° within the sandstone. The fault plane flattens drastically within the basement where the average dip is less than 35°. These listric structures commonly induced a normal vertical displacement of less than 5 m (Figure 4).

A complex collapse structure is produced at the intersection of two normal faults in the northern part of the pit (Figure 4). The two conjugate faults are separated by a downthrown trough-like region entirely composed of tectonized and altered sandstone. Locally, this collapse structure represents the structural footwall of the deposit. The unconformity indicates that the vertical normal displacement in this area is approximately 12 m downwards.

e) Topography of the Unconformity

Figure 13 presents the unconformity elevation contours drawn from 317 drill holes in the pit area. This surface

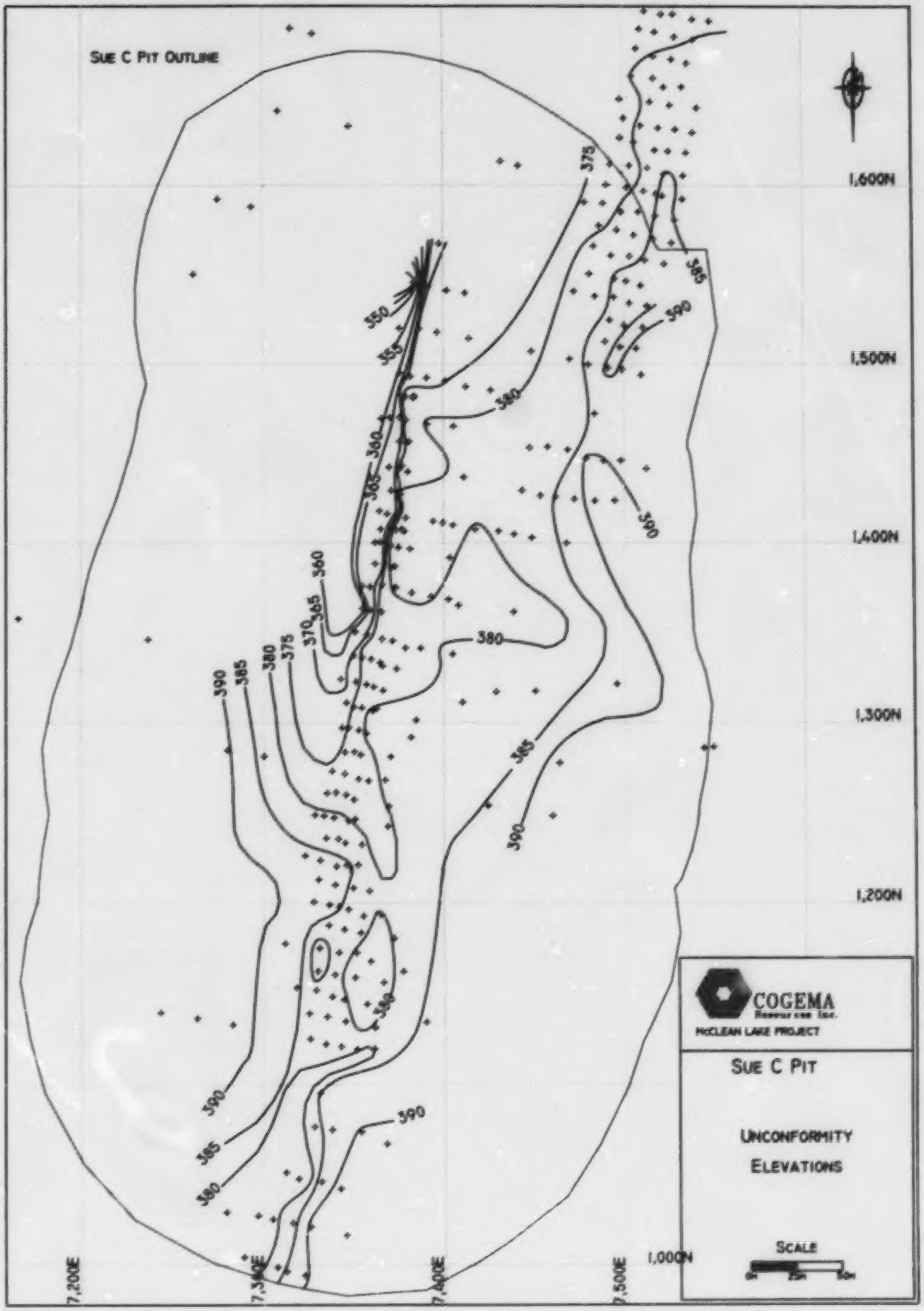
SUE C PIT OUTLINE
375
385
390
350
355
380
360
365
390
360
365
370
375
380
385
390
380
385
390
380
390
385
380
390
1,600N
1,500N
1,400N
1,300N
1,200N
1,000N
7,200E
7,300E
7,400E
7,500E
COGEMA
Resources Inc.
McCLEAN LAKE PROJECT
SUE C PIT
UNCONFORMITY
ELEVATIONS
SCALE
0M
25M
50M

Figure 13 - Unconformity elevation contours drawn from 317 drill holes in the pit area.

describes a paleoslope gently inclined to the north. The maximum elevation is at 408 m (≅40 m below the surface) in the west, southwest, and eastern parts of the open pit. The lowest exposed elevation of the unconformity is at 354 m (≅86 m below the surface) in the north-central part of the pit (Figure 13). The unconformity has an average slope of 10°, with a relief of approximately 40 m over a horizontal distance of 400 m.

The paleosurface is characterized by a marked linear, west-sloping feature in the central part of the pit demonstrated by close contour spacing (Figure 13). This feature coincides with a narrow, subvertical to steeply west-dipping fault. Field observations show that this topographic break represents a major north-northeast-trending structure overlying the principal orebody. At pit scale, this narrow structure is bounded by higher relief on the unconformity paleosurfaces to the north-northwest (350 to 360 m). This general topographic setting suggests that the major north-northeast structure probably represents a fault-controlled paleovalley carved into the non-resistant graphitic gneiss and bounded by competent quartzite ridges. This paleovalley may have controlled fluids involved in uranium deposition. Similar features have been described at a number of unconformity-type uranium deposits in Saskatchewan (see Wallis *et al.*, 1983 and references therein; Harvey, 1999).

In summary, the present relief of the unconformity surface appears to result from a combination of pre-Athabasca tectonism and erosion, and post-Athabasca faulting. The extent to which the post-Athabasca faulting has affected the final topography is significant as indicated by the displaced unconformity. Our structural observations are in agreement with this conclusion.

5. Conclusions

The study of the structural setting of the Sue C basement-hosted uranium deposit establishes the following principal points:

1) Cross-cutting relationships and superposition of structural elements show that the finite geometry of the mine sequence results from complex inhomogeneous progressive deformation related to three major deformation events:

    a) D1, an early subhorizontal nappe-style tectonic event, involving recumbent folding and subsequent development of subhorizontal thrust faults. The magnitude and sense of tectonic transport along these flat-lying faults is still unknown.

    b) D2, a major deformational event, chiefly characterized by development of large F2 folds with associated S2 regional foliation and extension lineations. The D2 strain increments record vertical dip-slip elongation seen as the steeply plunging mineral stretching lineations.

    c) A late phase of compressional deformation responsible for initiation of a major high-angle, thrust fault system developed parallel to the pervasive S2 foliation. Field relations indicate that faults were developed along S2 planes after this surface developed. The S2 foliation and the foliation-parallel thrust fault system can be related to a single bulk strain ellipsoid of the following orientation: a subhorizontal, east-west Z-axis trend; a north-south-trending, subhorizontal Y-axis; and a subvertical X-axis parallel to the transport direction. S2-parallel faults must, therefore, be due to west-northwest–east-southeast to east-west shortening. Mesoscopic structures indicate that the thrusting was west verging. The subvertical thrusts are not thought to be tilted flat-lying D1 structures. Finally, a late incremental stage of stress relaxation with concommittent normal faulting post-dated the shortening and reverse displacement events. Foliation-parallel normal faults clearly overprint previously developed compressional structures.

2) Uranium mineralization is essentially located within the prominent north- and north-northeast-trending thrust fault system. Mineralization is structurally controlled by these high-angle structures which were reactivated as extensional structures under conditions of high fluid pressure. Reactivation of faults and foliation planes during extension might have been a favorable factor for fluid mobility and emplacement.

3) Field observations support a pre-metamorphic origin for the quartzite unit occupying the structural footwall (west) of the deposit.

4) The paleogeographic setting of the deposit was dominated by high topographic relief to the west and southwest during conditions of post-orogenic tectonic instability. At that time the local topography was probably dominated by a north-south-trending paleovalley filled with quartzitic clasts locally derived from the erosion of Wollaston Group quartzites. This paleovalley was subsequently overlapped by Athabasca Group sandstones.

6. Acknowledgments

The authors would like to thank COGEMA Resources Inc. for full access to the mine site and for permission to publish this paper. The study has benefited from discussions with Kathy Bethune, Shawn Harvey, Hai Tran, and Gary Delaney. Brent Karstad, Ryan Bayne, Mike O'Brien, and Bill Slimmon are gratefully acknowledged for their assistance during preparation of photographs and figures. Critical reviews by Andrew Gracie, and later by Ken Ashton, have greatly helped to modify the initial version of the text.

7. References

Annesley, I.R., Madore, C., Shi, R., and Krogh, T.E. (1997): U-Pb geochronology and thermotectonic events in the Wollaston Lake area, Wollaston Domain: A summary 1994-1996; *in* Summary of Investigations 1997, Saskatchewan Geological Survey, Sask. Energy and Mines, Misc. Rep. 97-4, p162-173.

Ansdell, K.M., MacNeil, A., Delaney, G.D., Hamilton, M.A. (2000): Rifting and development of the Hearne craton passive margin: Age constraint from the Cook Lake area, Wollaston Domain, Trans-Hudson Orogen, Saskatchewan; GeoCanada 2000, Calgary, May 2000, Conference CD, ext abstr. #777.

Baudemont, D. and Pacquet, A., (1996): The Sue D and E uranium deposits, northern Saskatchewan: Evidence for structurally controlled fluid circulation in the Athabasca basin; *in* Ashton, K.E. and Harper, C.T. (eds.), MinExpo'96 Symposium–Advances in Saskatchewan Geology and Mineral Exploration, Sask. Geol. Soc., Spec. Publ. No. 14, p85-94.

Baudemont, D., Piquard, J.P., Ey, F., and Zimmerman, J. (1993): The Sue uranium deposits, Saskatchewan, Canada; Expl. Mining Geol., v2, no3, p179-202.

Bray, C.J., Spooner, E.T.C., Hall, C.M., York, D., Bills, T.M., and Kruger, H.M., (1987): Laser probe Ar/Ar and conventional K/Ar dating of illites associated with the McClean unconformity-related uranium deposits, northern Saskatchewan; Can. J. Earth Sci., v24, p1617-1625.

Cobbold, P. (1977): Description and origin of banded deformation structures: I. Regional strain, local perturbations and deformation bands; Can. J. Earth Sci., v14, p1721-1731.

Ghosh, S. K. and Sengupta, S. (1987): Progressive development of structures in a ductile shear zone; J. Struc. Geol., v9, p277-287.

Harvey, S.E. (1999): Structural geology of the Deilmann orebody, Key Lake, Saskatchewan; *in* Summary of Investigations 1999, Volume 2, Saskatchewan Geological Survey, Sask. Energy Mines, Misc. Rep. 99-4.2, p100-109.

Hoffman, P.F. (1990). Subdivision of the Churchill Province and extent of the Trans-Hudson Orogen; *in* Lewry, J.F. and Stauffer, M.R. (eds.), Geol. Assoc. Can., Spec. Pap. 37, p15-40.

Hudleston, P.J. (1986): Extracting information from folds in rocks; J. Geol. Educ., v34, p237-245.

Jaeger, J.C. (1969) : Elasticity, Fracture and Flow with Engineering and Geological Applications; Methuen & Co., London, 268p.

Lewry, J.F. and Sibbald, T.I.I. (1979): A review of pre-Athabasca basement geology in northern Saskatchewan; *in* Parslow, G.R. (ed.), Uranium Exploration Technioques, Sask. Geol. Soc., Spec. Publ. No. 4, p19-58.

Mandl, G. (1988): Mechanics of Tectonics Faulting; Elsevier, New York, 407p.

Platt., J.P. (1983): Progressive refolding in ductile shear zones; J. Struc. Geol., v5, p619-622.

Portella., P. and Annesley, I.R. (2000): Paleoproterozoic tectonic evolution of the sub-Athabasca basement, northern Saskatchewan: Intergrated magnetic, gravity, and geological data; GeoCanada 2000, Calgary, May 2000, Conference CD, ext. abstr. #647.

Ramaekers, P. (1990): Geology of the Athabasca Group (Helikian) in Northern Saskatchewan; Sask. Energy Mines, Rep. 195, 49p.

Ramsay, J.G. and Huber, M. (1987): The Techniques of Modern Structural Geology, Volume 2: Folds and Fractures; Academic Press, London, 700p.

Sibbald, T.I.I. (1983): Geology of the crystalline basement, NEA/AEA Athabasca Test Area; *in* Cameron, E.M. (ed.), Uranium Exploration in Athabasca Basin, Saskatchewan, Canada, Geol. Surv. Can., Pap. 82-11, p1-14.

Slimmon, W.L. (1996): Saskatchewan Precambrian geochronology chart: Athabasca Basin; *with* Summary of Investigations 1996, Saskatchewan Geological Survey; Sask. Energy and Mines, Misc. Rep. 96-4.

Tran, T.H. and Smith, M. (1999): Geology of the Cup-Keller-Schmitz lakes transect of the Wollaston-Mudjatik domains boundary; *in* Summary of Investigations 1999, Volume 2, Saskatchewan Geological Survey, Sask. Energy Mines, Misc. Rep. 99-4.2, p68-79.

Wallis, R.H., Saracoglu, N., Brummer, J.J., and Golightly, J.P. (1983): Geology of the McClean uranium deposits; *in* Cameron, E.M. (ed.), Uranium Exploration in Athabasca Basin, Saskatchewan, Canada, Geol. Surv. Can., Pap. 82-11, p71-110.

Detection of K-enrichment (Illite) Chimneys Using Ground Gamma Ray Spectrometry, McArthur River Area, Northern Saskatchewan

R.B.K. Shives [1], K. Wasyliuk [2], and G. Zaluski [2]

Shives, R.B.K., Wasyliuk, K., and Zaluski, G. (2000): Detection of K-enrichment (illite) chimneys using ground gamma ray spectrometry, McArthur River area, northern Saskatchewan; *in* Summary of Investigations 2000, Volume 2, Saskatchewan Geological Survey, Sask. Energy Mines, Misc. Rep. 2000-4.2.

Abstract

In the Athabasca Basin, previous work has shown that hydrothermal alteration chimneys may extend hundreds of metres above uranium mineralization into overlying rocks, and redistributed in glacially derived surficial materials, including boulders. In 2000, a brief field study was conducted in the McArthur River uranium mine area, to determine if ground gamma ray spectrometry can map radioactive element (K, eU, and eTh) variations associated with known illite enrichment in sandstone boulders.

Initial results show that, although the bedrock and overburden sampled contain very low concentrations of all three radioactive elements (K, eU, and eTh), potassium variations associated with illite enrichment in boulders can be measured using a portable gamma ray spectrometer. These subtle potassium patterns are enhanced through the use of eTh/K ratios. No obvious relationship has been discerned between eU or eTh concentrations and the boulder clay-fraction geochemical data. Further study may provide additional correlation.

The potassium concentration of sand deposits exceeds that of sandstone outcrop and boulders where measured. The sands can be distinguished from outcrop or boulder-rich tills by very low eTh/K ratios. In the mature Athabasca sandstone basin, where the background concentrations of radioactive elements are typically the lowest of all regions in Canada, radioactivity associated with these materials may produce anomalies in modern, high-sensitivity airborne gamma ray spectrometric surveys, thereby assisting exploration and surficial mapping.

1. Introduction

In 1990, Earle *et al.* described regional lithogeochemical patterns established through analysis of glacial boulder geochemical data at several uranium exploration properties in the eastern Athabasca Basin (Figure 1). They used major and trace element analyses to calculate proportions of illite, chlorite, and kaolinite following a technique described by Earle and Sopuk (1989). They compared the patterns with shallow bedrock drilling results in several areas, including the Read Lake and McArthur River properties, where hydrothermal alteration associated with uranium mineralization was known to subcrop. Despite extensive, locally thick (up to 75 m) overburden, bedrock alteration patterns were clearly reflected in the boulders as anomalies in the concentrations of illite, boron, chlorite, uranium, and lead.

In 1999, at the Saskatchewan Geological Survey's 30th Annual Open House in Saskatoon, Ken Wasyliuk delivered a talk entitled "Clay alteration in the Manitou Falls Formation". He presented additional information from the Read Lake–McArthur River property, including colour images of the boulder geochemistry. This presentation prompted the principal author to conduct a brief field study in August 2000 to determine if ground gamma ray spectrometry can be used to map potassium variation associated with the illite. The work was done under the Geological Survey of Canada (GSC)–Saskatchewan Energy and Mines (SEM) EXTECH IV Athabasca Uranium Multidisciplinary Study, sub-project 6. This paper provides a brief summary of the results of this work to date.

2. Gamma Ray Spectrometry

Fueled by early successes, radiometric surveys have played an obvious and significant role in the exploration history of many uranium deposits worldwide. In the Athabasca Basin, in northern Saskatchewan, airborne and ground scintillometer surveys have outlined uraniferous boulder trains associated with mineralization at Rabbit Lake, Cluff Lake, Key Lake, Midwest Lake, and Read Lake. The surveys are successful because the scintillometers are able to detect the relatively high radioactivity (relative to background) associated with uranium-enriched material eroded and transported from orebodies. The instruments typically use small detectors and measure only total radioactivity from all sources including uranium and thorium.

A modern, field-portable gamma ray spectrometer uses a much larger, more sensitive detector and is calibrated to provide accurate estimates of the three most common, naturally occurring radioactive elements, potassium, uranium, and thorium. This extends the

---

[1] Radiation Geophysics Section, Geological Survey of Canada, 573 - 601 Booth Street, Ottawa, ON K1A 0E8.
[2] Cameco Corporation, 2121 - 11th Street West, Saskatoon, SK S7M 1J3.

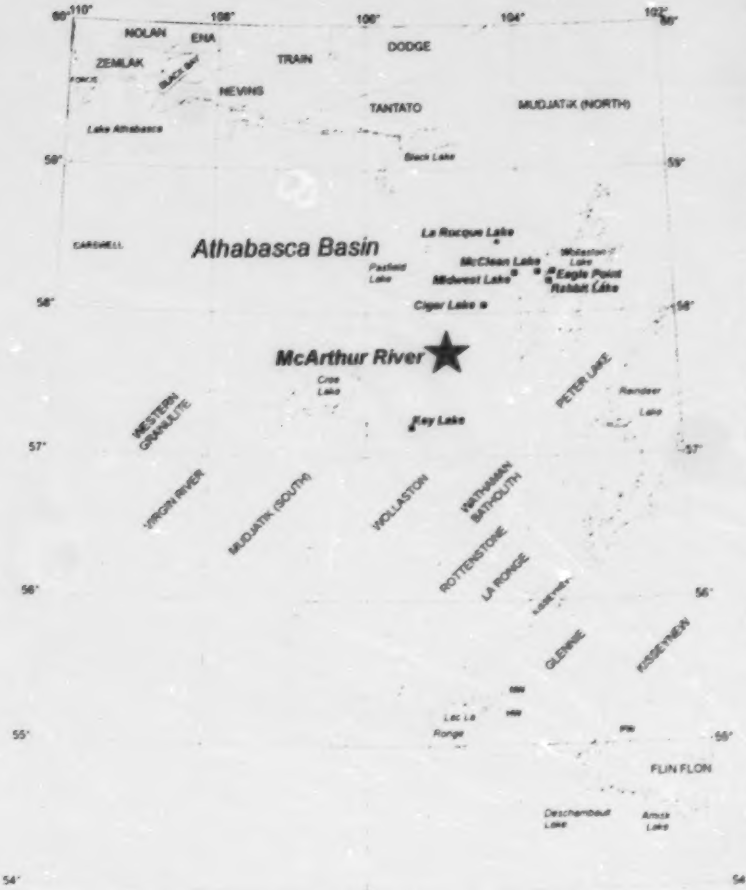

60° 110°
108°
106°
104°
102° 60°
NOLAN
ENA
ZEMLAK
BLACK BAY
TRAIN
DODGE
NEVINS
TANTATO
MUDJATIK (NORTH)
Lake Athabasca
Black Lake
59°
59°
CARSWELL
Athabasca Basin
La Rocque Lake
McClean Lake
Wollaston Lake
Midwest Lake
Eagle Point
Rabbit Lake
Cigar Lake
58°
58°
McArthur River
Cree Lake
WESTERN GRANULITE
PETER LAKE
Reindeer Lake
Key Lake
57°
57°
VIRGIN RIVER
MUDJATIK (SOUTH)
WOLLASTON
WATHAMAN BATHOLITH
ROTTENSTONE
LA RONGE
56°
56°
GLENNIE
KISSEYNEW
HW
NW
Lac La Ronge
PW
55°
55°
FLIN FLON
Deschambault Lake
Amisk Lake
54°
54°

Figure 1 - Location of the McArthur River mine property, northern Saskatchewan; PW, Pelican Window; HW, Hunter Bay Window, and NW, Nistowiak Window.

practical application of radioactivity surveys well beyond the search for uranium only.

In Canada, many studies (Shives *et al.*, 1995, 1997; Shives and Ford, in press) documented the application of gamma ray spectrometry to surficial mapping (glacio-fluvial deposits, tills, soils), bedrock mapping at regional to deposit scales, exploration for a wide variety of commodities (rare, base, and precious metals, granophile elements, and industrial minerals), and environmental studies. In Australia and elsewhere, where the effects of tropical weathering and landform development may significantly modify bedrock radioelement distribution (Dickson and Scott, 1997), the airborne patterns provided important information for soil, regolith, and geomorphology studies used for land management and mineral exploration strategies (Wilford *et al.*, 1997). The technique has been applied successfully to basin-scale studies at Mount Isa (Jayawardhana and Sheard, 1997) and hydrocarbon exploration (Sikka and Shives, in press). The latter example may be particularly relevant to work in the Athabasca Basin.

The use of gamma ray spectrometry to determine concentrations of elemental potassium, regardless of the associated potassium mineral species (orthoclase, microcline, biotite, illite, sericite, muscovite, etc.) enables alteration mapping in various geological settings. In the Sullivan Basin, British Columbia, airborne gamma ray spectrometric patterns provide useful regional stratigraphic mapping guides, but they also distinguish potassium associated with hydrothermal muscovite within the Sullivan Pb-Zn corridor, from the regional potassium distribution related to development of metamorphic biotite (Lowe *et al.*, 1997).

In general, mapping variations in the "normal" radioactive element content of detrital sedimentary rocks is made difficult by the typically low abundance of K, U, and Th, as shown in Table 1. Although borehole total radioactivity logs commonly delineate grit and quartz pebble conglomerate beds throughout the basin (Mwenifumbo *et al.*, this volume), courtesy of preserved thorium-bearing minerals, the majority of Athabasca sandstone is at the lowest ends of the radioactive element concentration ranges shown. This presents a challenge to gamma ray spectrometry in terms of stratigraphic mapping. However, in the search for ore, the extremely low background levels support detection of very small geochemical variations related to mineralizing, hydrothermal processes. Thus, given sufficient sensitivity, even very subtle increases in radioactive element composition may prove mappable.

3. Methodology

All ground spectrometric measurements were made using an Exploranium GR320 spectrometer with a 0.35 liter sodium iodide detector and 120 s counting time. The spectrometer weighs 4 kg and is carried in a backpack. Prior to fieldwork, the unit was calibrated on concrete pads containing known concentrations of potassium, uranium, and thorium, at the GSC's calibration facility in Ottawa. The instrument uses an internal cesium source to automatically maintain system stability, providing improved precision compared to older units. The unit displays properly corrected assays of K, equivalent U, and equivalent Th, in real time (the term "equivalent" or its abbreviation "e" is used to indicate that equilibrium is assumed

Table 1 - Radioelement concentrations in different classes of rocks.

Rock Type	Potassium (%)		Uranium (ppm)		Thorium (ppm)	
	Mean	Range	Mean	Range	Mean	Range
Acid Extrusives	3.1	1.0 – 6.2	4.1	0.8 – 16.4	11.9	1.1 – 41.0
Acid Intrusives	3.4	0.1 – 7.6	4.5	0.1 – 30.0	25.7	0.1 – 253.1
Intermediate Extrusives	1.1	1.1 – 2.5	1.1	0.2 – 2.6	2.4	0.4 – 6.4
Intermediate Intrusives	2.1	0.1 – 6.2	3.2	0.1 – 23.4	12.2	0.4 – 106.0
Basic Extrusives	0.7	0.06 – 2.4	0.8	0.03 – 3.3	2.2	0.05 – 8.8
Basic Intrusives	0.8	0.01 – 2.6	0.8	0.01 – 5.7	2.3	0.03 – 15.0
Ultrabasic	0.3	0 – 0.8	0.3	0 – 1.6	1.4	0 – 7.5
Alkali Feldspathoidal Intermediate Extrusives	6.5	2.0 – 9.0	29.7	1.9 – 62.0	133.9	9.5 – 265.0
Alkali Feldspathoidal Intermediate Intrusives	4.2	1.0 – 9.9	55.8	0.3 – 720.0	132.6	0.4 – 880.0
Alkali Feldspathoidal Basic Extrusives	1.9	0.2 – 6.9	2.4	0.5 – 12.0	8.2	2.1 – 60.0
Alkali Feldspathoidal Basic Intrusives	1.8	0.3 – 4.8	2.3	0.4 – 5.4	8.4	2.8 – 19.6
Chemical Sedimentary Rocks	0.6	0.02 – 8.4	3.6	0.03 – 26.7	14.9	0.03 – 132.0
Carbonates	0.3	0.01 – 3.5	2.0	0.03 – 18.0	1.3	0.03 – 10.8
Detrital Sedimentary Rocks	1.5	0.01 – 9.7	4.8	0.01 – 80.0	12.4	0.2 – 362.0
Metamorphosed Igneous Rocks	2.5	0.1 – 6.1	4.0	0.1 – 148.5	14.8	0.1 – 104.2
Metamorphosed Sedimentary Rocks	2.1	0.01 – 5.3	3.0	0.1 – 53.4	12.0	0.1 – 91.4

between the radioactive daughter isotope monitored by the spectrometer, and its respective parent isotope; uranium^{238} is estimated by measuring bismuth^{214} and thorium^{232} via thallium^{208}). Each reading is also stored internally as a 256-channel spectrum, for subsequent downloading and further analysis. An Exploranium GR101 scintillometer was used to continuously monitor changes in total radioactivity.

Positional data was gathered using a Trimble GeoExplorer II. Station locations were plotted manually on property-scale base maps (Figure 2). Traverses were positioned using the company boulder geochemistry maps (Figure 3), with emphasis on measuring boulders within highs and lows on the illite/(illite+kaolinite) x 100 map, to determine if spectrometry responds to the associated, very subtle changes in potassium concentration. Access was limited to areas accessible by truck or four-wheel drive all terrain vehicle.

For ground gamma ray spectrometry (GRS), large, angular sandstone boulders are the preferred sample medium as they are usually well exposed and provide a sufficiently large source to fill the sensitive volume of the sodium iodide detector, as required by the calibration procedure. Smaller boulders and less dense, unconsolidated materials depart from the ideal source geometry and density, yielding less quantitative results. For example, a reading of 1165 ppm eU from a small (50 cm) subrounded sandstone boulder from the Read Lake U-boulder train likely represents an underestimation, as the instrument assumes the detected radiation emanated from a larger volume of average density rock. In this study, the length and width of boulders measured ranged from 1 m by 1 m to over 6 m by 6 m, with the majority falling in the 2 m by 3 m range. In each case, the gamma ray detector was placed centrally, to avoid edge effects.

4. Initial Results

Evaluation of the results was not complete at the time of writing, however, several features are apparent from the 108 *in situ* GRS readings collected. Traverses and individual station locations are shown on a topographic base in Figure 2 and are superposed on the boulder geochemical maps in Figure 3. The main transect (stations 18 to 45 and 96 to 107) lies along a series of southwest-elongated, high-relief drumlinoid features, which dominate the area. The northernmost traverse (stations 61 to 82) lies along on a well-sorted outwash sand deposit, with local mixed-clast till.

Much of the colour variation present on the original boulder geochemical maps is lost in conversion to the greytone images (Figure 3) required for publication. For this reason, legends for the colour maps are not shown and tones have been labelled as either highs or lows. The dashed lines indicate the approximate surface trace of the P2 fault, which contains the P2 North (McArthur River) orebody and P2 Main uranium deposit, and curves to the southwest. The most striking feature illustrated by the maps is the strong zoning in calculated clay fraction compositions: high chlorite and low illite abundance west of the P2 fault, high illite and low chlorite east of the fault, and high boron along the fault.

Minimum, maximum, mean, and standard deviation for K, eU, eTh, and eTh/K values at all spectrometry stations are provided in Table 2, grouped separately for boulders, sand/till, and outcrop. XY-plots for these groupings are shown in Figures 4A (eU vs. K) and 4B (eTh vs. K). Uraniferous boulders at stations 2, 19, and 20 (6.9, 7.2, and 1164 ppm eU, respectively) are not included in the statistical summaries.

Mean K values are clearly higher in the outwash sand and till (0.55% K) than in the unsorted sandstone boulders (0.16% K) or outcrops (0.09% K). The ranges of eU and eTh values overlap considerably for all three media, and, as a result, eU/eTh ratio values (not shown) are very similar. The best discriminator for the

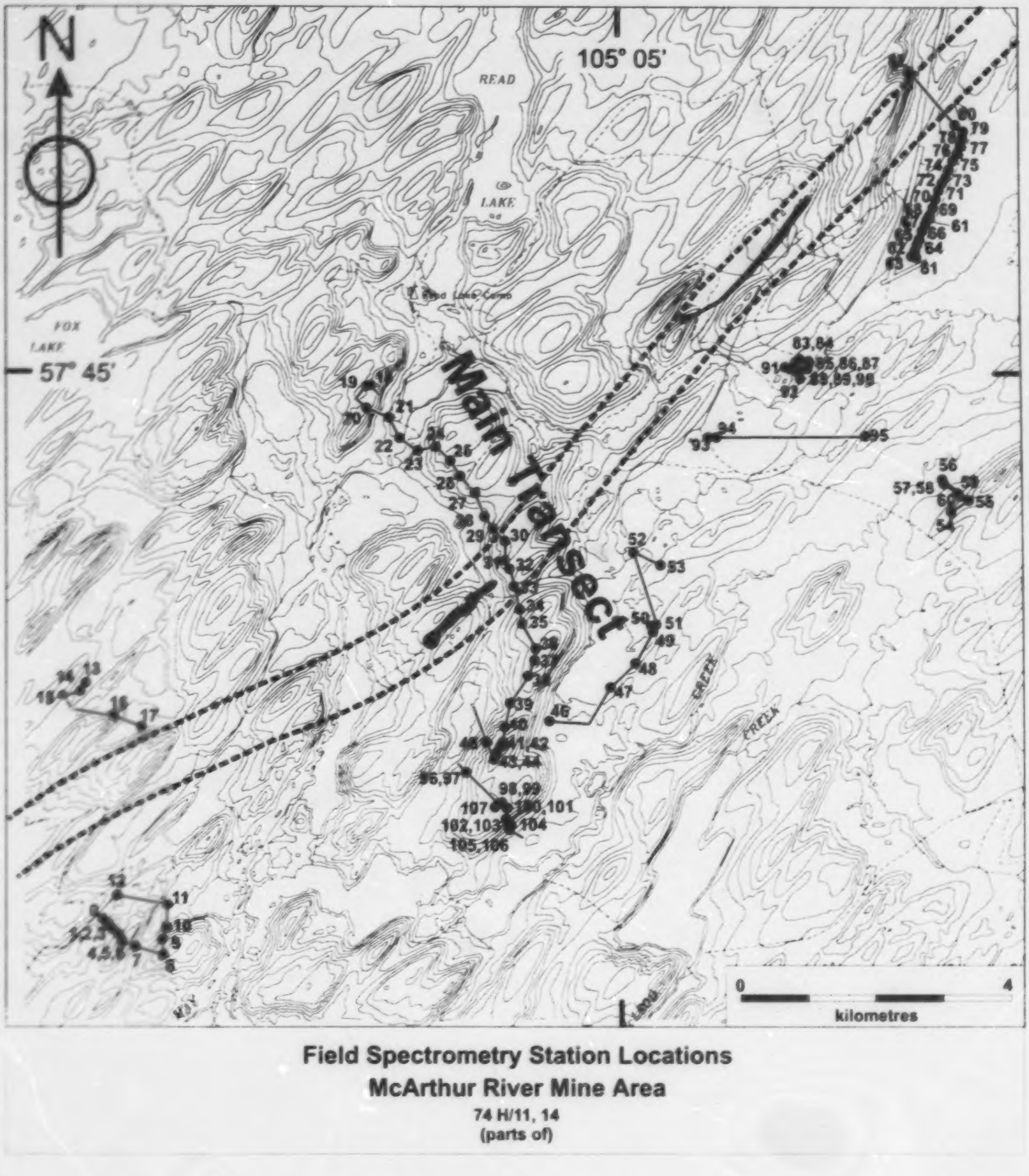
N
105° 05'
READ
LAKE
FOX
LAKE
Read Lake Camp
57° 45'
Main Transect
CREEK
CREEK
0
4
kilometres
Field Spectrometry Station Locations
McArthur River Mine Area
74 H/11, 14
(parts of)

Figure 2 - Location of ground spectrometry stations, July 27 to August 1, 2000.

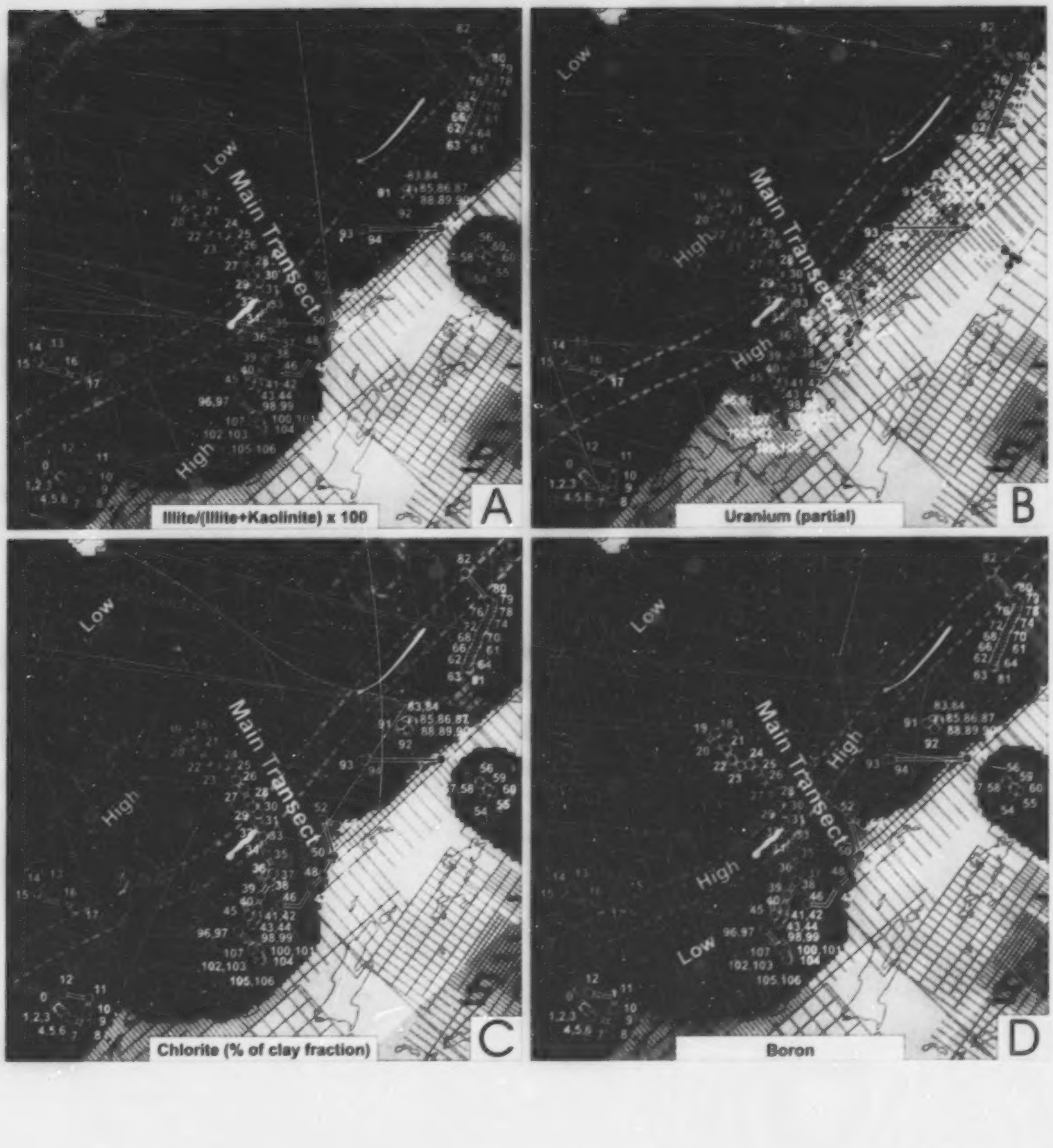
Low
Main Transect
High
Illite/(Illite+Kaolinite) x 100
A
Low
Main Transect
High
High
Uranium (partial)
B
Low
Main Transect
High
Chlorite (% of clay fraction)
C
Low
Main Transect
High
High
Low
Boron
D

Figure 3 - Ground spectrometry traverses plotted on greytone maps of sandstone boulder geochemical data (Earle et al., 1990) as labelled. Shades of relative high and low concentration are indicated, but are best-viewed in original colour versions. For gridding purposes, an inverse distance weighting algorithm (G. Zaluski) was used to extend each data point to 1000 m.

Table 2 - Statistical summary of in situ *gamma ray spectrometry results for all stations and sandstone, sand/till, and outcrop stations.*

		All Stations*	Sandstone Boulders	Outwash Sand/till	Sandstone Outcrop
K (%)	min	0.01	0.04	0.23	0.01
	max	1.00	0.34	1.00	0.15
	mean	**0.25**	**0.16**	**0.55**	**0.09**
	SD	0.20	0.06	0.18	0.04
eU (ppm)	min	0.17	0.35	0.42	0.17
	max	2.83	2.83	1.44	1.00
	mean	**0.95**	**1.01**	**0.83**	**0.61**
	SD	0.38	0.39	0.29	0.30
eTh (ppm)	min	0.74	0.74	0.88	2.71
	max	10.53	10.53	5.95	3.23
	mean	**3.18**	**3.16**	**3.32**	**2.94**
	SD	1.16	1.10	1.39	0.20
eTh/K	min	2.42	8.95	2.42	21.02
	max	271.05	167.89	11.62	271.05
	mean	**22.19**	**23.86**	**5.98**	**78.09**
	SD	31.08	20.76	1.65	96.61

Note: * excludes U-mineralized boulders at stations 2, 19, and 20.

different media appears to be the eTh/K ratio. The few outcrops sampled (n=5) were relatively siliceous and contained less K (highest value of 0.15% K in outcrop at station 17) than the mean K content of boulders in the illite-areas. As a result, the eTh/K ratios on outcrops are very high, with a mean value of 78. In strong contrast, the relatively potassium-rich sand/till sites produce very low eTh/K values, with a mean of six. These variations may be mappable using airborne gamma ray spectrometry.

Values obtained for K, eU, and eTh concentrations in boulders along the main transect are shown in Figure 5. Station number is indicated on the diagrams. The spatial relationship between the *in situ* GRS and boulder illite patterns in Figure 3A is clear. Stations 18 to 31 represent boulders occurring in the northwestern, low-illite area, and 96 to 107 are on boulders within the southeastern high-illite area. The intervening area contains spotty high and low patterns on the illite geochemical map, such as a weak low in the vicinity of station 37, and a moderate high just south of stations 25 and 29.

In Table 3 and Figure 6, results for the sandstone boulders only, are presented, grouped simply according to occurrence in either the illite-rich or illite-poor areas shown in Figure 3A. Again, mean values for eU and eTh (and ratios eU/eTh and eU/K) offer little discrimination between the two groups. However, with minor exceptions, there is clearly more potassium in the high-illite area boulders than in the low-illite areas, with mean values of 0.18 and 0.11 respectively. Corresponding eTh/K ratio values in the low-illite areas are twice those in the high-illite areas.

5. Discussion

To create the original colour grids, G. Zaluski used an inverse distance weighting algorithm to extend the influence of each data point to 1000 m. This facilitates interpretation of broad-scale features, but, by design, reduces site-to-site variations which may better explain variation in the spectrometry data.

In the composite boulder sampling program, small chips from 10 boulders within a 10 m radius were aggregated, at roughly 100 m intervals along lines spaced 300 to 500 m apart or wider (Earle *et al.*, 1990). Considering these factors, and the inherent 'nugget effect' in sampling boulders within glaciated terrain, correlation between the illite patterns defined by the geochemical data and the ground spectrometry results is surprisingly good.

Where information about variations in K, eU, or eTh is desirable, the relative ease and speed with which gamma ray spectrometry data can be collected may compare very favorably with boulder sampling techniques.

During ground GRS, variability in source material types (bedrock, boulders, overburden) can be controlled by the operator and treated as separate populations. In airborne GRS surveys, however, each measurement represents the average radioactive element composition of variable amounts of bedrock, overburden (highly variable in itself), surface water, soil moisture, and vegetation. In this brief study, we observed, through the use of ground GRS, that K enrichment can be detected in individual illite-altered sandstone boulders, and that well-sorted outwash sands are consistently K-rich, eTh-poor, resulting in low eTh/K ratios. Where similar boulders are abundant, or sand deposits are sufficiently large, modern, high-sensitivity airborne gamma ray spectrometric surveys may provide exploration and surficial mapping guidance within the Athabasca Basin. This potential will be further investigated (Campbell and Shives, this volume).

6. Conclusions

Initial results show that although the bedrock and overburden sampled contain very low concentrations of all three radioactive elements (K, eU, and eTh), potassium variations associated with illite enrichment in boulders can be measured using a portable gamma ray spectrometer. These subtle potassium patterns are enhanced through the use of eTh/K ratios.

No obvious relationship has been discerned between eU or eTh concentrations and the boulder clay-fraction geochemical data. Further study may provide additional correlation.

Potassium concentration of sand deposits exceeds that of sandstone outcrop and boulders, where measured.

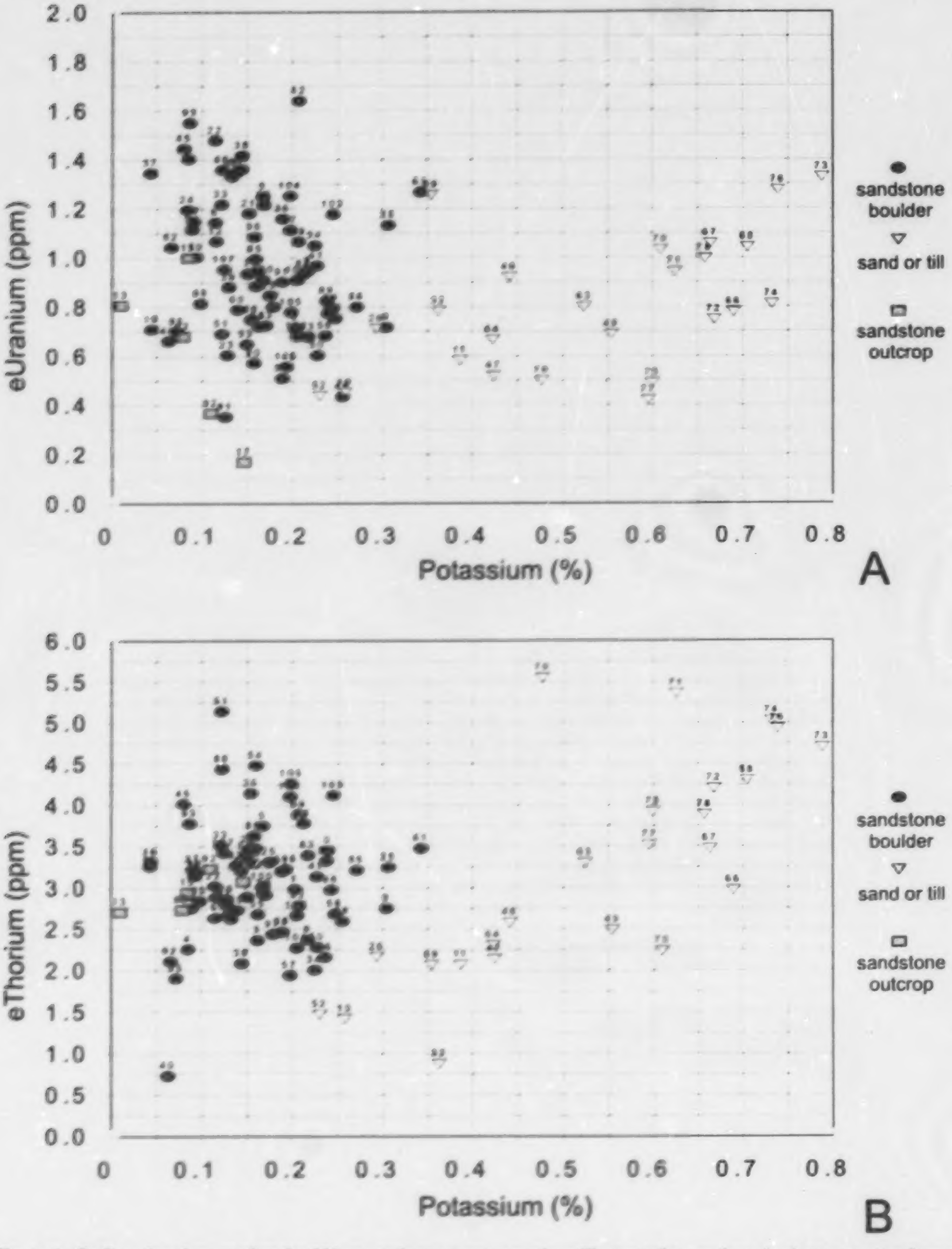

Figure 4 - Radioactive element plots for 106 ground spectrometry stations illustrate the very low absolute concentrations of eU (A), eTh (B), and K in sandstone outcrop, sandstone boulders, and unconsolidated sand/till. Ranges for eTh and eU are narrow and overlapping for all three media, but K values (and, especially eTh/K ratios, not illustrated) clearly distinguish sand/till from the boulders and outcrop.

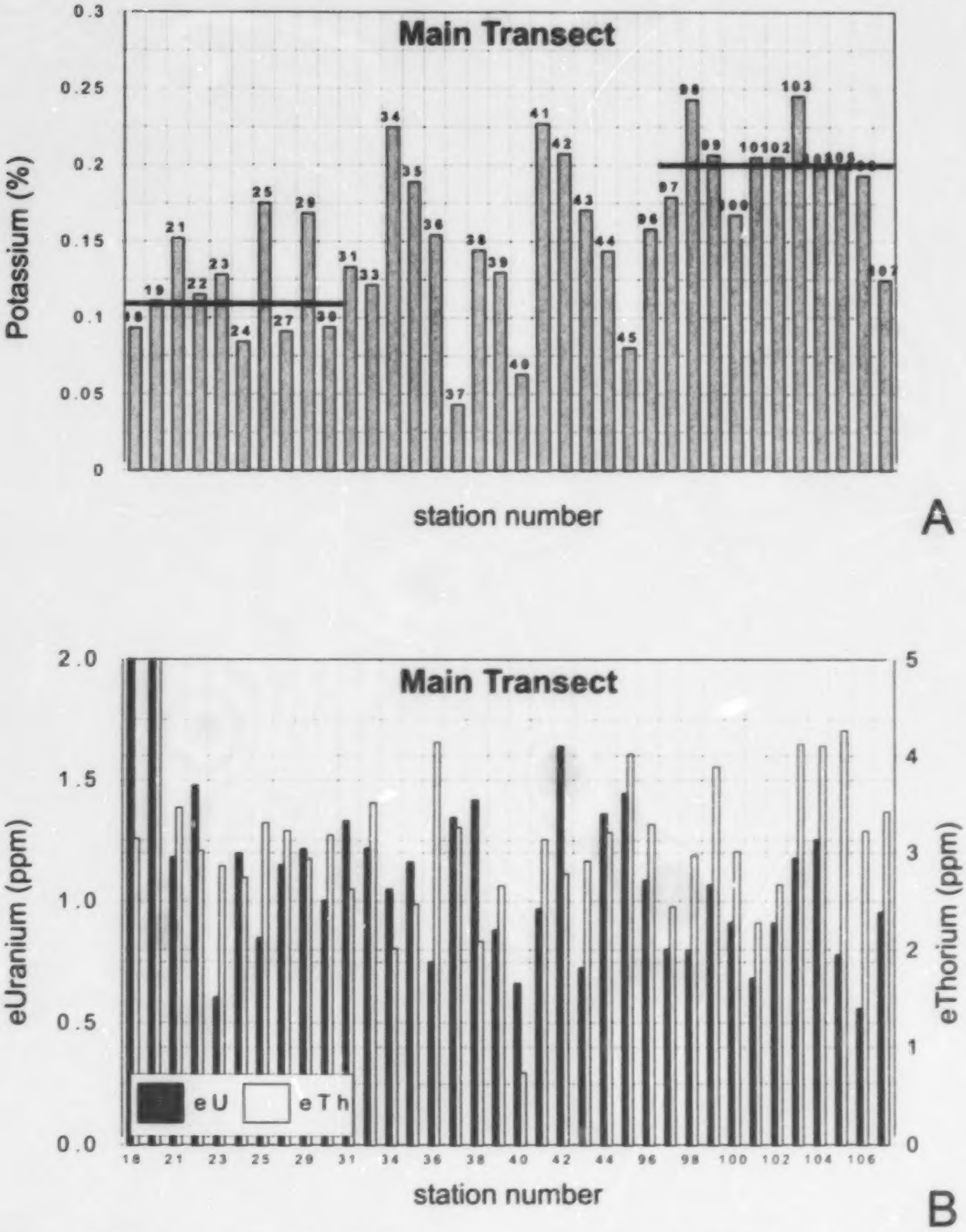

Figure 5 - Potassium concentrations (A) along the main transect correlate surprisingly well with relative illite enrichment shown in Figure 3A. Understandably, local variation between boulders creates spikes, but the general low- to high-illite (potassium) trend is apparent. Anomalous eU (B) at stations 18 and 19 reflect known, U-bearing sandstone boulders in a train extending southwesterly from Read Lake. Neither eU nor eTh reflect the boulder geochemical patterns in any obvious way.

Table 3 - Statistical summary of in situ gamma ray spectrometry results for sandstone boulders occurring within low- and high-illite areas defined by boulder geochemical patterns.

		Low-illite area	**High-illite area**
K (%)	min	0.04	0.06
	max	0.31	0.34
	mean	**0.11**	**0.18**
	SD	0.06	0.05
eU (ppm)	min	0.35	0.44
	max	2.83	1.64
	mean	**1.20**	**0.94**
	SD	0.56	0.27
eTh (ppm)	min	1.91	0.74
	max	10.53	5.15
	mean	**3.36**	**3.08**
	SD	1.70	0.76
eU/eTh	min	0.12	0.13
	max	0.90	0.90
	mean	**0.38**	**0.33**
	SD	0.16	0.14
eU/K	min	0.12	0.13
	max	0.90	0.90
	mean	**0.38**	**0.33**
	SD	0.16	0.14
eTh/K	min	10.60	8.95
	max	167.89	49.94
	mean	**38.74**	**18.45**
	SD	33.68	8.08

The sand can be distinguished from outcrop or boulder-rich tills by very low eTh/K ratios. In the mature Athabasca Basin, where the background concentrations of radioactive elements in the sandstones are typically the lowest of all regions in Canada, radioactivity associated with these materials may produce anomalies in modern, high sensitivity-airborne gamma ray spectrometric surveys, thereby assisting exploration and surficial mapping.

7. Acknowledgments

Cameco Corporation is thanked for approval to publish these preliminary results.

The principal author sincerely thanks several Cameco Corporation technical and support staff. At the McArthur River minesite: Dan Brisbin arranged logistical support; Larry Richardson provided office accommodation and well-presented summaries of the mine geology; Brian McGill freely shared valuable information about earlier boulder prospecting methods and results; Scott McHardy provided much appreciated logistical help and guidance concerning Read Lake boulder geochemical anomalies; and Lawson Forand offered background information on property exploration history. In the Saskatoon office, Ron Matthews ensured delivery of maps critical to field logistics and Wally Harildstad provided digital base

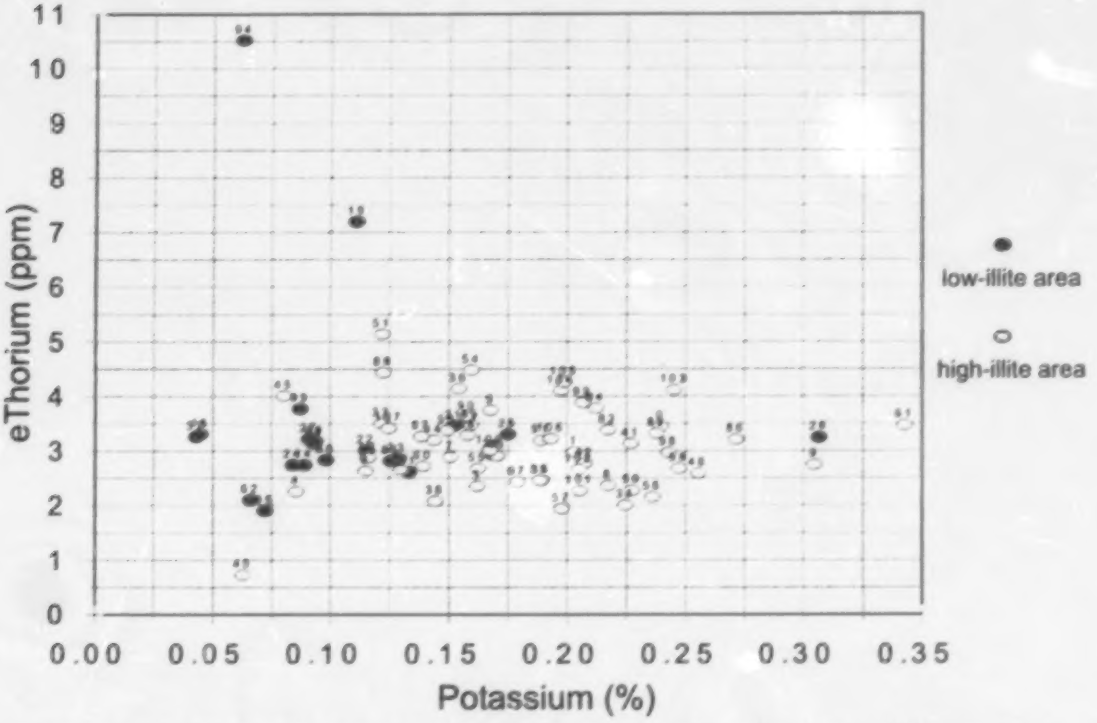

Figure 6 - A thorium/potassium plot of sandstone boulders only, clearly shows the elevated range of K concentrations (roughly 0.15 to 0.35% K) in boulders within high-illite areas, relative to those in low-illite areas. Higher eTh at stations 19 and 94 results from the presence of thorium-bearing minerals preserved in purple, heavy mineral-rich grit beds.

information. Excellent field assistance was provided by summer student Charley Murphy. Geological Survey of Canada Contribution Number 2000160.

8. References

Dickson, B.L. and Scott, K.M. (1997): Interpretation of aerial gamma ray surveys - adding the geochemical factors; AGSO J. Australian Geol. Geophys., v17, no2, p187-200.

Earle, S.A.M. and Sopuk, V.J. (1989): Regional lithogeochemistry of the eastern part of the Athabasca Basin uranium province, Saskatchewan, Canada; *in* Uranium Resources and Geology of North America, Proceedings of an IAEA Technical Committee Meeting, Sept. 1 to 3, 1987, Saskatoon, IAEA-TECDOC-500, p263-296.

Earle, S., McGill, B., and Murphy, J. (1990): Glacial boulder geochemistry: An effective new uranium exploration technique in the Athabasca Basin, Saskatchewan; *in* Beck, L.S. and Harper, C.T. (eds.), Modern Exploration Techniques, Sask. Geol. Soc., Spec. Publ. No. 10, p94-114.

Jayawardhana, P.M. and Sheard, S.N. (1997): The use of airborne gamma ray spectrometry by M.I.M. Exploration - a case study from the Mound Isa Inlier, North West Queensland, Australia; *in* Gubins, A.G. (ed.), Proceedings of Exploration 97, Fourth Decennial International Conference on Mineral Exploration, p765-774.

Lowe, C., Brown, D.A., Best, M., and Shives, R.B.K. (1997): East Kootenay multiparameter geophysical survey, southeastern British Columbia: Regional synthesis; *in* Current Research 1997-A, Geol. Surv. Can., p167-176.

Shives, R.B.K., Charbonneau, B.W., and Ford, K.L. (1997): The detection of potassic alteration by gamma-ray spectrometry - recognition of alteration related to mineralization; *in* Gubins, A.G. (ed.), Proceedings of Exploration 97, Fourth Decennial International Conference on Mineral Exploration, p741-752.

Shives, R.B.K., Ford, K.L., and Charbonneau, B.W. (1995): Applications of gamma ray spectrometric/magnetic/VLF-EM surveys - Workshop Manual; Geol. Surv. Can., Open File 3061, 82p.

Shives, R.B.K. and Ford, K.L. (in press): Mapping and exploration applications of gamma ray spectrometry in the Bathurst Mining Camp, northeastern New Brunswick; *in* Goodfellow, W.D., van Staal, C.R., McCutcheon, S.R., and Thomas, M.D. (eds.), Massive Sulphide Deposits of the Bathurst Mining Camp and Northern Maine, Econ. Geol. Mono.

Sikka, D.B. and Shives, R.B.K. (in press): Radiometric surveys of the Redwater oil field, Alberta: An early surface exploration case history (and similar case histories) suggest mechanisms for the development of hydrocarbon-related geochemical anomalies; Amer. Assoc. Petro. Geochem.

Wilford, J.R., Bierwirth, P.N., and Craig, M.A. (1997): Application of airborne gamma ray spectrometry in soil/regolith mapping and applied geomorphology; AGSO J. Australian Geol. Geophys., v17, no2, p201-216.

Status Report on the Surficial Geological Framework for the NEA-IAEA Study Area, Eastern Athabasca Basin [1]

Janet Campbell [2] and Rob Shives [3]

Campbell, J. and Shives, R. (2000): Status report on the surficial geological framework for the NEA-IAEA study area, eastern Athabasca Basin; *in* Summary of Investigations 2000, Volume 2, Saskatchewan Geological Survey, Sask. Energy Mines, Misc. Rep. 2000-4.2.

Abstract

This summer, as part of the Geological Survey of Canada (GSC)–Saskatchewan Energy and Mines' EXTECH IV Athabasca Uranium Multidisciplinary Study, a sub-project was initiated by the Saskatchewan Research Council to compile and upgrade in digital format the existing surficial geological framework and regional till geochemical database for the NEA-IAEA study area, eastern Athabasca Basin. The purpose of the surficial geology project is twofold. The compilation of the surficial geological framework supports the GSC's Gamma Ray Geophysics sub-project (sub-project 6) in the EXTECH IV program involving reprocessing and re-interpretation of previous regional and detailed gamma ray surveys for the Athabasca Basin. Secondly, the surficial geological framework will also assist mineral exploration and sustainable development in this region.

The compilation of data both from government and industry sources is underway. The 1:100 000 scale map of the Quaternary surficial deposits in the NEA-IAEA area will form the basis of the surficial geological framework. Limited fieldwork this summer involved collection of bulk till samples along existing roads in NEA-IAEA area. These samples, together with the analyses of archived drift samples, will provide a regional till geochemical framework and baseline data. Reprocessing of the NEA-IAEA airborne radiometric survey has been completed. Preliminary interpretation is underway, and several features not previously described have been recognized. The next step is the integration of the surficial geology and drift composition data with the airborne radiometric data to assess these features.

1. Introduction

This summer, as part of the EXTECH IV Athabasca Uranium Multidisciplinary Study, a project was initiated by the Saskatchewan Research Council (SRC), in cooperation with the Geological Survey of Canada (GSC), to compile and upgrade in digital format the surficial geological framework and regional till geochemical database in the NEA-IAEA study area, eastern Athabasca Basin of northern Saskatchewan (Figure1). The NEA-IAEA study area is the test area where a previous jointly sponsored GSC-SEM program compared different methods of exploration for uranium (Cameron, 1983).

The purpose of the surficial geology sub-project is twofold. Firstly, compilation of the surficial geological framework to support the Gamma Ray Geophysics sub-project (sub-project 6) of the EXTECH IV program. One component of the Gamma Ray Geophysics project involves the reprocessing and reinterpretation of the original ground and airborne radiometric data from the NEA-IAEA test area. The surficial geological framework is a component critical to the reinterpretation. Secondly, the surficial geological framework will also assist mineral exploration and sustainable development in this region. Both require knowledge of baseline conditions and geological models that describe the genesis, characteristics, and provenance of surficial sediments.

2. Methodology

a) General Remarks

The main component of the sub-project is the compilation of existing public and private domain Quaternary geological and surficial geochemical data into both digital databases and map formats for the NEA-IAEA study area. The data will be compiled and presented on 1:100 000 scale maps. The databases and maps will include: i) ice-flow indicators and summary of ice flow history, ii) dispersal trains and indicator erratics, iii) geochemical data (both existing and new analyses), iv) surficial geology, v) till compositional data (database only), and vi) drift thickness and bedrock surface topography maps based on existing digital drill hole data.

b) Data Sources

The interpretation of the Quaternary geological framework for the NEA-IAEA area is based on data compiled from geological reports, maps, drill hole logs, and databases. The sources of data include: university theses, published Quaternary geology maps and reports (i.e. Campbell *et al.*, 1999; Geddes, 1982; Schreiner, 1983, 1984a, 1984b, 1984c), exploration

---

[1] This project is jointly funded by the Saskatchewan Research Council and the Geological Survey of Canada.

[2] Saskatchewan Research Council, 15 Innovation Blvd., Saskatoon, SK S7N 2X8.

[3] Geological Survey of Canada, 601 Booth Street, Ottawa, ON K1A 0E8.

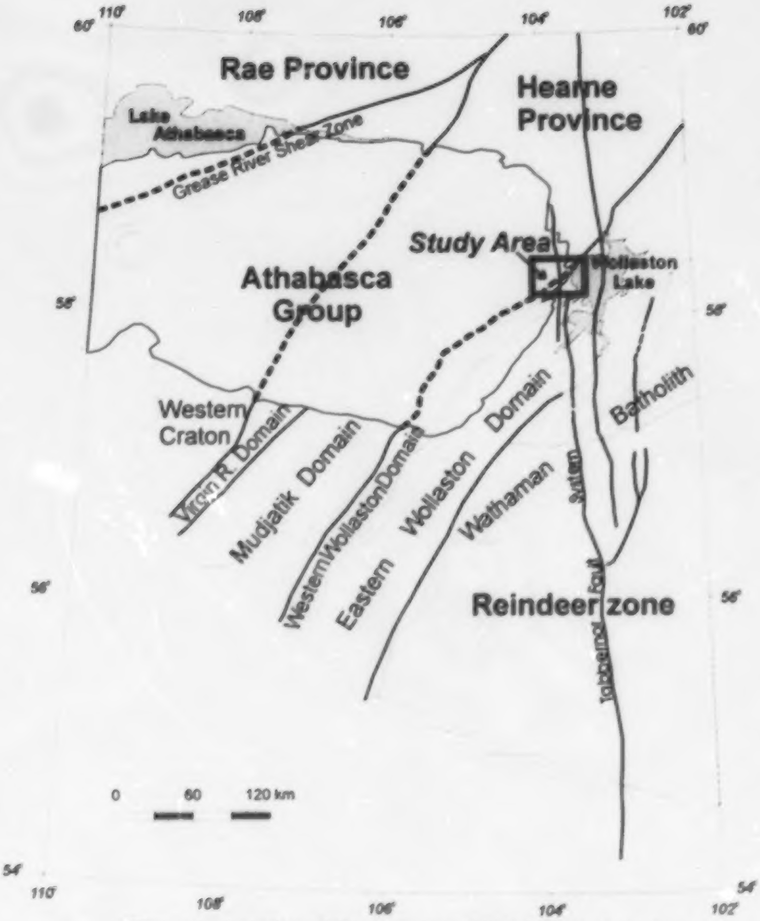

Figure 1 - Location of the study area (NEA-IAEA test area).

reports, industry-supported Quaternary geological investigations, geo-technical data and reports, and the Environmental Impact Statements (EIS) from the Rabbit Lake Operations, as well as the Midwest Lake and McClean Lake mine sites.

c) Surficial Sediment Geochemistry

The geochemical database will comprise regional geochemical data obtained from Schreiner's (1984a, 1984b, 1984c) reconnaissance mapping program augmented with exploration data from participating industry partners. Comprehensive geochemical analyses of selected archived samples from within the NEA-IAEA study area (Schreiner, 1983) will be done to assist with calibration of data obtained over several years, and by various analytical methodologies. These samples will be submitted for major and trace elements, partial and total uranium by fluorimetry, and boron analyses of the <63 Φm size fraction. Although the clay-size fraction is preferable, there is insufficient archive material to use this fraction.

Several days were spent in the field collecting 11 bulk till samples and field data from sites along the Black Lake and Points North roads. The samples were collected from a variety of till deposits as well as locations of both background and elevated total count airborne radiometrics to assist with the ground calibration of the radiometric data. These samples will provide a regional east-west ground-truth transect through the study area.

Data from these, together with the analyses of Schreiner's (1983) archived drift samples will provide a regional till geochemical framework and baseline data.

d) Integration of Data

Once the surficial geological framework and till geochemistry has been compiled, the data and maps will be incorporated into the EXTECH IV ArcView format database. The final step will be to integrate the surficial geology and drift composition data with existing remote sensing data and radiometric data to assist with the reinterpretation of the radiometric data.

3. Work in Progress

The compilation of data both from government and industry sources is underway. Schreiner's (1983) 1:100 000 scale map of the Quaternary surficial deposits in the NEA-IAEA area will be digitized. Data collected during the NEA-IAEA study were included in Schreiner's (1984) reconnaissance mapping program of the Quaternary geology of the Precambrian Shield region of Saskatchewan. Field and analytical data from these projects have never been published and are presently being compiled in an ACCESS database. These data provide the most comprehensive regional coverage of sediment-type distribution, stratigraphy, glacial history, and selected compositional properties of the surficial sediments in the study area to date. Data from industry activities including property-scale mapping of the surficial geology, surficial sediment geochemical surveys for selected areas, drill hole data, and related Quaternary geological investigations, will also be entered into the databases.

The inventory and selection of samples for geochemical analyses from Schreiner's (1983) archived drift samples is underway. As well, the bulk till samples collected this past summer are being processed to characterize their geochemical, lithological, and mineralogical attributes.

Reprocessing of the NEA-IAEA airborne radiometric survey has been completed. Preliminary interpretation is underway, and several features not previously described have been recognized.

4. Future Work

Characterization of the till compositional properties, and calibration of the geochemical data will be carried out once the geoanalytical work is complete. These data will be integrated with the re-processed radiometric data to assist with the new interpretation. The completed databases and maps will be integrated into the EXTECH IV ArcView GIS database. The results of this project will assist in determining the future direction of the surficial geological contribution to the EXTECH IV project.

5. Acknowledgments

The authors wish to thank COGEMA Resources Inc. and Cameco Corporation for providing logistical support in the field. Charlie Jefferson's (GSC) efforts in initiating and supporting this project are greatly appreciated.

6. References

Cameron, E.M. (ed.) (1983): Uranium Exploration in Athabasca Basin, Saskatchewan, Canada; Geol. Surv. Can., Pap. 82-11, 310p.

Campbell, J.E., Quirt, D.H., and Millard, M.J. (1999): The application of till geochemistry to mineral exploration in northern Saskatchewan, Canada; 19th International Geochemical Exploration Symposium, Vancouver, BC, April 12-16, 1999, Prog. Abstr., p8-9.

Geddes, R.S. (1982): The Vixen Lake indicator train northern Saskatchewan; *in* Davenport, P.H. (ed.), Prospecting in areas of glaciated terrain - 1982. Can. Inst. Min. Metall., p264-283.

Schreiner, B.T. (1983): Quaternary geology of the NEA/IAEA Athabasca test area; *in* Cameron, E.M. (ed.), Uranium Exploration in the Athabasca Basin, Saskatchewan, Canada, Geol. Surv. Can., Pap. 82-11, p27-32.

__________ (1984a): Quaternary Geology of the Precambrian Shield, Saskatchewan; Sask. Energy Mines, Rep. 221, 106p.

__________ (1984b): Quaternary geology of the Wollaston Lake area (NTS 64L), Saskatchewan; Sask. Energy Mines, Open File Rep. 84-14, 1:250 000 scale map.

__________ (1984c): Quaternary geology of the Pasfield Lake area (NTS 74I), Saskatchewan; Sask. Energy Mines, Open File Rep. 84-15, 1:250 000 scale map.

Synchrotron X-radiation Study of Illitic Clays from the Cigar Lake Uranium Deposit, Northern Saskatchewan

J.B. Percival [1], S. Skanthakumar [2], L. Soderholm [2], P.C. Burns [3], and A. Locock [3]

Percival, J.B., Skanthakumar, S., Soderholm, L., Burns, P.C., and Locock, A. (2000): Synchrotron X-radiation study of illitic clays from the Cigar Lake uranium deposit, northern Saskatchewan; *in* Summary of Investigations 2000, Volume 2, Saskatchewan Geological Survey, Sask. Energy Mines, Misc. Rep. 2000-4.2.

Abstract

Synchrotron X-ray absorption spectroscopy (XAS) was used to investigate U speciation and location within illite-rich clay separates from the Cigar Lake uranium deposit. Fluorescence experiments were carried out on the BESSRC beamline at the Advanced Photon Source facility at Argonne National Laboratory, Illinois. For each of the six samples analysed, from 10 to 15 spectra were collected and averaged to improve resolution. The U L_3-edge X-ray absorption near-edge structure (XANES) spectra obtained from the clay separates were compared with standard spectra for U^{4+} and UO_2^{2+} to provide insight into the speciation of U within the clays. The normalized spectra can be used to subdivide the samples into two sets that correlate, whether or not the samples contain free Fe-oxides. The bleached samples, which do not contain free Fe-oxides, have spectra consistent with U^{4+}. The XANES from the Fe-oxide bearing samples may indicate some oxidation of the U^{4+}, which would be consistent with the known U-Fe redox chemistry. Further refinement and analysis of the XAS data will enable determination of the U-U and U-O bond lengths that are necessary to confirm whether U occurs as UO_2, is adsorbed onto the clay surface, or occurs within the illite interlayer.

1. Introduction

In 1999, Natural Resources Canada and the National Research Council of Canada agreed to support the construction of the Canadian Light Source (CLS) Synchrotron facility in Saskatoon, Saskatchewan. Natural Resources Canada participated in the project on the basis that scientists would have access to the new facility. There was, however, a dearth of experience and understanding of geological applications of such a facility. As part of this initiative, a workshop was held to brief the scientific research community, stimulate discussion, and generate ideas for potential projects. Following the workshop (see report at www.nrcan.gc.ca/synchrotron/nrcan_activities/wkshop_e.htm), a call for proposals was sent out and 11 pilot projects were funded at existing facilities in the U.S.A. to facilitate training and develop new collaborations. We proposed to examine uranium-bearing illite-rich samples from the Cigar Lake alteration halo using XAS to determine the binding mechanism of uranium: whether it is incorporated into the illite structure, is adsorbed to the clay surfaces, or is present as extremely fine UO_2 (uraninite) crystallites.

a) Background

The world class Cigar Lake uranium deposit in northern Saskatchewan has been investigated by Atomic Energy of Canada Limited and others as a natural analogue of a high-level nuclear waste repository (Cramer and Smellie, 1994). Its simple geometry, occurrence above the unconformity entirely within the Athabasca Group, and depth from surface, which precludes effects from recent weathering and erosion, provided a unique opportunity to study trace element migration in an actinide- and lanthanide-rich environment. As part of this overall project, the clay mineral characteristics of the alteration halo around the deposit, as well as the origin and timing of fluids involved in the alteration and mineralization processes were studied (Percival, 1989; Percival *et al.*, 1993).

Clay minerals are sensitive indicators of low-temperature geological environments, modifying their composition, structure, and crystallinity with changes in temperature. Clay minerals can also act as sinks for heavy metals that are released and transported during weathering and hydrothermal alteration by mechanisms such as co-precipitation, adsorption, surface complex formation, and ion exchange. Partitioning of the metals among various substrates (e.g. clay minerals, organic matter) and mechanisms of retention can be determined using sequential extraction procedures in which a series of single, partial extractions attack samples with increasing severity. A sequential selective extraction procedure was developed to determine partitioning of U among: 1) exchangeable sites and carbonates, 2) uraninite and organic/sulphides, 3) amorphous Fe-oxides, 4) crystalline Fe-oxides, and 5) residual silicates including clay and other refractory minerals (Percival, 1989).

Results from sequential extraction experiments showed that up to 60% of the total U contained in some alteration halo samples was associated with the residual silicates fraction and that the proportion of U within this fraction increases away from the ore zone

---

[1] Geological Survey of Canada, 601 Booth Street, Ottawa, ON K1A 0E8
[2] Chemistry Division, Argonne National Laboratory, 9700 South Cass Avenue, Argonne, Illinois 60439
[3] Department of Civil Engineering and Geological Sciences, University of Notre Dame, Notre Dame, Indiana 46566

(Percival, 1989). Residual silicates are dominated by clay minerals but also contain trace amounts of refractory minerals such as ilmenite, rutile, and zircon. Autoradiography of representative samples taken from the alteration halo was used to map α-radioactivity associated with weakly radioactive mineral grains. In sandstone specimens, the α-activity appeared to be associated with heavy mineral layers rich in rutile, magnetite, pyrite, hematite, and zircon. Some U was detected in rutile by microprobe analyses. In highly altered sandstone samples, the α-activity was very high, especially in those containing pervasive hematite or sulphides. Microprobe analyses showed that U content was very low in pyrite and rutile, but high in the clay matrix surrounding these minerals. Analyses revealed that the clay matrix could contain from 3 to 16% UO_2 (Percival, 1989). However, it was difficult to determine whether U is present as isomorphic substitution in the clay mineral lattice, adsorbed onto the illite surface or within the interlayer, or if U occurs as micro-disseminated uraninite within the interstitial clay. Scanning electron microscope analyses did not reveal the location of the U.

2. Synchrotron Application

X-ray absorption spectroscopy (XAS) is an element-specific technique that can be used to examine the co-ordination, valence, and local bonding environment of a selected element. Each element has a set of characteristic X-ray absorption edges that are unique to that element. The absorption edges of elements heavier than P are in the keV energy range, and therefore it is often possible to target these elements or their ions *in situ*, and in complex systems that include the presence of other elements. XAS can be used to probe an element of interest in the gas phase, in solution or in the solid state.

An XAS spectrum, determined as a function of incident X-ray energy, is artificially divided into two regions to represent the contributions primarily from electronic and scattering processes that occur as X-rays are absorbed (Teo, 1986). The X-ray absorption near-edge structure or XANES region, which includes the edge itself, is sensitive to the electronic structure of the absorbing atom because the absorption process involves the excitation of a core, or inner-shell electron into an empty shell of the appropriate symmetry. For example, the L_3-edge involves the excitation of a core p-state to an unoccupied d state. The energy at which absorption occurs is modified slightly by the valence and local co-ordination environment of the absorbing ion. The intensity of the non-normalized absorption is proportional to the concentration in the sample of the absorbing ion. Unfortunately, there is not yet a fundamental understanding of the detailed electronic and scattering processes that contribute to an observed XANES spectrum. However, information can be obtained by comparison of spectra obtained from well-characterized standard samples. At higher energies, a free photoelectron is generated, which is scattered by neighbouring ions. The resulting standing waves, dependent on the identities of scattering-elements and their distances from the absorbing ion, are manifested as small oscillations in the intensity of the X-ray absorption, extended X-ray absorption fine structure (EXAFS). After appropriate background subtraction, the Fourier transform of the EXAFS spectrum yields metrical information about the identity and distance of the absorbing ions near neighbours.

3. Sample Selection and Experimental Set-up

A suite of six clay-sized (<2 µm) to silt-sized (2 to 20 µm) powder samples was investigated. These samples have variable characteristics and were taken from above the ore zone within the intense clay alteration halo (Table 1). Samples were selected based on several criteria including the total U content of the bulk material, the proportion associated with the residual fraction (high and low), and sample availability. The powders were pressed into rectangular slots in aluminium or cardboard sample holders and held in position using Kapton® tape. The sample holders were placed inside a standard secondary sample chamber.

Table 1 - General characteristics of samples selected for detailed study.

				Extractable Uranium (%)[3]					
Sample No.	**Lithology**[1]	**Depth (m)**	**Total U**[2]	Step 1	Step 2	Step 3	Step 4	Step 5	**Illite**[4] **(%)**
44-10	Clst	407.7	1920	37	49	1	7	6	99
44-15	Cl-Sst	410.9	366	–	–	–	–	–	95
44-16	Cl-Sst	411.1	1980	–	–	–	–	–	94
44-21	Clst	413.1	2160	24	42	5	19	10	91
49-12-bulk	Clst	418.9	318	6	24	1	11	58	
49-12-clay	Clst		1215	12	28	1	13	46	100
60-10	Cl-Sst	413.6	2040	–	–	–	–	–	88

Notes:

[1] Clst, sandy claystone and Cl-Sst, clayey sandstone

[2] Total U in ppm as determined by Neutron Activation Analysis-Delayed Neutron Counting method

[3] step 1, exchangeable sites and carbonate-bound, step 2, uraninite and organic/sulphide-bound, step 3, amorphous Fe-oxide-bound, step 4, crystalline Fe-oxide-bound, step 5, residual silicate-bound, and –, indicates not determined

[4] percent illite in the <2 µm fraction

The U L_3-edge X-ray absorption data were collected at the 7 GeV Advanced Photon Source (APS) on the Basic Energy Science Synchrotron Radiation Center (BESSRC) station 12-BM-B. This bending-magnet beamline is equipped with Si<111> crystals mounted in a double-crystal monochromator. Focusing is accomplished with Pt mirrors that also serve for harmonic rejection. The incident X-ray intensity was monitored by a standard ion chamber filled with Ar gas. The incident X-ray energy was calibrated from a Zr foil spectrum by setting the maximum in the first derivative to 17.998 keV. The U fluorescence lines were detected using a Canberra 9-element Ge detector operating with a 1 µsec shaping time. It was necessary to tightly window the energy spectrum because of the high concentrations of Sr in the samples. The Sr K-emission lines at 14.165 and 14.098 keV interfere with the emission lines from the U L_3 edge at 13.615 and 13.439 keV. Similarly, L_2-edge absorption data were vitiated by the presence in the sample of significant concentrations of Mo and/or Nb. Fluorescence intensity at the detector was attenuated with high purity Al foil. Typically 10 to 15 data sets were averaged from each sample. Data analyses were performed using WinXAS (Ressler, 1998) with the single scattering U-O phase and oxygen backscattering amplitude obtained from FEFF8.00 (Rehr *et al.*, 1991).

4. Results and Discussion

Table 1 summarizes the general characteristics of the samples used in this study. Note that the information pertains to bulk or whole rock samples rather than the clay-size separates, with the exception of sample 49-12. The samples are subdivided into two sets: bleached (samples 44-10, 44-15, 44-16, and 49-12) and hematite-bearing (samples 44-21 and 60-10). Three of the bulk and one clay-size sample were subjected to the sequential extraction procedure described above. The bulk samples containing the lowest concentrations of U, in general, contained the highest proportion association with the residual silicate fraction (step 5). Those with higher concentrations tended to have the highest proportion associated with the uraninite or sulphide/organic-bound fraction (step 2). Note that the clay-size fraction of sample 49-12 contains more U (1215 ppm) than its bulk equivalent (318 ppm), but still has a high proportion associated with the residual silicate fraction (46% total U). All samples are rich in illite with the remainder comprising trace to minor kaolinite, chlorite, and hematite (and goethite in sample 60-10).

The average XAS spectrum for all samples is shown in Figure 1 plotted relative to U^{4+} and U^{6+} standard spectra. As exemplified in the figure, the EXAFS oscillations from all of the geological samples appear to dampen out very quickly, suggesting that the samples do not exhibit significant long-range order about the U ion. The XANES regions of all the spectra are compared in Figures 2 and 3. The absorption-edge positions of all the samples, as defined by both the maximum intensity and the maximum in the first derivative, are listed in Table 2. The edge positions

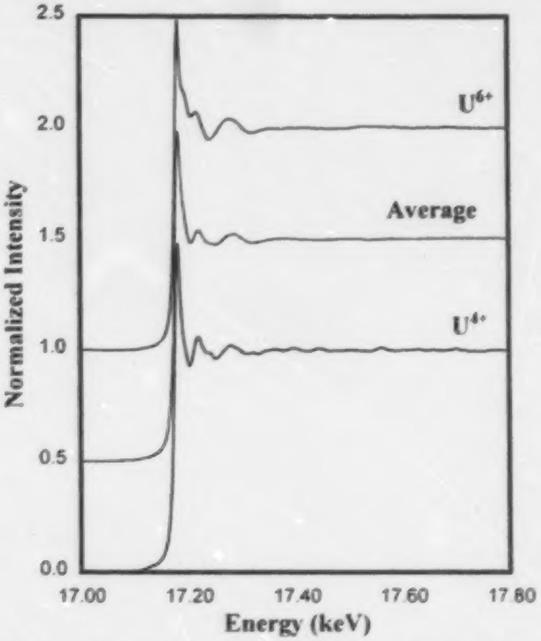

Figure 1 - Normalized average X-ray absorption spectrum for all samples compared to standards for U^{4+} (in UO_2) and U^{6+} (UO_2^{2+}) in acidic solution.

determined from the maximum in the edge energy do not correlate well with either standard or among the samples. This result reflects the significant differences between samples, in the width of the resonant-white line observed at the edge. Widths of resonant lines may depend on a wide variety of factors, including the d-final state splitting, hybridization, cluster size, and differences in co-ordinating ligands and central-ion environment. The various contributions to changing line widths are not fundamentally well understood. However, it has been observed that a decreased line intensity in conjunction with the occurrence of a second feature at about 15 eV higher energy than the resonant line, are signatures of the uranyl, O-U-O, moiety (Hudson *et al.*, 1995). This feature is present in our uranyl UO_2^{2+} standard spectrum, but is not clearly evident in any of our sample spectra (Figures 2 and 3). The absence of this strong feature in the sample data indicates that the samples do not contain primarily U^{6+}.

The maximum in the first derivative, which reflects the rising edge of the resonance, correlates well between samples (Table 2). From the first derivative data, it appears that all samples have edge energies intermediate between the two standards. The XANES spectra can be split into two groups based on these data, those of the bleached samples and those containing hematite. The hematite-bearing samples (44-21 and 60-10) have slightly higher energies than those of the bleached samples. The standard reduction potentials of UO_2^{2+} and Fe^{3+} show that the oxidation of

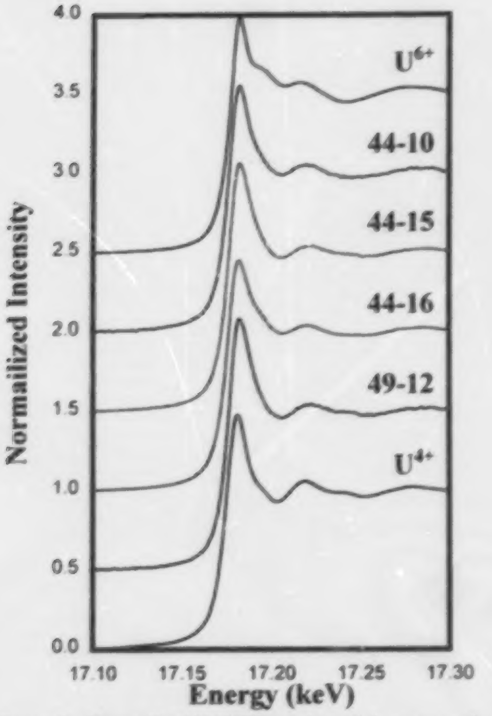

Figure 2 - Normalized XANES portion of the spectra for each of the bleached samples compared to the standards for U^{4+} and U^{6+}. Note the similarity of the shape of the spectra of the samples with the U^{4+} spectrum.

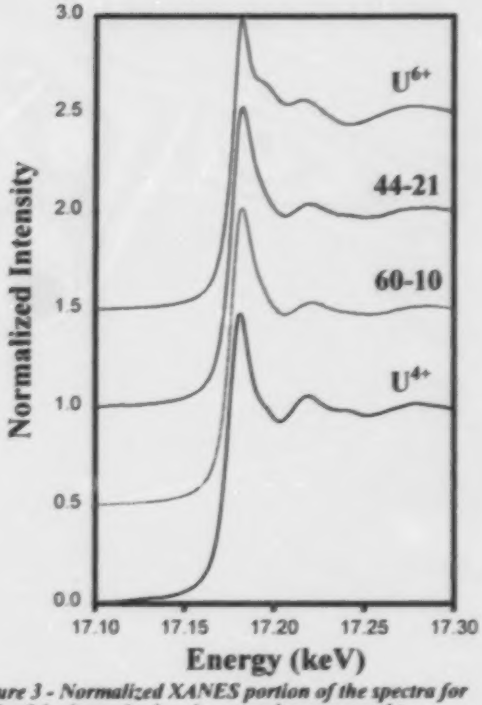

Figure 3 - Normalized XANES portion of the spectra for each of the hematite-bearing samples compared to standards for U^{4+} and U^{6+}. Note the similarity of the shape of the spectra of the samples with the U^{4+} spectrum, however, they exhibit slightly higher peak energies than the bleached samples in Figure 2.

U^{4+} by Fe^{3+} is thermodynamically allowed. However, the data discussed herein are not able to distinguish a slight oxidation of U^{4+} from other factors that may shift the edge energy slightly, such as changes in particle size or co-ordination of the U.

Further studies will address the details of uranium speciation in the clay samples. There are three possibilities in this regard: 1) uranium may be adsorbed onto the clay mineral surfaces, 2) uranium may be present as disseminated microcrystals of uraninite or some other U^{4+}-bearing mineral, or 3) uranium may be incorporated directly into the clay mineral structure. Identification of the valence state of uranium in the samples will provide insight into which of these mechanisms dominates. If the uranium is mainly U^{6+}, the most probable binding mechanism is sorption onto the clay mineral surfaces. Substitution of the uranyl ion (UO_2^{2+}) into the tetrahedral-octahedral sheets of illite is very unlikely, and with a length of 3.6 Å, incorporation of uranyl into the interlayer of illite also seems unlikely, given the typical $^{[XII]}$K-O bond length is 3.0 Å. Conversely, the presence of U^{4+} is consistent with sorption onto clays, the presence of disseminated uraninite, and possibly the incorporation of the uranous cation into the interlayer of illite, assuming appropriate charge-balance mechanisms can occur. The ionic radius of U^{4+} is 0.97 Å, considerably smaller than of $^{[XII]}K^{+}$ at 1.64 Å, suggesting that incorporation into the interlayer sites of illite is the least likely of these speciation mechanisms. Further refinement and analysis of the XAS data will enable determination of the U-U and U-O bond lengths that are necessary to confirm the binding mechanisms of U in these samples.

Table 2 - A comparison of the U L_3-edge XANES peak positions for the different samples determined by the maximum in the observed intensity and by the maximum in the first derivative.

Sample No.	Peak Position (keV ±1.2 eV) Intensity Maximum	Peak Position (keV ±0.5 eV) First Derivative Maximum
U^{4+} Standard	17.1820	17.17763
U^{6+} Standard	17.1817	17.17479
44-10	17.1819	17.17608
44-15	17.1821	17.17608
44-16	17.1817	17.17608
44-21	17.1821	17.17660
49-12	17.1822	17.17608
60-10	17.1821	17.17660

5. Summary and Conclusions

Six clay to silt-size illite-rich powder samples from the alteration halo above the Cigar Lake uranium deposit were analyzed by synchrotron X-ray absorption spectroscopy (XAS) to determine U speciation and location. The U L_3-edge X-ray absorption near-edge structure (XANES) spectra from the clay separates were compared to standard U^{4+} and UO_2^{2+} spectra. The bleached and hematite-bearing samples are readily subdivided based on their normalized XAS spectra. The bleached samples, which do not contain free Fe-oxides, have spectra consistent with U^{4+}. The XANES from the Fe-oxide-bearing samples may indicate some oxidation of the U^{4+}, which would be consistent with the known U-Fe redox chemistry. Further refinement and analysis of the XAS data is necessary to determine the U-U and U-O bond lengths to confirm the binding mechanisms and speciation of U.

6. Acknowledgments

We thank Guy Jennings (APS) for technical assistance, and S.R. Wasserman (APS) for fruitful discussions. Preliminary results were obtained at the COM-CAT beamline under the direction of S. Wasserman. We appreciate the services received from the infrastructures of the BESSRC CAT and the Actinide Facility at ANL. Two of the authors (LS and SS) acknowledge support from the U.S. DOE. BES. Chemical Sciences and the Advance Photon Source is supported by the U.S. DOE, Material Sciences, all under contract W-31-109-ENG-38. Support for this project from the NRCan Synchrotron Committee is gratefully acknowledged. We are grateful to D.C. Grégoire (GSC) for reviewing the manuscript. GSC Contribution No. 2000161.

7. References

Cramer, J.J. and Smellie, J.A.T. (1994): Final Report of the AECL/SKB Cigar Lake Analog Study; Atomic Energy of Canada Limited, Whiteshell Laboratories AECL-10851 (COG-93-147, SKB TR 94-04), 393p.

Hudson, E.A., Rehr, J.J., and Bucher, J.J. (1995): Multiple-scattering calculations of the uranium L_3-edge X-ray absorption near-edge structure; Phys. Rev., B52, p13815-13826.

Percival, J.B.M. (1989): Clay mineralogy, geochemistry, and partitioning of uranium within the alteration halo of the Cigar Lake uranium deposit, Saskatchewan, Canada; unpubl. Ph.D. thesis, Carleton Univ., 343p.

Percival, J.B., Bell, K., and Torrance, J.K. (1993): Clay mineralogy and isotope geochemistry of alteration associated with the Cigar Lake deposit; Can. J. Earth Sci., v30, p689-704.

Ressler, T. (1998): WINXAS: A program for X-ray absorption spectroscopy data analysis under MS-Windows; J. Synchrotron Radiat., v5, p118-122.

Rehr, J.J., Mustre de Leon, J., Zabinsky, S.I., and Albers, R.C. (1991): Theoretical X-ray absorption fine structure standards; J. Amer. Chem. Soc., v113, p5135-5140.

Teo, B.K. (1986): EXAFS: Basic Principles and Data Analysis; Springer Verlag, Berlin, 284p.

C. Athabasca Basin: Other Contributed Papers

Paleotopography and Clay Mineral Alteration Associated with the Deilmann Uranium Orebody, Key Lake, Saskatchewan

S.E. Harvey [1] and K.M. Bethune [1]

Harvey, S.E. and Bethune, K.M. (2000): Paleotopography and clay mineral alteration associated with the Deilmann uranium orebody, Key Lake, Saskatchewan; *in* Summary of Investigations 2000, Volume 2, Saskatchewan Geological Survey, Sask. Energy Mines, Misc. Rep. 2000-4.2.

Abstract

The Deilmann uranium deposit is one of two orebodies comprising the Key Lake mine at the southeastern edge of the Athabasca Basin. The orebodies are at the unconformity between sandstone of the Paleoproterozoic Athabasca Group and highly deformed and metamorphosed Paleoproterozoic supracrustal rocks and Archean granitoids of the Wollaston Domain. The unconformity surface exposed in the Deilmann Pit is recognized to be the northern slope of a paleovalley marked by onlap of basal strata of the Manitou Falls Formation onto the unconformity surface. Analysis of diamond drill hole data revealed a linear, northeast-trending topographic depression that slopes gently northeast, parallel to the main structural grain of basement rocks. The paleovalley sides have slopes of 6° to 7°. The onlapping relationship of the lower Manitou Falls Formation here indicates that it is a valley-fill deposit. The distribution of uranium mineralization suggests that flow of mineralizing fluids was in part controlled by the paleovalley.

Near-infrared reflectance spectrometry (Pima II) analyses of samples from the Deilmann Pit revealed a number of alteration phases. Dickite is prevalent in the northeastern corner of the pit and is interpreted as part of the regional background signature. Illite occurs everywhere, but is most abundant along the outer edges of the pit. It may represent part of a regionally extensive (up to 30 km) illite halo that encompasses the major deposits in the southern Athabasca Basin. Kaolinite is spatially associated with faults where it strongly overprints illite alteration. In the basement, kaolinite zones are 2 to 20 m wide, whereas in the Athabasca sandstone they are at least 200 to 300 m wide. Within the sandstone, a zone of dravite, up to 30 to 60 m wide, also coincides with faults. Chlorite is ubiquitous throughout the basement rocks, but as yet, no meaningful patterns have been delineated. Overall, the patterns documented in the pit suggest an earlier background dickite-illite signature was overprinted by a later phase of fluid flow along late faults.

1. Introduction

This report stems from a M.Sc. thesis investigation of the relationships between structure, lithology, alteration, and mineralization in rocks which host the Deilmann orebody of the Key Lake uranium mine. Key Lake is located at the southeastern margin of the Mesoproterozoic Athabasca Basin (Figure 1). The uranium orebodies are located at the unconformity between highly deformed and metamorphosed Paleoproterozoic and Archean basement rocks and overlying, unmetamorphosed fluviatile sandstone of the Athabasca Group. The basement rocks are part of the Wollaston Domain which consists of Paleoproterozoic passive margin sedimentary rocks (Wollaston Group) overlying Archean Rae-Hearne orthogneiss in the hinterland of Paleoproterozoic Trans-Hudson Orogen (Lewry and Sibbald, 1979).

2. General Geology

The Key Lake deposit consists of two orebodies: the Deilmann orebody, to the northeast, and the Gaertner orebody, to the southwest (Figure 2). Both orebodies are located on the northwest-limb of a regional F_2 antiform cored by Archean basement. Basement exposed in the pit comprises Paleoproterozoic supracrustals and derived granitoids. The dominant rock types are graphite-bearing pelitic and psammopelitic rocks, along with non-graphite-bearing psammopelitic and minor calc-silicate bearing-

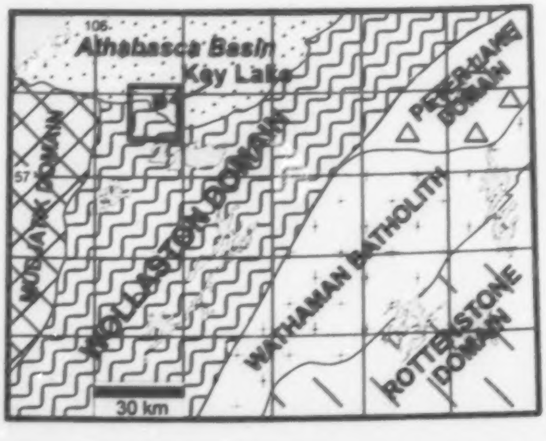

Figure 1 - Location map of the Key Lake uranium mine.

---

[1] Department of Geology, University of Regina, Regina, SK S4S 0A2.

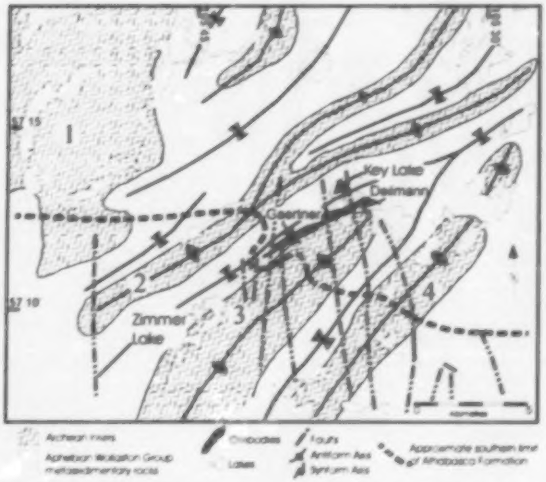

Figure 2 - Sub-Athabasca Precambrian geology of the Key Lake area (modified from Ray, 1977); 1, Orchid Lake inlier; 2, unnamed inlier; 3, Zimmer Lake inlier; and 4, McMillan Lake inlier.

psammitic rocks (Ruhrmann, 1987; Dahlkamp, 1978; Harvey, 1999). These metasedimentary rocks contain abundant partial melt material and are cut by pegmatitic rocks of various ages. The unconformably overlying Manitou Falls Formation of the Athabasca Group comprises up to 60 m of non-marine fluvial quartz sandstone and minor conglomerate bedded at decimetre to metre scale (Ruhrmann, 1987). The alteration history of both the basement rocks and the sandstones of the Athabasca Group is complex and involves regolith development on the unconformity surface, and later silicification, dickitization, illitization, kaolinitization, chloritization, hematitization, and dravitization. The sub-Athabasca unconformity surface exhibits irregular relief, and locally defines a paleovalley with its axis parallel to the main regional structural trends (Harvey, 1999). This linear depression is the result of both primary (erosional) and secondary (faulting) effects. In the pit itself, basal conglomeratic beds of the Athabasca Group onlap onto the unconformity surface, most likely indicating an early valley fill in the subdued basement topography (Harvey, 1999).

3. Rock Types

Basement rocks in the Deilmann pit are represented by: 1) Wollaston Group metasedimentary rocks and 2) Hudsonian intrusive rocks which include two pegmatite suites. The most important units, both lithologically and structurally, are the graphite-bearing pelitic rocks. These rocks are characterized by 5 to 35% graphite along with rarely preserved cordierite and garnet porphyroblasts (Harvey, 1999). The graphitic units are structurally important because they appear to have facilitated early shearing and later faulting. The other metasedimentary units in the basement include non-graphite-bearing and graphite-bearing psammopelitic rocks, along with minor psammitic and calc-silicate-bearing psammitic rocks (Ruhrmann, 1987; Dahlkamp, 1978; Harvey, 1999). Hudsonian intrusive rocks are represented by an early white- to yellow-weathering pegmatite that typically occurs as decimetre- to metre-wide sheets oriented sub-parallel to the main S_1 fabric. These pegmatitic rocks are most commonly concentrated in the sheared graphite-bearing units. A second suite of pegmatitic rocks is represented by a relatively undeformed, irregular, pink, and more alkalic pegmatite that cross-cuts S_1.

The overlying Athabasca Group sedimentary rocks belong to the MFb member of the Manitou Falls Formation. This member consists of quartz sandstone, and subordinate conglomerate which becomes more abundant near the base (Ramaekers, 1990).

4. Structural Geology

Five phases of deformation have been recognized (Harvey, 1999) (Table 1). The first phase of deformation (D_1) resulted in the development of a regionally penetrative foliation (S_1) defined by migmatitic, gneissic layering oriented sub-parallel to the Archean basement/Wollaston Group contact. The S_1 foliation is generally oriented east-northeast and dips moderately to the north. It is paralleled by transposed compositional layering and isoclinal F_1 fold axial planes. Syn- to late-D_1 high-strain zones are defined by proto-mylonitic to locally mylonitic fabrics commonly developed in the graphite-bearing units. Regionally, these high-strain zones may be related to early thrusting in the Wollaston Domain as discussed by Tran *et al.* (1999). Deformation nomenclature has been modified from previous reports (e.g. Harvey, 1999) with previous D_2 involving tight to isoclinal folding, now being considered part of D_1. This is based on the premise that these folds are broadly continuous and coeval with D_1 (Table 1).

The second phase of deformation (D_2) gave the Wollaston Domain its characteristic northeast-southwest-trending structural grain. During this event, the earlier formed S_1 and sub-parallel high-strain fabrics were folded about moderately northeast-plunging axes, forming a set of major, open to tight and typically Z-asymmetric folds. Rarely, an axial planar foliation (S_2) is preserved in the hinge zones of these folds. The axial planes of F_2 folds dip moderately to steeply to the southeast.

D_2 fold limbs are locally cross-cut by post-D_2 ductile to brittle-ductile faults which are oriented sub-parallel to the main foliation (S_1). These high-strain zones are locally and rarely folded by very open F_4 folds.

The third phase of deformation (D_3) formed open- to very open northwest-trending subvertical folds. F_3 folds are fairly rare and are generally expressed only by gentle warping of previous structures (Harvey, 1999).

Table 1 - Correlation between deformation events distinguished in the Wollaston Domain.

Event	This paper	Harvey (1999)	Tran *et al.* (1999); Yeo and Savage (1999)
Regional foliation, isoclinal folds, local mylonite zones	D_1	D_1	D_1
Very tight to isoclinal folds	D_1	D_2	D_2
Dominant open to tight folds	D_2	D_3	D_3
Ductile-brittle shear zones	post-D_2	post- D_3	late- to post D_3
Open to very open folds	D_3	D_4	D_4
Brittle to brittle-ductile faults (east-west-trending in Key Lake area)	D_4	D_5	D_5
Brittle, subvertical faults (northwest-trending in Key Lake area)	D_5	D_6	D_6

D_4, the fourth deformation event, is represented by a system of brittle faults that are generally oriented east-west, dip moderately to steeply to the north and are oriented sub-parallel to the main S_1 foliation (Figure 3) (Harvey, 1999). The fault system is dominated by one main fault, the Key Lake Fault, and an associated group of smaller, anastomosing faults. These structures are believed to represent reactivation of the ductile to brittle-ductile, post-D_2, pre-D_3, faults that cross-cut F_2 folds (Harvey, 1999). In the basement, the faults appear to have been concentrated in the previously sheared (late-D_1) graphitic-units. Remobilization of graphite into the fault structures has caused enrichment of graphite (up to 60% graphite) which has imparted a black colour to fault rocks. The fault system was clearly active after deposition of the Athabasca sandstone and resulted in up to 10 m of vertical offset of the unconformity surface along with major brecciation in the Athabasca sandstone. This sense of offset is consistent with reverse slip and moderately plunging slickenstriae indicate an oblique component whereby the hangingwall moved towards the southwest over the footwall.

The last phase of deformation (D_5) is represented by a set of brittle, northwest-trending, subvertical faults that are generally curvilinear and anastomosing (Figure 3) (Harvey, 1999). These faults are well developed in the basement rocks and only locally penetrate into the overlying sandstone. In the basement, they display sinistral-oblique offset, whereas in the overlying sandstone minor normal and reverse senses of displacement have been observed, likely indicating several phases of reactivation.

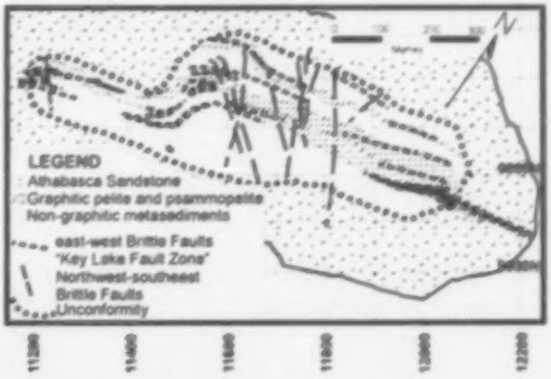
LEGEND
Athabasca Sandstone
Graphitic pelite and psammopelite
Non-graphitic metasediments
east-west Brittle Faults "Key Lake Fault Zone"
Northwest-southeast Brittle Faults
Unconformity
N
11200
11400
11600
11800
12000
12200

Figure 3 - General structural geology of the Deilmann Pit.

5. Unconformity Surface

In 1999, a shallow sub-Athabasca paleovalley was identified in the Deilmann pit (cover photo; Harvey, 1999). Specifically, it was proposed that, prior to Athabasca sandstone deposition, there was preferential erosion of weaker graphitic rocks and fault zones, which resulted in negative topographic relief. Further relief of the unconformity surface was generated by post-Athabasca reactivation of these faults. Following the 1999 field season, depth to basement (unconformity) data from approximately 2200 diamond drill holes was used to obtain a three dimensional form of the depression. The paleovalley has an east-northeast-trending axis and varies in width from tens of metres to greater than 500 m (Figure 4). The paleovalley is asymmetric in cross-section, with the northern slope steeper than the southern one. Maximum paleo-relief is about 55 to 60 m, with an average slope of 6° to 7°. The elevation of the paleovalley axis grades from about 490 m in the west to about 420 m in the east, giving a slope angle of approximately 1°. It is clear that the main Key Lake Fault parallels the axis of this lineament although the relative contribution of topographic relief (paleovalley) versus fault-induced relief is difficult to assess. Drill hole data indicates that the fault offset is sharp, implying that much of this paleotopography is primary. Further work will be directed at confirming this by removing fault offset(s).

The onlap of basal Manitou Falls Formation (MFb) conglomerates and sandstones onto the basement erosion surface in the Deilmann pit suggests that the basal strata represent an episode of valley fill (Figure 5) (Harvey, 1999). Following infill of the paleotopographic lows, the area was buried by relatively sheet-like upper Manitou Falls Formation (MFb) strata, shed from the east. An intraformational disconformity may cap the valley-fill sediments. Stratigraphic sections in the Deilmann pit have yet to be analyzed in detail, but preliminary work by Yeo *et al.*, this volume) suggests that such a change in sedimentation is present. Such a disconformity, if present, may have exerted control on later uranium-bearing fluid flow.

The relationship between the paleovalley and uranium mineralization is notable. In particular, the orebodies

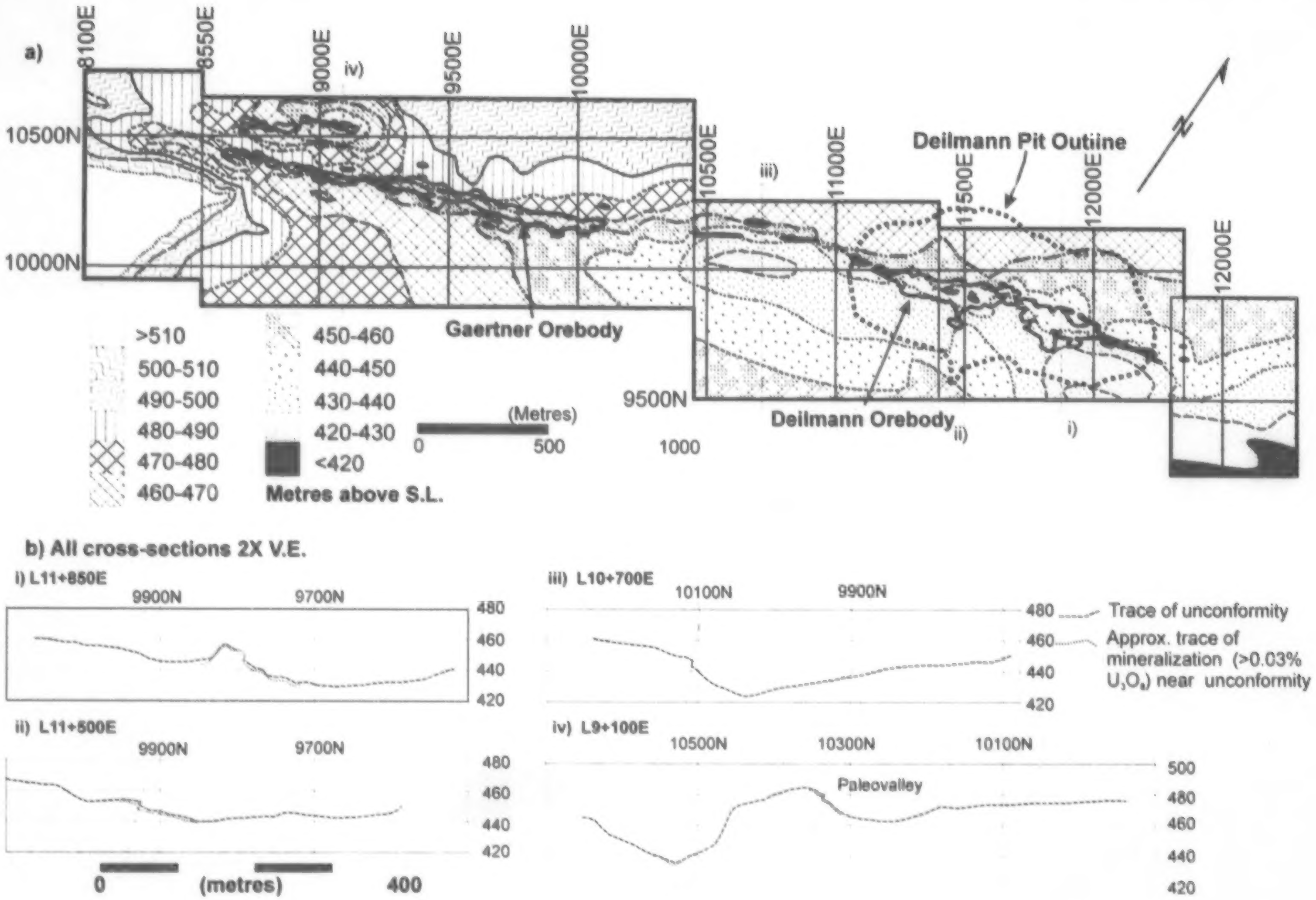
a)
8100E
8550E
9000E
iv)
9500E
10000E
10500E
iii)
11000E
11500E
12000E
12000E
10500N
10000N
9500N
Deilmann Pit Outiine
Gaertner Orebody
Deilmann Orebody
ii)
i)
>510
500-510
490-500
480-490
470-480
460-470
450-460
440-450
430-440
420-430
<420
Metres above S.L.
(Metres)
0
500
1000
b) All cross-sections 2X V.E.
i) L11+850E
9900N
9700N
480
460
440
420
ii) L11+500E
9900N
9700N
480
460
440
420
0
(metres)
400
iii) L10+700E
10100N
9900N
480
460
440
420
Trace of unconformity
Approx. trace of mineralization (>0.03% U3O8) near unconformity
iv) L9+100E
10500N
10300N
10100N
Paleovalley
500
480
460
440
420

Figure 4 - a) Contour map of basement elevation (above sea level) in the Key Lake area. Contour interval is 10 m; b) Cross-sections through the axis of the topographic depression, with 2X vertical exaggeration.

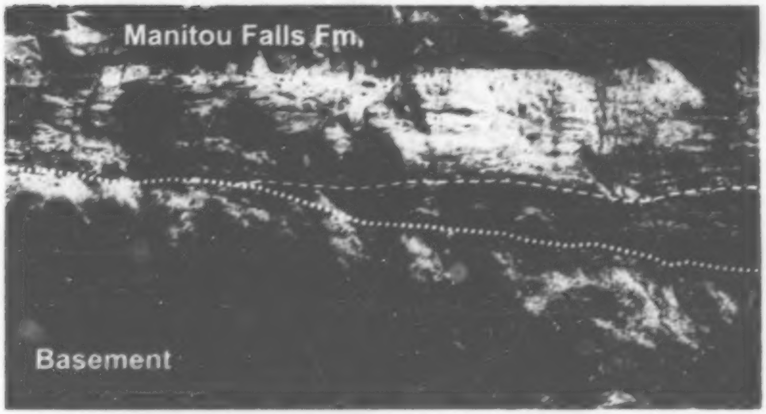

Figure 5 - Lower Manitou Falls Formation conglomeratic layers onlapping the unconformity surface illustrating sedimentation within a paleovalley; upper wide dashed line, onlapping conglomeratic layer and lower narrow dashed line, unconformity (staff for scale).

are spatially associated with the northern slope of the paleovalley, coincident with the main Key Lake Fault, and not the axis of the paleovalley (Figure 4). An interesting feature is a small depression north of the main paleovalley between lines 8600N and 9300N (Figures 4a and 4b iv). This feature has a relatively steep slope of 20° to 25° and drops to a depth of less than 440 m from about 480 m. It is intimately associated with a satellite zone of mineralization lying off the main trend of the major Gaertner and Deilmann orebodies.

6. Alteration

Clay minerals are sensitive indicators of low-temperature changes and record the diagenetic and burial history of sedimentary basins or of host-rock alteration associated with some ore deposit types (Hoeve and Quirt, 1984; Dunoyer de Segonac, 1970). Although the approximate thickness of the Athabasca Group is now about 2 km, Pagel (1975) estimated that it once attained a thickness of approximately 5 km. At such depths, high-grade diagenesis of the sandstone and clay mineral alteration would have occurred (Hoeve and Quirt, 1984). Within the Athabasca Basin, much work has been done on clay mineral paragenesis at both regional and deposit scales (e.g. Earle and Sopuck, 1989; Hoeve and Quirt, 1984; Earle *et al.*, 1999). Most studies utilized X-ray diffraction (XRD) and/or geochemical analysis, but recently the use of near-infrared reflectance spectrometry (PIMA) has become prevalent (Earle *et al.*, 1999). Although opinions vary greatly on clay mineral paragenesis, the main clay constituents in the Athabasca sandstone are generally agreed to be illite, kaolin-minerals, dravite, and chlorite. Total clay contents appear to vary with depth: the upper Athabasca Group sedimentary rocks contain approximately 5%, whereas the lower formations have more variable clay contents of 5 to 20% (Earle and Sopuck, 1989).

Although original detrital clay minerals in the Athabasca sandstone are difficult to assess, Hoeve and Quirt (1984) argued that since the basement source rocks preserve a kaolinitic paleoweathering profile, kaolinite was likely a main constituent. Other clay minerals likely included smectite and related clays, illite and chlorite (Earle and Sopuck, 1989). As burial diagenesis progresses, original clay minerals are converted to other clay minerals (Dunoyer de Segonzac, 1970). At relatively low level diagenetic temperatures of about 100°C, kaolinite can be converted to illite, provided there is sufficient K, Fe or Mg available for reaction (Kisch, 1983; Hoeve and Quirt, 1984). Traditionally, the regional background clays in the Athabasca Group have been reported to be sub-equal amounts of illite and kaolinite. Since temperature is believed to have reached approximately 200°C (Pagel, 1975), kaolinite would likely have been long converted to illite. This raises the question as to why there is still so much kaolinite in the sandstone matrix. The presence of the kaolinite suggests it was either preserved or formed during prograde diagenesis (Earle and Sopuck, 1989). If the kaolinite was the result of prograde diagenesis then the appropriate dilute- and acid-forming formation waters must have been present (Dunoyer de Segonzac, 1970). Recently, the idea that kaolinite is actually a major constituent of the background matrix has been reinterpreted with the notion that dickite (a kaolin polymorph), rather than kaolinite, is the kaolin-mineral in question (Earle *et al.*, 1999). Kisch (1983) proposed that if the sedimentary detritus is alkali- and Fe- or Mg-depleted, kaolinite may persist until it is converted to dickite. Thus, it is possible that the regionally observed kaolin mineral is dickite that was converted from kaolinite (Earle *et al.*, 1999). Alternatively, Hoeve and Quirt (1984) postulated that kaolinite is present as the result of retro-diagenetic kaolinitization along fault-controlled zones. This method seems unlikely as the regional kaolin-rich areas are generally not associated with fault zones (Earle and Sopuck, 1989). The lack of smectites also indicates that temperatures were greater than 100°C, because at that temperature smectites would have been progressively converted to illite (Hoeve *et al.*, 1981).

Fine-grained illite is predominantly formed by the conversion of kaolin minerals (dickite?) (Hoeve and Quirt, 1984). Illitization in the eastern Athabasca Basin appears to vary from north to south. In the north, major kaolin replacement by illite is restricted to areas that are generally less than 5 to 10 km wide and closely associated with mineralization (e.g. Midwest, Cigar

Lake, and McClean Lake; Earle and Sopuck, 1989). In the south, a very large (up to 30 km wide) illite halo encompasses all of the known mineralization in the area (Earle and Sopuck, 1989), but all of the deposits lie in small illite-depleted zones within the larger illite anomaly.

Illite crystallinity can be used as a measure of diagenetic grade. In particular, illite crystallinity changes progressively with depth and temperature and can be used to distinguish the zone of diagenesis from that of low-grade metamorphism (Kubler, 1968). Following early work by Kubler (1968), Esquevin (1969) refined Kubler's technique by plotting Kubler's index against the intensity ratios of (002) and (001) reflections (considered proportional to illite composition). Dunoyer de Segonzac (1970) later subdivided Esquevin's diagram into five distinct fields ranging from incipient diagenesis to low-grade metamorphism (Figure 6; Hoeve *et al.*, 1981). Samples from the eastern Manitou Falls Formation (MFa and b) have variable Kubler values of between 2 and 8, with an average of about 5.45 (Hoeve *et al.*, 1981; Percival *et al.*, 1993) indicating that the illite formed under conditions of high-grade diagenesis (zone III) to anchizone (transition between high-grade diagenesis and low-grade metamorphism). Hoeve and Quirt (1984) observed that samples of illite from the Athabasca sandstone at Key Lake generally have lower Kubler index values (approx. 3.83) than the regional values (Figure 6), which may reflect somewhat higher temperatures at the site of this deposit.

Illite polytypes also change with increasing depth of burial and temperature, reflecting increasing stability, from 1Md (disordered form) to 1M, 2M, and, more rarely, 3M (Kisch, 1983). Regionally, the 1M and 2M illite polytypes are typical (Percival *et al.*, 1993; Hoeve and Quirt, 1984). At many deposits (Key Lake, Cigar Lake, Midwest, McClean Lake, and Collins Bay) the 3M polytype is observed proximal to mineralization (Wilson *et al.*, 1987; Percival *et al.*, 1993). The presence of the 2M and 3M polytypes in the alteration halos suggest temperature was higher than regional estimates (180° to 220°C). This implies that regional high-grade diagenesis locally reached anchizonal conditions (Percival *et al.*, 1993).

Chloritization associated with a 20 to 45 m thick paleoregolith on the basement rocks is observed throughout the Athabasca Basin (Macdonald, 1980). Locally, near mineralization, a hydrothermal chlorite alteration, typically associated with illitization, overprints the paleoregolith (Wilson and Kyser, 1987). At Key Lake, Wilson and Kyser (1987) defined a Mg-chlorite halo, a few tens of metres in diameter, surrounding mineralization, and a Fe-Mg-chlorite halo very close to, and within, the mineralization. The same features are observed at Cigar Lake, where a more distal Mg-chlorite and illite halo gives way to a proximal Fe-Mg chlorite halo near mineralization (Percival *et al.*, 1993).

a) Alteration in the Deilmann Pit

Procedure

Approximately 300 samples of both the Athabasca sandstone and the basement rocks were collected from the periphery of the Deilmann pit for the identification of clay mineral type and abundance (Figure 7a). The deepest parts of the pit were not sampled as they have been flooded. Samples were collected every 10 m along eight sections across-strike (Figure 7a). Near-infrared reflectance spectrometry was used to identify clay minerals with clay content quoted in the relative proportion of clay species. The clay reflectance spectra were acquired using an Integrated Spectronics PIMA-II spectrometer. Many of the sandstone samples were pretreated by heating in a microwave to drive off excess moisture.

Analyses were normalized using the MINSPEC algorithm, a computer program created by Steven Earle (Earle *et al.*, 1999). The MINSPEC algorithm utilizes peak-height ratios and slopes of the spectral curves within the 1300 to 2500 nm wavelength range to estimate proportions of illite, chlorite, dickite, kaolinite, halloysite, and dravite (Earle *et al.*, 1999). The analysis of the basement samples should be treated with caution, as the MINSPEC algorithm was developed on the basis of Athabasca Group samples for which clay mineral proportions had been determined by other techniques. A reference 'library of clay minerals' for the basement has not yet been developed.

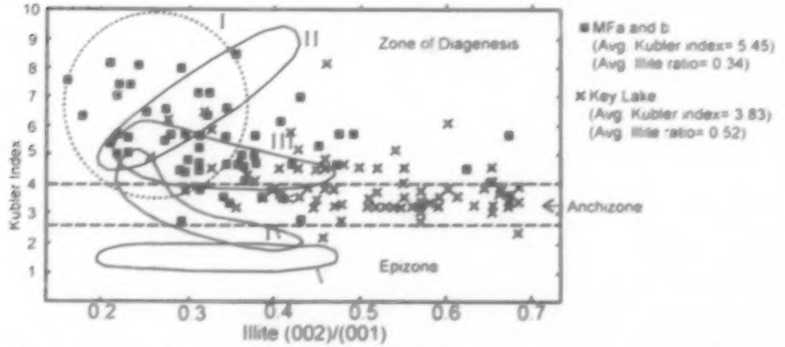

Figure 6 - Esquevin plot with de Segonzac's fields of: I) incipient diagenesis; II) low-grade diagenesis; III) high-grade diagenesis; IV) anchizone; and V) epizone. Samples for the Manitou Falls Formation a and b members in the eastern Athabasca Basin, and Manitou Falls b samples from Key Lake (modified from Hoeve and Quirt, 1984).

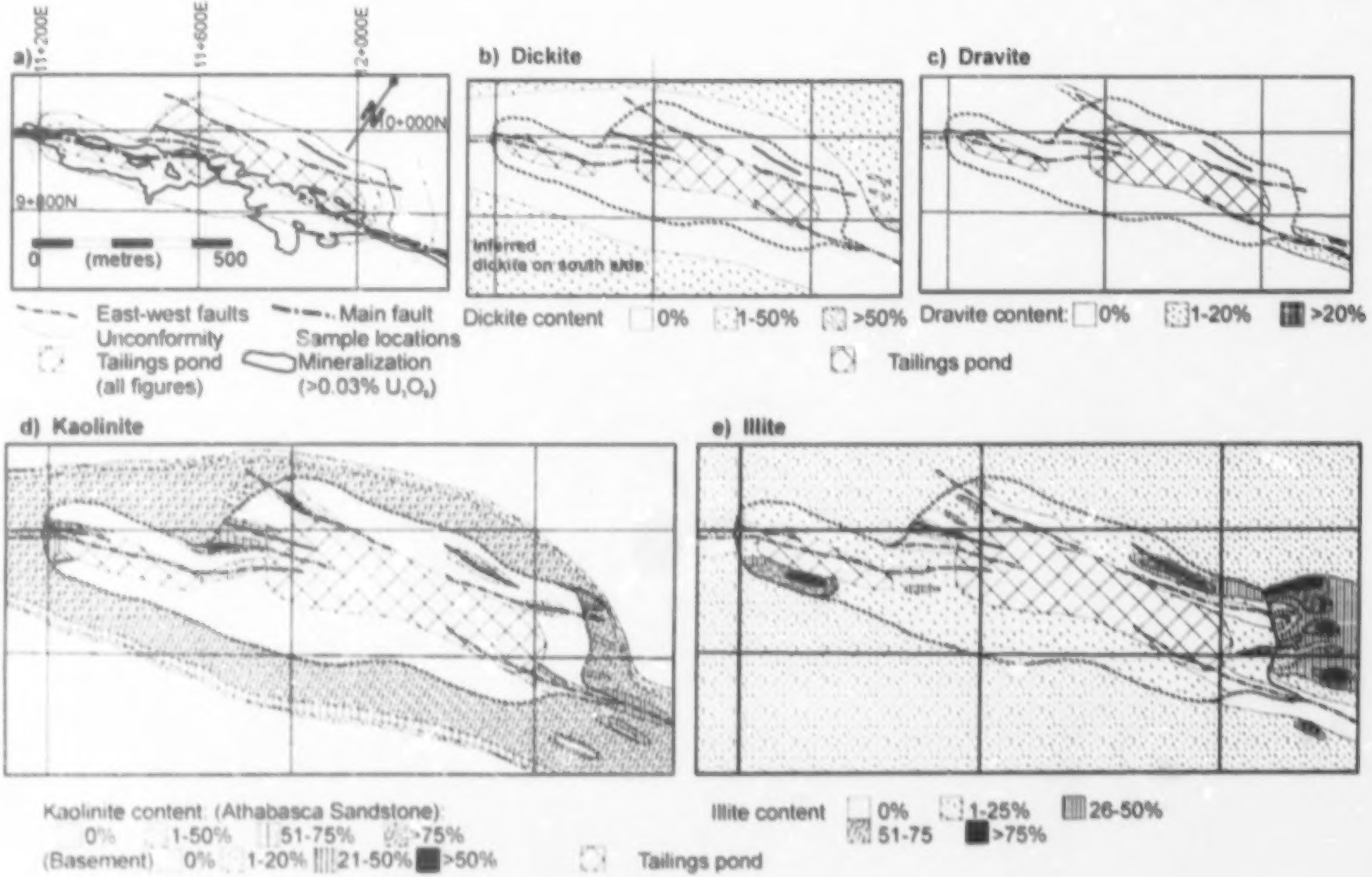
a)
11+200E
11+600E
12+000E
10+000N
9+800N
0
(metres)
500
East-west faults
Main fault
Unconformity
Sample locations
Tailings pond (all figures)
Mineralization (>0.03% U_3O_8)
b) Dickite
Inferred dickite on south side
Dickite content
0%
1-50%
>50%
c) Dravite
Dravite content:
0%
1-20%
>20%
Tailings pond
d) Kaolinite
Kaolinite content: (Athabasca Sandstone):
0%
1-50%
51-75%
>75%
(Basement)
0%
1-20%
21-50%
>50%
e) Illite
Illite content
0%
1-25%
26-50%
51-75
>75%
Tailings pond

Figure 7 - a) Sample locations and general pit geology. Distribution of clay minerals: b) dickite, c) dravite, d) kaolinite, and e) illite. Unconformity as in Figure 3.

Results

Dickite is only present within the Athabasca sandstone in the east-northeast part of the Deilmann pit and varies greatly in quantity, from near 0 up to 72% (Figure 7b). It is never found less than 80 m from the main Key Lake Fault. Outside the limits of the study area it probably constitutes the main "background" (regional) kaolin mineral previously interpreted as kaolinite (Earle and Sopuck, 1989; Earle *et al.*, 1999). Dickite was not detected in basement rocks.

Illitization takes place at the expense of kaolin-group minerals subsequent to kaolinite-to-dickite transformation (Ruhrmann, 1987). The same paragenesis was observed in the Rotliegend sandstone reservoir (North Sea) where kaolinite is inferred to have been converted to dickite followed by illitization of the kaolin minerals (Lanson *et al.*, 1996). Illite, ranging from 0 to 100%, is found in both the Athabasca sandstone and underlying basement rocks (Figure 7e). Generally, illite comprises less than 50%, with small enriched areas containing greater than 50% (Figure 7e). There does not appear to be any trend away from the main fault zone in the basement rocks, possibly indicating that the entire basement sequence in the study area is within the illite-chlorite alteration halo described by Wilson and Kyser (1987). This illite alteration may be a part of Earle and Sopuck's (1989) regional (<30 km wide) illite anomaly that encompasses all the deposits in the southern part of the eastern Athabasca Basin.

Although there are no apparent trends in the illite anomaly, there are local illite depleted zones, both in the basement and the sandstone, that are intimately associated with fault zones where there is also evidence of enrichment of secondary kaolinite. Illite is very depleted near subsidiary faults and is completely absent from the zone of mineralization associated with the main Key Lake Fault (Figure 7e). This correlates with the pattern observed in many other mineralized fault zones in this part of the basin where illite depletion in the basement rocks correlates with anomalous concentrations of late-stage kaolinite (Earle and Sopuck, 1989).

In the Athabasca sandstone, the kaolinite alteration zone is at least 200 to 300 m wide and contains some areas consisting of 100% kaolinite (Figure 7d). The limit of this halo is probably not far beyond the southern margin of the pit. Similar kaolinite halos have been recognized only in the southern deposits of the eastern Athabasca Basin, and, as mentioned earlier, are generally located immediately above mineralization where they overprint the regional illite signature (Earle and Sopuck, 1989). Deposits in the northern part of the basin lack equivalent kaolinitic halos (Hoeve and Quirt, 1984; Earle and Sopuck, 1989). In the basement rocks, kaolinite is rare and is only observed in association with east-west-trending D_4 faults (Figure 7d). This kaolinite alteration zone is generally less than 30 m wide and is widest along the main Key Lake Fault. In these basement fault zones, kaolinite contents average approximately 25%, with some areas containing up to 85% kaolinite. Thus, it appears that late kaolinite alteration is clearly fault-controlled as postulated by Hoeve and Quirt (1984).

Within the Deilmann pit, a strong dravite halo is found within the Athabasca sandstone above the mineralization associated with the main fault at both ends of the pit (Figure 7c). The dravite halo is about 30 to 60 m wide with dravite contents averaging about 26% of the clay matrix, and kaolinite making up the rest. Another small zone of dravite alteration is associated with a fault in the north-central part of the pit. This alteration zone correlates well with fault-related kaolinitization and depletion of illite in the basement rocks (Ruhrmann, 1987). In the basement rocks, dravite is observed only as vein fillings associated with euhedral quartz associated with the main Key Lake Fault.

Chlorite is ubiquitous in the basement rocks, but is not observed of the Athabasca sandstone. The chlorite content in the basement rocks averages 70%, but is highly variable. The overprinting of hydrothermal chlorite on regolith chlorite makes alteration patterns very difficult to assess. At this stage, Mg-rich and Fe-Mg-rich hydrothermal chlorite has not yet been differentiated.

7. Summary and Discussion

a) Unconformity Surface

Contouring depth to basement data has revealed a significant east-northeast-trending topographic depression. Onlapping of basal Manitou Falls strata onto the northern slope of this depression exposed in the Deilmann pit shows that it is, at least in part, a paleovalley. This feature parallels the main structural trend of basement rocks and its northern slope coincides with the Key Lake Fault. The depression has a north-south asymmetry, with the north slope being steeper than the south (Figure 4). Mineralization is generally concentrated on the north slope of the paleovalley where it is cut by the Key Lake Fault. Complexities in the Gaertner area include a small zone of mineralization coincident with an elliptical, satellite depression located north of the main lineament (Figure 4).

This data supports and augments the existing interpretation of the area (Harvey, 1999, Harvey and Bethune, 2000) which holds that early shearing in the basement (late-D_1) was concentrated near the Archean/Wollaston Group contact where graphite-bearing sedimentary rocks were highly sheared and locally mylonitized. Later faulting (D_3 and D_4) was also concentrated in the weaker graphitic units. Preferential erosion of the sheared and faulted metasedimentary rocks between Archean inliers in Paleoproterozoic time resulted in the development of a paleovalley. Early Manitou Falls strata filled in the topographic depressions (paleovalley). Subsequently, the area was buried beneath sheet-like strata shed from the east. The pattern of mineralization suggests that fluid flow was, in part, controlled by topographic relief on the unconformity surface. It is also possible that an intraformational disconformity separates valley fill from overlying Manitou Falls strata.

b) Alteration

The paragenetic sequence of clay minerals in the Deilmann mineralization developed over a long time and is complex. The original clay constituents in the Athabasca sandstone (likely kaolinite, illite, smectite and chlorite) were replaced and converted to other clay minerals during progressive diagenesis. The presence of dickite in the northeastern corner of the pit is interpreted as a part of the regional background signature (Figure 8) (Earle *et al.*, 1999) reported as kaolinite by earlier workers (e.g. Hoeve and Quirt, 1984). The dickite probably results from detrital kaolinite having been progressively converted to the dickite polymorph under K-, Fe- or Mg-depleted conditions of burial diagenesis. According to Kisch (1983), the replacement of kaolinite by dickite is common in quartz-rich sandstone with a predominantly kaolinite matrix analogous to the Athabasca sandstone.

The overprinting of the regional dickite-dominated clay matrix by illite is exemplified by the outer edges of the Key Lake alteration halo. Illitization of dickite is observed in an area that encompasses the entire pit, and, according to Earle and Sopuck (1989), is part of a regionally extensive illite halo up to 30 km wide. Illitization was possibly due to an influx of K, Fe or Mg, or an increase in temperature (Lanson *et al.*, 1996). Illite contents are highly variable, but show clear depletion in fault zones associated with later kaolinite enrichment (Figure 8).

The spatial association of intense kaolinite halos with faults indicates they are the result of late fluids flowing along reactivated east-west trending fault planes (Hoeve and Quirt, 1984). This alteration must have occurred after mineralization, as temperatures of approximately 200°C are believed to have been present during mineralization and at such temperatures, dickite would be the stable kaolin-polymorph, not kaolinite. This late kaolinitization clearly occurred at the expense of illite in the clay matrix, as evidenced by the coupling of zones of illite depletion and kaolinite enrichment (Figure 8).

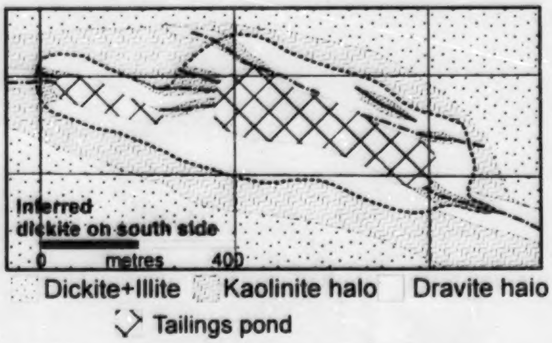

Figure 8 - Compilation of major alteration features in the Deilmann Pit.

The occurrence of dravite also corresponds closely to zones of faulting and mineralization (Figure 8). Dravite formation may have been accompanied by silicification, as dravite typically occurs in basement veins with euhedral quartz, and such zones were only identified below a wide zone of silicification within the Athabasca sandstone. The timing of dravitization is unclear, but Wilson and Kyser (1987) determined $\delta^{18}O$ values of euhedral quartz which constrain isotope equilibration temperatures between 190° to 230°C. As this is the approximate temperature postulated for uranium mineralization (Pagel, 1975), it follows that if the same generation of euhedral quartz is related to dravitization then dravitization, is syn-mineralization.

8. Acknowledgments

Much appreciation goes out to Ken Wasyliuk (Cameco Corporation) and the Cameco Corporation for the use of, and assistance in, PIMA analysis. Financial and logistical assistance from the Cameco Corporation, PNC Exploration Ltd., and COGEMA Resources Inc. is greatly appreciated. Discussions with: Gary Yeo, Gary Delaney, and Ghislain Tourigny (SEM); Dan Brisbin and Vlad Sopuck (Cameco Corporation); Charlie Jefferson (GSC); and numerous field trip participants contributed greatly to this report. Further logistical support was provided by SEM. The review and comments made by SEM geologists and Dan Brisbin is greatly appreciated.

9. References

Dahlkamp, F. J. (1978): Geologic appraisal of the Key Lake U-Ni deposits, northern Saskatchewan; Econ. Geol., v73, p1430-1449.

Dunoyer de Segonzac, C. (1970): The transformation of clay minerals during diagenesis and low-grade metamorphism: A review; Sediment., v15, p281-346.

Earle, S. and Sopuck, V. (1989): Regional lithogeochemistry of the eastern part of the Athabasca Basin uranium province, Sask.; *in* Muller-Kahle, E. (ed.), Uranium Resources and Geology of North America, International Atomic Energy Agency, TEDOC-500, p263-352.

Earle, S., Wheatley, K., and Wasyliuk, K. (1999): Application of reflectance spectrometry to assessment of alteration mineralogy at the Key Lake uranium deposit, Saskatchewan; *in* Ashton, K.E. and Harper, C.T. (eds.), MinExpo'96 Symposium–Advances in Saskatchewan Geology and Mineral Exploration, Sask. Geol. Soc., Spec. Publ. No. 14, p109-123.

Esquevin, J. (1969): Influence de la composition des illites sur leur cristallinite; Bull. Cent. Recher. Pau, v3, p147-153.

Harvey, S.E. (1999): Structural geology of the Deilmann orebody, Key Lake, Saskatchewan; *in* Summary of Investigations 1999, Volume 2, Saskatchewan Geological Survey, Sask. Energy Mines, Misc. Rep. 99-4.2, p100-109.

Harvey, S.E. and Bethune, K.M. (2000): Geology of the Key Lake unconformity-type uranium deposit, Deilmann pit, northern Saskatchewan; *in* GeoCanada 2000, Calgary, May 2000, Conference CD, ext. abstr. #601.

Hoeve, J., Rawsthorn, K., and Quirt, D. (1981): Uranium metallogenic studies: Clay mineral stratigraphy and diagenesis in the Athabasca Group; *in* Summary of Investigations 1981, Saskatchewan Geological Survey, Sask. Energy Mines, Misc. Rep. 81-4, p76-89.

Hoeve, J. and Quirt, D. (1984): Mineralization and host rock alteration in relation to clay mineral diagenesis and evolution of the middle-Proterozoic, Athabasca Basin, northern Saskatchewan, Canada; Sask. Resear. Counc., Tech. Rep. 187, 187p.

Kisch, H.J. (1983): Mineralogy and petrology of burial diagenesis (burial metamorphism) and incipient metamorphism in clastic rocks; *in* Larsen, G. and Chilingar, G.V. (eds.), Developments in Sedimentology- Diagenesis in Sediments and Sedimentary Rocks 2, Elsevier, p289-495.

Kubler, B. (1968): Evaluation quantitative du metamorphisme par la cristallinite de l'illite; Bull. Cent. Recher. Pau, v2, p385-397.

Lanson, B., Beaufort, D., Berger, G., Baradat, J., and Lacharpagne, J. (1996): Illitization of diagenetic kaolinite-to-dickite conversion series: Late-stage diagenesis of the Lower Permian Rotliegend sandstone reservoir, offshore of the Netherlands; J. Sed. Resear., v66, p501-518.

Lewry, J.F. and Sibbald, T.I.I. (1979): A review of the pre-Athabasca basement geology in northern Saskatchewan; *in* Parslow, G.R. (ed.), Uranium Exploration Techniques, Sask. Geol. Soc., Spec. Publ. No. 4, p19-58.

Macdonald, C.C. (1980): Mineralogy and geochemistry of a Precambrian regolith in the Athabasca Basin; unpubl. M.Sc. thesis, Univ. Sask., 151p.

Pagel, M. (1975): Determinations des conditions physiochemiques de la silicification diagenetic des gres Athabasca (Canada): Au moyen des inclusions fluides; Acad. Sci. [Paris] Comptes Rendus, v280, p2301-2304.

Percival, J.B., Bell, K., and Torrance, J.K. (1993): Clay mineralogy and isotope geochemistry of the alteration halo at the Cigar Lake uranium deposit; Can. J. Earth Sci., v30, p689-704.

Ramaekers, P. (1990): Geology of the Athabasca Group (Helikian) in Northern Saskatchewan; Sask. Energy Mines, Rep. 195, 49p.

Ray, G.E. (1977): The Geology of the Highrock Lake–Key Lake Vicinity; Sask. Dep. Miner. Resour., Rep. 197, 36p.

Ruhrmann, G. (1987): The Gaertner uranium orebody at Key Lake (northern Saskatchewan, Canada) after three years of mining: An update of the geology; *in* Gilboy, C.F. and Vigrass, L.W. (eds.), Economic Minerals of Saskatchewan, Sask. Geol. Soc., Spec. Publ. No. 8, p120-137.

Tran, H.T., Yeo, G., and Bethune, K. (1999): Geology of the McKenzie Falls area, Haultain River, Wollaston-Mudjatik domain boundary (NTS 74B-7 and -8); *in* Summary of Investigation 1999, Volume 2, Saskatchewan Geological Survey, Sask. Energy Mines, Misc. Rep. 99-4.2, p55-67.

Wilson, W.R., Kyser, T.K., Mehnert, H.H., and Hoeve, J. (1987): Changes in the H-O-Ar isotope composition of clays during retrograde alteration; Geochim. Cosmochim. Acta, v51, p869-878.

Wilson, W.R. and Kyser, T.K. (1987): Stable isotope geochemistry of alteration associated with the Key Lake uranium deposit, Canada; Econ. Geol., v82, p1540-1557.

Yeo, G. M. and Savage, D. A. (1999): Geology of the Highrock Lake area, Wollaston Domain (NTS-74H-3 and -4); *in* Summary of Investigation 1999, Volume 2, Saskatchewan Geological Survey, Sask. Energy Mines, Misc. Rep. 99-4.2, p38-54.

Paleoproterozoic Thermotectonic Evolution of the Eastern Sub-Athabasca Basement, Northern Saskatchewan: Integrated Geophysical and Geological Data

Philippe Portella [1] and Irvine R. Annesley [2]

Portella, P. and Annesley, I.R. (2000): Paleoproterozoic thermotectonic evolution of the eastern sub-Athabasca basement, northern Saskatchewan: Integrated geophysical and geological data; *in* Summary of Investigations 2000, Volume 2, Saskatchewan Geological Survey, Sask. Energy Mines, Misc. Rep. 2000-4.2.

Abstract

The Cree Lake Zone of northern Saskatchewan forms the southeastern margin of the Archean Hearne craton. It was deformed and metamorphosed during the ca. 1.8 Ga continent-continent collision of the Trans-Hudson Orogen (THO). The Cree Lake Zone is overlain by the ca. 1.7 Ga Athabasca Basin and is the site of numerous unconformity-type uranium deposits and ongoing exploration.

The fold belt nature of the southeastern margin of the Hearne craton was recognized and documented in the 1960s. The thrust belt nature has only been documented in the last 10 years, and more recently, a strike-slip transpressional component of the fold-thrust belt has been identified. A new interpretation of the Paleoproterozoic tectonic evolution of the eastern sub-Athabasca basement advocates that Archean/ Paleoproterozoic rocks in the eastern sub-Athabasca basement experienced the following deformation history:
a) Early D_1 Collisional Stage (1860 to 1835 Ma),
b) D_2 Collisional Stage (1835 to 1820 Ma),
c) D_2 Oblique Collisional Stage (1820 to 1805 Ma),
d) Early D_3 Oblique Collisional Stage (1805 to 1795 Ma),
e) Late D_3 Oblique Collisional Stage (1795 Ma? to 1775 Ma),
f) D_4 Post-Collisional Stage (1775 to 1760 Ma), and
g) D_5 Late Post-Collisional Stage (1760 to 1720 Ma).

Our proposed thermotectonic model is compatible with both geological and geophysical observations/ interpretations, and as well for limited seismic images of the present crustal structure in the region. A critical aspect of the model is that the geological characteristics of the eastern Cree Lake Zone changed significantly from 1860 to 1720 Ma as a consequence of the collision of the THO. This resulted in the southeastern Hearne craton evolving from a foreland collisional (i.e. compressional) fold-thrust belt to a steeply-dipping transpressional plate boundary. Transpression was probably followed by extension from 1760 to 1720 Ma, the time that the Athabasca Basin was being formed.

1. Introduction

The Cree Lake Zone of northern Saskatchewan forms the southeastern margin of the Archean Hearne craton. It was deformed and metamorphosed during the ca. 1.8 Ga continent-continent collision of the Trans-Hudson Orogen (THO). The THO extends from Baffin Island through central Canada (Manitoba and Saskatchewan) to the north-central United States (Hoffman, 1989). The Cree Lake Zone is overlain by the ca. 1.7 Ga Athabasca Basin (Figure 1) and is the site of numerous unconformity-type uranium deposits and ongoing exploration (Matthews *et al.*, 1997). To better understand the genesis of these deposits, the geology of the Wollaston Group and its underlying Archean basement has been studied over the last twelve years (Annesley and Madore, 1991; Annesley *et al.*, 1996, 1997, 1999; Matthews *et al.*, 1997; Tran and Yeo, 1997; Tran *et al.*, 1998, 1999; Madore *et al.*, 1999; Tran and Smith, 1999; and references therein).

Fold-thrust belts are common worldwide. Their main localities include: 1) the foreland side of collisional orogenic belts, 2) restraining bends of strike-slip faults, 3) passive-margin sedimentary basins, and 4) Andean-type backarc regions. The fold belt nature of the southeastern margin of the Hearne craton was recognized and documented in the 1960s by Money (1968) and Weber *et al.* (1975). The thrust belt nature has only been documented in the last 10 years by Annesley and Madore (1991), Hajnal *et al.* (1997), Tran and Yeo (1997), and Tran *et al.* (1998, 1999, 2000). More recently, the strike-slip transpressional component of the fold-thrust belt has been identified by Annesley *et al.* (1996, 1997), the senior author (1999), and Portella and Annesley (2000).

With this in mind, we present a new twist to the interpretation of the Paleoproterozoic tectonic evolution of the eastern sub-Athabasca basement by integrating aeromagnetic data, gravity data, and ground geophysical data with detailed geological studies (Portella and Annesley, 2000).

---

[1] COGEMA Resources Inc., 817 - 825 45th Street West, Saskatoon, SK S7K 3X5; E-mail pportella@cri.ca

[2] Saskatchewan Research Council, 15 Innovation Blvd., Saskatoon, SK S7N 2X8.

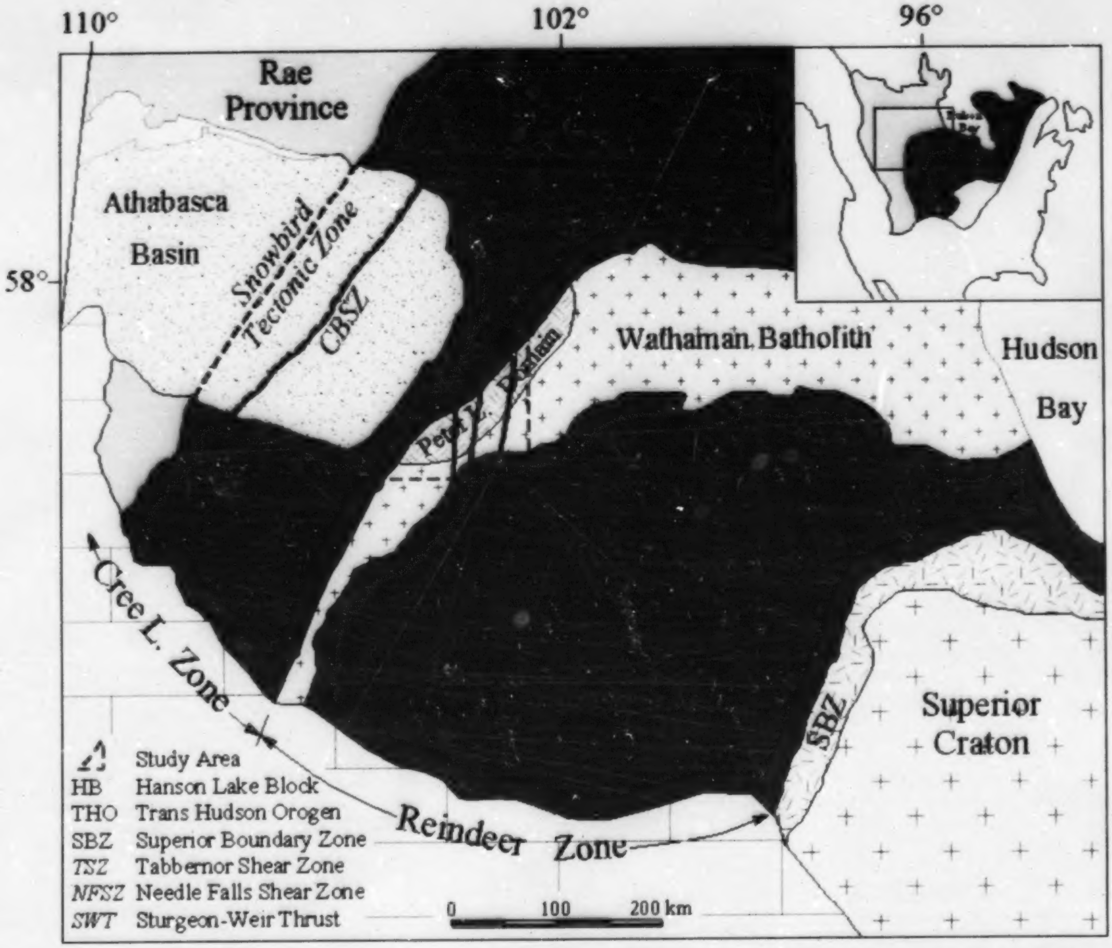
110°
102°
96°
58°
Rae Province
Athabasca Basin
Snowbird Tectonic Zone
CBSZ
Wathaman Batholith
Hudson Bay
Peter L. Domain
Cree L. Zone
Reindeer Zone
SBZ
Superior Craton
Study Area
HB Hanson Lake Block
THO Trans Hudson Orogen
SBZ Superior Boundary Zone
TSZ Tabbernor Shear Zone
NFSZ Needle Falls Shear Zone
SWT Sturgeon-Weir Thrust
0 100 200 km

Figure 1 - Location of the study area and the lithotectonic domains of northern Saskatchewan; CBSZ, Cable Bay Shear Zone.

2. Regional Geology

Basement to the eastern part of the Athabasca Basin comprises rocks of the Wollaston and Mudjatik domains, two of the major lithotectonic subdivisions of the Cree Lake Zone (Lewry and Sibbald, 1977), and also part of the Hearne Province (Bickford *et al.*, 1990; Hoffman, 1989, 1990; Lewry and Collerson, 1990). The Wollaston Domain is a northeast-trending fold-and-thrust belt composed of Paleoproterozoic Wollaston Group metasediments overlying Archean granitoid gneisses, whereas the Mudjatik Domain is a northeast-trending, in part shear-bounded belt consisting mainly of Archean felsic gneisses. The rocks of these domains have been subjected to a complex history of polyphase deformation and metamorphism (Lewry and Sibbald, 1977, 1980; Sibbald, 1983; Annesley and Madore, 1991; Annesley *et al.*, 1996, 1997, 1999; Tran and Yeo, 1997; Tran *et al.*, 1998, 1999, 2000; Madore *et al.*, 1999; Orrell *et al.*, 1999), which can only be unraveled through integrated studies of geological and geophysical data.

Five main deformation phases are recognized. Metamorphic grade in the area varies from amphibolite to granulite facies under high T/medium to low P conditions. These deformation and metamorphic events can be correlated with the thermotectonic evolution of the Trans-Hudson Orogen (Lewry and Sibbald, 1980; Lewry *et al.*, 1985; Lewry, 1987; Machado, 1990; Clowes *et al.*, 1999).

Four main groups of rocks are identified in the basement to the eastern Athabasca Basin. These include: 1) Archean orthogneisses and subordinate rocks, 2) high-grade Paleoproterozoic Wollaston Group metasediments, 3) deformed calc-alkaline granitoids and subordinate gabbroids, and 4) peraluminous granitoids of different petrochemical types.

Four lithostructural sub-domains from east to west are distinguished in the basement: eastern Wollaston Domain (ED), western Wollaston Domain (WD), Wollaston-Mudjatik Transition Zone (WMTZ), and Mudjatik Domain (MD) (Figures 2, 3, 5, 7, 8, and 9). These sub-domains form a paired northwest-dipping hinterland and southeast-dipping foreland to the northwestern THO. The eastern Wollaston Domain corresponds to an aeromagnetic high and comprises a Paleoproterozoic upper sequence of calc-silicate- and magnetite-bearing siliciclastic metasediments overlying a Paleoproterozoic lower sequence of magnetite-rich to magnetite-poor pelitic to psammitic gneisses with locally infolded Archean orthogneisses. The western Wollaston Domain corresponds to an overall aeromagnetic low and consists mainly of a Paleoproterozoic lower sequence of graphitic pelitic gneiss, garnetite, pelitic gneiss, calc-pelitic gneiss, psammopelitic gneiss, psammitic gneiss, and meta-quartzite overlying and intercalated with Archean orthogneisses. This domain and the WMTZ are structurally complex, comprising elongated Archean granitoid domes (mega-boudins), interpreted thrust- and strike-slip structures, and related duplex structures. The authors interpret the WMTZ as a curvilinear deformation front of a foreland fold-thrust belt related to the THO collision. The mega-boudins are less deformed and larger in the WMTZ, suggesting that the deformation front has propagated from southeast to northwest. Also, this front possibly delineates the transition from thick-skin (east) to thin-skin tectonics (west). The Mudjatik Domain is composed mainly of variably reworked Archean orthogneisses with a thin skin of polydeformed Wollaston Group metasediments.

3. A Model for Thermotectonic Evolution of the Eastern Sub-Athabasca Basement

A recent structural interpretation of the eastern Athabasca Basin by the senior author complements the history of late- and post-collisional thermotectonic events by Annesley *et al.* (1996, 1997) for the Archean/Paleoproterozoic basement complex of the Wollaston Lake area and the basement to the southeastern Athabasca Basin.

Archean/Paleoproterozoic rocks in the eastern sub-Athabasca basement were involved in five major stages of deformation and metamorphism (Figures 2, 3, 5, 7, 8, and 9), outlined below.

a) Early D_1 Collisional Stage (1860 to 1835 Ma)

The D_1 deformation is responsible for rootless isoclinal folds (F_1), a regional axial planar foliation (S_1), and a basement/cover décollement surface (Figure 2). This stage is poorly understood.

b) D_2 Collisional Stage (1835 to 1820 Ma)

The D_2 deformation produced the regionally penetrative S_2 gneissic foliation and the northeast-trending, doubly-plunging regional folds. This stage included a continuation of stage one metamorphism along a prograde clockwise P-T-t path at peak pressures (6 to 9 kbar) and approaching peak temperatures (Annesley *et al.*, 1996, 1997; Madore *et al.*, 1996, 1999; Tran and Yeo, 1997; Tran *et al.*, 1998, 1999).

c) D_2 Oblique Collisional Stage (1820 to 1805 Ma)

Steep, sinistral strike-slip shear zones were produced during this late D_2 transpressional stage (Figure 3). The area south of McArthur River is characterized by a system of sinistral strike-slip ductile shear zones, which define three or more north-northeast-trending tectonic corridors with an internal clockwise rotation of D_1/D_2 folds (Figure 3B). This system is interpreted as part of a 'lateral extrusion' feature of the THO collision. This stage involved complex modification of the Wollaston Group metasediments and the upper part of the Archean basement (Figure 4) at peak metamorphic temperatures (750° to 850°C, see Figure 9 of Madore *et al.*, 1999) with intrusion of abundant leucogranites and pegmatites (Annesley and Madore, 1999). Recent geological mapping by Yeo and Savage (1999) supports this interpretation of the late D_2 sinistral shears.

Table 1 - Comparison of proposed deformation events proposed for the basement to the eastern Athabasca Basin.

Annesley *et al.* (1996, 1997, 1999)	Portella and Annesley (2000, this study)	Wallis (1970, 1971)	Lewry and Sibbald (1980)	Tran and Yeo (1997)	Tran and Smith (1999) Tran *et al* (1999) Yeo and Savage (1999)
Age			**Deformation Events**		
1860 to 1835 Ma	D_1	D_1	D_1	D_1	D_1/D_2
1835 to 1820 Ma	D_2	D_2	D_3	D_2	D_3
1820 to 1805 Ma	late D_2				
1805 to 1795? Ma	early D_3			D_3	
		D_3	D_2		D_4
1795? to 1775 Ma	late D_3			late D_2	
1775 to 1760 Ma	D_4	D_4	D_4		D_5
1760 to 1720 Ma	D_5		D_5	D_4	D_5

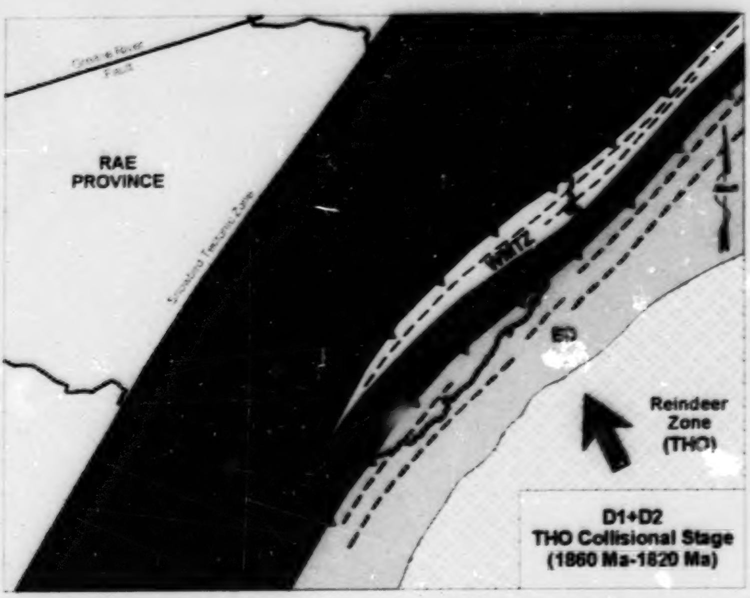

Figure 2 - Interpretation of the early D_1/D_2 collisional stage in the eastern Athabasca region. Note the WMTZ which dies out towards the southwest. Structural elements and lithotectonic domains for Figure 2 and the following figures are interpreted from aeromagnetic geophysical data and correlated with existing ground geophysical, drill hole, and outcrop data. Dashed lines are schematic fold axes, and barbed solid lines are actual thrust structures.

d) Early D_3 Oblique Collisional Stage (1805 to 1795? Ma)

The D_3 deformation produced broad open, upright, northwest-trending folds, kinks, and crenulations (Figures 5 and 6).

e) Late D_3 Oblique Collisional Stage (1795? Ma to 1775 Ma)

This late stage of transpression included development of amphibolite-facies shear zones with a strong dextral strike-slip component and retrograde movement of older shear zones. It involved the Needle Falls Shear Zone (NFSZ) and Cable Bay Shear Zone (CBSZ) (Figure 7A and 7C), and the generation of 070°, 090°, and 110° structures between them. These structures controlled the location of major unconformity-type uranium deposits (e.g. Cigar Lake, Figure 7B). The movement along these structures is revealed by drag folding with anti-clockwise rotation of D_2 folds (Figure 7C). It also included apparent rotation of the main shortening axis and development of accommodation features due to vertical uplift (i.e. extension). The authors interpret this stage to be the result of the oblique collision of the east Alberta Orogen (Ross *et al.*, 1995, 2000) with the Hearne Province, as late THO transpression and uplift was ongoing.

f) D_4 Post-Collisional Stage (1775 to 1760 Ma)

The D_4 deformation gave rise to north-northeast-trending, sinistral, oblique-slip reverse faults and reactivation of late D_2 sinistral shear zones (Figure 8). This stage involved continued localized adjustments along an essentially isobaric cooling path under ductile-brittle conditions.

g) D_5 Late Post-Collisional Stage (1760 to 1720 Ma)

This stage involved continued crustal adjustments under essentially brittle conditions. D_5 deformation produced north-northwest- and northwest-trending sinistral faults (Figure 9), which include the northern extension of the Tabbernor fault system.

4. Discussion

We have developed a thermotectonic model that is compatible with both geological and geophysical observations/interpretations, and as well for limited seismic images of the present crustal structure in the eastern part of the Athabasca Basin (Hajnal *et al.*, 1997; Matthews *et al.*, 1997). A critical aspect of the model is that the geological characteristics of the eastern Cree Lake Zone changed significantly from 1860 to 1720 Ma as a consequence of the collision of the THO (Annesley *et al.*, 1997). This resulted in the southeastern Hearne craton evolving from a foreland collisional (i.e. compressional) fold-thrust belt to a steeply-dipping transpressional plate boundary. Transpression was probably followed by extension from 1760 to 1720 Ma, the time that the Athabasca Basin was being formed.

When compared with the plastic deformation models of Beaumont *et al.* (1995, 1996) and Ellis (1996), the tectonic models from our research allow the following observations and interpretations. The WMTZ corresponds to a retroshear zone, which would be a zone of heterogeneous high strain that is overall southeast-dipping. Southeast-dipping shear zones are well shown on the seismic images of the Points North road profile (Hajnal *et al.*, 1997). This model also accommodates an increase in vertical uplift westward across the WMTZ to the Mudjatik Domain with the exposure of deeper crustal rocks. Higher pressure granulite facies rocks are intersected in drill core as one proceeds to the northwest (Madore and Annesley, unpubl. data). This is also compatible with a thinner veneer of Wollaston Group supracrustals in the Mudjatik Domain (Lewry and Sibbald, 1977, 1980).

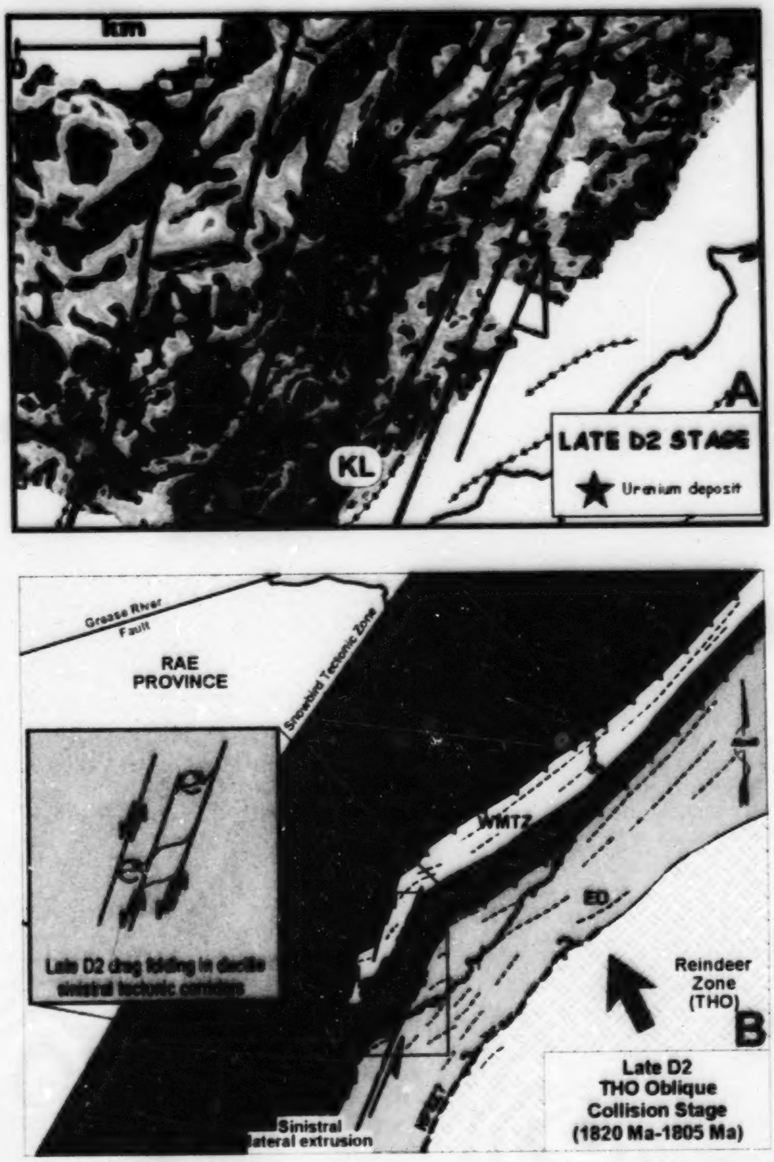
km
0
KL
A
LATE D2 STAGE
Uranium deposit
Grease River Fault
RAE PROVINCE
Snowbird Tectonic Zone
e
e
Late D2 drag folding in ductile sinistral tectonic corridors
WMTZ
ED
Reindeer Zone (THO)
B
Late D2 THO Oblique Collision Stage (1820 Ma-1805 Ma)
Sinistral lateral extrusion
NFSZ

Figure 3 - A) Vertical gradient anomaly map, plotted as grey scale, of the southeastern Athabasca Basin showing the interpreted late D_2 sinistral shears. Lines with dots represent D_2-folded foliation trends, which correspond to EM conductors. These shear zones are confirmed by drill hole geological data (COGEMA, int. rep., 1999) and outcrop mapping along the Key Lake road (see Figure 4, from Annesley and Madore, 1991). *KL is the Key Lake uranium deposits.
B) Structural interpretation of the late D_2 oblique collision stage. Inset box shows the details of our interpretation for the late D_2 drag folding within the ductile sinistral tectonic corridors. NFSZ, Needle Falls shear zone.

Our model is also consistent with the plastic deformation models of Beaumont *et al.* (1995, 1996) and Ellis (1996) in that northwest-dipping proshear zones of presumed Hudsonian age lie beneath the Peter Lake Domain and extend beneath and into the eastern parts of the Wollaston Domain. Tran and Yeo (1997) documented some major northwest-dipping shear zones in the eastern Wollaston Domain.

5. Conclusions

The eastern sub-Athabasca basement records a complex deformation history related to the THO. This orogenic fold-and-thrust belt is comparable to recent continent-continent collision zones, like the Himalayas (Haq and Davis, 1997). We interpret the eastern sub-Athabasca basement deformation to have been even more complicated than the Himalayan model because of the interaction of an adjacent continent-continent collision zone to the west: the eastern Alberta orogen (Ross *et al.*, 2000). The CBSZ could be considered as a post-collisional escape feature of this other Hudsonian orogen.

6. Acknowledgments

The authors acknowledge the support of, and the permission to publish from, COGEMA Resources Inc. and the Saskatchewan Research Council. The review and critical comments by Saskatchewan Energy and Mines geologists are greatly appreciated.

7. References

Annesley, I.R. and Madore, C. (1991): The Wollaston Group and its underlying Archean basement: Final Report; Sask. Resear. Counc., Publ. R-1230-4-C-91, 140p.

__________ (1999): Leucogranites and pegmatites of the sub-Athabasca basement, Saskatchewan: U protore?; *in* Stanley, C.J. need other authors (eds.), Mineral Deposits: Processes to Processing, Balkema, v1, p297-300.

Annesley, I.R., Madore, C., Shi, R., and Krogh, T.E. (1996): U-Pb geochronology and thermotectonic history of the Wollaston Domain in the Wollaston Lake area, Hearne Province, Saskatchewan; Geol.

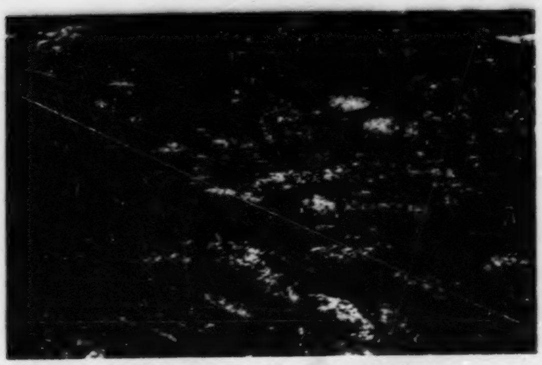

Figure 4 - Field photo of highly sheared Archean orthogneisses (A89-013) from south of Key Lake. Note the hammerhead at upper right corner for scale. Photo taken of flat-lying surface looking southeast.

Figure 6 - Field photo of F_3 folds in metaquartzites (A94-012) from an island outcrop east of Rabbit Lake. Photo taken looking southeast. Note the penknife at center of photo for scale.

Assoc. Can./Miner. Assoc. Can., Prog. Abstr., v21, pA-4.

__________ (1997): U-Pb geochronology of thermotectonic events in the Wollaston Lake area, Wollaston Domain: A summary of 1994-1996 results; *in* Summary of Investigations 1997, Saskatchewan Geological Survey, Sask. Energy Mines, Misc. Rep. 97-4, p162-173.

Annesley, I.R., Madore, C., Krogh, T.E., Kwok, Y.Y., and Kamo, S.L. (1999): New U-Pb zircon and monazite geochronological results for Archean and Paleoproterozoic basement to the southeastern part of the Athabasca Basin, Saskatchewan; *in* Summary of Investigations 1999, Volume 2, Saskatchewan Geological Survey, Sask. Energy Mines, Misc. Rep. 99-4.2, p90-99.

Beaumont, C., Ellis, S., Hamilton, J., and Fullscak, P. (1995): A geodynamical model of the transition from subduction to collision tectonics and its application to the eastern Trans-Hudson Orogen; *in* Trans-Hudson Orogen Transect, LITHOPROBE Rep. 47, p231-243.

__________ (1996): Mechanical model for subduction-collision tectonics of Alpine-type compressional orogens; Geol., v24, p675-678.

Bickford, M.E., Collerson, K.D., Lewry, J.F., Van Schmus, W.R., and Chiarenzelli, J.R. (1990): Proterozoic collisional tectonism in the Trans-Hudson Orogen, Saskatchewan; Geol., v18, p14-18.

Clowes, R., Cook, F., Hajnal, Z., Hall, J., Lewry, J., Lucas, S., and Wardle, R. (1999): Canada's LITHOPROBE Project (Collaborative, multidisciplinary geoscience research leads to new understanding of continental evolution); Episod., v22, p3-20.

Ellis, S. (1996): Forces driving continental collision: Reconciling identification and mantle subduction tectonics; Geol., v24, p699-701.

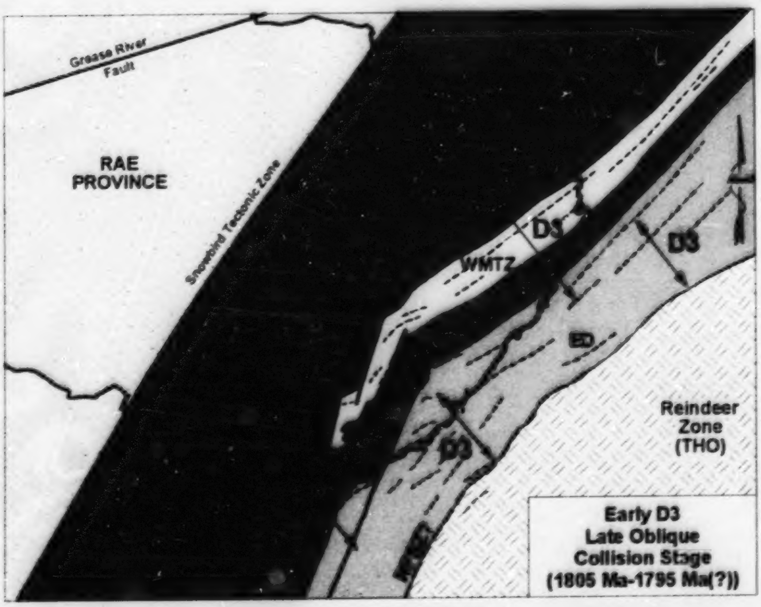

Figure 5 - Structural interpretation of the early D_3 late oblique collisional stage. Double-end arrows indicate D_3 shortening direction. NFSZ as in Figure 3.

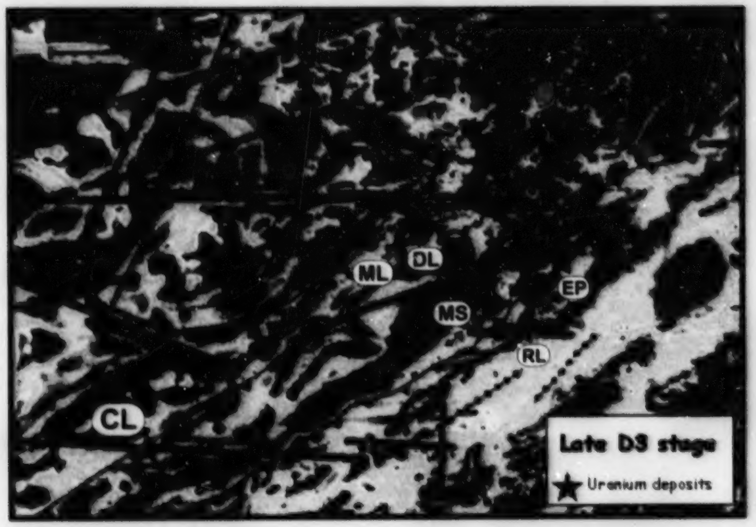
ML
DL
EP
MS
RL
CL
Late D3 stage
Uranium deposits

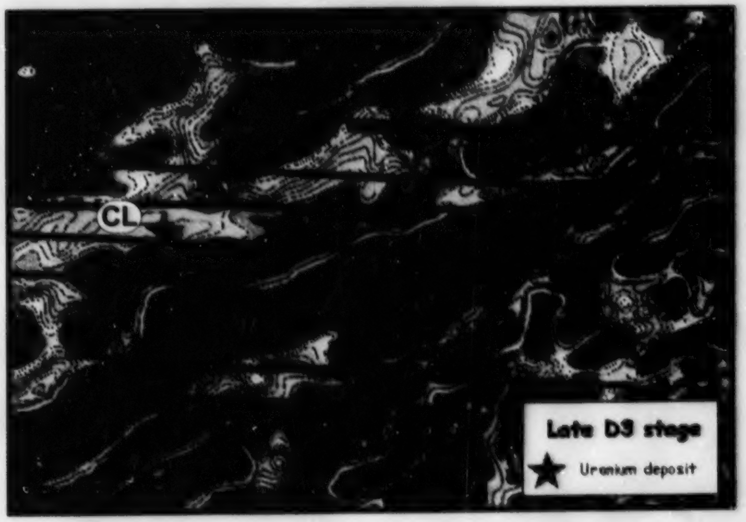
CL
Late D3 stage
Uranium deposit

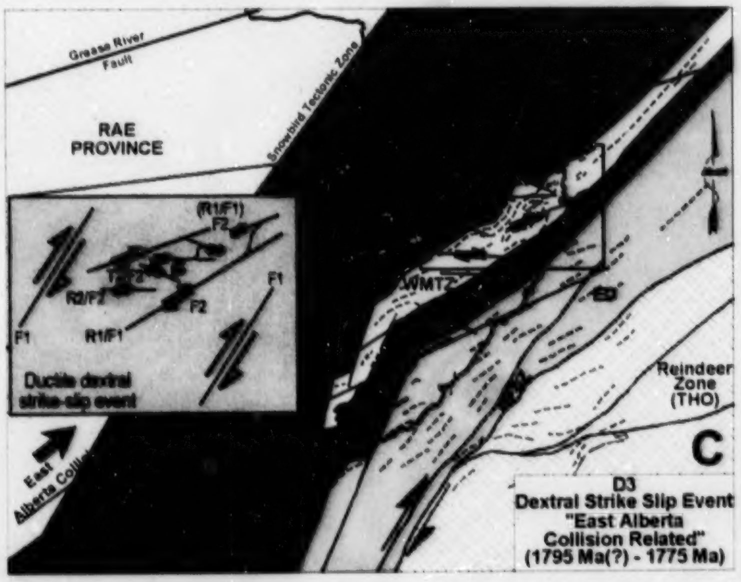
Grease River Fault
Snowbird Tectonic Zone
RAE PROVINCE
(R1/F1)
F2
R2/F2
F1
R1/F1
F2
F1
Ductile dextral strike-slip event
WMTZ
Reindeer Zone (THO)
C
East Alberta Coll
D3
Dextral Strike Slip Event
"East Alberta Collision Related"
(1795 Ma(?) - 1775 Ma)

Figure 7 - A) Vertical gradient anomaly map, plotted as grey scale, of the eastern Athabasca Basin showing the late D_3 dextral shears from Cigar Lake to northeast of Eagle Point. Dotted lines represent D_2-folded foliation trends, which correspond to known EM conductors. Stars represent: CL, Cigar Lake; ML, Midwest Lake; DL, Dawn Lake; MS, McClean Lake/Sue; RL, Rabbit Lake; and EP, Eagle Point uranium deposits.
B) Enlargement of magnetic anomaly trend at Cigar Lake showing the major east-west tectonic corridor. The eastern extension of this dextral shear zone is observed on island outcrops in Wollaston Lake. Measured kinematics give oblique dextral slip movement with a 30° plunge.
C) Structural interpretation of the dextral strike-slip component of the late D_3 oblique collisional stage. Inset box shows the details of our interpretation for the generation of 070°, 090°, and 110° structures. NFSZ as in Figure 3.

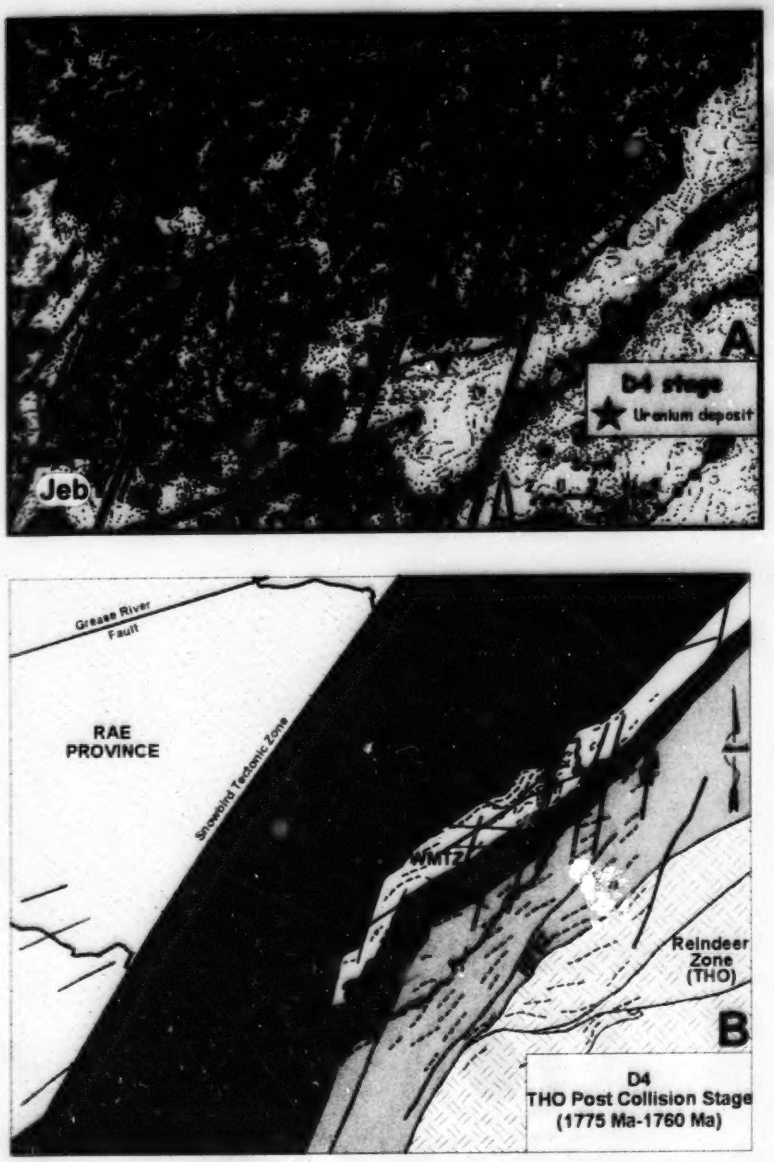

Figure 8 - A) Vertical gradient anomaly map, plotted as grey scale, of the Hatchet Lake area showing the D_4 post-collisional, sinistral ductile-brittle shears. Dotted lines represent D_2-folded foliation trends. Barbed lines correspond to interpreted D_1 /D_2 thrusts. Star denotes the Jeb uranium deposit.
B) Structural interpretation of the D_4 post-collisional stage. This interpretation implicates reactivation of late D_2 sinistral faults. The sinistral displacement for each fault is 1 to 5 km in magnitude. NFSZ as in Figure 3.

Hajnal, Z., Annesley, I.R., White, D., Matthew, R.B., Sopuck, V., Koch, R., Leppin, M., and Ahuja, S. (1997): Sedimentary-hosted mineral deposits: A high-resolution seismic survey in the Athabasca Basin; *in* Gubins, A.G. (ed.), Proceedings of Exploration 97, Fourth Decennial International Conference on Mineral Exploration, p421-432.

Haq, S.S.B. and Davis, D.M. (1997): Oblique convergence and the lobate mountain belts of western Pakistan; Geol., v25, p23-26.

Hoffman, P.F. (1989): Precambrian geology and tectonic history of North America; *in* Bally, A.W. and Palmer, A.R. (eds.), The Geology of North America - An Overview, Geol. Soc. Amer., vA, p447-512.

_________ (1990): Subdivision of the Churchill province and extent of the Trans-Hudson Orogen; *in* Lewry, J.F. and Stauffer, M.R. (eds.), The Early Proterozoic Trans-Hudson Orogen of North America, Geol. Assoc. Can., Spec. Pap. 37, p15-39.

Lewry, J.F. (1987): The Trans-Hudson Orogen: Extent, subdivisions, and problems; Geol. Assoc. Can./Miner. Assoc. Can., Prog. Abstr., v12, p67.

Lewry, J.F. and Collerson, K.D. (1990): The Trans-Hudson Orogen: Extent, subdivision and problems; *in* Lewry, J.F. and Stauffer, M.R. (eds.), The Early Proterozoic Trans-Hudson Orogen of North America, Geol. Assoc. Can., Spec. Pap. 37, p1-14.

Lewry, J.F. and Sibbald, T.I.I. (1977): Variation in lithology and tectonometamorphic relationships in the Precambrian basement of northern Saskatchewan; Can. J. Earth Sci., v14, p1453-1467.

_________ (1980): Thermotectonic evolution of the Churchill Province in northern Saskatchewan; Tectonophys., v68, p45-82.

Lewry, J.F., Sibbald, T.I.I., and Schledewitz, D.C.P. (1985): Variation in character of Archean rocks in the western Churchill Province and its significance; *in* Ayers, L.D., Thurston, P.C., Card, K.D., and Weber, W. (eds.), Evolution of Archean Supracrustal Sequences, Geol. Assoc. Can., Spec. Pap. 28, p239-261.

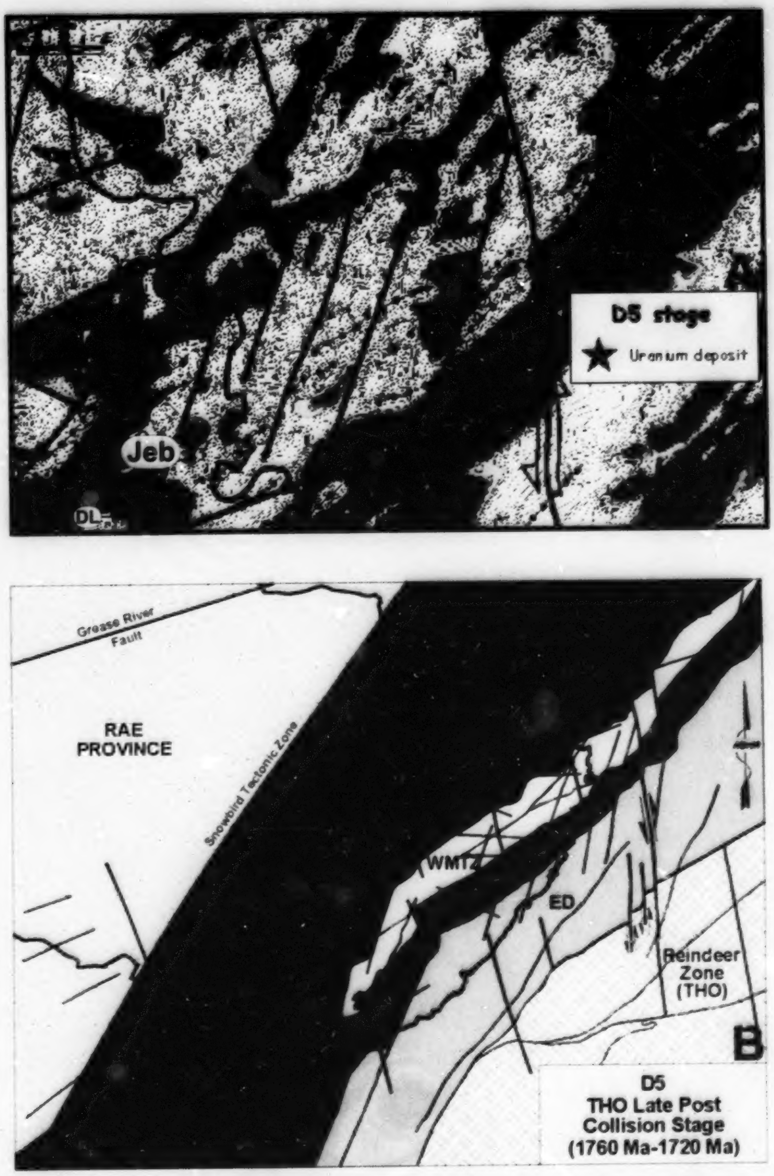

Figure 9 - A) Vertical gradient anomaly map, plotted as grey scale, of the Hatchet Lake area showing the main D_5 sinistral brittle faults. The D_5 faults are sub-vertical with overall steep slickensides. Star denotes the Jeb Lake uranium deposit. B) Structural interpretation of the D_5 late post-collisional stage.

Machado, N. (1990): Timing of collisional events in the Trans-Hudson Orogen: Evidence from U-Pb geochronology for the New Quebec Orogen, the Thompson Belt, and the Reindeer Zone (Manitoba and Saskatchewan); *in* Lewry, J.F. and Stauffer, M.R. (eds.), The Early Proterozoic Trans-Hudson Orogen of North American, Geol. Assoc. Can., Spec. Pap. 37, p433-441.

Madore, C., Annesley, I.R., and Shi, R. (1996): Regional metamorphism in the Wollaston Lake area, Wollaston Domain, Hearne Province, Saskatchewan; Geol. Assoc. Can./Miner. Assoc. Can., Abstr., v21, pA-61.

Madore, C., Annesley, I.R., and Tran, H.T. (1999): Petrology and geochemistry of Paleoproterozoic Wollaston Group metasediments from the eastern Keller Lake–Siemens Lake area, Saskatchewan: A preliminary interpretation; *in* Summary of Investigations 1999, Volume 2, Saskatchewan Geological Survey, Sask. Energy Mines, Misc. Rep. 99-4.2, p80-89.

Matthews, R., Koch, R., Leppin, M., Powell, B., and Sopuck, V. (1997): Advances in integrated exploration for unconformity uranium deposits in Western Canada; *in* Gubins, A.G. (ed.), Proceedings of Exploration 97: Fourth Decennial International Conference on Mineral Exploration, p993-1002.

Money, P.L. (1968): The Wollaston Lake Fold Belt System, Saskatchewan, Manitoba; Can. J. Earth Sci., v5, p1489-1504.

Orrell, S.E., Bickford, M.E., and Lewry, J.F. (1999): Crustal evolution and age of thermotectonic reworking in the western hinterland of the Trans-Hudson Orogen, northern Saskatchewan; Precamb. Resear., v95, p187-223.

Portella, P. and Annesley, I.R. (2000): Paleoproterozoic tectonic evolution of the eastern sub-Athabasca basement, northern Saskatchewan: Integrated magnetic, gravity, and geological data; GeoCanada 2000, Calgary, May 2000, Conference CD, ext. abstr. #647.

Ross, G.M., Eaton, D.W., Boerner, D.E., and Miles W. (2000): Tectonic entrapment and its role in the evolution of continental lithosphere: An example from the Precambrian on western Canada; Tectonics, v19, p116-134.

Ross, G.M, Milkereit, B., Eaton, D., White, D., Kanesewich, E.R., and Burianyk, M.J.A. (1995): Paleoproterozoic collisional orogen beneath the western Canada sedimentary basin imaged by LITHOPROBE crustal seismic reflection data; Geol., v23, p195-199.

Sibbald, T.I.I. (1983): Geology of the crystalline basement, NEA/IAEA Athabasca Test area; *in* Cameron, E.M. (ed.), Uranium Exploration in Athabasca Basin, Geol. Surv. Can., Pap. 82-11, p1-14.

Tran, H.T., Lewry, J.F., Bethune, K., Ashton, K., Yeo, G., and Ansdell, K. (2000): Crustal thrusting and tectonic imbrication in the Cree Lake Zone, northern Saskatchewan: Implications for the tectonic evolution of western foreland of the Trans-Hudson Orogen; GeoCanada 2000, Calgary, May 2000, Conference CD, ext. abstr. #543.

Tran, H.T. and Smith, M. (1999): Geology of the Cup-Keller-Schmitz lakes transect of the Wollaston-Mudjatik domains boundary; *in* Summary of Investigations 1999, Volume 2, Saskatchewan Geological Survey, Sask. Energy Mines, Misc. Rep. 99-4.2, p68-79.

Tran, H.T. and Yeo, G.M. (1997): Geology of the Burbidge Lake–northern upper Foster Lake area, eastern Wollaston Domain (NTS 74A-14); *in* Summary of Investigations 1997, Saskatchewan Geological Survey, Sask. Energy Mines, Misc. Rep. 97-4, p72-89.

Tran, H.T., Yeo, G.M., and Bethune, K. (1999): Geology of the McKenzie Falls area, Haultain River, Wollaston-Mudjatik domains boundary (NTS 74B-7 and -8); *in* Summary of Investigations 1999, Volume 2, Saskatchewan Geological Survey, Sask. Energy Mines, Misc. Rep. 99-4.2, p55-67.

Tran, H.T., Yeo, G.M., Bradley, S., and Lewry, J.F. (1998): Geology of the Daly-Suttle-Middle Foster lakes area, eastern Wollaston Domain (NTS 74A-5, -11, and -12); *in* Summary of Investigations 1998, Saskatchewan Geological Survey, Sask. Energy Mines, Misc. Rep. 98-4, p48-65.

Wallis, R.H. (1970): The Geology of the Dufferin Lake Area (West Half), Saskatchewan; Sask. Dep. Miner. Resour., Rep. 132, 60p.

__________ (1971): The Geology of the Hidden Bay Area, Saskatchewan; Sask. Dep. Miner. Resour., Rep. 137, 75p.

Weber, W., Anderson, R.K., and Clark, G.S. (1975): Geology and geochronology of the Wollaston fold belt in northwestern Manitoba; Can. J. Earth Sci., v12, p1749-1759.

Yeo, G.M. and Savage, D.A. (1999): Geology of the Highrock Lake area, Wollaston Domain (NTS 74H-3 and -4); *in* Summary of Investigations 1999, Volume 2, Saskatchewan Geological Survey, Sask. Energy Mines, Misc. Rep. 99-4.2, p38-54.

Uraninite-bearing Granitic Pegmatite, Moore Lakes, Saskatchewan: Petrology and U-Th-Pb Chemical Ages

Irvine R. Annesley [1], Catherine Madore [1], Richard T. Kusmirski [2], and Tom Bonli [3]

Annesley, I.R., Madore, C., Kusmirski, R.T., and Bonli, T. (2000): Uraninite-bearing granitic pegmatite, Moore Lakes, Saskatchewan: Petrology and U-Th-Pb chemical ages; *in* Summary of Investigations 2000, Volume 2, Saskatchewan Geological Survey, Sask. Energy Mines, Misc. Rep. 2000-4.2.

Abstract

This paper documents the first results of a detailed study of uraninite-bearing granitic pegmatite, which occurs near unconformity-type uranium mineralization in the Moore Lakes area in the southeastern part of the Athabasca Basin. Drilling has revealed that granitic pegmatites comprise <5 to 10% of the basement complex with half estimated being radioactive. Relatively fresh, radioactive granitic pegmatite, the subject of this investigation, was intersected in drill hole ML00-08. The pegmatite is 10 m thick and occurs 55 m below the unconformity with sandstones of the overlying Athabasca Group.

The pegmatite is fine to coarse grained, sheared and foliated, and essentially unaltered. It is composed mainly of quartz, grey feldspar, and biotite, with subordinate amounts of apatite, zircon, uraninite, and ilmenite. Uraninite and U-rich zircon are the dominant uranium-bearing accessory minerals. Some uraninite grains are zoned. SEM and microprobe results showed that uraninite alteration is greatest along grain boundaries and fractures, with significant U loss and Pb gain/loss.

The pristine parts of the uraninite grains are composed mostly of U (66.42 $\leq UO_2/U_3O_8 \leq$ *72.40 wt %), Th (3.24* $\leq ThO_2 \leq$ *8.84 wt %), and Pb (12.92* $\leq PbO \leq$ *19.15 wt %). U-Th-Pb chemical dating of the uraninite grains yielded a crystallization age of ≥1772 ±88 Ma and other age clusters of 1429 to 1649 Ma and 1169 to 1233 Ma, which imply that the uraninite grains started experiencing disturbances of their U-Th-Pb isotopic system. We correlate these ages of isotopic disturbance to the Stage 1 and Stage 2 U mineralization events documented for other unconformity-type uranium deposits in the Athabasca Basin. Post-Athabasca alteration of these pegmatites may have provided some U for unconformity-type uranium mineralization in the Moore Lakes area.*

1. Introduction

Unconformity-type uranium deposits of the Athabasca Basin in northern Saskatchewan are the world's highest grade uranium resources. Most of these deposits have common characteristics. Many researchers today attribute their genesis to some variation of the diagenetic-hydrothermal model proposed by Hoeve and Sibbald (1978), which invokes the mixing of highly saline oxidized basinal fluids with variably reduced basement fluids. More recent research shows that the transport and precipitation of uranium is controlled by basin paleohydrology, basement topography, large-scale reactivated basement structures, fluid flow, heat flow, and physiochemical traps (Hoeve and Quirt, 1984, 1987; Wilson and Kyser, 1987; Kotzer and Kyser, 1991, 1992, 1995; Fayek and Kyser, 1997; Quirt, 1997). There are several hypotheses as to the source of the uranium. Pagel *et al.* (1980) and Dahlkamp (1993), amongst others, speculated that uranium is derived from the basement. The regolith in the Archean/Paleoproterozoic basement has been proposed by Pagel (1991) as a major source of uranium. In contrast, Hoeve and Sibbald (1978) suggested that uranium was derived from sandstones of the Athabasca Group. Recent work by Fayek and Kyser (1997) favored this option and suggested that most of the uranium was leached from detrital zircons in the sandstones of the Athabasca Group. More recent research by Annesley and Madore (1999c) in the southeastern part of the Athabasca Basin and by Hecht and Cuney (2000, in press) in the western part of the Athabasca Basin advocated that granitic rocks (i.e. monazite-bearing leucogranites, granitic pegmatites, and potassic orthogneiss) were the major source of uranium.

This paper documents the first results of a detailed study of uraninite-bearing granitic pegmatite, which occurs near unconformity-type uranium mineralization in the Moore Lakes area (The Northern Miner, 2000). The aim of this work is: 1) to characterize petrographically and geochemically the uraninite-bearing granitic pegmatite; 2) to characterize the nature of the uranium-bearing accessory minerals; 3) to document their behavior during hydrothermal alteration; 4) to date the age of the granitic pegmatites and the hydrothermal events that affected them, using U-Th-Pb geochemistry of uraninites; 5) to determine the crystallization temperature of the pegmatite using biotite-apatite geothermometry; and 6) to compare these results with similar data collected from outcrop and from core beneath the eastern Athabasca Basin (Annesley, 1989, 1990; Annesley and Madore, 1988,

---

[1] Saskatchewan Research Council, 15 Innovation Blvd., Saskatoon, SK S7N 2X8.
[2] JNR Resources Inc., Suite 921, 470 Granville Street, Vancouver, BC V6C 1V5.
[3] Department of Geological Sciences, University of Saskatchewan, 114 Science Place, Saskatoon, SK S7N 5E2.

1989a, 1989b, 1990a 1990b, 1991a, 1991b, 1999; Annesley *et al.*, 1996, 1997a, 2000; Madore *et al.*, 2000).

2. Geological Setting

The Moore Lakes area is located in the southeastern part of the Athabasca Basin (Figure 1A), approximately 40 km northeast of the Key Lake mine and 35 km southeast of the McArthur River uranium deposit.

Basement comprises rocks of the Wollaston Domain (Lewry and Sibbald, 1977; Gilboy, 1983; Lewry *et al.*, 1985; Hoffman, 1990; Lewry and Collerson, 1990), which is subdivided into two subdomains, separated by a linear break, on the basis of aeromagnetic data. These subdomains are characterized by rocks of high magnetic total field and those of low total field, respectively.

Four main groups of basement rocks are distinguished: 1) Archean orthogneisses and subordinate rocks, 2) high-grade Paleoproterozoic Wollaston Group metasediments, 3) deformed calc-alkaline granitoids and subordinate gabbroids, and 4) peraluminous granitoids of different petrochemical types.

These rocks have been subjected to polyphase deformation and metamorphism (Lewry and Sibbald, 1977, 1980; Sibbald, 1983; Gilboy, 1983; Annesley and Madore, 1991a; Annesley *et al.*, 1996, 1997b; Tran and Yeo, 1997; Tran *et al.*, 1998, 1999, 2000; Madore *et al.*, 1999a; Orrell *et al.*, 1999). Five main deformation events (Table 1) are recognized. Metamorphic grade varies from amphibolite to granulite facies under high T/medium to low P conditions. Metamorphic mineral assemblages record two main phases of mineral growth, coeval with D_1 and D_2 deformation and followed by various retrograde events during D_3, D_4, and D_5. Peak metamorphism (M_2)

Table 1 - Summary of Paleoproterozoic deformation and metamorphic events for the basement to the eastern Athabasca Basin (after Portella and Annesley, this volume).

Age (Ma)	Deformation	Metamorphism	Thermotectonic Stage
1860-1835	D_1	M_1	Early collisional
1835-1820	D_2	M_2	Collisional
1820-1805	late D_2	M_2	Oblique collisional
1805-1795	early D_3	M_3	Oblique collisional
1795-1775	late D_3	M_3	Late oblique collisional
1775-1760	D_4	M_4	Post-collisional
1760-1720	D_5		Late post-collisional

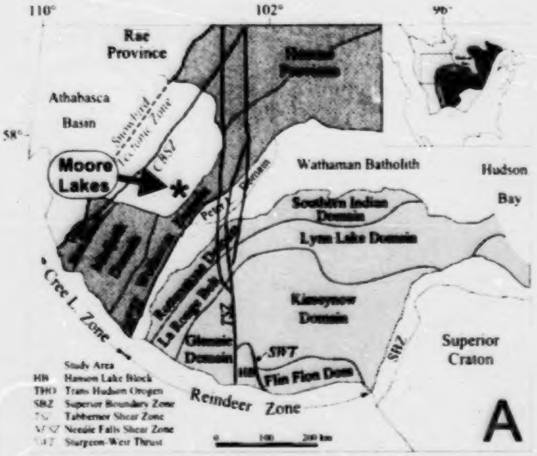
110°
102°
96°
58°
Rae Province
Athabasca Basin
Snowbird Tectonic Zone
CBSZ
Moore Lakes
Wathaman Batholith
Hudson Bay
Southern Indian Domain
Lynn Lake Domain
Kisseynew Domain
Superior Craton
Cree L. Zone
Reindeer Zone
Glennie Domain
La Ronge Belt
SWT
HB
Flin Flon Dom
SBZ
TSZ
Study Area
HB Hanson Lake Block
THO Trans Hudson Orogen
SBZ Superior Boundary Zone
TSZ Tabbernor Shear Zone
NFSZ Needle Falls Shear Zone
SWT Sturgeon-Weir Thrust
0 100 200 km
A

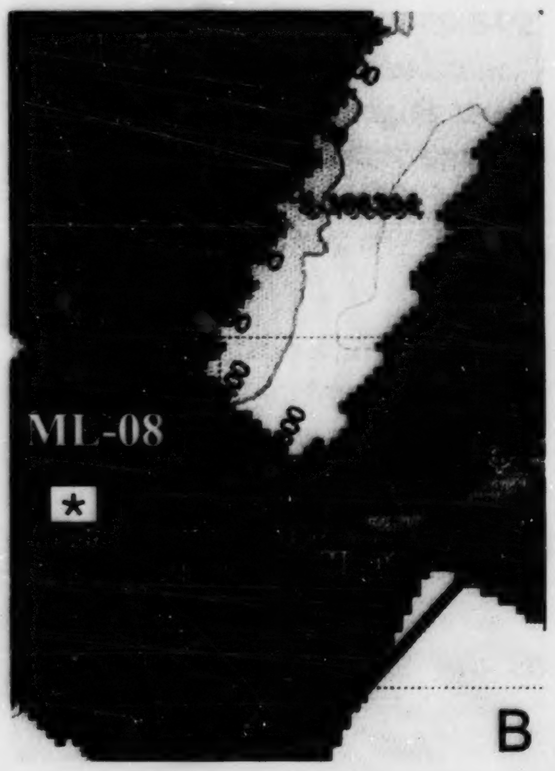

Figure 1 - A) Location of the study area in the southeastern part of the Athabasca Basin and B) location of the drill holes in the study area.

was synchronous with calc-alkaline plutonism at 1820 to 1800 Ma. Pegmatites of S-type affinity yield ages of 1820 to 1800 Ma (Annesley *et al.*, 1997b). Decompression, uplift, and cooling took place during D_3 transpression under amphibolite-facies conditions, and the timing of this deformation is constrained by monazite ages of 1806 to 1790 Ma and titanite age of 1800 to 1775 Ma. These deformation and metamorphic events are related to the thermotectonic evolution of the Trans-Hudson Orogen (Lewry and Sibbald, 1980; Lewry, 1987; Bickford *et al.*, 1990; Lewry and Collerson, 1990; Clowes *et al.*, 1999; and references therein).

Inliers of Archean/Paleoproterozoic rocks occur in the study area as part of the Moore Lakes Complex. The Moore Lakes Complex comprises Archean orthogneisses, Wollaston Group metasediments, and extensive diabase intrusions. Geological features of the complex were mapped and documented by Forsythe (1980), Ray (1983), and Ramaekers (1975, 1990). Recently, MacDougall and Williams (1993), and MacDougall and Maxemiuk (1995) mapped and sampled the Moore Lakes Complex for detailed petrochemical work of diabases.

The Moore Lakes area is the site of ongoing uranium exploration by JNR Resources Inc. and Kennecott Canada Exploration Inc. Results from a 10-hole drilling program have identified significant unconformity-type mineralization (drill hole ML00-03) near the footwall of a 125 m wide (i.e. downhole) structural zone (The Northern Miner, 2000). This drilling revealed that granitic pegmatites comprise <5 to 10% of the basement complex with half estimated being radioactive. Relatively fresh, radioactive granitic pegmatite was intersected in drill hole ML00-08, 400 m west of drill hole ML00-03. The pegmatite is 10 m thick and occurs 55 m below the unconformity with sandstones of the overlying Athabasca Group. Intensely clay-altered pegmatite with similar textural characteristics to the ML00-08 pegmatite was intersected by more recent drilling (ML00-11, unpubl. JNR Resources Inc. data), immediately west of drill hole ML00-03.

3. Analytical Methods

The focus of this paper is relatively fresh uraninite-bearing granitic pegmatite from drill hole ML00-08. Three samples of pegmatite were collected from the following intervals: 321.5 to 322.0 m, 322.0 to 322.5 m, and 322.5 to 323.0 m. Petrographic studies and whole-rock geochemistry were carried out at the Saskatchewan Research Council. The microprobe and SEM studies were performed at the Department of Geological Sciences, University of Saskatchewan.

4. Preliminary Petrographic Observations

The pegmatite is greyish to bluish grey mottled black, is holocrystalline, partly recrystallized, inequigranular-pegmatitic, fine to coarse grained, sheared and foliated, and essentially unaltered. It is composed mainly of quartz, grey feldspar, and biotite, with subordinate amounts of apatite (5 to 7 modal %), zircon (2 to 5 modal %), uraninite (trace to 2 modal %), and ilmenite (Figures 2, 3, 4, 5, and 6). Other accessory minerals include pyrite. Radioactivity reaches up to 1000 cps.

Quartz grains, which are partly recrystallized, form polycrystalline aggregates elongated parallel to the foliation cleavage. Quartz grains range from 0.20 to 4.00 mm in width and up to 6.00 mm in length. K-feldspar grains are variably recrystallized and are intergrown with the quartz grains. Their grain size varies from 0.45 to 4.30 mm in width and up to 5.30 mm in length. Biotite flakes form massive clusters along the foliation planes. The flakes range from 0.20 to 1.00 mm in width and up to 4.60 mm in length. They exhibit a pale brown to dark brown pleochroism. Apatite grains, which are distributed within biotite-rich clusters, are euhedral and blocky to stumpy prismatic in shape. The grains vary from 0.15 to 0.55 mm in width and up to 1.30 mm in length. The grains are colourless and strongly fractured. Two generations of zircon are identified (Figure 7). The first generation (Zrn1) is irregular in shape, strongly corroded, and overgrown by the second generation of zircon (Zrn2). Zircon (2) grains are euhedral, very well zoned, and contain inclusions of biotite. Their grain size varies from 0.06 to 0.40 mm in length. It is interpreted that the first generation of zircon was inherited from the source rock and the second generation was formed during the crystallization of the pegmatite. Uraninite grains are cubic in shape and 0.05 to 0.50 mm in size. The grains are found within biotite flakes. They show a dark grey metallic tint under reflected light and a dark pleochroic halo is developed around their grain margin. Some of the grains are highly fractured and variably altered. Trace amounts of rammelsbergite are developed around uraninite. Rammelsbergite displays a white metallic tint under reflected light. Its anisotropism is very strong, varying from blue to red-brown. Pyrite grains are subhedral to cubic in shape. They are concentrated within biotite-rich clusters. Their grain size varies from 0.06 to 0.40 mm in diameter. Ilmenite grains are elongated to acicular in shape. They range from 0.25 to 0.40 mm in length. The grains are altered and pseudomorphed by titanite grains.

5. Occurrence and Mineral Chemistry of Uraninite

Petrographic and SEM observations revealed that uraninite and U-rich zircon are the dominant uranium-bearing accessory minerals in the granitic pegmatite. SEM observations showed that some uraninite grains are zoned. SEM results and EDS spectra also revealed that the uraninite grains are highly altered in the vicinity of microfractures.

The pristine parts of the uraninite grains (Table 2) are composed mostly of U ($66.42 \leq UO_2/U_3O_8 \leq 72.40$ wt %), Th ($3.24 \leq ThO_2 \leq 8.84$ wt %), and Pb

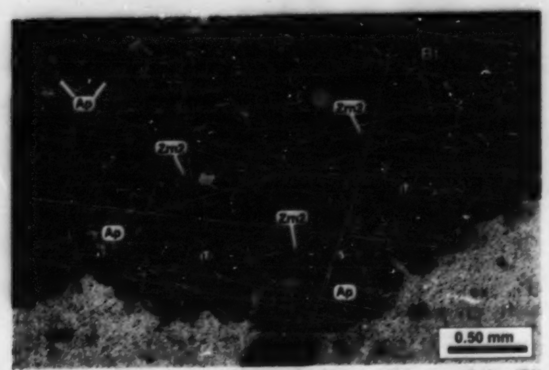
Bt
Ap
Zrn2
Zrn2
Zrn2
Ap
Ap
0.50 mm

Figure 2 - The photomicrograph shows cubic uraninite (U) grains intergrown with apatite (Ap) and zircon (Zrn 1 and 2) grains. Uraninite occurs in biotite-rich clusters, under plane-polarized light.

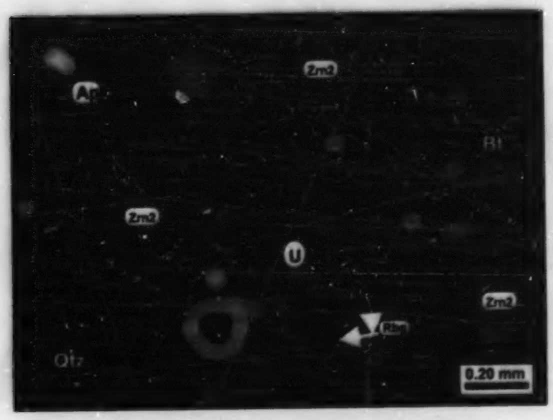
Zrn2
Ap
Bt
Zrn2
U
Zrn2
Rbg
Qtz
0.20 mm

Figure 3 - Close-up view of a cubic uraninite (U) grain surrounded by a thin film of rammelsbergite (Rbg), under reflected light

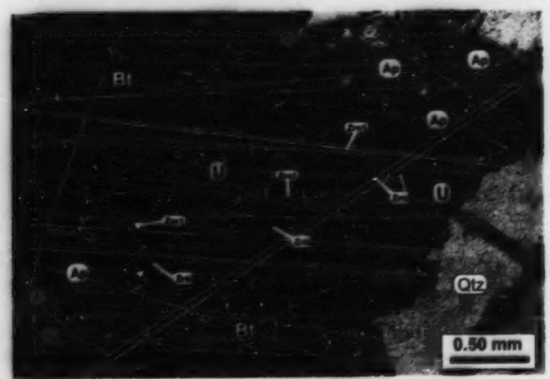
Bt
Ap
Ap
Ap
U
U
Ap
Qtz
Bt
0.50 mm

Figure 4 - The photomicrograph displays a complex intergrowth of biotite (Bt), apatite (Ap), uraninite (U), and zircon (Zrn 1 and 2), under plane-polarized light.

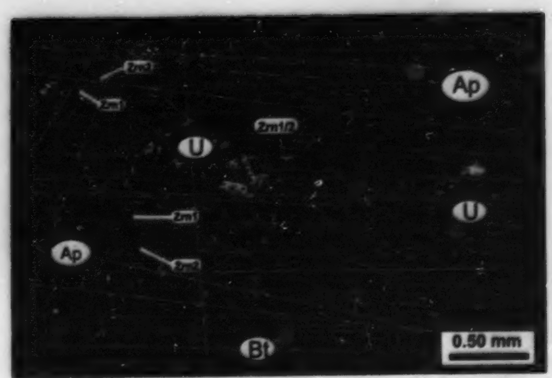
Zrn2
Zrn1
Ap
Zrn1/2
U
U
Zrn1
Ap
Zrn2
Bt
0.50 mm

Figure 5 - Same photomicrograph as Figure 4, but under reflected light.

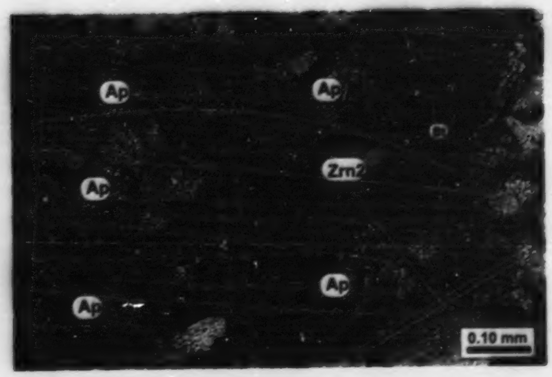
Ap
Ap
Bt
Zrn2
Ap
Ap
Ap
0.10 mm

Figure 6 - The photomicrograph shows an intergrowth texture composed of apatite (Ap), biotite (Bt), and well zoned zircon (Zrn 1 and 2), under plane-polarized light.

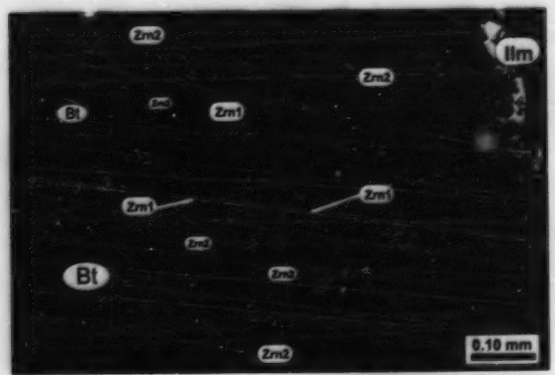
Zrn2
Ilm
Zrn2
Bt
Zrn1
Zrn1
Zrn1
Zrn2
Bt
Zrn2
Zrn2
0.10 mm

Figure 7 - Close-up view of well zoned zircons (Zrn 1 and 2) under reflected light.

Table 2 - Microprobe analyses of uraninite from ML00-08 granitic pegmatite.

Analysis Number	SiO_2 (wt %)	ThO_2	UO_2	V_2O_5	Nb_2O_5	P_2O_5	Ce_2O_3	Dy_2O_3	CaO	PbO	Total
U-1	0.00	6.18	70.61	0.01	0.00	0.06	0.38	0.30	0.10	18.30	95.94
U-2	0.00	7.15	68.19	0.00	0.06	0.08	0.43	0.30	0.50	15.11	91.82
U-3	0.55	6.14	72.40	0.00	0.10	0.31	0.49	0.22	0.76	12.92	93.89
U-5	0.20	5.63	70.20	0.00	0.08	0.04	0.37	0.26	0.28	15.87	92.92
U-6	0.02	6.50	69.10	0.05	0.17	0.00	0.35	0.39	0.00	17.89	94.46
U-7	0.00	3.93	70.82	0.00	0.03	0.23	0.36	0.51	0.34	15.81	92.04
U-8	0.22	4.27	70.89	0.00	0.04	0.12	0.30	0.32	0.01	18.44	94.59
U-9	0.00	5.89	69.74	0.00	0.00	0.00	0.25	0.37	0.21	16.29	92.75
U-10	0.00	5.10	71.15	0.00	0.01	0.07	0.46	0.36	0.00	18.75	95.91
U-11	0.00	3.73	71.74	0.00	0.03	0.01	0.40	0.32	0.00	18.43	94.68
U-13	0.00	7.99	67.64	0.06	0.00	0.00	0.28	0.16	0.00	19.15	95.28
U-15	0.00	5.16	71.30	0.03	0.05	0.00	0.21	0.30	0.08	17.69	94.82
U-17	0.00	8.84	66.42	0.04	0.08	0.00	0.39	0.28	0.00	19.05	95.10
U-18	0.01	3.95	73.14	0.00	0.00	0.00	0.25	0.59	1.10	13.36	92.40
U-19	0.03	3.24	70.37	0.00	0.06	0.04	0.29	0.29	0.00	19.30	93.63
U-21	0.14	7.16	68.73	0.00	0.00	0.13	0.27	0.27	0.00	16.43	93.12
U-22	0.19	7.44	70.60	0.00	0.00	0.00	0.26	0.36	1.41	12.33	92.58
U-23	0.26	7.83	69.09	0.00	0.00	0.24	0.39	0.30	0.59	15.24	93.93
U-24	0.67	6.61	68.66	0.00	0.00	0.26	0.41	0.35	0.24	16.41	93.61
U-25	0.04	7.52	67.80	0.00	0.02	0.00	0.39	0.35	0.04	18.11	94.28
U-4	2.39	5.53	46.15	0.04	0.00	0.00	0.23	0.23	0.50	24.02	76.09
U-12	4.24	4.18	55.20	0.09	0.06	0.00	0.29	0.31	0.46	24.65	89.47
U-16	11.32	5.43	47.89	0.04	0.00	0.61	0.47	0.10	0.65	11.84	78.34
U-20	2.96	3.69	49.83	0.12	0.00	0.03	0.25	0.36	0.91	10.68	68.83

($12.92 \leq PbO \leq 19.15$ wt %). The rare earths, Ce_2O_3 and Dy_2O_3, are always present at the tenths of a wt % level ($0.21 \leq Ce_2O_3 \leq 0.49$ wt %, and $0.16 \leq Dy_2O_3 \leq 0.59$ wt %). Other rare earths are invariably present at these levels, as well as Y. Calcium concentrations are highly variable at the tenths of a wt % level. Niobium, P, and V contents vary from <0.01 to 0.31 wt %. The totals of least altered uraninite are close to 96% (Table 2, U-1 and U-10). The other REE and Y could bring the totals close to 100%.

The altered parts of the uraninite grains show loss of $U0_2/U_30_8$ with either Pb gain (U-4, U-12) or Pb loss (U-16, U20, Table 2). Silica enrichment is also noted with this uraninite alteration.

The chemistry of the pristine uraninite grains is consistent with a magmatic origin. They contain Th and REE, which are rare or largely absent in hydrothermal and low-temperature sedimentary-hosted uraninite (Frondel, 1958). These impurities in the uraninite are important in understanding uraninite stability and uraninite-fluid interactions (Friedrich *et al.*, 1987; Finch and Ewing, 1992; Finch and Murakami, 1999).

6. Petrochemistry

The pegmatites (Table 3) are moderately rich in alkalis ($K_20+Na_20 = 4.95$ to 6.27 wt %) and weakly peraluminous (ASI=1.00 to 1.15). The oxides TiO_2, $Fe_2O_{3\,tot}$, and MgO values are highly variable, reflecting biotite content of the sample analyzed. Samples with high biotite content have high TiO_2, $Fe_2O_{3\,tot}$, MgO, Li, Nb, and Sc, and low SiO_2 values. Elevated concentrations of P_2O_5, CaO, HREE, and Y are related to the high apatite content. The strong to very strong enrichment of U-Th-Pb and Zr-Hf reflects the high to very high concentrations of uraninite and zircon, respectively, in the analyzed samples, when compared to other pegmatites in the area (Table 3).

The very high values of Hf, Pb, Th, U, Zr, and HREE suggest that an igneous enrichment process has taken place since these values exceed greatly the maximum values for solubility in both water-saturated and water-undersaturated granitic melts at high temperatures (Watson and Harrison, 1983; Puziewicz and Johannes, 1990; Pichavant *et al.*, 1992).

7. U-Th-Pb Chemical Age Dating

Radioelement-rich accessory minerals have the potential for U-Th-Pb_{tot} age dating by electron microprobe analysis (e.g. Suzuki and Adachi, 1991; Suzuki *et al.*, 1994; Montel *et al.*, 1996; Rhede *et al.*, 1996; Förster, 1998, 1999). Recently, most chemical age research has focussed on monazite and other minerals of the monazite group, as these minerals are less susceptible to radiation damage with metamictization and resultant hydration. In the Athabasca Basin, uraninite and pitchblende have been successfully used for U-Th-Pb_{tot} dating of the various U mineralization events (Parslow *et al.*, 1985; Fayek and Kyser, 1997; McCready *et al.*, 1999; among others). These chemical ages have been calculated

Table 3 - Whole-rock geochemistry of uraninite-bearing granitic pegmatite and other granitic pegmatite from the Moore Lakes area.

Sample	ML00-08 321.5-322.0	ML00-08 322.0-322.5 (this study)	ML00-08 322.5-323.0	MAC-64 292.3	MT-21 265.6
SiO_2 (wt %)	71.00	57.70	71.80	95.2	62.7
TiO_2	0.53	1.62	0.40	0.25	0.04
Al_2O_3	13.00	11.50	13.00	1.31	17.27
$Fe_2O_{3\,tot}$	2.71	7.30	2.41	0.01	4.36
FeO	1.40	3.00	1.20	0.50	0.50
MnO	0.05	0.15	0.04	0.01	0.01
MgO	2.59	6.78	2.83	0.76	5.61
CaO	2.70	4.43	1.63	0.46	0.73
Na_2O	2.56	0.15	1.58	0.16	0.06
K_2O	2.39	6.12	3.69	0.60	1.63
P_2O_5	0.71	2.89	0.25	0.25	0.16
LOI	2.20	1.80	2.20	0.70	6.40
Total	**100.43**	**100.44**	**99.82**	**100.78**	**99.37**
Ba (ppm)	400	671	689	19	77
Be	1.6	1.6	1.6	1.2	4.4
Cd	0.3	0.2	<0.2	0.2	0.2
Co	5	14	5	3	4
Cu	12	38	8	25	1
Ga	21	27	20	6	27
Hf	45.3	95.0	41.1	25.5	0.6
Li	47	105	78	23	98
Mo	4	21	10	1	1
Nb	15	39	7	23	1
Ni	3	5	3	11	61
Pb	296	630	210	4	1
Sc	11	35	10	3	20
Sn	4	5	2	1	4
Sr	158	59	114	6	71
Th	88	219	66	17	3
U	950	2400	880	9.8	2.8
V	13	38	10	20	56
W	2	2	1	1	1
Y	108	290	61	11	45
Zn	165	285	92	13	3
Zr	1530	2810	1360	792	51
La (ppm)	17	37	23	1	20
Ce	41	96	46	4	46
Pr	6	16	6	1	5
Nd	33	100	27	2	30
Sm	13.1	33.6	8.9	1.1	6.4
Eu	2.1	2.6	1.6	0.6	0.3
Gd	13.7	39.1	8.1	2.4	5.5
Tb	3.5	9.0	1.9	0.3	0.9
Dy	17.2	49.4	9.8	1.6	6
Ho	5.3	13.7	3.9	0.4	1.3
Er	10.9	31.9	7.0	0.9	3.7
Tm	1.4	3.2	0.6	0.3	0.7
Yb	11.9	31.2	8.5	2.4	6.3
Lu	1.9	4.9	1.3	0.8	1

assuming that the Pb_{tot} in the samples is entirely of radiogenic origin and that Pb loss or gain has not occurred since mineral crystallization (Bowles, 1990).

Fifteen grains of uraninite were analyzed for U, Th, Pb_{tot}, and other elements (Table 2). All grains show inhomogeneity related to fracturing, alteration, and possibly core-outer rim effects. Single-point ages were calculated by four different methods using the equation ($Pb = U\,[0.99276 \exp(\lambda_1 t) - 1 + 0.007196 \exp(\lambda_2 t) - 1] + Th \exp(\lambda_3 t - 1)$) for the radioactive decay of U and Th. The first term of the equation is related to the decay of ^{238}U to ^{206}Pb, the second term to the decay of ^{235}U to ^{207}Pb, and the third term to the breakdown of ^{232}Th to ^{208}Pb. The decay constants (λ) for each of these terms are $\lambda_1 = 0.00015512$ Ma^{-1}, $\lambda_2 = 0.00098485$ Ma^{-1}, and $\lambda_3 = 0.000049475$ Ma^{-1}, respectively. The largest proportion of Pb comes from the decay of ^{238}U to ^{206}Pb, and as noted by Bowles (1990), a simple approximation of the age is given by t (Ma) = Pb (wt %) x 100 (i.e. Method 1 in Table 4). Empirical formulas by Ranchin (1968) and Bowles (1990) have been fitted to the radioactive decay of U and Th to Pb. Our results using these formulas are presented as Methods 2 and 3 in Table 4. As pointed out by Bowles (1990), the Ranchin (1968) formula gives results that are too old for samples >200 Ma. Our research supports this observation. Method 3 gives good results, but does not take into account the contribution of Pb from the decay of Th. In most cases, this is not a factor, but the uraninites analyzed in this study contain significant amounts of Th. Therefore, we have used the rigorous iteration method of Bowles (1990) to produce a best fit between the measured Pb and the calculated Pb from the equation for production of radiogenic Pb by the decay of U and Th. By this method, uraninites with greater than 50 wt % U yielded ages of 1772 to 1169 Ma (Method 4, Table 4). The older group of ages 1772 to 1648 Ma, from least altered uraninite, are interpreted as a minimum age of crystallization. These are younger than the precise U-Pb zircon and monazite ages of 1820 to 1803 Ma for granitic pegmatites of the eastern sub-Athabasca basement (Annesley *et al.*, 1997a,

Table 4 - U-Pb-Th chemical age dating results for uraninite from ML00-08 granitic pegmatite.

Pt#	U (wt %)	Th (wt %)	Pb (wt %)	Ma Method 1	Ma Method 2	Ma Method 3	Ma Method 4	(± Ma) error
1	59.88	5.43	16.99	1699	2074	1757	1648	85
2	57.82	6.28	14.03	1403	1763	1530	1439	70
3	61.40	5.39	12.00	1200	1430	1259	1199	60
5	59.53	4.95	14.73	1473	1814	1557	1472	74
6	58.59	5.71	16.61	1661	2068	1755	1644	83
7	60.06	3.46	14.67	1467	1807	1539	1464	73
8	60.11	3.75	17.12	1712	2103	1762	1663	86
9	59.14	5.18	15.12	1512	1871	1603	1511	76
10	60.34	4.48	17.40	1740	2120	1782	1676	87
11	60.84	3.28	17.11	1711	2083	1743	1649	86
13	57.36	7.02	17.78	1778	2242	1897	1759	89
15	60.47	4.54	16.43	1643	1997	1691	1595	82
17	56.32	7.77	17.68	1768	2258	1918	1772	88
18	62.03	3.47	12.40	1240	1479	1286	1233	62
19	59.68	2.85	17.92	1792	2229	1846	1742	90
21	58.28	6.29	15.25	1525	1902	1636	1534	76
22	59.87	6.54	11.44	1144	1388	1234	1169	57
23	58.59	6.88	14.14	1414	1748	1523	1429	71
24	58.22	5.81	15.23	1523	1907	1636	1537	76
25	57.50	6.61	16.81	1681	2120	1803	1680	84

Notes:

Method 1 - Bowles (1990) - age(t) = Pb x 100

Method 2 - Ranchin (1968) - age(t) = Pb x 7550 / (U + 0.36Th)

Method 3 - Bowles (1990) - age(t) = (1/0.000155125) x ln ((1.104 x Pb/U) + 1)

Method 4 - Bowles (1990) - age(t) calculated by iteration program using U, Th, and Pb

Error estimate = 5 percent of the Pb analyses

1997b, 1999a, 1999b, 1999c, 2000; Madore *et al.*, 1999b).

8. Discussion and Conclusions

The diagenetic hydrothermal model of Hoeve and Sibbald (1978) is the favored model for the genesis of unconformity-type uranium deposits, however, the source of uranium is still debated. Some researchers appeal to the basement as a direct source of the uranium, still others to the basement regolith (Pagel, 1991), whereas some researchers (Fayek and Kyser, 1997) and most exploration geologists favor sandstones of the Athabasca Group as the main source. Annesley and Madore (1999) suggested that the radioelement-enriched leucogranite suite is the most important basement source of uranium in the eastern part of the Athabasca Basin. High-U monazite and uraninite are the major contributors of uranium. Likewise, Hecht and Cuney (2000, in press) from a ca. 1500 km^2 area suggested that granitic rocks of the sub-Athabasca basement are the most important source of uranium in the western Athabasca Basin. These researchers demonstrated that hydrothermal alteration of basement lithologies beneath the paleoweathered zone down to at least 200 m below the unconformity resulted in substantial mobilization and redistribution of uranium. This post-regolith hydrothermal alteration is present in thick (tens of metres) zones of highly fractured basement rocks, and comprises chloritization, sericitization, and clay alteration. Their preliminary fluid inclusion work confirms the circulation of brines in these hydrothermally altered rocks. The mobilization and redistribution are marked by the replacement of monazite by a Th-silicate phase with concurrent liberation of approximately 75% of the U, P, and LREE. This monazite (±uraninite) alteration by brines provides an attractive mechanism for releasing uranium.

Our study adds to the research of Hecht and Cuney (2000, in press) by demonstrating weak to locally moderate mobilization of uranium from a weakly altered, variably fractured granitic pegmatite. SEM and microprobe results showed that uraninite alteration is greatest along grain boundaries and fractures, with significant U loss and Pb gain/loss.

U-Th-Pb chemical dating of uraninite grains yields a crystallization age of ≥1772 ±88 Ma. This chemical dating also yielded age clusters of 1429 to 1649 Ma and 1169 to 1233 Ma, which imply that the uraninite grains in this paper started experiencing disturbances of their U-Th-Pb isotopic system. We correlate these ages of isotopic disturbance to the Stage 1 and Stage 2 U mineralization events of Fayek and Kyser (1997). Preliminary drill hole observations and geophysical logging (R. Kusmirski, pers. comm., 2000) from nearby, highly altered pegmatites indicate that significant mobilization/redistribution of uranium may have occurred. If this post-regolith alteration covers a large area or zone with approximately 5% radioactive pegmatites, do we have enough uranium for mobilization, redistribution, and precipitation? Mass-balance calculations for an east-west structural corridor (10 km long by 0.5 km wide by 2.0 km deep) gives a volume of 1.0 x 10^{16} cm^3. Five percent pegmatite with a density of 2.66 g/cm^3 would give a mass of 1.33 x 10^{12} kg. If the granitic pegmatite for the corridor averaged 30 ppm U, then 3.99 x 10^7 kg of uranium would be available for leaching. Five percent mobilization, redistribution, and precipitation of this amount would give 2 000 000 kg (4,400,000 lb) U, whereas 25% would give 10 000 000 kg (22,000,000 lb) U.

We conclude that relatively fresh uraninite-bearing granitic pegmatites in the Moore Lakes area record the age of Stage 1 and Stage 2 U mineralization events in the basin. We also suggest that post-Athabasca alteration of these pegmatites may have provided some

U for unconformity-type uranium mineralization in the Moore Lakes area.

9. Acknowledgments

The authors acknowledge the support of JNR Resources Inc. and Kennecott Canada Exploration Inc. for providing samples and background information to this study. Funding for the first and second authors was provided by Saskatchewan Research Council. The senior author thanks Dr. Alistair McCready of Belfast University for the introduction to chemical age dating. The review and critical comments by Saskatchewan Energy and Mines geologists are gratefully acknowledged.

10. References

Annesley, I.R. (1989): The Wollaston Group and its underlying Archean basement in Saskatchewan: An Update; Sask. Resear. Counc., Publ. R-855-5-E-89, 86p.

__________(1990): The Wollaston Group and its underlying Archean basement in Saskatchewan: Interim Report; Sask. Resear. Counc., Publ. R1240-1-C-90, 27p.

Annesley, I.R. and Madore C. (1988): The Wollaston Group and its underlying Archean basement in Saskatchewan: Preliminary Report; *in* Summary of Investigations 1988, Saskatchewan Geological Survey, Sask. Energy Mines, Misc. Rep. 88-4, p54-60.

__________(1989a): A re-examination of the Wollaston Group and its underlying Archean basement in northern Saskatchewan; Geol. Assoc. Can./Mineral. Assoc. Can., Prog. Abstr., pA39.

__________(1989b): The Wollaston Group and its underlying Archean basement in Saskatchewan: 1989 fieldwork and preliminary observation; *in* Summary of Investigations 1989, Saskatchewan Geological Survey, Sask. Energy Mines, Misc. Rep. 89-4, p87-91.

__________(1990a): The Wollaston Group and its underlying Archean basement in Saskatchewan: Appendices to Interim Report, Volumes 1 and 2; Sask. Resear. Counc., Publ. R-1240-2-C-90, 389p.

__________(1990b): The Wollaston Group and underlying Archean basement in Saskatchewan: Subsurface and bedrock geological mapping in 1990; *in* Summary of Investigations 1990, Saskatchewan Geological Survey, Sask. Energy Mines, Misc. Rep. 90-4, p48-54.

__________(1991a): The Wollaston Group and its underlying Archean basement: Final Report; Sask. Resear. Counc., Publ. R-1230-4-C-91, 140p.

__________(1991b): The Wollaston Group and its underlying Archean basement: Appendices A, B, C, D, E, and F of the Final Report (Volumes 1, 2, and disk); Sask. Resear. Counc., Publ. R-1230-5-C-91, 472p.

__________(1999): Leucogranites and pegmatites of the sub-Athabasca basement, Saskatchewan: U protore?; *in* Stanley, C.J. *et al.* (eds.), Mineral Deposits: Processes to Processing, Balkema, v1, p297-300.

Annesley, I.R., Madore, C., Kamo, S.L., and Krogh, T.E. (1999a): U-Pb zircon and monazite ages from the sub-Athabasca basement of the P-patch uranium deposit, Wollaston Domain, Saskatchewan; Geol. Assoc. Can./Miner. Assoc. Can., Abstr., v24, pA-3.

Annesley, I.R., Madore, C., and Krogh, T.E. (1997a): U-Pb geochronology of peraluminous pegmatites from the Wollaston Lake area, northern Saskatchewan; Geol. Assoc. Can./Miner. Assoc. Can., Abstr., v22, pA-4.

Annesley, I.R., Madore, C., Krogh, T.E., and Kamo, S.L. (1999b): Anomalous U-Pb values in monazites from peraluminous leucogranites and pegmatites near unconformity-type uranium mineralization, eastern Athabasca, Saskatchewan; Geol. Assoc. Can./Miner. Assoc. Can., Abstr., v24, pA-3.

Annesley, I.R., Madore, C., Krogh, T.E., and Kwok, K.K. (1998): New U-Pb zircon and monazite dates from the sub-Athabasca basement, Wollaston Domain, Hearne Province, Saskatchewan; Geol. Assoc. Can./Miner. Assoc. Can., Abstr., v23, pA-5.

Annesley, I.R., Madore, C., Krogh, T.E., Kwok, Y.Y., and Kamo, S.K. (1999c): New U-Pb zircon and monazite geochronological results for Archean and Paleoproterozoic basement to the southeastern part of the Athabasca Basin, Saskatchewan; *in* Summary of Investigations 1999, Volume 2, Saskatchewan Geological Survey, Sask. Energy Mines, Misc. Rep. 99-4.2, p90-99.

Annesley, I.R., Madore, C., Kamo, S., Andrade, N., and Portella, P. (2000): Petrochemistry and U-Pb geochronology of peraluminous leucogranite from Cigar Lake, Hearne Province, northern Saskatchewan, GeoCanada 2000, Calgary, May 2000, Conference CD, ext. abstr. #983.

Annesley, I.R., Madore, C., Shi, R., and Krogh, T.E. (1996): U-Pb geochronology and thermotectonic history of the Wollaston Domain in the Wollaston Lake area, Hearne Province, Saskatchewan; Geol. Assoc. Can./Miner. Assoc. Can., Prog. Abstr., v21, pA-4.

__________(1997b): U-Pb geochronology of thermotectonic events in the Wollaston Lake area, Wollaston Domain: A summary of 1994-1996 results; *in* Summary of Investigations 1997, Saskatchewan Geological Survey, Sask. Energy Mines, Misc. Rep. 97-4, p162-173.

Bickford, M.E., Collerson, K.D., Lewry, J.F., Van Schmus, W.R., and Chiarenzelli, J.R. (1990): Proterozoic collisional tectonism in the Trans-Hudson Orogen, Saskatchewan; Geol., v18, p14-18.

Bowles, F.J.W. (1990): Age dating of individual grains of uraninite in rocks from electron microprobe analyses; Chem. Geol., v83, p47-53.

Clowes, R., Cook, F., Hajnal, Z., Hall, J., Lewry, J., Lucas, S., and Wardle, R. (1999): Canada's LITHOPROBE Project (Collaborative, multidisciplinary geoscience research leads to new understanding of continental evolution); Episod., v22, p3-20.

Dahlkamp, F.J. (1993): Uranium Ore Deposits; Springer-Verlag, Berlin, 460p.

Fayek, M. and Kyser, T.K. (1997): Characterization of multiple fluid-flow events and rare earth element mobility associated with the formation of unconformity-type uranium deposits in the Athabasca Basin, Saskatchewan; Can. Mineral., v35, p627-658.

Finch, R.J. and Ewing, R.C. (1992): The corrosion of uraninite; J. Nuclear Materials, v190, p133-156.

Finch, R.J. and Murakami, T. (1999): Systematics and Paragenesis of Uranium Minerals; *in* Burns, P.C. and Finch, R. (eds.), Uranium: Mineralogy, Geochemistry and the Environment, Mineral. Soc. Amer., Reviews in Mineralogy, v38, p91-179.

Förster, H.-J. (1998): The chemical composition of REE-Y-Th-U-rich accessory minerals in peraluminous granites of the Erzgebirge-Fichtelgebirge region, Germany. Part I. The monazite-(Ce)-brabantite solide solution series; Amer. Mineral., v83, p59-272.

__________ (1999): The chemical composition of uraninite in Variscan granites of the Erzgebirge, Germany; Mineral. Mag., v63, p239-252.

Forsythe, L.H. (1980): Geology of Part of the Geikie River (East) Area, Part of NTS Area 74H (east); Sask. Dep. Miner. Resour., Rep. 204, 12p.

Friedrich, MH, Cuney, M., and Poty, B. (1987): Uranium geochemistry in peraluminous leucogranites; Uranium, v3, p353-385.

Frondel, C. (1958): Systematic Mineralogy of Uranium and Thorium; U. S. Geol. Surv., Bull. 1064, 400p.

Gilboy, C.F. (1983): Sub-Athabasca Basement Geology Project; *in* Summary of Investigations 1983, Saskatchewan Geological Survey, Sask. Energy Mines, Misc. Rep. 83-4, p28-31.

Hecht, L. and Cuney, M. (2000): Mechanism of uranium mobilization in the Athabasca Basin and basement by hydrothermal and/or diagenetic fluids; GeoCanada 2000, Calgary, May 2000, Conference CD, ext. abstr. #191.

__________ (in press): Hydrothermal alteration of monazite in the Precambrian crystalline basement of the Athabasca Basin (Saskatchewan, Canada): implications for the formation of unconformity-related uranium deposits; Mineral. Dep.

Hoeve, J. and Quirt, D. (1984): Mineralization and host rock alteration in relation to clay mineral diagenesis and evolution of the middle-Proterozoic Athabasca Basin, northern Saskatchewan, Canada; Sask. Resear. Counc., Tech. Rep. 187.

__________ (1987): A stationary redox front as a critical factor in the formation of high grade, unconformity-type uranium ores in the Athabasca Basin, Saskatchewan; Can. Bull. Mineral., v110, p157-171.

Hoeve, J. and Sibbald, T. (1978): On the genesis of Rabbit Lake and other unconformity-type uranium deposits in northern Saskatchewan, Canada; Econ. Geol., v73, p1450-1473.

Hoffman, P.F. (1990): Subdivision of the Churchill province and extent of the Trans-Hudson Orogen; *in* Lewry, J.F. and Stauffer, M.R. (eds.), Early Proterozoic Trans-Hudson Orogen of North America, Geol. Assoc. Can., Spec. Pap. 37, p15-39.

Kotzer, T. and Kyser, T.K. (1991): Retrograde alteration of clay minerals in uranium deposits: Radiation catalysed or simply low-temperature exchange?; Chem. Geol., v86, p307-321.

__________ (1992): Isotopic, mineralogic and chemical evidence for multiple episodes of fluid movement during prograde and retrograde diagenesis in a Proterozoic Basin; *in* Kharaka, Y.K. and Maest, A. S. (eds.), Proc. 7th Inter. Symp. on Water-Rock Interaction, Utah, July 13-18, p1177-1181.

__________ (1995): Petrogenesis of the Proterozoic Athabasca Basin, northern Saskatchewan, Canada, and its relation to diagenesis, hydrothermal uranium mineralization and paleohydrogeology; Chem. Geol., v120, p45-89.

Lewry, J. F. (1987): The Trans-Hudson Orogen: Extent, subdivisions, and problems; Geol. Assoc. of Can./Miner. Assoc. Can., Prog . Abstr., v12, p67.

Lewry, J.F. and Collerson, K.D. (1990): The Trans-Hudson Orogen: Extent, subdivision and problems; *in* Lewry, J.F. and Stauffer, M.R. (eds.), The Early Proterozoic Trans-Hudson Orogen of North America, Geol. Assoc. Can., Spec. Pap. 37, p1-14.

Lewry, J.F. and Sibbald, T.I.I. (1977): Variation in lithology and tectonometamorphic relationships in the Precambrian basement of northern Saskatchewan; Can. J. Earth Sci., v14, p1453-1467.

__________ (1980): Thermotectonic evolution of the Churchill Province in northern Saskatchewan; Tectonophys., v68, p45-82.

Lewry, J.F., Sibbald, T.I.I., and Schledewitz, D.C.P. (1985): Variation in character of Archean rocks in the western Churchill Province and its significance; *in* Ayers, L.D., Thurston, P.C., Card, K.D., and Weber, W. (eds.), Evolution of Archean Supracrustal Sequences, Geol. Assoc. Can., Spec. Pap. 28, p239-261.

MacDougall, D.G. and Maxemiuk, L.M.T. (1995): Moore Lakes revisited-gold and palladium concentrations in altered diabase from the Moore Lakes Complex (part of NTS 74H-6 and -7); *in* Summary of Investigations 1995, Saskatchewan Geological Survey, Sask. Energy Mines, Misc. Rep. 95-4, p68-78.

MacDougall, D.G. and Williams D.H. (1993): The Moore Lake Complex, Neohelikian olivine diabase lopoliths in the Athabasca Group (part of NTS 74H-6 and -7); *in* Summary of Investigations 1993, Saskatchewan Geological Survey, Sask. Energy Mines, Misc. Rep. 93-4, p86-91.

Madore, C., Annesley, I.R., and Tran, H.T. (1999a): Petrology and geochemistry of Paleoproterozoic Wollaston Group metasediments from the eastern Keller Lake–Siemens Lake area, Saskatchewan: A preliminary interpretation; *in* Summary of Investigations 1999, Volume 2, Saskatchewan Geological Survey, Sask. Energy Mines, Misc. Rep. 99-4.2, p80-89.

Madore, C., Annesley, I.R., and Wheatley, K. (2000): Petrogenesis, age, and uranium fertility of peraluminous leucogranites and pegmatites of the McClean Lake/Sue and Key Lake/P-Patch deposit areas, Saskatchewan, GeoCanada 2000, Calgary, May 2000, Conference CD, ext. abstr. #1041.

Madore, C., Annesley, I.R., Kwok, K.K., and Krogh, T.E. (1999b): Petrography, geochemistry, and age of granitic pegmatites from the Close Lake and Epp Lake areas, Mudjatik Domain, Saskatchewan; Geol. Assoc. Can./Miner. Assoc. Can., Abstr., v24, pA-77.

McCready, A.J., Annesley, I.R., Parnell, J., and Richardson, L.C. (1999): Uranium-bearing carbonaceous matter, McArthur River uranium deposit, Saskatchewan; *in* Summary of Investigations 1999, Volume 2, Saskatchewan Geological Survey, Sask. Energy Mines, Misc. Rep. 99-4.2, p110-120.

Montel, J.-M., Foret, S., Veschambre, M., Nicollet, C., and Provost, A. (1996): Electron microprobe dating of monazite; Chem. Geol., v131, p37-53.

Orrell, S.E., Bickford, M.E., and Lewry, J.F. (1999): Crustal evolution and age of thermotectonic reworking in the western hinterland of the Trans-Hudson Orogen, northern Saskatchewan; Precamb. Resear., v95, p187-223.

Pagel, M. (1991) Lateritization and paleogeomorphology: Their roles in the genesis of unconformity-type uranium deposits in Saskatchewan, Canada; *in* Pagel, M. and Leroy, L. (eds.), Source, Transport, and Deposition of Metals, Balkema, Rotterdam, p331-332.

Pagel, M., Poty, B., and Sheppard, S.M.F. (1980) Contribution to some Saskatchewan deposits mainly from fluid inclusion and isotope data; *in* Ferguson, S. and Goleby, A. (eds.), Uranium in the Pine Creek geosyncline; IAEA, Vienna, p639-654.

Parslow, G.R., Brandstatter, F., Kurat, G., and Thomas, D.J. (1985): Chemical ages and mobility of U and Th in anatectites of the Cree Lake zone, Saskatchewan; Can. Mineral., v23, p543-551.

Pichavant, M., Montel, J.-M., and Richard, L.R. (1992): Apatite solubility in peraluminous liquids: Experimental data and an extension of the Harrison-Watson model; Geochim. Cosmochim. Acta, v56, p3855-3861.

Puziewicz, J. and Johannes, W. (1990) Experimental study of a biotite-bearing granitic system under water-saturated and water-undersaturated conditions; Contrib. Mineral. Petrol., v104, p397-406.

Quirt, D. (1997): Geochemistry, host-rock alteration, mineralization, and uranium metallogenesis of the Wollaston EAGLE Project Area; *in* Thermotectonic and Uranium Metallogenic Evolution of the Wollaston EAGLE Project Area, Sask. Resear. Counc., Publ. No. R-1420-2-C-97, 98p.

Ranchin, G. (1968): Contribution à l'étude de la repartition de l'uranium à l'état de traces dans les roches granitiques saines les uranites à teneur élévée du Massif de Saint-Sylvestre (Limousin - Massif Central Français); Sci. Terre., v13, p161-205.

Ramaekers, P. (1975): Athabasca Formation, southeast edge (74H): Part 1: Reconnaissance geological mapping; *in* Summary of Investigations 1975 by the Saskatchewan Geological Survey, Sask. Miner. Resour., p48-52.

__________ (1990): Geology of the Athabasca Group (Helikian) in Northern Saskatchewan; Sask. Energy Mines, Rep. 195, 49p.

Ray, G.E. (1983): Compilation Bedrock Geology, Geikie River, NTS Area 74H; Sask. Energy Mines, Rep. 229 (1:250 000 scale map with marginal notes).

Rhede, D., Wendt, I., and Förster, H.-J. (1996): A three-dimensional method for calculating independent chemical U/Pb- and Th/Pb-ages of accessory minerals; Chem. Geol., v130, p247-253.

Sibbald, T.I.I. (1983): Geology of the crystalline basement, NEA/IAEA Athabasca Test area; *in* Cameron, E.M. (ed.), Uranium Exploration in Athabasca Basin, Geol. Surv. Can., Pap. 82-11, p1-14.

Suzuki, K. and Adachi, M. (1991): Precambrian provenance and Silurian metamorphism of the Tsubonosawa paragneiss in the South Kitakami terrane, northeast Japan, revealed by the chemical Th-U-total Pb isochron ages of monazite, zircon and xenotime; Geochem. J., v25, p357-376.

Suzuki, K., Adachi, M., and Kajizuka, I. (1994): Electron microprobe observations of Pb diffusion in metamorphosed detrital monazites; Earth Planet. Sci. Lett., v128, p391-405.

The Northern Miner (2000): JNR sizes up Moore Lake drill core; v86, no20, p16.

Tran, H.T. and Yeo, G.M. (1997): Geology of the Burbidge Lake–northern upper Foster Lake area, eastern Wollaston Domain (NTS 74A-14); *in* Summary of Investigations 1997, Saskatchewan Geol. Surv. Misc. Rep. 97-4, p72-89.

Tran, H.T., Yeo, G.M., and Bethune, K., (1999): Geology of the McKenzie Falls area, Haultain River, Wollaston-Mudjatik domains boundary (NTS 74B-7 and -8); *in* Summary of Investigations 1999, Volume 2, Saskatchewan Geol. Surv., Sask. Energy Mines, Misc. Rep. 99-4.2, p55-67.

Tran, H.T., Yeo, G.M., Bradley, S., and Lewry, J.F. (1998): Geology of the Daly-Suttle-Middle Foster lakes area, eastern Wollaston Domain (NTS 74A-5, -11, and 12); *in* Summary of Investigations 1998, Saskatchewan Geol. Surv., Sask. Energy Mines, Misc. Rep. 98-4, p48-65.

Tran, H.T., Lewry, J.F., Bethune, K., Ashton, K., Yeo, G., and Ansdell, K. (2000): Crustal thrusting and tectonic imbrication in the Cree Lake Zone, northern Saskatchewan: implications for the tectonic evolution of western foreland of the Trans-Hudson Orogen; GeoCanada 2000, Calgary, May 2000, Conference CD, ext. abstr. #579.

Watson, E.B. and Harrison, T.M. (1983): Zircon saturation revisited: Temperature and composition effects in a variety of crustal magma types; Earth Planet. Sci. Lett., v64, p295-304.

Wilson, M.R. and Kyser, T.K. (1987): Stable isotope geochemistry of alteration with the Key Lake Uranium Deposit, Canada; Econ. Geol., v82, p1540-1557.

Appendix 1: Microprobe Analytical Technique

Microprobe analyses were performed on polished thin sections using a JEOL 8600 Superprobe electron microprobe analyzer housed at the University of Saskatchewan, Department of Geological Sciences. The probe was operating at an accelerating voltage of 20 kV, beam current of 10 ηA and a beam diameter of <5 µm. High purity metals were used as standards for U, Th, V, and Nb. Quartz was used as standard for Si, diopside for Ca, apatite for P, cerium phosphate for Ce, dysprosium phosphate for Dy, and crocoite for Pb.

All elements with the exception of Th and Pb were analyzed using a count time of 40 s. Th and Pb were analyzed using 100 s count times. Matrix and ZAF corrections were performed using formulas modeled after Heinrch/Duncumb-Reed.

D. Industrial Minerals Studies

Origin of Saskatchewan Sodium Sulphate Deposits – A Progress Report[1]

Lynn I. Kelley

Kelley, L.I. (2000): Origin of Saskatchewan sodium sulphate deposits – a progress report; *in* Summary of Investigations 2000, Volume 2, Saskatchewan Geological Survey, Sask. Energy Mines, Misc. Rep. 2000-4.2.

Abstract

In the 2000 field season, study was focused on an individual deposit. Lydden Lake is located about 30 km west of Biggar, Saskatchewan. It is underlain by an evaporite deposit of approximately 800 000 tonnes of anhydrous sodium and magnesium sulphates that have never been mined. Lydden Lake occupies a northwest-oriented closed basin about 5000 m long and 300 to 500 m wide. Fieldwork has been geared to solving components of the solute mass balance that are fundamental to understanding the genesis of these deposits. Fieldwork initiated during the 2000 field season included: the electrical resistance tomography (ERT) survey described in the paper by Zimmerman et al. (this volume); establishing, through compilation of drill logs and completion of five stratigraphic test holes, a regional hydrostratigraphic framework for the Lydden Lake area; measurement of hydraulic properties of near-surface sediments through aquifer tests in shallow piezometers and seep meters; collection of lake brine and groundwater samples for detailed geochemical analysis; and meteorological studies aimed at quantifying lake fluxes due to snowmelt runoff, precipitation, and evaporation.

1. Introduction

Reconnaissance hydrogeochemical studies reported in Kelley and Holmden (1999) and Kelley *et al.* (1998) constituted initial steps in investigating the processes leading to the formation of lacustrine evaporite deposits mined for sodium sulphate in Saskatchewan. In the 2000 field season, the study focused on an individual deposit. Lydden Lake is underlain by an evaporite deposit of approximately 800 000 tonnes of anhydrous sodium and magnesium sulphates. It is located about 30 km west of Biggar, Saskatchewan (Figure 1), and has never been mined. Lydden Lake occupies a northwest-oriented closed basin about 5000 m long and 300 to 500 m wide. Another lake, Springwater Lake, occupies a valley of similar size that is parallel to, and about 500 m south of, Lydden Lake. Springwater Lake is a fresh water lake that may recharge local groundwater. Fieldwork has been geared to solving components of the solute mass balance that are fundamental to understanding the genesis of these deposits.

2. Geophysical Surveys

The electrical resistance tomography (ERT) survey of Lydden Lake is described in the paper by Zimmerman *et al.* (this volume). The survey, and companion EM31 and EM34 surveys, were carried out to investigate whether high-specific-gravity salt water seeps through the lakebed and exits the lake, driven by gravity. The ERT pseudo-sections make a strong case for the existence of saline plumes extending up to 60 m inland from the lakeshore. Piezometers will be installed to intercept the most well-developed plume to confirm whether the low resistivity layer evident on the pseudo-sections is indeed a gravity-driven plume of saline water.

3. Regional Hydrostratigraphy

Water well logs archived in the SaskWater Corp. water well database were compiled to establish a regional stratigraphic framework. This was supplemented by drilling of five stratigraphic test holes completed September 18 to 25, 2000. A single hole completed in the lake basin was terminated in the Bearpaw Formation (field determination). The two deepest holes, drilled outside the lake basin, reached approximately 170 m below surface and terminated in the Judith River Formation. No significant bedrock aquifers were penetrated in any of the holes. Inter-till sands were penetrated in every hole, but the number and aggregate thickness of inter-till sand varies widely amongst the holes. Piezometers were installed in two of the holes to facilitate head measurement and water sampling.

4. Physical Hydrogeology

Shallow piezometers and seep meters were installed at two locations on the shore of Lydden Lake, in order to estimate the water and solute flux in the springs and seeps evident at various locations along the lakeshore. At each location, two piezometers were installed at nominal screen depths of 2 m and 1 m. Analysis of data from these devices was not complete at the time of writing, but it was evident that at least some of the piezometers recovered very rapidly during slug tests, indicating high hydraulic conductivity in the near-surface sediments. An upward vertical gradient on the

---

[1] Funded in part by the Saskatchewan Strategic Initiatives Fund.

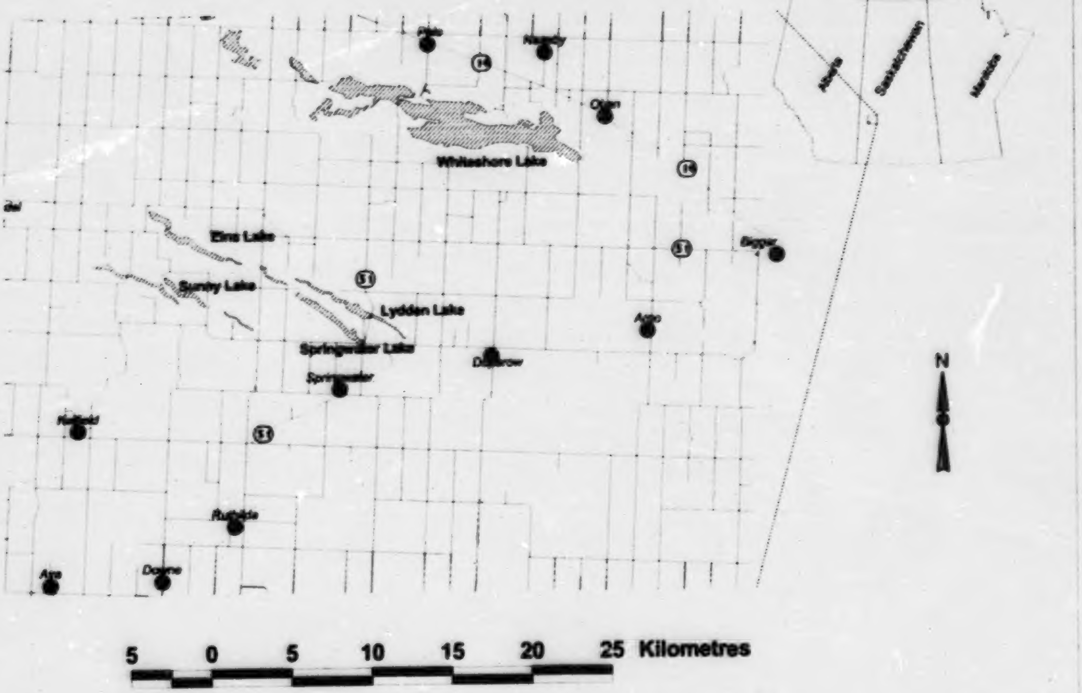

Figure 1 - Location map.

order of 0.1 is indicated from preliminary head measurements.

5. Detailed Geochemistry

A network of shallow piezometers that permit sampling of most of the springs and seeps on the margin of Lydden Lake has been established. Two rounds of samples have been collected and analyzed for major ions. All farm wells in the vicinity of Lydden Lake have been sampled and analyzed for major ions and water isotopes.

6. Meteorological Studies

A snowpack survey was carried out in March 2000, in order to estimate the amount of snowmelt runoff available for recharge of shallow groundwater and direct runoff to Lydden Lake. An automated rain gauge and two class A evaporation pans were installed near Millar-Western Industries sodium sulphate mine at Whiteshore Lake, about 15 km north of Lydden Lake, in order to monitor local precipitation and evaporation rates. One evaporation pan was filled with fresh water and a saturated sodium sulphate solution was maintained in the other. Data for the full season have not been analyzed, but field indications are that the evaporation rate from the saturated solution is a large fraction of that of the fresh water.

7. Future Work

Current plans through 2001 call for:

1) Completion of the shallow drilling and piezometer installation to investigate the origin of the low-resistivity layer mapped in the ERT surveys.
2) Compilation of deep drilling results and interpretation of regional hydrostratigraphy.
3) Incorporation of geochemical data from lake waters and groundwater and meteorological data into a solute mass balance for Lydden Lake.
4) Installation of seepmeters or piezometers in lakebed springs.
5) Begin detailed study of solute transport in groundwater.

8. References

Kelley, L.I. and Holmden, C. (1999): Reconnaissance study of strontium isotopic composition of lake brines and groundwater associated with sodium sulphate deposits, southern Saskatchewan; *in* Summary of Investigations 1999, Volume 2, Saskatchewan Geological Survey, Sask. Energy Mines, Misc. Rep. 99-4.2, p208-212.

Kelley, L.I., Smith, J.J., and Holmden, C. (1998): Stable isotope and chemical composition of groundwater associated with sodium sulphate deposits, southern Saskatchewan; *in* Summary of Investigations 1998, Saskatchewan Geological Survey, Sask. Energy Mines, Misc. Rep. 98-4, p136-141.

Electrical Resistivity Imaging of a Brine Plume under the Margin of a Sodium Sulphate Lake [1]

E.P. Zimmerman [2], L.R. Bentley [2], M. Hayashi [2], L.I. Kelley, and C. Holmden [3]

Zimmerman, E.P., Bentley, L.R., Hayashi, M., Kelley, L.I., and Holmden, C. (2000): Electrical resistivity imaging of a brine plume under the margin of a sodium sulphate lake; *in* Summary of Investigations 2000, Volume 2, Saskatchewan Geological Survey, Sask. Energy Mines, Misc. Rep. 2000-4.2.

Abstract

Electrical resistivity tomography (ERT) is a modern technique for imaging two-dimensional resistivity cross-sections in areas with complex subsurface geology. We used ERT to investigate the interface between relatively fresh groundwater and dense lake brine at the margins of a modern lacustrine evaporite deposit of sodium sulphate in west-central Saskatchewan. Six ERT profiles were oriented perpendicular to the shoreline of Lydden Lake and three parallel to the shore. Anomalously low resistivity is evident at depths of 5 to 25 m along the lake shore. We interpret the source of the anomalously low resistivity to be dense lake brine seeping from the lake bed under the influence of gravity. The zones of anomalously low resistivity intrude over 60 m inshore in areas where the lakeshore slopes gently, and a much shorter distance in areas where the shoreline is flanked by cliffs. The difference in length of the brine plume is interpreted to be related to a lower hydraulic gradient in areas where the shoreline slopes gently.

1. Introduction

Saline lakes are common hydrogeological features in arid and semi-arid climatic zones. In most saline lakes in the prairie region, lake water contains sulphates of Na and Mg (Salama *et al.*, 1999) .The total dissolved solids (TDS) content in some of these lakes exceeds 200,000 ppm. High concentration of dissolved salts leads to the formation of crystalline salt beds, which are mined for Na_2SO_4 – a valuable industrial mineral. From the hydrogeological viewpoint, sodium sulphate lakes are the focus of groundwater discharge and the high TDS concentration is the result of evaporation. Subsurface resistivity imaging provides insight into the interaction between saline and fresh waters on the margins of the lake. The study of these processes is essential to our understanding of the genesis of evaporite deposits in the saline lakes.

2. Site Description and Methodology

a) Lydden Lake Site

Lydden Lake is situated 35 km west of Biggar, Saskatchewan (Figure 1). The area is underlain by approximately 100 m of unconsolidated glacial, glaciofluvial, and glaciolacustrine deposits. Beneath the glacial drift, Mesozoic and Paleozoic rocks form a sequence of nearly horizontal sedimentary layers approaching 2000 m in thickness (Macdonald and Slimmon, 1999). Like most of the Na_2SO_4-producing lakes of the region, Lydden Lake is in a narrow river-like valley (Last and Slezak, 1987). It is approximately 5000 m long and 300 to 500 m wide. Most of the shoreline is marked by 5 to 15 m high cliffs, but on the southern shore, a bay with a very gentle slope is present. Lydden Lake is underlain by a well-developed crystalline salt bed, estimated to contain 800,000 short tons (700 000 tonnes) of anhydrous sodium and magnesium sulphates. In mid-summer, the lake brine reaches a maximum concentration of 200,000 ppm TDS, with Na^+, SO_4^{2-}, and Mg^{2+} being the dominant ion species.

b) Electrical Resistivity Tomography

Electrical resistivity tomography (ERT) is a modern technique for imaging two-dimensional resistivity cross-sections in areas with complex subsurface geology (Loke and Barker, 1996). The electrical current is injected through two current electrodes and the resulting voltage difference is then measured at two potential electrodes. The depth of penetration (and therefore imaging) depends on the spacing between the electrodes and the type of the array. For this investigation we used the Wenner array, which resulted in the least amount of noise with the deepest penetration. From the current (I) and voltage (V) values, the apparent resistivity (ρ_a) is calculated by:

$$\rho_a = kV / I \qquad (1)$$

where k (m) is a geometric factor, which depends on the arrangement and spacing of the electrodes (Loke, 1999). The ERT unit consists of a large number of electrodes (in our case up to 56) connected to a single cable and set out at a constant spacing.

---

[1] Partially funded by the Saskatchewan Strategic Initiatives Fund.

[2] University of Calgary, Department of Geology and Geophysics, 2500 University Drive NW, Calgary, AB T2N 1N4.

[3] Department of Geological Sciences, University of Saskatchewan, 114 Science Place, Saskatoon, SK S7N 5E2.

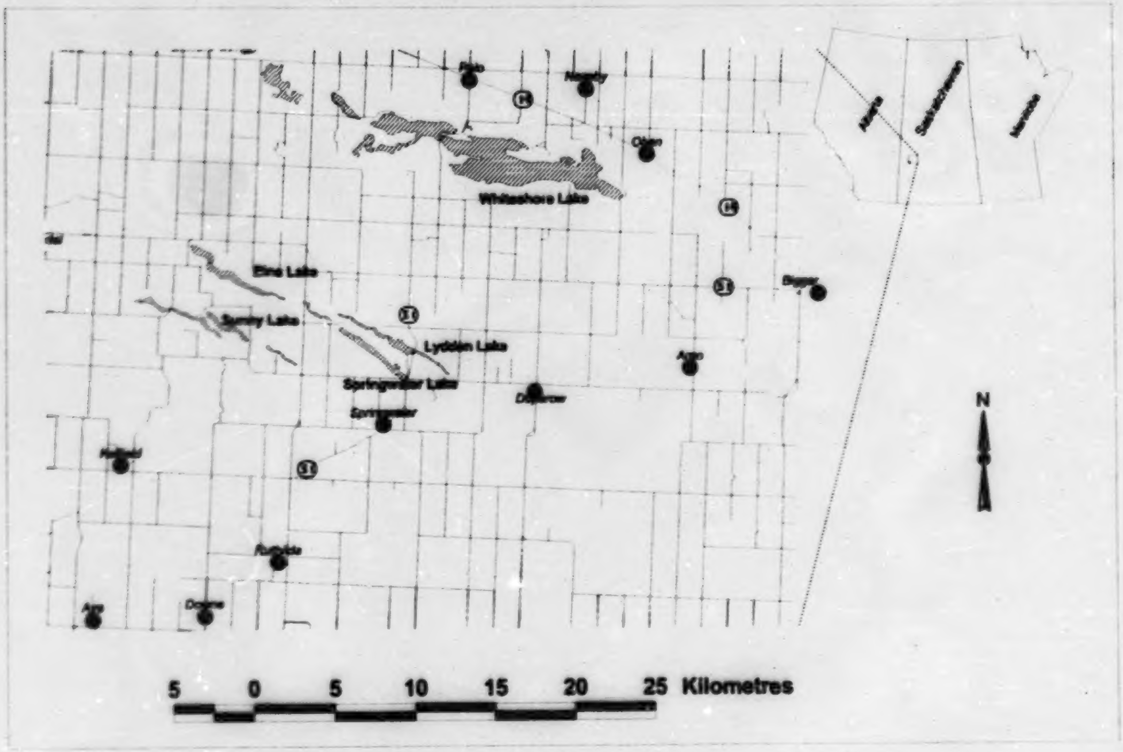

Figure 1 - Location of the study area.

The cable is laid out in a straight line and a computer-controlled system is then used to automatically select four active electrodes for each measurement (individual array). Measurements are then taken and stored in the computer. The minimum distance between neighbouring electrodes in an individual array is the set-up spacing. As the distance between neighbouring electrodes increases, the number of individual arrays that can be used decreases and so does the number of measurements at a given depth level. Therefore the interpretation is most accurate for the top half of the profile (Loke, 1999).

The data obtained is commonly arranged and contoured in the form of a pseudo-section. The relation between the true resistivity of the subsurface and the apparent resistivity is complex. An inversion algorithm (Loke and Barker, 1996) was used to estimate the true soil resistivity from the apparent resistivity values and to produce a model of resistivity cross-section.

3. Results

a) General

Six ERT profiles were run perpendicular to the shoreline of the Lydden Lake and three were oriented parallel to the shore (Figure 2).

To characterize the marginal processes, the ERT profiles were carried out on both steep and gentle shores of Lydden Lake. Four lines (12, 13, 14, and 15) were run where the shoreline was marked by 5 to 10 m high cliffs and five (lines 1, 2, 9, 10, and 11) were run from a bay on the southern shore that had a gentle slope (Figure 2). The elevation of the bay's slope gradually increases inland from 663 to 665 m. The shoreline extends for about 500 m within this bay (Figure 2).

The depth of imaging reached 40 to 50 m, with electrodes spaced between 4 and 6 m. The images obtained were of good quality. The amount of noise increased for the profiles run across complicated topographical features (e.g. cliffs, valleys).

The images from the profiles run perpendicular to the shoreline showed an area of lower resistivity starting from the lake's margin and extending inland in some cases for more than 60 m.

b) Response Along Gently-sloping Shoreline

On line 1, the resistivity values near the shore and at 5 to 25 m depth are consistently below 3 Ω-m while the background resistivity values exceed 20 Ω-m. We interpret the source of these anomalies to be brine intrusions from the lake. The brine plume has a tongue shape in longitudinal section and significant inland

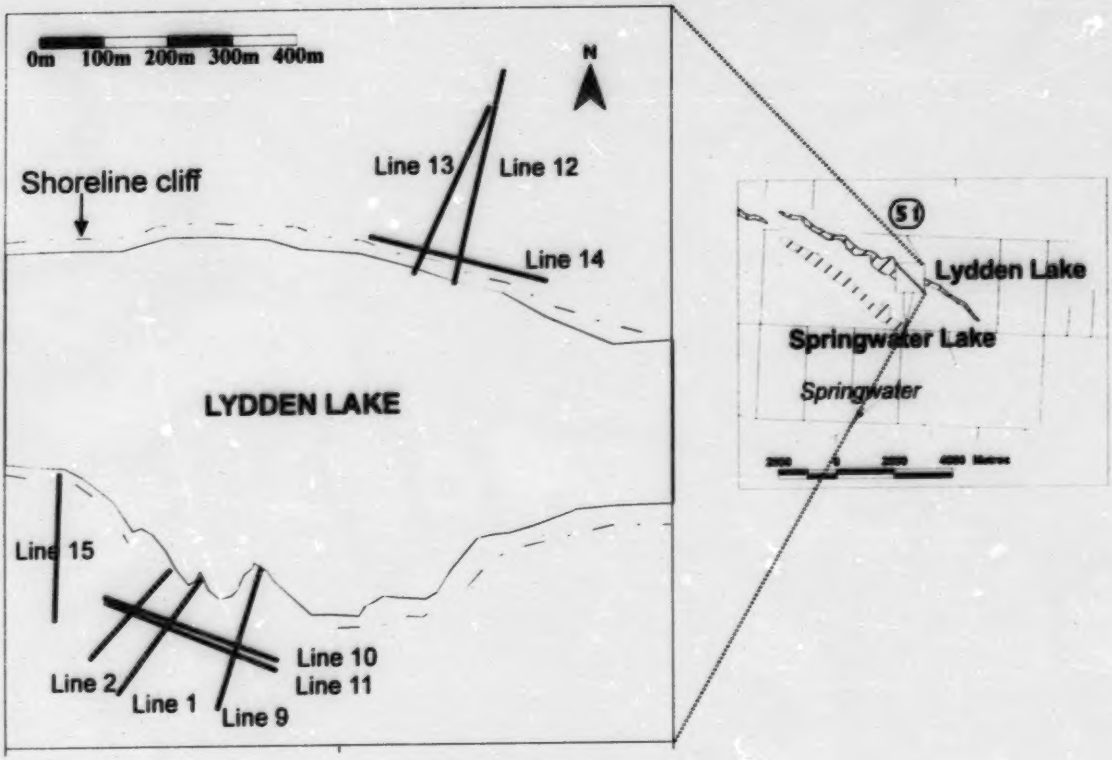
0m 100m 200m 300m 400m
N
Shoreline cliff
Line 13
Line 12
Line 14
LYDDEN LAKE
Line 15
Line 10
Line 11
Line 2
Line 1
Line 9
51
Lydden Lake
Springwater Lake
Springwater

Figure 2 - The ERT survey scheme.

extension in the case of line 1 where the shore slopes gently (Figure 3). Lines 2 and 9 (not shown) were oriented sub-parallel to line 1 and yielded images similar to Figure 3. The area of lower resistivity on top of the plume is interpreted as groundwater discharge having much lower salt content than the lake water.

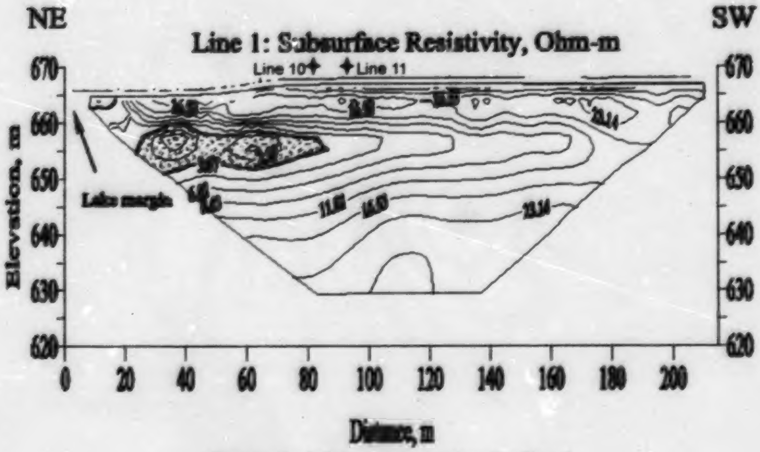

Figure 3 - ERT pseudo-section for line 1.

The plume occurs between 660 and 640 m and the water level in Lydden Lake is at 663 m. A layer of lower hydraulic conductivity may control the location of the bottom of the plume. A single drill hole completed east of the study area penetrated fine sand between 5 and 15 m below surface, roughly coincident with the elevation of the anomalously low resistivity. The sand is underlain by clay-rich glacial till.

The tongue-like shape of the brine plume is evidently three-dimensional, based on pseudo-sections oriented parallel to the shore and perpendicular to line 1. Figure 4 shows the image obtained along line 10.

The cross-section of brine plume on line 11 (not shown), that was run farther inland than line 10 is smaller, thus confirming that the plume thins away from the lake.

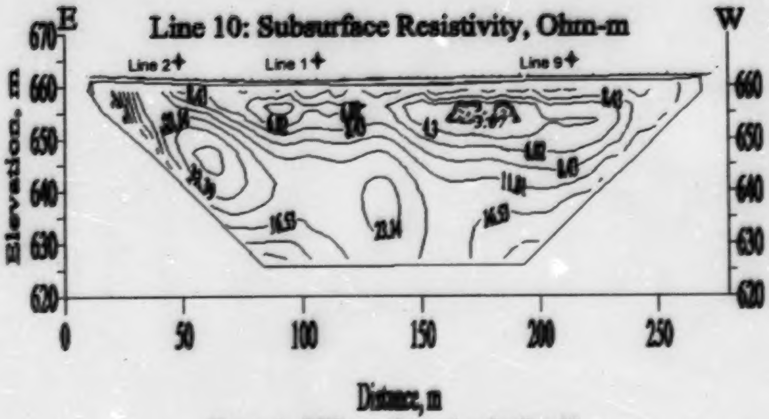

Figure 4 - ERT pseudo-section for line 10.

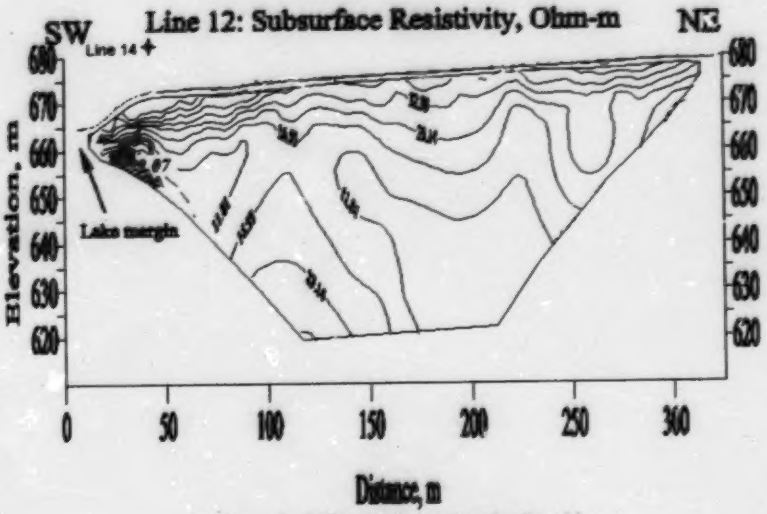

Figure 5 - ERT pseudo-section for line 12.

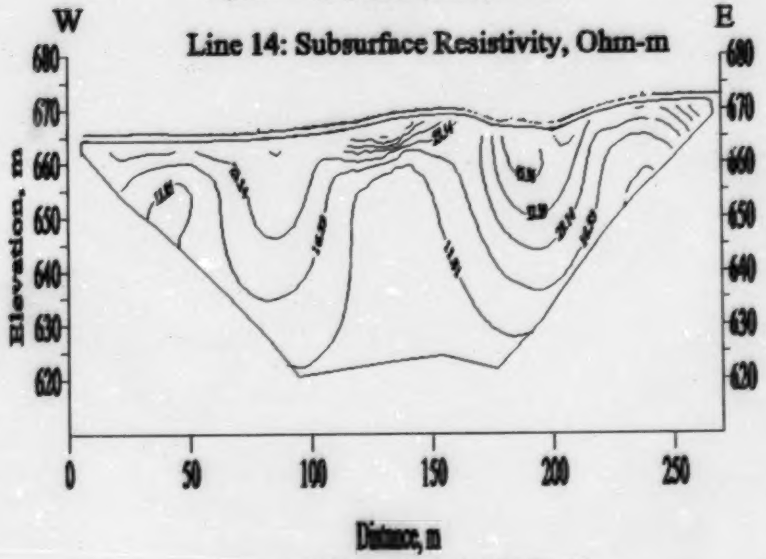

Figure 6 - ERT pseudo-section for line 14.

c) Response Along Shoreline Cliffs

Where a cliff forms the lakeshore, the plume becomes shorter, and appears not to advance inland beyond the cliff break (Figure 5).

Line 14 was run parallel to the shore on the bluff of the cliff (Figure 6). This image does not have an area of lower resistivity, which is consistent with the conclusions that the plume does not advance past the top of the bluff on the shores formed by a cliff (Figure 5).

4. Discussion

A shallow saline-freshwater interface was described along the margins of the Dead Sea in Quaternary deltaic sandy gravel overlying upper cretaceous carbonates (Yechieli, 2000). Our study suggests that a similar process of saltwater intrusion is occurring on the margins of a significantly smaller saline lake. The tomography at Lydden Lake is interpreted to indicate two water bodies under the margins of the lake. The uppermost is relatively fresh groundwater, flowing into the lake from the watershed. The hydraulic head decreases towards the lake that is the focus of this groundwater discharge. Beneath the freshwater is a body of saline groundwater. This denser brine seeps from the lake bed and pushes inshore in the opposite direction to the flow of relatively fresh groundwater. On the margins of Lydden Lake, the hydraulic gradient is lower under the gentle shore flanking the bay and the brine plume extends farther inshore. In contrast, where the lake is flanked by cliffs, the hydraulic gradient is steeper and the brine plume does not extend far inland.

5. Conclusions

Electrical resistivity tomography was successfully used to image subsurface resistivity under the margins of a sodium sulphate lake.

Drilling and groundwater sampling are planned to quantify the groundwater salinity variations presumed to be the cause of the low-resistivity plumes imaged in the ERT survey.

6. References

Last, W.M. and Slezak, L.A. (1987): Sodium sulphate deposits of western Canada: Geology, mineralogy, and origin; *in* Gilboy, C.F. and Vigrass, L.W. (eds.), Sask. Geol. Soc., Spec. Publ. No. 8, p197-205.

Loke, M.H. (1999): Electrical imaging surveys for environmental and engineering studies, a practical guide to 2-D and 3-D surveys; http://www.agiusa.com/literature.shtml, accessed 10 Feb 2000.

Loke, M.H. and Barker, D. (1996): Rapid least-squares inversion of apparent resistivity pseudosections by a quasi-Newton method; Geophys. Prospect., v44, p131-152.

Macdonald, R. and Slimmon, W.L. (compilers) (1999): Geological Map of Saskatchewan; Sask. Energy Mines, 1:1 000 000 scale.

Salama, R.B., Otto, C.J., and Fitzpatrick, R.W. (1999): Contribution of groundwater conditions to soil and water salinization; Hydrogeol. J., v7, p46-64.

Yechieli, Y. (2000): Fresh-saline groundwater interface in the Western Dead Sea area; Ground Water, v38, no4, p615-623.

The Diamond Potential of Saskatchewan 2000: A Study in Progress

Brent C. Jellicoe [1], Phil Robertshaw [2], Gary Billingsley [3], and Bruce Kjarsgaard [4]

Jellicoe, B.C., Robertshaw, P., Billingsley, G., and Kjarsgaard, B. (2000): The diamond potential of Saskatchewan 2000: A study in progress; *in* Summary of Investigations 2000, Volume 2, Saskatchewan Geological Survey, Sask. Energy Mines, Misc. Rep. 2000-4.2.

Abstract

Since the first discoveries at the end of the 1980s, more than $50 million has been expended in exploration for diamonds in Saskatchewan. The authors have, along with the Saskatchewan Geological Survey, the Geological Survey of Canada, and several industry partners, committed to complete and publish a comprehensive study of the province's diamond potential. The study will summarize all data pertaining to diamond exploration that resides in the public domain. The study is intended to facilitate and to promote diamond exploration in the province. Publication is targeted for November 2001.

This year, a significant resurgence in diamond exploration in Saskatchewan has been signaled by an increase in exploration programs and expenditures. Much of the expected expenditure of $5 million is targeted for the evaluation of previously discovered diamondiferous kimberlites, rather than exploration for new kimberlites.

Diamond exploration in Saskatchewan has undergone significant evolution since Gent (1992) summarized preliminary investigations for a number of geological anomalies, some of which were then known, or later proven, to be associated with the occurrence of diamond-bearing rocks such as kimberlite. This publication also presented the first descriptions of the character and distribution of diamonds extracted from the kimberlites. Diamond exploration exploded in response to the identification of this potential. Annual diamond exploration expenditures incurred on projects in Saskatchewan ranged from $1.7 million to $11 million during 1989-2000, with peak outlays in 1993, 1996, and 2000. In total, about $50 million has been expended on diamond exploration in Saskatchewan during the past ten years.

Much of the data generated from these exploration ventures, as well as that from several surveys conducted by provincial and federal agencies, have not been systematically compiled and evaluated. The potential for new discoveries remains high as over 70 kimberlite bodies, of which at least 50 are diamondiferous, have been found in central Saskatchewan. Encouraging new results continue to be announced. We believe that a summary and synthesis of all relevant diamond exploration data will be timely and useful as evaluation of known targets continues and new targets are sought.

The authors, the Saskatchewan Geological Survey, the Geological Survey of Canada, and several industry partners have committed to complete and publish a comprehensive study of the province's diamond potential, building on the work of Jellicoe *et al.* (1998). The primary objective of the study is to integrate and synthesize the data and geological concepts pertinent to diamond exploration currently within the public domain, particularly that which has been amassed since 1992. The study will identify corridors or zones of diamond source rock (kimberlite or lamproite) potential and present a rationale for prioritization of these areas based on clear resolution of geological, geochemical, and geophysical anomalies. An additional objective of the study is to summarize exploration methods used in the past and to evaluate which methods are most applicable to Saskatchewan.

Six areas of interest will be addressed that ultimately will be integrated to support the primary objective.

1) Regional Archean and Proterozoic geology and relevant structural considerations.
2) Regional geology of kimberlite host rocks.
3) Regional geophysics including magnetic surveys, resistivity, and downhole logs.
4) Exploration targets - revisiting selected prospects of Gent (1992) and outlining current areas of exploration interest and history.
5) Proven exploration plays - including summaries of known kimberlite fields including: Fort-à-la-Corne, Star Lake, Candle Lake, and other drill-proven kimberlites; emplacement models, geochemistry, stratigraphy, and exploration history; and investigations of any potential kimberlite intersections or suspect structures in oil and gas drill holes.
6) Regional indicator mineral abundance and geochemistry (integrating historical and recently completed work through Saskatchewan Energy and Mines).

---

[1] Jellicoe Resource Associates, #210 - 3502 Taylor Street East, Saskatoon, SK S7H 5H9.
[2] Robertshaw Geophysics, 111 Middleton Crescent, Saskatoon, SK S7J 2W5.
[3] Great Western Gold Corp., #303, 416 - 21st Street East, Saskatoon, SK S7K 0C2.
[4] Geological Survey of Canada, 1 Observatory Crescent, Ottawa, ON K1A 0E8.

The study is intended to facilitate and to promote diamond exploration in the province of Saskatchewan. The target publication date for a digital open file report is November 2001.

References

Gent, M.R. (1992): Diamonds and precious gems of the Phanerozoic Basin, Saskatchewan: Preliminary investigations; Sask. Energy Mines, Open File Rep. 92-2, 67p.

Jellicoe, B.C., Robertshaw, P., Williamson, P., and Murphy, J. (1998): Summary of exploration activities and results for the Fort-à-la-Corne diamond project, Saskatchewan; *in* Summary of Investigations 1998, Saskatchewan Geological Survey, Sask. Energy Mines, Misc. Rep. 98-4, p144-157.

E. Appendices

Titles and Abstracts of Recent Saskatchewan Energy and Mines Publications and Papers by Staff of the Saskatchewan Geological Survey

---

1. Miscellaneous Reports and Papers

Bennett, R.W. (1998): Assessment Work Catalogue, Saskatchewan; Sask. Energy Mines, Misc. Rep. 98-6, Part 1, p1-650.

__________ (1998): Assessment Work Catalogue, Saskatchewan; Sask. Energy Mines, Misc. Rep. 98-6, Part 2, p651-1302.

Gracie, A.J. and Lafrance, B. (1998): Saskatchewan exploration and development highlights 1998; Sask. Energy Mines, 16p.

Gracie, A.J. and Bennett, R.W. (1999): Saskatchewan exploration and development highlights 1999; Sask. Energy Mines, 14p.

Gracie, A.J. and Tourigny, G. (in press): Saskatchewan exploration and development highlights 2000; Sask. Energy Mines.

2. Maps

Macdonald, R. and Slimmon, W.L. (compilers) (1999): Geological Map of Saskatchewan; Sask. Energy Mines, 1:1 000 000 scale.

Saskatchewan Energy and Mines (1999): Mineral Resource Map of Saskatchewan; Sask. Energy Mines, 1:1 250 000 scale.

3. Digital Products

***Slimmon, W.L.** (1998): Geological Map of Saskatchewan; Sask. Energy Mines, CD-ROM, version 1.*

__________ (1999): Geological Atlas of Saskatchewan; Sask. Energy Mines, CD-ROM, version 2.

__________ (2000): Geological Atlas of Saskatchewan; Sask. Energy Mines, CD-ROM, version 3.

4. External Papers

(Saskatchewan Energy and Mines staff are indicated by **bold** type face)

*Ansdell, K.M., Corrigan, K., Stern, R., and **Maxeiner, R.O.** (1999): Shrimp U-Pb geochronology of complex zircons from Reindeer Lake, Saskatchewan: Implications for timing of sedimentation and metamorphism in the northwestern Trans-Hudson Orogen: Geol. Assoc. Can.–Mineral. Assoc. Can. Joint Annual Meeting, Sudbury 1999, Abst. Vol., p3-4.*

Amphibolite-grade sedimentary and magmatic rocks of the northwestern margin of the Trans-Hudson Orogen are exposed on Reindeer Lake, Saskatchewan, within north-dipping structural panels. As part of the multidisciplinary La Ronge–Lynn Lake Bridge Project, zircons were obtained from five clastic metasedimentary rocks, chosen to constrain the age and provenance of sediments now preserved at different structural levels. These were analysed by the GSC SHRIMP II ion microprobe.

Detrital zircons have overgrowths, and complex cores, which include fragments of igneous zircons with lobate recrystallization textures. The northernmost sample, the Milton Island turbidites (MT), yielded core ages ranging from 1864 ±11 to 2829 ±8 Ma. This indicated a significant older component to the source, potentially the Hearn craton, but also constrains sedimentation to between 1864 and 1859 +3/-2 Ma, the age of the crosscutting Butler Island diorite. The north-dipping Duck Lake shear zone (DLSZ), separates MT from the structurally-underlying McLennan Group (ML), and Levesque Bay assemblage (LB). Probability distribution plots emphasize that ML basal conglomerate and overlying psammite contain a major population of 1845 to 1850 Ma zircons, whereas deeper water metapelites to the south are dominated by 1855 to 1860 Ma zircons. The LB, which pre-dates the 1867 ±4 Ma tonalite, are imbricated with these rocks within the Levesque Bay thrust zone. The ages also suggest that the ML and equivalents, the LB sediments were likely derived from the La Ronge/Wathaman continental arc system. In contrast to the MT, older >1.9 Ga zircons are rare to the south of the DLSZ.

Metamorphic overgrowths and grains are especially common in the more pelitic MT and LB samples, and exhibit uniform cathodoluminescence characteristics, low Th/U (~0.02), and high U concentrations (~1000 ppm). Zircon growth occurred between 1818 and 1805 Ma in the LB, but as late as 1789 Ma in the MT. The former ages are characteristic of peak regional metamorphism throughout most of the Trans-Hudson Orogen, although the significance of the younger age is presently unclear. The contrast in type and age of sedimentation, and difference in timing of metamorphic zircon growth does suggest that the DLSZ represents a major tectonic break.

*Ansdell, K.M., MacNeil, A., **Delaney, G.D.**, and Hamilton, M.A. (2000): Rifting and development of the Hearne craton passive margin: Age constraint from the Cook Lake area, Wollaston Domain, Trans-Hudson Orogen, Saskatchewan; GeoCanada 2000, Calgary, May 2000, Conference CD, ext. abstr. #777.*

***Ashton, K.E.**, Froese, E., and Legault, A. (1999): Recognition of felsic volcanic rocks and* *hydrothermal alteration in moderately to highly metamorphosed parts of the Flin Flon volcanic belt;* in *Ashton, K.E. and Harper, C.T. (eds.), MinExpo'96 Symposium–Advances in Saskatchewan Geology and Mineral Exploration, Sask. Geol. Soc., Spec. Publ. No. 14, p27-43.*

In the amphibolite facies terrains north of Flin Flon, the Flin Flon volcanic belt is represented both as continuous extensions (e.g. the Wildnest-Mirond and Kisseynew lakes areas) and more isolated occurrences (e.g. Sherridon and Scimitar Lake areas). In the absence of primary features, it has generally been assumed that the felsic gneisses in these terrains were derived from plutonic or sedimentary precursors. However, the composition of many of these felsic gneisses could also indicate volcanic protoliths, and the spatial association of intermediate to mafic gneisses, amphibolite, VMS-type sulphide mineralization (e.g. Sherridon, FON, Teejay, and DRS deposits), and metamorphosed hydrothermal alteration supports a volcanic origin.

Four alteration types are recognized: calcic (clinopyroxene, epidote, calcite), ferromagnesian (cordierite, garnet, orthoamphibole, cummingtonite), potassic (muscovite, biotite), and aluminous (aluminum silicates). Several of these commonly occur together (e.g. at Sherridon and Wildnest Lake), which allows easy recognition of potentially mineralized areas. The association of altered rocks with felsic gneisses and amphibolites is particularly interesting and should act as an incentive for more detailed exploration of these high-grade terrains.

Ashton, K.E. *and* ***Harper, C.T.*** *(editors) (1999): MinExpo'96 Symposium–Advances in Saskatchewan Geology and Mineral Exploration, Sask. Geol. Soc., Spec. Publ. No. 14, 163p.*

Ashton, K.E.*, Hartlaub, R.P., Heaman, L.M., and Card, C.D. (2000): The northeastern Rae Province in Saskatchewan; GeoCanada 2000, Calgary, May 2000, Conference CD, ext. abstr. #696.*

Ashton, K.E.*, Heaman, L.M., Lewry, J.F., Hartlaub, R.P., and Shi, R. (1999): Age and origin of the Jan Lake Complex: A glimpse at the buried Archean craton of the Trans-Hudson Orogen; Can. J. Earth Sci., v36, p185-208.*

The largely buried Sask Craton is a continental fragment or microcontinent that collided with and underthrust the Paleoproterozoic Flin Flon–Glennie protocontinent along the Pelican Décollement Zone at 1840-1830 Ma. Rocks of the Sask Craton are exposed in three tectonic windows. Those of the Pelican Window have been named the Jan Lake Complex and comprise ≥2960 Ma arc-derived leucocratic orthogneisses, migmatitic paragneisses, and a tholeiitic, within-plate igneous suite comprising 2488 Ma dioritic to gabbroic rocks and 2450 Ma enderbitic and charnockitic rocks including the Sahli Granite. Ages of ca. 2450 Ma are also common from the other two tectonic windows to the Sask Craton, suggesting that emplacement of the igneous suite was widespread and perhaps part of the coeval Matachewan Igneous Event. The absence of rocks in the ≥2960 and ca. 2450 Ma age ranges on both the adjacent Superior and Rae-Hearne cratonic margins makes it improbable that the Sask Craton was derived by simple fragmentation without large-scale tectonic transport. The overthrust Paleoproterozoic rocks represent a high-grade northwestern extension of the Flin Flon volcanic belt and include 1856 Ma leucotonalite and 1843 Ma quartz monzodiorite. An 1830 Ma suite of homogeneous, calc-alkaline enderbitic rocks, which intrude Burntwood semipelitic migmatites throughout the Kisseynew Domain, has also been emplaced in mylonites of the Pelican Décollement Zone. Zircon and monazite ages in the 1812-1803 Ma range record a high-grade metamorphic event that resulted from collision between the Sask Craton and Flin Flon–Glennie Complex.

Card, C.D., Bethune, K.M., ***Ashton, K.E.****, and Heaman, L.M. (2000): The Oldman-Bulyea Shear Zone: The Nevins Lake Block–Train Lake Domain Boundary, eastern Rae Province, northern Saskatchewan; GeoCanada 2000, Calgary, May 2000, Conference CD, ext. abstr. #596.*

Christopher, J.E., ***Gilboy, C.F., Paterson, D.F.****, and Bend, S.L. (eds.) (1998): Eighth International Williston Basin Symposium, Sask. Geol. Soc., Spec. Publ. No. 13, 290p.*

Coolican, J., ***Ashton, K.E.****, and Card, C.D. (2000): Geochemistry and tectonic setting of meta-igneous rocks within the Train Lake and Dodge domains, eastern Rae Province, Saskatchewan; GeoCanada 2000, Calgary, May 2000, Conference CD, ext. abstr. #706.*

Corrigan, D., Lucas, S.B., Thériault, R., ***Maxeiner, R.O.****, and Ansdell, K.M. (1999): Terrane assembly and tectonomagmatic evolution of the northwestern Reindeer Zone, Trans-Hudson Orogen: Insights from the Reindeer Lake Transect; Geol. Assoc. Can.–Mineral. Assoc. Can. Joint Annual Meeting, Sudbury 1999, Abst. Vol., p26.*

The northwestern Reindeer Zone along Reindeer Lake, Saskatchewan, forms a north-northwest dipping imbricate stack that consists of juvenile volcanic arc rocks, sedimentary basins of various ages and tectonic setting, plutonic rocks including the ca. 1.86 Ga Wathaman Batholith, and the Archean Peter Lake Domain. The structurally lowest level (Kisseynew Domain) consists of <1.84 Ga fluvial sediments (McLennan/Sickle Group) that appear to grade southwards into Burntwood Group turbidites, suggesting the deepening of a sedimentary basin in that direction. Geological relationships in the McLennan/Burntwood transition zone are obscured by high strain zones and the occurrence of narrow thrust slices comprising supracrustal rocks older than ca. 1.87 Ga and tentatively correlated with the La Ronge arc.

The Kisseynew Domain is overthrust along its northern flank by the La Ronge Domain, which consists of ca. 1.88-1.89 Ga volcanic and associated sedimentary rocks (Central Metavolcanic Belt) intruded by 1.86-1.85 Ga calc-alkaline plutons. Turbiditic sediments (Milton Island assemblage) structurally and stratigraphically overly the volcanic rocks and are interpreted as remnants of another basin, flanking the Central Metavolcanic Belt.

North of the La Ronge Domain, higher-grade equivalents of the Central Metavolcanic Belt, Milton Island assemblage, and a ca. 1.89 Ga orthogneiss complex of dioritic to granitic composition yielding a juvenile ε-Nd signature can be traced to the south margin of the Wathaman Batholith, where they are intruded by the latter. This assemblage corresponds to the Rottenstone Domain, which appears to represent the higher-grade equivalent of the La Ronge Domain in the study area.

A recently identified assemblage of clastic metasedimentary rocks (Park Island assemblage) occurring immediately south of the Wathaman Batholith consists of polymictic conglomerate grading stratigraphically upwards into arkosic sandstone, calcareous sandstone and siltstone. Structural relationships suggest that the Park Island assemblage was deposited on previously folded rocks of the La Ronge Domain and subsequently intruded by the Wathaman Batholith. We speculate that the Park Island assemblage was deposited in the forearc basin between the Hearne margin and the advancing La Ronge arc shortly before the emplacement of the Wathaman Batholith. The present day crustal architecture can be inferred to be the result of continued post-collisional convergence.

Delaney, G.D. *(1999): Gold in the Glennie Domain: Relationship to a major temporal break in the supracrustal succession;* in *Ashton, K.E. and Harper, C.T. (eds.), MinExpo '96 Symposium–Advances in Saskatchewan Geology and Mineral Exploration, Sask. Geol. Soc., Spec. Publ. No. 14, p71.*

The Glennie Domain of the Trans-Hudson Orogen, northern Saskatchewan, contains in excess of eighty gold occurrences and one gold producer, the Seabee mine at Laonil Lake. Nearly all occurrences are within or adjacent to greenstone belts; by far the greatest number of showings, including the Seabee orebodies, are hosted in the Pine Lake Greenstone Belt. Gold-quartz veins occur in shear zones in a variety of rock types including volcanics, volcaniclastics, sediments, intrusions (both subvolcanic and younger post-volcanic suites), and migmatites. They are also in close spatial association with a major stratigraphic break that separates two distinct assemblages of supracrustal rocks and two major suites of intrusions. The older supracrustal assemblage, which is commonly more volumetrically extensive, consists of ca. 1890 Ma mafic to intermediate volcanic, volcaniclastic, and subvolcanic intrusive rocks emplaced in anomalous island arc settings. The older suite of intrusions comprises granodioritic and tonalitic plutons emplaced between 1846 and 1859 Ma. The younger supracrustal assemblage is a ca. 1840 Ma succession of volcaniclastic, sedimentary, and minor intermediate to felsic volcanic rocks, which at least locally are overlain by a thick sequence of arkose, grit, and conglomerate. A second, volumetrically more restricted suite of granodioritic to granitic intrusions were emplaced between 1828 and 1836 Ma.

Gold mineralization occurs in secondary or tertiary shear zones typically developed in areas of lithologic heterogeneity during D2 regional deformation. Gold is associated with quartz veins, alteration phases, and sulphide minerals and is paragenetically late. D3 and/or D4 deformation events and syn- to post-D3 amphibolite facies metamorphism are superimposed.

Dunn, C.E., ***Haidl, F.M.****, Yeager, J.R., Butrenchuk, E., Dorval, D., and Larson, B. (1998): Surface geochemical patterns derived from selective leaching of soils over a deep Ordovician oil pool, Bromhead, southeastern Saskatchewan;* in *Christopher, J.E., Gilboy, C.F., Paterson, D.F., and Bend, S.L. (eds.), Eighth International Williston Basin Symposium, Sask. Geol. Soc., Spec. Publ. No. 13, p254-265.*

Surface geochemical detection of deeply seated hydrocarbons is an inexact science. It has been firmly established that there is upward movement of chemical compounds from hydrocarbon reservoirs. Therefore the challenge is to develop economical methods to assist in differentiating those seismic anomalies that represent barren structures from those that host hydrocarbons.

The recently developed enzyme leach method of extracting elements loosely bound to amorphous manganese oxide coatings on soil particles has been tested in southeastern Saskatchewan. The target, an Ordovician Red River reservoir at a depth of 2850 m, was studied by collecting soil samples from 74 sites within a one square mile (2.6 km^2) section. A 3-D seismic structure that is quite pronounced at the Ordovician Winnipeg–Red River formation level is outlined by a number of element enrichments in the soils that flank its surface projection. Of note are relative enrichments of the halogens (Br, I, Cl) and of Mo, Re, W, V, As and Sb. Copper, Ni, Ba, Cd, Sr and U also show positive but less distinctive relationships to the structure.

Fanton, K., Holmden, C., Nowlan, G., and ***Haidl, F.M.*** *(1998): Nd and C isotope stratigraphy of Ordovician carbonates in the Williston Basin;* in *Christopher, J.E., Gilboy, C.F., Paterson, D.F., and Bend, S.L. (eds.), Eighth International Williston Basin Symposium, Sask. Geol. Soc., Spec. Publ. No. 13, p8.*

Nd and C isotopic profiles were constructed for a section of Ordovician cores from southeastern Saskatchewan in order to investigate Nd and C isotopic distributions within the Williston Basin. The Yeoman and Herald formations show large (3‰) variations in $\delta^{13}C$ values which mirror changes in lithology. In contrast, C isotopic values are more uniform within the Hartaven, Gunn and first 10 m of the Gunton members of the Stony Mountain Formation. This correspondence between $\delta^{13}C$ values and lithology reflects carbon cycling within the Williston Basin and therefore suggests a method for correlating carbonate sequences, provided that factors operative in southeastern Saskatchewan are representative of the whole basin.

Minute amounts of Nd dissolved in seawater are derived from river inputs and the isotopic composition reflects the average age of the surrounding crust. Previous studies have shown that a substantial shift in the isotopic composition of Nd in Lower Paleozoic clastics indicates that a major change in the age of emergent continental crust had occurred throughout North America. We have found this Nd isotopic shift within the Yeoman Formation of the Williston Basin. Pre-shift epsilon values are -17, whereas post-shift epsilon values range between -7 and -9 for the rest of the sampled section. The magnitude and singularity of this shift within the Ordovician provide another means of correlating strata within the Williston Basin. The pre-shift values are a result of river inputs from Precambrian rocks, including those exposed on the Transcontinental Arch. Less negative post-shift values indicate a source terrain substantially younger in crustal age. The similarity in εNd values (-7 to -9) within the Williston Basin to εNd values (-6 to -9) of Appalachian clastics suggests an emergence of a common Taconic watershed and submergence of the intervening Transcontinental Arch during deposition of the Yeoman. The persistence of the less negative εNd values (-7 to -9) throughout the rest of the section may be interpreted to reflect continued submergence of the arch.

__________ *(2000): Nd isotope stratigraphy of Late Ordovician carbonates; GeoCanada 2000, Calgary, May 2000, Conference CD, ext. abstr. #526.*

***Gilboy, C.F., Haidl, F.M.**, Casswell, C., Edwards, B., and McMaster, L. (2000): Dancing on rocks: Geosciences and our communal future–the Saskatchewan experience; GeoCanada 2000, Calgary, May 2000, Conference CD, ext. abstr. #914.*

Grieve, R.A.F., ***Kreis, L.K.**, and Therriault, A.M. (1998): Impact structures of the Western Sedimentary Basin of North America: New discoveries and hydrocarbon resources;* in *Christopher, J.E., Gilboy, C.F., Paterson, D.F., and Bend, S.L. (eds.), Eighth International Williston Basin Symposium, Sask. Geol. Soc., Spec. Publ. No. 13, p189-201.*

Seven impact structures are now known from the Western Sedimentary Basin of North America. This contribution reports on the discovery of shock metamorphic effects at three of these structures: Elbow, Maple Creek and Viewfield, all in Saskatchewan. It also describes their general character and that of the other impact structures in the basin. Particular emphasis is placed on the production of hydrocarbons from these structures, which ranges from none to 1000 BOPD (at Red Wing Creek, North Dakota). Other hydrocarbon-producing impact structures in Canada, Mexico and the United States are briefly characterized along with their productivity. Most production at impact structures occurs from structural traps in the rim and central uplift and from brecciated target rocks, including crystalline rocks. The most productive impact-related hydrocarbon reservoir rocks are breccias in the Gulf of Mexico believed to be genetically linked to the K/T impact that formed the Chicxulub structure on the Yucatan Peninsula, Mexico. Many impact structures remain to be discovered throughout the world. For example, the current estimate of the terrestrial cratering rate indicates that as many as 12 ±6 impact structures with diameters of 10 km or greater remain to be discovered in the Williston Basin. If half of them have reserves similar to the 9 km diameter Red Wing Creek structure, the cumulative potential impact-related reserves are in the order of 1 BBO and 600 BCFG in the Williston Basin alone.

***Haidl, F.M.**,* ***Kreis, L.K.**, Miles, W.,* ***Nickel, E.**, and Ware, M.J. (2000): Relationships between Phanerozoic sedimentation, erosion, hydrocarbon accumulations, and basement tectonics: Examples from Lower Paleozoic strata in southeastern Saskatchewan; GeoCanada 2000, Calgary, May 2000, Conference CD, ext. abstr. #933.*

Hamilton, M.A. and ***Delaney, G.** (2000): New U-Pb geochronological constraints on the age of basement and cover in the eastern Wollston Domain, Saskatchewan, and evolution of the SE Hearne Province; GeoCanada 2000, Calgary, May 2000, Conference CD, ext. abstr. #1103.*

***Harper, C.T.** (1999): Structural styles in, and transitions from, the La Ronge, Kisseynew and Glennie domains, Waddy Lake–Southend region;* in *Eighth LITHOPROBE Trans-Hudson Orogen Transect Workshop, Saskatoon, Feb. 25-26, 1999.*

Recent geological mapping of the northeastern extension of the La Ronge Domain, including parts of the MacLean Lake Belt (Kisseynew Domain) and northern extremity of the Glennie Domain in the region between Waddy Lake and Southend (Harper, 1996, 1997, 1998; Maxeiner, 1996), has revealed some interesting structural features and contrasts. Each of the three domains has a different lithological character and structural style. The structural transitions between the domains can be correlated to the LITHOPROBE seismic reflection Line S2B, which transects part of this area.

The Central Metavolcanic Belt (CMB) of the La Ronge Domain in the Waddy Lake area comprises ultramafic to felsic volcanic and plutonic rocks with minor volcaniclastics (Harper, 1984, 1985). The CMB essentially acted as a rigid structural domain preserving less deformed and lower metamorphic grade rocks. It is typified by steep to subvertical dips, regional homoclinal to isoclinal folds, and pressure-shadow style deformation around the 1855-1850 Ma plutons and tighter deformation aureoles around the younger 1835 Ma plutons. Small-scale folds are rare in the CMB. The boundary with the adjacent sedimentary belts is marked in part by an unconformity, locally represented by a basal polymictic conglomerate, but also by a high-strain zone, which places the CMB structurally above the younger metasediments of the MacLean Lake Belt (MLB).

The MacLean Lake Belt (MLB), which is more appropriately considered part of the Kisseynew Domain, mainly comprises psammitic to pelitic gneisses, with lesser amphibolitic (mafic volcanics) and calc-silicate gneisses. Feldspathic psammites and minor conglomerate of the McLennan Group represent the youngest near shore sediments of the sequence. Intrusive sheets of ultramafic to felsic composition are a minor component. Deformation and metamorphism increase in intensity and grade (attaining granulite grade) away from the CMB. The MLB is characterized by decreasing dips away from the contact with the CMB, becoming very shallow to subhorizontal SE of the Stanley Shear Zone (SSZ). The SSZ also marks a change in structural style. To the NW are strongly linear, highly attenuated structures disrupted by numerous parallel thrust faults producing a complicated structural interleaving of metasediments and metavolcanics. A well-developed stretching lineation plunges shallowly NNE. This imbricate thrust zone extends northeast to and across Reindeer Lake (Maxeiner, 1997, 1998; Corrigan *et al.*, 1997, 1998). Southeast of the SSZ are large-scale, open dome and basin and mushroom-shaped interference structures, which refold an earlier formed porphyroclastic texture. As a result of the folding, the equivalent stretching lineation is highly variable in attitude. The transition to the Glennie Domain, along the NW margin and along the east margin near Southend, is marked by a prominent mylonite zone affecting rocks of both domains. The early-formed porphyroclastic-textured mylonite is folded and refolded. Pseudotachylite veins and blebs occur in the mylonite locally. Delta wing porphyroclasts and shear folds show a consistent sinistral shear sense consistent with the Kisseynew Domain (and La Ronge Domain) being thrust southwestwards.

The northern margin of the Glennie Domain comprises highly strained, upper amphibolite to granulite grade, mafic to felsic plutonic rocks, termed the Gloeckler Lake Intrusive

Suite (Harper, 1998), and predominantly pelitic metasediments with minor amphibolitic and calc-silicate gneisses interpreted as thrust nappes of Kisseynew gneisses on the Glennie Domain. This part of the Glennie Domain has shallow to moderate dips with a well-developed stretching lineation of variable attitude because of refolding as in the MLB. The mylonitized margin gives way to larger, open interference structures involving the Kisseynew nappes. The Glennie Domain also acted as a more rigid block, with the more plastic Kisseynew metasediments squeezed between it and the La Ronge Domain.

Previous structural interpretations of the seismic reflection line S2B, that followed highway 905 north from the junction with highway 102, show several features which need to be addressed. Hajnal *et al.* (1996) show a narrow strip of Glennie Domain at the southern end of the transect. This is in fact part of the MLB (Kisseynew Domain) with the nearest part of the Glennie Domain being exposed at Street Lake (Harper, 1998) about 4.5 km to the SE. At an average dip of 30 degrees, the Glennie–Kisseynew domain boundary would intersect the plane of the transect at a depth of about 2.5 km, below the prominent reflector indicated on the section. The wedge shaped area beneath the southern end of line S2B could be all Glennie Domain or could include part of the Sask Craton.

In the LITHOPROBE Phase V Proposal volume (Clowes, 1997), the interpretive drawing of Line S2B shows a much narrower La Ronge Domain compared to the Rottenstone Domain which doesn't agree with the geology of the transect. The second point is that the entire wedge-shaped area beneath the southern end of Line S2B is depicted as being Sask Craton. This would mean that a very thin slice of the profile would be representative of the Kisseynew Domain. Also if that interpretation were correct, the Sask Craton would project to surface at the same position as the Kisseynew–Glennie boundary at Street Lake, or could be at a shallow depth beneath a thin skin of Glennie Domain granitoid rocks. Certainly dating rocks of the Gloeckler Lake Intrusive Suite would provide some valuable information on the northern margin of the Glennie Domain.

At this time there are still a number of unanswered questions regarding the northern part of the Reindeer Zone.

1. Although we know that volcanism, plutonism and sedimentation among the La Ronge, Glennie and Flin Flon arcs were contemporaneous, we are still uncertain whether they were linked in any way. Perhaps they were related in a similar fashion as the southwest and western Pacific.

2. What was the role of the Sask Craton? Was it an indentor, driving beneath the Flin Flon–Glennie arc terrain or was it also a transporter, carrying the over riding Glennie and Kisseynew thrust plates northward to collide and be overthrust by the La Ronge Domain?

3. How far north does the Sask Craton extend and is it imaged in the seismic reflection Line S2B? If one of the structural interpretations of Line S2B is correct, is the Sask Craton exposed in the northern Glennie Domain? Isotopic studies on pegmatites from this region and further geochronological studies could provide the answers.

4. If the Kisseynew basin represents some combination of back-arc or interarc basin, was there any oceanic crust developed and if there was where is it? It could have been entirely subducted. Geological mapping and geochemical studies of the amphibolite gneisses of the MLB (Harper, 1996, 1997, 1998; Hasanie and Harper, 1997; Hasanie, 1998; Harper and Hasanie, this meeting) have shown that they are primarily derived from pillowed metabasalts. The amphibolites have a consistent ocean floor basalt (or N-MORB) chemical affinity with some transitional affinity to volcanic arc basalts which is characteristic of back arc basalts. Therefore, these rocks are the best candidates for the missing oceanic crust.

Harper, C.T. and Hasanie, R. (1999): Geochemistry and tectonic implications of amphibolite gneisses of the MacLean Lake Belt, Waddy Lake–Southend Region; **in *Eighth LITHOPROBE Trans-Hudson Orogen Transect Workshop, Saskatoon, Feb. 25-26, 1999.***

Amphibolites of the MacLean Lake belt (MLB) have been variously interpreted to be derived from sedimentary, volcanic, and plutonic protoliths. This diversity of opinion in part reflects the high-metamorphic grade, the lack of preserved primary structures, and misinterpretation of the effects of early carbonate alteration of the amphibolites. During recent remapping of the region between Waddy Lake and Southend (Harper, 1996, 1997, 1998), the nature and origin of these rocks were investigated through field examination, petrography, and whole rock and trace element geochemistry (Hasanie and Harper, 1997), which formed the basis of an honours thesis by Hasanie (1998). The earlier results are augmented by additional geochemical data obtained during the 1998 mapping season.

The amphibolites commonly cap prominent topographic ridges and are generally better exposed than other rock types of the MLB. They are interlayered with metasediments of the MLB (part of the Kisseynew Domain) and are very commonly associated with a calc-silicate assemblage (marble, quartzite/metachert, calcareous psammopelite) of sedimentary derivation. The amphibolites also have a calcareous component consisting of pods, lenses, and bands comprising variable amounts of epidote, diopside, carbonate, plagioclase, quartz, garnet, sphene, and sulphides. This component, which is interpreted as representing early alteration of mafic volcanics, commonly produces a streaky to banded habit, which undoubtedly caused some workers to think of them as metasediments.

Johnston (1969 , 1970, 1982, 1983), who mapped this region at 1:63,360 scale in the mid 60's to early 70's, had recognized pillow structures in a few places and generally considered the amphibolites to be metabasalts. Harper (1996, 1997, 1998) also considers the amphibolites to be primarily of volcanic origin based on recognition of pillow structures, together with fragmental textures, intercalation of minor intermediate to felsic varieties, and the early volcanogenic calcareous and siliceous alteration.

The amphibolites comprise massive and well banded varieties. The massive type tends to be a black to dark greenish black, coarser gained hornblende-plagioclase rock that in places has a rectilinear net-veined character. Locally this type may have a spotted appearance caused by abundant plagioclase porphyroblasts, some of which have a core of garnet. The massive types may represent thicker flows or intrusive sills. The banded type has alternating dark green to black hornblende-rich layers and pale to medium green diopside-bearing layers. Calcite is locally abundant and weathers recessively. In most outcrops of this type flattened ovoid shapes, V-shaped intersections, and amphibole±biotite±garnet-rich 'selvages' suggest that these rocks originated from altered pillowed flows.

Rock samples used for geochemical studies were selected on the basis of the least evidence of alteration and compositional homogeneity. Samples collected in 1996 were analyzed by Bondar Clegg, Vancouver, in 1997 by Acme Analytical Laboratories Ltd., Vancouver, and in 1998 by Activation Laboratories Ltd., Ancaster. Except for the rare earth elements (REE) the analyses from the three companies were very consistent. For comparative purposes metabasalts from the southeastern margin of the Central Metavolcanic Belt (CMB) of the La Ronge Domain are included.

The amphibolites have a narrow range of silica, from 48 to 51 percent, and show little evidence of alkali mobility on Harker type plots. On silica versus alkalis plots the amphibolites display subalkaline and low to medium potassium basaltic characteristics as do the CMB metabasalts. On the Jensen cation plot, the amphibolites mainly cluster in the high-iron tholeiite field compared to a broader spread for the CMB basalts, which cover high iron, high magnesium tholeiite and some calc-alkaline basalt fields. This probably reflects more diversity and/or alteration effects in the CMB rocks.

Immobile element basalt discrimination diagrams help resolve the tectonic setting in which the rocks were formed. The Ti/100-Zr-Yx3 ternary diagram (Pearce and Cann, 1973) shows the amphibolites and CMB basalts overlap the low potassium tholeiite (LKT) and ocean floor basalt (OFB) fields. On the Zr versus Ti diagram (Pearce and Cann, 1973) the generally higher Ti content of the amphibolites begins to show more of a distinction between them and the CMB basalts. The amphibolites plot near the upper limit of the LKT field as well as in the OFB and in the area where the two types overlap. Most of the CMB basalts plot near the lower end of the LKT field. On the Ti/100-Sr-Sr/2 ternary diagram (Pearce and Cann, 1973) the split is more evident, with the majority of the amphibolite samples plotting in the OFB field and a few falling in the island arc basalt (IAB) field. The CMB basalts mostly plot in the IAB field with several near or in the cal-alkaline basalt (CAB) field. The Cr versus Ti diagram (Pearce, 1975) shows a clear distinction with the amphibolites showing a relatively tight cluster and plotting entirely in the OFB field and the CMB basalt, except for two samples, plot within the LKT field. On the Nbx2-Zr/4-Y ternary diagram (Meschede, 1986) amphibolite samples from 1998 plot in the overlapping N-MORB and volcanic arc basalt field.

A primitive mantle normalized REE plot of the amphibolites shows a relatively flat profile which compares well with N-MORB and back-arc basalt (BAB) profiles of young basalts (Jenner, 1996). Similarly a MORB normalized spider plot for the amphibolites is most like the BAB profile (Jenner, 1996).

The chemical signatures of the amphibolites and CMB basalts generally indicate that they were derived from different magmatic sources and in different tectonic settings. The amphibolites typically show an OFB affinity with some transitional VAB character, whereas the CMB basalts generally show a VAB affinity. The locally preserved pillowed character of the amphibolites is also consistent with an OFB setting. The OFB and transitional VAB character together with the association with Kisseynew basin sediments is also consistent with the amphibolites having formed in a back arc tectonic setting. The interlayering of the amphibolites and sediments may be in part primary, but probably also due to thrust tectonics as the Kisseynew basin was destroyed between the colliding La Ronge and Glennie domains. The amphibolites potentially represent the missing oceanic crust of the Kisseynew basin.

Harper, C.T., *Heaman, L.M., and Prokopiuk, T.C. (2000): Glassy pseudotachylite preserved in Paleoproterozoic Gloeckler Lake Mylonite Zone at the Kisseynew Domain–Glennie Domain boundary, Street Lake area, northern Saskatchewan; GeoCanada 2000, Calgary, May 2000, Conference CD, ext. abstr. #124.*

Hertlaub, R.P., Heaman, L.M., Chacko, T., and **Ashton, K.E.** *(2000): The Murmac Bay group, southern Rae Province: Evidence for an Archean ensialic basin?; GeoCanada 2000, Calgary, May 2000, Conference CD, ext. abstr. #948.*

Hilgers, C., Büker, C., Urai, J.L., Littke, R., Post, A.D., van der Zee, W., and **Kraus, J.** *(2000): Field study on an exhumed lower Devonian high pressure reservoir; European Geophysical Society, XXV General Assembly, Millennium Conference on Earth, Planetary & Solar Systems Sciences, Nice, France.*

We present a field-based study on a thick lower Devonian deltaic sand-shale sequence. The rocks studied are present in excellent quality outcrops around the shores of the Rur Lake (Rhenish Massif, Germany), and allow us to study processes occurring in a depth range not yet explored by drilling. We studied microstructure evolution in transmitted light microscopy, combined with fluid inclusion microthermometry and basin modelling. Microstructures indicate that the burial was initially at near-hydrostatic pore pressures. During compaction cohesion was built up by cementation. Then, pore pressure rose to values around the (horizontal) minimum principal stress, as evidenced by a suite of layer-perpendicular quartz veins in the sandstones, which show mode one trans-granular fracturing. The period of overpressuring was long-lived, in a setting of moderate tectonic extension, as shown by up to ten percent layer-parallel extension by crack-seal processes. Basin modelling helped to constrain the influence of gas generation and clay dewatering on overpressure build-up. Onset of tectonic shortening and rotation of principal stress direction is reflected by the development of layer-parallel reverse faults and associated quartz veins. Shear stress levels have increased as indicated by quartz microstructures, probably associated with a rise in pore pressure. Where the reverse faults crosscut bedding in small ramps, large amounts of quartz veins with complicated structures were formed, suggesting that these were major pathways for fluid migration. The early thrusts were overprinted by progressive folding and the development of a slaty cleavage in the pelitic layers.

Kelley, L.I. *(1998): Industrial minerals of Saskatchewan: An overview of geology, production, and prospects; Focus on Industrial Minerals, Canadian Institute of Mining and Metallurgy, Vancouver, October 1998, Abst., p65-67.*

Industrial mineral production contributes on the order of CDN$1.5 billion per year to the economy of Saskatchewan. Potash is the primary industrial mineral produced in the province, followed by aggregate, sodium sulphate, salt, potassium sulphate, peat, clays, silica sand, calcium chloride brine, and "clinker". Potentially economic deposits of kaolin, diamond, and building stone are under evaluation.

__________ *(1999): Industrial minerals of Saskatchewan;* in *Johnson, K.J. (ed.), Proceedings of the 34th forum on the geology of industrial minerals, Norman, OK, Oklahoma Geological Survey Circular 102, p309-312.*

Industrial-mineral production contributes on the order of CDN$1.5 billion per year to the economy of Saskatchewan, Canada. Potash is the primary industrial mineral produced in the province, followed by aggregate, sodium sulphate, salt, potassium sulphate, peat, clays, silica sand, calcium-chloride brine, and "clinker". Potentially economic deposits of kaolin, diamond, and building stone are under evaluation. All of the major deposits of commodities discussed here are located south of lat. 56°30'N.

Kelley, L.I. *and Holmden, C. (1999a): Geochemistry of groundwater associated with economic deposits of sodium sulfate (mirabilite) in saline lakes of Saskatchewan, Canada; Seventh International Conference on Salt Lakes, Death Valley, California, Sept. 1999, abstr.*

Sodium sulfate has been mined from evaporite deposits in post-glacial, groundwater-fed, endorheic lake basins in Saskatchewan since 1918. Sodium sulfate is used in the manufacture of detergents, fresheners, glass, paper and textiles. Recently, Saskatchewan companies have pioneered the use of sodium sulfate in the value-added manufacture of potassium sulfate used as a fertilizer for chloride-sensitive crops.

We have begun a five-year project to advance understanding of the origin of these deposits as modern ore-forming systems. Because groundwater continues to supply ions to the lake basins through spring discharge, our approach is hydrogeological, with the major objective of quantifying fluid and chemical mass balances.

Our initial efforts are focused on evaluating which portion of the groundwater flow system supplies ions to the lake basins. Hydrogen and oxygen isotopes demonstrate that relatively shallow (<200m) systems are the source of groundwater that discharges in springs near sodium sulfate deposits. Preliminary work with strontium isotopes shows that different inter-till aquifers appear to have different ^{87}Sr/^{86}Sr ratios. In some cases the lake brine isotopic composition matches that of groundwater discharging from springs. The challenge ahead is to determine whether strontium isotopes can be used to fingerprint specific aquifer inputs in a context of potential ^{87}Sr/^{86}Sr evolution along groundwater flow paths.

__________ *(1999b): Origin of sodium sulphate deposits of southern Saskatchewan, Canada: 1. Stable isotope and chemical composition of groundwater; 35th Forum on the Geology of Industrial Minerals, Salt Lake City, May 1999, abstr.*

Sodium sulphate is used in the manufacture of powdered detergents, carpet fresheners, plate (float glass), kraft paper and textiles. It is also reacted with potash to produce potassium sulphate. Sodium sulphate has been mined from lacustrine evaporite deposits in southern Saskatchewan since 1918. In 1997, three companies operated four sodium sulphate operations, and two other companies extracted sodium sulphate for potassium sulphate production. The total value of sodium sulphate and potassium sulphate produced in Saskatchewan in 1997 was approximately $CDN 40 million.

The deposits occupy post-glacial endorheic (closed) lake basins in a belt that stretches from northwestern North Dakota and northeastern Montana across southern Saskatchewan to east-central Alberta. Previous workers generally acknowledge the empirical relationship between evaporitic mineralization and the presence of active lake-bottom or peripheral springs. Groundwater discharging into the lake basins contains 1000 to 5000 ppm of total dissolved solids (TDS). Most of the TDS load is Na^+ and $SO_4^=$. Groundwater is viewed as a causative agent, but workers disagree on the ultimate origin of the groundwater (e.g. connate water, deeply circulating brines, or recent meteoric water) and the source of dissolved ions (e.g. Paleozoic evaporites deep in the sedimentary section, bentonite in Cretaceous mudstones, or till). None of the previous workers tested their hypotheses.

Hydrogen and oxygen isotope results for groundwater sampled from six sodium sulphate deposits suggest that the spring systems that currently supply ions to alkali lakes in southern Saskatchewan are not hydraulically connected to Paleozoic saline aquifers. Major ion chemistry suggests that the groundwater may be at least partly from a pre-Wisconsinan aquifer, perhaps mixed with shallow groundwater during ascent.

__________ *(2000): Reconnaissance hydrogeochemical investigations of economic lacustrine evaporite deposits in post-glacial basins, Saskatchewan; GeoCanada 2000, Calgary, May 2000, Conference CD, ext. abstr. #326.*

Kraus, J. *(2000): Back-rotation during crenulation cleavage development: Implications for structural facing and cleavage-forming processes: Discussion; J. Struc. Geol., v22, p149-151.*

Kraus, J. *and Williams, P.F. (1999): The structural development of the Snow Lake Allochthon and its role in the evolution of the southeastern Trans-Hudson Orogen in Manitoba, Central Canada; Can. J. Earth Sci., v36, p1881-1899.*

The Snow Lake Allochthon is a zone of tectonic interleaving of sedimentary rocks of an inverted marginal basin (Kisseynew Domain) with island arc and oceanic rocks. It is located in the southeastern part of the exposed internal zone of the Trans-Hudson Orogen in Manitoba, Canada, near the external zone (Superior collision zone or Thompson Belt), which constitutes the local boundary between the Trans-Hudson Orogen and the Archean Superior craton. The Snow Lake Allochthon formed, was deformed, and was metamorphosed up to high grade at low to medium pressure during the Hudsonian orogeny as a result of the collision of Archean cratons ~1.84-1.77 Ga ago. Four generations of folds (F_1-F_4) that formed in at least three successive kinematic frames over a period of more than 30 m.y. are described. Isoclinal to transposed southerly verging F_{1-2} structures are refolded by large open to tight F_3 folds and, locally, by open to tight F_4 folds. The axes of the F_{1-2} folds are parallel or near-parallel to the axes of F_3 folds, owing to progressive reorientation of the F_{1-2} axes during south- to southwest-directed tectonic transport, followed by F_3 refolding around the previous linear anisotropy. A tectonic model is presented that reconciles the distinct tectonometamorphic developments in the Snow Lake Allochthon and the adjacent part of the Kisseynew Domain on the one hand, and in the Thompson Belt on the other, during final collision of the Trans-Hudson Orogen with the Superior craton.

***Kraus, J.** and Williams, P.F. (in press): The structural and metamorphic history of the Snow Lake area, internal Trans-Hudson Orogen: A synopsis; LITHOPROBE Trans-Hudson Orogen Transect, Report.*

__________ (in press): A new spin on "non-rotating" porphyroblasts: Implications of cleavage refraction and reference frames; J. Struc. Geol.

***Lafrance, B.**, Corrigan, D., and **Sibbald, T.I.I.** (1999): The Grease River Shear Zone: Proterozoic reactivation along the margin of the Archean East Athabasca Mylonite Triangle in the Snowbird Tectonic Zone; Geol. Assoc. Can.–Mineral. Assoc. Can. Joint Annual Meeting, Sudbury 1999, Abst. Vol., p65-66.*

The East Athabasca mylonite triangle (EAMT) is a deep-crustal mylonite zone at the boundary between the Rae and Hearne provinces. The EAMT is exposed over 75 km along the north shore of Lake Athabasca, Saskatchewan, but it disappears under the ca. 1.7 Ga Athabasca Basin, south of the lake. Deep-crustal shearing at ca. 2.6 Ga produced the regional, granulite-grade mylonitic foliation, which characterized the EAMT. The EAMT is bounded by narrow greenschist-grade shear zones, the Grease River Shear Zone (GRSZ), to the west and the Black Lake Fault to the east. The two shear zones have been previously interpreted as products of strain localization of the deep-crustal deformation into narrow strike-slip structures during Late Archean exhumation of the granulite terrain.

Mapping of the GRSZ along Lake Athabasca and geochronological constraints suggest that the GRSZ is a Proterozoic shear zone, which overprints and reactivates the Archean structure with minor Proterozoic reworking, as previously inferred. The GRSZ forms the western margin of a wider, greenschist-grade, strain zone, which extends over 6 km in the EAMT. In this strain zone, the Archean mylonitic foliation is folded by open to tight folds with an axial planar cleavage, defined by flattened biotite and muscovite knots replacing garnet porphyroblasts. In the GRSZ, folding is more intense, and the folds, which plunge 40-50 degrees to the NE, consistently have dextral asymmetry. With increasing shear, the folds tighten, their axial planes rotate in clockwise fashion, and the folds become bounded by biotite-rich décollement zones parallel to the Archean mylonitic foliation. These structures and dextral shear bands are indicative of dextral transcurrent shear along the GRSZ. Muscovite- and biotite-bearing pegmatites and aplites cut across the Archean mylonitic foliation and are overprinted by the folds. Preliminary isotopic work produced a Proterozoic U-Pb zircon crystallization age for the dykes, suggesting a Proterozoic age for the GRSZ. A ca. 1.9 Ga, deformed, leucogranite dyke, 2.6 km northeast of the study area, cuts across the greenschist-grade foliation of the GRSZ, and further supports a Proterozoic age for the GRSZ.

*Lucas, S.B., Syme, E.C., and **Ashton, K.E.** (1999): New perspectives on the Flin Flon Belt, Trans-Hudson Orogen, Manitoba and Saskatchewan: An introduction to the special issue on the NATMAP Shield Margin Project, Part 1; Can. J. Earth Sci., v36, p135-140.*

A new tectonic framework for the Flin Flon Belt in southeastern Reindeer Zone of the Trans-Hudson Orogen has emerged in recent years through four-dimensional studies (bedrock and subsurface mapping, seismic reflection profiling, U-Pb geochronology) associated with the NATMAP Shield Margin Project and LITHOPROBE Trans-Hudson Orogen Transect. This special issue contains 10 papers covering a wide variety of topics related to the NATMAP Shield Margin Project.

*Lucas, S.B., **Ashton, K.E.**, Syme, E.C., Stern, R.A., White, D.J., Ansdell, K.M., and Ryan, J.J. (1999): Four-dimensional mapping of the Flin Flon Belt through interdisciplinary NATMAP and LITHOPROBE studies;* in *Ashton, K.E. and Harper, C.T. (eds.), MinExpo'96 Symposium–Advances in Saskatchewan Geology and Mineral Exploration, Sask. Geol. Soc., Spec. Publ. No. 14, p4-25.*

The southeastern Reindeer Zone is marked by a northeast-dipping, crustal-scale stack characterized by three principal elements which were juxtaposed during 1.84 to 1.80 Ga collisional deformation: 1) 3.20 to 2.40 Ga metaplutonic rocks and paragneisses of the 'Sask craton', exposed in the Pelican window; 2) 1.92 to 1.87 Ga juvenile arc and oceanic rocks, 1.88 to 1.84 Ga plutons, 1.87 to 1.85 Ga volcano-sedimentary packages (Schist-Wekusko assemblage), and 1.85 to 1.84 Ga alluvial-fluvial sandstones (Missi Group); and 3) 1.85 to 1.84 Ga marine turbidites (Burntwood Group) and distal facies of the Missi Group sandstones at the highest structural levels (Kisseynew Domain). The middle element in the stack comprises the Flin Flon Belt (now including the Attitti Block and Paleoproterozoic rocks in the Hanson Lake Block) and Glennie Domain (including the Scimitar Complex) and is here termed the Flin Flon–Glennie Complex (FFGC). The previous stratigraphic framework for Flin Flon Belt 'greenstones' (Amisk Group) is insufficient to account for the range in lithological and geochemical associations, Sm/Nd isotopic signatures, and U-Pb zircon ages. As a result, a series of 1.92 to 1.87 Ga arc and ocean floor assemblages have been distinguished. These assemblages are stitched together by cross-cutting plutons (1.88 to 1.84 Ga) and some are separated by early high-strain zones, suggesting that they were accreted to form a tectonic collage at 1.88 to 1.87 Ga. Post-accretion plutons and volcanic rocks (1.88 to 1.84 Ga) are attributed to younger successor arc(s) which were imposed on the collage contemporaneously with regional steepening of the early collision-accretion structures. Uplift and erosion, development of a paleosol and deposition of voluminous turbidites (Burntwood Group) and continental sedimentary rocks (Missi Group) occurred ca. 1.85 to 1.84 Ga, coeval with the waning stages of successor arc magmatism. Assembly of the crustal thrust stack occurred in response to collision of the Sask craton with the overriding FFGC. Due to structural interleaving, the boundary between the FFGC and Kisseynew Domain is best described as a structural-stratigraphic transition zone. In contrast, the boundary between the Sask craton and FFGC is a broad ductile shear zone termed the Pelican décollement zone. Initial thrusting was coeval with 1.84 to 1.83 Ga mafic-felsic calc-alkaline magmatism and ongoing continental sedimentation (Missi Group), and continued through peak regional metamorphism at 1.82 to 1.80 Ga. Oblique collision with the Superior craton occurred at about 1.81 Ga and led to post-collisional sinistral transpression of eastern Trans-Hudson Orogen (THO), with wrench faulting and refolding of the thrust stack producing considerable structural relief. The Namew Gneiss Complex, mapped beneath the Phanerozoic cover south of Flin Flon, represents the middle crust of the intraoceanic terrane juxtaposed against the exposed upper crustal levels by post-collisional wrench faulting.

Maxeiner, R.O.*, Corrigan, D., and* ***Harper, C.T.*** *(2000): Geology of the northwestern Reindeer Zone, southern Reindeer Lake, Saskatchewan: Insights from regional mapping, geochemistry and geochronology; GeoCanada 2000, Calgary, May 2000, Conference CD, ext. abstr. #467.*

Maxeiner, Ralf O. *and* ***Sibbald, Tom I.I.*** *(1999): Redefining contact relationships between McLennan Group and surrounding lithotectonic elements in the southern La Ronge Domain, Trans-Hudson Orogen, Saskatchewan; in Ashton, K.E. and Harper, C.T. (eds.), MinExpo'96 Symposium–Advances in Saskatchewan Geology and Mineral Exploration, Sask. Geol. Soc., Spec. Publ. No. 14, p55.*

The McLennan Group, a lithotectonic element of the La Ronge Domain, has traditionally been viewed as a molasse deposit lying unconformably upon rocks of the Central Metavolcanic Belt (CMB) and the MacLean Lake Belt (MLB). Structurally, it lies between these two northwest dipping belts, and is overthrust along much of its length by the CMB along the McLennan Lake Tectonic Zone. At the south end of the domain, the exposed relationship between the McLennan Group and the CMB is clearly interpreted to be an unconformity.

Based on recent remapping of parts of the region, two typically distinct supracrustal assemblages are recognized. Assemblage A (> ca. 1855 Ma), a predominantly volcano-plutonic assemblage that is exclusively made up of CMB rocks, comprises mafic to intermediate and minor felsic volcanics which are intruded by simple to multiphase plutons. Assemblage B (≤ 1855 Ma) is formed by polymictic volcanogenic conglomerate, psammite, calcareous psammite, psammopelite, trachytic-textured intermediate volcanics, amphibolite, and arkosic rocks including those of the McLennan Group. It is intruded by quartz-phyric granite porphyry, mafic to felsic dykes and sills, and multiphase granites. The basal parts of Assemblage B are characterized by a heterogeneous volcano-sedimentary succession that is gradational into and intercalated with overlying McLennan arkoses and arkosic conglomerates. Local unconformity exists between quartz-phyric granite porphyry, which intrudes polymictic volcanogenic conglomerate and overlying McLennan arkose, and arkosic conglomerate. However, major regional unconformity exists between Assemblage A and Assemblage B.

The basal, heterogeneous part of Assemblage B is of economic interest because it contains a diversity of gold occurrences which differ markedly from the shear zone-hosted deposits of the CMB. Examples of such occurrences are provided by showings at Greywacke Lake, Ramsland Lakes, and North Lake. The extended package of ca. 1840 to 1855 Ma supracrustals, overlying the CMB, and the similarly aged 'auriferous' volcano-sedimentary package now identified throughout the Glennie Domain, clearly represent a metallotect that has been underexploited because of a lack of deposit models.

Maxeiner, R.O., Sibbald, T.I.I., Slimmon, W.L.*, Heaman, L.M., and Watters, B.R. (1999): Lithogeochemistry of volcano-plutonic assemblages of the southern Hanson Lake Block and southeastern Glennie Domain, Trans-Hudson Orogen: Evidence for a single island arc complex; Can. J. Earth Sci., v36, p209-225.*

This paper describes the geology, geochemistry, and age of two amphibolite facies volcano-plutonic assemblages in the southern Hanson Lake Block and southeastern Glennie Domain of the Paleoproterozoic Trans-Hudson Orogen of east-central Saskatchewan. The Hanson Lake assemblage comprises a mixed suite of subaqueous to subaerial dacitic to rhyolitic (ca. 1875 Ma) and intercalated minor mafic volcanic rocks, overlain by greywackes. Similarly with modern oceanic island arcs, the Hanson Lake assemblage shows evolution from primitive arc tholeiites to evolved calc-alkaline arc rocks. It is intruded by younger subvolcanic alkaline porphyries (ca. 1861 Ma), synvolcanic granitic plutons (ca. 1873 Ma), and the younger Hanson Lake Pluton (ca. 1844 Ma). Rocks of the Northern Lights assemblage are stratigraphically equivalent to the lower portion of the Hanson Lake assemblage and comprise tholeiitic arc pillowed mafic flows and felsic to intermediate volcaniclastic rocks and greywackes, which can be traced as far west as Wapawekka Lake in the south-central part of the Glennie Domain. The Hanson Lake volcanic belt, comprising the Northern Lights and Hanson Lake assemblages, shows strong lithological, geochemical, and geochronological similarities to lithotectonic assemblages of the Flin Flon Domain (Amisk Collage), suggesting that all of these areas may have been part of a more or less continuous island arc complex, extending from Snow Lake to Flin Flon, across the Sturgeon-weir shear zone into the Hanson Lake Block and across the Tabbernor fault zone into the Glennie Domain.

Miles, W.F., Roest, W.R., ***Kelley, L.****, and Gent., M. (2000): Rationalized detailed gravity data, southern Saskatchewan; Geol. Surv. Can. Open File D3883, Sask. Energy Mines Open File 2000-1, CD.*

More than 150 detailed gravity surveys acquired for the exploration industry and archived as Bouguer anomaly maps at Saskatchewan Energy and Mines (SEM) cover much of southern Saskatchewan. Most of the available maps have been digitized, however, individual gravity surveys were tied to arbitrary datums and the Bouguer anomaly corrections were calculated with many different crustal rock densities. In order to generate a gridded data set suitable for regional scale interpretation it was necessary to level the data to a single datum and regenerate Bouguer anomalies with standard densities. The levelled data are presented as a flat file of principal facts with a FORTRAN program to extract data and recalculate anomalies based on user-specified Bouguer densities and geoid models.

Variations in the force of gravity are due to variations in the mass of underlying materials. Gravity surveys acquire data that map these small variations. The data are useful for geological interpretation and have applications in oil, gas, and mineral exploration. The gravity field is also used to define the geoid, which is the ideal shape of the Earth, or mean sea level if the Earth were completely covered with water.

Norford, B.S., Nowlan, G.S., ***Haidl, F.M.****, and Bezys, R.K. (1998): The Ordovician-Silurian boundary interval in Saskatchewan and Manitoba; in*

Christopher, J.E., Gilboy, C.F., Paterson, D.F., and Bend, S.L. (eds.), Eighth International Williston Basin Symposium, Sask. Geol. Soc., Spec. Publ. No. 13, p27-45.

Biostratigraphic data based on macrofossils and conodonts from wells and outcrops in the Williston and Hudson Bay basins permit new interpretations of stratigraphic units within the Ordovician-Silurian boundary interval. On the basis of conodont data, the Ordovician-Silurian boundary has been restricted to an 8 cm interval that essentially coincides with the top of the upper t-marker in the Stonewall Formation in Saskatchewan and within a 2 m interval associated with the t-marker in other outcrops and wells in Manitoba. Correlations in the Hudson Bay region are less precise because of sparse data. A major disconformity is documented within the Stonewall Formation of the Williston Basin with the associated hiatus ranging from latest Ordovician (Gamachian) to probably earliest Silurian (part of the Rhuddanian). Cyclic sedimentation related to relative sea-level changes is suggested by the repetition of carbonate lithologies separated by marker beds that probably represent disconformities of uncertain duration. The late Rhuddanian brachiopod *Virgiana decussata* (Whiteaves) occurs at the base of the Interlake Group in the Williston Basin and in the Severn River Formation of the Hudson Bay Basin, indicating the probable connection of the two basins at that time. In northern Manitoba, conodont data clearly indicate that the type section of the Port Nelson Formation is entirely Late Ordovician (Richmondian) and is correlated with the Stonewall Formation in the Williston Basin. The name Port Nelson Formation is advocated to replace the name Red Head Rapids.

Osadetz, K.G., Kohn, B.P., O'Sullivan, P., Feinstein, S., Hannigan, P.K., Everitt, R.A., ***Gilboy, C.F.,*** *Bezys, R.K., and Stasiuk, L.D. (1998): Williston Basin thermotectonics: Variations in heat flow and hydrocarbon generation;* in *Christopher, J.E., Gilboy, C.F., Paterson, D.F., and Bend, S.L. (eds.), Eighth International Williston Basin Symposium, Sask. Geol. Soc., Spec. Publ. No. 13, p147-165.*

Apatite fission-track (AFT) thermochronology and organic maturity data indicate spatial and temporal variations in the thermal history of the Williston Basin. Variations of oil windows are associated with crustal structure. Oil windows are elevated by ~750 m to ~1250 m and heat flow, as determined from maturity models, is at least 18% higher in the North American Central Plains Conductivity Anomaly than in adjacent regions. The persistent difference in heat flow between regions is attributed to crustal compositional changes originating during the Precambrian Trans-Hudson Orogeny. In the same region, some deduce that current geothermal gradients are still high. Analysis of apatite fission track (AFT) data indicates complicated temporal and geographical heat flow variations in the Williston Basin and on the adjacent Canadian Shield. On the Canadian Shield and in the thin wedge of peripheral Williston Basin strata, AFT data typically record a Late Precambrian epeirogeny followed by episodic Phanerozoic heating and cooling, the pattern of which corresponds to Williston Basin sedimentation history. Elsewhere the record of Late Precambrian cooling is obliterated by a resetting of AFT clocks during the Permian. The regions affected include both a basin central zone, with a radius of more than 300 km, where the Phanerozoic succession is more than 1500 m thick; and a linear zone at shallower depths, trending northwesterly from Yorkton to Lake Athabasca in Saskatchewan. The Permian thermal anomaly is intrinsic to the mechanism of Williston Basin subsidence, in that, in addition to the foregoing, it is associated with a major erosional event and originates in the basement. With geohistory constraints, the AFT models suggest Permian heat flows that were at least 184% of Mesozoic to present values. Neither the timing nor magnitude of this thermal event is considered by current tectonic models. Everywhere the pre-Mesozoic thermal history is partially to totally obscured by heating accompanying the Rocky Mountain Foreland sedimentation that extended beyond the Williston Basin onto the Canadian Shield. In most locations and strata the main stage of hydrocarbon generation began no sooner than latest Cretaceous to Early Tertiary time, although Permian heating has a significant potential to affect organic maturity histories in select locations and in lower parts of the Phanerozoic succession. The Deadwood Formation, which may be a source of a regionally significant, but poorly described hydrocarbon system, is predicted to have reached the main hydrocarbon generation stage during the Late Paleozoic, as a direct consequence of the Permian heating.

Pratt, B.R., Bernstein, L.M., and ***Haidl, F.M. (1998):*** *Upper Ordovician reef in Red River strata, subsurface Saskatchewan;* in *Christopher, J.E., Gilboy, C.F., Paterson, D.F., and Bend, S.L. (eds.), Eighth International Williston Basin Symposium, Sask. Geol. Soc., Spec. Publ. No. 13, p26.*

A 2.8 m thick boundstone unit occurs at the base of the Lake Alma Member, Yeoman Formation (Upper Ordovician), in the LVR *et al.* Steelman 7-28-4-4W2 well. It overlies 0.4 m of laminated lime mudstone and fine-grained grainstone which in turn overlie 3.4 m of bioclastic rudstone rich in laminar and low-relief domal stromatoporoid-like fossils. The reef is capped by 0.8 m of lime mudstone and fine-grained grainstone.

The reef is thrombolitic, in that it consists of millimetre- to centimetre-sized, knob-like digits and crusts of microbial origin, which impart a mottled appearance to the core. This microbial framework is composed of variable proportions of clotted micrite and hemispheroids of laterally juxtaposed, radiating micrite-walled tubes attributable to Ortonella (or Cayeuxia). Many clotted micrite knobs exhibit a radial fabric, and their outer portions are locally laminated and therefore stromatolitic.

Locally common are undulating laminar and rarely columnar stromatoporoid-like fossils 0.5 cm thick and several centimetres wide. Intergrown or incorporated into the clotted micrite are horizontal meandering to loosely coiled tubular skeletons 0.5 to 1 mm wide of unknown affinity, micrite-walled, Terebella-like 'worm' tubes, rare Wetheredella (foraminifer?) and ramose bryozoans. In the matrix are abundant ostracodes, scattered brachiopods, gastropods, crinoid ossicles and possible bivalves. Small cavities contain geopetal micrite peloids. Larger pockets and intercalated thin beds and laminae of lime mudstone exhibit multiple generations of Planolites burrows suggestive of increasing induration. Isopachous fibrous submarine cement is common. Replacive anhydrite is ubiquitous and the rock is dolomitized.

This framework composition is unique among Upper Ordovician reefs which tend to exhibit a more diverse biota. Somewhat similar frameworks are known from the Alpine Triassic and Mediterranean Miocene and point to a marine but somehow ecologically stressed environment. The reef points to a more complex arrangement of facies in the Red River succession than hitherto believed.

Ridgley, J.L., McNeil, D.H., ***Gilboy, C.F.****, Fisher, C.G., Condon, S.M., and Obradovich, J.D. (2000): Interplay of structure, facies, and unconformities on sites of biogenic gas accumulation in Upper Cretaceous Belle Fourche and Greenhorn formations–Alberta, Saskatchewan, and Montana; GeoCanada 2000, Calgary, May 2000, Conference CD, ext. abstr. #313.*

Roberts, R. Gwilym and ***Maxeiner, R.O.*** *(1999): The Anglo-Rouyn Deposit, La Ronge, Saskatchewan: A Besshi-type massive sulphide deposit;* in *Ashton, K.E. and Harper, C.T. (eds.), MinExpo'96 Symposium–Advances in Saskatchewan Geology and Mineral Exploration, Sask. Geol. Soc., Spec. Publ. No. 14, p44-55.*

The Anglo-Rouyn deposit is on the northwest shore of Lac La Ronge, approximately 35 km northeast of La Ronge, Saskatchewan. Between 1966 and 1972, 1.7 million tonnes of ore with an average grade of 1.7 percent Cu, 1.2 g/t Au, and 5.5 g/t Ag were extracted from three orebodies of chalcopyrite, pyrite, pyrrhotite, magnetite, and trace amounts of sphalerite. The property consists of: 1) a northeast-trending, northwest-facing sequence of metabasaltic flows and tuffs, accompanied by greywacke-type metasediments; 2) overlying footwall rocks of calc-silicate gneiss, hornblende-plagioclase gneiss and laterally equivalent, gneissic magnetite iron formation; and 3) the ore zone rocks, which consist of the host quartz-hornblende-plagioclase gneiss and quartz-plagioclase gneiss in the hanging wall.

The rocks of the area have undergone three episodes of deformation. The first of these is the most significant, since it established the structural architecture of the region and coincided with the regional, amphibolite facies metamorphism. The units of the mine area are on the northwest limb of an antiform that closes to the southeast. Both regional- and property-scale structural evidence indicate that the units face, as well as dip, to the northwest. The Jepson Lake granite, a regional-scale, sill-like body, was intruded into the hanging-wall units before or during deformation.

Major and trace element whole rock geochemistry was used in association with the geological data to determine the protoliths of the gneissic rocks associated with the ore. The stratigraphic succession in the mine area records the history of a volcano-sedimentary package in a volcanic arc environment as it evolved from mafic volcanism and siliceous greywacke-type sedimentation into a basin in which both clastic and exhalative, chemical sediments were deposited. The exhalative component in the footwall rocks changed from carbonate-silica in the sediments overlying the mafic volcanics to iron oxide-carbonate in the sediments underlying the ore zone. The clastic component is similar in each unit and was derived from the underlying mafic volcanics, probably by a combination of near-surface, submarine alteration and sedimentary processes. The cupriferous sulphides of the Anglo-Rouyn ore immediately overlie the magnetite iron formation, and the maximum development of sulphides in the basin appears to be at the fringes of the iron oxide-rich sediment (the magnetite iron formation). The units of the ore zone (quartz-hornblende-plagioclase gneiss and quartz-plagioclase gneiss) signify a stage in the development of the volcanic-sedimentary basin when exhalative sedimentary processes dominated over clastic sedimentation. The rocks are believed to be isochemically metamorphosed, mixed clastic-exhalative sediments.

The Anglo-Rouyn is an exhalative deposit and several characteristics, listed below, point to its classification with Besshi-type massive sulphide deposits: 1) the metal content of the sulphide ore is Cu, ±Zn, Au, low Pb; 2) the association of the ore body with mafic volcanic rocks and greywacke sediments in a probable back-arc setting; 3) the sheet-like form of the sulphide units, and the absence of any evidence of focused discharge sites; and 4) the close association of the ore with a succession of exhalative-clastic sediments, in which silica-carbonate exhalite is widely dispersed and the sulphide ore is associated with the more restricted iron oxide exhalite (magnetite iron formation).

Rostron, B.J., Holmden, C., and ***Kreis, L.K.*** *(1998): Hydrogen and oxygen isotope compositions of Cambrian to Devonian formation waters, Midale area, Saskatchewan;* in *Christopher, J.E., Gilboy, C.F., Paterson, D.F., and Bend, S.L. (eds.), Eighth International Williston Basin Symposium, Sask. Geol. Soc., Spec. Publ. No. 13, p267-273.*

Hydrogen and oxygen isotopic compositions of formation waters from the Williston Basin are reported from drill stem tests and produced waters for a stratigraphic section near Midale, southeastern Saskatchewan. Above the Prairie aquitard, the Birdbear and Duperow aquifers exhibit the highest δD (-17‰) and $\delta^{18}O$ (6.9‰) values known from the Williston Basin. They are substantially more D and ^{18}O enriched than formation waters from equivalent aquifers 160 to 360 km farther north and northeast in stratigraphic sections above three potash mines. Below the Prairie aquitard, the three deepest aquifers at the Midale site yielded lower δD and $\delta^{18}O$ values than the Birdbear and Duperow aquifers and are relatively uniform in isotopic composition down to the Precambrian basement. The new data, in conjunction with data from the literature, show that Williston Basin formation waters vary substantially in isotopic composition between aquifers in stratigraphic section and within the same aquifer regionally. These large isotopic variations reveal the potential of H and O isotopes in Williston Basin formation waters for tracing petroleum migration pathways and for fingerprinting sources of contaminant water encountered during drilling and production of hydrocarbons.

Sibbald, T.I.I. *(1999): Nicholson Bay Uranium-Gold-PGE Deposits;* in *Ashton, K.E. and Harper, C.T. (eds.), MinExpo'96 Symposium–Advances in Saskatchewan Geology and Mineral Exploration, Sask. Geol. Soc., Spec. Publ. No. 14, p139.*

Between 1953 and 1982, the Beaverlodge uranium district produced some 25 000 t of uranium metal from 17 main mines. The producing deposits, as well as numerous other radioactive showings in the area, are predominantly classical epigenetic vein-type pitchblende occurrences. Most are hosted by rocks of the metamorphic basement although veins are also present in rift-deposited immature clastics and alkalic basalts of the unconformably overlying Paleoproterozoic (1700 to 1800 Ma) Martin Group. Mineralization is also known in the younger Mesoproterozoic (1450 to 1700 Ma) mature sandstones of the Athabasca Group.

The epigenetic deposits can be divided into two groups, respectively showing simple and complex mineralogy. In the former, pitchblende is accompanied by brannerite, chalcopyrite, pyrite, galena and nolanite, and uranium by a simple suite of elements (Cu, Pb, Fe, V, and S). In the latter, pitchblende and thucolite are accompanied by arsenides, sulphides, selenides and native metals, and uranium by a diverse group of elements (Cu, Ni, Co, As, Pb, Fe, V, Y, Se, Ag, Au, and PGEs).

The association of uranium, gold, and platinum group metals was first described in 1955, but only more recently has exploration interest for the precious metals gained importance. Impetus was provided by: 1) discovery of a potentially economic zone of gold-platinum group metal mineralization, adjacent to the historically mined Coronation Hill uranium-gold deposit, in the South Alligator River Uranium Field (SARUF) in the Northern Territory of Australia, and 2) recognition that Coronation Hill and other deposits in the SARUF show many similarities of mineralogy and geological setting to complex pitchblende veins in the Beaverlodge district. The regional geological analogy is further enhanced by the undoubted resemblance of the nearby world-class unconformity-type uranium deposits of the Alligator River Uranium Field to those within the Athabasca Basin of Saskatchewan. Exploration around Nicholson has identified, adjacent to historic uranium prospects, more extensive zones of gold and platinum group metal mineralization than previously recognized (Nicholson #2 zone) and has also resulted in new discoveries (Quartzite Ridge).

Cryptic gold and platinum group metal mineralization occurs within alteration zones commonly adjacent to uranium veins of complex mineralogy. These zones are characterized by: 1) hematization, silicification, and talcification of host dolomitic marbles, diopsidic calc-silicates, and quartzites; 2) extensive fracturing; and 3) development of vugs containing euhedral quartz, specular hematite, and carbonates. There is a close spatial relationship to the sub-Martin Group and/or sub-Athabasca Group unconformities, and detailed field relationships and U/Pb (pitchblende) age data suggest mineralization after deposition of the Athabasca Group. Preliminary fluid inclusion studies from secondary euhedral quartz and carbonates from the altered/mineralized zones indicate fluids with temperatures in the range 150° to 200°C and high salinities. Similar fluids characterize the unconformity-type uranium mineralization of the Athabasca Basin.

The uranium-gold-platinum group metal deposits of the Beaverlodge district and SARUF represent a new type of low-temperature, hydrothermal precious metal mineralization. Their economic potential is as yet unknown, as is the exploration potential of the Paleo- to Mesoproterozoic sandstone basins to which they appear related.

Syme, E.C., Lucas, S.B., Zwanzig, H.V., Bailes, A.H., ***Ashton, K.E.****, and* ***Haidl, F.M.*** *(1998): Geology, NATMAP Shield Margin Project Area, Flin Flon Belt, Manitoba/Saskatchewan accompanying notes; Geol. Surv. Can. Map 1968A, Manit. Energy Mines Map A-98-2, Sask. Energy Mines Map 258A, 54p.*

The regional compilation maps of the Paleoproterozoic Flin Flon Belt, southern Kisseynew Domain and interpreted sub-Phanerozoic basement (six sheets, 1:100,000 scale), and adjacent Phanerozoic cover (Fig. 1a, 1:325,000 scale), represent synthesis products stemming from the NATMAP Shield Margin Project. These maps are the culmination of efforts by the project partners (Manitoba Geological Services Branch (MGSB), Saskatchewan Geological Survey (SGS), and Geological Survey of Canada (GSC)) and build on the rich history of geoscience mapping in the Flin Flon Belt. A companion set of surficial geology maps has been produced at 1:100,000 scale (see below). A preliminary CD-ROM containing digital maps and an integrated geoscience knowledge base was released in 1993 (Broome *et al.*, 1993; Broome and Viljoen, in press). The final synthesis maps, more detailed maps, and most other geological, geophysical, and geochemical information sets pertinent to the project area are planned for release in digital format in a final project CD-ROM in 1999.

The National Geoscience Mapping Program (NATMAP) aims to foster a multidisciplinary team approach to bedrock and surficial mapping and related research, combine the efforts of federal, provincial and university scientists, and utilize digital information technology for more efficient interdisciplinary research and map publication. The Shield Margin Project, initiated in March 1991, was an inaugural NATMAP venture (Lucas *et al.*, in press a, b). Its purpose was to study the Paleoproterozoic rocks of the Flin Flon Belt and their continuation below gently dipping Paleozoic carbonates and the Quaternary cover. The region was chosen in part because of its economic significance: the Flin Flon greenstone belt is the largest Paleoproterozoic volcanic-hosted massive-sulphide (VMS) district in the world (e.g. Galley, 1996, and references therein), and also contains producing gold deposits.

The Shield Margin Project is closely tied to a variety of initiatives, including the Partnership Agreements on Mineral Development (1990-95) in Manitoba and Saskatchewan, the Snow Lake Exploration Technology (EXTECH) project, LITHOPROBE's Trans-Hudson Orogen Transect (THOT), the International Metamorphic Map program, and the Industrial partners Program (with Hudson Bay Mining and Smelting Co.). The NATMAP project team has brought together over 50 participants from government surveys, universities (Calgary, Saskatchewan, Regina, Manitoba, Queen's, Ottawa, UQAM, Concordia, McGill, UNB) and the minerals industry.

Tran, H.T., Lewry, J.F., Bethune, K., ***Ashton, K.****,* ***Yeo, G.****, and Ansdell, K. (2000): Crustal thrusting and tectonic imbrication in the Cree Lake Zone, northern Saskatchewan: Implications for the tectonic evolution of western foreland of the Trans-Hudson Orogen; GeoCanada 2000, Calgary, May 2000, Conference CD, ext. abstr. #579.*

Wright, D.M., Ansdell, K.M., Corrigan, D., and ***Maxeiner, R.O.*** *(2000): Metamorphic petrology and tectonic setting of variably altered Paleoproterozoic volcanic rocks, Reindeer Lake, northern Saskatchewan; GeoCanada 2000, Calgary, May 2000, Conference CD, ext. abstr. #543.*

Yeo, G.M. *(1999): Is the Janice Lake unconformity a link between the Hearne Craton and the La Ronge–Lynn Lake volcanic arc?; Institute on Lake Superior Geology Proceedings, 45th Annual Meeting, Marquette, MI, 1999, v45, Part 1, p59-60.*

The Wollaston Domain, a NE-trending, 75 km wide belt of 2076-1860? Ma paragneisses, overlying Archean orthogneisses along the eastern edge of the Hearne Craton in Saskatchewan, is separated from 1910-1875 Ma arc volcanics and sediments of the La Ronge Domain by (a) Archean orthogneisses, poorly known supracrustal rocks, and minor Proterozoic plutons of the Peter Lake Domain, (b) 1855 Ma monzogranite to quartz diorite of the Wathaman Batholith, and (c) the Rottenstone Domain, a migmatitic belt of sediments, similar to those of the La Ronge Domain, intruded by tonalite. The boundary between Wathaman Batholith and Wollaston and Peter Lake domains is the Needle Falls–Parker Lake Shear Zone. While this is a fundamental break between ancient crust to the west and juvenile crust of Trans-Hudson Orogen to the east, there is no evidence that it is a collisional suture.

Within the Wollaston supracrustal succession, the Janice Lake Conglomerate, which can be traced discontinuously for 245 km along the eastern margin of the belt, marks a major unconformity. The conglomerate is polymictic, with clasts derived from underlying strata predominating. Locally, it includes fanglomerate. Although the conglomerate cannot be traced westward, younger calc-silicate bearing strata, locally resting on various older lithostratigraphic units, mark the presence of a profound unconformity. A correlative unconformity has been recognized in the Manitoba segment of Wollaston Domain, another 200 km to the northeast.

In the absence of any evidence for thermal uplift (i.e. igneous activity), uplift and extension in Janice Lake time must be due to mechanical flexure of the crust. A probable cause is tectonic loading of the eastern margin of the Hearne craton as the La Ronge–Lynn Lake volcanic arc converged towards it over an east-dipping subduction zone. Volcanism in the La Ronge–Lynn Lake arc began about 1910 Ma and reached a peak about 1880 Ma. Following arc-craton collision at about 1860 Ma, the sense of subduction was reversed and the Wathaman Batholith was emplaced at about 1855 Ma. Geochemical evidence suggests that the La Ronge segment of the arc developed in a transitional crust setting, close to or partly over marginal continental crust.

Tectonic loading of the outboard margin of the Hearne Craton would have resulted in an inboard flexural bulge, with consequent normal faulting and erosion over its crest and deposition of coarse clastics on its flanks. As convergence proceeded, the bulge would have migrated cratonward and died out, creating a diachronous regional unconformity. Preservation of coarse clastics would be favoured only on the trailing, eastern flank of the bulge, however. The approaching volcanic arc would have become a barrier to the open ocean, and accumulation of evaporites and carbonates in the resulting restricted basin would have been increasingly favoured.

This hypothesis also explains the dramatic change in sedimentation recorded by the Wollaston paragneisses. Following 2100 Ma rifting, the widespread Lower Sequence of psammopelites, pelites, and feldspathic psammites accumulated on a passive margin. As arc-craton convergence proceeded, coarse clastics were shed off a migrating flexural bulge ahead of the arc. Upper Sequence calc-silicate rich strata subsequently accumulated in the developing foreland basin.

Yeo, G.M. *(1999): Low-resolution sequence stratigraphy of early Proterozoic paragneisses, Wollaston Domain, Saskatchewan; Institute on Lake Superior Geology Proceedings, 45th Annual Meeting, Marquette, MI, 1999, v45, Part 1, p61-62.*

The Wollston Domain is a NE-trending, 75 km wide belt of early Proterozoic paragneisses, overlying Archean orthogneisses along the eastern edge of the Hearne Craton; west of the Trans-Hudson Orogen. Bimodal volcanics near the base of the paragneiss succession give a U-Pb zircon age of 2.08 Ga, while minor gabbro and granitic plutons range from 1.81 to 1.84 Ga. A three-year, 1:20,000 scale mapping project was begun in 1997 in the southern part of Wollaston Domain to improve understanding of the stratigraphy and structure of the gneisses, which underlie the unconformity-type uranium deposits of Athabasca Basin. A basic strategy of the project is to map outward from Archean inliers so as to be able to work out the stratigraphic succession in spite of complex deformation and high metamorphic grade.

Four episodes of regional deformation can be distinguished. D1 involved isoclinal folding, local basement overthrusting, and transposition of primary layering into the S1 foliation. D2 involved tight to isoclinal folding about NE-trending axes, superposition of a strong S2 foliation, and local thrust faulting. D3 involved local open folding about SW to NW axes, and local brittle-ductile fault movement. D4 involved minor sinistral offset on a series of N to NNW trending brittle faults.

Two episodes of high T-low P (upper amphibolite–lower granulite facies) metamorphism are associated with D1 and D2 deformation. Peak P-T conditions, reached during D2, were about 750°C and 5 kbar. Along the eastern margin of the belt, however, metamorphic grades are relatively low (upper greenschist–lower amphibolite facies).

Two widespread paragneiss successions are distinguished in Wollaston Domain: a lower Pelite Unit, and an overlying Psammite Unit. These can be subdivided into at least eight subunits in the Foster-Daly lakes area. Two restricted successions are also recognized: a basal package (Courtenay Lake and Souter Lake Formations), preserved locally along the eastern margin of the domain, and the heterogenous Hidden Bay Assemblage of interlayered quartzites, pelites, amphibolites, calc-silicates, and marbles, which likely overlies or is correlative with the Psammite Unit near Wollaston Lake. The Courtenay Lake Formation has been demonstrated to be a rift succession, while a passive margin setting is inferred for the overlying Pelite and Psammite units. Attempts to determine the depositional setting of individual lithologic units, however, have been restricted to the low-grade rocks along the eastern margin of the domain.

Although sequence stratigraphy has become a standard technique for analysis of platform and craton margin strata, there have been few attempts to apply it to metamorphosed and deformed rocks. As demonstrated here, it has great potential in interpreting strata in which obliteration of primary features limits application of facies models or comparison with modern sedimentary environments.

Two major sequence boundaries subdivide the succession. The unconformity on Archean basement can be recognized without difficulty. The base of the Janice Lake Conglomerate (Unit Wo) marks a second unconformity. To the west, where the conglomerate is absent, this unconformity corresponds to the base of the calcareous rocks that overlie it. Within each sequence, the mapped lithofacies units can be assigned to a succession of systems tracts.

Yeo, G., Delaney, G., *and Tran, H. (2000): Paleoproterozoic stratigraphy of the Wollaston Supergroup, Saskatchewan; GeoCanada 2000,*

Calgary, May 2000, Conference CD, ext. abstr. #588.

Acknowledgments

Saskatchewan Geological Survey project leaders acknowledge the assistance in the field and office of the following, hired under the Saskatchewan Student Summer Employment Program: Sarah Allen, Danielle Bovin, Erin Chorney, Brent Collier, Grant Cranfield, Cameron Demans, Sarah Ehman, Amanda Gaze, Aaron Grimeau, Russell Hartlaub, Geoff Heggie, Douglas Hobson, Ryan Morelli, Kevin Radke, Andy Tong, and Asha Yanko.

The scientific and production editors are grateful for assistance given the editing and production process by Ken Ashton, Jagdish Bilkhu, Lynn Kelley, Ralf Maxeiner, Dave MacDougall, Laura Smith, and Gary Yeo.

The preliminary field maps, in the associated but separately released map package, were produced using AutoCAD and FieldLog software. Bill Slimmon was primarily responsible for implementing the assembly of the digital maps. Ryan Bayne and Ken Tong were variously involved in the production of these maps.

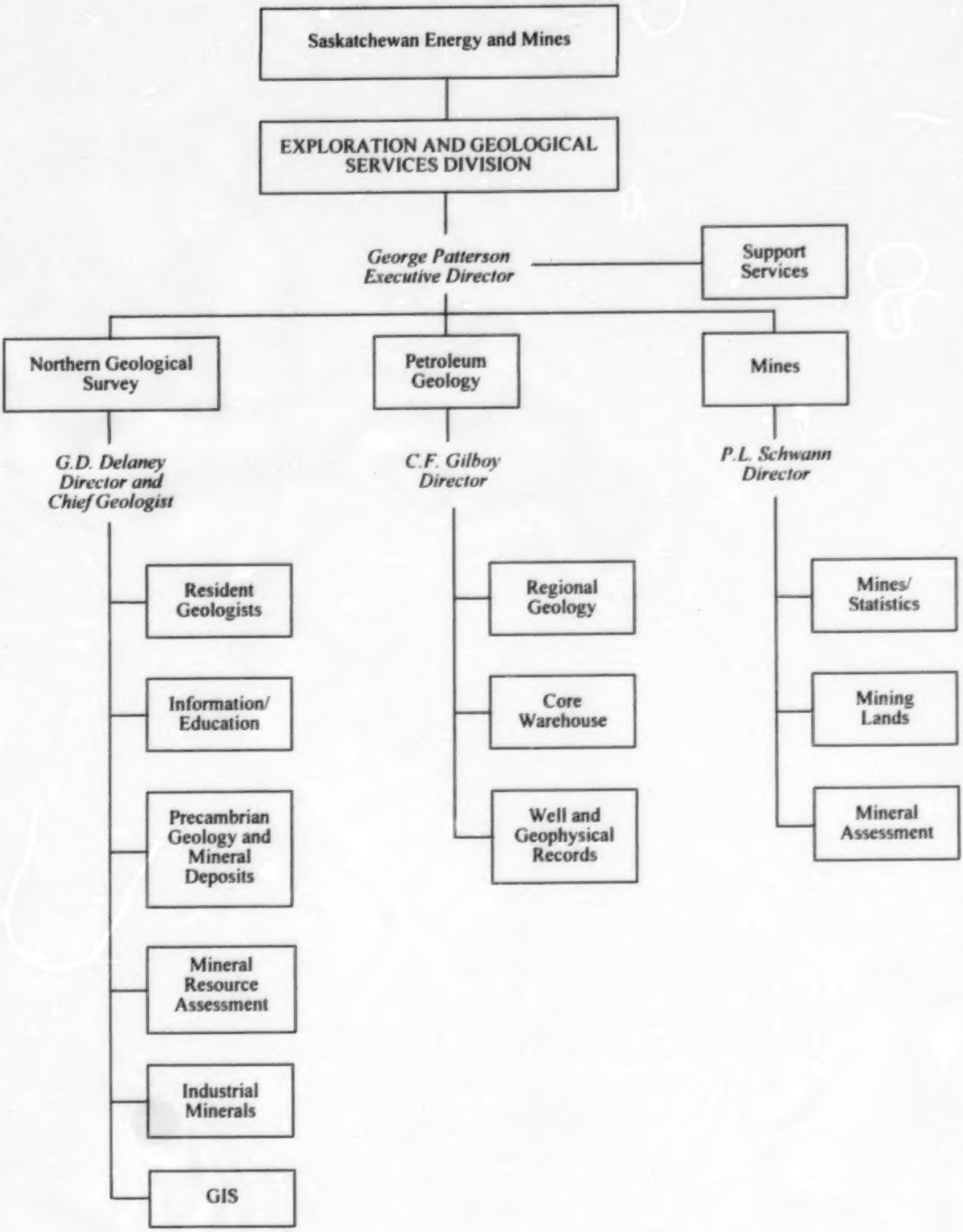
Saskatchewan Energy and Mines
EXPLORATION AND GEOLOGICAL SERVICES DIVISION
George Patterson Executive Director
Support Services
Northern Geological Survey
Petroleum Geology
Mines
G.D. Delaney Director and Chief Geologist
C.F. Gilboy Director
P.L. Schwann Director
Resident Geologists
Information/ Education
Precambrian Geology and Mineral Deposits
Mineral Resource Assessment
Industrial Minerals
GIS
Regional Geology
Core Warehouse
Well and Geophysical Records
Mines/ Statistics
Mining Lands
Mineral Assessment

The Saskatchewan Geological Survey comprises the geoscience activities of the Northern Geological Survey and Petroleum Geology.

Staff as of December 1, 2000

Exploration and Geological Services Division
Administration

2101 Scarth Street, Regina, SK S4P 3V7

Executive Director George Patterson, *Ph.D., P.Geo.* (787-2560)
E-mail: gpatterson@sem.gov.sk.ca
Secretary .... J. Adams (787-2476)

Northern Geological Survey Branch

2101 Scarth Street, Regina, SK S4P 3V7
FAX: 787-1284

Director and Chief Geologist .... G.D. Delaney, *Ph.D., P.Geo.* (787-1160)
E-mail: gdelaney@sem.gov.sk.ca

Precambrian Geology:
Project Geologists .... K.E. Ashton, *Ph.D., P.Geo.* (787-1909)
E-mail: kashton@sem.gov.sk.ca
Jurgen Kraus, *Ph.D., G.I.T.* (787-3931)
E-mail: jkraus@sem.gov.sk.ca
R. Maxeiner, *M.Sc., P.Geo.* (787-2553)
E-mail: rmaxeiner@sem.gov.sk.ca
G. Yeo, *Ph.D., P.Geo.* (787-2568)
E-mail: gyeo@sem.gov.sk.ca

Scientific Editor/Project
Geologist .... C.T. Harper, *Ph.D., P.Eng., P.Geo.* (787-2578)
E-mail: charper@sem.gov.sk.ca

Industrial Minerals:
Geologist .... Lynn Kelley, *M.Sc., P.Geo.* (787-2646)
E-mail: lkelley@sem.gov.sk.ca

GIS Geologist .... W.L. Slimmon, *M.Sc., P.Geo.* (787-9181)
E-mail: bslimmon@sem.gov.sk.ca

GIS Technician .... Ken Tong, *B.Sc.* (787-2436)
E-mail: ktong@sem.gov.sk.ca

Geological Information/Education:
Geologist .... D.G. MacDougall, *B.Sc.(Hons.), P.Geo.* (787-2579)
E-mail: dmacdougall@sem.gov.sk.ca

Mineral Resource Assessment:
Geologist .... M. Rogers, *M.Sc., P.Geo.* (787-1932)
E-mail: mrogers@sem.gov.sk.ca
Technician .... Ryan Bayne, *B.Sc. (Hons.)* (787-7284)
E-mail: rbayne@sem.gov.sk.ca

Secretary .... J. Bilkhu (787-2585)
E-mail: jbilkhu@sem.gov.sk.ca

Warehouse Operator (part-time) .... I.P. Gaw (787-2491)

Mineral Assessment/Mineral Deposits Index:
FAX: 787-2488

Geologist .... R.W. Bennett, *B.Sc.(Hons.), P.Eng., P.Geo.* (787-2569)
E-mail: rbennett@sem.gov.sk.ca
Clerk .... L. Smith, *B.Sc.* (787-2582)
E-mail: lsmith@sem.gov.sk.ca

Resident Geologist Offices:

La Ronge:
P.O. Box 5000, La Ronge, SK S0J 1L0
FAX 425-4471

Geologists .... A.J. Gracie, *Ph.D., P.Eng., P.Geo.* (425-4499)
E-mail: agracie@sem.gov.sk.ca
Ghislain Tourigny, *Ph.D.* (425-4564)
E-mail: gtourigny@sem.gov.sk.ca
Clerk .... T. Beck (425-4498)

Creighton:
P.O. Box 70, Creighton, SK S0P 0A0
688-8800

Support Services Section

2101 Scarth Street, Regina, SK S4P 3V7
FAX: 787-1284

Manager/
Production Editor .... C.L. Brown, *B.Sc.(Hons.)* (787-2590)
E-mail: cbrown@sem.gov.sk.ca

Petroleum Geology Branch

201 Dewdney Avenue East, Regina, SK S4N 4G3
FAX: 787-4608

Director .... C.F. Gilboy, *Ph.D., P.Eng., P.Geo.* (787-2573)
E-mail: cgilboy@sem.gov.sk.ca

Regional Geology:
Geologists .... F.M. Haidl, *M.Sc., P.Geo.* (787-6116)
E-mail: fhaidl@sem.gov.sk.ca
L.K. Kreis, *M.Sc., P.Geo.* (787-2620)
E-mail: kkreis@sem.gov.sk.ca
E. Nickel, *B.Sc., G.I.T.* (787-0169)
E-mail: enickel@sem.gov.sk.ca
Part-time Geologists .... D. Harvey, *B.Sc., G.I.T.* (787-2621)
A. Nimegeers, *B.Sc. (Hons.), G.I.T.* (787-2621)

Warehouse:
Supervisor .... M. Mongrain (787-2622)
Staff .... D. Gallant (787-2622)
R. McCall (787-2622)
T. Mounstephen (787-2622)
Part-time Staff .... K. Desjarlais (787-2622)
Secretaries .... C. Boyle (787-1393)
R. Lavigne (787-2621)

2101 Scarth Street, Regina, SK S4P 3V7
FAX: 787-2488

Well and Geophysical Records:
Geologist .... D.R. Troyer, *M.Sc., P.Eng., P.Geo.* (787-2562)
E-mail: btroyer@sem.gov.sk.ca
Engineer .... T. Badger, *P.Eng.* (787-2492)
E-mail: tbadger@sem.gov.sk.ca
Horizontal Well Coding Clerk .... R. Ferner (787-2550)
E-mail: rferner@sem.gov.sk.ca
Well File Clerks .... L. Mikenas (787-3804)
B. Russell (787-7416)
G. Schick (787-1363)
L. Siapno (787-7373)
Coding Clerks .... N. Bhasin (787-7420)
A. Landry (787-7412)
P. McMillen (787-7421)
D. Read (787-2443)
C. Syrota (787-2398)
J. Tanouye (787-2757)
G. Ziegler (797-7413)
E-mail: geodata@sem.gov.sk.ca
Geophysical Clerk .... L. Merkel (787-2558)
E-mail: geophysical@sem.gov.sk.ca

Mines Branch

2101 Scarth Street, Regina, SK S4P 3V7
FAX: 787-1284

Director .... P.L. Schwann, *M.Sc., P.Geo.* (787-2584)
E-mail: pschwann@sem.gov.sk.ca
Administrator .... L. Troesch (787-2537)
E-mail: ltroesch@sem.gov.sk.ca
Mining Recorder .... K. Klyne (787-2538)
E-mail: staking@sem.gov.sk.ca
District Mineral Officer (La Ronge) .... M. O'Brien (425-4600)
E-mail: mo'brien@sem.gov.sk.ca
Clerk .... S. Bond (787-8247)
Industrial Minerals Clerks .... D. Buckshaw/M. Zaron (787-2539)
Assessment Geologist .... H. Stolz, *B.Sc., P.Eng.* (787-2564)
E-mail: hstolz@sem.gov.sk.ca
Mining Engineer .... G. Lopez, *B.Sc., P.Eng., P.Admin.* (787-2559)
E-mail: glopez@sem.gov.sk.ca
Clerk .... V. Bohn (787-7631)
E-mail: minestats@sem.gov.sk.ca
Data Processing Geologist .... N. Lee, *B.Sc., P.Eng.* (787-2574)
E-mail: nlee@sem.gov.sk.ca